Institute of Robotics and Mechatronics Status Report: **Scientific Results** 2005–2008

Publisher	Deutsches Zentrum für Luft- und Raumfahrt e.V. in der Helmholtz-Gemeinschaft
Director of the Institute	Prof. Dr.-Ing. Gerd Hirzinger
Address	Oberpfaffenhofen 82230 Wessling
Telephone *Telefax* *WWW*	+49 8153 282400 +49 8153 281134 www.robotic.dlr.de
Editor	dr Patrick van der Smagt
Print	Druckerei Thierbach GmbH 45478 Mühlheim an der Ruhr
Publication date	January, 2009

DLR
Institute of Robotics and Mechatronics
Status Report: **Scientific Results**
2005–2008

I Overview

This status report describes DLR's Institute of Robotics and Mechatronics (DLR-RM) with respect to the scientific technological results achieved in the period 2005–2008. In this first chapter a short overview is given, in particular regarding the institute's "mission", structure and major achievements.

1 On the Institute's "Mission" and Goals

The main scientific-technological focus of the institute is the multidisciplinary (virtual) design, computer-aided optimisation, and realisation of mechatronic systems and man-machine interfaces. We thus aim at the **development of intelligently controlled mechanisms** (in particular **robots, small satellites, aeroplanes, vehicles**). These typically exhibit some kind of autonomy, but also should allow for human intervention at any time, e.g., based on "shared control". **Mechatronics,** as the **fundamental technological basis** of our institute, for us not only means the utmost integration of mechanics, optics, electronics, and information technologies in one functional unit, but also the holistic, computer-aided 3-D simulation and design optimisation: **concurrent engineering**. Therefore we aim at the parallel design and simulation of all dynamical and physical effects and their interactions, e.g., multibody dynamics, spatial integration of electronic components into 3-D CAD design, simulation of electronic circuits and their heat transfer characteristics, as well as design and simulated verification of control and feedback algorithms to be realised in embedded computer chips. For critical aerospace and vehicle applications we develop new **control engineering techniques** and tools for modelling, simulation, and control design.

The intelligently controlled mechanisms as mentioned above need sensory perception and feedback up to the cognitive level. Thus, the higher-level control systems that we develop (in addition to the dynamic modelling and simulation), comprise advanced telerobotic and telepresence concepts with full and "shared" local autonomy as well as multi-sensory 3-D world-modelling, object recognition, and motion planning.

Our technological developments over the past years are classified and subdivided into DLR's programmatic key areas:

- **Space flight:**
  - space robotics
  - advanced space technologies
- **Aeronautics**:
  - flight dynamics and control
  - more electric aircraft systems
- **Transportation**:
  - vehicle dynamics and control
  - innovative mechatronic subsystems.

The development of remotely controlled and (semi-)autonomous robots or robonauts for space has traditionally been a central focus of the institute's work. In January 2006 the organisational unit Optical Information Systems OS in Berlin has become an integral part of the institute (RM-OS) and has widened the space flight theme (for the scientific-technical results—advanced space technologies—see Chapter II.2). Technology transfer and "cross transfer" synergies (including contributions to the wide field of security) is gaining even more importance in the institute now. The next page visualises present structures of the institute and the main contributions of the departments to the programmatic areas.

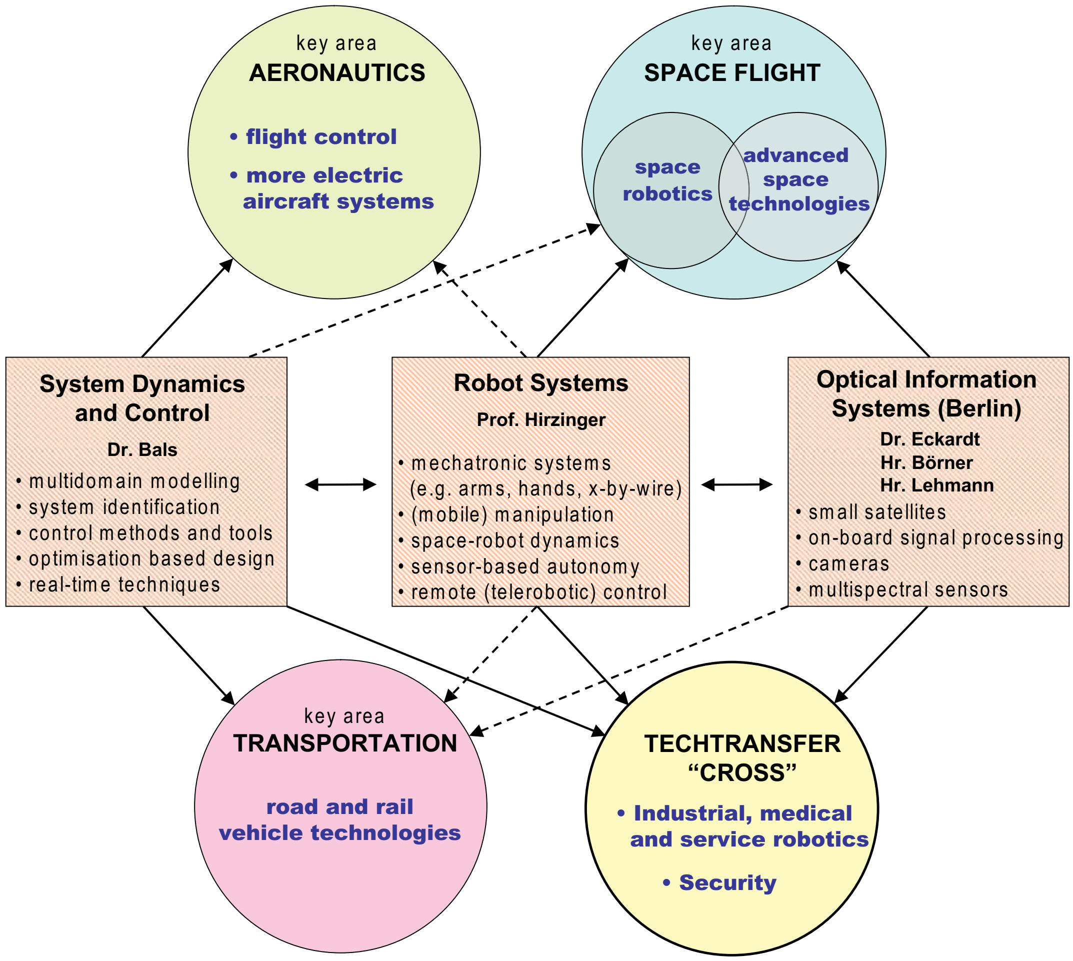

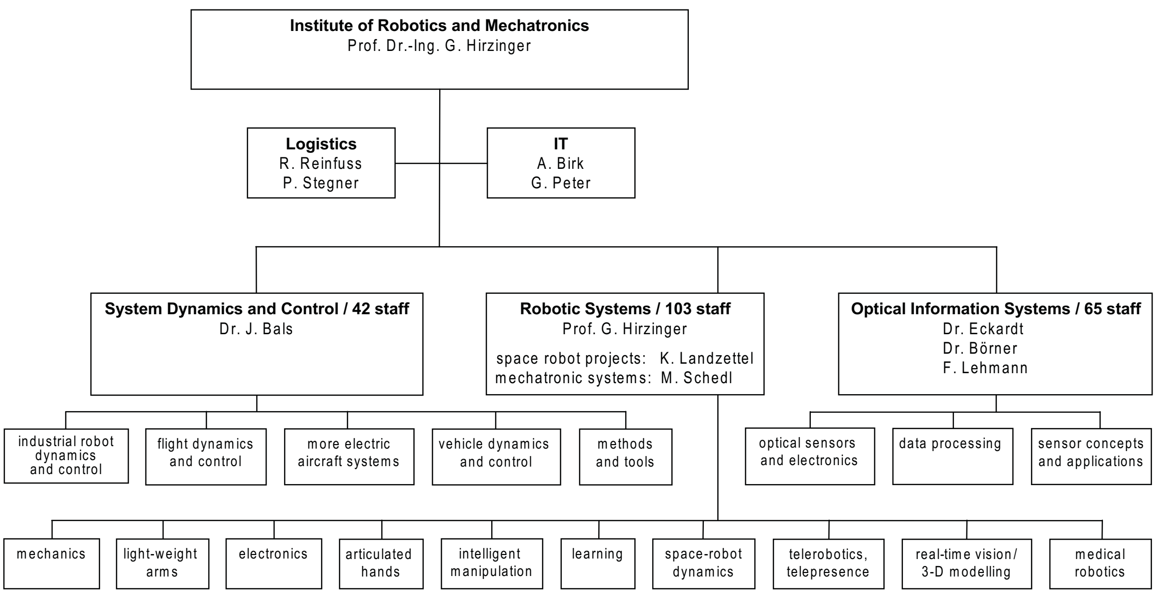

Fig. 1 Organisation and Fields of Research of DLR's Institute of Robotics and Mechatronics

Presently our **technology transfer efforts** (including the founding of spin-off companies) are focused on various areas, e.g.:

- sensors, actuators, man-machine interfaces;
- industrial and service robotics;
- medical technologies (artificial organs, surgical robots), prostheses;
- drive-by-wire in automotive systems;
- software tools (Modelica model libraries, MOPS optimisation environment);
- education in mechatronics.

2 Major Achievements – a Brief Excerpt

2.1 Space Flight

ROKVISS on the ISS

In January 2005 we have launched the ROKVISS (Robotic Components Verification on ISS) experiment for the International Space Station ISS. The experiment aims at the qualification/verification of DLR's lightweight robot technology under outer-space conditions and at the first demo of high-fidelity telepresence including teleoperation via stereo visual feedback and haptic feedback via a force-reflecting hand controller.

From March 2005 onwards, we gained a lot of data, e.g. concerning changes in joint friction etc. The robot still is working perfectly and the successful project—originally planned for one year—has been prolonged twice. Thus our torque-controlled lightweight robot joints have proven their perfect performance in outer space, though they had undergone only low-cost qualification, i.e., most of the electronic components are off-the-shelf and had been qualified by own radiation, vibration and temperature tests. The institute now has the worldwide longest experience with the remote control of robots in earth orbit.

DEOS

With ROKVISS closing our last technological gaps in space robotics, we have initiated the consequent next step towards orbital servicing in space, namely the technology experiment DEOS. Phase A is in progress. DEOS is supposed to demonstrate the autonomous grasping of a (non-cooperative) target satellite with our 7 degree-of-freedom lightweight arm mounted on a service satellite, performing numerous experiments in compound mode, too and finally deorbit the target satellite safely into the Ocean. In close cooperation with the Technical University of Munich (cooperate research area "telepresence") we have demonstrated the necessary telepresence concepts via geostationary relays. Thus, we intend to massively push forward the concepts of remotely ground controlled operations in space with modest cost.

S-OLEV

There have been strong indicators in the recent past, that prolonging the lifetime of expensive geostationary satellites that are running out of gold gas, might become the first business case for orbital servicing. The concepts, originally proposed by the institute and now refined by an industrial consortium, aim at the automatic docking of a life-extension satellite, using the institute's capture tool technology, and overtaking attitude control of the compound system via ionic thrusters over years.

The core technology "capture tool" has been totally redesigned meanwhile, provided with redundant inductive sensing and an innovative drive mechanism. A radiation hard, space qualified version, is already in preparation.

We presume that S-OLEV (Orbital Life Extension Vehicle) will become one of our central space projects in the coming years.

ExoMars Rover and Crawler

We have considerably enforced our efforts in the area of planetary exploration.

Meanwhile they comprise the development of innovative actuation and mobility technologies for all kind of mobile systems on planetary surfaces, the development of novel stereoscopic and panoramic camera techniques for space use, as well as 3-D world modelling algorithms.

At present, our main objective is the design of the rover of ESA's Mars mission ExoMars, where in a consortium with Swiss and German industry and the ETH Zürich we have developed the complete drive system for the rover breadboard wheels. In detail, we have integrated torque-controlled light-weight drives as space qualified in the ROKVISS experiment, which would be ideally suited to drive a rover on Mars or Moon with minimal weight and power losses.

Powerful modelling, including modelling of contact dynamics, and simulation tools have been created to demonstrate the driveability and the overall mobility performance of any kind of rover kinematics and dynamics, specifically w.r.t. stability performance (e.g. rover turn-over might be a total mission design stopper).

With respect to mobility we developed a prototype of a small six legged crawler based on the finger technology implemented in DLR's robot hand II. Such a system can serve as scout to explore the surface properties in the vicinity of a planetary lander.

The Anthropomorphic "Robonaut" System JUSTIN

Our internationally highly acknowledged torque controlled and kinematically redundant light-weight robots have become kind of a technology standard for pushing forward the paradigm of "soft robotics" that allows for direct interaction with humans. The performance of the arms in terms of high-fidelity impedance control has been permanently improved. In the same way our torque-controlled four-finger hands have been steadily improved e.g. in terms of reliability and dynamics. The "ball catching" experiment with light-weight arm and hand has become one of the most well known demonstrations for robot skills in the international community.

But the biggest step in the report period was the design and realisation of the two-arm-two-hand upper body JUSTIN with a 3-DoF torso and a multi-sensory head (3D-Modeller) including stereovision and laser-scanning.

With its 43 torque-controlled joints, JUSTIN is one of the most complex robot systems ever built. And in 2008 JUSTIN has been equipped with a powerful mobile basis consisting of an omnidirectional wheel system mounted on four "legs", which can be stretched out or withdrawn depending on the static stability needed in special situations. JUSTIN's mobility is supported meanwhile by optical navigation.

Telerobotics and Autonomy

For the remote control of space robot systems we have developed and verified universal and flexible telerobotic concepts combining elements of task-level teleprogramming in virtual environment with telepresence concepts, thus covering the range of operational modes from on-line direct interaction, shared control (direct interaction with local, autonomous refinement of gross commands) to supervised autonomy (operator supervises autonomous actions). With respect to telepresence (where we focus on real-time stereo video and force feedback), we have reached a high level of transparency for the operator and, thus, we were able to develop new passivity-based bilateral control strategies that guarantee stability in the overall loops, even with significant delays.

For autonomous actions the fusion of force and video signal feedback is, in our view, of crucial importance and has led to convincing assembly demonstrations on moving objects in our lab, laying foundations for robotic rendezvous and docking in space, too.

With our two-arm upper body JUSTIN, we have investigated the potentials and limits of two-handed autonomous manipulation.

Robust recognition of every-day objects and impedance-controlled grasping has enabled some first demonstrations of complex manipulation tasks.

The rising complexity of humanoid robots has cried for new software concepts which support modularity, concurrent and distributed execution while guaranteeing hard real-time constraints. Our "agile Robot Development" (aRD) concept takes advantage of modern multi-core computing resources and fast communication links in the gigabit range between the computers and the robot components. It is efficiently usable not only in JUSTIN but in any kind of teleoperated multi-arm setup in space robotics.

In this context, the institute has become partner of the excellence cluster Cognitive Technical Systems CoTeSys of the Technical University of Munich. And in the framework of a "virtual institute" as defined in the HGF the development of autonomous airships and octocopters ("flying robots") has been initiated and has led to convincing results.

Camera Technologies

During the last five years the institute could achieve a leading position in Europe in the field of high resolution focal planes for spaceborne and airborne sensor systems. Lines scanners with more than 20.000 pixels, stereo cameras for airborne applications, multispectral systems and imaging spectrometers in the infrared range are impressive examples for our scientific and technological capabilities. According to user requirements sensor systems with high geometrical, radiometrical and spectral resolution can be designed, deployed, calibrated and verified.

ESA project MERTIS, the development of Kompsat3 for the Korean space agency, infrared payload on TET-1 and the MFC cameras are the main projects in this successful business field.

Small Satellite Technologies

BIRD's heritage put the institute in the position to develop innovative components for small satellites. Intelligent board computers on reconfigurable hardware platforms and attitude and orbit control systems based on multi-sensor inputs are key technologies for future space missions. Besides, the work was focussed on contributions to mechanical construction, power supply and system simulation for small satellites. System parameters can be verified in hardware in the loop configurations at a small satellite laboratory equipped with a high tech air bearing test stand. The institute plays a key role in both German small satellite programs – TET and compact satellite.

2.2 Aeronautics

Flight Dynamics Modelling and Simulation

The Modelica-based DLR Flight Dynamics Library was re-designed and considerably expanded (e.g. landing gear dynamics, navigation equipment). For generation and integration of model data behind flight dynamics models, a dedicated model integration process was defined and successfully applied in-house as well as in industrial cooperations (e.g. flight loads analysis for Airbus A350 and A400M).

We further enhanced functionality and performance of our 3-D stereo flight simulator. It has become a major attraction at various public events, like ILA2006 and the Public Day 2008 in the Federal Chancellery. The simulator allows a fully flexible aircraft to be interactively flown in real time, while airframe deformations, external loads, the environment, etc. are shown in 3D. A network-based coupling between the automatic landing system and a real-time GPS+GBAS simulation of the Institute of Communication and Navigation (KN) was established, allowing for automatic landing demonstrations using the future Galileo satellite navigation system.

Robust Flight Control Design

In the frame of numerous national and international projects and industrial cooperations our methods and tools for multidisciplinary flight control law design could be significantly improved and successfully applied to solve complex problems. The major developments were:

Dynamic Inversion: Based on the new Modelica Flight Dynamics Library generation of nonlinear dynamic inversion-based control laws has been improved and facilitated for by-wire aircraft ground control augmentation. The latter was done in the GARTEUR Action Group FM(AG17) on Nonlinear Analysis and Synthesis Techniques in Aircraft Control. The AG consortium was awarded as the "Best GARTEUR Action Group of 2008".

LFT-model generation: The tool chain for generation of Linear Fractional Transformation (LFT) models for highly non-linear aeronautic models has been completed and made more efficient. The application to real industrial problems such as flexible aircraft and missiles became possible (projects: EU-COFCLUO, cooperation with MBDA-Systems).

Fault detection and isolation (FDI): Numerically stable algorithms and accompanying robust software has been developed for the synthesis of model based residual generators applicable for fault tolerant control and health monitoring systems (projects: ADDSAFE, MOET).

Multi-objective parameter synthesis: The tool has been further improved and matured especially with respect to (global) optimisation algorithms, statistical analysis and efficient worst case search. It has been used in completely new fields of application not only in aeronautics.

Active Loads Control

In the areas of active load alleviation, real-time estimation of atmospheric disturbances and aeroelastic model identification we achieved remarkable improvements within international and national projects like EU-AWIATOR and MODYAS. These achievements resulted in several industrial cooperations and requests from industry to overtake a leading role in actual and future projects on active loads control like EU-ACFA2020 and CleanSky "Smart Fixed Wing".

More Electric Aircraft Systems

Our first project POA (power optimised aircraft) in this field was finished in 2006. The analysis and optimisations using our newly developed virtual iron bird (VIB) tool were the basis for the final performance evaluation of more electric aircraft architectures by our industrial partners.

In the follow on project MOET (more open electrical technologies) we are now responsible for developing a coherent design and validation environment for future high voltage aircraft electrical networks. For this purpose we developed an integrated architecture analysis and optimisation tool with the capability to simulate different normal and failure operating modes of electric system architecture and with automated features for component power sizing, weight, and reliability analysis. This novel tool is considered to be one of the major project achievements so far.

Because of our involvement in POA and MOET important industry partners invited us to lead the modelling and simulation activities in the frame of the Management of Energy part of the recently started CleanSky project "Systems for Green Operations".

2.3 Transportation

Road Vehicle Dynamics Modelling

We have been creating various automotive Modelica libraries (PowerTrain, AlternativeVehicles, VehicleInterfaces, VehicleControls) on our own and in multiple cooperations. Furthermore, a new generic Modelica package provides interfaces for interactive simulations and a new generic visualisation system for the generation of a persuasive 3-D visualisation of the whole driving scene. From this collection of libraries, we can and do compose complex and real time vehicle models covering all necessary aspects.

An interactive driving simulator for several vehicle models compiled from components of the various libraries gained attention in the exhibition of FISITA 2008 World Automotive Congress. A separate screen showed a virtual motion simulation by means of an industrial KUKA robot model.

Integrated Road Vehicle Control

A generic approach for Integrated Chassis Control has been developed which allows for the synergetic management of an arbitrary number of mechatronic chassis actuators in all driving situations. It aims at optimal performance with respect to vehicle dynamics, reliability, safety, efficiency, and tire wear. Primarily, the approach is suitable for comparative assessment of multiple chassis configurations in simulations even in a very early design phase. Therefore, we experience a great demand for the concept from automotive companies, actually resulting in commencing cooperations. Furthermore, our approach has the potential for application to real time control of real vehicles in the future.

Railway Vehicle Dynamics

In the past four years, we have developed highly accurate multibody modelling approaches for railway vehicle systems. Therefore, we meet the emerging challenges regarding a refined simulation of wheel/rail forces and the associated deformations in the higher frequency range up to 6 kHz and introduce thermoelastic effects in brake system analysis.

The multibody methodology is innovated and opened to relevant applications such as acoustics, longitudinal wear (corrugation, out-of-round wheels), virtual homologation and multi-field problems.

We are applying these modelling approaches for elastic, thermoelastic and rotor structures with industrial partners such as Knorr-Bremse, which we could win for a close cooperation even on the strategic technological level of railway brake design and control.

To organise an across-the-board commercial dissemination we implement these methods twice: in the Modelica environment, see the EUROSYSLIB project and the Modelica FlexibleBodies library and in the world's leading multibody software tool Simpack, initially developed at our institute as well.

Next Generation Train

Since vehicle dynamics is a key technology of railway vehicles we play a leading role in the DLR project Next Generation Train. We proposed and analysed a 400 km/h-high-speed vehicle concept that will be further advanced in cooperation with other DLR experts.

We suggested and assessed a novel mechatronic running gear concept in low-floor-design using simulations. The advantages in running stability and extraordinary low wear and noise characteristics by active steering and running gear control will be demonstrated at our existing scaled M 1:5 roller rig.

2.4 Technology Transfer

Our technology transfer efforts have found not only a lot of acknowledgement in industry, government and public, they are a major source of third-party funding meanwhile.

- Based on the success we had in the past in our cooperation with the leading European robot manufacturer KUKA, a large strategic cooperation between the institute and KUKA has been installed recently. It aims at the development of advanced service robots, especially production assistants and personal assistants (elderly care). In this context KUKA has started to commercialise the institute's light-weight robot in license. Other fields of cooperation are the development of innovative flight and vehicle simulators using large 6-axis robot systems on rails and mobility concepts including visual navigation.
- There is an intensive and established cooperation over the past ten years with respect to industrial robots, the core business of KUKA. The success of this cooperation is demonstrated in permanent improvements of the dynamic behaviour of the industrial robots. DLR Know-how is used in nearly all KUKA industrial robots, having an annual production volume of around 8,000. Innovative model-based control algorithms have been included in the industrial robots software.
- The company Schunk has started to commercialise the DLR/HIT Hand-I (jointly developed with Harbin Institute of technology) in license. Several of these hands are already in operation at different institutions, of which many closely cooperate with the institute.
- A spin-off company RoboDrive was founded, which commercialises the new light-weight motor technologies in different application fields, e.g., vehicle technology, motion platforms, demining robots, etc.
- In the medical field, the development of our first medical robot KINEMEDIC is about to be commercialised in close cooperation with KUKA and BrainLAB. These efforts have been awarded with the EURON technology transfer award of the European robotics research community. Meanwhile, a complex minimally invasive surgery system MIROSURGE has been developed, which US-analyst Oppenheimer denotes as the only visible competitor for the worldwide monopolist Intuitive Surgical (the DaVinci system).
- The institute's development of an innovative artificial heart, distinguished by a number of technology awards, has led to the founding of a new company DUALIS with DLR as shareholder.
- The institute's wedge brake technology has gained enormous public interest. Our spin-off company eStop was bought by Siemens VDO and the wedge brake was optimised and redeveloped in order to reach the technical matureness of a mass product for the automotive market. However, in 2007 Continental, a market leader in hydraulic "wet" brakes, bought Siemens VDO. Therefore the short-term future of the wedge brake is unsure. It has, however, frequently been denoted as one of the most important automotive innovations of the last years.

II Space Flight

1 Space Robotics

1.1 Background/Motivation

Already in 2003 the European Parliament has called upon Europe to work out an international leading position in the field of "Orbital Serving in space". Space systems above approx. 500km flight path altitude are not accessible for astronauts by means of shuttle and therefore excluded from any kind of repair. But precisely in that sphere there are many satellites needed for earth observation, which may need maintenance. For instance, "parking spaces" are firmly allotted in geostationary orbit (GEO) which under no circumstances may be left and endanger neighbours. In future, remotely controlled satellites equipped with robot arms, so-called robonauts (e.g., with two arms, two hands, and a multi-sensory head), should assist or replace astronauts during routine and maintenance work on LEO (low earth orbit) space stations, capture uncontrollably tumbling satellites, repair them or deorbit them if necessary. And they might refuel, maintain and repair GEO satellites or clear parking spaces in GEO.

Robotics is just over 40 years old and can be adapted to outer space conditions at comparatively small expense. In connection with efficient remote-control and telepresence technology, robotics will become an important augmentation for manned space flight, the more when their remarkable manipulative skills are compared with those of an astronaut in clumsy spacesuits and gloves. The question as to when robots become really intelligent and can work autonomously is of minor importance. Once we have understood and implemented the basic concepts of the "extended arm in space", we can switch quite flexibly between all levels of "shared autonomy" between the ground operator and the robot in space, from high fidelity telepresence up to the highest possible on-board autonomy level, according to the respective state-of-the-art.

Telepresence allows an operator on ground to seamlessly work at the remote site, providing real-time feedback of (mainly) stereo images and forces/torques. Round-trip signal delays, however, should not be longer than ½ second for guaranteeing e.g. high fidelity haptic feedback. Concerning LEO (low earth orbit systems), we may restrict ourselves to the 7–8 minutes direct sight during overflight and then have only 20msec delays or so. For longer operations with up to 40 minutes contact, new communication infrastructures are needed in space, (not really available so far) with preferably KA-based links from LEO satellite (using an automatically served antenna) to a GEO relay. Then we can indeed meet the half-second delay request in all LEO orbits. If the robot would have to work in GEO, the situation is even simpler due to permanent contact and only ¼ sec round-trip delay (Fig. 2).

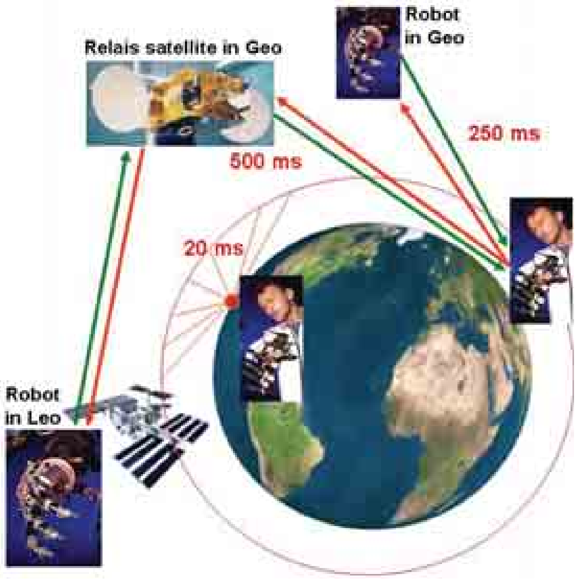

Fig. 2 Minimal round trip signal propagation delay to robots in LEO 0.5 sec., to robots in GEO 0.25 sec

Fig. 3 shows the idea of a free-flying "robonaut" (a term invented by NASA) catching a problematic satellite.

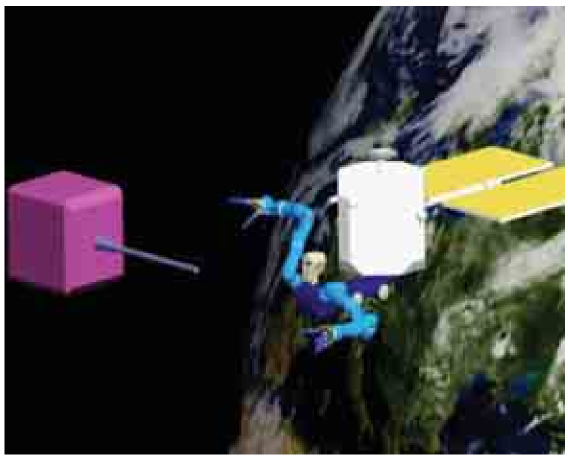

Fig. 3 Free-flying robonaut

The term “Exploration”, on the other hand, is above all associated with research of planets and the solar system. Here robotics is even more so the cost-saving support and alternative to manned spaceflight.

The demonstration of rover mobility performance requires the use of powerful modelling and simulation tools, for analyzing the interaction between the wheels and the uneven and rough terrain (Terramechanics). Of crucial importance is the development of highly efficient (i.e. low weight, low power losses) drive mechanisms and mobility concepts (wheeled rovers, legged crawlers, combined systems).

In this context, special attention should be given to “rovonauts”, i.e. humanoid “upper bodies” mounted on rovers or multi-legged platforms (Fig. 4). They should be able to collect rock samples, either autonomously or via high-level commands from earth, possibly analyse them, and prepare the stay of human beings on distant planets. Due to the high signal propagation delays (approx. 15 min.), a robot on Mars must work autonomously as far as possible with the operator on earth defining only the gross goals. Thus it must have (real-time) 3-D world modelling capabilities, be able to navigate independently, recognise objects and know how these objects are grasped and handled.

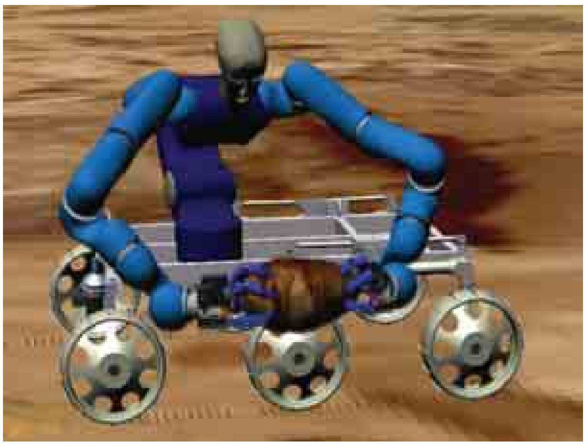

Fig. 4 Rovonauts for Mars sample return

In summary, our real challenge focuses on “low-cost operations in space either remotely controlled from ground or via interaction with astronauts” using the most innovative mechatronic and cognitive capabilities of advanced robotics. For the development of “robonauts” and “rovonauts” in space, ultra light-weight arms with articulated hands, minimal power consumption and high autonomy as well as 3-D world modelling capabilities on one side, but teleoperational control capabilities on the other side are the key issues, rendering space flight as a real technology driver.

And space robotics has an enormous “dual use” transfer potential with great market-economy relevance in terrestrial applications (Fig. 5). These aspects also belong to DLR’s major challenges.

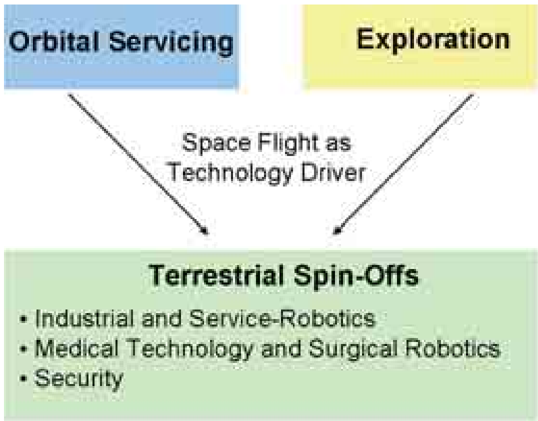

Fig. 5 Space Robotics and its terrestrial transfer potential

In this Chapter, we briefly describe the programmatic issues, projects and studies w.r.t. space robotics, while what we call the enabling technologies are in more detail outlined in the Advanced Robot Technologies (Chapters III.1–6).

1.2 On-Orbit Servicing

1.2.1 Preparatory Work / State of the Art

For more than 20 years we have consequently pursued the goal of preparing operations in space via remotely controlled intelligent mechanisms. As one result, DLR today has the longest experience with remote control of robot systems in earth orbit. The first important step had been ROTEX, the worldwide first remotely controlled space robot, flown in 1993 inside the COLUMBIA shuttle. Multi-sensory gripper technology, sensor-based teleprogramming, on-line teleoperation based on shared autonomy and delay-compensating predictive graphics had been key issues. In 1999 we were able (Project GETEX) to remotely control Japan’s free-flying space robot ETS VII, demonstrating the next level of task level teleprogramming in virtual reality and in particular verifying and analysing (active) dynamic interaction between a satellite-mounted robot and its free-floating carrier satellite.

ROTEX 1993 ETS VII 1999

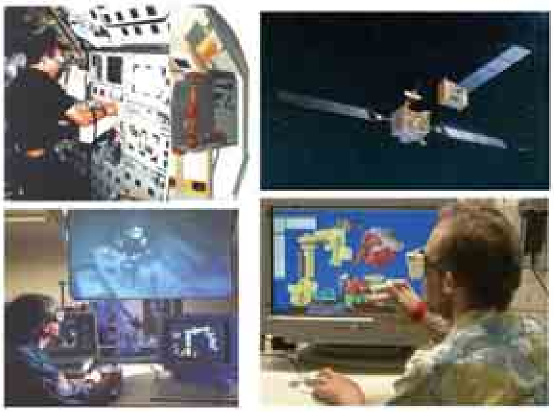

Fig. 6 Our first space robot experiments

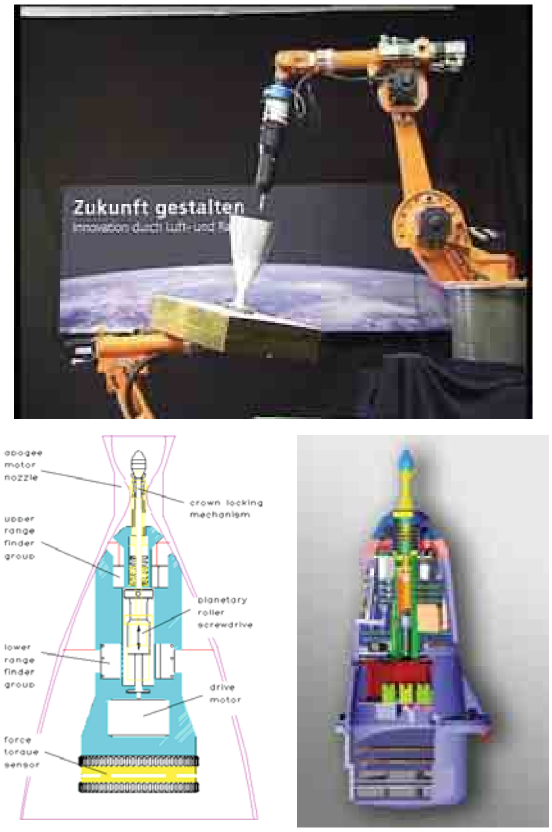

Fig. 7 DLR's original capturing technology

In parallel, we had built up a laboratory simulator that allows to study these dynamic interactions using two industrial robots (Fig. 7 below), one carrying a tumbling target satellite, the other one a "servicing and repair robot", virtually mounted on a servicing satellite, and equipped with an innovative multi-sensory capture tool (Fig. 7), with stereo cameras, radial laser range finders, force sensing and a grasping mechanism. Indeed we had found out that the only way to grasp large communication satellites was to rendezvous and dock with this capture tool at the apogee motor, the nozzle which brings satellites into geostationary orbit. As any kind of unexpected contact might jeopardise the capturing process, we had to develop contact dynamics and latching mechanics calculations. Innovative image processing techniques have been developed for tracking the nozzle with sufficient reliability.

1.2.2 Actual and Planned Projects

ROKVISS on the ISS

After ROTEX, the small two-joint robot arm, ROKVISS (Fig. 8) is the second space robot experiment proposed and realised by our institute in cooperation with the German space companies EADS-ST, Kayser-Threde, and vHS (von Hörner & Sulger) as well as the Russian Federal Space Agency ROSKOSMOS and RKK Energia. While the project was started in 2002, the ROKVISS hardware was mounted outside at the Russian Service Module of the ISS in January 2005 (Fig. 9). Since February 2005, ROKVISS is operated by us, closely supported by ZUP, the ISS ground station in Moscow.

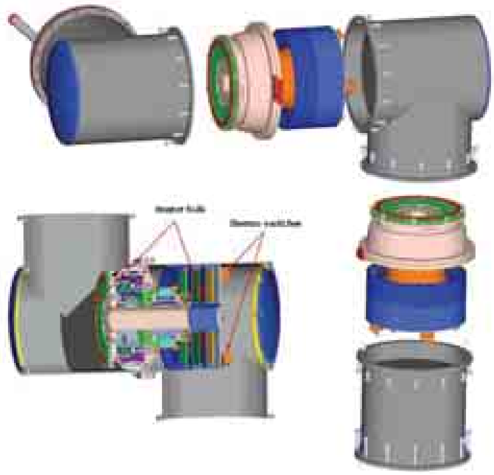

Fig. 8 The two-joint ROKVISS manipulator

ROKVISS aims at the in-flight verification of highly integrated modular light-weight robotic joints as well as the demonstration of different control modes, reaching from high system autonomy to force feedback teleoperation (telepresence mode). Meanwhile, the experiment operates for more than three years in free space, delivering lots of interesting data concerning the joints reliability and the telepresence mode performance. ROKVISS is a further step forward to provide space-robotics hardware and powerful control concepts for on-orbit servicing and for planetary exploration as required in upcoming manned and unmanned space missions.

The two robot joints are extensively tested and identified (dynamics, joint parameters) by repetitively performing predefined robot tasks in an automatic mode, or based on direct operator interaction. The automatic mode is necessary due to the fact that communication constraints limit the direct link experiment time to frames of only up to eight minutes length, when the ISS passes over the German Space Operations Centre's (GSOC) tracking station.

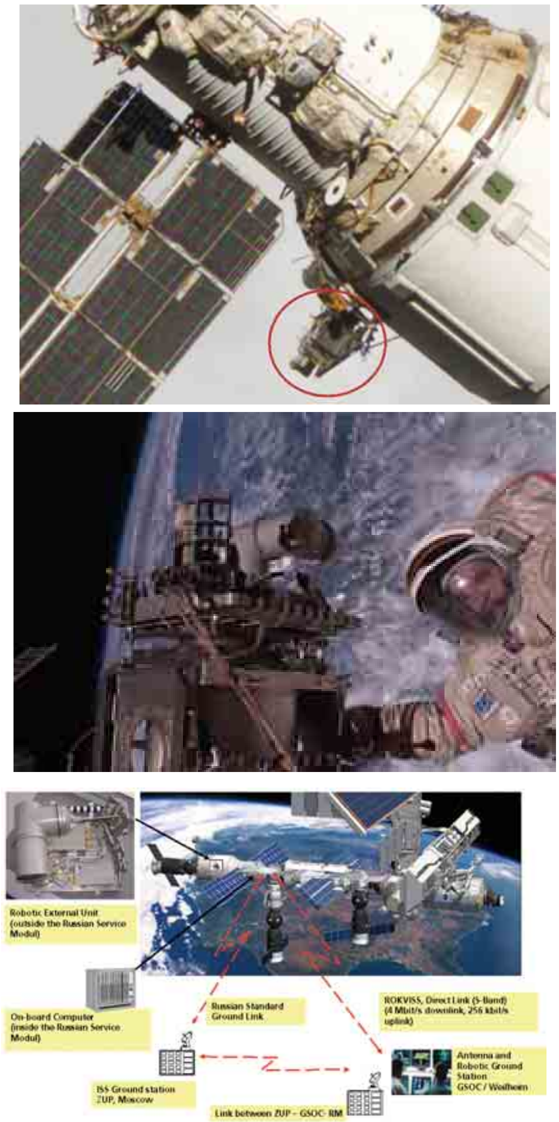

Fig. 9 ROKVISS on ISS

The main goals of ROKVISS are:

- the verification of DLR's modular light-weight, torque-controlled robotic joints in outer space, under realistic mission conditions, and the identification of their dynamic and friction behaviour over time. The joints are based on DLR's new high energy motor RoboDrive and they are identical to those used in DLR's seven joint light-weight robot. This technology is the basis for our future "robonaut" developments;
- the verification of force-reflecting telemanipulation in order to show the feasibility of telepresence methods for future satellite servicing tasks, as we are convinced that the inclusion of the human ground operator into the control loop is a must in many situations.

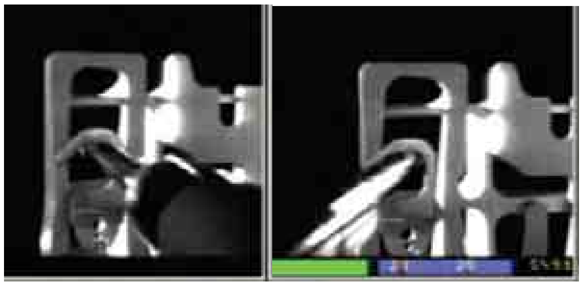

Fig. 10 ROKVISS pulling a spring

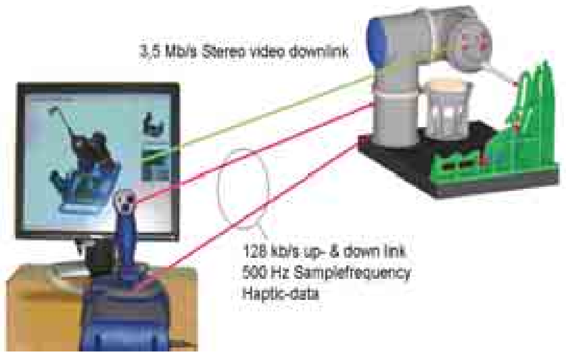

Fig. 11 Telepresence based upon DLR's high-fidelity force reflecting joystick and stereo visual feedback

Qualification Approach

As mentioned above, the ROKVISS joint development is based on DLR's light-weight intelligent joints. One basic idea for the ROKVISS project was to get rid of bulky and expensive radhard components for a space-born application in favour of highly integrated circuits used with terrestrial devices. To come to a first assessment of the applicability of the joint mechatronics for free space, we performed a radiation, an EMC and a thermal test with one of the existing joints. The results of all these tests were very convincing; no basic problem could be identified.

Despite of these encouraging test results, it was clear that some kind of redesign had to be done:

- exchange cross roller bearing against two angular ball bearings;

- exchange all electrolytic capacitors against tantalum types;
- all heat emitting electronic parts need to be thermally coupled to the robot's structure to allow for heat dissipation;
- the optical SERCOS bus ring topology was modified into a point to point connection via copper wires. Each joint is coupled via SERCOS with the main computer (OBC). The advantage of the point to point structure is that even if one joint electronic fails, the remaining joint is still operable;
- a latch-up protected power supply circuit had to be implemented;
- electronic parts with extended temperature range (-45°C to +85°C) are used.

All these modifications led to the joint design as shown in Fig. 12.

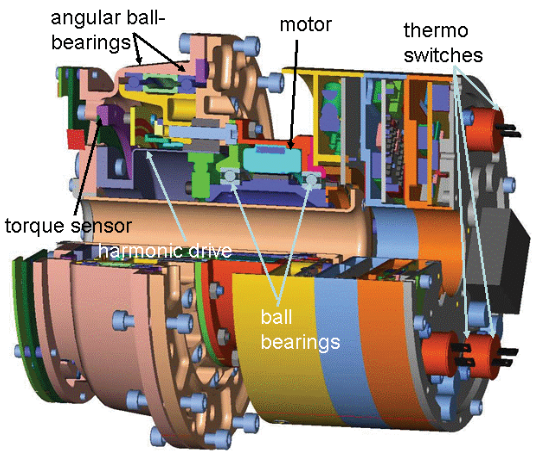

Fig. 12 ROKVISS joint unit

The drawback for using components off the shelf is the probability of latch-ups, which may destroy a CMOS circuit when hit by a heavy ion or proton. Based on the fact, that neither a hot nor a cold redundant configuration for the joint electronics was intended, a latch-up protected power supply circuit had to be implemented. The task of the latch up protection circuit (Fig. 13) is to prevent burn out of the device hit and hence to protect it. It is self-evident that the power supply itself must be latch up immune and able to handle latch up situations. Therefore it must be built with radiation tolerant parts (with the temp. range: -55°C to +125°C) in order to guarantee the correct functionality during the whole mission.

To prevent burn-out of the device being hit, it is surely not sufficient to switch off the power, because the charge stored in the smoothing capacitors will permanently damage the device. So, in addition to switching off the supply, one must shorten the output by use of a so-called crow bar circuit.

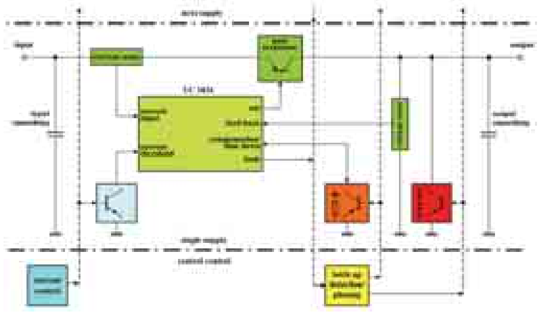

Fig. 13 The new latchup protection system

Joint Parameter Identification

Accurate dynamic models were required for both the pre-mission development and testing phase as well as the in-flight operations phase. By using 3-D CAD programs for the mechanical design, the problem of determining the parameters of the rigid robot dynamics becomes straightforward, since they can be generated with high accuracy from the design data. This, of course, requires a detailed modelling of all components, including motors, gears, and electronics. The parameters which still have to be identified are the friction parameters, the motor constant, and the joint stiffness. The objectives of the technological experiments during the mission were:

- to identify important dynamic non-linear system parameters in micro-gravity environment, and to validate the underlying multibody system models;
- to increase modelling fidelity and hence performance quality for future space robotic missions.

For the design of the joint controllers (position, torque, and impedance control), recursive least-squares methods have been developed, which identify the stiffness and damping, as well as the friction parameters. Starting from the model and the corresponding identification measurements, a modified time-efficient, on-line version has been tested on ground and is used during the mission.

To identify the different parameter groups we perform dedicated measurements that enable independent identification for each group. This procedure avoids complex online optimisation problems which, in our earlier experiments, always got stuck in local minima, with parameters very different form the real physical parameters.

Joint Friction Identification Results

For the identification of the motor side friction the following signals are available: the commanded motor current, the measured motor position and hence, by differentiation, the motor velocity, as well as the measured joint torque. The identification procedure determines the motor torque constant k_m, the Coulomb friction τ_C, the friction coefficient for the load dependent component, and the viscous friction coefficient b_1.

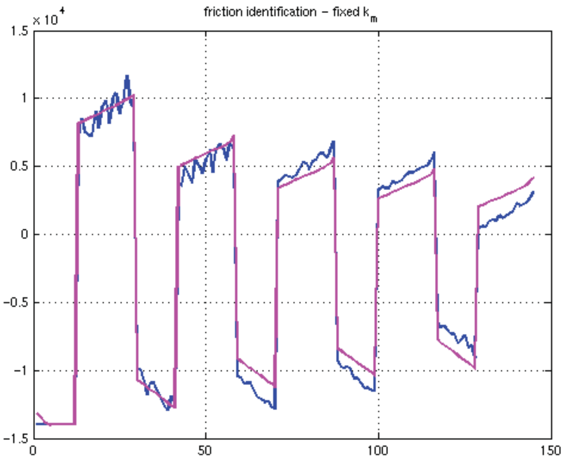

Fig. 14 Commanded current and estimated current after the identification of the friction parameters. The movements are performed with 30.0, 20.0, 10.0, 5.0, and 1.0deg/s.

Table 1 Friction parameters for joint 1 in space

	with fixed k_m	with optimised k_m
k_m [Nm/inc]	345.62	337.39
τ_C [Nm]	28.5	29.1
μ	0.272	0.302
b_1 [Nms/rad]	12.25	12.51

The identification of these parameters can be formulated as a static, linear optimisation problem. This means that for a properly chosen trajectory, which independently excites all parameters, a fast and reliable parameter convergence can be obtained. Such a trajectory is given when pulling the springs of the test setup using a saw-tooth trajectory with different constant velocities (Fig. 10). Due to the variable load torque, the reversion of the movement direction, and the coverage of the entire velocity range, all parameters are well excited. A typical identification plot is given in Fig. 14 as well as the numerical results for the friction values (measured on 2005-07-22 during an automatised on-orbit experiment) are given in Table 1.

In order to test the reliability of the identified values, the motor constant k_m was also identified on a separate motor test-bed and the optimisation was performed only for the remaining parameters. Table 1 shows that the results for the two cases are very similar.

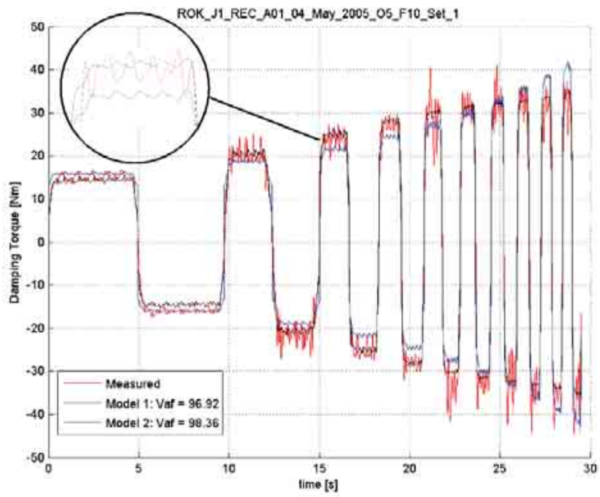

Fig. 15 Two different models for the friction torque are compared. vaf (= variance accounted for) defines a statistical measure to judge the quality of the identification results and, hence, the underlying model: The ideal value vaf=100% means that we have total agreement between model and measurement.

In addition to identifying the parameters of a fixed model, we also try to improve the model itself. For the previously presented triangular trajectory with varying frequency (i.e. velocity amplitude) and undergoing spring load, a nonlinearity of the viscous friction term can be noticed. Fig. 15 compares two further model versions in terms of their degree of complexity and the modelling accuracy on a similar trajectory. Model 1 is a simplified one that accounts only for Coulomb friction and linear viscous damping. Those two damping terms had been identified before in ground experiments to be of dominant influence. The second model, Model 2, is regarded as an improvement of Model 1, and accounts now for more damping terms such as viscous damping of quadratic and cubic velocity dependence, and a term regarding the load dependent effect on

Coulomb damping:

$$T_{damp} = (\tau_C + \mu \,|\, T_{out} \,|)\mathrm{sign}(\nu) + b_1\nu + b_2\nu \,|\, \nu \,|\, + b_3\nu^3$$

where $|T_{out}|$ is the magnitude of the output torque (e.g. spring load) and ν is the angular velocity. The second model fits the measurements considerably better.

Time and Temperature Dependency

The results of the on-orbit identification show that shortly after launch the Coulomb friction for joint 1 in space increased by about 50% compared to the friction on ground, taken at 20°C, under normal atmospheric pressure. However, only a small further change of the parameters can be observed (Fig. 16). This suggests the conclusion that the lubricant changed its properties when exposed to outer space conditions at the beginning of the mission and afterwards reached an operating state with slow parameter variation.

A heating system is used to regulate the operating temperatures on-orbit between -20°C and +30°C. Within this range, a temperature dependency of the parameters is not clearly recognisable. The parameter variation over temperature is thus obviously lower than their variation over time.

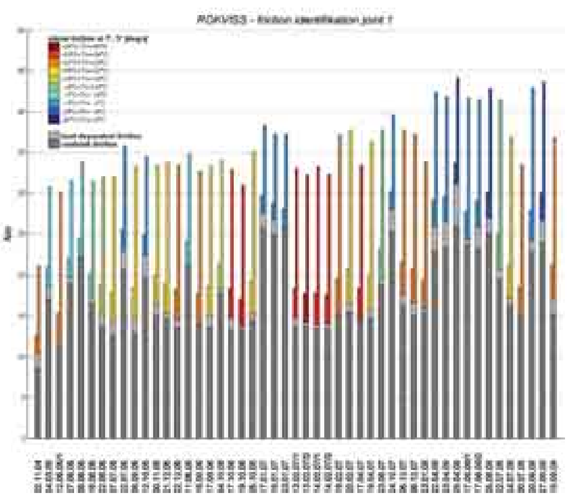

Fig. 16 Time evolution of total friction

Contact Dynamics Experiments

The ROKVISS facility is also used to study how the space environment affects the behaviour of bodies interacting in a contact situation. Compared with joint dynamics changes, strong dependency of temperature variations and space radiation upon surface material properties is expected for the impact and contact cases. In impact and contact dynamics, the proper knowledge of both the energy dissipation and the tangential forces (damping, static and dynamic and friction of Coulomb type) is of our primary interest. These experiments are conducted in cooperation with CSA, the Canadian Space Agency. Specifically, the energy dissipation occurring during intermittent impact events (in normal and oblique impact) is measured, as well as the frictional forces acting between two bodies while they are moving w.r.t. each other in a lasting contact situation (Fig. 17).

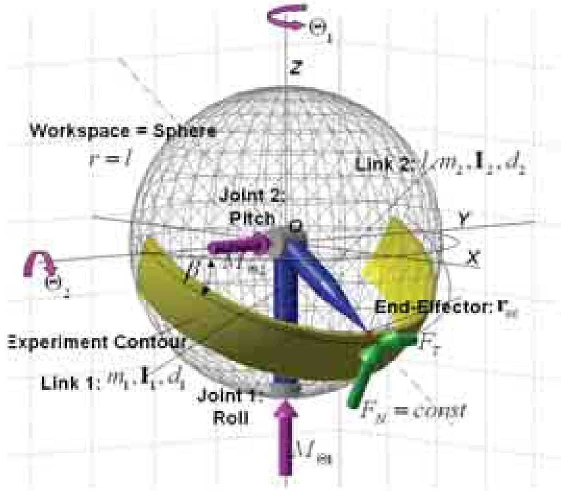

Fig. 17 ROKVISS manipulator: contact case, stylus moving on a given trajectory. This figure is part of an animation: the length of the arrows is varying according with time. The arrows indicate the torques of the two joints exerted during motion and the reaction force at the contact surface.

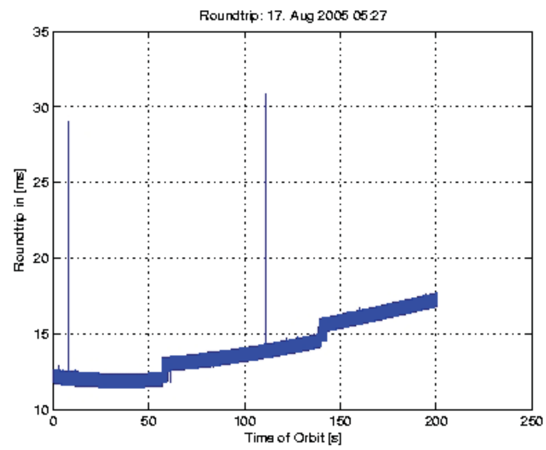

Fig. 18 Roundtrip delay measured during an experiment on Aug. 17, 2005

Telepresence Results

One important step to achieve high-fidelity telepresence with stereo video and haptic feedback was to design a fast communication link between the on-board system and the ground operating system. The requirement has been a low latency data link with small jitter (<1ms). This has been reached by a dedicated communication protocol based on CCSDS, but with reduced overhead. In Fig. 18 a typical measurement of the round-trip delay is depicted. It indicates that the delay varies depending on the distance between the ground antenna and the ISS from about 12ms to 18ms. This is a reasonable value for direct force-feedback.

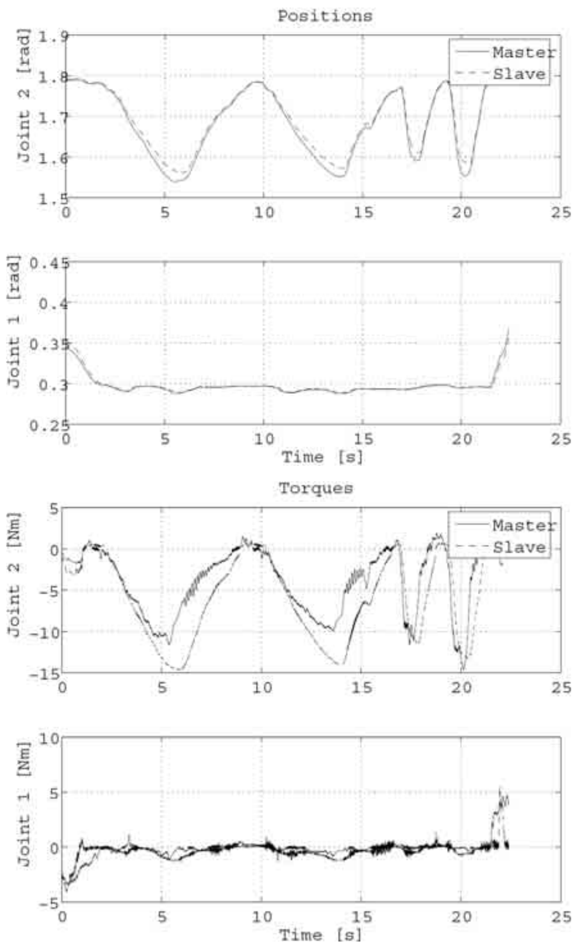

Fig. 19 Data recordings during telepresent operation on vertical spring. First figure shows positions of joints. Second presents the torques.

Beside the real stereo image the haptic feedback is one major component to achieve realistic feedback from the remote system, allowing an intuitive exploration and manipulation of the remote environment. The ROKVISS experiment has been used to evaluate the application to the principles of telepresence, including various bilateral control architectures (see Sec. III.5.2), in a robotic space experiment [Preusche *et al.* 2006[c]].

As example an experiment operating one spring is shown in Fig. 19. Here the human operator telepresently pulls the vertical spring, such that the spring acts on joint 2 of the manipulator. A four channel like control architecture has been used in this specific experiment. The system was moved with different speeds, which had no differences on the results. Position tracking is good and only disturbed by the delay of the system. In the torque recordings an oscillation occurs between 6–7.5s and 14–15s (plus smaller ones later). The reason for this is a very slight slip-stick effect in the manipulator joint, which is amplified by the controller on the master side.

ROKVISS Activities Continued

Since March 2005, we gathered a lot of data concerning changes in joint friction etc., but the robot still is working perfectly and the successful project—originally planned for one year—has been prolonged three times.

Fig. 20 ROKVISS communication links

A real time communication link between the ground station in Weilheim and the institute was developed and established at the beginning of 2007. Thus from this time on the ROKVISS experiments are conducted from the ground control station located in our institute.

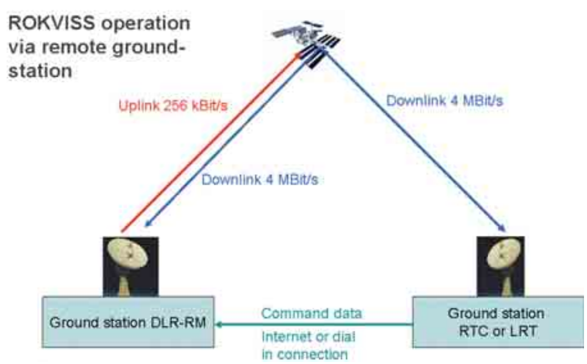

Fig. 21 ROKVISS operation via internet

This link adds approximately 2.7ms to the overall round trip time of ~18ms.

In a close cooperation with the Russian State Scientific Centre for Robotics and Technical Cybernetics, structures for telepresence control are implemented in order to operate the ROKVISS system over the internet (Fig. 21).

DEOS

The project DEOS (Deutsche Orbitale Servicing Mission) is a consequent next step towards robotic servicing in space (Fig. 23). A carrier satellite (the "servicer"), equipped with our 7-DoF light-weight arm mounted on it would be launched together with a smaller target satellite (the "client") to demonstrate the maturity of technologies and systems for OOS (On Orbit Servicing).

Fig. 22 DEOS servicer (left) and client (right)

The 7-DoF manipulator arm is based on the ROKVISS development as well as the telepresence control mode which shall be used to perform satellite capturing and maintenance operations.

After separating the two satellites, the arm would have to:

- grasp the client (autonomously and teleoperated);
- perform prototype manipulation tasks on the client (module exchange, re-fuelling, mating electrical connectors, etc);
- act as a coupling element between both satellites during orbital manoeuvres;
- support a controlled de-orbiting at the end of the mission.

The most challenging DEOS experiment is the grappling of a non-cooperative, uncontrolled tumbling satellite, which can be subdivided into the following steps:

- determination of the client's motion in 6 DoF out of image sequences;
- identify the moments of inertia, the centre of gravity (CoG) and the motion of the CoG;
- estimate the client's motion;
- path-planning regarding the dynamic interaction between manipulator and satellite platform;
- execution of the pre-planned motion and refinement of the grasp-trajectory by visual servoing;
- grapple the client and diminish the relative motion between both satellites.

After grasping (including mastering the dynamic interaction), the robot might fix the client by means of a docking mechanism, thus getting the arm free for "assembly" or "repair" activities on the target. Finally (e.g. after one year) the satellite-compound would be de-orbited in a dedicated way into the Atlantic or Pacific Ocean by firing the servicer's thrusters.

New communication structures (Fig. 23) should be tested, using automatically servoed (with respect to a geostationary relays satellite) KA-band antennas thus assuring the minimal round trip delay of approximately 0.5 seconds for at least 40 minutes contact time.

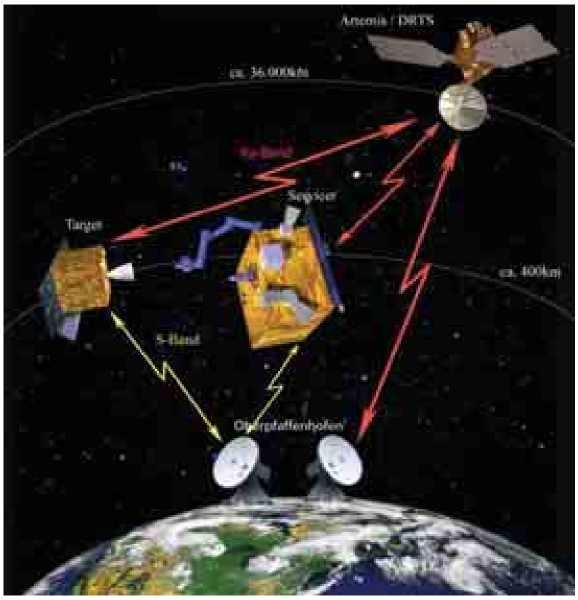

Fig. 23 DEOS communication links

The MARCO architecture, as used in the ROKVISS experiment, was redesigned [Stelzer 2007r] to realise a framework for On-Orbit-Servicing, where different spacecraft subsystems have to communicate while the entire system has to be supervised during all mission phases. The new MARCO architecture provides real-time data-streams which may be established (by the ground-operator) during runtime between subsystems needing fast and direct data transfer.

The new architecture (Fig. 24) can be seen as an extension to the core avionics of a satellite. This means that a standard core avionics can be kept as it is, guaranteeing overall system stability.

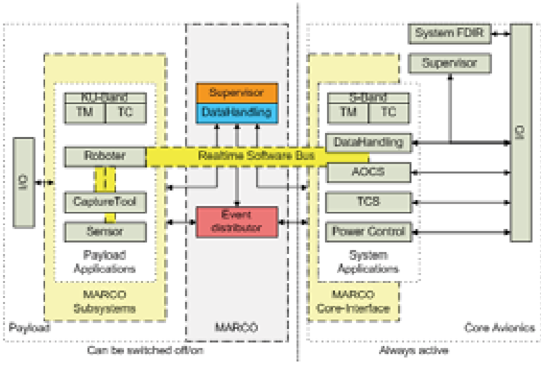

Fig. 24 Architecture overview

The communication between MARCO subsystems as well as the real-time data exchange among specific subsystems is realised through a common generic interface. This enables MARCO to be used in every system configuration, because each subsystem has to provide the same interface. Interaction with applications owned by the core avionics is realised by MARCO-subsystems that are just acting as interfaces to the core avionics.

DEOS is currently in a phase A state which should be followed by a phase B in spring of 2009. A direct and consequent continuation of the project could lead to launch of the DEOS mission in 2012/13. DEOS is the best suited opportunity to demonstrate and manifest Germany's leadership in space-robotics for On-Orbit Servicing.

S-OLEV

A special case of orbital servicing, the service life prolongation of geostationary satellites, which run low of cold gas and thus will loose attitude control, is currently investigated by a European commercial consortium under the leadership of Orbital Satellite Services Ltd. With the participation of the industrial partners Kayser-Threde GmbH (responsible for the docking payload, Swedish Space Corporation (responsible for the platform) and the Spanish Sener Ltda. (responsible for the hardware and software of the Guidance and Navigation Control system) a proposal with the name of OLEV (Orbital Life Extension Vehicle) is being finalised and is close to realisation (Fig. 25).

This application is based on the capture of operating geostationary communications satellites via the multi-sensory capture tool from our institute (Fig. 26) with which practically any of these satellites can be grasped via their always-present apogee nozzle. Their attitude can then be stabilised for years with a set of ion propulsion engines provided by the service satellite.

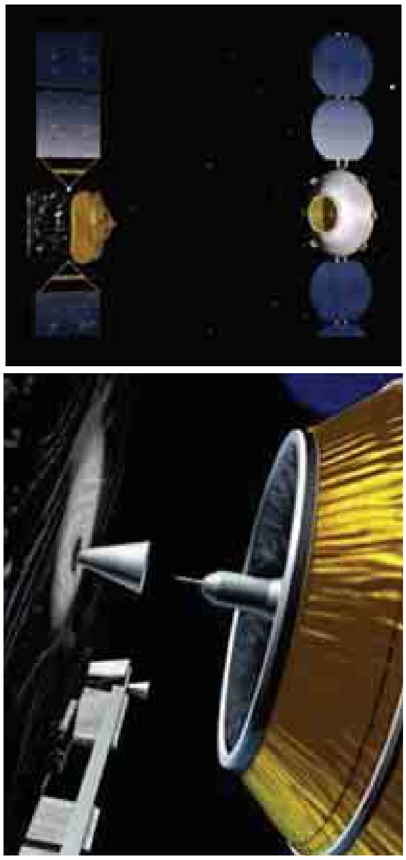
Fig. 25 Orbital Life Extension Vehicle OLEV

Besides service life prolongation, customers also have the option of fleet management to constantly achieve the optimal position over Earth through customised positioning of the fleet vehicles in orbit.

In this context the capture tool has been totally redesigned, provided with redundant sensing and an innovative drive and locking mechanism. The locking mechanism may be applied for motor nozzles with a throat diameter between 16mm and 24mm. The design phase B for the radiation hard, space qualified version of the capture tool is already concluded.

We contribute to the S-OLEV project with the above mentioned capture tool, the control strategies for the final approach from 5m distance until docking (teleoperated or autonomously by means of image processing (see chapter III.4.1 "Robot Vision"), and the simulations of these critical mission phases.

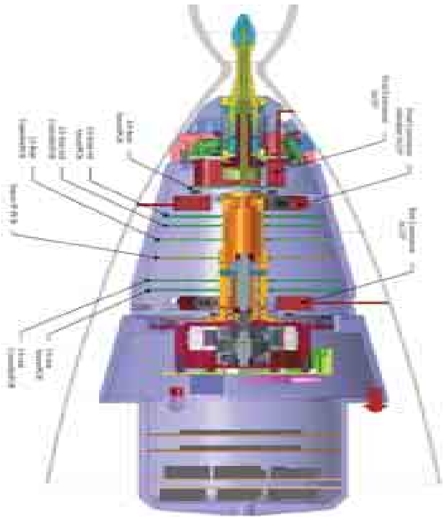

Fig. 26 S-OLEV Capture tool

Docking Simulations for OLEV Missions

A simulation environment has been developed to demonstrate the feasibility of the proposed docking and undocking procedures. The Matlab/Simulink models are implemented according to the classical Multi-Body Simulation (MBS) method.

The following list gives an overview of the models, which have been created and integrated within the simulation environment.

1. environmental model (zero gravity in GEO)
2. servicing spacecraft
   a. 6-DoF kinematics and dynamics;
   b. flexible appendages (solar panel)
   c. AOCS
   d. docking payload
      i. docking stereo camera and image processing (Fig. 27)
      ii. capture tool deployment mechanism and control (Fig. 28)
      iii. capture tool with Locking Crown, sensors (radial laser distance sensors and contact switches) and control (Fig. 29)
      iv. client support brackets
3. client spacecraft
   e. 6-DoF kinematics and dynamics
   f. flexible appendages (solar panel)
   g. AOCS
   h. momentum wheels
   i. docking components
   j. apogee kick motor nozzle
   k. launch adapter
4. contact dynamics models for the physical interaction between the spacecrafts during docking
5. ground operator model

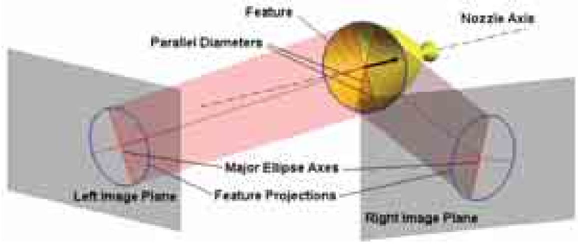

Fig. 27 Camera model

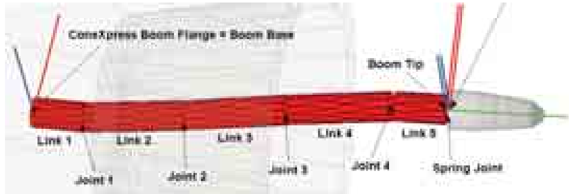

Fig. 28 Deployment mechanism

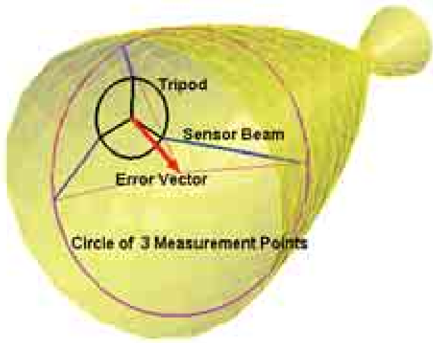

Fig. 29 Capture tool model

Contact Dynamics Models

In order to simulate the docking and undocking procedure with the highest level of fidelity, in particular without any kinematical assumptions or constraints, a contact dynamics model was implemented in the simulation environment representing the physical contact between

1. the capture tool body and the client's nozzle;
2. the locking crown and the client's nozzle throat;
3. the client support brackets and the client's launch adapter.

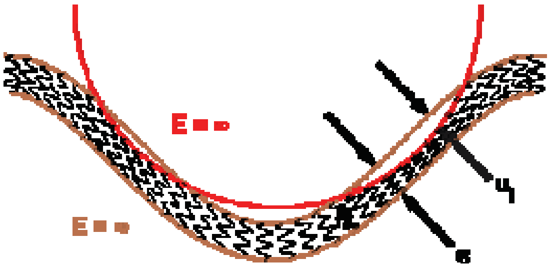

Fig. 30 Elastic Foundation Model

The surfaces of both components of the three contact pairings are modelled as triangle meshes, which are utilised within the polygonal contact model (PCM) algorithm for computation of physical contact forces. PCM applies the elastic foundation layer theory (Fig. 30). It implies that all physical parameters like stiffness, damping and friction are concentrated on a thin elastic surface layer while the rest of the body behaves like a rigid body, which fits very well to the requirements of MBS systems.

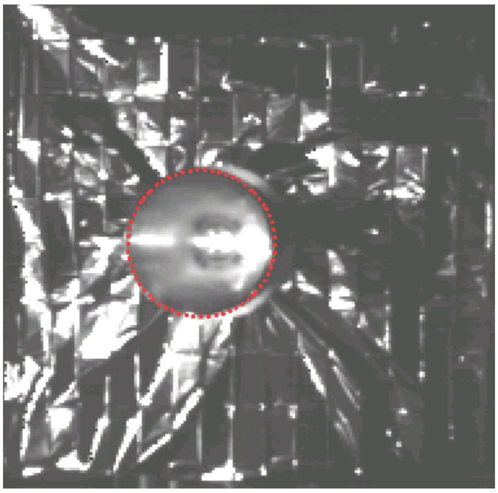

Fig. 31 Tracking of nozzle with circular overlay by ground operator

Model of the Ground Operator

The operation of the stereo camera image processing is supposed to be autonomous on ground. However, due to many uncertainties in terms of optical conditions the operation may fail. In these cases the tracking of the client nozzle rim has to be performed by a human ground operator. In the model the human operator is represented by a transfer function that was derived from results of experimental investigations. The test person had to track the nozzle rim in the movie by a circular overlay that could be adjusted in terms of diameter and position with a SpaceMouse input device (Fig. 31).

Simulation Results/Mission Inputs

Within the OLEV project, a large number of simulations have been performed with specific scopes depending on the status of the project and specific questions of the customer. The proposed solution is the docking from a parking position. Here, the servicing satellite remains in a short, constant distance in front of the client and deploys the capture tool for docking. In order to minimise potential contact shocks between capture tool and the nozzle, the deploying velocity will be controlled depending on the clearance and the distance from the final capture tool position. After adapting the models to the new docking strategy the feasibility of docking could be confirmed by simulation results. The robustness of the strategy has been proven by simulations with different clients and variations of the sensor accuracies.

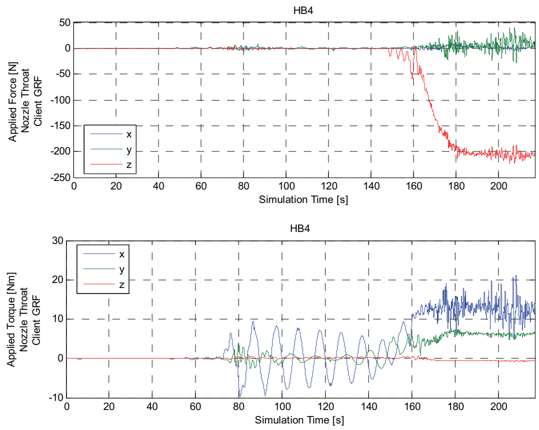

Fig. 32 Force/Torque impact at the client nozzle throat during docking 0–70s; capture tool insertion; 70–80s; locking and rigidising; 80–150s; CDM retraction; 150– >200s

As a next step the results of these plain software simulations shall be validated with hardware in the loop simulations. For this purpose the existing EPOS facility will be modified such that it is possible to simulate contact dynamics effects (Fig. 33).

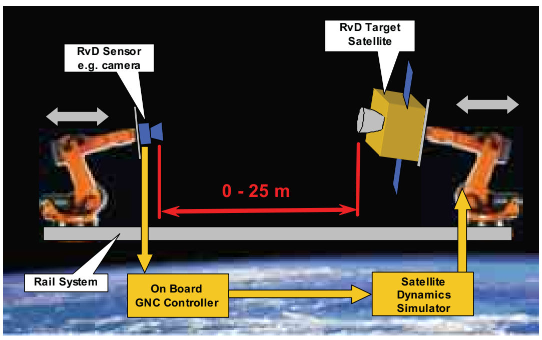

Fig. 33 DLR's new rendezvous and docking simulator at GSOC

1.3 Exploration

1.3.1 Preparatory Work/ State of the Art

It is well recognised that robotics will play a key role for future space exploration missions. The German national interest for exploring our Moon and planets gains increased importance. Actual examples of such missions with participation of our institute are the ESA ExoMars mission, ESA's Next Lunar Lander study, and planned lunar and Mars missions within the ILN and iMars groups. Our activities in Planetary Exploration comprise the development of innovative actuation and mobility technologies for all kind of mobile systems on planetary surfaces, the development of novel stereoscopic and panoramic camera techniques for space use, as well as 3-D world modelling.

We entered exploration around 2003, when we developed an innovative navigation system for Mars rovers in an ESA study (Fig. 34).

It was based on a lander stereo camera and tiny LED's on the rover. Since then we have developed highly efficient real-time stereo algorithms for cameras on rovers, aiming at 3-D world modelling "on the fly" (see Sec. III.4.2). Based on this experience, we started to develop innovative methods for the processing of stereo cameras on orbiters. We used DLR's MarsExpress stereoline camera HRSC as test system, not only processing Mars data however, but also terrestrial data gained by flying with small aeroplanes. Meanwhile, the new stereo algorithm developed, denoted as SGM (semiglobal matching) has often been declared as an internationally leading stereo algorithm based on robot and machine vision concepts, with a number of obvious improvements compared to classical photogrammetry (Fig. 35).

And, even more important, with this excellent algorithmic background we succeeded meanwhile in developing new "true" stereo colour line cameras, e.g., a 3-colour line camera MFC with highly reduced noise features; 5 and 11 line cameras are in preparation for moon and Mars orbiters (Fig. 36), see Sec. II.2.2.

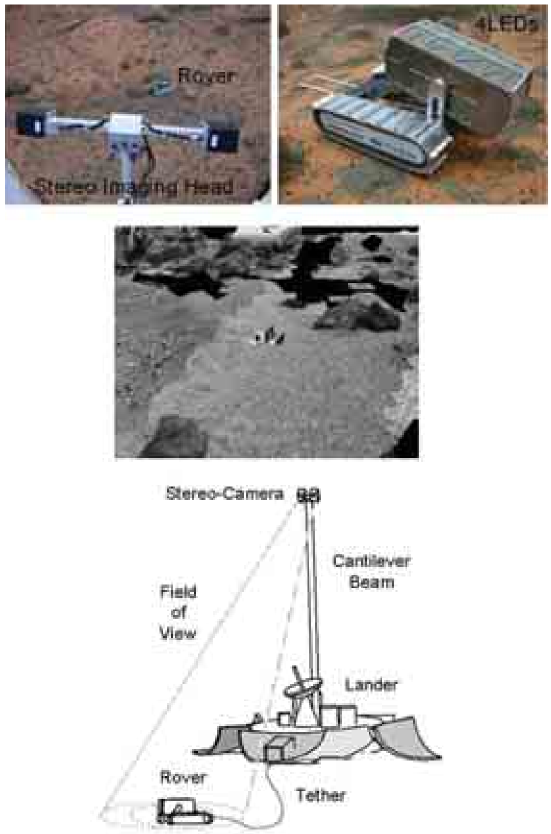

Fig. 34 Innovative navigation system for Mars rovers in an ESA study


Fig. 35 3-D world modelling with stereo line camera HRSC and the innovative SGM processing (top and middle: Mars surface/bottom: Zugspitze-area)

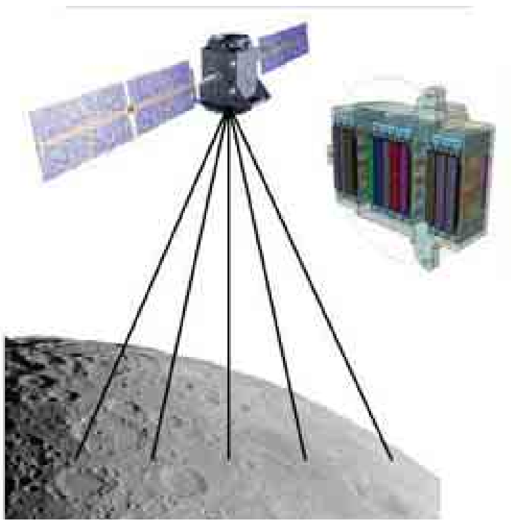

Fig. 36 New MFC cameras for moon/planetary orbiters

1.3.2 The ExoMars Rover Project

Ascertaining the existence or non-existence of life on Mars or earth-like planets and moons is one of the principal outstanding scientific tasks of our time. This knowledge also is a necessary prerequisite to prepare for the future human exploration endeavours. To achieve this important objective, ESA intends to launch the ExoMars mission in 2013 (most probably shifted to beginning of 2016), whose primary element is a 6-wheeled vehicle (rover, Fig. 37) that transports instruments to scientifically interesting surface locations, and takes soil samples.

Fig. 37 ExoMars rover (courtesy ESA)

We are partner in a consortium with Swiss and German industry and the ETH Zürich, which is responsible for developing the rover chassis and locomotion system. Our major contributions are: First, design and realisation of drives for wheel driving and steering of a breadboard rover while making use of the in-house developed light-weight and powerful ROBODRIVE motors. Second, DLR-RM is fully responsible for the complete modelling and simulation part of the rover's dynamical motion behaviour, where the interaction between the wheels and the uneven terrain is a great challenge, varying from soft soils with remarkable wheel sinkages to hard and stony surfaces. Third, for autonomous navigation of any kind of planetary mobile systems (e.g. rovers, legged crawlers) we are going to apply our efficient 3-D image reconstruction methods for localisation and environmental mapping, and hence for developing safe driving strategies (cooperation with CNES).

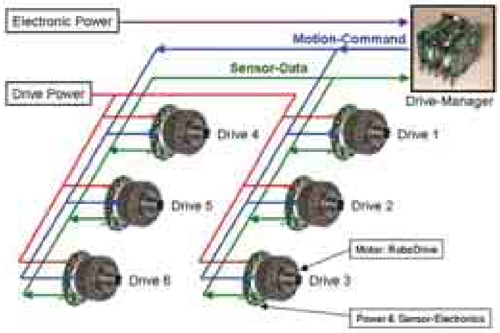

Fig. 38 DLR's motors RoboDrive for the ExoMars rover breadboard

Fig. 39 ExoMars-Rover breadboard (testbed at Oerlikon Space, Zürich)

To be more specific, we have developed the complete torque-controlled light-weight drive system for the rover breadboard wheels, which have already been space qualified in the ROKVISS experiment. They would be ideally suited to drive a rover on Mars or Moon with minimal weight and power losses (Fig. 38 and Fig. 39). In addition, a more advanced actuator system has been proposed that combines wheel driving and steering by using a bevel-gear-like system.

Powerful modelling and simulation tools have been created to demonstrate the drive-ability and the overall mobility performance of any kind of rover kinematics and dynamics, specifically w.r.t. stability performance (e.g. rover turn-over might be a total mission design stopper). Besides the integration of efficient terramechanics models, we have integrated highly efficient contact dynamics models in order to precisely determine contact forces while driving over obstacles, thus simulating the motions of the most diverse rover bodies (Fig. 40 and Fig. 41).

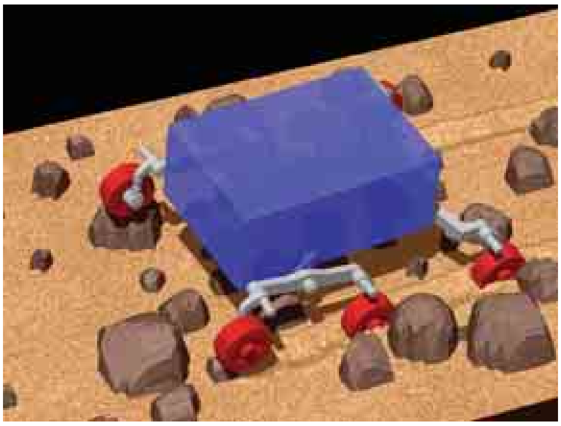

Fig. 40 Powerful 3-D simulation tool for rover mobility performance

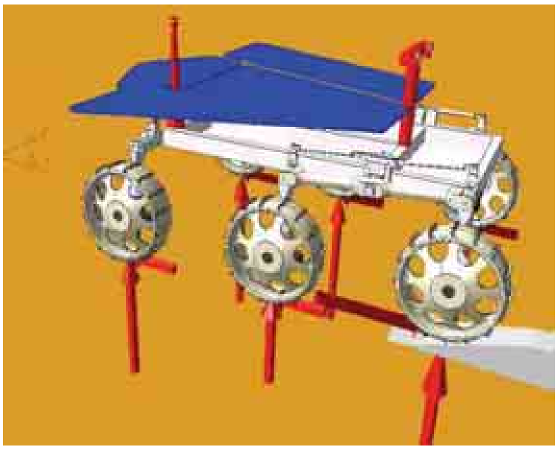

Fig. 41 Modelling the terramechanics and contact forces of a rover

1.3.3 New Actuator Concept for Rover Driving and Steering

Within the institute's participation in the ExoMars Phase B1 study for the development of the rover's chassis and locomotion subsystem, we have developed a new actuator concept for driving and steering of the wheels, reducing weight and volume. This concept has already been used in several other applications of the institute (medical robots, 4-finger-hand II) that favourably make use of the highly integrated robotic drive systems. Major advantage is the use of our novel brushless DC motors (RoboDrive) in combination with a very compact bevel gear drive system. Compared to conventional brushed motors, these motors are almost free from wear and can be used in space environments with no atmosphere, like for Moon exploration. Furthermore, due to low gear ratio by high motor effective power, the friction losses are very low.

Fig. 42 shows two different designs of the proposed actuator concepts: The left one uses two RoboDrive motors each connected with Harmonic Drive gears and both are coupled by the bevel gear. This allows distributing the power of each motor by appropriate controller design continuously between the driving and the steering axis. Hence, this design concept guarantees to use the power of both motors for driving and steering. The right figure shows a similar design, whereas the driving axis now is not arranged off-set to the wheel axis, but is centrically located between a pair of wheels.

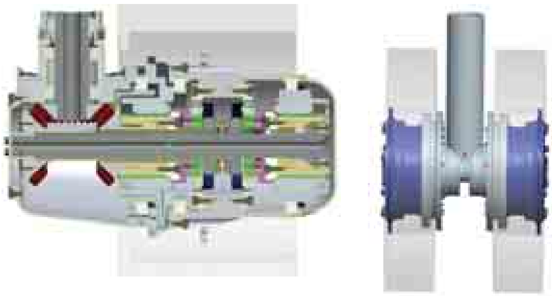

Fig. 42 Two bevel gear actuator concepts: off-set (left) and centred (right, twin-wheel concept) driving axis

1.3.4 Studying Moon and Planetary Exploration

Besides its participation in the ExoMars mission, the institute has been and still is engaged in national and international study activities that involve robotic and mechatronic systems for planetary exploration, since mobility and manipulability are dominant functions to be addressed to any autonomous in-situ exploration. Our findings in light-weight robotic construction, robotic end effectors and tools development for payload handling and increased autonomy by using multiple sensor information and advanced control concepts are therefore the drivers for our engagement. The following studies and projects have been or are performed with our contributions:

- LUROP Lunar Robotic Payload Study, teaming with Kayser-Threde (2007-08);
- Mission Moon 2016 – Technology Platform for extraterrestrial research, study initiated by DLR-AS (2006-07);
- Moon Exploration Study, initiated by DLR-RY (2007);
- Planetary Evolution and Life, a HGF Alliance funded by HGF, led by DLR-PF, (started 2008);
- participation in working groups of ILN (International Lunar Network) and iMars (International Mars Architecture for the Return of Samples).

Fig. 43 Combined rover and manipulator concept for science payload handling and instrument deployment on a planetary surface

Fig. 44 "Rovonaut" design study (rover equipped with our 2-arm torso JUSTIN)

Fig. 43 gives a typical example of combining the advantages of mobility and manipulability in order to place science payloads at certain rocks ("science-on-the-go") and to deploy special instruments (e.g. ISRU-Demonstrators, drop-and-go) to any planetary surface.

System study of a rover equipped with our 2-arm torso JUSTIN is under way. JUSTIN (see Sec. III.2.3) would give a rover sensorial and handling capabilities. The system should serve as a robotic agent and/or crew assistant for set-up and operation of planetary surface exploration and exploitation infrastructures (Fig. 44).

1.3.5 The DLR Crawler: A Testbed for Actively Compliant Hexapod Walking

Both, for planetary exploration as well as for search and rescue scenarios walking robots pose a promising alternative to wheeled or tracked vehicles. Their property of using discrete footholds and their omnidirectional mobility allow them to smoothly negotiate unstructured terrain. Further, they show remarkable climbing capabilities and are able to manipulate the environment either using their legs or their body as a tool holder.

Fig. 45 The DLR Crawler

The DLR Crawler is the first walking robot developed in our institute. It is intended to serve as a laboratory testbed for the development and test of leg and gait control algorithms as well as for research on vision based navigation and exploration strategies (see Chapter III.4).

Being modular, highly integrated and equipped with a broad set of sensors, the fingers of DLR Hand-II are well suited to be used as legs for this walking robot prototype. In addition to potentiometers and hall sensors to measure joint and motor angles respectively, joint torque sensors and fingertip force-torque sensors are available. These allow using active compliance control algorithms, which remarkably enhances the quality of gaits. Furthermore, they allow a fast detection of collisions along the leg and a quick response thereafter, which is crucial for the motion in unstructured terrain.

In addition to the proprioceptive sensors of the fingers of DLR Hand-II the Crawler is equipped with a FireWire stereo camera head, which enables the use of vision based exploration algorithms. Further sensor interfaces are prepared allowing to add an inertial measurement unit (IMU) as well as other sensors in future.

In order to enable statically stable walking and to grant some redundancy, the Crawler is built in a hexapod configuration. The final geometric setup is a result of a detailed workspace analysis of the fingers of DLR Hand-II and an optimisation of the body geometry minimising the contact forces for all legs over a nominal gait cycle, while maximising the stability margin, [Görner *et al.* 2008[c]].

The Crawler employs an external 24V power supply as well as an external QNX based realtime PC to perform all computations. Using the SpaceWire standard, FPGAs and two fibre-optic cables, a fast 1Gbit/s communication is implemented between the Crawler and the external PC. Even though not being autonomous at this stage, the powerful PC allows testing of different gait and exploration algorithms with low and high computational complexity.

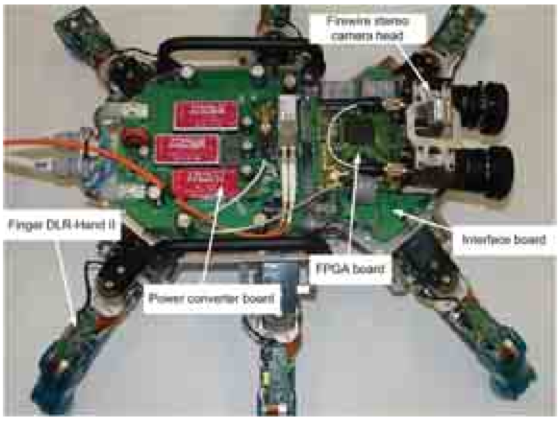

Fig. 46 The Crawler's hardware layout

In order to control the Crawler, joint compliance controllers developed for the fingers of DLR Hand-II are implemented. The gaits are generated using two different methods. The first is a tripod gait based on a fixed coordination pattern. In this case, the foot step trajectories are generated using fourth order polynomials to achieve smooth swing-stance transitions. Step height, step length, walking velocity and the posture of the robot can be altered online. Smooth gait transitions are designed to allow changes between forward and backward walking, turning as well as sideways walking.

The second method is biologically inspired by coordination rules that were found for the stick insect. In this case, each leg in stance dynamically alters its admissible workspace depending on the state of its neighbouring legs. As soon as it crosses its virtual workspace boundary a step is initiated. Hence, different gaits emerge according to the desired walking velocity and direction. This algorithm results in truly omnidirectional motion capabilities without the necessity of gait transitions. In combination with a stretch reflex and an elevator reflex, implemented for each leg, it allows the Crawler to walk on gravel and to overcome unstructured terrain with larger height differences, [Görner *et al.* 2008[c]]. Both methods work in conjunction with manual SpaceMouse control as well as vision based navigation algorithms.

Further developments of the 6-legged crawler concept will focus on its use for coming space missions w.r.t. to reconstruction, power autonomy and payload accommodation.

As it is not yet clear what the optimal form of mobility on a planetary surface is, we additionally studied e.g. the combination of legs and wheels (Fig. 47).

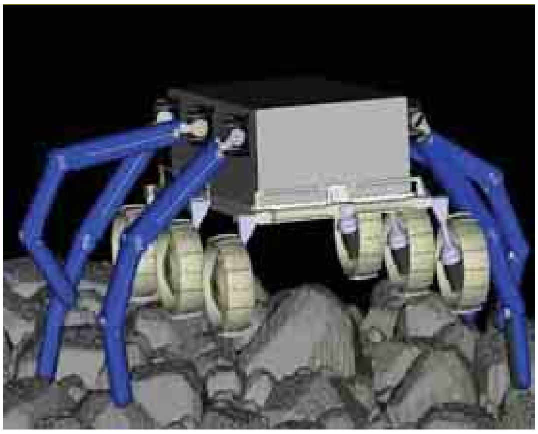

Fig. 47 Hybrid mobility system: combination of legs and wheels

Generally speaking we design heterogeneous, reconfigurable mobile robots, which combine the advantages of crawlers (high mobility and manipulation) with rovers (high payload, low energy consumption on flat terrain) to enhance the horizon of future missions regarding application areas, duration, and operational distance.

2 Advanced Space Technologies

2.1 Small Satellite TET

Heritage

There have been numerous contributions from DLR to space missions by sensors, sub systems, ground segment, mission control and data processing in the past.

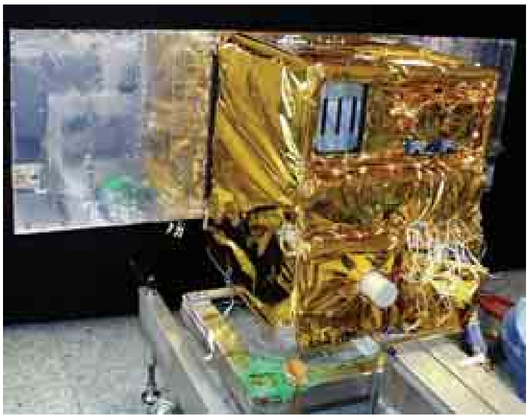

Fig. 48 Small satellite BIRD

In particular the small satellite BIRD (Fig. 48) as developed by our department Optical Information Systems in Berlin (RM-OS) successfully demonstrated DLR's capabilities to design, manufacture and operate a complete satellite. The BIRD mission successfully introduced an advanced and unique hot spot (fire) recognition sensor system with sub-pixel resolution (down to $4m^2$).

BIRD introduced new technologies in space, for example:

- a high-precision on-board navigation system based on GPS data and gravity field model on board (demonstrated 5m accuracy in each dimension);
- micro satellite structure with high mechanic stability, adoptable for various "piggy-back" launch platforms;
- newly developed sophisticated board computer, composed of four identical computers, protected against latch-ups with error detection;
- on board classification system based on artificial neural networks;
- fibre optical links on board;
- demonstration of a small ground station for local users;
- new precise and intelligent reaction wheels for satellite attitude control.

New special test units and laboratories were established. Based on the BIRD experiences it was possible to design a new attitude control test stand.

BIRD was operated in a new multi-mission concept by the GSOC together with the missions Champ and Grace.

New Technologies

As a key part of DLR's On-Orbit Verification Program, the small satellite Project "TET" started successfully into the project phase A in 2006. Based on the BIRD satellite bus, the new satellite TET will open the door for commercial German space products and shall improve the chances to capture the market.

Technology research objectives within the TET program were defined by the German Aerospace Agency, e.g., the establishment of a new gigabit optical link from satellite to ground, in combination with precise attitude control, new navigation systems, or the test of new infrared sensors.

In parallel the new TET satellite bus will be used as a base for a DLR compact satellite mission.

The TET initiative will also provide the opportunity to validate and to promote new approaches in the ground system field like the Intelligent Compact Control Center (ICCC), developed in an earlier DLR initiative for Intelligent Ground Systems.

The expected results are in the field of high-precision attitude control for optical payloads and optical data links. They are closely related to new actuator systems as are micro-machined reaction wheels, new control concepts, and on-board sensor autonomy.

Actually first tests of the new star-cameras were done. Two of theses new products, to be integrated in TET later, will help to increase precision of the attitude control system. This is needed for the geo-referencing of the IR-Sensor data product. Here a pointing accuracy of 26 arcsec has to be reached. The geometrical calibration is taking place in the camera calibration laboratory in Berlin.

For the TET-Mission new attitude modes are needed: The development of a target pointing mode will be tested at the DLR test facilities. This is done in the attitude control laboratory at the air-bearing table. Here a complete hardware-in-the-loop simulation with all sensors and actuators from TET is used for the validation of the attitude modes. For telemetry and telecommand of TET new approaches will be implemented in cooperation with DLR GSOC: now the mission control tool SCOS2000 is tested in the laboratory for the TET application.

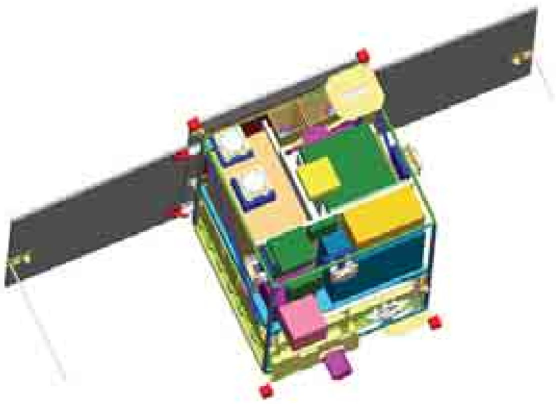

Fig. 49 The TET CAD design

In the system engineering part new software drivers for sensors and actuators are in the developing and test stage. A new magnetometer is integrated in the spacecraft bus computer application software.

The next milestone is related to TET project phase C. In November 2008 the critical-design-review of the bus of TET will give the kick-off to manufacture the TET bus.

The new compact satellite development of DLR's research and development program (planned Phase A) depends on one hand on the needs of the studies of the mission proposals, and on the other hand it will be a platform for new satellite technology as mentioned above.

Our activities will concentrate on TET and DLR's compact satellite program for the next five years. Including next generation infrared sensor technologies this could be the way to install a world wide fire observation system confirming our leading role in the field of fire detection from space.

2.2 Innovative Sensor Systems for Space

2.2.1 High Resolution Focal Plane Technology for Kompsat

Introduction

Our Berlin department RM-OS is part of the industrial consortium led by EADS Astrium GmbH in Friedrichshafen which won the international contract for the optical payload of the Kompsat3 project. In this particular project, DLR is responsible for the development of the camera electronics unit (CEU), one of the technological challenges associated with the development of the focal plane assembly (FPA).

Table 2 KompSat3 system parameters

Nr. of Pixels PAN	24,000
PAN-Sensor	2 × 12,080-TDI
Line Rate PAN	0.5-14 [nom 10] kHz
CCD Output Rate	< 16 × 25MPixel/s
Data Rate	3.84Gbit/s
MS-Sensor	8 × 6,000-TDI
Line Rate MS	0.5-7 [nom 2.5] kHz
CCD Outp. Rate MS	< 2 × 25MPixel/s
Data Rate MS	4 × 240Mbit/s
Pitch PAN	8.75µm
Pitch MS	2 × 17.5µm
Anti Blooming	yes
Operating tempera-	10°-25°C
Length of Image	22cm
Dynamic Range	14 Bit
PRNU	yes
DSNU	yes
SNR-PAN	>200
SNR MS	>200
Bandwidth PAN	450nm-900nm
Bandwidth NIR	760nm-900nm
Bandwidth RED	630nm-690nm
Bandwidth GREEN	520nm-600nm
Bandwidth BLUE	450nm-520nm
Supply Voltage	28VDC
Power CEU	< 200W

Korean multi-purpose satellite (Kompsat) is the name of the South Korean Satellite program started in the 90ies and highlighting in 1999 with launching Kompsat1 the first time.

The development of the Kompsat3 satellite with a ground resolution of 0.7m is the next step within the development of high resolution satellites.

FPA (Focal Plane Assembly) Technology

One of the most common approaches for increasing the optical performances for Earth observation is the application of so-called TDI (time delay and integration) detectors. To meet all of the requirements, the used TDI detectors had to be developed and optimised for the Kompsat3 application. The optical payload is comparable to the existing satellite class of Quick-Bird by a doubled swath width.

For Kompsat3, FPA and CEU were developed based on a new generation of technologies using a modular sensor concept. This technology has been developed over the last years in our department. Table 2 lists important system parameters.

This information gained during the development technology guaranties a distinct export advantage to the German space industry over other competitors.

Development Results

The development phase commenced with a Kick-Off Meeting in June 2006 in Berlin. The Preliminary Design Review was performed in November 2006, Pre-Shipping Readiness Review for the engineering model December 2007, and the Critical Design Review in March 2008. We are currently working on the verification of the qualification model (QM). The planned delivery date for the QM is February 2009.

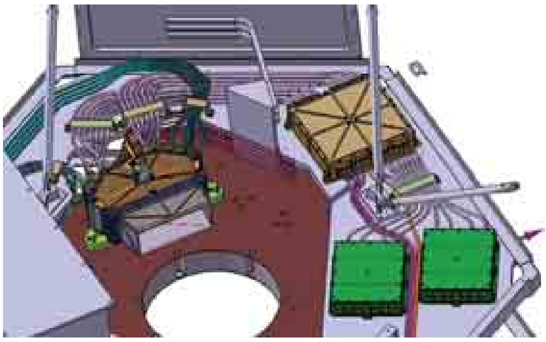

Fig. 50 Arrangement of KompSat3 modules and interfaces

Fig. 50 shows the arrangement and interfaces for components development for the satellite. The two green boxes are the main and redundant power supplies; the brown box contains the main and redundant camera controller including the main and redundant focus mechanism controller. The focus mechanism will be used for the controlling of the secondary mirror of the telescope to solve the zero G problems. The focal plane assembly was in focus for the development because of the performance relevance. One of the main functions of this FPA is the high accuracy of the assembly of the different TDI detectors by flatness better than ±7µm. The readout and analogue processing electronics is situated directly in line to the detector. The concept allows a reduced rms channel noise down to 21 electrons, resulting in a 6LSB rms noise by an ADC of 14 Bit.

Fig. 51 shows the implementation of this electronics concept.

Fig. 51 Focal Plane Assembly of KompSat3

One important point during the development phase was the thermal design. The simulated result fits exactly the reality by measurement. Fig. 52 illustrates the thermal behaviour of the FPA module stack and shows the maximum thermal differences over the detector line of lower than 1K.

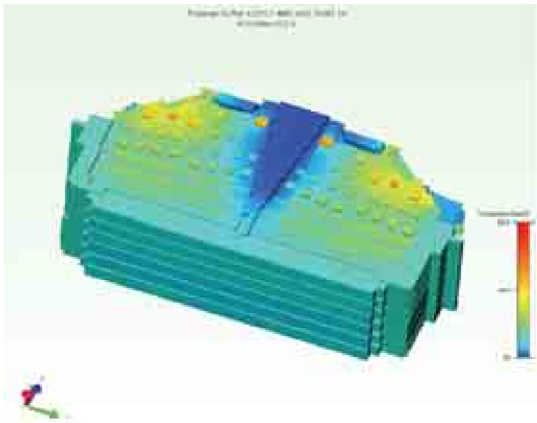

Fig. 52 Example for thermal load at KompSat3 FPA

The performance verification yielded excellent results—sensor's modulation transfer function (MTF) of 52% at Nyquist frequency, linearity better 1.8% for 1 million electrons full well and signal-to-noise ratio better 200 over the total dynamic range. In conjunction with the availability of qualified space parts, special industrial components were taken into account for space qualification.

Unique Selling Point

Companies such as ITT, Alcatel, and El-Op are also in the position to develop focal plane assemblies for high-resolution satellites; however none of these companies are in the position to develop such compact technology. Nevertheless the very good relationship established with Fairchild Imaging in the USA for the development of the detectors guaranties the success of this leading edge technology.

2.2.2 MERTIS

Introduction

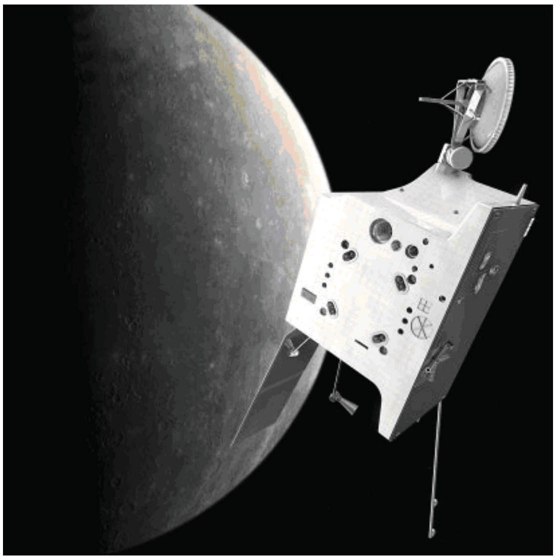

Fig. 53 BepiColombo Satellite (ESA)

MERTIS (MErcury Radiometer and Thermal Infrared Spectrometer) is one the scientific payloads of the ESA deep space mission BepiColombo. BepiColombo will be launched in 2014 toward Mercury to observe the planet from 2020 on.

The MERTIS state-of-the-art instrument design is based on a highly integrated and miniaturised concept, featuring low mass of only about 3kg and low power consumption. It is an imaging spectrometer obtaining hyper-spectral data in the thermal and mid-infrared wavelength range with a medium spatial resolution. An un-cooled bolometer array provides spectral separation and spatial resolution according to its two-dimensional shape and operates close to room temperature.

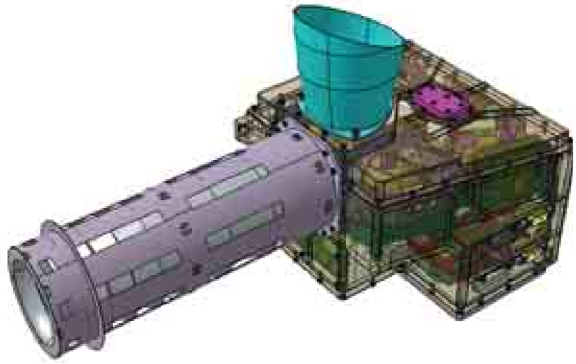

Fig. 54 MERTIS instrument

The operational concept is characterised by an intermediate scanning of the planet surface and three different calibration targets – deep space and two on-board black body sources. Sharing the same optical path a pushbroom radiometer is integrated allowing measurements of the Mercury surface temperature.

The general instrument architecture comprises two separate parts—the sensor head including optics, detectors, shutter and proximity detector electronics, and the electronics unit containing instrument control and driving electronics as well as power supply. This highly integrated measurement system is completed by a pointing device which orients the optical path to the planet and the in-flight calibration targets.

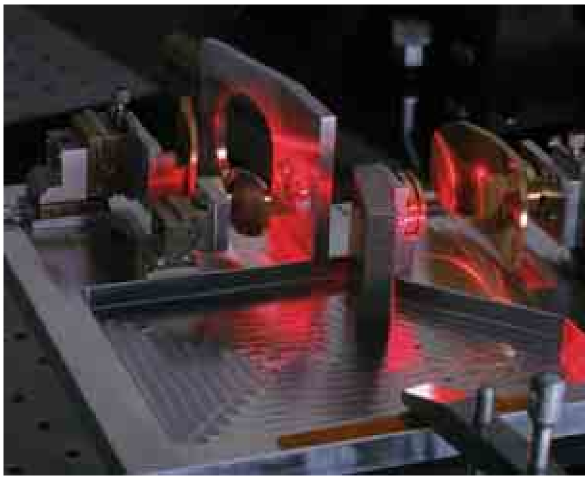

Fig. 55 Optics breadboard

RM-OS proposed and developed the instrument concept and design, coordinates the developments of its sub-systems and verifies the overall performance based on theoretical modelling, laboratory investigations and final instrument calibrations. The MERTIS development runs in close cooperation with the University of Münster, the DLR Institute of

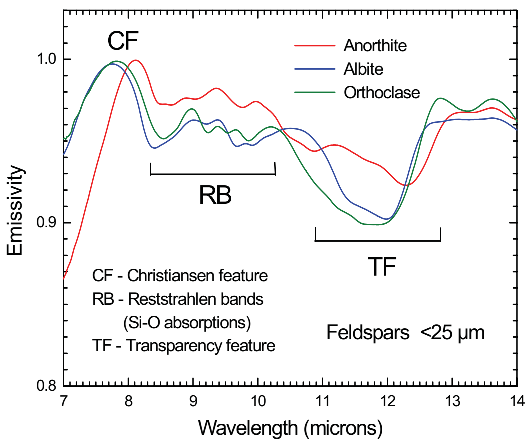

Fig. 56 Characteristic spectral features

Planetary Research, international institutions and several companies of the German industry.

Scientific Requirements

The scientific goal of MERTIS is to provide detailed information about the mineralogical composition of Mercury's surface layer by measuring the spectral emittance in the spectral range from 7–14m (Fig. 56) with a high spatial and spectral resolution. Furthermore MERTIS will obtain radiometric measurements in the spectral range from 7–40µm to study the thermo-physical properties of the surface material. Top level requirements are shown in Table 3.

Table 3 MERTIS performance requirements

Spectral coverage	7–14µm
Spectral resolution	< 200nm
SNR for whole spectral range	> 100
Spatial resolution for global mapping	500m
Targeted observation with better than 500m	5-10% of the surface
NETD at 100K surface temperature	1K

Instrument Design and Performance

The MERTIS instrument design is driven by a strong need for miniaturisation and a modular combination of the functional units, at the same time using several new technologies. The complexity of internal interfaces requires a complex design functionally consisting of the sensor head and the electronics unit with the pointing/calibration units in front of the optical entrance.

All sub-systems are designed (partially by cold redundancy) to withstand the extreme environmental conditions such as are high temperature and cosmic radiation, as well as to fulfil the quality requirements, e.g. a long life time over about eight years mission operation.

A functional block diagram is shown in Fig. 57. The sensor head structure contains the entrance and spectrometer optics, the bolometer and radiometer focal plates, its proximity electronics, the calibration devices (shutter and 300K black body). It provides thermal interfaces to the spacecraft to achieve the required high thermal stability.

Table 4 MERTIS performance parameters

Spectrometer	**Radiometer**
Focal length (F): 50mm	
F–number (F#): 2.0	
Optical efficiency (ηopt): 0.54	
Detector technology	
Bolometer matrix array	Thermopile line array
Number of pixels / size (illuminated pixels)	
160x120 @ 35µm (100 spatial, 80 spectral)	2x15 @ 250µm
Spectral range (λ)	
7–14µm	7–40µm
Spectral channel width (λδ)	
90nm / pixel	Line array 1: 7–14µm Line array 2: 7–40µm
Spectral resolution (λ/λδ) **Spectral sampling distance (SSD)**	
78–156	-
Detectivity	
NEP < 15pW	D*=7*10^8 cm$Hz^{1/2}$ W^{-1}
FOV (field of view) / Instantaneous FOV	
4° / 0.7mrad	4° / 5mrad
Ground sample distance (GSD)/Dwell time (τ)	
@ Periherm 400km	
280-1400m / 109msec	2000m / 775msec
@ Apoherm 1500km	
1050m / 784msec	7500m / 5597msec
Swath width: 28km	
Instrument dimensions: 180 × 180 × 130 mm³ **External baffles: 200 × ø75 & 90 × ø75 mm³**	
Mass: 3.3kg	
Power consumption (cold case heating) 9–13W (<19W)	
Instrument telemetry data rate: 1–1263KBit/s	

At its optical entrance, a pointing device is located which directs the incoming infrared beam from four different targets, three for in-flight calibration purposes (300K black body view, 700K black body view, space view and the planet baffle view).

This segment as well as the sensor head is mounted into the electronics unit (see Fig.

58) which contains common cold redundant electronics for instrument control and power supply, including electrical interfaces to the spacecraft, electronics for bolometer temperature stabilisation, the 700K black body with its electronics, and the shutter electronics. It also serves as the housing for the sensor head and the pointing unit as well as the mounting interfaces of the planet and space baffles.

A summary of the MERTIS performance parameters are shown in Table 4.

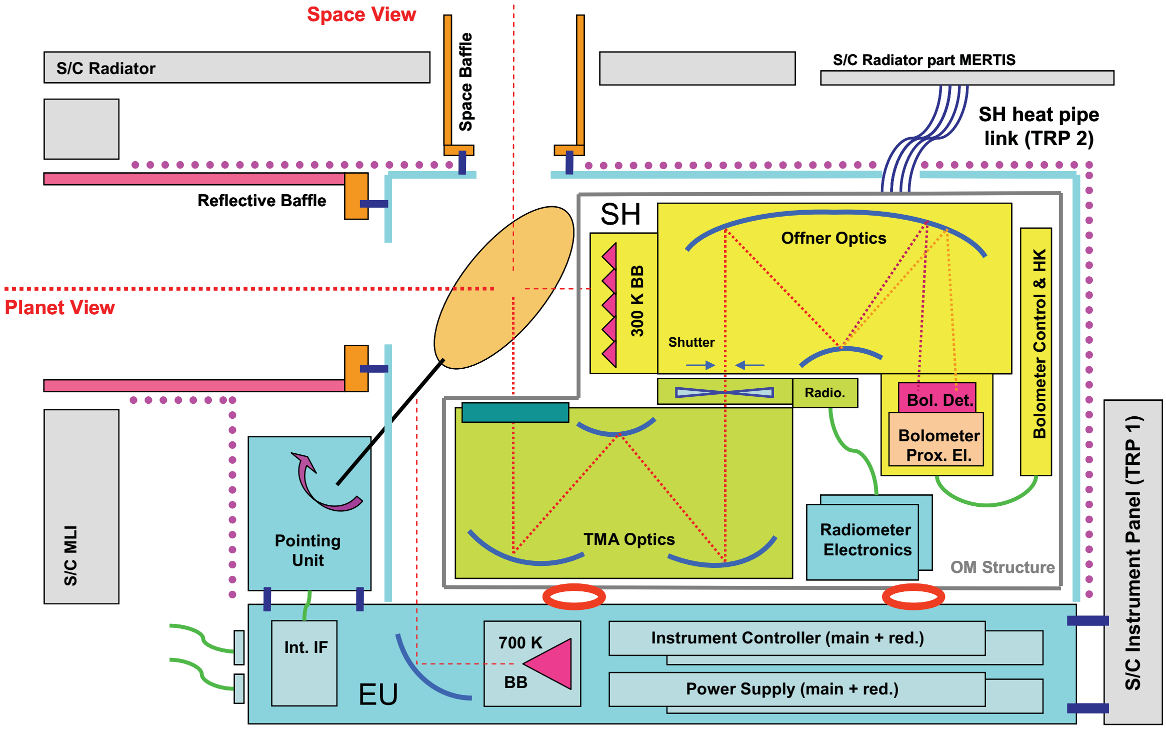

Fig. 57 MERTIS functional block diagram

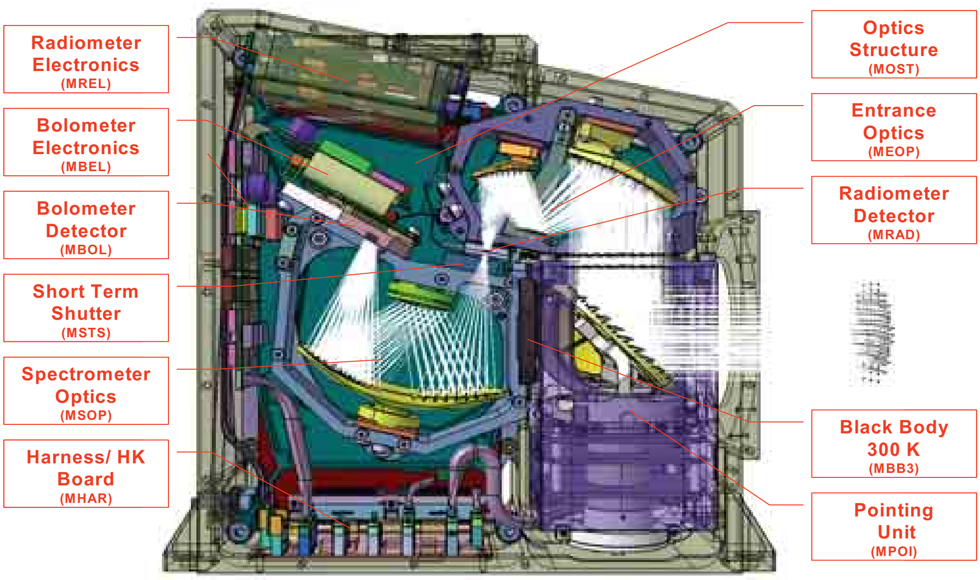

Fig. 58 MERTIS sub-systems (without baffles, instrument controller and power supply)

2.2.3 Infrared Sensor Systems

Introduction

Most of the knowledge of the institute in the field of infrared systems is based on the small satellite project BIRD. This satellite was designed, deployed, calibrated and operated at DLR. It aimed at the investigation of hot spot events (e.g., detection and monitoring of fires) as well as technological experiments. BIRD was launched in 2001 and performed its tasks till 2007 very well.

Project TET-IR

The OS department now deploys an infrared payload for the small satellite mission TET funded by the German Space Agency. Based on the detectors, focal plane array and cooling machines of BIRD, an improved camera system was developed. Two infrared channels with 1024 pixels each and three visible channels (R, G, B) with about 5,000 pixels will provide images with a ground sampling distance of 356m and 42m, respectively. This ground resolution is sufficient to detect fires with an area smaller than 10m².

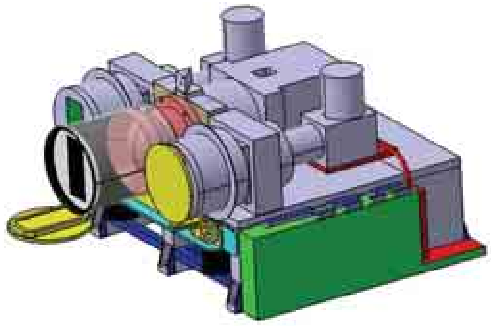

Fig. 59 Infrared payload for TET, CAD model

Project Signature Camera

This project is designed to investigate spectral signatures of hot temperature events in the infrared range of the electromagnetic spectrum. In addition to the measurement of temperature and emissivity other object properties can be determined. Hot temperature events can be classified much more accurately.

Project Fuegosat

The institute supports the definition phase of GMES infrared segment by determining user requirements and providing BIRD data. Fuegosat is funded by ESA.

Fig. 60 Signature camera

Project Earthquake

This project was acquired in order to investigate the possibility to detect earth quakes with the help of spaceborne infrared sensors. The detection of earthquake precursors in form of thermal anomalies uses sea surface temperature and land surface temperature maps obtained from infrared satellite sensor data. To overcome the uncertainties resulting from non-accurate surface emissivity measurements with conventional Earth observation sensors a spaceborne hyper-spectral thermal infrared imaging sensor appears as the "right tool".

Technology Experiments

A number of technological investigations are executed in RM-OS. Modern detectors are evaluated, e.g. Mercury-Cadmium Telluride (MCT) arrays, and micro bolometer. Geometric, radiometric and spectral calibration facilities including turntables, collimators, black bodies, spectrometers are at our disposal. These experiments put the institute in the position to propose own payload concepts for future space missions for Earth observation and planetary exploration.

2.2.4 3-D Line Cameras

Introduction

Three-dimensional data sets are very important inputs for governmental decision makers and commercial products. Applications like city planning, assistance systems, vehicle simulators and crisis management systems rely on high quality models of urban and rural regions. Above all, the generation of 3-D city models turned out to be a big challenge to engineers and scientists working in the fields of cameras and signal processing.

Due to the technological developments (e.g., detectors, inertial measurement units, computers, algorithms), considerable improvements have been made.

Cameras

The department of optical information systems developed a multi-functional camera (MFC, Fig. 61) which can be used for the generation of imagery as basic input data for 3-D world models.

Fig. 61 MFC camera family, MFC-5, MFC-1, MFC-3 (from left to right) with 5, 1 and 3 CCD lines module

MFC is a CCD line-based digital camera. Each CCD line with 6k, 8k, 10k or 14k pixels each (RGB or panchromatic) is glued on a separate focal plane module. This module includes heat pipes for thermal control. Furthermore, it carries two boards containing the front end electronics. These boards are soldered directly on to the CCD, therefore very short ways for analogue signals are achieved. Front end electronics is responsible for A/D conversion, for reduction of systematic noise effects (e.g., photo response non-uniformity) and data compression (lossy or lossless). All these tasks are performed in a field programmable gate array (FPGA). Digital data are transmitted via a USB2 interface to a receiving unit (e.g., internal PC104, external Laptop, or 19" industrial computer) and stored in an internal or external mass memory system (hard disk or solid state). Up to five focal plane modules are aligned and fixed sequentially in relation to the optical axis (Fig. 15). Additionally, DLR also operates other sensor systems.

Future spaceborne and airborne camera systems (e.g., HRSC-L for Germany's LEO mission to the moon and AMS for defence applications) are phased in our current development process.

Calibration

The radiometric calibration of the MFC consists of the correction of the electronic offset, a correction of the dark signal non uniformity (DSNU), and a homogenising of the different sensitivities for each single pixel of a CCD line. The latter is corrected by the photo response non uniformity (PRNU) function. The PRNU includes also the luminosity gradation of an optic system; therefore the PRNU is measured with a diffuse homogenous emitter (e.g., Ulbricht sphere). At last a linear factor for a white balance correction is estimated for different colour temperatures. The geometric calibration is different from standard photogrammetric approaches.

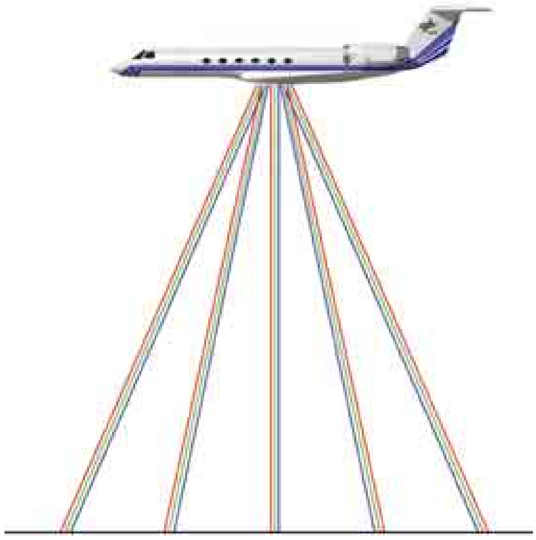

Fig. 62 Principle of 5 line stereo camera

Instead of describing the deviations of a linear Gaussian optic with interior orientation parameters a direct measurement of single pixels of a CCD-line is preferred. Therefore, the camera is mounted on a two-axis manipulator. A widened collimator ray illuminates a single pixel. The respective angles for a measured pixel corresponding two the effective line of sight. The resulting geometric calibration is within high subpixel accuracy. This is reproducible before and after different measuring campaigns.

Data Processing

In order to enable direct georeferencing of the MFC-images, an accurate determination of the cameras exterior orientation is needed. For this purpose an integrated GPS/INS (inertial navigation system) is used (e.g., the IGI AEROControl IId, Applanix POS-AV 510). A precise time synchronisation of the

MFC and the GPS/ INS-system is mandatory. The original MFC-images, scanned line by line, are heavily distorted due to non-linear movements of the MFC's platform (e.g. aeroplane, car, robot, etc.). After synchronisation and correction of the measured orientation, each captured line of the original MFC image is projected onto a virtual reference plane at the average scene depth. The projected images are clear from distortion and geometrically corrected.

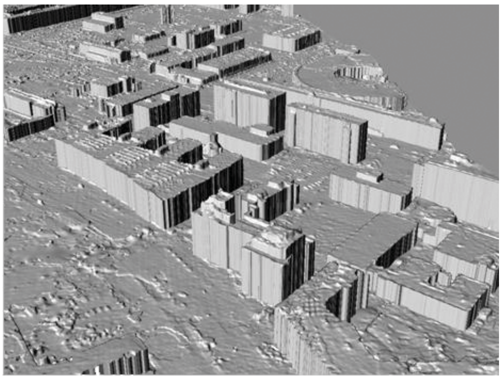

Fig. 63 Digital terrain model, computed from MFC imagery and the SGM algorithm

The pre-processed images as well as the intrinsic calibration data and the extrinsic movement path serve as input for stereo matching. In order to minimise the search region for correspondence finding, the epipolar geometry is required. In case of dynamic applications on moving platforms like aeroplanes or cars, epipolar lines are not straight. The computation of epipolar lines is done point by point, by reconstruction of pixels in different distances and projection into other images using the intrinsic calibration data as well as all extrinsic camera positions and orientations. It is assumed that the camera calibration and especially the extrinsic movement path are accurate enough to compute the epipolar lines with an accuracy of 0.5–1 pixel. Stereo processing itself (see Fig. 63) relies on the Semi-Global Matching (SGM) method as developed by our robot vision group (see Sec. III.4.2).

2.2.5 DIOPTER

Introduction

Geometrical calibration is an essential need for using opto-electronical sensors within applications where high accurate coordinate measurement is needed. It is the goal to determine physical camera parameters. An approved method is to determine the line of sight for a subset of pixels by single pixel illumination with collimated light. A manipulator construction is used to adjust angles which define the line of sight of a pixel. Large construction and amount of time for calibration are disadvantages of this method. Alternative calibration methods use test patterns which are imaged from different positions and viewing directions. The images are processed by appropriate algorithms, interior orientation of the camera is determined.

Diffractive Optical Elements (DOE)

Diffractive optical elements are designed to manipulate amplitude and phase of coherent light. They can be used to split an incoming laser beam with a certain wavelength into a number of beams with well-known propagation directions (Fig. 64 and Fig. 65). As the image on the sensor is a Fraunhofer diffraction pattern, each projected image point represents a point at infinity, denoted in 3-D projective space in the camera.

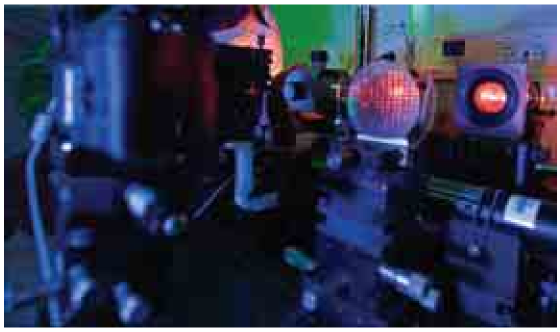

Fig. 64 DOE and diffraction pattern

Table 5 DOE parameters

	29×29	71×71
Grating period	0.4×0.4 mm	0.041×0.041 mm
Element diameter	45mm	75mm
Angular spacing	4.27°	0.88°
Highest diffraction order	[362, 362]	[35, 35]
Max. diffraction angle	59.96°	49.39°

Table 5 summarises the important parameters of the two different DOEs used in the experiments with the laser wave length of 676.4nm.

The angular accuracy was checked with a collimator-goniometer arrangement, finding only minor deviations from the computed values of less than 0.001°.

Calibration Setup

The principle scheme for geometrical sensor calibration is illustrated in Fig. 65. A mixed gas argon/krypton ion laser is used which offers a selection of wavelengths in the visible spectral range. The beam is collimated and enlarged with a beam expander to a diameter of 78mm. The enlarged beam is then diffracted by a DOE which is located directly in front of the camera optics.

The diameter of the incident laser beam and that of the DOE active area should be at least equal to the aperture diameter of the camera lens. Each of the diffracted beams is focused within the image plane of the camera. In order to obtain spots over the whole camera sensor area, the maximum diffraction angle of the DOE should be larger than the field of view of the camera. No further alignment steps are necessary, because firstly the mapping of the diffraction points is invariant against translation, and secondly the rotation of the DOE in terms of the collimation system as well as the exterior orientation of the camera is modelled and can thus be determined.

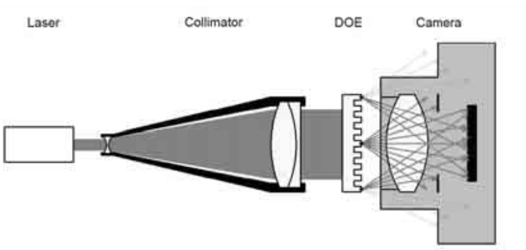

Fig. 65 Scheme of camera calibration with DOE

Experimental Results and Discussion

The experiments were conducted with a Dalsa 1M28-SA, which is a monochrome CMOS camera, and the semi-professional digital single-lens reflex camera Nikon D2X. In Table 2 the important camera parameters are listed. Both cameras were calibrated with a wavelength of 676.4nm. After aligning, the DOE to the collimator system within 200", the cameras are initially aligned to the DOE system by direct lens reflections which determine the principal point for the Dalsa and for the Nikon. This method allows an accuracy of about 3 to 4 pixels.

The standard deviation of the residuals between model and measurement points is less than 0.2 pixel (<2μm) with a maximum error of 1 pixel for each dataset. The results are also comparable to the results realised with chessboard pattern calibration. The distortion of the 4.8mm wide-angle lens is very strong and the used distortion model just suitable in this case (see Fig. 66).

Table 6 Main camera parameters

	Dalsa 1M28-SA	Nikon 2DX
Resolution	1024×1024	4288×2848
Pixel Size	10.6μm	5.5μm
Focal length	4.8mm	24mm
IFOV	0.12°	0.013°
FOV	97°	99°

The second test series with the Nikon D2X were done in order to prove that the method also works with high resolution cameras. Here the 71x71 DOE with a higher density of diffraction points was used. In accordance to the wavelength used for calibration only the red channel was evaluated. It was noticeable that an exact alignment of the DOE with respect to the incident laser beam is apparently not required for obtaining a steady calibration result. For all measurements a better resolution compared to the Dalsa and therefore a more accurate sub-pixel position as well as a better fitting distortion model leads to better results with a standard deviation of less than 0.1 pixels (<0.4μm) and a maximum residual of less than 0.3 pixel for each dataset.

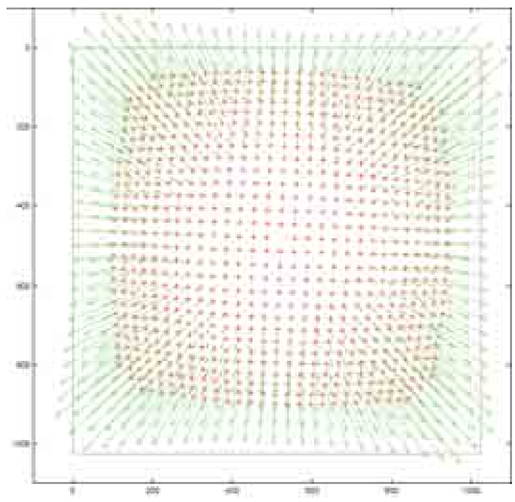

Fig. 66 Calibration pattern (red) with radial distortion vectors (green) for Dalsa 1M28-SA

Conclusion

RM-OS developed a new approach for geometrical sensor calibration which uses custom-made diffractive optical elements as beam-splitters with precisely known diffraction angles. The compact calibration setup in principle allows in-field calibration. By using not only a single but different reference wavelength the presented method also allows the determination and correction of chromatic aberrations.

III Advanced Robot Technologies

1 Background / Motivation

For us the realisation of a new generation of advanced robotic systems for servicing and exploration in space is the primary motivation for research and development in robotics. Space robonauts cooperating with astronauts must be of the "soft robotics" type, not harming humans even when in direct contact. At the same time, space missions, with their requirements for minimal weight, minimal power consumption and high-level interaction, are a real technology drive for terrestrial robotic applications, too.

After decades of intensive research, it seems that we are getting closer to the time when robots will finally leave the cages of industrial robotic workcells and start working in near and with humans. This opinion is not only shared by many robotics researchers, but also by leading automotive and IT companies and, of course, by some clear-sighted industrial robot manufacturers. Several technologies required for this new kind of robots have reached the necessary level of performance, e.g., computing power, communication technologies, sensors, electronics integration, actuators with high energy density, high level dynamics simulation, and code generation tools.

However, it is clear that these human-friendly robots interacting with people or with unknown environments will look very different from today's industrial robots. Rich sensory information, light-weight design, advanced manipulation and interaction control features as well as algorithms for autonomous action and immersive teleoperation are required to reach the expected performance and safety. The achieved advances in technology pave the way towards new application fields, such as industrial co-workers, service and household robots, advanced surgical robots, prostheses, and rehabilitation devices.

In this Section, we will give an overview on the advanced humanoid robotic components and systems developed in the Institute as well as on the main research topics addressed therefore. According to the definition of the IEEE Robotics and Automation Society, a robot is a device which *embodies* the intelligent interconnection between *perception* and *action* (Fig. 67). In accordance to this definition, our research activities focus on three major fields:

- The **mechatronic** development of new **robotic systems**. This includes the concurrent design of the hardware (mechanics and electronics, see Chapter III-2) and of their control (Chapter III-3). We present our two main approaches for reaching the aforementioned compliant interaction and robust manipulation features. The first one is the meanwhile matured technology of torque-controlled light-weight robots (even space qualified via ROKVISS, see Sec. I.2.1) developed over the past decade in the institute: arms, hands, a humanoid upper body, and a crawler. Several products resulted from this research and are currently being commercialised through cooperations with different industrial partners (DLR-KUKA LWR, DLR/HIT-Schunk Hand, DLR-BrainLAB Medical Robot). The second technology, our newest topics of research in this area, is based on variable-compliance actuation that implements the soft-robotic features mainly in hardware. Robots closer to human performance and morphology, and stronger inspired by human biomechanics are aimed for in this context.
- A fundamental research topic for the addressed new robotic application fields is **perception**. Since the robots are supposed to act in unknown, dynamically changing environments, it is obvious that efficient perception, internal representation, and recognition of the surroundings are indispensable prerequisites for autonomy. Research in the institute includes on one side the development of sensors for stereo vision, 3-D modelling, tactile and haptic information. On the other side, a strong focus is on the development of algorithms for data processing (in particular for image processing), as well as methods for 3-D representation and localisation of objects and whole environments, see Chapter III-4.

- The third major challenge addressed in this Part is to develop methods which enable the effective **action** of robots (esp. space robots) in complex environments. Various levels of human involvement in the action planning and execution are addressed, starting from haptic feedback and telepresence, where the human is controlling the robot, to shared autonomy, as in telerobotics, up to full autonomy. In the former cases, the focus is on high-fidelity interaction control of the robots, even in the case of large communication delays, see Chapter III-5. In the latter case, the planning of tasks and motions as well as fast online reactive behaviours are the primarily addressed topics. A few examples of autonomously acting robots will be finally presented in Chapter III-6.

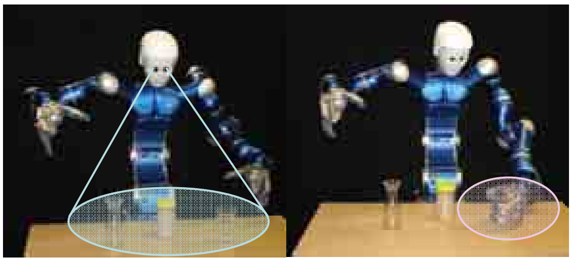

Fig. 67 Robots physically embody the link between perception and action

2 Humanoid Robot Technologies

2.1 Light-Weight Robot III

The third generation of light-weight robots (LWR-III), an early version of which was presented by the institute in 2002, has become a central engine for the institute's research towards future space and service robotics. Many demonstrators have been set up to show the sensitiveness, versatility and performance of the system. The arms are used in an industrial context, e.g.,. for force controlled assembly operations, as well as for humanoid robotics experiments.

The LWR consists of joint units with Harmonic Drive gears, DLR's own RoboDrive motors and torque sensors, all operated by integrated joint electronics. The joints are linked by carbon fibre exoskeleton structures to form a robot arm, weighing 14kg, which is capable to handle 14kgs of load with excellent dynamics.

Fig. 68 DLR LWR-III with Hand-II

Since the first presentation of the LWR-III important improvements have been made to increase its capabilities.

2.1.1 Hardware Design

From the first prototype to the actual revision, several hardware parts have been redesigned, including:

- the joint structures and mechanical parts have been altered to increase the robot's stiffness, improve the assembly process and reduce the costs;
- the piezoelectric brakes have been replaced by optimised magnetic safety brakes due to problems inherent to the piezo material;
- the motor-side position sensing in the robot has been replaced by a newly developed magneto resistive (MR) sensor concept, which especially matches the RoboDrive motors and the hollow shaft design of LWR-III. This new commutation sensor enabled a huge step of improvement in control of the robot and has become an internal standard for drive development;
- the joint electronics has been redesigned to meet the requirements of the commutation via MR Sensor, to improve reliability and to shorten initial operation

in order to ease the prospected serial production.

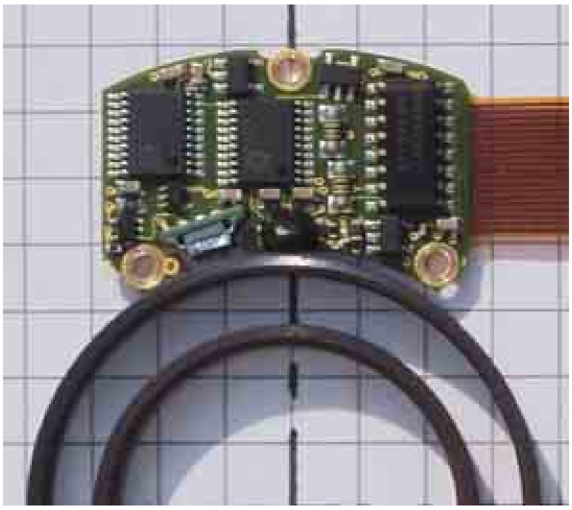

Fig. 69 DLR Magnetoresistive (MR) Encoder

2.1.2 Towards Robot Standards

The LWR-III is used in different applications, one of which should be a "CoWorker" for industrial production tasks. Thus it has to be easy to use, reliable, exact and easy to adapt to its task. Several efforts have been taken to prove or improve its suitability:

- long-term tests with extended payload in cooperation with KUKA have proven reliability;
- ISO standard accuracy tests for robots attested the same precision for the LWR that industrial robots have;

Fig. 70 DLR quick-release interface for grippers

- an extremely compact quick release interface with internal power and data supply was developed so the robot can be equipped with different grippers without external cabling (Fig. 70). The interface has to be very thin, because every additional length between the robot's wrist frame and the manipulation object decreases the robots manipulation range by twice its length. The interface has become a standard part for robots and is now manufactured and marketed by Schunk GmbH.

2.2 Multifingered Hands

2.2.1 Design Modifications on the DLR Hand-II

The DLR Hand-II was used in numerous demonstration experiments in the past years. Experience from these applications as well as the upcoming dual arm and hand demonstrator JUSTIN, required a substantial redesign of the hand. Several optimisations in the mechanical, electronic and even kinematic design were made. As the basic technology and construction remained the same, its name was chosen to be DLR Hand-IIb.

Fig. 71 DLR Hand-II (left) and IIb (right)

To enhance the grasping capabilities of the hand, the range of motion of the finger's base joints were modified such that even very small objects could be handled by the fingers. The joint limit for the abduction of the fingers base was increased by 20°.

Furthermore, the palm geometry was optimised to support a large variety of power (enveloping) grasps. In addition, the palm elements were equipped with silicone pads with high-frictional coefficients, to increase grasp robustness. This way, the new hand can now grasp objects with a small diameter (e.g., the hammer in Fig. 72) and perform lateral pinch grasps (brush).

Even with the superior sensor-equipped hand, robustness of the manipulation actions carried out was far below human capabilities. To increase robustness, the use of biomimetic fingertips turned out to be very useful. We studied the mechanical properties of the human fingertip and derived a novel robotic fingertip that consists of a bone with fingernail that resembles the properties of the human fingertip bone surrounded by skin-like material (Fig. 73) [Potdar 2007[r]].

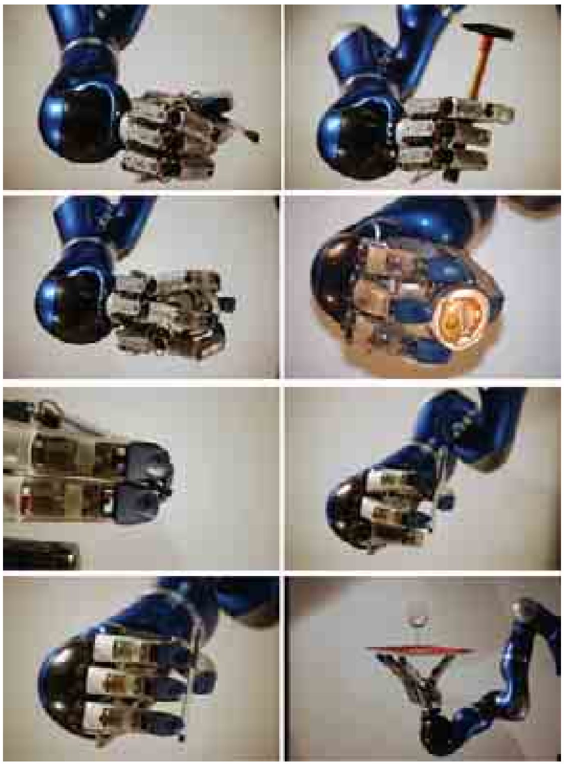

Fig. 72 DLR Hand-II can handle a large variety of objects

Through the variable compliance of the fingertip, grasp robustness increases drastically, such that we can even manipulate delicate objects, like the fragile glass in Fig. 76. Furthermore, the area on the fingertip that is suitable to contact objects was increased leading to more flexibility and dexterity in manipulation.

The maximum velocity of the finger joints was improved to 550°/s in the base joint and 480°/s in the distal joint, thus enabling grasping speeds similar to human performance.

To simplify the integration of the hand device into more complex robotic systems such as JUSTIN, the power supply board, as well as the communication device on the host computer, were completely redesigned.

Fig. 73 Novel biomimetic fingertip consisting of a bone, skin, and a fingernail

Due to better EMC-compatibility and better integration on mobile platforms powered by accumulators, the former 20kHz AC power supply was replaced by a new power supply supporting 24V DC input voltage. As the form factor and the technical specification were fixed, a commercial solution was not available. Therefore a two-stage power supply board with a down converter on the input side and a planar transformer on the output side was developed.

Fig. 74 Power supply board for DLR's Hand-IIb

By use of a synchronous rectifying scheme and using a smart control to the first stage of the power supply, the stability of the output voltage is such that no output voltage control is needed. This in turn eliminates the need for a galvanically separated voltage feedback. A patent claim has been filed for this design.

Fig. 75 FPGA PMC Module to communicate with two DLR Hands-IIb as, e.g., used in JUSTIN

Due to the compact configuration, the passive input filter for the motor supply and the necessary emergency stop circuit for the motor current could also be integrated.

Fig. 76 Even a fragile glass can be gently—but stably—held

To allow the seamless integration of the hand in our agile Robot Development framework (aRD), the communication to the real-time control computer was also changed. Previously, a customised VME card was used to collect the hand sensory data. For this hand release, the communication protocol IEEE 1355 was implemented on a commercially available FPGA board. This module allows the operation of two hands on a single board, which suits well for two-handed manipulation. For the integration in our control framework, customised QNX drivers were developed to assure low latency and computational load for data acquisition.

The quick fastener that is used to attach the hand to the robot wrist was redesigned with the goal to minimise the distance between arm and hand. This way, the workspace w.r.t. to the orientation of the hand was increased.

2.2.2 DLR/HIT Hand-II

DLR and HIT (Harbin Institute of Technology) have jointly developed a modular (i.e. all actuators integrated) DLR/HIT Hand-I in 2004 and 2005. It has four fingers with in total thirteen DoFs, each finger having three DoFs in four joints—as in the DLR Hand-II, the most distal joints are mechanically coupled. To achieve a high degree of modularity, all four fingers are identical. Rather than using an expensive VME bus board, control has been realised by a custom-made DSP/FPGA board. An outer shell, mimicking the looks of a human hand, completes the hand.

Fig. 77 The backside electronics and nice envelop of the DLR/HIT Hand-I

The packing of the DLR/HIT Hand-I (Fig. 77) is realised by extra plastic parts mounted on the finger bodies and palm. It needs more space and makes the hand relatively large. The whole size of the hand is about 1.5 times the adult human hand. Because of its modular construction, it can be easily configured as a left or right hand using the same components. In 2006 this hand has been distributed by Schunk as the "Schunk Anthropomorphic Hand" (SAH), and is used since then by various universities and institutes worldwide.

Feedback on these developments revealed interest in a smaller hand with five rather than four actuated fingers. To this aim, DLR and HIT have been jointly developing a second generation hand. To decrease the size of the hand while increasing is maximal fingertip force (up to 10N), not only the mechanical design had to be overhauled but also new actuators, more powerful gears, new sensors and miniaturised electronics were introduced. In particular, super flat BLDC motors, harmonic drives, and (w.r.t. electronics) Ball Grid Arrays were used, leading to a new modular hand design: the DLR/HIT Hand-II.

Mechanical Structure of the Hand

The DLR/HIT Hand-II is a multi-sensory and integrated five-fingered hand with in total fifteen DoFs, as shown in the right of Fig. 78. To achieve a high degree of modularity, all five fingers are identical. Each finger has three DoFs and four joints, the most distal two joints again being mechanically coupled. All actuators, gears, electronics, and communication controllers for one finger are fully integrated in the finger's base or body.

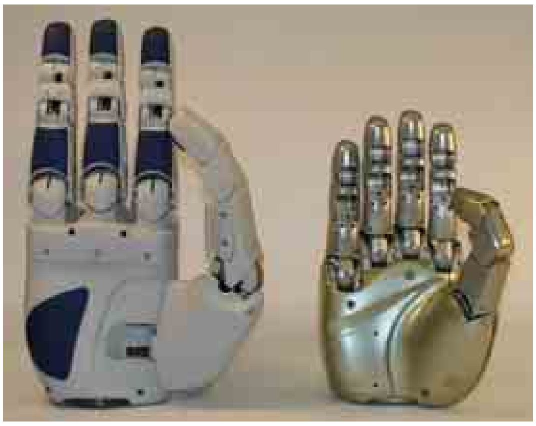

Fig. 78 DLR/HIT Hand-I (left) and DLR/HIT Hand-II (right) compared

On the basis of the DLR/HIT Hand-I, super flat BLDC motors have replaced traditional BLDC motors. The motor measures only 20mm in diameter and 10mm in height, weighing only 15g. The rated speed and torque of the motor are 6000rpm and 3.2mNm, respectively. In each finger's distal joint, a 2.1:1 mechanical transmission is realised by a timing belt instead of bevel gears, thus reducing transmission noise. The coupling mechanism in the last two joints of the finger is realised by steel wires with a fastening mechanism. This makes the transmission ratio exactly 1:1 in the whole movement range. Also, at the base joint actuation unit, two tiny harmonic drives with timing belts have replaced the previously used planetary gears and bevel gears. A comparison of the mechanical transmission in the DLR/HIT Hand-I and II is shown in the next table.

	Type	Ø /mm	H/mm	Wt/g
Hand-I	BLDCM	16	35	31
	Planetary gear	16	25.3	28
Hand-II	BLDCM	21.2	10.4	15
	Harmonic drive	20	13.6	15

Fig. 79 Robotic finger and human hand

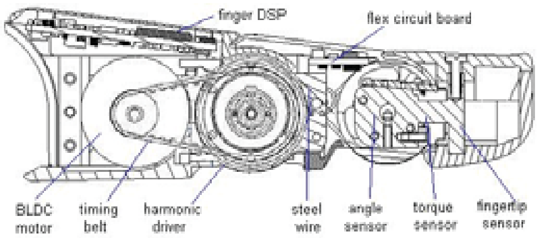

Fig. 80 Finger unit

One modular finger consists of two independent units: a finger body and a finger base. In the finger body unit (Fig. 80), there is a super-flat BLDC motor and a tiny harmonic drive. They are mounted in parallel and transmitted by a high-speed timing belt with a reduction ratio of 1:2.1. The harmonic drive with reduction ratio of 100:1

measures only 20mm in diameter and 13.4mm in length. The maximal driving torque can reach 2.4Nm. The BLDC motor controller and driver are integrated in the back side of fist linkage. The finger flexible circuit board is a hard-flexible combination for sensors conditioning and communication, which runs through the rotational joint. This kind of arrangement saves much space because there is no need for extra electric connectors.

In the finger base unit (Fig. 81), the two rotational axes intersect. Because the effectiveness of bevel gear differential transmission has been successfully demonstrated in the DLR Hand-II, this scheme has been also adopted in the base joint design. For curling/extension motion the motors apply a synchronous motion to the bevel gears using the torque of both motors. For abduction/adduction motion the motors turn in contrary directions. This causes a curling motion on the fingertip. Using the torque of both motors means that we can use small motors and reducers while reaching double output force on the fingertip. Instead of motor and planetary gear combination in the DLR/HIT Hand-I, the finger base actuation unit is similar as in the finger body. Two flat BLDC motors are placed in parallel in the bottom of the base and two harmonic drives are also mounted in parallel between motors and bevel gears.

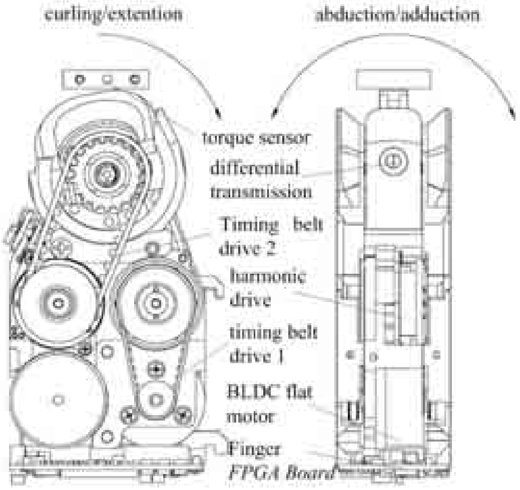

Fig. 81 Finger base joint

From experiences with the DLR/HIT Hand-I, we concluded that the extra DoF in the base of the thumb is hardly used for manipulation. Therefore, in the new hand the thumb is fixed in an appropriate orientation of the palm.

Hardware Architecture

The DLR/HIT Hand-II hardware architecture consists of a PCI-based central floating point DSP/FPGA processor for hand control, a palm FPGA controller for local processing and data communication; finger base FPGAs for 2-DoF base-joint motor control and a miniature DSP for the finger joint motor control (Fig. 82), allowing for stand-alone use.

Software Architecture

The software architecture has been developed according to the principle of multi-level structure and modularity. As shown in Fig. 83, all data processing and control algorithms of the hand are realised in five levels. In Lower Control Level, sensor data acquisition and motor actuation are implemented by finger DSP board and FPGA board.

Fig. 82 DLR/HIT Hand-II hardware components

The Data Process Level performs all data processing and communication needed to pack all digital sensor values from Lower Control Level and distribute command signals to each finger. The Higher Control Level implements all computation for the hand and provides basic client interface for External Command Level, such as PC and data glove. The control cycle for the hand is 200μs.

Envelope Design of the Hand

Hand envelop design is very important for the appearance and protection and also for optimal grasping of the hand. In the DLR/HIT Hand-I, we implemented a nice cover for the hand with extra plastic parts, and thus considerably increased its size. In Hand II, the fingers are directly designed in a human-like fashion (Fig. 83).

Fig. 83 From artist design to the real hand

2.3 JUSTIN and Rollin' JUSTIN

As a first step towards a robonaut system, the institute aimed at building a humanoid service robot capable of sensor based manipulation tasks. As a platform for bimanual grasping and environment interaction, the service manipulator JUSTIN was built. JUSTIN is based on the modular 7-DoF DLR Light-Weight Robot III (LWR-III) and the four-fingered DLR Hand-II. It is designed as a versatile platform for research on two-handed manipulation and service robotics in everyday human environments. This work extends the manipulation capabilities demonstrated with the Robutler system presented in the previous reporting period.

Fig. 84 DLR's humanoid upper body system: JUSTIN

2.3.1 Mechanical Design

The main design goal was to combine two arms to manipulate objects with two hands. Due to the modular design of the LWR as well as of Hand-II, it was immediately possible to set up both a left-hand and right-hand configuration. The robots' common base holds the arms mounted 60 degrees from the vertical in a sideways direction. This allows the elbow to travel fore and aft below the shoulder and up to horizontal height without passing through singularities.

To extend the manipulation range, the robot base is held by a four degree-of-freedom torso.

A vertical roll axis, followed by two pitch joints and a third, passive pitch axis which keeps the arm base upright, allows movements to the side, in vertical and horizontal directions. Through this configuration "JUSTIN" is capable of lifting objects from the floor, reaching over normally deep tables and even reaching objects on a shelf of about two metres height

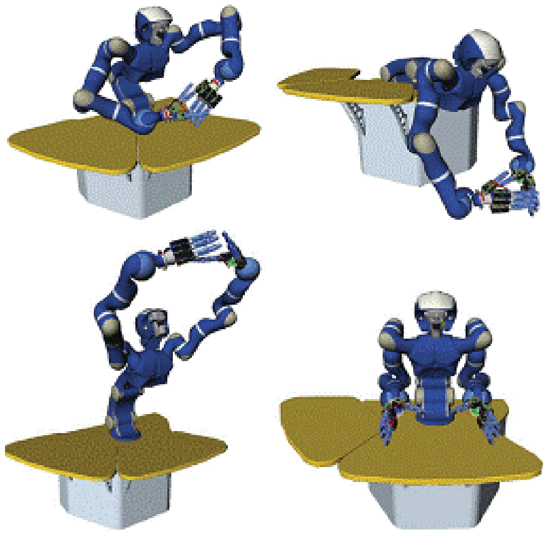

Fig. 85 Workspace design for the humanoid JUSTIN

To maintain the DLR robot philosophy, the torso joints consist of the same functional components as the arm joints, allowing full torque control for the setup. "JUSTIN" can detect and react to contact forces applied anywhere on its structure.

To gain further sensor information about the environment, the institute's 3D-Modeller was integrated on a 2-DoF pan-tilt unit in order to allow for scene analysis based on stereo vision and laser range sensors.

Since it was planned from the very beginning to integrate the system on a mobile platform, it was designed to be slim enough to pass standard doorways of about 90cm width. The backward seated position allows for a lower centre of gravity. This is useful to prevent tipping over in curves despite the overall weight of approximately 45kg. Mounted on a 60cm table or platform, the torso reaches a human-like shoulder height of up to 150cm. The below table gives an overview of the 43 actuated DoF.

Subsystem	Arm	Hand	Torso	Neck	Σ
DoF	2x7	2x12	3	2	43

Fig. 86 The newly designed torso

Fig. 87 To increase the stiffness while preserving the extreme low weight of the mechanical structure foamed aluminium was used

2.3.2 Control System Design

Control of the humanoid manipulator is very challenging due to the large number of degrees of freedom and the resulting redundancy. Using joint-level control, complex planning algorithms would be needed to accomplish given tasks. For intuitive operation and hence short development times, high-level control interfaces are needed. Even more important, for many tasks it is desirable to define impedance behaviour in task space. Therefore, flexible control laws are used that implement impedances on joint level, on end-effector level, and on object level. The controllers are based on well-known compliance control laws and combine several suitable potential functions.

Fig. 88 JUSTIN balancing soccer balls

The performance of the controllers is demonstrated by several experiments:

- *Gravity-compensated mode, showing coupling stiffness between the arms, which can be moved freely in space.* Three soccer balls are manipulated in Fig. 88 using a coupling between the two arms which squeezes the small ball while the hands are power-grasping the large balls in joint impedance control.
- *Emptying of a trash bin.* A trash bin is picked up with both hands, moved around the workspace, and emptied. A compatible combination of coupling stiffness and world stiffness for the arms is selected. Human interaction during task execution is presented as well.
- *Unscrewing of a can.* The vision system locates the can which is then opened using both hands. For the unscrewing of the can, an object-level control law is employed that maps onto the hands as well as onto the arms.
- *Motion of a box and human interaction.* The pose of the box is commanded on object level. Note that the control law maps onto the whole kinematic struc-

ture, including fingers, arms, and torso, to hold the box.

In order to ensure safe physical human-robot interaction the disturbance observer (see Sec III.3.1.1) has been integrated. It is based only on the capabilities of the two-arm system and provides a filtered version of the external torque. The torque estimation is used to scale time increments in the trajectory generation and allows the user to push the robot intuitively back and forth along its desired trajectory.

This work has been distinguished with the Best Video Award at the IEEE International Conference on Robotics and Automation in Rome, 2007.

2.3.3 Mobile Base

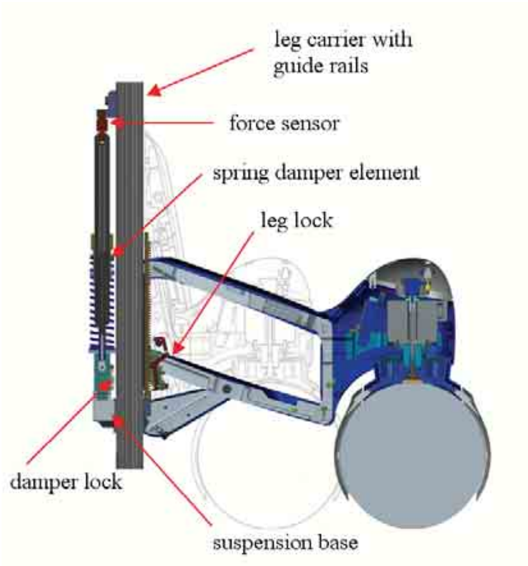

Fig. 89 Wheel design for variable footprint

Service robots supporting humans at home or on planetary surfaces need mobility. The mobile platform enables the system to interact with humans, e.g. in carrying objects, and brings the development towards a universal service robotics platform.

An extendable robot base is required in order to take advantage of the large workspace and the dynamics of the upper body, while providing the stability of the overall system. In contrast for a reliable and easy navigation, compact dimensions are necessary. To meet both requirements, our mobile platform has four legs which can be individually extended via a parallelogram mechanism. Each leg carries an endlessly rotating wheel for omnidirectional movement.

Furthermore, each leg incorporates a lockable spring damper system. This enables the whole system to move over small obstacles or to cope with the unevenness of the floor, as well as to sustain reaction forces under heavy load. By itself, the mobile platform has a weight of 120kg. Mounted on the mobile platform, Rollin' JUSTIN has a shoulder height of up to 1.6m. The whole system is powered by a Lithium-Polymer battery block and has an operating time of about 3h.

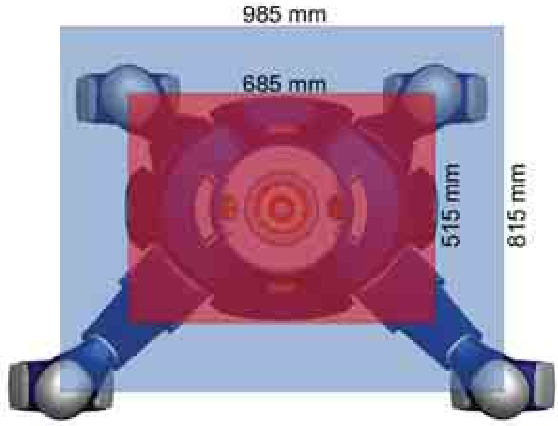

Fig. 90 Variable footprint of Rollin' JUSTIN's mobile base

2.3.4 System Architecture

An important design guideline for building the platform was a compact construction and the use of off-the-shelf components. Therefore the components were chosen upon their size and suitability for the functional needs, but not on the homogeneity of bus and communication protocols. This requires the communication concept to cope with several different real-time protocols and bus systems.

The hub motor wheels communicate via CAN 2.0B at a command rate of 16ms. The digital servo drivers (Whistle) for the steering motors use CANopen (4ms). The absolute encoders for the steering angle and the leg extension deliver their values via an SSI connection and the values from the force sensors have to be read by an analogue-digital-converter. The position of the servo drives for the locking functions in the wheel suspensions can be commanded by a digital output signal. Arms, torso and head of JUSTIN use the real-time bus SERCOS and the hands use HIC (Heterogeneous Interconnect, IEEE 1355). The whole upper body system has a control loop rate of 1kHz.

Similar to the JUSTIN control concept, all the sensor data should be available in hard real-time on a single PC, such that the robot can be used within a Simulink environment as hardware in the loop system. Normally this would require a lot of driver programming, several PCI slots and cards for the different bus systems and a lot of CPU power consumed by data acquisition, which makes the design of the control system difficult and error-prone.

Fig. 91 The mobile manipulator Rollin' JUSTIN as presented at the 2008 AUTOMATICA fair

For Rollin' JUSTIN, a commercially available PLC communication concept from Beckhoff is used. A single PC is dedicated as data collector platform which retrieves the data from the CAN 2.0b, the OpenCAN, the analogue, the SSI and the SERCOS PLC components and transfers them in real-time to an EtherCAT bus. The data collector acts as EtherCAT Master. All the timing constraints and data conversions are configured using the standard software TwinCAT from Beckhoff. On the dedicated control PC for the platform and torso control only an EtherCAT Slave PCI card is present, providing all sensor data of the entire system via mapped memory. Therefore the communication overhead on the real-time control PC is small and there is only one fairly simple driver for the EtherCAT slave which has to be programmed. On the data collector PC however, the communication overhead is quite high, but there an industry approved system is used. No driver has to be programmed. Only PLC components to start and stop the communication system have to be configured, which is also sometimes a challenge, but less labour-intensive than programming the protocol drivers itself. Fig. 92 shows an overview of the real-time communication concept of Rollin' JUSTIN.

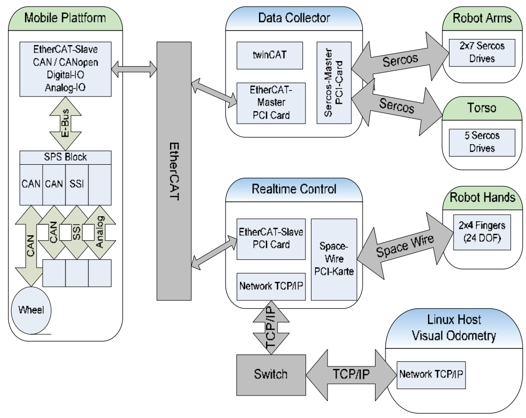

Fig. 92 Real-time communication concept of Rollin' JUSTIN

Besides the real-time part there are also components that do not need to communicate in real-time. Video cameras, PMD cameras, inclination sensor and status display are connected to the standard I/O interfaces (Ethernet, USB, IEEE 1394) of the Linux computer. The Linux PC is also the gateway to the control hosts outside the platform attached via WLAN interface.

This way the platform has all components on board, to perform autonomous mobile manipulation tasks.

2.4 Hand-Arm Systems for Future Service Robotics

After more than a decade of service robotics research, the results of the community regarding major challenges such as grasping, manipulation, and mobility still are not really satisfying and seem to stagnate. In our observation, this is related to major shortfalls in the tool chain and especially the hardware. Since robotic systems get increasingly complex, the danger of damage increases. A single collision during operation may cost huge amounts of money and time. Therefore application developers have to be very conservative when testing new methods and strategies. This slows down progress dramatically und hardly gives a chance to develop radically different control/motion planning strategies.

What's more, the dynamical properties of actuators are not sufficient for several human tasks. Particularly in cyclic tasks (e.g., running) or highly dynamic tasks (throwing), the actuators cannot provide the required energy during peak loads without getting to bulky and heavy.

Therefore we are convinced that major steps in space and service robotics are only possible if future robotic systems have two major characteristics: (1) They have to be robust against "every-day" impacts, and (2) they have to be able to store energy short-term.

This can be achieved by introducing variable passive compliance into future robotic systems. For this reason, we realise a highly anthropomorphic hand-arm system using these promising approaches.

2.4.1 DLR's Anthropomorphic Hand-Arm System

The coming DLR Hand-Arm System is a robotic system mimicking the kinematic, dynamic and force properties of the human arm using modern mechatronic technologies. What's more, it should allow us to make a next major step towards autonomy in service robotics. It is based on a variable stiffness drive concept with joint structures as close to the biological counterpart as possible.

The system (Fig. 93) is designed as a fully integrated hand- arm system that no longer allows the isolated use of the hand or arm, as was the case with the previous modular hands.

Nevertheless it still can be logically divided into a forearm and hand, including the wrist, on one side, and the arm consisting of a 3-DoF shoulder and a 2-DoF elbow, on the other. The requirements of the hand and arm are quite different. For example, vibration damping is of no relevance for the fingers (finger dynamics are negligible in relation to the applied forces), whereas a good vibration damping performance of the arm, especially in the shoulder, is crucial for the whole hand-arm system. Therefore the design aspects must be separately analysed for both systems.

Fig. 93 Rendering of DLR's Hand-Arm System

2.4.2 Anthropomorphic Hand

In the design of an anthropomorphic hand, our goal is to closely copy the properties of the human hand rather than its intrinsic structure. The solutions found in biology must be transferred to technical components and evaluated before they can actually be used.

Anatomy of the Human Hand

The human hand consists of a palm with metacarpal bones and finger bones. The index, middle and ring finger are similar in their structure and configuration, whereas the thumb and little finger differ considerably; the latter has a bone structure similar to the middle fingers, but its tendons, ligaments and muscles resemble those of the thumb. Furthermore, a thorough understanding of the hand's joints is imperative for realising an anthropomorphic hand, since joints found in biology are radically different from technical joints.

The human hand mainly uses three kinds of joints, which can be divided into 1-DoF and 2-DoF joints. The 1-DoF joints in the hand all are hinge joints; 2-DoF joints can be divided into two types. The metacarpal (second down) joint of the thumb is a saddle joint but with non-orthonormal axes and has been described geometrically by Kuczynski by the saddle of a scoliotic horse. In contrast, the metacarpal (3^{rd} down) joints of the fingers are condyloid. The main difference between saddle and condyloid joints is that condyloid joints have (roughly) intersecting axes, which saddle joints do not have. For the thumb, the axes of the metacarpal are non-orthogonal screws (Fig. 94).

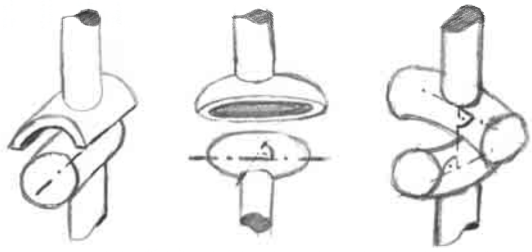

Fig. 94 Joint types of the human hand: hinge, condyloid, and saddle joint

The thumb can be assumed to be the most important part of the human hand. This is most obvious in hand surgery: a lost finger can be coped with, but a lost thumb is generally solved by pollicisation (replacement of a missing thumb by finger or toe) of, e.g., the index finger or a toe.

Since the coupling of the bones in the human hand is not stiff, compliant motion in almost every direction is possible. Subsequently, there are several opinions how many degrees of freedom the metacarpal and thus the first interphalangeal joint of the thumb has. Kapandji hypothesises two degrees of freedom in the metacarpal and 2 in the first interphalangeal joint, while Benninghoff suggests three DoF in the metacarpal and one in the first interphalangeal joint. Following Kapandji, we consider the metacarpal of the thumb is a 2-DoF saddle joint. The interphalangeal joints of the thumb are similar to those of the fingers. Kapandji proposes that the fifth DoF of the thumb is located in the proximal interphalangeal joint as a limited range DoF along the longitudinal axis of the medial phalanx. One hint to prove this is that the proximal interphalangeal joint of the thumb is not a hinge joint but a condyloid joint. Based on the experiences from pollicisation, this degree of freedom can be assumed less important; after all, near-perfect hand functionality can be regained by replanting the index finger as a thumb.

Putting it Together: The Design of DLR's Anthropomorphic Hand

The condyloid joints of the human fingers imply an additional movement of the finger in the longitudinal direction, since the ellipsoidal contact surfaces cannot be generated using a 2-DoF motion and a common geriatrix. First, this leads to complications calculating the inverse kinematics of the finger. Furthermore, extended wear is to be expected at the contact surfaces. For these reasons, hyperboloid joints are more applicable. Simulations showed that the use of non-intersecting axes of hyperboloid joints reduces the functionality of the hand only marginally, if the main axis of the finger (flexion/extension) is distal to the secondary axis of the finger (adduction/abduction) (Fig. 95).

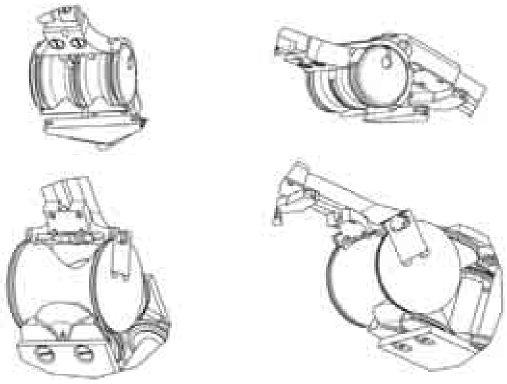

Fig. 95 Biologically inspired overload-proof joints

Fig. 96 First finger prototype on testbed

The structure of the finger is designed as an endoskeleton with bionic joints. The metacarpal joint is designed as a hyperboloidally shaped saddle joint, whereas the interphalangeal finger joints are designed as hinge joints. The proximal interphalangeal joint of the thumb is, in contrast to biology, also designed as a hinge joint. This circumvents the negative side effects of technical condyloid joints, while leaving out the thumb's fifth degree of freedom is not problematic. The kinematics of the new hand is closely adapted to the human hand. So every finger differs in "bone"-length, size and kinematics. For example, the fifth finger PIP joint has to have an inclination of about 15° to enable opposition to the thumb, while the index and middle finger only have minimal inclination. All joints enable dislocation of the “bones” without damage in case of overload, using the elasticity in the drive train.

In addition to the known assets, such as robustness and short-term energy storage, the use of antagonistic actuation enables us to cope with geometric inaccuracy which is one of the major problems of known tendon-driven mechanisms. In contrast to standard tendon routed systems with inherent constant tendon length, unaligned pulley-axes and other geometrical errors do not overstretch or slacken the tendons, since these are inaccuracies compensated by the elastic elements in the drive train. Therefore no tendon tensioner is needed.

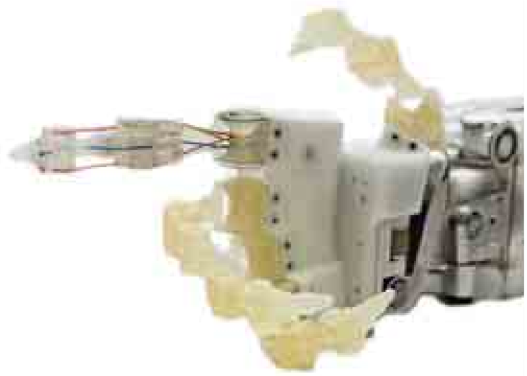

Fig. 97 Prototype of hand with final index finger design

A fully functional version of the finger, using alloy structure and steel cables, has been attached to an antagonistic drive unit (8 motors). This enabled the development of control strategies and to test mechanical parameters of the system such as maximum forces, friction in joints and tendon guides, accuracy, and wear (Fig. 96). Based on the results of these tests, a second version of the index finger was designed (Fig. 97). Based on this design, the middle, ring and 5th finger has been designed differing in size, angle of axes (inclination), strength, and even number of DoF. The design of the index finger also has been partly used for the thumb to keep machining and cost effort as low as possible. The design of all fingers is now finished, and the mechanical parts of the fingers are being machined (Fig. 98) [Grebenstein & Smagt van der 2008[j]].

Fig. 98 Final hand design virtually grasping a 0.5l glass

Wrist and Forearm of DLR’s Hand-Arm-System

Wrist

To reduce friction by keeping the angle of tendon deflection minimal, as well as to downsize coupling between wrist and finger motion, a 4-bar mechanism wrist, forming a 3-D anti-parallelogram, has been developed (Fig. 99). It enables routing the tendons as close to the neutral position as possible and in addition centres and therefore stabilises the wrist if maximum tension (totalling >6kN) is erroneously applied to the tendons. The wrist is actuated by 4 mini servo units located between the elbow and forearm base frames.

Forearm

Since the hand itself has no drives or electronics, these have to be integrated into the forearm. To realise antagonistic drives for the total of 19 DoF (4 DoF thumb, index, middle finger, 3 DoF ring finger, and 4 DoF little finger), 38 actuators, 38 elastic elements and 76 position sensors have to be located in the forearm. These actuators are realised as mini servo units consisting of motor (DLR's ILM25), gear, and nonlinear elastic element. All required sensors and electronics are integrated into the “mini servo unit”. A high-resolution angular rotor position sensor has been realised as well as an angular MR sensor to measure the deflection of the elastic elements lever. These sensors as well as the drive unit itself can be addressed directly via BISS sensor-/actuator interface (unified sensor/actuator bus with very small footprint). This allows reducing the number of communication protocols and thus the needed design space to a minimum.

Fig. 99 Wrist integrated in forearm prototype

The "mini servos" are integrated into two base frames which are connected at the base of the wrist and can be separated for easy maintenance of tendons, springs, etc. They also hold the water-based cooling channels to keep the system thermally stable, even during operations which require high strength for a prolonged period (Fig. 100).

Fig. 100 Inside view of forearm prototype with opened base frames

All 19 "mini servos" are connected via BISS to a set of PCBs forming the digital and communication electronics on the outside of the base frames. These also hold the FPGAs running the position controllers for the mini servos and the calculation of couplings. As in DLR's medical Robot MIRO, the high-level communication is realised using an up to 1Gb/s SpaceWire bus, connecting the two halves of the forearm, the elbow and shoulder modules, and the real-time controller.

Shoulder and Elbow

Similar to the hand of the new Hand-Arm System, the arm (consisting of a 3-DoF shoulder and a 2-DoF elbow) is as close to the human archetype as possible in terms of kinematics, dynamics, and force. Again the target must be not to copy nature, but rather to understand the principles and transfer them to a technical system.

Since the arm requirements are rather different from the hand requirements, different actuation principles were investigated and will be integrated. The arm has to carry much higher loads than the fingers: the actuators have to apply the necessary force to counter gravity for the whole arm, which is negligible for the fingers. Furthermore, angular accuracy is much more important, and the dynamics within the system are not negligible, so vibration damping performance is essential for proper functioning of the whole hand-arm system.

Fig. 101 Quasi-antagonistic joint prototype

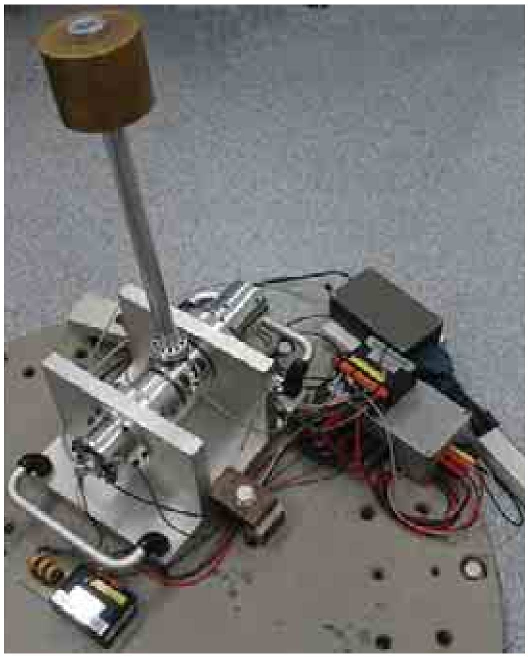

Fig. 102 Variable stiffness actuator prototype

To ensure the capability of the arm to perform human tasks in every position within the workspace, ergonomics data for every joint of the human arm were analysed.

From this, the final dimensioning of the drives has been derived [Panzer *et al.* 2008[c]].

Of course the actuation of the arm has to be capable of storing short-term energy. Furthermore, the energy consumption of the system has to be minimised, thus leading to an approach which does not favour antagonism. We investigated two different types of variable stiffness actuators (see Sec. III.3.3) to find the most suitable approach and verify its controllability (Fig. 101, Fig. 102). The design of the final arm joints is currently under development.

2.5 Biomechatronic Systems

In the development of robotic systems, inspiration on biological examples is an important instrument. In the development of the Institute's robotic systems (arms, hands, upper body, …) such "inspirations" are clear: they are based on specific parts of the human body. In the last few years this cross-fertilisation was extended, investigating biological systems and using these findings in robotic and technical environments. In this section, the most prominent examples are explained.

2.5.1 Artificial Skin

Touch and haptic sensory inputs are crucial and fundamental to the sensorimotor tasks in our everyday behaviour. These noisy, high-resolution local sensing systems allow us to grasp, handle, and identify even the smallest objects in our hands. Robotic hands, on the other hand, depend on high-precision, low-dimensional sensory signals, e.g., indicating a single force vector per finger tip. Such signals do not suffice for fine manipulation to, e.g., light a match or unbutton a shirt.

A detailed study of the properties of the human skin lays a path for artificial touch sensor development. A human index finger tip had a two-point discrimination threshold of less than 2mm; a corresponding robotic finger tip would require 100 to 200 taxels (tactile elements; i.e., the sensor elements) with 3-D continuous values, or around 400 per finger. Such data amounts cannot be easily transported from the finger to the processing unit. The Institute therefore develops a new generation of tactile sensors.

Sensor Principle

The foremost goal is to obtain a sensor with sensitivity near to that of the human skin, while reducing the number of wires coming out of the skin. In a first solution, we developed piezoresistive material, consisting of an elastomeric nonconductive matrix material and a electrically conductive filler (e.g., carbon black). Conductivity of the compound material results from the filler particles forming conductive pathways. Applying pressure to this material has the same effect as increasing the content of filler particles: the electrical resistance decreases.

Sensor Layout

For the first sensor prototypes injection moulded the material around metal wires. These wires form a matrix, while the wires do not physically touch (Fig. 103).

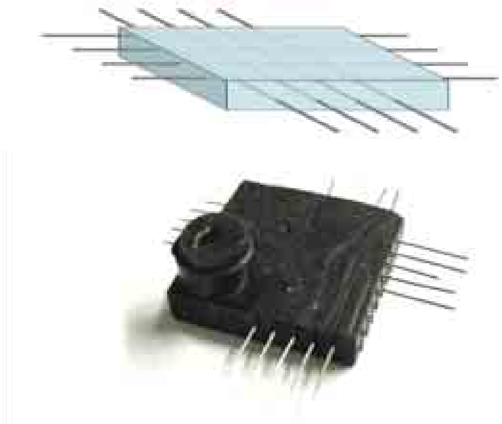

Fig. 103 (top) Sensor layout (bottom) Sample patch

The number of crossing points increases quadratically with the number of wires used. Pressure on the "skin" is measured through the resistances between wire pairs. Thus, with a relatively low number of wires we achieve a high number of read-out points [Smagt van der 2007[p]].

In the manufactured patches, a granulated polymer filled with carbon black was used for injection moulding (Fig. 103). The manufactured samples are 2.5 millimetres thick with a side length of 11mm. Five wires were embedded in two orthogonal layers, resulting in ten wires in total and 25 taxels.

Results

The manufactured prototype patches clearly show a piezoresistive effect. But tests of the patches on the testbed also showed an unexpected behaviour: If the indentation speed is faster than 500µm/s, the measured voltage shows an unexpected dip (Fig. 104).

To explain this behaviour, the patches were examined using scanning electron microscopy (SEM). This revealed the most likely reason for the observed phenomena: The unsatisfying adhesion between the SEBS matrix and the cast-in steel wires. SEM of the cast-in and pulled out steel wires shows that no matrix material at all adhered to the metal wires (see Fig. 105).

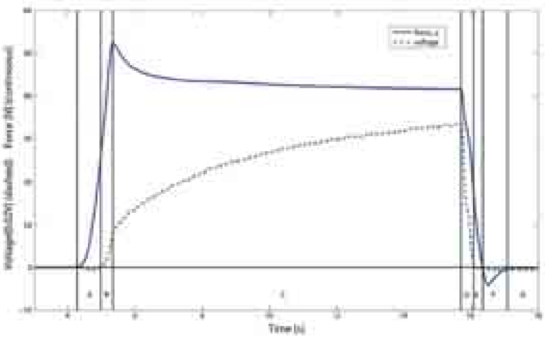

Fig. 104 Piezoresistive behaviour. A fast increase of the applied force (blue solid) leads to an initial increase of resistance (dotted green), followed by a slow decrease of sensor resistance.

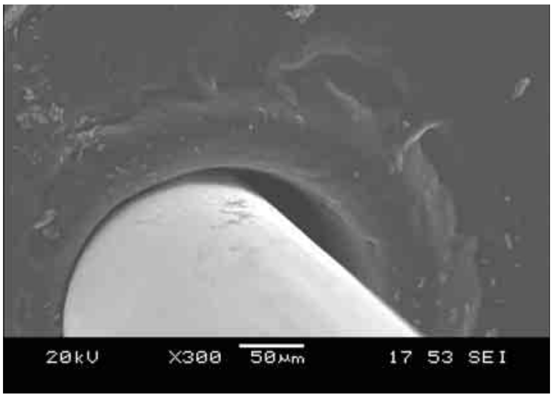

Fig. 105 SEM image of a metal wire in the filled polymer (magnification factor 300)

In a follow-up approach, flexible wires composed of highly conductive elastomers form the basis for a sensor setup. If two elastic wires of cylindrical shape are crossed, a sensitive area (taxel) is formed at each crossing point. Mechanical load presses the wires against each other, increasing the contact surface between the wires and thus decreasing transition resistance. With this approach the disadvantages of the previous sensor setup can be avoided. The proposed sensor setup no longer relies on the piezoresistive effects within the conductive elastomer; rather, it is based on the change of the transition resistance between two wires at the crossing points [Smagt van der 2008[P]].

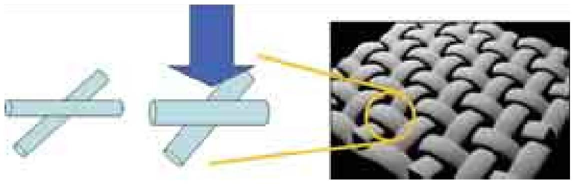

Fig. 106 Woven-type sensor, consisting of wires of flexible, conductive material

Applying standard textile production techniques, the wires can be woven to form a sensitive tissue. This enables the production of literally tailored tactile sensors at low cost. Large sensitive surfaces providing variable spatial resolution can be realised.

2.5.2 Micro Movements

Movements in humans consist of successive micro movements. Such movements (also known as submovements) were first detected in the context of small correcting movements, and are executed at a rate of just below 10Hz. Micro movements are coded in the brain, although the exact location (motor cortex, premotor cortex or (more likely) cerebellum) is yet unknown. Related timing and muscle control is done by the cerebellum.

There have been preliminary simulations which proved the principal functional efficiency of the micro movement approach, for a hand-chosen micro movement set, as well as a (larger than necessary) random micro movement set.

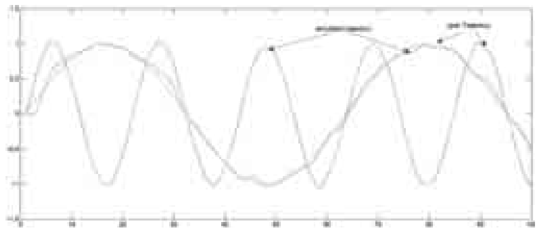

Fig. 107 A 2-D robot following a trajectory defined by the joint angles. The trajectory lasted for 10 seconds (100·0.1s). The set contained 20 random Micro Movements.

Building on these results, methods for learning the forward model—predicting the outcome of a single micro movement—have been investigated. Among others, the most important methods were an enhanced Growing Neural Gas algorithm, and the LWPR, a very sophisticated radial basis function network including a dimensionality reduction, and local linear model fitting. However, learning the forward dynamics and kinematics of a robot was unsatisfactory for all but the simplest robots, due to the highly coupled nonlinear dynamics. The nature of the micro movements, being very tiny parts of a movement, required detailed forward models, which are not always available; also, they then provide little advantage w.r.t. classical methods using the Jacobian.

2.5.3 EMG

The capturing of poses and forces of the human hand via surface EMG electrodes positioned at the lower arm enables the capturing of fine manipulation tasks without the use of inconvenient force sensors directly at the fingers, hindering the movement and falsifying the haptic feedback. We have studied lower arm EMG for a prolonged period and have managed to present unequalled results. Based on learning approaches (SVM, LWPR, feed-forward networks), our methods are able to classify 11 different finger movements (flexion and extension of all fingers separately, plus abduction/adduction) as well as the exerted finger force.

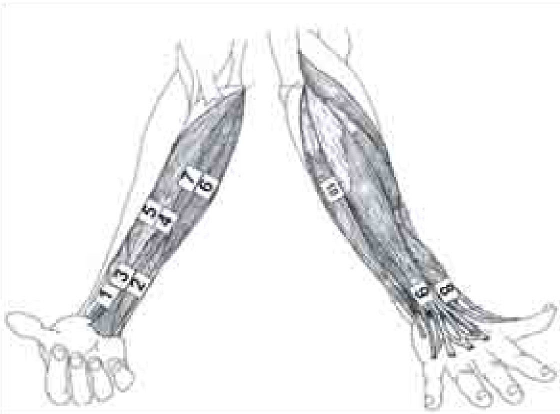

Fig. 108 Placement of the 10 electrodes on the healthy lower arm

In a first study, we investigated the relationship between lower arm surface EMG patterns and the corresponding finger movement (extension and flexion of all fingers separately, as well as finger abduction/adduction) [Bitzer & Smagt van der 2006[c]; Maier & Smagt van der 2008[c]].

EMG signals are recorded using ten commercial Otto Bock active double differential electrodes, each amplifying the signal by a factor 4,000 and rectifying it. Correct positioning of the EMG electrodes on the lower arm is key for successful distinction of the different finger movements. Since the extension and flexion muscles are located in the human lower arm, placement on the lower arm is essential (Fig. 108). Classification of EMG signals to finger movements is done with Support Vector Machines (SVM) using a Gaussian rbf kernel.

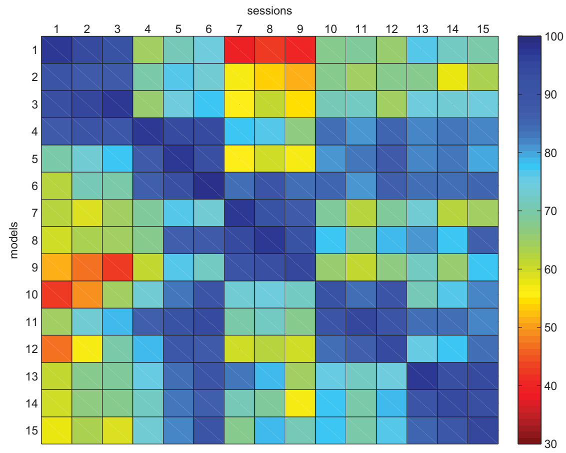

Fig. 109 EMG Classification results. Values on the diagonal indicate classification directly after learning; off-diagonal results are obtained after removing and replacing the EMG electrodes without relearning

Classification results are depicted in Fig. 109. For these results, flexion and extension of the thumb, index finger, middle finger and ring finger are investigated, plus combined finger movements; these are the major candidates for most grasps. In a session in which the classification capabilities are tested directly after a training session, accuracy of 95.37% ± 2.85% is obtained. When the electrodes are removed and put back, we obtain 74.38% ± 12.27%.

Driven by this success, in a second study the relationship between EMG signal and finger flexion force was investigated, thus allowing a patient to control grasp strength.

The nature of the data again made us revert to learning approaches. In this particular case, we experimented with three approaches: (a) a simple feed-forward neural network with one hidden layer, (b) a support vector machine with radial basis function kernel, and (c) locally weighted projection regression. Our analysis consists of a preliminary phase in which several models have been built in a batch fashion, in order to understand how to deal with the non-stationarity of EMG. To deal with this problem while keeping the number of samples down, we devised a method called Online Uniformisation (OU).

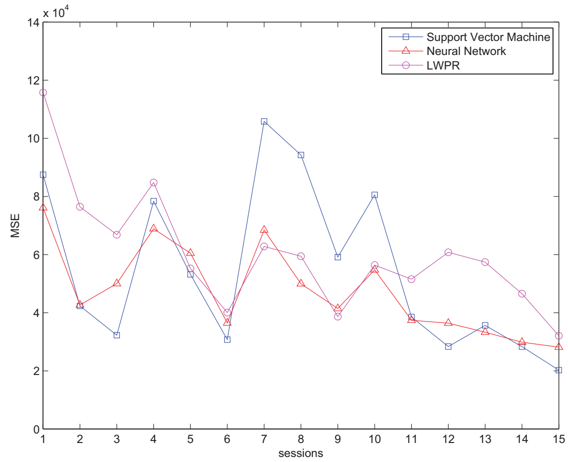

Fig. 110 RMS error of predicting the grasp force from EMG data

OU is based upon the simple idea of keeping a minimum inter-sample Euclidean distance, in order to uniformly sample the input space. The selected samples are then used to periodically re-train the system. Using this approach, the applied force can be predicted with an average percentage error of 7.89% ± 0.09%, meaning 4.5N over a range of about 57N (Fig. 110). Fig. 111 shows an example of predicting the grasp force of a single finger from EMG data [Castellini *et al.* 2008[c]; Castellini & Smagt van der, 2008[j]].

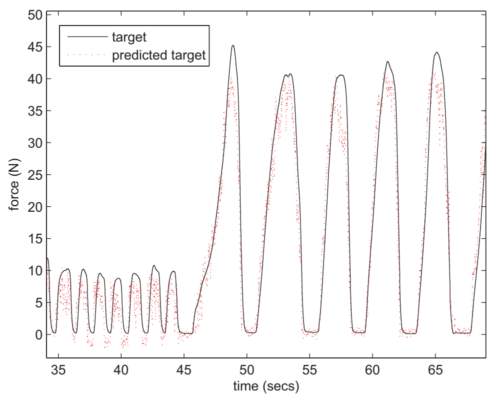

Fig. 111 Human grasp force measured by a hand-held force sensor (solid black) and predicted by lower arm EMG (dotted red)

These approaches are currently being investigated in clinical trials. First results show that, despite reduced musculature, similar accuracies are obtained with hand amputees.

2.5.4 Human Catching

In order to allow a better interpretation of the results with the DLR robot catcher (see Sec. III.6.3), we investigated human ball catching strategies. Although many of such experiments have been done in 1 and 2-dimensional settings, 3-D catching has been ignored in the literature to date. The most prominent results are from Flash and Hogan in 1985, setting up the minimum jerk law: human arm movement follows a trajectory in which the acceleration of the wrist changes as little as possible, thus saving energy. With this approximate model, a complete trajectory can be computed from fixed start and end conditions.

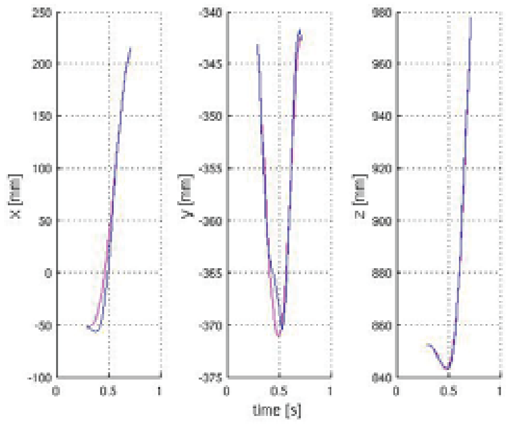

Fig. 112 Movement of the hand over time in x, y and z (blue) compared to trajectories generated with minimum jerk (magenta)

To investigate fast human reaching movements in 3D, ball catching experiments were executed. Eleven right-handed persons were tracked while catching a tennis ball. Three optical tracking cameras were used to track markers at the human hand, elbow and shoulder, recognising the marker's position and orientation. To ensure equal trajectories of the ball a catapult was used to throw the ball from three different positions, approximately 4m in front of the catcher. The catcher was instructed to catch with the right hand only and to place his hand at the same place before every throw. In a second experiment, eye trackers were used to investigate the catching strategy and balls were air-perturbed with help of a compressor.

Results show that the tangential velocity profile of the hand is bell-shaped and that the hand movements coincide with the well known results for 2-D point to point movements and 2-D catching experiments like minimum jerk theory or the 2/3 power law. Furthermore the two phases of fast reaching and slower fine movements at the end of the placement can clearly be seen. Besides it seems that the catcher's gaze follows the ball throw the whole flight, but predicts its trajectory as the same time (catchers were very confused about the perturbed balls).

In most cases, the trajectory of the hand closely followed a minimum jerk trajectory (Fig. 112); in some cases, the trajectory could be closely modelled by a sequence of minimum jerks: apparently, a (visual) sensory signal instigated a recomputation of the trajectory, leading to a change in motion.

2.5.5 Human Hand Kinematics

The human hand, in combination with the arm, is one of the most intricate biomechanical structures, in which evolutionary optimality can clearly be distinguished. Optimised for both power and precision grasp, its structure with a thumb opposing four fingers is perfectly suited to solve every kind of daily task, be it precise grasping and handling or heavy duty lifting and grasping. Various important factors of the hand allow for this unmatched diversity in tasks. Not taking the sensing aspect into account, these include

- the dexterity of the thumb, having 4 or 5 degrees of freedom, allowing it to oppose any of the four fingers;
- the rotation of the finger tips of the index, middle, ring, and little fingers towards the thumb, so as to optimise opposition with the thumb.

Fig. 113 Segmenting the proximal phalanx of the little finger in Amira. (left) Automatic segmentation with manual correction in per slice; (middle) Corrected slice segmentation; (right) Segmented area mapped on the recording of the bone, resulting in an 8-bit representation of the bone

The DLR integrated hand-arm system (see Sec. III.2.4) is targeted to copy human kinematics and dynamics as closely as possible. In order to construct this system, the kinematics of the human hand must be precisely modelled. The precise number of degrees of freedom of the human thumb needs to be identified; furthermore, the exact finger movement must be quantified in order to obtain optimal opposition of the fingers of the hand. Using a very large number of 3-D MRT recordings of the human hand in vivo, we reconstruct a precise computational model of the human hand, describing its kinematic behaviour in detail. This model will be used for a simulation of human hand kinematics, as well as in the construction of the highly anthropomorphic robotic hand-arm system.

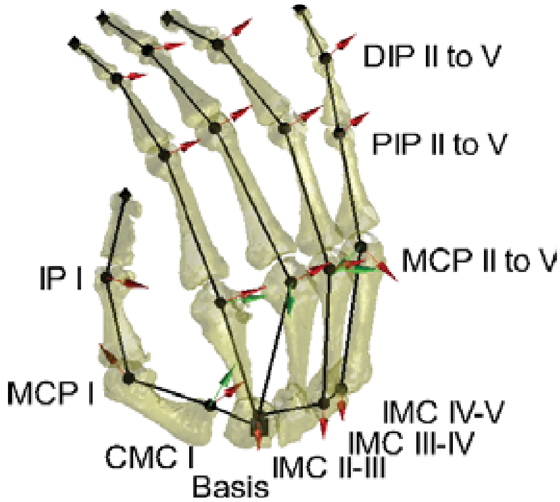

Fig. 114 The hand model

The kinematics of the hand is reconstructed from the movement of its bones, as obtained from the MR images. As a first step, we needed to know the position and orientation of each bone in each image. This is done by segmenting the bone and 6-D localising it. This works by drawing point triples from two images and comparing point triples with similar edge lengths. The motion that is suitable to make most of these triangle pairs congruent is considered the best estimation for the motion of the bone from one image to the next.

Building a Model

We modelled the human hand as a set of five kinematic chains, one for each finger (Fig. 114). The metacarpo-phalangeal (MCP) joints of the fingers and the carpometacarpal (CMC) joint of the thumb are modelled as 2-DoF rotational joints with intersecting axes. The proximal (PIP) and distal interphalangeal (DIP) joints and the thumb IP joint are modelled as 1-DoF rotational joints. For each joint, three sets of parameters were to be calculated:

- the positions of the centres of rotation;
- the orientations of the axes of rotation;
- the scope of the rotation angles.

The basis for the calculation of the above parameters is the relative motion of the distal bone of a joint with respect to the proximal bone.

This approach has led to a computational model of the human hand with parametrisable joints [Smagt van der & Stillfried 2008[c]] and will be formed to a simulation and used in the DLR integrated hand-arm system.

3 Manipulation and Interaction Control

The robotic systems developed at DLR (arms, hands, and the humanoid manipulator JUSTIN) are designed for interaction with humans in unstructured environments. Typical applications are assembly processes in which a robot works in immediate vicinity of humans and possibly in direct physical co-operation with them, as, e.g., mobile service robotics in space and on earth, and medical applications. In such applications, high absolute positioning accuracy cannot be exploited due to limited accuracy of position information about the surrounding environment. At the same time, the corresponding side-effects in design, namely high stiffness and mass are clearly undesired. Therefore, for the light-weight robot concepts developed at DLR, a strong emphasis is on control laws that can provide robust performance with respect to positioning and model uncertainty, as well as active safety for the human and the robot during their interaction. The following aspects are of particular importance:

- one needs a position controller which is able to deal with the structural elasticity and to provide accurate motion that incorporates active vibration damping;
- the most important feature in the control of the DLR robots, however, is the use of the joint torque sensors for so-called soft robotics control, including compliance and force/torque control, as well as for collision and failure detection and reaction.

3.1 Motion Control

Position control for the light-weight robots has to compensate for the effects of the intrinsic structural robot elasticity (such as vibrations or the steady state position displacement) to ensure the performance of positioning and trajectory tracking. This problem exists (although in a reduced amount) also for industrial robots moving at high velocities. In the control of the DLR robots, the torque sensing in each joint plays a key role. These sensors constitute an essential feature compared to most other robots: they measure the joint vibration behind the gear-box and therefore enable an active vibration damping. The complete state is given by position and velocity (as for the second order rigid robot model), and additionally by the torque and its derivative. Although basic methods for motion control were developed in the last reporting period, new, more powerful algorithms have been developed over the last years [Ott *et al.* 2005[c], 2008[j]; Albu-Schäffer *et al.* 2007a[j], 2007b[r], 2008[j]]. Furthermore the robustness and performance has been extended to product maturity for the commercialisation of the light-weight arm in cooperation with KUKA Roboter GmbH and of the KINEMEDIC/MIRO arms with BrainLAB AG. Moreover, during performance tests at KUKA it turned out that despite of the light, elastic structure and the high payload, the robots can have motion accuracy comparable to industrial robots. In fact, in a direct comparison, the DLR-KUKA robot outperformed a standard industrial robot in three of five test categories. The aspects contributing to this performance increase are:

- new automatic algorithms for optimal parameterisation of the controller gains depending on the robot configuration and load;
- a new disturbance observer which effectively compensates friction as well as the gearbox and motor ripple. Especially in the low velocity range this is critical for precision applications. [Le-Tien *et. al*. 2008[c]] (see Sec. 3.1.1);
- the design of Multi-Input-Multi-Output (MIMO) controllers instead of the earlier decentralised controllers, in order to optimally address the elastic couplings be-

tween the joints [Le-Tien *et al.* 2007c] (see Fig. 115).

The last two methods have been first developed and tested for the KINEMEDIC/MIRO Robot and then applied to the DLR Light-Weight Robot LWR. Due to the flexible and automatic controller parameterisation, its extension and application to the whole humanoid JUSTIN was a straight-forward task.

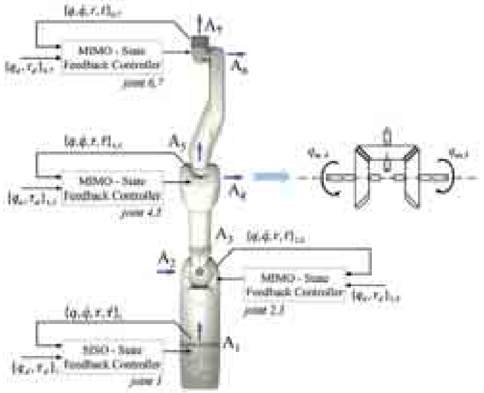

Fig. 115 Motion control structure for the coupled joints of MIRO

3.1.1 Disturbance Observers

Since the control of the DLR robots is fundamentally relying on accurate models of the robot dynamics, friction torques and external interaction torques (from humans or the environment) are a critical source of errors if not estimated correctly. Therefore, we developed a new disturbance observer concept. This allows the independent estimation of friction and external collision torques using the same observer structure by exploiting the joint torques signals τ_J (see Fig. 116).

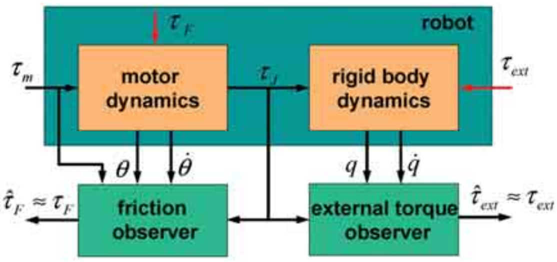

Fig. 116 Disturbance observers for identification of friction and external interaction torques

The friction observer allows for high performance motion control as mentioned in the previous section, while the external torque observer is used for safe human-robot interaction, described in section 3.4. A passivity based design ensured the direct control of the energy amount injected by the friction compensator and therefore fits into the general passivity based framework developed for the DLR robots.

3.2 Compliant Manipulation Control

Advanced manipulation skills gained recently more and more attention within the robotics community. For JUSTIN (i.e., its arms and hands), as well as for the medical robots systems we developed a set of impedance controllers which are based on a unified, passivity-based approach that accesses the joint torque interface.

Measuring the torque after the gears is essential for implementing high-performance soft-robotics features. When implementing compliant control laws, the torque signal is used both for reducing the effects of joint friction and for damping the vibrations related to the joint compliance. Motor position feedback is used to impose the desired compliant behaviour. The control framework (for both position and impedance control) is constructed from the perspective of passivity theory. It is giving a simple and intuitive physical interpretation in terms of energy shaping to the feedback of the different state vector components.

- A physical interpretation of the joint torque feedback loop is given as the shaping of the motor inertia.
- The feedback of the motor position can be regarded as shaping of the potential energy.

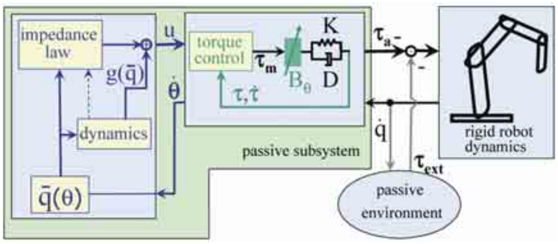

Fig. 117 Passive representation of the impedance controller

These interpretations allow a passivity representation (see Fig. 117) and thus a straightforward stability analysis and enable also a consistent generalisation to Cartesian impedance control. In this operation mode the robot is controlled to display independently adjustable compliance and damping in each translational and rotational direction in space. The basics for these new methods were developed in the last reporting period for the light-weight arms. They were now optimised, generalised, and extended to the medical robots (Fig. 118) and JUSTIN.

Fig. 118 KINEMEDIC in impedance-control mode

3.2.1 Control of the DLR Hand-II

Similar to the LWR, the DLR Hand-II is equipped with joint torque sensors in addition to joint position measurements. This enables the implementation of several impedance controllers on the DLR Hand-II. Thus, a uniform framework was created that enabled the development of control laws to coordinate finger, arm and torso motion. Furthermore, due to its flexibility, this framework served as the basis for the development of the DLR crawler [Görner *et. al,* 2008[c]].

The DLR hands are particularly designed for physical contact with different objects and, therefore, the concepts of impedance control can be fully exploited. For power (enveloping) grasps joint level impedance control is generally applied, which makes it is easy to, e.g., grasp an aerosol or to catch a ball.

In the case that the fingers have to be independently positioned, Cartesian fingertip control is applied. Typical examples are the use of a touchpad or playing the piano, (Fig. 119). In this application, impedance control is used to decrease the stiffness along the direction of contact, whereas the stiffness for the lateral positioning over the keyboard is set to high values. Fig. 119 shows the recorded piano sound amplitude over time while one note is played with increasing attack.

Fig. 119 DLR Hand-II realising dynamic attack in piano playing

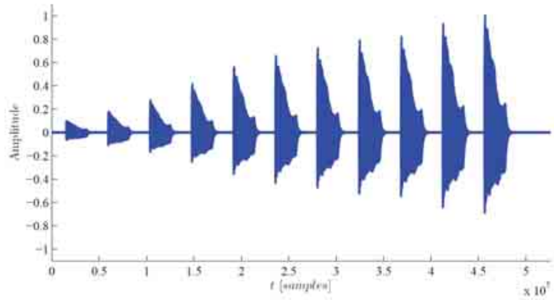

Fig. 120 DLR Hand-II realising dynamic attack in piano playing: Microphone recording

The most interesting case from a control point of view for a hand is fine manipulation of a grasped object since all degrees of freedom of the hand can contribute to its motion. In this case the combined robot hand object system represents a parallel structure (see Fig. 121).

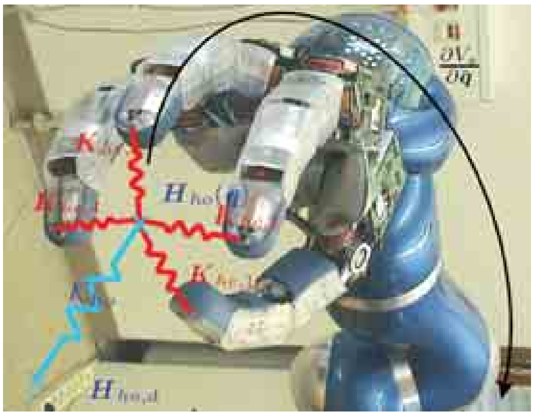

Fig. 121 DLR Hand-II is controlled by superimposing virtual spatial springs

The purpose of the developed hand controllers for fine manipulation is two-fold:

- to control the overall motion of the grasped object;
- to generate internal grasping forces.

The concepts to realise grasping forces can be divided into impedance control and force control. A force control strategy is only meaningful during stable contact, but it is not suited to handle the transition between contact and non-contact. Therefore, different impedance based grasp controllers were developed and analysed.

In [Wimböck *et al.* 2006[c], 2008a[c]] we introduced and demonstrated the performance of such passivity-based object level controllers that are based on the compliance control for a multifingered hand.

3.2.2 Impedance Control for Two-Handed Manipulation

The humanoid robot JUSTIN represents a unique platform to manipulate objects in various ways, e.g. an arm holding a large bin while one hand grasps a small object and inserts it into the bin. A natural extension of the impedance control approaches for the arms and hands allows formulating intuitive compliance behaviours also for more complex anthropomorphic manipulators like the humanoid manipulator JUSTIN.

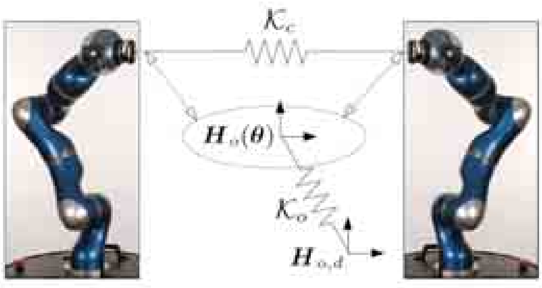

Fig. 122 Two-arm impedance behaviour by combining a coupling spring with an object level spring

Similar to multifingered hands, the compliance control of two arms has to handle the grasping forces between the arms as well as the forces which the two arms exert cooperatively on the environment, e.g. to move a grasped object [Ott *et al.* 2006a[c]]. In this case the implementation can be done by combining two spatial springs. One spatial spring defines the relative (coupling) stiffness between the arms. The second spring is attached with one end to a virtual object (which generally corresponds to the grasped object) and with the other end to a virtual equilibrium pose (see Fig. 122). In combination with the coupling stiffness, one thus can intuitively define an impedance behaviour which is useful for grasping large objects with two arms as, e.g. a large bin (Fig. 123).

Fig. 123 Moving a bin by using Cartesian compliance control

In case of a two-handed system such a compliant behaviour can easily be combined with the object level compliance controller designed for the artificial hands in a hierarchical fashion [Wimböck *et al.* 2007[c]]. Therefore, the virtual visco-elastic springs are attached now to the virtual object frames of the hands instead of attaching them directly to the end-effectors of the arms (see Fig. 124, Fig. 125).

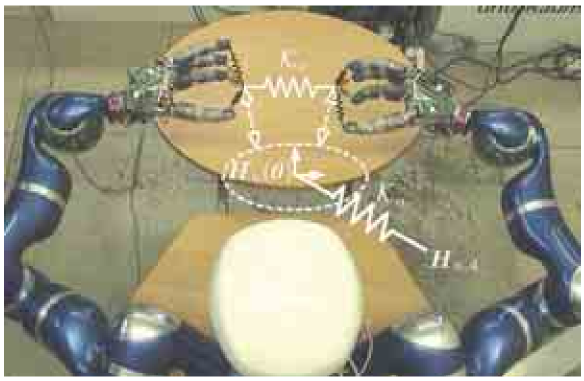

Fig. 124 Two-hand impedance behaviour by combining the object level impedances of the hands and the arms

All spatial springs generate joint torques for the arms, hands, as well as for the torso by computing the total derivative of the potential function with respect to the generalised coordinates of the complete mechanism. The presented control approach results in a passive closed loop system. Moreover, the chosen set of virtual spatial springs allows for a conceptually simple physical interpretation and consequently for an intuitive parameterisation in any higher-level planning stage. The resulting motion of the hands and fingers is very human-like, since they are based on the natural inertia properties of the robot and the intuitive elastic force fields.

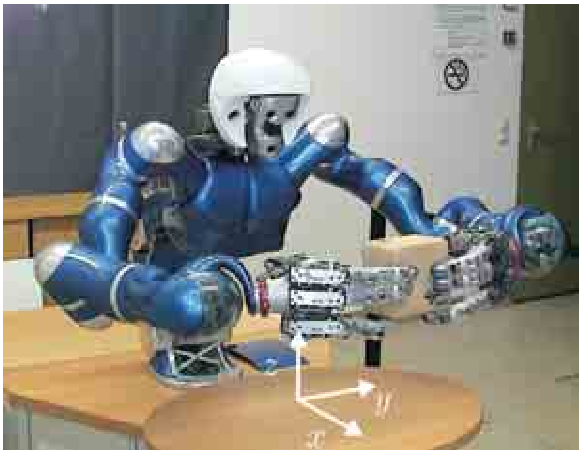

Fig. 125 Experimental verification of two-handed impedance behaviour

3.2.3 Control of a Mobile Base with Variable Footprint

The mobile platform of JUSTIN is designed to provide full planar mobility to the robot so as to allow the execution of complex dual handed manipulation tasks with increased (possibly infinite) workspace capabilities, (Fig. 126). The platform is equipped with four independent centred steering wheels that ensure, through suitable coordination, the possibility to realise arbitrary linear/angular velocities (omnidirectionality). In addition, the "legs" connecting each wheel to the central body are free to extend/retract in the horizontal direction without affecting the platform height. No special motor is dedicated to the leg actuation: each wheel, by rolling on the ground, is responsible for producing the force needed to extend the leg along its sliding direction, and to move the platform at the same time. This completely new kinematic structure requires special control algorithms in order to allow a coordinated motion. With fixed leg lengths, the wheels have to be oriented such that all axes intersect in one point, the so called Instantaneous Centre of Rotation (ICR), see Fig. 126, otherwise the wheels would block each other. For the extendable leg case, the coordination constraints are even more complex and necessitate the development of a new control approach [Robuffo-Giordano *et. al*, 2008c]. Given desired trajectories (translations and rotations) of the basis, a control law on acceleration level is computed and then integrated to desired rolling and steering velocities of the wheels. The acceleration level approach is required since the system is omnidirectional but non-holonomic, i.e., the platform can move in any direction, but not instantaneously (it possibly has to rotate the wheels in place before).

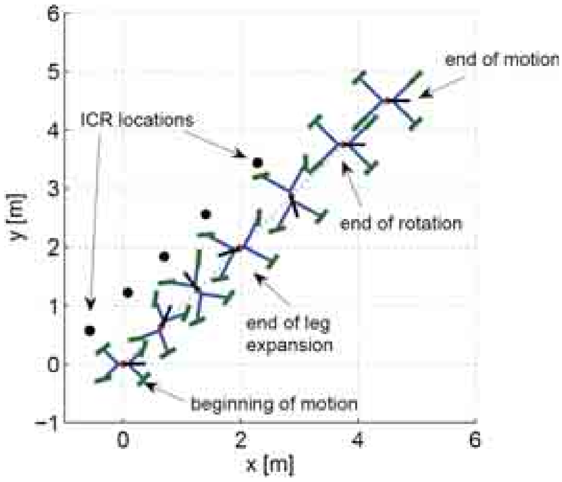

Fig. 126 Synchronised wheel motion for platform translation, rotation, and leg extension

Using the abovementioned Cartesian platform velocity interface, the Cartesian compliance controllers of the upper body were extended to incorporate also the platform. Therefore, a virtual admittance was introduced between the torso and the mobile base (see Fig. 127). The forces that appear at the upper body are mapped to the base of the torso and act as inputs to the admittance controller (which represents a virtual mass and damper). The controller generates a corresponding velocity signal which in turn is sent to the mobile platform. This way, when pushing and pulling JUSTIN, the platform will follow. This enables several applications such as, e.g. intuitive teaching of positions, cooperatively carrying bulky objects, or even dancing as an entertainment feature.

The methods for compliance control were also transferred to the medical scenario of MIRO (Fig. 128) and are currently in development for the parallel structure robot implementing a heart-beat simulator for minimal invasive surgery (see Sec. VII.4.1).

The work on compliant control of the DLR arms received numerous awards, such as at-Automatisierungstechnik, Best Paper Award 2005, DLR Research Award 2007, Industrial Robot Journal Outstanding Paper Award 2008.

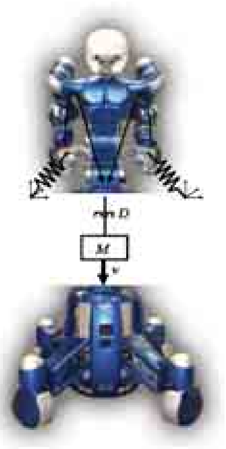

Fig. 127 Coordinated compliance control from the hand to the mobile base involving 51 controlled DoF

Fig. 128 Application of impedance control for the MIRO surgical system

3.3 From Actively Controlled to Passive Compliance

Based on the experience gained with the successful torque controlled robot approach, we were trying to identify also its limitations in terms of performance and control and to recognise new directions of research for further increasing the performance and safety of robots. The limitations of the compliance achievable by active control especially becomes an issue when considering the protection of the robot joint from external overload [Haddadin *et al.* 2007e[c], Haddadin *et al.* 2008[j]] or protecting the human from high velocity impacts. This is due to the limited sensor precision, model accuracy, and sampling time as well as the motor torque saturation. These threats can be diminished by deliberately introducing mechanical compliance into the joint. Furthermore, future robotic systems are supposed to execute tasks with similar speed and dexterity to humans, while current robots are still less performant than humans in terms of peak power. Therefore, the elastic element in the joint serves as an energy storage mechanism, possibly decreasing the energy consumption of the entire system during the task execution, e.g., when playing drums or during running. Furthermore, the stored energy can be used to considerably increase the link speed as exemplified in the ''Experimental Validation of Joint Robustness and Performance'' section [Wolf & Hirzinger 2008[c], Haddadin *et al.* 2008f[j]]. These considerations regarding the desired intrinsic dynamic behaviour and the control properties lead to the design of a new type of joints, namely variable compliance actuators.

3.3.1 New Hardware Design Concepts

The biologically motivated concept of antagonistic actuation can already be found in some robotic systems. In these realisations, two opposing actuators of similar size, each in combination with a series elastic element, were used (see Fig. 129a). Current work at DLR regarding robot arm joints is focused on a second option, in which one motor changes the link position and the other one the link stiffness almost independently [Albu-Schäffer *et al.* 2008[j]]. Mechanical compliance is introduced by a spring mechanism. This system leads to reduced dynamic losses and allows for stiffness adjustment independent from the link speed. Two different mechanical compliant joint principles (patents pending) are derived from the previous considerations.

The elastic mechanism of the Quasi Antagonistic Joint is derived from the antagonistic principle: Two progressive elastic elements oppose each other with a variable offset supporting the link with variable range of elastic motion (Fig. 129b).

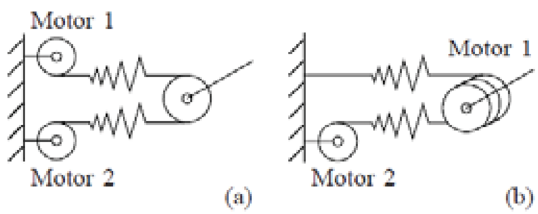

Fig. 129 Variable stiffness actuator with nonlinear progressive springs in antagonistic (a) and quasi antagonistic (b) realisation. In the later case, Motor 1 moves the joint while Motor 2 is adjusting the stiffness.

The concept of the Variable Stiffness Joint

(VS-Joint) as presented in [Wolf & Hirzinger 2008[c]] contains two motors of different size. The high power motor changes the link position. The joint stiffness is adjusted by a much smaller and lighter motor, that changes the characteristics of the supporting mechanism (see Fig. 130).

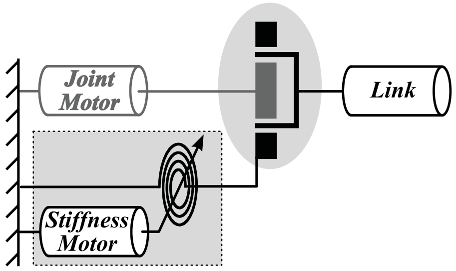

Fig. 130 Principle of the Variable Stiffness Joint mechanism. The circular spline of the harmonic drive gear is supported by the new mechanism.

Both joints were modelled and evaluated in simulation. The models and the developed controller structures were furthermore validated experimentally on joint test beds. Moreover, first experiments proving the expected increase in robustness and performance were done, as reported below.

3.3.2 Experimental Validation of Joint Robustness and Performance

The impact of the joint at a predefined velocity with a test object was evaluated. Two stiffness setups are realised via the passively compliant VS-Joint. The most compliant as well as the stiffest configuration were chosen and compared to a stiff realisation without variable compliance. As shown in Fig. 131, the maximum peak torque limit of the joint gear is almost reached with the stiff joint at an impact velocity of ≈ 3.7m/s, whereas the compliant VS-Joint is still far in the safe torque region [Haddadin *et al.* 2008[j]].

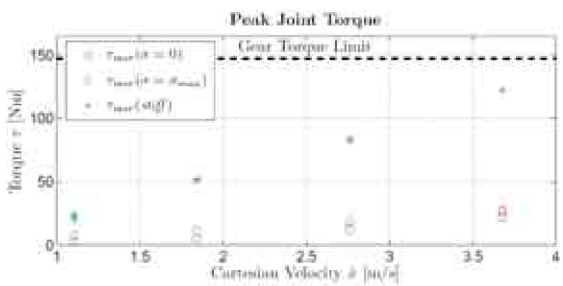

Fig. 131 Peak joint torque during impacts with the VS-Joint. The impact velocity ranges up to the maximum velocity of the R500/Robocoaster on which the joint was mounted for the experiment.

Fig. 132 Throwing distance of a ball with a flexible link using energy storage in the springs (6.0m) and a stiff link (0.8m)

Ball throwing shows the performance enhancement gained by the VS-Joint in terms of maximal velocity and power (Fig. 132). The link velocity of a stiff link corresponds to the velocity of the driving motor. In contrast, for a flexible joint the potential energy stored in the spring can be used to additionally accelerate the link relatively to the driving motor. The joint uses the resonance effect of the mass spring system to maximise joint velocity. A speed gain of 265% between the stiff and the compliant joint was achieved for the link velocity, increasing the throwing distance from 0.8m to approximately 6m.

3.3.3 Control for Robots with Variable stiffness

Our approach to the control of the VSA arms is to extend the passivity based control framework developed for the torque controlled light-weight robots to the VSA case. Following aspects are particularly relevant for the arm control:

- Due to the high compliance of the joint, a separate torque sensor is not required. The torque can be well estimated based on the motor and link position [Wolf & Hirzinger 2008[c]].
- An active compliance control will be used only for stiffness components which cannot be realised by the mechanical springs. Examples are zero stiffness or the joint coupling stiffness needed by arbitrary Cartesian stiffness matrices.
- The joints have very low intrinsic damping. While this is useful for cyclic move-

ments, involving energy storage (e.g. for running), damping of the arm for fast, fine positioning tasks has to be realised by active control. This is a challenging task, regarding the strong variation in inertia and stiffness. Control methods addressing this topic have been developed and tested on a joint prototype and for the whole robot in simulation.

- Absolute accuracy of fine manipulation has to be realised using additional external sensing at the tip.

The control of tendon-driven joints for robot hands has been an important subject of research. The advantages of relocating the motors into the forearm play a crucial role in achieving the goal to obtain human size and power. Due to the mechanical structure of such a tendon network the robot joints are coupled. Another important aspect of such systems is the capability to adjust the mechanical stiffness of the joints when tendons with nonlinear stiffness characteristic are employed. In an early stage, a feedback-linearisation control was investigated [Palli *et al.* 2007[c]].

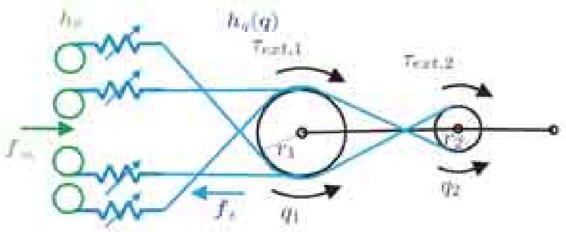

Fig. 133 Physical model of a variable stiffness tendon driven robot

For the control of tendon driven variable stiffness robots (Fig. 133), and in particular for the new multifingered hand following aspects have been considered and investigated [Wimböck *et al.* 2008b[c]]:

- parallel structures have to be treated, since at least two tendons are attached at each robot joint;
- the consideration of linear joint elasticity has to be extended to nonlinear tendon elasticity enabling to define a variable joint stiffness;
- the determination of the effective stiffness that is a combination of the variable stiffness of the mechanical transmission and the active controller stiffness;
- the pulling constraint of the tendons has to be ensured, i.e. tendons can only pull and not push the joints.

These considerations led to the development of an impedance controller for tendon-driven variable stiffness mechanisms.

3.4 Safety in Human-Robot Interaction

Physical human-robot interaction and cooperation has become a topic of increasing importance and of major focus in robotics research. An essential requirement of a robot designed for high mobility and direct interaction with human users or uncertain environments is that it must in no case pose a threat to the human user. Following aspects have to be primarily addressed especially in the context of unexpected collisions between robot and human:

- define and classify impact types;
- select the appropriate measure(s) to estimate human injury;
- evaluate the potential injury of the human during human-robot impacts;
- evaluate the influence of the relevant robot parameters determining the human injury;
- develop and evaluate countermeasures for injury prevention by means of robot design, control, and planning.

3.4.1 Possible Injuries: A Summary

One of the major outcomes of our work in human-robot safety is to give for the first time in robotics an overview of possible injuries during robot-human impacts. We introduced a general classification of injury types and selected adequate injury severity measures for their quantification. The goal of this work was to assemble a full image of injury mechanisms in human-centred robotics, since such an overview was missing completely in the literature up to now [Haddadin *et al.* 2007c[c]]

This synopsis is the generic outcome of the detailed investigations described in the following.

3.4.2 Crash Testing in Robotics

In order to analyse safety issues during physical human-robot interaction we investigated real-world threats via impact tests at standardised crash-test facilities of the German Automobile Club (ADAC) [Haddadin *et al.* 2007d[c], 2007b[c], 2007e[c]], cf. Fig. 134. These led to fundamental new insights for this still open topic of robotics. In order to quantify the potential danger emanating from the DLR LWR-III, impact tests at the crash-test centre of the German Automobile Club (ADAC) were conducted and evaluated. The outcome of these dummy crash-tests indicated a very low injury risk with respect to evaluated injury criteria for rigid impacts with the LWR-III. Furthermore, they show that a robot, even with arbitrary mass moving not much faster than 2m/s is not able to become dangerous to a non-clamped human head with respect to typical severity indices.

Fig. 134 Standardised impact tests with the LWR-III and various industrial robots. The tests were performed with standardised equipment of the German Automobile Club (ADAC).

These strong statements were confirmed by crash-tests with several industrial robots [Haddadin *et al.* 2007a[c], 2008c[c], 2008e[c]] (see Fig. 135). As an example the resulting Head Injury Criterion (HIC), an injury indicator used in the automobile industry, is depicted for various robots of varying weight.

After evaluating free impacts between humans and robots we analysed dynamic and constrained impacts at high robot speeds as well.

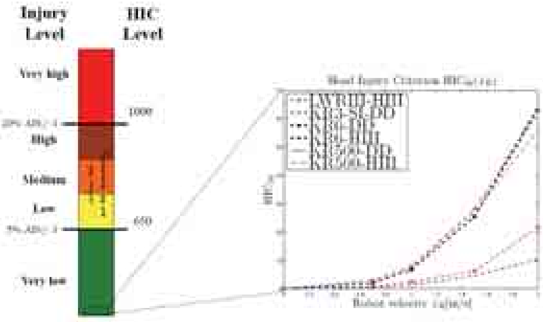

Fig. 135 Resulting HIC values at varying impact velocities for robots of different weights

As can be seen in Table 7 this is a major source of potential injury especially for massive robots [Haddadin *et al.* 2007c[c], 2008d[c]], clearly requiring light-weight robot design for human-robot interaction. Apart from such dynamic clamping impacts certain situations were identified in which low-inertia robots as the LWR-III could theoretically become seriously dangerous as well [Haddadin *et al.* 2007c[c]]. However, we were recently able to show that full prevention of this type of situation is possible by the collision detection and reaction methods which we have developed. This mechanism, vital for safe human-robot interaction, is described in Sec. 3.1.1, and shall now be shortly discussed.

Table 7 Chest injury during constrained robot-human impacts

ROBOT	CC[mm]	VC[m/s]	F^x_{ext}[N]
LWRIII	14.4(0.0)	0.035	741.6(1.3)
KR3 (Cat.0)	31.2(0.0)	0.1	851.9(1.4)
KR6 (Cat.0)	65.5(2.0)	0.25	2836.1(2.7)
KR6 (Cat.1)	66.6(2.1)	0.25	2904.6(2.7)
KR500 (Cat.0)	228.0(6.0)	0.84	14282.0(6.0)
KR500 (Cat.1)	245.0(6.0)	0.89	15491.0(6.0)

3.4.3 Collision Detection and Reaction

Using a light-weight robot as the LWR-III that was especially designed for interactive and cooperative tasks, we have shown how collision detection and reactive control strategies can significantly contribute to ensuring safety to the human during physical interaction [De Luca *et al*. 2006[c]; Borst *et al.* 2007[c], Haddadin *et al.* 2008a[c]]. Several collision tests were carried out, illustrating the feasibility and effectiveness of the proposed approach. Fig. 116 depicts a schematic view of the collision detection scheme which realises a precise estimation of external disturbances. This enables us to distinguish between desired interaction and unexpected collisions. After isolating a collision as such, various sophisticated reaction schemes are possible which go beyond simply stopping the robot.

This work [Haddadin *et al.* 2008a[c]] has been awarded the "Best Application Paper Award" at the IEEE/RSJ International Conference on Intelligent Robots and Systems (IROS 2008).

3.4.4 Soft Tissue Injuries in Robotics

In our latest research we carried out an analysis of soft-tissue injuries caused by sharp tools which are mounted on, or grasped by a robot as the next step down the road to a full safety analysis of robots for HRI (Fig. 136). The entire evaluation is based on available biomechanical and forensic data and, to our knowledge, for the first time in robotics presents various experimental results with biological tissue which validate the analysis [Haddadin *et al.* 2008b[c]]. There, we provide empirically relevant limit values for injury prevention for the case of sharp contact. Furthermore, the previously described collision detection and reaction enables the LWR-III to reduce injury significantly during stabbing and entirely for cutting with sharp tools.

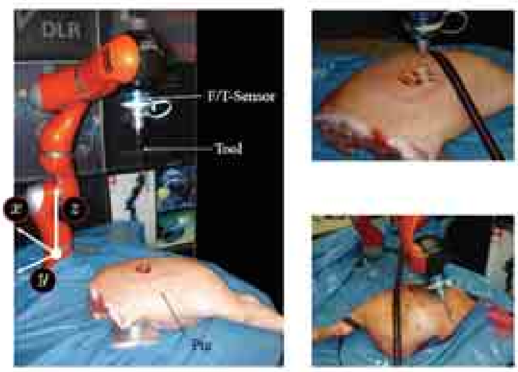

Fig. 136 Pig testing series with the LWR-III for investigating the mechanisms of stabbing and cutting

Various video-clips on related experiments are available on the institute's web server.

3.4.5 Collision Avoidance

For complex kinematic structures such as JUSTIN, avoiding collisions with the surrounding persons, objects or even itself in free-floating, gravity compensated mode or during compliant behaviour is a fundamental safety requirement. A passivity based method has been developed, which can make use of proprioceptive sensors and the estimated position of the surrounding objects for generating repulsive force fields which prevent the robot from collision (Fig. 137). These forces sum up with the control torques, such that the robot still tries to fulfil the task while avoiding the (possibly moving) obstacles [De Santis *et al.* 2007[c]].

Fig. 137 Elastic force field-based collision avoidance

3.5 Free-Flying Robots

The research on the free-flying robot application has evolved in the last years in the areas of dynamic modelling, parameter identification and control.

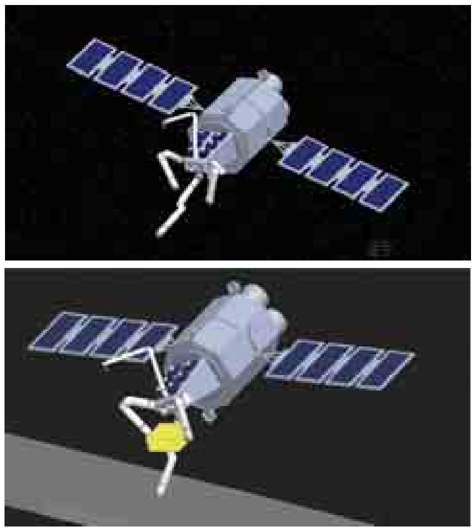

Fig. 138 Free-flying robot with four arms: free open branched chain (above); grappled closed loop (below)

Further advances have also been made in developing tools for the autonomous grasping of a tumbling target satellite (see also

Sec. II.1.2). These activities will be addressed in the following subsections.

3.5.1 Dynamic Modelling

A new algorithm for the efficient computation of the dynamics of structure-varying kinematic chains was developed [Lampariello *et al.* 2008[c]]. Typical structure changes for free-flying robots include open branched chains and closed loops, in free and grappled conditions (see Fig. 129). The algorithm is intended to contribute to the efficiency of motion planning for robots which require different kinematic structures for a given task. Since structural variations are handled on-line, there is no need to prepare every possible kinematic chain in advance for a given system.

This work also gave rise to a dynamic library which, with simple codes, allows the computation of any free-flying robot model, for any kinematic structure, based on dynamics principles (acceleration level) or momentum conservation principles (velocity level). The latter also allows easily computing the free-flying robot Jacobian matrix, which is used for solving important problems, such as inverse kinematics and open-loop control.

Furthermore, the dynamic library includes the operational space dynamics formulation for free-flying robots. The dynamics in operational space for space robots is more complicated than that of the ground based robot, due to the lack of a fixed base. However, by considering this unique characteristic, a computational efficient algorithm of operational space formulation was developed [Abiko & Hirzinger 2008[c]].

The dynamic library is already been extensively used to support motion planning and control algorithms, addressed in the following sections.

3.5.2 Parameter Identification

A method was developed for the identification of the inertial parameters of a free-flying robot directly in orbit [Lampariello & Hirzinger 2005[c]]. This may serve to improve the path planning and path tracking capabilities of the robot, as well as its efficiency in energy consumption.

The method was applied in simulation to a single-arm free-flying robot, for the identification of the parameters of the satellite base and of the load on the end-effector, assuming those of the robot arm to be known from CAD data. Emphasis was also given to the experimental design. This resulted in a means to derive optimal exciting robot manoeuvres for the identification, within the operational orbital constraints, such as limited robot joint velocities.

The problem of the identification of the full system, i.e. with unknown robot inertial parameters, was also addressed in its theoretical aspects. This resulted in a description of the identifiability of free-flying robot inertial parameters.

The experience from the GETEX Dynamic Motion experiments performed on the ETS-VII satellite in 1998, has allowed determining a most suitable orbital dynamic model for the identification. The work described here was performed in view of the experiments to be performed within the DEOS project (see Sec. II.1.2.2).

3.5.3 Control

Advances in the control of free-flying robots have been made by addressing the following problems, explained hereafter:

1. motion compensation control;
2. differential flatness control;
3. grasping control;
4. path tracking control.

The first control task involved the dynamics and control of a cable-suspended, two-arm robotic system shown in Fig. 139 [Lampariello *et al.* 2006[c]]. One manipulator arm was commanded to fulfil a user defined task. The second arm was then controlled to compensate for the disturbances on the cable-suspended platform arising from the motion of the first.

Model-based feed-forward control, stemming from the momentum conservation equations of a free-floating robot, was developed for the motion compensation problem. Furthermore, due to model uncertainty, sensor-based feedback control was introduced, to account for undesired oscillatory motions of the system. The latter control problem reduces to the dissipation of the oscillatory energy of the system, by means of adequate robot control. Both control methods were implemented and tested on the experimental setup shown in Fig. 139.

This work gave great insight into two-arm free-flying robot control. The developed feed-forward control described above would in fact be very useful to minimise the disturbances of one robot arm on the satellite platform, by means of a second arm.

The second control problem, more theoretical in nature, involved the search for a differentially flat mathematical representation of the free-floating robot dynamics [Agrawal *et al*. 2006[c]]. The dynamics described as such, allows an easier treatment of the non-integrable angular momentum equations and of the construction of point-to-point manoeuvres in the robot's configuration space.

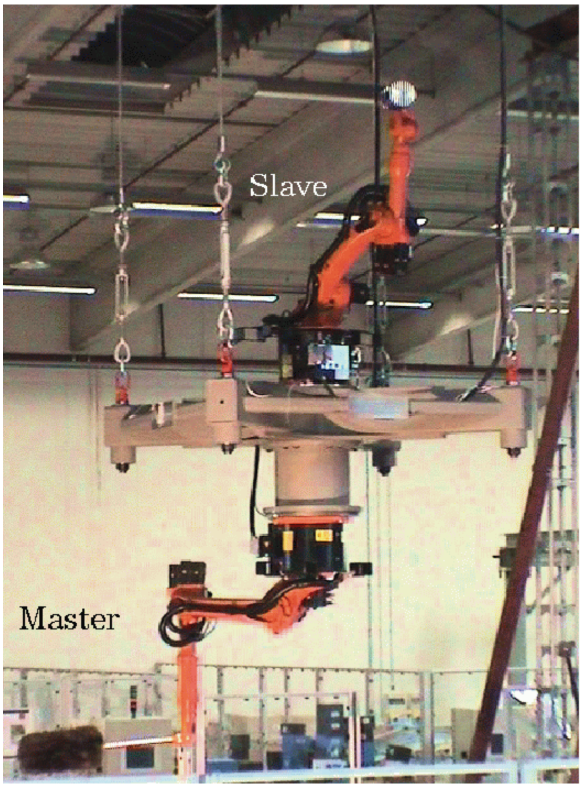

Fig. 139 Experimental setup of two-arm cable-suspended system: the master is provided with a long duster, the slave with a heavy dumbbell

The result of this work was that of finding a differentially flat representation for a three-joint free-flying robot with a particular design. The design is such that the centre of mass of the last link falls onto its own axis of rotation.

The third control problem addressed the grasping of a freely-tumbling target satellite by means of a free-flying robot (see Fig. 139). The particular goal was to dampen out the motion of the target satellite relative to the grasping satellite. Considering the grasped target satellite as a disturbance force on the robot end-effector, the control is independent of the target inertial parameters and the damping-out control can be achieved in the presence of model uncertainty. The control can also deal with unexpected impact at the time of grasping. [Abiko *et al*. 2006[c]].

The path tracking in operational space of a free-flying robot is greatly influenced by the dynamic parameter of the system. Even the kinematic mapping from joint space to Cartesian space is dependent on the dynamic properties, unlikely for ground based robot system. Therefore, model uncertainty gives rise to a deviation of the tracking in operational space.

To tackle this issue, several control solutions can be found in sensor-based feedback control or robust control. In our work, an adaptive control for free-flying robots was developed. The control adjusts the dynamic parameters adaptively by using the tracking error during the path tracking phase. Furthermore, the control was extended by combining the information of the reaction force and the tracking error, which improves the convergence to the desired trajectory [Abiko & Hirzinger 2007a[c], 2007b[c]].

3.5.4 Autonomous Grasping of a Tumbling Target Satellite

In the control section above, the control problem of grasping a freely-tumbling target satellite by means of a free-flying robot was addressed (see also Sec. II.1.2.2). The aim is to perform this task in the autonomous operational mode, where planning and control algorithms will provide, through automatic processing of the onboard sensor's output, the necessary grasping commands. This is opposed to the telepresence mode, for which the commands are provided by a human operator.

For this purpose, motion prediction and motion planning tools have been and are being developed. The first addresses the task of long-term motion prediction of the target satellite (~ 100 seconds), to support a subsequent motion planning task for the robot's grasping motion. The motion prediction involves building a dynamic model of the target satellite, the parameters of which are to be identified after a prolonged observation period of its motion. This dynamic model will then be used to predict the motion of the target up to a suitable grasping point. The motion observation period delivers, by means of camera images and robot vision tools a description of the satellite motion parameters in time (see Sec. III.4.1.1). These are then fed to an inertial parameter identification algorithm, which defines the dynamic model to match the observed motion. The details of this work can be found in [Hillenbrand *et al.* 2005c].

The developed method was applied to simulated noisy data, for different target satellite tumbling motions. For some cases the prediction was found to be successful, whereas cases where found for which the excitation of the relevant parameters during the observation phase was not sufficient for a successful identification (the observation time was limited for practical purposes to 100 seconds).

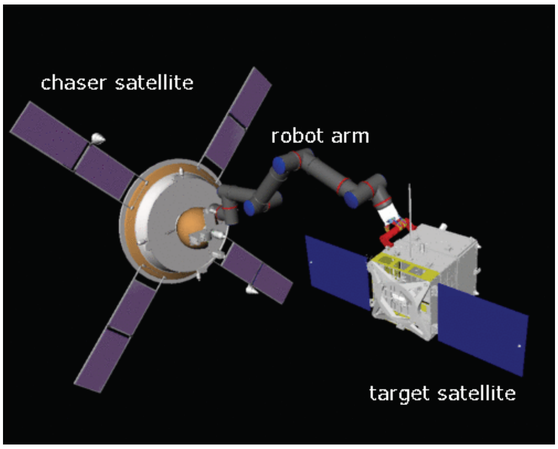

Fig. 140 A robot mounted on a chaser satellite grasping a target satellite

For the purpose of the autonomous grasping operational mode, the motion prediction algorithm will then be fed into a robot motion planner, which computes a feasible and safe robot trajectory to grasp the target satellite. This motion planning problem is already being addressed and is solved with an algorithm based on nonlinear optimisation. This allows to account for operational constraints, such as limited actuation forces and limited workspace, and to minimise user-defined cost functions, such as energy or disturbances on the satellite due to the robot motion.

Fig. 141 Example sequence of a grasping manoeuvre (simulation): i) initial relative position between target and chaser; ii) approach; iii) tracking; iv) grasping; v) stabilisation

4 Perception

The two major perceptual modalities for a robot are vision and touch. Vision is characterised by its long range and contact-free acquisition, while touch sensing is local and is based upon physical interaction with the environment. In robot systems, as in humans, the two modalities can provide complementary information on the environment.

Visual information processing may be categorised according to whether its goal is the faithful representation or modelling of the environment geometry or appearance, or the extraction of a few environmental parameters or states relevant to a specific robotic task.

Accordingly, we here cover our work in robot vision, 3-D modelling, and force and touch sensing.

4.1 Robot Vision

4.1.1 Motion Estimation

Appearance-Based Object Tracking in 6 DoF

When a rigid object moves in 3-D space relative to a camera, it is often interesting to know how its relative pose changes in all 6 degrees of freedom (DoF). The problem of 6-DoF tracking arises in the context of numerous applications within and beyond robotics, such as manipulation of moving objects, navigation of a mobile robot or vehicle, or pose estimation of a handheld sensing device.

In general, the approaches to vision-based pose estimation can be divided into two classes depending on the level of the considered detail: appearance-based pose estimation, for a single though detailed representation of the object, and feature-based pose estimation, for multiple independent local appearance-cues. By their nature, appearance-based approaches aim at non-homogeneously textured objects while line-feature-based approaches, for instance, only support low textured, polyhedral objects on largely uncluttered background.

In this research project, we have explored appearance-based object tracking dealing with the following challenges:

- the projective camera model for accurate tracking is numerically expensive;
- object or camera motion changes the view, and hence the appearance of the object;
- object motion may change the illumination, and hence the appearance, of the object.

We developed an appearance-based tracking algorithm for monocular cameras, which is based on a textured 3-D point cloud representing the geometric and photometric properties of the object. Accordingly, arbitrary object geometries are supported such as, for instance, planar, polyhedral, and free-form object shapes (Fig. 142 and Fig. 143).

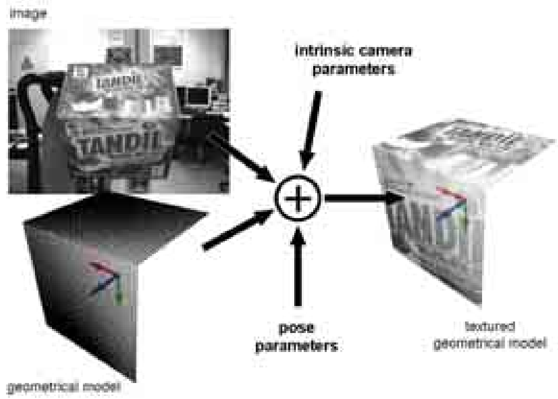

Fig. 142 The registration process: a textured 3-D object model is generated by registering the geometrical information given by a 3-D point-cloud with photometric information contained in a reference view on the object

Furthermore, a full-perspective camera model is considered and free object motion is allowed in all 6 DoF. This comprehensive physical model allows to accurately predict the object appearance in non-occluding scenes and, hence, inversely allows to determine the 6-DoF object pose that most likely generates a captured image.

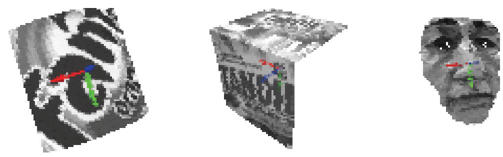

Fig. 143 Textured shape models. Left: 3-D cylinder. Centre: 3-D edge. Right: 3-D face.

In addition to appearance changes caused by object motion, changes in appearance due to variations in illumination are considered, too. In detail, three approaches of different complexity have been analysed and compared, which either keep track of the changes or which explicitly model the object radiance depending on the lighting conditions [Sepp, 2005[c]]. The evaluation of the approaches under real-time conditions and with limited computational resources favours the application of efficient intensity-difference normalisation methods [Sepp 2008[c]].

For the estimation of the most likely 6-DoF object pose, two algorithms have been developed: A single-hypothesis approach and a multi-hypotheses approach. The former allows tracking object poses at frame rate with a Gauss-Newton method given initially a single, reliable pose hypothesis. By contrast, the multiple pose hypotheses approach uses an annealed particle filter, thus considering also less reliable pose estimates [Sepp *et al.* 2006[c]].

The accuracy and robustness of the single-hypothesis method is substantially increased by improving the real-time efficiency of the Gauss-Newton method. Here, an explicit expression for the image Jacobian is derived allowing the prediction of appearance changes induced by motion at arbitrary object pose, given only a reference image and the corresponding object pose [Sepp, 2006[c]]. Accordingly, we succeed in tracking objects (Fig. 144) at an inter-frame displacement of 3mm and at a frame rate of 50Hz (Core2 2.4GHz). The achievable accuracy is better than 1mm in translation and 1 degree in rotation.

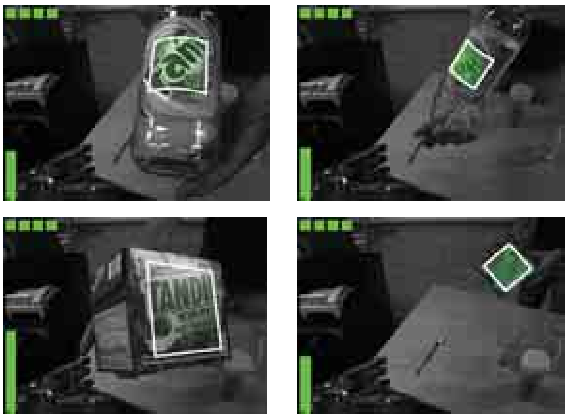

Fig. 144 Screenshots of successfully tracked objects under motion and incurred changes of illumination. Top: bottle object, bottom: box object

Feature-Based Eye Tracking in 5 DoF

Human-computer interaction in general and human-robot interaction in particular rely on the perception of human behaviour and human intention for the generation of appropriate (graphical or physical) actions. In this project, we investigate methods for tracking eye positions in 3-D space aiming at the view-dependent rendering of 3-D content on computer displays. In combination with the latest developments in auto-stereoscopic displays, this allows an operator to perceive a scene in 3-D, which is especially useful for telepresence applications; see, e.g., the DLR MIROSURGE system for robotic endoscopic surgery, Sec. VII.4.1.5.

In this project, we investigated three different approaches to the localisation and tracking of the two eyes of a human face: texture-based tracking (cf. previous section), tracking with Haar-like features (i.e. responses to a set of local linear filters), and tracking the reflections caused by an active infrared light source.

Face shape and appearance differ from person to person. Hence and in contrast to the above section on texture-based tracking, a geometric and photometric object model is not known in advance. Instead, the required textured 3-D point cloud is constructed online and individually for each user through dense stereo image processing [Hirschmüller, 2005[c], 2008[j]].

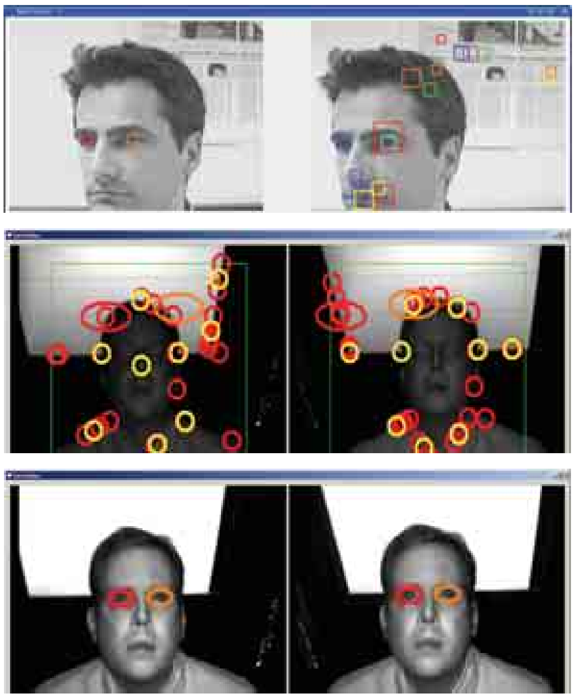

Fig. 145 Top: eye detection with Haar-like feature classification; all hypotheses (right), correctly selected hypotheses (left). Centre: eye detection with reflection features: spurious hypotheses. Bottom: correctly selected pair of reflection features.

In order to automatically determine the eye region in the camera images, experiments have been carried out for locating eyes with Haar-like features (Fig. 145). Though the method achieves a recognition rate of up to 95%, the localisation accuracy of 1.3cm has been identified as too low for application with auto-stereoscopic displays.

Hence and in order to gain independence of ambient lighting conditions, a third method has been developed using an active infrared light source and a specific feature detector for the associated reflections of the light source in the eyes (Fig. 145). In combination with geometric constraints for the reliable selection of the eye-related responses, the devised eye tracker proofs highly robust for subjects wearing no glasses. Moreover, the method exhibits a superior performance in terms of localisation accuracy, frame rate and latency, critical properties for seamless 3-D visualisation.

ToF-Camera-Based Object Tracking in 6 DoF

We have explored tracking of rigid object motion based on the data from time-of-flight (ToF) cameras (O3D100 and SR3100). To this end, a two-stage incremental pose estimation procedure is set up.

On the first stage, the initial pose is estimated by a particle filter approach. On the second stage, the incremental object movement is estimated by an iterative closest point (ICP) tracking. Both methods are based on the same target representation and error function but differ in the maximum number of hypotheses and radius of convergence. The convex target object is modelled by a set of 3-D points. Additionally, corresponding normals are used to decide whether a model point is seen by the camera or occluded. The ToF camera observes the scene and provides a point cloud. The model points are fitted into this point cloud in order to estimate the pose of the target. The coordinate root mean squared (CRMS) error between the model and the point cloud is a measure for the match quality and the likelihood of the estimated pose. As a result, the pose is estimated with a mean accuracy of 5° orientation and 10mm translation. Thus, the pose can serve as control variable in a visual servoing loop or as desired frame in a grasping task.

Non-Rigid Motion Tracking

Apart from rigid objects, which may have previously known geometries, deformable objects pose particular challenges for motion tracking. For such non-rigid objects like organ surfaces, vision approaches able to deal with unknown and dynamically changing objects are required. For the goal of motion tracking and compensation of the beating human heart as required in a medical technology transfer project (see Sec. VII.4.1 on surgical robotics), a tracking scheme based on natural landmarks has been developed [Gröger *et al.* 2005b[c]]. Based on robust landmark tracking, motion correction algorithms have been developed to assist the surgeon by stabilising image motion arising from the beating heart [Gröger & Hirzinger 2006a[c], 2006b[c]]. More detail on this project and its medical background can be found in Sec. VII.4.1.7 within the technology transfer example of surgical robotics.

Motion Estimation for System Identification

The identification of dynamic system parameters from visual observation requires motion estimation along an extended trajectory. For instance, autonomous on-orbit servicing of a satellite by a robotic spacecraft (cf. Sec. II.1.2) requires identification of the long-term motion of the free-floating target. Indeed, to plan an approach and grasping manoeuvre, the satellite motion has to be predicted over a time span on the order of minutes ahead.

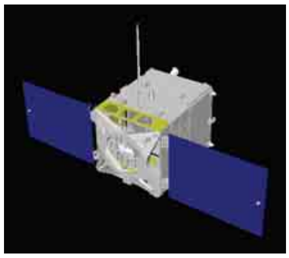

Fig. 146 Target satellite model from the TECSAS scenario

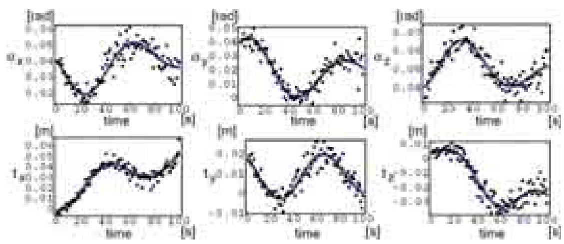

Fig. 147 Example trajectory (blue dots) and motion estimates (black dots) of the free-floating target satellite. Rotations are plotted in canonical coordinates (top row), translations in vector components (bottom row).

For an uncooperative satellite, estimation may either be based upon range data of the target satellite or on ordinary camera images. The advantage of using range data for motion estimation lies in its independence from any prior knowledge about the target.

Range data may be obtained from stereo image processing or laser ranging. Depending on the nature of the sensor, the target surface, and the image processing algorithms, three types of range data may be available:

- sparse 3-D data points, computed from local image features, with known correspondences between consecutive time frames;
- sparse 3-D data points, computed from local image features, with unknown correspondences between time frames;
- dense 3-D data points, computed from dense image disparities or measured with a laser ranger, without correspondences between time frames.

Note that the not considered case of sparse 3-D data points without correspondences between time frames would not allow for motion estimation without a geometric object model.

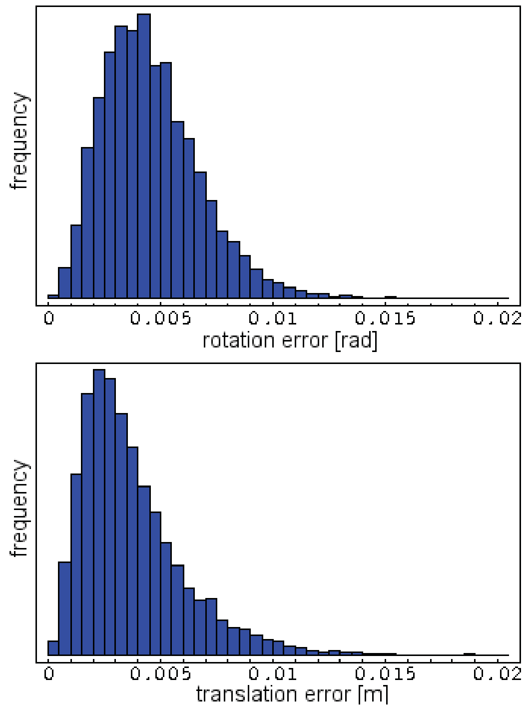

Fig. 148 Histograms of rotation and translation estimation errors for sparse range data with known correspondences

We have studied the three scenarios of model-free motion estimation [Hillenbrand & Lampariello 2005c] by simulating adequate range data and target motions. Gaussian measurement noise with a standard deviation of 5mm has been assumed, which is a rather high value, and occlusion and surface slant taken into account. Furthermore, no knowledge of target geometry or dynamics has been provided to the motion estimator. Fig. 146 shows a view of the target satellite model used in this study, Fig. 147 an example trajectory along with the motion estimates.

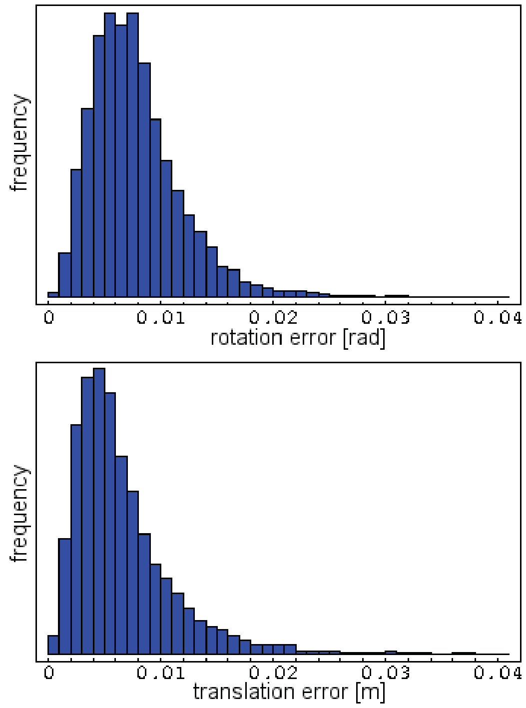

Fig. 149 Histograms of rotation and translation estimation errors for sparse range data with unknown correspondences

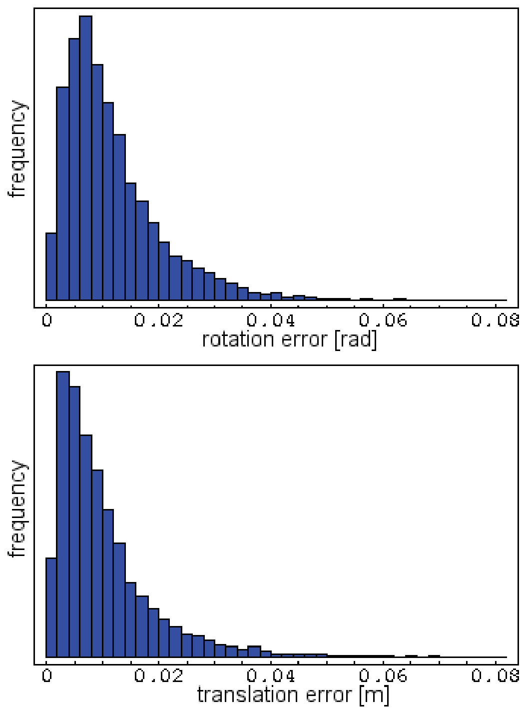

Fig. 150 Histograms of rotation and translation estimation errors for dense range data without correspondences

In case of known correspondences of data points between time frames, a straightforward least-squares estimator produces optimal results; see Fig. 148.

Without knowing any correspondences between time frames, those have to be established during the estimation procedure. We have achieved this using a robust M-estimator for the cases of sparse and dense range data; see Fig. 149 and Fig. 150.

The method investigated for motion estimation proves able to track small motions with high precision. It turns out that the loss in estimation accuracy, brought about by not knowing point correspondences, is not dramatic. However, the case without point correspondences in the data proves a lot less suitable for long-term prediction, even with a 100-fold increase in data density. Moreover, the computation time increases at least linearly with the number of data points, such that scenarios that can rely on few points are preferable.

4.1.2 Pose Estimation

Pose estimation refers to the process of determining the position and orientation of an object or of the environment relative to a sensor frame. In general, no prior knowledge of pose parameters is available. We are hence faced with a global estimation problem.

A rigid motion has to be estimated from a model frame, where a model of the object or the environment is defined, to the sensor frame, where the sensory data is given. In general, no correspondences between the model and the data are known in advance. We hence have to employ a robust estimator that will also find those correspondences.

We have studied a class of global, robust estimators that is based upon location statistics in parameter space, as opposed to error statistics in data space. In its general form, we refer to this algorithm as *parameter clustering* [Hillenbrand, 2007[i]].

In the context of pose estimation, the algorithm consists of the following steps:

1. randomly draw a subset of scene data;
2. randomly draw a subset of model data consistent (geometrically, photometrically, etc.) with the drawn scene data;
3. compute the rigid motion between the scene subset and the model subset;
4. compute and store the six pose parameters associated with the motion;
5. repeat steps 1 through 4 until a significant cluster of pose parameters has emerged;
6. estimate the location of the parameter density peak from the stored parameter samples and return it as the parameter estimate.

The relevant data subsets for computing each pose hypothesis depend on the nature of the data. In case of range data, 3-D point triples are a possible choice, but information on surface normals may also be exploited. In case of ordinary camera images, sets of pixel coordinates and values or their spatial derivatives can be used.

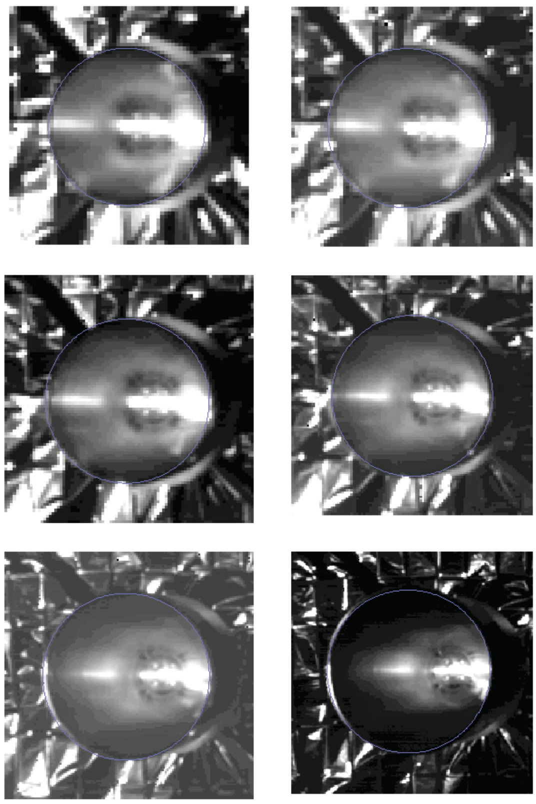

Fig. 151 Nozzle regions of images from a sequence of an approaching satellite; the detected nozzle rim is outlined in blue

An application example from the domain of on-orbit servicing is estimating the position of the target satellite through detection of the rim of its apogee motor nozzle in camera images. The nozzle model is just a circle. The challenge lies in detecting the nozzle rim in images of highly reflective surfaces, where the contrast polarity of nozzle to background changes and disappears many times along the rim and over the sequence.

We have studied image sequences of a moving satellite model taken at the DLR EPOS facility; see Fig. 151. The lighting conditions were arranged to mimic those of orbital sun light.

The nozzle position and scale in the images are estimated by computing thousands of hypotheses for each image from triples of high-contrast pixels, followed by locating their maximum density in parameter space through a mean-shift procedure.

The Parameter Space

Unlike for data space methods, for parameter clustering the estimation result depends on the choice of parameter space. Theoretical arguments of statistical consistency [Hillenbrand, 2007[j]] suggest using a parameterisation that yields a uniform Haar measure of the parametric group to be estimated. We refer to such a parameterisation as being consistent for clustering. For pose and motion estimation, we have derived a consistent parameterisation and conducted quantitative studies of its advantage over the canonical parameterisation of motions [Hillenbrand 2007[j]; Nölle 2008[r]]. These studies have been based on random data sets and on the Princeton Shape Benchmark data set, a publicly accessible database of 3-D object models.

The consistent parameterisation turns out to consistently outperform the canonical parameterisation. The orientation error with canonical parameterisation can be more than an order of magnitude larger than with consistent parameterisation. The size of the effect depends on the variant of parameter clustering and the quality of the data; see Fig. 152.

Range Data Sources

Stereo image processing has become a fast and cheap source of range data, but cannot reconstruct scenes that lack sufficient photometric structure for the correspondence search.

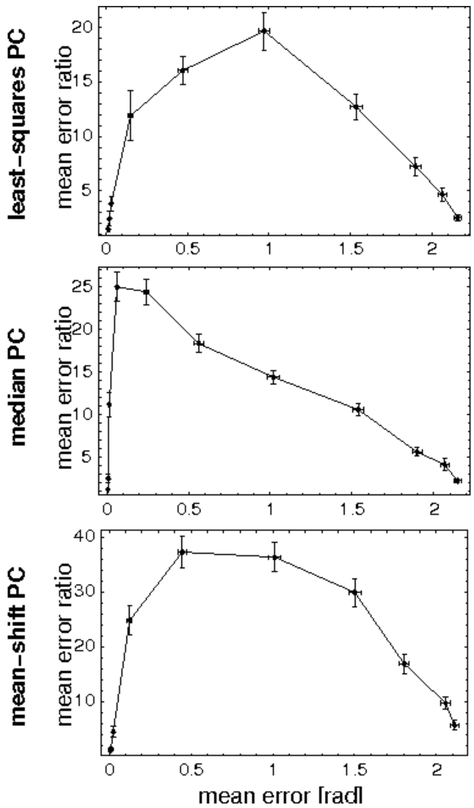

Fig. 152 Mean ratio of canonical to consistent rotation estimation errors for three variants of parameter clustering (least-squares PC, median PC, and mean-shift PC) as a function of the mean consistent rotation estimation error; bars indicate standard errors of the means

A recent competitor to stereo image processing is a camera based on a chip that measures the time of flight (ToF) of emitted modulated light. A simultaneous measurement of distances to scene surfaces in a pixel array is thus obtained. One of the current problems, however, is the low lateral and depth resolution achievable, especially in the short range, i.e., in the workspace for robotic manipulation.

We have conducted quantitative studies to evaluate the relative utility of correlation-based stereo data and ToF data (O3D100 camera) for the task of pose estimation for manipulation [Hillenbrand 2008[c]].

Fig. 153 shows an image of a test scene with a cardboard grid box that contains metal pieces. A model of the box was acquired by the same sensor—stereo cameras or ToF camera—that was also used for scene sensing. Fig. 154 shows stereo data from a test scene with the matched model data of the box, Fig. 155 shows the same for ToF data.

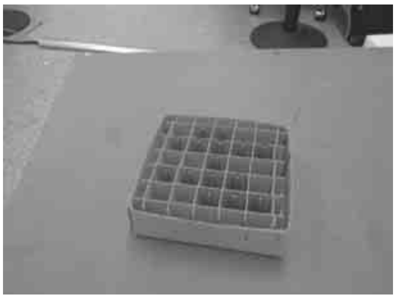

Fig. 153 Test scene with cardboard grid box (approximate dimensions: 170×170×50mm)

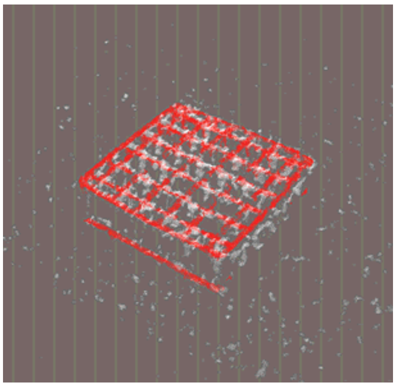

Fig. 154 Stereo data points of a test scene (white) and box model points (red) in the estimated pose

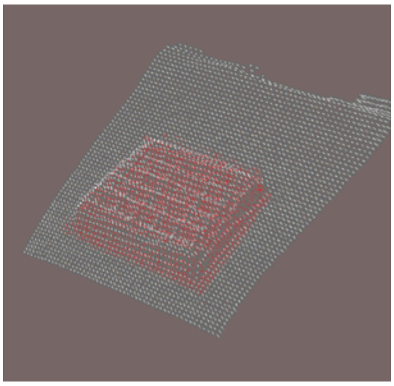

Fig. 155 ToF data points of a test scene (white) and box model points (red) in the estimated pose

Using the same 16 variants of pose clustering algorithm, it turns out that pose estimation from stereo data is about one order of magnitude more accurate and faster than pose estimation from ToF data (see Fig. 156 and Fig. 157).

The dramatic drop in accuracy and increase in computation time when using ToF data is partly due to the lower spatial resolution of each ToF data point. Another factor lies in the nature of ToF data providing a representation of object surfaces, while correlation-based stereo data emphasise object edges. Edges can be a stronger cue to object pose than surfaces, as they usually impose stronger constrains on pose hypotheses.

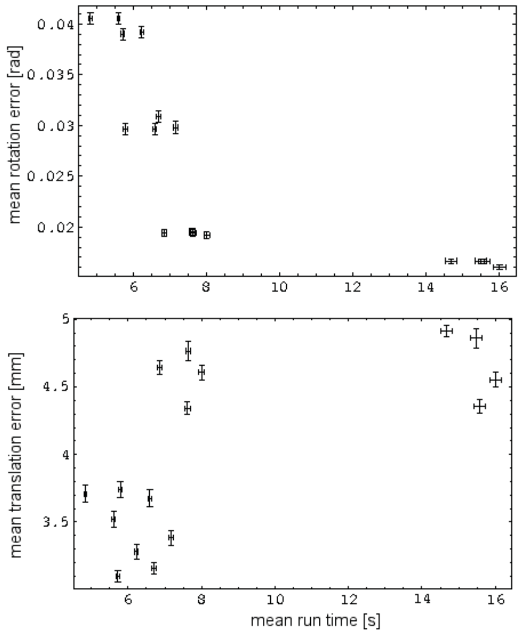

Fig. 156 Mean error/runtime trade-off for rotation and translation estimates from stereo data; bars indicate standard errors of the means. It is interesting to note that the translation error actually increases for variants with longer run time, while the rotation error decreases.

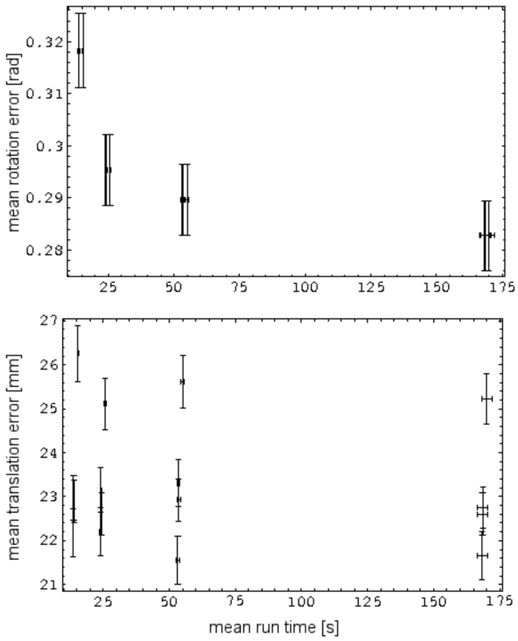

Fig. 157 Mean error/runtime trade-off for rotation and translation estimates from ToF data; bars indicate standard errors of the means. The rotation error decreases while the translation error remains roughly the same for variants with longer run time.

However, ToF data may be made more useful for pose estimation than is apparent from this study. For instance, by taking additional measurements such as fusion of multiple views or with other sensors (cameras), the spatial resolution of the range data may be enhanced. Moreover, additional processing of ToF data can overcome the inherent drawback of surface data for pose estimation.

Finally, it is clear that ToF data may be applicable in cases where stereo image processing fails, such as when images lack sufficient structure.

4.1.3 Object Recognition

Object Recognition through Robust Pose Estimation

Since robust pose estimation establishes correspondences between model and scene data, it effectively selects for each object model the best-matching part of the data. For pose clustering (cf. Sec. 4.1.2), the maximum parameter density is then a measure of match quality. Object recognition along with pose estimation can thus be achieved in scenes with multiple objects.

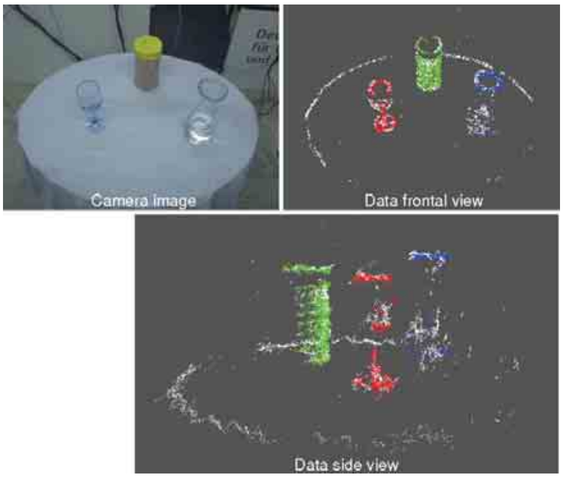

Fig. 158 Scene with objects used by the humanoid "JUSTIN" for preparing an instant-tea drink: camera image and stereo data points (white) superposed with model points of the recognised objects (coloured)

In a service robot scenario, pose clustering from stereo data has been used to recognise and locate typical objects from a kitchen environment (bottles, glasses, jars, spoons) [Hillenbrand 2008[c]]; see Fig. 158. DLR's humanoid robot JUSTIN is thus able, e.g., to prepare a glass of instant tea [Ott *et al.* 2005[c], 2006b[c]; Borst *et al.* 2007[c]], a demonstration that has run regularly in our lab; see Sec. III.2.3.

Recognition of Planar Shapes

Shape recognition of planar objects is a traditional problem in computer vision, arising in many applications. We have studied Arbter's affine invariant Fourier descriptors and the popular 7 Hu's invariant moments for shape recognition in the context of an assembly task with planar parts; see Sec. III.6.4 [Stemmer *et al.* 2006[c], 2007[c]; Robuffo *et al*. 2008[c]]. Both methods are known to be computationally highly efficient and hence suitable for real-time applications.

Fig. 159 The set of planar objects from a slanted camera view

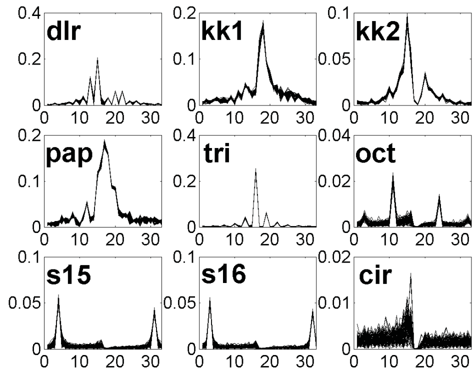

Fig. 160 Signatures (superimposed values) of 33 Arbter invariants (affine invariant Fourier descriptors) taken from 80 observations at different camera views. The invariants prove to be sufficiently insensitive to quantisation noise and different viewing angles (robustness) and show specific patterns from class to class (distinctiveness). tri=triangle, oct=octagon, cir=circle, s15=15-teeth star, s16=16-teeth star, dlr=DLR logo, pap=PAPAS logo, kk1=KUKA logo—lower part, kk2=KUKA logo—upper part.

We used 8 different objects which were chosen to span a range of planar shape types: polygonal and free form, with rotational symmetry (triangle, octagon, 15-teeth star, 16-teeth star, and circle) and without (logos of DLR, PAPAS and KUKA); see Fig. 159. The Arbter invariants have turned out to be robust to spatial quantisation effects (sensor chip of the camera) as well highly discriminative over the complete set of shapes; see Fig. 160 and Fig. 161. The Hu invariants, on the other hand, could not discriminate the rotationally symmetric shapes of a symmetry order higher than 3 (this is here 8, 15, 16, and ∞) without ambiguities; see Fig. 161.

As a result, Arbter invariants outperform Hu invariants in terms of discrimination of rotational symmetries.

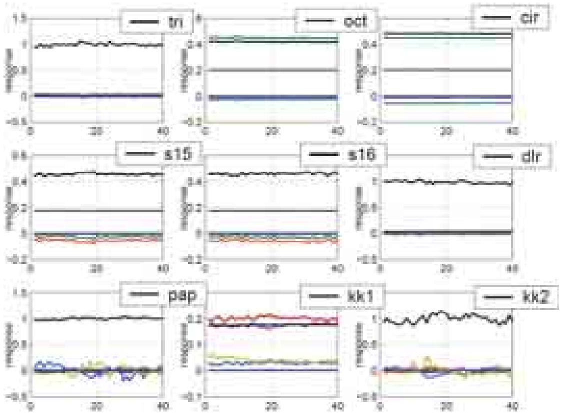

(a)

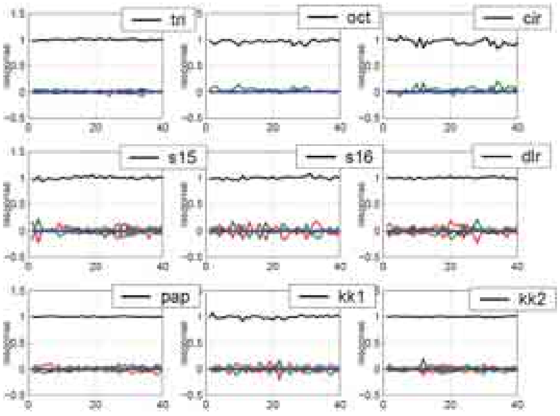

(b)

Fig. 161 Responses of two linear classifiers to 40 test data sets (views) for each object. (a) Responses to Hu invariants; (b) responses to Arbter invariants. A response of 1 indicates a high level of confidence in class membership, 0 indicates high confidence in class non-membership. Arbter invariants are unambiguous with respect to the given classes, in contrast to the popular Hu invariants.

4.2 3-D Modelling

Three-dimensional perception of the environment is crucial for robotic applications in motion planning, grasping, mapping or navigation to mention just a few examples. Basically, there are several approaches in order to contactlessly sense the spatial structure of an environment and scene respectively. State-of-the-art approaches either use laser-scanners or cameras. While the first directly provide spatial data, the latter reconstruct the scene from consecutive images, e.g. Structure-From-Motion, or from at least two images captured by a stereo camera system. These approaches are common, exhaustive investigated and regarding the laser-scanners very accurate. Especially the spread of image based methods goes along with an increasing performance of processors and decreasing prices for hardware, e.g. cameras and processors.

4.2.1 The 3D-Modeller

The second generation of the 3D-Modeller (Fig. 163 and Fig. 162) is a device for geometric and visual perception of the world [Suppa *et al.* 2007[c]]. It combines multiple sensors: Our laser-range scanner, a laser-stripe profiler and stereo vision consisting of two digital Firewire cameras. Common perception tasks in robotics include object modelling and recognition, visual servoing, exploration, collision avoidance, path planning, and simultaneous localisation and mapping.

Fig. 162 The 3D-Modeller

For making the 3-D digitisation of an object convenient and versatile, the Modeller is used as if it were an aerosol can, thus simplifying the digitisation of large or complex objects. Due to its low weight and generic mechanical interface, it can also be such as JUSTIN (Chapter III.2). The 3D-Modeller is flexibly applicable, not only in research but also in industry, especially in small batch assembly.

In order to acquire a 3-D model of the environment, the position and orientation (pose) of the Modeller is measured while sensing. Either the pose is given by a robot in automated use or by a tracking system for hand-guided purpose. Meanwhile, we have succeeded in estimating the pose is estimated by visual odometry (Sec. III.4.2.3).

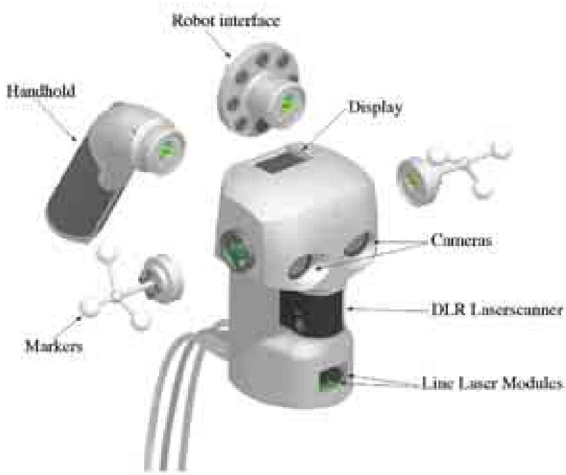

Fig. 163 3D-Modeller Components

Design Considerations

The various applications have different and conflicting demands w.r.t. sensor range, view angle, lighting, precision, and acquisition speed. These demands can only be met by integrating multiple sensors in the same hardware platform.

The first version of the Modeller, the DLR hand-guided multi sensor device, only served for 3-D object digitisation. The increased requirements demanded an updated hardware platform: On the one hand the components and the hand-held operation had to be improved, and on the other hand the fields of applications have extended, especially for robot vision. The former system was not suitable for robot use, due to extensive cabling and lack of couplers.

Sensors

The sensors support each other both in accuracy and range. In this way not only a large sensing field is covered to satisfy the diverging demands of the numerous applications, but also the sensor principles differ, thus increasing the applicability.

As in the former system, the institute's rotating Laser Range Scanner is integrated in the 3D-Modeller. With its high precision in short range and robustness against environment lighting and textures, it is suitable for high-resolution modelling. Its high-view angle is advantageous in robot vision.

The Stereo Vision System is very efficient for textured environments. A stereo sensor acquires large areas of the environment at once. The accuracy is usually low, but the sensor covers a large range. The base distance and the focal length of the lenses of the cameras define the minimal and maximal sensing range. It is desired to cover a range from approximately 250mm up to 2000mm.

The single Laser Stripe Profiler consists of a laser beam that illuminates a stripe on a surface plus a camera that records its reflection. Using a second laser line, perpendicular to the first, yields the Dual Crosshair Profiler using both cameras and lasers alternately. Benefits are no scanning movement constraints and a higher data rate [Suppa *et al.* 2007[c]].

Communication

The communication concept of the 3D-Modeller (Fig. 164) brings together the different control tasks. These tasks are to control the laser modules, active markers and the synchronisation signal generator, to manage a LCD display and an input device as user interface and to establish an interconnection from the 3D-Modeller to the sensor PC.

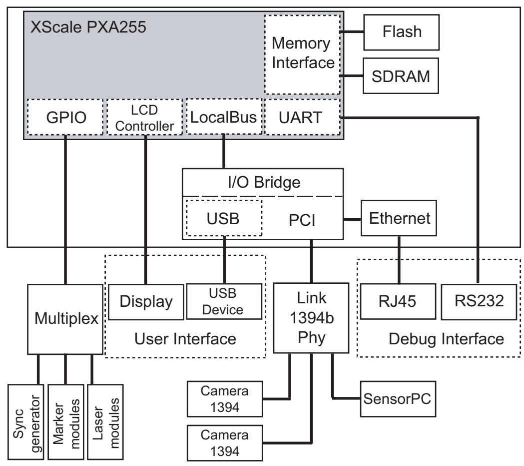

Fig. 164 Communication concept

The Modeller is equipped with an embedded PC running Linux. This architecture provides display control, Firewire interfaces for the cameras as well as external data exchange, active marker and laser control, and a sync generator. Further interfaces such as Ethernet and USB are used for debugging and user interaction purposes (i.e. via handheld). The high integration level leads to only one Firewire 800 connection to the sensor PC transmitting both electric power and data.

Synchronisation and Interfacing

The fusion of multiple range sensors and positioning devices (e.g. robots, tracking systems) for the task of 3-D scanning requires a reliable communication concept that allows for synchronisation and concurrent access to both hardware resources and sensor data.

The former is achieved combining hardware synchronisation clocks with software messages. The latter consists of a primary abstraction layer for common classes of peripherals and a secondary, unified sensor abstraction for generic types of range sensors and pose sensors. The proposed framework has been implemented and tested for the DLR multi-sensory 3D-Modeller. Finally, an implementation on the basis of the DLR multi-sensory 3D-Modeller is introduced and applications are identified. The concept is extendable to other range sensors [Bodenmüller *et al.* 2007[c]].

4.2.2 Sensor Calibration

The geometric reconstruction achieved with the 3D-Modeller is based on sensors that work on the principle of triangulation. For these sensors to work accurately, the estimation of their own geometric structure plays a pivotal role. The process of accurately estimating the geometric structure of sensors given an adequate sensor model is within the reach of competence of calibration algorithms.

Camera Calibration

For our purposes, camera calibration cannot be performed following traditional photogrammetric approaches. Therefore, new approaches had to be developed to master the problem. In our Institute different shortcomings were identified in camera calibration approaches for computer vision, and eventually fixed [Strobl & Hirzinger 2006[c], 2008[c]]. In addition, a camera calibration toolbox was developed in order to both simplify camera calibration and maximise accuracy. The toolbox is freely available on the internet for non-commercial purposes.

The Camera Calibration Toolbox CalDe and CalLab were developed in order to provide a platform independent application. The procedures for features detection were detached from the parameters estimation application. The former task is performed by the program CalDe, whereas the latter task is exclusively performed by CalLab.

CalDe: The detection toolbox CalDe serves the need for localising landmarks/corners on a chessboard-like 2-D calibration panel with sub-pixel accuracy. Finally, files containing the correspondences between the landmarks of the calibration object and their (stereo) image coordinates may be produced. These are the starting points for CalLab. In contrast to the vast majority of similar free available toolboxes, here the operation is fully automatic. Additionally, the calibration pattern no longer has to be fully visible within the images. Implications are twofold: First, the calibration of the lens distortion, too, in the peripheral regions of the image is enabled. Secondly, it facilitates the calibration of stereo-cameras and eye-in-hand or eye-to-hand systems, since partially visible patterns suffice for calibration.

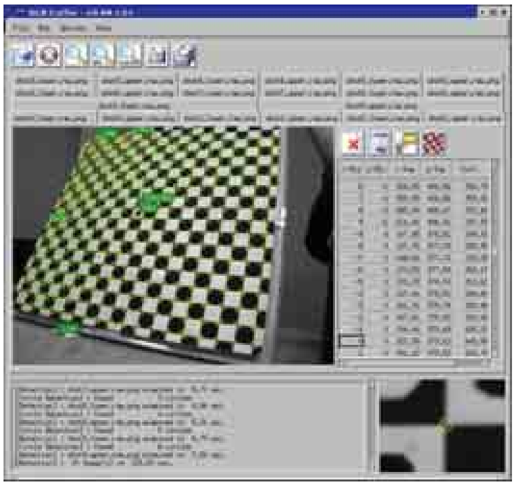

Fig. 165 GUI of CalDe

CalLab: DLR CalLab estimates both the intrinsic and extrinsic parameters of either a single camera or a stereo-camera based on previously detected image features (e.g. from DLR CalDe).

Intrinsic parameters describe the perspective projection, the lens and sensor distortions, and the digitisation process [Strobl & Hirzinger 2008[c]]. These define the nonlinear transformation between coordinates in the camera frame. In the case of a stereo-camera calibration, the rigid-body transformation(s) between cameras might also be considered as an intrinsic parameter of the stereo-camera.

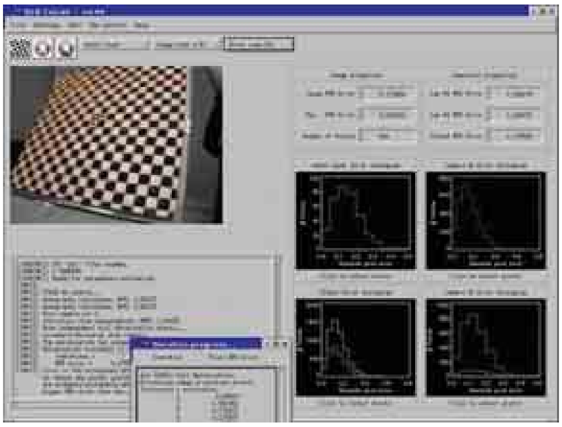

Fig. 166 GUI of CalLab

Extrinsic parameters describe the rigid-body transformations between the (main) camera frame and either the world frame or the Tool Centre Point (TCP) frame. The former transformation changes at different instances (camera stations), whereas the latter remains constant as long as the camera(s) remain rigidly attached to the TCP. For the camera to TCP calibration (generally known as hand-eye calibration) several previously stated methods, as well as the novel one presented in [Strobl & Hirzinger 2006[c]] were implemented.

Range Calibration of Laser Sensors

At the Institute a self-calibration approach for estimating the geometry of active laser triangulation sensors (e.g. the Laser-Range Scanner or the Laser Stripe Profiler) has been developed. The procedure requires little work and, most importantly, yields very accurate results. Self-calibration is performed by measuring a planar surface with adequate scanning movements and refining the structure parameters by flattening the resulting 3-D point cloud.

Range Calibration of Time-of-Flight Sensors

Time-of-Flight cameras (ToF-cameras) provide a monochromatic image allowing for classical image processing algorithms and additionally measure distances for all pixels. Thereto, the observed scene is illuminated with modulated infrared light. The reflected light features a phase delay which is detected within the pixels and directly translated into a distance value. Thus, the ToF-camera provides depth information of dynamic or static scenes at video frame rate, irrespective of the object's texture. These properties allow for a wide range of applications.

Depth measurements with ToF-cameras are characterised by systematic and unsystematic errors. Due to the complex electronic measuring principle, the measured distances depend on exposure time and reflectivity of the observed objects. The understanding of these errors and the development of appropriate error models are main research topics in order to improve the ToF-camera in terms of a measurement device.

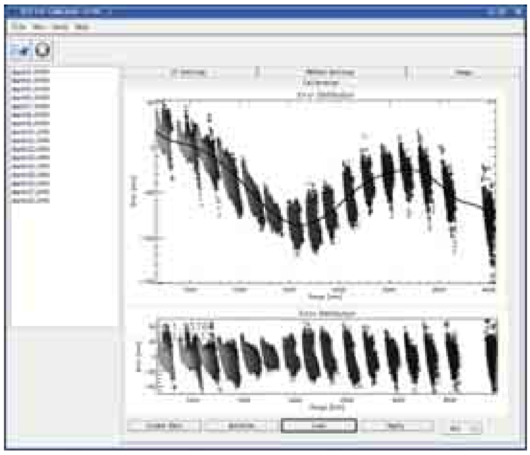

Fig. 167 Screenshot of the ToF-camera calibration GUI for identifying the depth measurement errors

There are three significant non-systematic errors. First, a bad signal-to-noise ratio distorts the measurement and cannot be suppressed. The solution is either to carefully increase the exposure time and to amplify the illumination respectively or to filter the measured values that are marked with low amplitudes. Second, the so-called multiple ways reflection occurs in concave objects, e.g. corners or hollows. Here, the remitted near-infrared (NIR) signal is superposed by NIR light that has travelled a longer distance. Third, light scattering of close objects influences the depth measurement of pixels that belong to far distant objects. The latter two effects are unpredictable, since the topology of the observed scene is unknown a priori.

Furthermore, there are four systematic errors. First, there is a distance-related error (also called wiggling error or circular error) stemming from the asymmetric response of a NIR-LED-signal. This asymmetric response causes a non-harmonic sinusoidal illumination of the scene. Since a harmonic sinusoidal illumination is the basic assumption in the principle of modulation interferometry, the computed phase-delay and distance respectively are inaccurate. Second, due to non-linearities of the semiconductor and its imperfect separation properties, a different number of photons at a constant distance cause different distance measurements. This so-called amplitude-related error also depends on the actual distance. Third, there is a latency-related error. Since the emitted and remitted signals are correlated at the sensor array directly, different latencies for every pixel have to be considered. Finally, there is a fixed pattern noise (FPN) that comes along with the latency-related error. FPN is related to latencies and different material properties in each CMOS-gate. Thus, a constant pixel offset for each pixel can be identified.

These four systematic errors are manageable by an appropriate calibration. The manufacturers of ToF-cameras encounter these problems only partially with different calibration procedures. The used calibration methods are costly because the entire working range is taken into account although many users only run the camera within a limited working range.

For this reason, we improved the camera calibration methods in order to calibrate the ToF-camera in a common manner regarding the intrinsic and extrinsic parameters. Furthermore, we have investigated the depth measurement errors and thus developed a new procedure for a depth calibration. This depth calibration procedure is primarily appropriate for ToF-cameras attached to a robot (but also for non-robotic applications) and integrated into a GUI (see Fig. 167). As a result the accuracy of ToF-camera measurements is increased accompanied with only marginally higher effort since the depth calibration is performed almost concurrently with the intrinsic and extrinsic calibration [Fuchs & Hirzinger 2008[c]].

4.2.3 Self-Positioning from Images

In order to gain complete models of the objects, it is required to see the object from different vantage points. For this reason it is common to use an external positioning system (e.g., a robotic manipulator or a tracking system).

Fig. 168 Features for monocular navigation

However, this conventional approach is inconvenient for either hand-guided scanning operation or unconstrained robotic operation. The application area of the scanner is restricted to the range of the external positioning system and a change of the workspace yields cumbersome transport and calibration work. Further, the errors of both algorithms, the one for the localisation and the one for the 3-D reconstruction, correlate. In addition, the system's cost becomes primarily determined by the external positioning system, which in reality is accessory to 3-D modelling. For this reason it was decided to conduct research on algorithms for visual positioning of the 3D-Modeller using the same images acquired by its own stereo-camera for 3-D modelling. This information will only be useful if these positioning estimations are of very high accuracy and are calculated in real-time. Our work on accurate system calibration laid the basis for accurate pose estimation from images.

Fig. 169 (right) Real putto, (left) 3-D point cloud of the putto

Having real-time capability in mind, the algorithm was extended for sequential mapping. The resulting system is a world-wide novelty by providing accurate positioning data in real-time while scanning the object with complementary sensors at the same time.

4.2.4 Accurate Stereo Reconstruction

Images capture two spatial dimensions of three dimensional scenes. The third dimension (i.e. depth) can be recovered from two or more images of the same scene, taken from spatially different viewpoints. This is done by automatically determining corresponding points using stereo matching methods and triangulating them by using the pre-calibrated intrinsic and measured extrinsic camera geometry.

Stereo matching is an inherently ill-posed problem without a unique solution. There is a lot of research activity world-wide, which concentrates on either local or global stereo methods. Local methods are typically fast and suitable for real-time applications, but have a low quality, e.g. blurred object boundaries, etc. Global methods are much more accurate, especially at object boundaries, but slow and memory intensive and therefore not suitable for most practical problems.

Semi-Global Matching

The Semi-Global Matching (SGM) has been developed [Hirschmüller 2005[c], 2006[c], 2008[j]] for accurate, pixel-wise matching. It attempts the minimisation of a global cost function along one dimensional paths, which go in all directions through the image and are joined at each pixel. This can be done quite efficiently. Similar to local methods, SGM is complemented by a left-right consistency check, sub-pixel disparity estimation and post-filtering. Multi view matching is also possible.

The SGM algorithm is based on minimising a global cost function with a data and a smoothness term. The data term computes pixelwise matching using Mutual Information for being robust against a wide range of radiometric distortions. The smoothness term adds a penalty for all pixels with neighbours that have a different disparity. The goal of stereo matching is to find the disparity image that minimises this global cost function. The implemented algorithm includes a consistency check and blunder elimination. Sub-pixel accuracy is achieved be applying quadratic interpolation. SGM works with image pairs. If more than two images are available, pairwise matching and subsequent median filtering is executed in order to determine disparity values robustly from redundant measurements. High-resolution images are processed by sub-dividing one data set into small patches. Geo-referencing is implemented by projection into a suited coordinate system. Orthophotos can be calculated using the 3-D surface model as well as the interior calibration and exterior positions and orientations by common mapping procedures. Sec. II.2.2.4 illustrates results of the SGM matching. Even steep slopes (e.g., walls of buildings) are reconstructed exactly and small details are preserved. This is due to the pixelwise matching as used by SGM.

The quality of SGM disparity images is as high as disparity images from global stereo methods, but SGM is several magnitudes faster than most global methods. Its complexity is the same as that of a local, correlation based method (i.e. linear to the number of pixels and the disparity range). An ongoing on-line evaluation of stereo methods (vision.middlebury.edu/stereo) shows that SGM can compete with the best global methods. Additionally, its efficiency makes it very attractive for using it in practice.

Radiometric Insensitive Matching Costs

The comparison of pixels of different images requires the consideration of radiometric differences (e.g. different brightness, noise, etc). These differences are caused by the cameras due to slightly different settings, the vignetting effect, image noise, etc. Further differences may be caused by non-Lambertian surfaces, for which the amount of reflected light depends on the viewing angle. Another source of radiometric differences is that the positions or strength of the light sources may change when images are acquired at different times. For larger scenes, image acquisition will take some time and it may not be possible to control the light source (e.g., the sun outdoors).

It is important to note that some, but not all causes of radiometric differences can be pre-calibrated. Therefore, matching should be done tolerant to radiometric differences. An extensive evaluation of 15 different stereo matching costs in combination with a local, a global stereo method and SGM on ten stereo image pairs with ground truth and simulated and real radiometric changes has been done [Hirschmüller & Scharstein 2007[c]]. It showed that matching with Mutual Information, Census and background subtraction using a bilateral filter are quite effective for handling even large radiometric differences. Furthermore, these costs are also best on images with very little or apparently no radiometric differences. This study allows the selection of appropriate matching costs for practical applications.

Real-Time Semi-Global Matching

The hierarchical SGM algorithm with Mutual Information as matching cost is efficient, but a software implementation on a PC is still too slow for most real-time applications. A rectified VGA image (i.e. 640x480 pixel resolution) with 128 pixel disparity range can be processed in about 3.5s on a 2.66MHz Xeon PC.

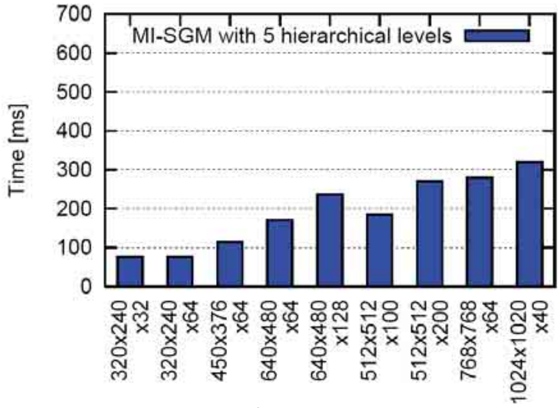

Fig. 170 Run times of the GPU implementation on a NVIDIA GeForce 8800 ULTRA

Modern graphics cards offer massive by parallel processing power. They have now become flexible enough for general purpose processing. Hierarchical SGM with Mutual Information (MI) as matching cost has been implemented in OpenGL/Cg. This implementation can compute VGA images with 128 pixel disparity range in just 237ms, including the transfer time between main memory of the computer and the graphics card [Ernst & Hirschmüller 2008[c]]. This is 4.2 frames per second, which is almost 15 times faster than the CPU implementation and already sufficient for some real-time applications. The current graphics card implementation is suitable for images up to 1024x1020 pixels.

Higher frame rates can currently only be achieved by hardware implementations. An FPGA implementation is currently under development. The goal is 25 frames per second of VGA sized images. The computation of the matching costs can be performed by Census or Mutual Information. However, the FPGA implementation uses Census, because it is better suited for a FPGA implementation. The advantage of a FPGA implementation is not only a high frame rate, but making stereo processing independent from a desktop or laptop computer. Furthermore, there are certified FPGAs for extreme temperature and radiation environments, e.g. for space applications.

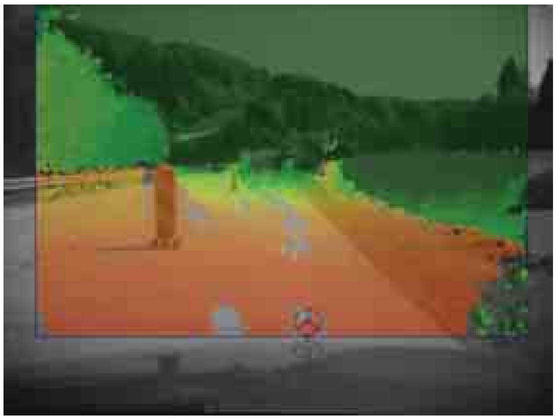

Fig. 171 The first Mercedes cars drive with a real-time distance map as driver assistance system based on the SGM algorithm

The Environment Perception Group at Daimler AG in Böblingen has independently developed a FPGA implementation of SGM that works on quarter VGA images (i.e. 320x240 pixel resolution). The system is currently tested in cars for supporting various driver assistance tasks. This indicates the current industrial interest in the SGM method for real-time applications.

3-D Modelling from Image Sequences

Aerial or space images are taken from well defined viewpoints and directions. This directly supports fusion into a 2.5-D orthographic model. However, real 3-D models cannot be created using this recording geometry.

Current work includes stereo matching and fusion of image sequences taken along an almost arbitrary path. This allows full 3-D modelling. However, it requires the generalisation of the underlying geometric models and the development of an appropriate error model. The currently developed fusion strategy eliminates or reduces errors by utilising image and matching information from all available viewpoints.

Applications include hand held modelling of small statues, etc as well as automatic environmental modelling from driving, crawling and flying robots (e.g., octocopter).

Fig. 172 3-D Model from a stereo image sequence using the stereo camera of the hand held 3D-Modeller around a model of Neuschwanstein castle

Fig. 173 Textured 3-D model

4.2.5 Surface Reconstruction from 3-D Live Streams

The challenge in surface reconstruction of range data directly from a sensor's real time stream is that in general no a priori knowledge concerning the shape or the size of the surface is available and the data from the stream is not spatially ordered. Moreover, new data has to be integrated dynamically and fast by extending and refining the existing surface model incrementally. Further, the sampling of the surface is not necessarily homogeneous or at least sufficient in some regions, due to the manual movement of the device. Especially for devices that allow full 6-DoF motion, a uniform movement of the device is difficult for a human operator. Here, the challenge is on the one hand to detect undersampled regions or faulty measurements and not to integrate these data into the surface model until more sample points are added. On the other hand, one wants to generate a coarse surface approximation as early as possible and refine it consecutively with new sample points.

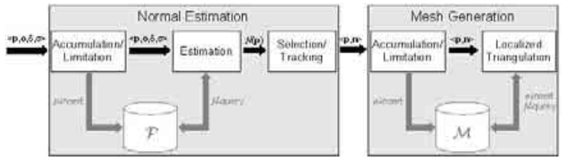

Fig. 174 Reconstruction pipeline

The developed surface reconstruction method meets these challenges. It is based on the approach by Bodenmüller, but major improvements have been made. The goal of our reconstruction approach is to generate successively a single triangle mesh (which approximates the unknown, measured surface) by incrementally inserting 3-D points from a live stream that is generated by a 3-D scanner. The approach can be described as a process chain, as shown in Fig. 174.

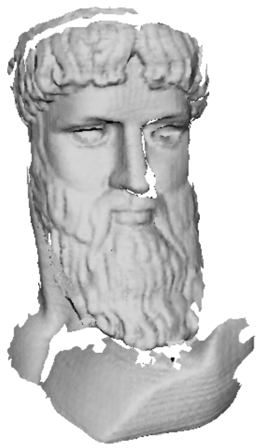

Fig. 175 Surface model of a Zeus bust. The data was acquired using a laser-stripe profiler.

The incoming stream data is assumed to consist of a coordinate, an orientation, a resolution, and a deviation as described in the previous chapter. This point data is received in the normal estimation stage at the Accumulation and Limitation step and stored in a suitable data structure. The point density is moreover limited here, so that the computational effort in successive stages will be bounded. In the successive Surface Normal Update influenced points are identified and the respective surface normals are re-estimated. Finally, at the Selection and Tracking module the previously estimated normals are validated and rejected if not feasible. Additionally, changes in the direction of the estimated normals are tracked and notified to successive stages.

The outgoing stream of points, each with corresponding surface normal, is now passed to the mesh generation stage. Here, the points are again accumulated and limited. The stored points represent the vertices of the growing mesh that is generated and refined in the Localised Triangulation. The result is shown in Fig. 175.

4.2.6 Feature-Based Global Registration of Homogeneous Triangle Meshes

When generating complete 3-D models from sensory data, a common problem is the acquisition of the object's backside or downside. Then, parts of the object are generated as separate meshes, i.e. surface models.

A feature based algorithm is used in order to estimate the transformation between two surface models of the same object, assuming a rigid motion transformation. The used surface models are homogeneous triangle meshes, merely curvature-based features are used.

The algorithm allows for fast global registration of slightly overlapping surface models, even overlaps of about 25% can be handled. The use of features has two purposes: data reduction and finding of correspondences. The algorithm even holds for inhomogeneous triangle meshes or point clouds, if appropriate feature points can be calculated. It has been applied for patient registration in medical robotics and in reconstruction of surface models in the field of cultural heritage and industrial robotics.

Outline of the Algorithm:

- calculation of a (scalar or multidimensional) feature for each vertex and assignment of feature classes;
- calculation of a histogram of the features. Removal of all points with high occurrence in this histogram;
- assignment of corresponding points based on the feature classes;
- search for the best rotation: calculation of all possible translations between corresponding points for each rotation (of a discretised space of rotations). The correct rotation is given by the largest cluster in this set of translations;
- refinement of estimation with Iterative-Closest-Point Algorithm.

Fig. 176 Work piece (left) and its complete textured 3-D model (right)

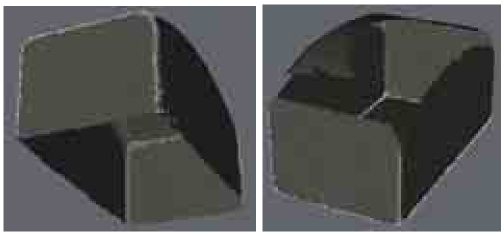

Fig. 177 Incomplete surface models and reduced feature points (white)

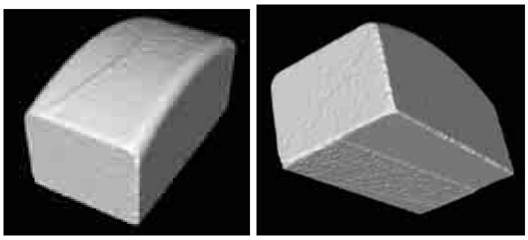

Fig. 178 Complete surface model after registration and re-meshing

In Fig. 176 to Fig. 178, the generation of a complete surface model of a wooden work piece (Fig. 176, left picture) for an SME is shown. After registration of the two incomplete original models (Fig. 177), the raw point clouds calculated from sensor measurements are transformed correspondingly and re-meshed (Fig. 178). As post processing step hole-filling [Liu R. *et al*. 2007b[c]] and texture-mapping are performed, resulting in a complete textured 3-D surface model (Fig. 176, right picture). The complete process has been published in [Hirzinger *et al.* 2005[c]].

4.2.7 Multi-Scan Registration for Building Interiors

For the 3-D reconstruction of interiors of historic buildings, we apply a marker-free automatic registration approach to align different views together, because GPS does not work indoors and the placement of markers is not allowed. We use the automatic matching process [Liu & Hirzinger 2005a[c]], which employs a novel algorithm, Dynamic Matching Tree technique, for a fast and stable coarse-matching to achieve the automatic pre-alignment of two point clouds and uses modified ICP to do a fine matching efficiently.

The whole process is divided into three consecutive steps:

1. Preprocessing: In this stage, we segment each point cloud. Then, we use a form descriptor to generate corresponding segment-pairs. By the characteristics of the surfaces, the model in one view is segmented into diverse objects. Here, the difference between normal vectors between adjacent points is treated as segmenting criteria. If the difference between the normal of two neighbouring points is large, the boundary between two objects will be set through here.
2. 2-View Matching: A coarse-to-fine matching process is applied, which consists of two steps: The coarse matching solves the pre-alignment problem, using a novel algorithm, denoted "Dynamic Matching Tree (DMT)". In the following fine matching, two views are aligned using the ICP algorithm.
3. Fine Matching: After the fine two-view matching, all the scans are in a common coordinate system. We generate the corresponding point pairs of the multiple views, and make a bundle adjustment to homogenise all point clouds.

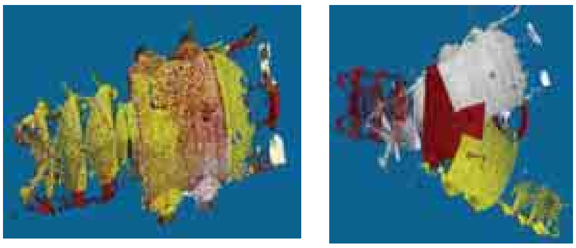

Fig. 179 Registration process: scans before registration (left) and after registration (right)

In Fig. 179 the result of registration is shown for the Seefeld church. The method has been used in various applications [Liu *et al*. 2005a[c], 2007c[c]].

4.2.8 Offline Scene Reconstruction

A generation of photorealistic models requires accurate capture of geometry and real textures. Thereby, a common problem is to gain coloured panoramic 3-D data, which is highly accurate and has a high resolution. Aligned colour and range data is the basis for subsequent modelling tasks, e.g. textured surface generation [Hirzinger *et al.* 2005[c]] or 3-D object recognition.

We apply a multi sensor calibration and registration to yield highly accurate and robust coloured panoramic 3-D data. To achieve this, we use a panoramic 2.5-D laser scanner in combination with a colour camera and an electronic spirit-level. The calibration and registration software suite was developed and designed by the laser scanner manufacturer Zoller+Fröhlich in close cooperation with DLR. It has advantages compared to many camera-only based approaches commonly used today, concerning efficiency, robustness, and computational effort.

Fig. 180 Panoramic image of the Seefeld church interior

The spatial resolution of the scanner we use (Z+F Imager 5006) is dense and requires high precision for sensor calibration and for the registration of geometry and colour. For capturing the colour data, two different types of sensors are used.

Either, we mount an array camera on a vertical tilt unit: overlapping colour images are acquired by rotating the entire system horizontally and the tilt unit vertically by predefined angle increments.

Alternatively, we use a high resolution line-camera, the DLR-MFC (Fig. 180). It was originally developed in our institute for space missions and has the advantage that we only need to acquire one single image. In this case, the scanner and the camera are not used as a combined system, but as two independent sensors.

For stabilising the registration between these viewpoints, an electronic spirit-level is used to compensate the horizontal tilt of the system. This increases the automation of the approach in various field scenarios.

In our approach, the registration between the sensors is based on corresponding points between the data sets: in our cooperation with Z+F, we developed automated feature-based matching methods which focus on the multi-modal characteristics of the data. Afterwards, we used the registered colour images, to colourise the geometry. Here, we use a *z*-buffering technique which is optimised for fast processing of huge data sets at low memory consumption.

Fig. 181 3-D model of the working room at castle Neuschwanstein. Left: model with grey scale textures based on laser reflectance. Right: model with coloured textures acquired with a digital camera

Our framework already was applied in a broad variety of scenarios: Within the scope of the project "Virtuelles Bayern" initiated by our institute, we already successfully applied the system on cultural heritage sites, e.g. castle Neuschwanstein (Fig. 181) and the monastery church of Andechs.

4.2.9 2.5-D Modelling from Aerial and Space Images

The SGM method has originally been developed for 2.5-D terrain and city modelling from aerial images. This is done by fusing the matching results of all images into a digital elevation model (DEM). Thereafter, the images are used for computing a true ortho-image as well as tilted views for texturing the model from all sides [Hirschmüller 2008[i]]. All processing steps are fully automatic.

The methods have been implemented on a processing cluster that consists currently of 66 CPU's in different configurations (e.g. dual core workstations or blade systems). The cluster has already processed terrestrial terrain models and ortho-images of almost 40,000km^2 in resolutions of 5-25cm/pixel. Most of the data has been captured in 15-20cm/pixel by the terrestrial version of the High Resolution Stereo Camera (HRSC) [Hirschmüller *et al.* 2005[c]] that has been developed at the Institute of Planetary Research (DLR) and is used on-board the ESA Mars Express probe.

Fig. 182 Mountain "Zugspitze" in Bavaria, captured by HRSC in 20 cm/Pixel

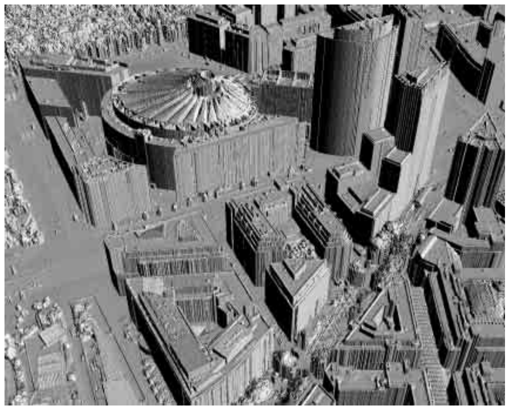

Fig. 183 DEM of Berlin, captured by UltraCam in 7cm/Pixel

Fig. 184 Automatically textured DEM of Berlin in 7cm using UltraCam data (Sony Center)

HRSC is a multi-line pushbroom camera. Equally, data from other aerial pushbroom cameras like the ADS 40 from Leica (originally developed at our department Optical Information Systems in Berlin) and the new MFC (developed from the same group) have been successfully processed. Furthermore, aerial high resolution full frame images like Vexcels UltraCam are regularly processed with the same methods (Fig. 184).

Finally, it has been shown [Hirschmüller *et al.* 2006[c]] that modelling of Martian terrain from HRSC images of Mars Express equally results in high quality models.

4.2.10 Active Localisation

Localisation of robots in a known environment is the problem of finding the robot's pose in its environment model, represented by a map. If the robot acts autonomously, we talk about active localisation.

Navigation is the planning and execution of movements in a known or unknown environment.

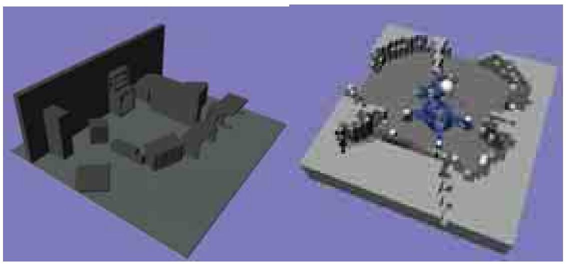

Fig. 185 The voxel-maps used for localisation. Left: the global map the robot has to localise in. Right: the local map used for active localisation, exploration, path planning and collision avoidance.

We use a particle filter resulting in a Monte-Carlo localisation approach for active localisation. The global map is 3-D, the unknown state consists of the robot's 2-D position and orientation. For the JUSTIN platform (Sec. IIII.2.3), four time-of-flight (ToF) cameras provide depth measurements to gather information about the robot's vicinity.

Surface models as well as volume models for the global map can be handled as they are internally converted into a voxel map representation (Fig. 185, left picture). Following the goal of fully autonomously localising and navigating a local 3-D map of the robot's vicinity is calculated by means of the 3-D depth measurements (Fig. 185, right picture). This allows for intelligent exploration strategies, path planning and collision avoidance. The map building process presented in section III.4.2.12 is used, employing a Fuzzy-Update method [Suppa 2008[t]].

Outline of the localisation algorithm:

1. Get the last odometry reading and resample the particles accordingly;
2. Perform depth measurements with the four sensors, i.e. ToF cameras;
3. Update the local map with Fuzzy-Update. Weight new particles by their Gaussian depth measurement likelihood;
4. Resample particles by their weights;
5. Check if localisation is achieved by making use of the particles covariance. Plan and execute next movement and return to step 2, if localisation is not achieved.

The algorithm has been successfully applied on the mobile robot platform JUSTIN. In Fig. 185 and Fig. 187 the application of actively localising and navigating the platform to a table in order to execute some manipulation tasks is depicted.

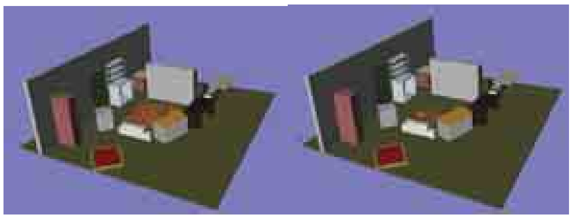

Fig. 186 Progress in localisation and navigation to the destination area. Left: Initially the particles are spread throughout the space. Right: convergence of the particle distribution in progress.

Initially the particles are spread over the entire map (Fig. 186, left picture). After some iteration the distribution quickly converges to the correct state of the robot. When convergence is achieved (Fig. 186, right picture) navigation to the destination area in front of the table is performed using both global and local map. The particle distribution at the destination is shown in Fig. 187, the corresponding local map in Fig. 185, right picture.

While navigating to the destination, the localisation is concurrently updated in order to guarantee correction of pose errors due to wrong odometry readings or inconsistencies in the global map.

After successful navigation to the destination area, a tracking method (Sec. III.4.1) is used to accurately reposition and park the platform at a destined pose relative to the table.

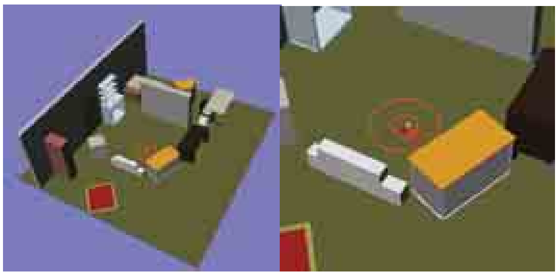

Fig. 187 The robot has reached its destination. Converged particles in the destination area, the corresponding local map is shown in Fig. 185, right picture.

4.2.11 Visual Navigation and SLAM

Mobile robots are being developed for servicing tasks, hazardous environment as well as space applications. Many mobile robotics researchers use simplifying assumptions, such as moving on absolutely planar ground, which is acceptable for urban environments, but not for natural terrains as found on other planetary bodies.

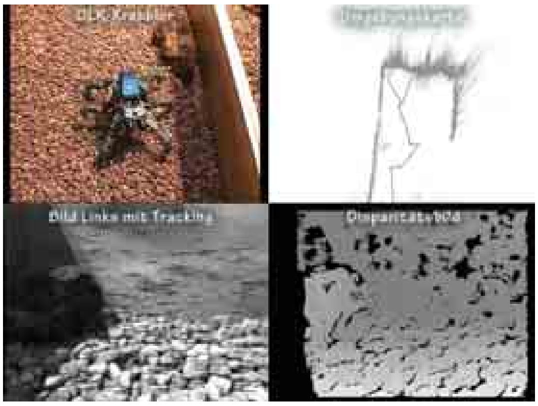

Fig. 188 Real-time stereo processing, ego-motion estimation and mapping on the DLR crawler

The own movement of the robot (i.e. ego-motion) could be tracked by a wheel or leg based odometry. However, there is typically a lot of slip in natural environments. Furthermore, the robot needs to perceive its environment three dimensionally for accomplishing certain tasks. Therefore, a calibrated stereo camera is used. A fast, correlation based stereo method computes a depth image. Based on this information, a stereo camera based ego-motion method determines corresponding points between consecutive frames and computes the camera motion with six degrees of freedom. This works robustly, even for large camera motions between frames (e.g. low frame-rate). Both information (i.e. the sequence of depth images and motion) is fused into a fuzzy logic based environment map for higher level processing [Görner *et al.* 2008[c]].

Since the ego-motion computation is purely incremental, a drift is unavoidable. This is compensated by a particle filter based Simultaneous Location and Mapping method (SLAM). The method corrects the ego-motion and consistently closes loops if it detects that it has reached a place where it has been before.

These steps are complemented by a path planning algorithm for uneven terrain. It uses the depth image and the ego-motion information for creating a 2.5-D elevation model. Then, the terrain is classified according to steepness and space considerations. This forms the base for a modified D* algorithm that computes the path with the lowest cost for reaching a predefined goal (e.g. reaching a certain coordinate or going into a certain direction).

A visual navigation system including sensor fusion with a low cost IMU has been developed by our colleagues from the University of Stuttgart in the context of the autonomous airship ALUSTRA (Sec. III.6.2).

4.2.12 Robot Work Space Exploration

In most applications, the full knowledge of the environment is not available to the robot. Therefore, the lack of information must be compensated by sensing operations, i.e. exploration. As sensing requires motion and measurement cost, an optimisation on the sensing locations is performed.

The research focuses on sensor-based approaches to robotic exploration of partly unknown environments. Aiming at facilitating automated work processes in flexible work cells, an efficient and reliable task-dependent exploration is performed by integration of flexible sensor systems, probabilistic environment representations, view and motion planning designed to acquire a maximum amount of knowledge while using a minimal number of view points, and the fusion of information. Safety for motion planning is achieved by multi-sensory data acquisition. The methods and sensors are evaluated in 3-D simulations. Experiments for exploration of work space (Fig. 189), regions of interest in physical space, and combined missions are successfully performed. The methods, considering environment uncertainty in the planning process, enable flexible information gain-driven missions such as view planning for object recognition or grasp planning.

Fig. 189 Robotic work cell: Red blocks denote regions of high information gain. The greyscale values depict the occupancy state.

The exploration of partially known environments, enabling a robotic system to act autonomously [Suppa 2008[t]] requires knowledge of: mechatronics, computer graphics, computer vision, and motion planning, to name a few. Various approaches cover subsets of the entire problem. Our work follows an integrated consolidation:

- the approach (method and implementation) combines imprecise sensing in sensor-based exploration in physical space (under consideration of work space constraints) with a general view planning in physical space, verified in real experiments;
- the sensor data is fused in maps. A comparison of map update methods for 3-D occupancy grids in multi-scale representations is performed;
- uncertain information on the physical space is used for weakening the ideal sensing assumption towards planning with uncertainty, while in computational geometry these methods assume ideal sensing;
- a general measure of information based on entropy is developed, serving as a task-specific driving force for exploration, fusing physical and work space exploration into a common framework;
- design criteria for the development of versatile exploration sensors are defined, which enable robots with complex geometry and kinematics to identify safe-for-motion regions under presence of uncertain sensing. Requirements for exploration of the work space in combination with task-specific goals are considered, resulting in the development of a multi-purpose vision platform. Thus, the autonomous operation of robots in flexible work cells is enabled.

These developments have been partially published at international conferences and in journals: Parts of the synchronisation concept and calibration are published in [Bodenmüller *et al.* 2007[c] ; Suppa *et al*. 2007[c]]. The consideration of noise in the planning stage of motion planning in 2-D environments is presented in [Suppa 2008[t]]. Multi-sensory exploration is addressed in [Suppa & Hirzinger 2005[j]].

In [Suppa & Hirzinger 2007[j]] the application of the approach to flexible work cells is extensively discussed.

4.3 Force and Touch Sensing

Humans use their perceptional abilities of touch excessively, when they are exploring or manipulating objects. This sub-skill is often referred to as "perception-by-touch". The haptic sense of the human is divided into proprioception and tactility.

Robots, which interact with humans and/or have humanlike abilities, also need the sensorial equipment to feel the environment. We therefore have been developing and using force and torque sensors in our robots for a long time. Like in human beings force and touch sensing uses various different sensors to perceive the interaction between the robot and its environment.

The kinesthesia or proprioception, which refers to the force interaction, is measured by the internal torque sensors and external 6-D force sensors in the fingertips and/or the wrist of the robot arm.

The tactile impression is detected by artificial skin, which is under development (see below).

Design of Stiff Force/Torque Sensors

With the experience of the former developed stiff force/torque sensors design principles for the measurement body have been stated. One mayor weakness of an integrated wrist sensor is the mechanical coupling between the sensor and the robot, which conveys disturbances from the robot. This implies that electronics and cables are mounted on the fixed part of the measurement body. Furthermore the mechanical joint between the beam bendings and the screw holes should be thin enough to protect the measurement body against stresses forced while tightening the screws.

In the FEM design of the measurement body the focus lies on symmetrical distribution of the strains, to allow the use of full bridges. In general a four-spoke architecture, if sufficient space is available, outscores a design with three spokes, which is sufficient for a 6-DoF force/torque measurement. The overdetermined system of the four-spoke sensor allows reducing the coupled error of the strain gauges measurements. Furthermore manufacturing process can be simplified, if all strain gauges are mounted in one plane.

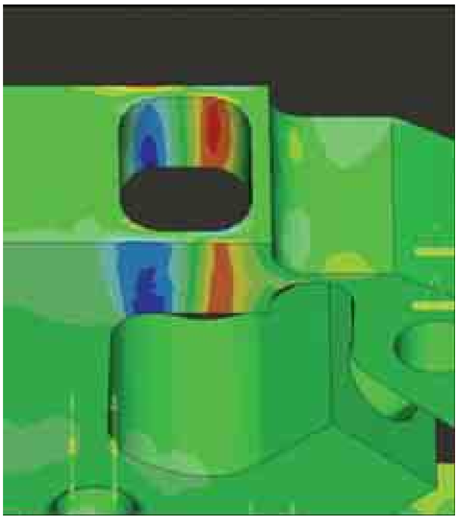

Fig. 190 FEM analysis of measurement body

The length of the spokes and the resulting dimension of the sensor are responsible for the ratio between force and torque - longer spokes allow better distinguishing between force and torque. The decision has to be taken according to the application of the sensor.

Improved Implementation of Wrist Sensor

Following these design principles an improved body of the DLR wrist force/torque sensor has been implemented together with new version of the integrated electronics. As a result the influence of external disturbances, e.g. ripple of the gearbox, has been significantly reduced and the force/torque resolution increased. On side of the electronics the analogue part has been enhanced to increase the signal-to-noise ratio, which results in a higher accuracy of the sensor.

The communication between the sensor and the control systems has been accelerated by use of the EtherCAT protocol to cope with the requirements of fast control loops for reactive behaviour. Additionally the power consumption has been optimised, such that the sensor can be supplied through the Ethernet connection via PoE (Power over Ethernet).

Calibration of Force/Torque Sensors

The calibration procedure of the force/torque sensors has been optimised and automated. A standard industrial robot serves as handling device to generate a well defined load on the sensor along its axis. A Matlab/Simulink program controls the robot and automatically collects the signals of the strain gauges. The resulting calibration matrix is calculated and optimised from this data by an algorithm. So the calibration is finished in less than an hour and several sensors can be calibrated in parallel.

Artificial Skin

For the evaluation of the artificial skin patches (see Sec. III.2.5) we used a calibration approach based on learning methods. In an early stage, a simple, 2-layer feed-forward neural network was used for interpreting the values from the skin readout system. We used four different objects to apply force to the skin patch with the goal of classifying them correctly. Forces were applied using a spherical, cylindrical, conical, and a 4-point indenter. The neural network was trained using two sets for each indenter and then tested with other two sets for the same indenters in a sequence (spherical, cylindrical, conical, and a 4-point indenter).

The neural network was able to classify the 8 sets correctly. The skin was indented two times successively by the same indenter in a sequence specified above. This concluded that the shape (geometry) of the indenter was correctly classified using simple neural networks.

Similar indenting experiments were done also in a real-time system. A recurrent neural network was modelled with an objective of classifying different indenting position on the skin patch independent of the type of indenter. Readings were obtained at 5 different positions on the skin patch using 3 indenters by applying repetitive force of 5N. We were able to classify the indentations at different positions correctly with an accuracy of about 98%.

Fig. 191 Indenting the artificial skin with different indentors (top) lead to clearly distinguishable readouts (bottom)

Thus the skin, along with the neural network, classified different geometries and positions. In the future, this approach will be used in future for classifying different forces (magnitude and direction) along with movements.

5 Telerobotics and Telepresence

In telerobotics, a human operator commands a remote robot (so-called teleoperator) e.g. in outer space. The separation of robot and human operator may occur due to spatial distance, hazardous environmental conditions, scaling, or even matter for virtual environments. Hence, human high-level cognitive processes are decoupled from the physical execution by the robot, and technical means are needed to overcome this separation [Niemeyer *et al.* 2008[b]].

In telerobotics, the human is part of the control loop. Depending on the abstraction of the human commands and the time delay in the communication link, two modes can be distinguished: supervisory (or shared) control and telepresence. In telepresence, the human operator will immerse into the remote environment and control the teleoperator on a motion/force level. By means of a multimodal (vision, audio, haptic) human machine interface (HMI) the human perceives and acts as in the real world. The main channels are (stereo-)visual and haptic feedback. On the other side, an operator using supervisory control gives gross commands, which are refined in local control loops by the robotic system. With an increasing level of shared autonomy on the telerobotic system the operator can use higher command languages, even voice commands to operate the remote systems. This increasing autonomy requires motion and task planning abilities of the robot.

Supervisory control can also provide an immersive virtual environment, which is updated to the real one by sensor information and in which the user can pre-simulate the real robot actions. For physical immersion into a remote or virtual environment a key feature is haptic user interaction, including suitable devices, control aspects, and rendering [Preusche & Hirzinger 2007[j]].

5.1 Haptic User Interaction – a Key Element in Telepresence

This chapter deals with three important topics of haptic user interaction: haptic feedback devices, stability analysis, and algorithms for haptic rendering.

5.1.1 Haptic Feedback Devices

Haptic devices for both kinaesthetic and tactile feedback, as required for immersive multimodal HMI, have been developed at the Institute, including end-effectors for connecting the human arm to the device, and encountered-type haptic displays.

Kinesthetic Feedback

The DLR Light-Weight Robot (LWR) is well suited for human-robot interaction, as described in Sec. III.3.4. Due to its properties—it is equipped with torque sensors in each joint, its workspace is fairly similar to that of a human arm, and a control rate of 1kHz allows for a highly dynamic behaviour—the LWR is well suited as a haptic interaction device [Hulin *et al.* 2008b[c]].

In order to generate kinaesthetic feedback to both human hands, a human-scale bimanual haptic interface, consisting of two LWR that are horizontally attached to a column, has been created (see Fig. 192). Two sectional drawings of the workspace are shown in Fig. 193.

Fig. 192 Human-scale bimanual haptic interface

The spheres represent possible end-effector positions in the overlapping workspaces of the two LWR. At each position, three dimensional orientations of the end-effector are checked for reachability [Zacharias *et al.* 2007[c]]. Blue spheres mark points at which the robot can reach more than 75% of all possible three dimensional orientations, whereas red spheres mark points with less than 8% reachability, respectively.

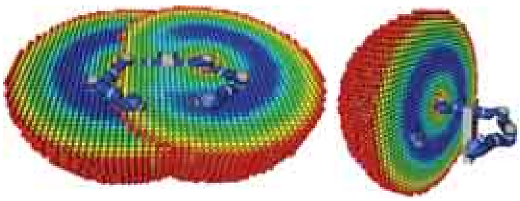

Fig. 193 Sectional drawings of the workspace

Connecting the Robots to Humans

Three different interfaces that connect the robot to the human hand have been developed [Hulin *et al.* 2008b[c]]: a magnetic clutch, a grasping force controller and a joystick handle. All these devices can be attached to the robot by a quick tool changing system.

The magnetic clutch attaches the human hand in a way that fingers are free to move (Fig. 194, left). Therefore, this interface can be used in combination with a tactile finger feedback device or a finger-tracking device.

Fig. 194 Magnetic clutch (left), grasping-force interface (middle) and joystick handle (right)

The geometry of the clutch, the arrangement of the magnets and their strength define the holding force and torque. The current version is able to transmit forces up to about 100N and torques up to approximately 10Nm. If the applied forces or torques exceed these values, the user gets detached from the robot and the integrated emergency stop circuit is disconnected so that the robot is stopped immediately for safety reasons.

Our grasping force controller is a one-dimensional actuated haptic interface, which is operated by a human using the forefinger (Fig. 194, middle). This additional DoF can be used to control the grasping force in a virtual reality simulation, to explore virtual objects, or to control a multi-DoF device such as the DLR Hand-II [Wimböck *et al.* 2006[c]].

The joystick handle (Fig. 194, right) is equipped with a mini joystick, a switch, and several buttons, including a deadman function, enabling the user to change parameters online, including those of haptic interaction, telemanipulation, visualisation, or VR simulation.

Encountered–Type Haptic Device

The specific characteristic of this type of haptic device is that no end-effector needs to be held permanently by the human. Rather than using an in-between medium (as the joystick grip) for manipulating, the user's hand "encounters" and gets in contact with a grasping primitive attached to the robot end-effector, which renders the remote/virtual environment. Thus, in free environment situations, the device tracks the human hand maintaining a short gap between the primitive and the hand, allowing movements without perceiving any resistance. In contact situations the human hand gets in contact with the grip-primitive, rendering thus the virtual/remote solid environment.

This type of device can achieve more immersive systems compared to conventional Held-Type devices. In Held-Type devices the user is constrained to the use of a tool, such as a joystick-like end-effector, which he permanently holds for manipulating and interacting with a given virtual or remote environment tool. However, this sort of interaction is sometimes not very intuitive and poses constraints in the manipulation dynamics, which decreases the immersion of the human operator.

Fig. 195 DLR encountered-type haptic device

The DLR Encountered-Type haptic device [Bellana 2007[r]] uses the DLR LWR-III to drive a 15cm platform as end-effector primitive, which the user contacts to render remote and virtual walls with high stiffness (see Fig. 195). Further, a controller switching mechanism allows switching between admittance mode, which is convenient for the free environment, and impedance, which allows better stiffness definition.

Tactile Feedback

To increase immersion and to obtain a more intuitive impression of a virtual scenario, all the mentioned interfaces can be used in combination with a vibro-tactile feedback device [Schätzle 2006[r]; Hulin *et al.* 2007[c]] for haptic feedback to the forearm, shown in Fig. 196.

Twelve motor groups can be controlled independently in intensity of vibration [Schätzle 2006[r]] to display position and strength of collisions within VR environments or to display information from telepresence applications.

Fig. 196 Vibro-tactile feedback device

5.1.2 Control and Stability of Haptic Interaction

In order to assure a safe and realistic feedback with the presented devices, the overall haptic system must be stable. Most theoretical approaches presented in the past dealing with ensuring stability for haptic interfaces are passivity-based approaches. Although ensuring passivity of haptic devices is a valid approach for telemanipulation, it has the disadvantages of being conservative for haptic rendering in terms of stability and of requiring the presence of mechanical damping.

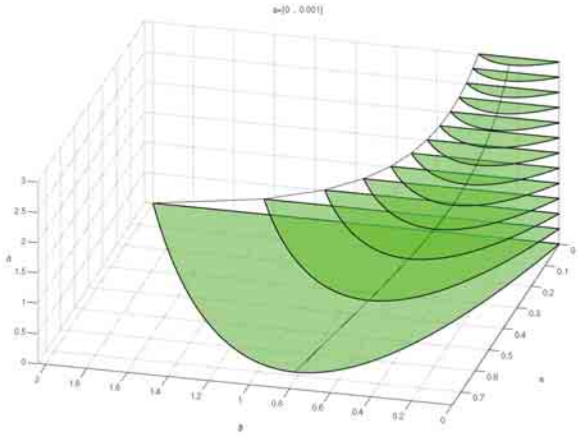

Fig. 197 Stable regions in a three dimensional parameter space

In order to be able to optimally control haptic devices, the relation of the parameters of a haptic system must be well understood. Therefore, a detailed stability analysis has been performed, investigating the parameters of a haptic device and those of the virtual world [Hulin *et al.* 2006b[c]]. Time-delay has been also considered as a parameter. Due to normalisation rules, generic stability boundaries for haptic rendering could be obtained (see Fig. 197).

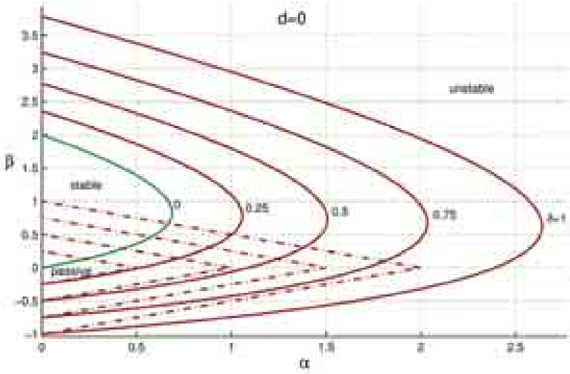

Fig. 198 The passive regions are sub-regions inside the stable ones

A more general research investigates the influence of the haptic device's damping [Hulin *et al.* 2006c[c]], yielding a relation between passive and stable regions (see Fig. 198). Moreover, this has been the basis for an easy-to-use linear stability condition, which allows setting the parameters of the virtual world such that the system is stable [Gil *et al.* 2007[c]]. An experimental study proves that this condition and the stability boundaries hold well for real systems [Hulin *et al.* 2006a[c]].

The influence of a human operator, who is holding a haptic device, as illustrated in Fig. 199, has been investigated in [Hulin *et al*. 2008a[c]]. This research shows the impact of the human arm on the stability of a haptic system. It also proves that the linear stability condition is not affected by the human arm. In addition, this work gives an explanation of why the passivity condition for haptic rendering is conservative in terms of stability: the stiffness of the human arm is bounded, while the passivity condition remains valid even for infinite stiffness.

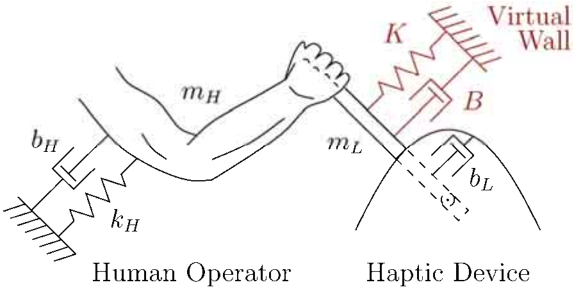

Fig. 199 Simplified model of a human arm interacting with a 1-DoF haptic device

5.1.3 Haptic Rendering

Including the haptic modality in applications like virtual assembly verification or training of mechanics (see Sec. III.5.4) improves considerably the efficiency of such tasks.

Haptic rendering algorithms detect collisions between virtual objects and compute appropriate collision forces in order to feed back haptic information to the user via a haptic device. A fast and constant update rate of at least 1kHz is necessary to achieve immersive systems with realistic contact sensations.

Voxmap-PointShell Algorithm

The used haptic rendering algorithm is an adapted version of the Voxmap-PointShell (VPS) Algorithm [Otterbach 2005[r]; Hulin *et al.* 2005[c]; Sargadia 2008[r]; Sargadia *et al.* 2008[c]]. The VPS algorithm allows to detect collisions and to compute collision forces between virtual objects at a constant sampling rate, even for arbitrarily complex virtual scenarios. Furthermore, it can be used for VR scenarios with two moving objects, as enabled by the bimanual kinaesthetic device [Hulin *et al.* 2008b[c]].

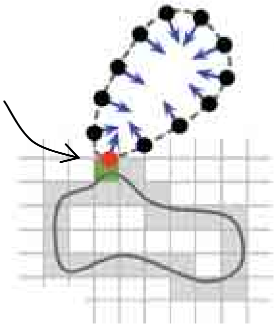

Fig. 200 Voxmap-PointShell Algorithm: when a point of the dynamic object collides with a surface-voxel of the static object a collision force is computed

Two data-structures are used to compute collision responses [Sargadia 2008[r]]: voxmaps and pointshells, as shown in Fig. 200 and Fig. 201. Voxmaps are voxelised volume structures representing the static part of the virtual environment. Pointshells, on the other side, represent dynamic or moving objects through clouds of points; each point is located on the surface of the polygonal model and possesses a normal vector pointing inwards the object. Using these vectors, determining the direction of the collision forces is possible.

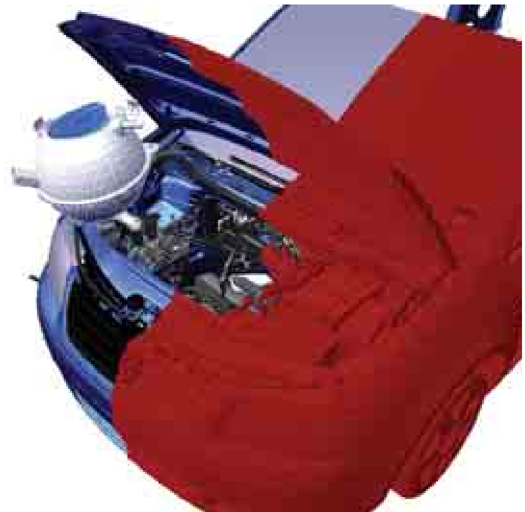

Fig. 201 A coolant tank (with pointshell-points on its surface) is assembled inside the car (half of it visualised with surface-voxels, that form the voxmap structure)

These haptic data-structures must be generated, i.e., the voxmap and the pointshell. Both data-structures are generated offline from the polygonal models that are used for visualisation. The new algorithms, developed at the Institute, generate the data-structures much faster and more accurately than previous algorithms [Sagardia 2008[r]; Sargadia *et al.* 2008[c]]. For instance, models like the car in Fig. 201, with more than three million triangles, can be voxelised in less than eight minutes, whereas previous algorithms required almost three hours to obtain structures even with lower quality values on the same computer.

As shown in Fig. 200, every time a point is inside a surface-voxel, a single collision is detected. For each colliding point a corresponding single collision force is computed immediately using the normal vectors and the penetration of the colliding point. Finally, all the collision forces summed together yield the total repulsion force.

5.2 Telepresence

As afore described, enable telepresence systems humans to interact directly with remote environments. Developing such complex systems requires infrastructures for communication and control as well as advanced control strategies and novel evaluating criteria.

Within a multimodal telepresence system there is a lot of data exchange, as most components located at the human machine interface (HMI) require data from the teleoperator and the other way round. Some components require data from other components at the same site to achieve a high fidelity system, like an aural feedback requires the head position.

On a higher layer, the design encompasses the so-called real-time control. This is responsible for stability and performance of both, master and slave robots. The software must allow engineers to build local and distributed complex control schemes for any hardware device and to easily manage those [Artigas *et al.* 2006[b]]. A real-time operative system and a flexible and modular methodology are determinant underlying factors for the system design.

A distributed control loop incorporating human operators and possibly large delays requires advanced control strategies, as well as novel evaluation criteria.

The Institute's advances herein are described in the following.

5.2.1 Communication Infrastructure

To be able to integrate a new component, or even to exchange a whole subsystem, without the need of a complete redesign of the overall system, a framework to define interfaces is required. Using such a framework, all available data can be distributed into different streams, to which all components can connect to. To exchange data between teleoperator and HMI these streams are multiplexed and de-multiplexed into and from two single data streams, a reliable but slow and an unreliable but fast one, in each direction.

A typical example of exchanging a complete subsystem, in this case the haptical part of the HMI is shown in Fig. 202. The robotic hand arm system is teleoperated in the first case by using an optical tracking system and tactile feedback, described in [Hulin *et al.* 2007[c]] and in the second case using a LWR to command the remote robotic arm and a grasping force controller [Hulin 2008b[c]] to command the robotic hand. In the first case the only feedback is a tactile feedback at the fingertips of the human operator, in the second case the human operator gets full haptic feedback from the arm and a one dimensional grasping force from the grasping force controller.

Fig. 202 Teleoperating a robotic hand arm system using an optical tracking system and a tactile feedback

If the component does not provide vital data to the telepresence system, it can be plugged into the system or removed, without any further effort. A typical example for this kind of enhancement would be auditive feedback.

For the Institute's telepresence system, as described later on [Artigas *et al.* 2006a[c]], the communication is implemented as standard IP traffic (TCP for the reliable channel and UDP for the unreliable one). Therefore, the connection is realised using local network, or if the components are separated, using the Internet or even satellite links. To provide a variety of possible realistic communication channels, an emulator is employed. It is based upon the implementation of a satellite link simulator, described in [Schroth 2006[r]] with computed satellite link parameters derived in [Schroth *et al.* 2007[c]]. This emulator is able to compensate for the jitter introduced using unreliable connections, as well as add time delay and packet loss.

5.2.2 Control Infrastructure

Control methods are nowadays tightly related to soft computing techniques. From this relationship a new area in software engineering has emerged, which explores the interplay between control theory and software engineering worlds. In [Artigas *et al.* 2006[b]] a software architecture for robotic and telerobotic applications, which supports the real-time control, is presented. The software is device independent and distributed control oriented. The architecture allows designers to easily build complex control schemes for any hardware devices, easily control and manage them, and communicate with other devices with a plug-in/-out modular concept. The need to create a platform where control engineers could freely implement their algorithms, without needing to worry about the device driver and programming related issues, further motivated this project.

The core of the so called DIMSART consists of a dynamic data base surrounded by a frame and modules. The frame contains the communication and interface with the hardware device, i.e. the driver. The modules are atomic routines which contain control algorithms. Both communicate through the data base, an element which stores static and dynamic information of each module and frame. During the real-time operation an engine schedules the calls of each active module, which in turn executes the different algorithms which implement the real-time control task. Fig. 203 shows a block diagram of the DIMSART overview. Furthermore, in a higher layer, a Graphical User Interface (GUI) has been developed to configure the specific robotic control scheme.

This architecture has been used in the ROKVISS experiment [Preusche *et al.* 2006[c]], and signifies the core of the bilateral control for both, master device and slave robot.

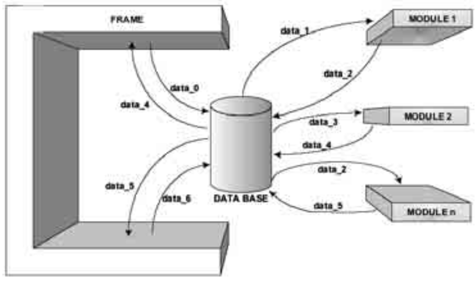

Fig. 203 DIMSART Concept Diagram

5.2.3 Bilateral Control

Bilateral Control is the discipline which investigates the closed haptic loop created between the human operator and the remote/unreachable environment. Special control methods are hereby applied in order to stabilise a closed loop, whose communication delay, package loss, unavoidable nonlinearities, and the inclusion of a human operator in the control loop make it especially challenging to tackle.

Besides stability, the main goal of a telepresence system is transparency, meaning ideally that the user is not able to distinguish remote presence from local presence. The pursuit of stability often compromises transparency once the system constraints are established. This trade-off is a common denominator in every single approach dealing with bilateral control. Further, it signifies one of the main research areas within the telepresence framework at the Institute. In this sense, one of the most accounted issues in haptic telemanipulation scenarios is the aforementioned time delay present in the communication channel. This often forces to design conservative control laws in order to achieve unconditional system stability, which in turn often results in system transparency losses.

Fig. 204 shows a general network representation of the haptic channel of a telepresence system. It can be seen how the human operator is part of the system and thus becomes energetically coupled to the remote environment through a master haptic device and slave robot. Further, master and slave controllers connect both sides, i.e., the bilateral control together with the communication channel.

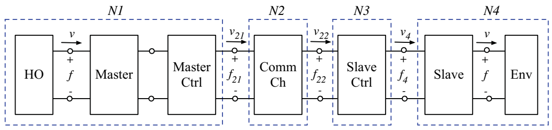

Fig. 204 General network diagram of a telepresence system

Among the most remarkable approaches in dealing with time-delayed telepresence, are those based on passivity criteria. The appeal of passivity-based approaches is the property that system passivity (and therefore, stability) is granted by passivity of its subsystems. Passivity can be proved without the need of precise modelling the analysed system. Thus, it is a useful tool to study a system where some of its elements are difficult to model or unknown, i.e. the human operator, the remote environment, and the communication channel. In particular, the communication channel can be active due to the inclusion of time delay, and the generated energy must be dissipated using some specific techniques such as Wave Variables-based methods or the novel Time Domain Passivity approach, which are both gaining appeal and acceptance within the international community [Artigas & Preusche 2005[c]].

Wave Variables–Based Methods for Varying Time Delay and Package Loss

By using the electrical-mechanical analogy, the wave variables transformation uses the power conjugated variables of force and velocity to define wave variables, the same way voltages and currents are related to energy waves in transmission lines. A *wavy* system has the interesting feature that passivity is preserved even though time delay incurred by the data to travel from one point to the other. Thus, the two-port network created by a communication channel with time delay described in terms of wave variables is a passive system, which will therefore, not compromise stability for any amount of constant time delay. However, real communication channels have been shown to be variable in regard to the time delay magnitude, and highly dependent on the communication medium, which in turn introduces a non negligible package loss. Within the scope of the telepresence subdivision, the Institute has put special emphasis upon these two issues, which are fundamental for the real implementation of haptic telepresence missions, and has extended this method to make it feasible for time-varying and package loss scenarios [Hosseini *et al.* 2008[c]].

Bilateral Passivity Controller and Energy Transfer

The Time Domain Passivity (TDP) approach provides the mean to analyse passivity in real-time (as opposed to the Wave Variable approach based on the frequency domain), and bases its control on the real-time observability of the system energy. Thereby, passivity is no longer a design constraint which fixes controller rules (and thus compromising transparency), but rather an on-the-fly observation and correction of passivity of the system [Ryu *et al.* 2005[j]].

Originally thought as a method for making virtual environments passive, the Institute has contributed and extended this novel method to the time delayed telepresence context [Artigas *et al.* 2006b[c], 2007[c]], tolerating varying time delay as well as package loss. By placing the so-called forward and backward passivity controllers (FPC and BPC) at each side of the communication channel, the system created by these three elements becomes a passive network. Another approach under research is the passive control of the energy flow in the communication channel, which separately observes and controls the transmitted energy in the forward and backward direction [Ryu *et al.* 2005[j]].

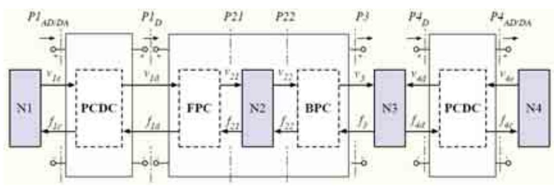

Fig. 205 Network representation of Bilateral Passivity Controller-based architecture

In [Artigas *et al.* 2008[c]], the previous methods are extended to introduce the concept of Bilateral Energy Transfer, to convey the energy introduced in the master side robot toward the slave robot (and vice versa), as accurately as possible, with regard to the system passivity. Thus, two main characteristics are sought in the design of the control architecture: To limit unneeded energy dissipation and to convey the energy, even in the presence of unavoidable transmission delay (Fig. 205).

5.2.4 Transparency Measurement

Measuring performance becomes a tricky aspect in haptic contexts since human perception is part of the system.

Only a few studies on this matter are reported in the literature. The authors of [Radi *et al.* 2008[b]; Stoll *et al.* 2008[j]] investigate and extend two methods which aim at determining a quantitative transparency coefficient: an analytical model-based method and an empirical approach based on the Z-width concept, which allows to measure transparency without the need of precise knowledge about the system. The methods are validated using a velocity-force haptic telepresence system testing for different control parameters and different time delays in the communication channel, as can be seen in Fig. 207.

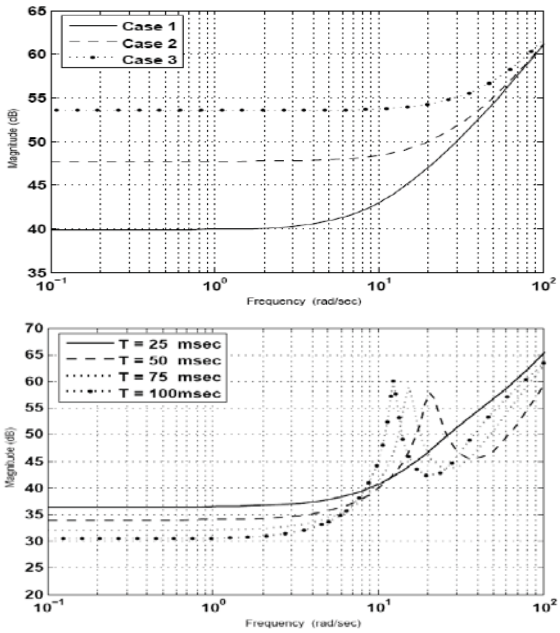

Fig. 206 Different transparency measurements for (top) different control parameters cases and (bottom) different communication time delays

Furthermore, psycho-physical evaluation using expertise from psychologists was conducted to measure the cognitive impact upon an array of sixty test people who had to actively perform as human operator for telemanipulating the OOS testbed (Sec. III.5.4.1).

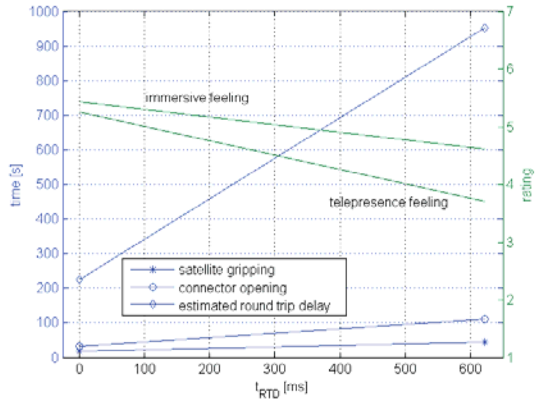

Fig. 207 Psychophysiological transparency measurement

The analysis evaluated several factors of the system, but it mainly aimed at determining a psycho-physical transparency coefficient as a function of bilateral control parameters and the communication time delay. Further, this research investigated the question about which amount of communication delay is tolerable for executing the telemanipulation task. The conclusion resulted in telepresence being feasible up to delays of 650ms (see Fig. 207).

5.3 Telerobotics

Telerobotic systems, in contrast or in combination to telepresence systems, are implemented if the delay is too large to include the human operator directly into the control loop or if the task can be performed semi-autonomously, i.e. the teleoperator acts according to its pre- or tele-programmed behaviour and the operator supervises the task execution. The elements for this operation mode are a virtual world, which is updated with real sensor readings, a programming-by-demonstration interface and a shared autonomy functionality.

5.3.1 Task-Oriented Programming

Since 1996 the AOP ("Aufgabenorientiertes Programmiersystem"), developed as key element for our telerobotic concepts, has been used for almost all demonstration scenarios and applications where control methods and higher level tasks had to be programmed. The system is used for:

- the ROTEX workcell;
- the Experimental Servicing Satellite demonstrator;

- the Japanese ETS VII robot;
- the Canadian Space Station Manipulator Simulator SSRMS;
- the BallCatcher demonstrator;
- the Robutler Service Robot.

The system has been closely integrated into the Robot Control/Robot Sensor Interface (RC/RSI) which has been the standard robot control software supporting all available robots at that time. The robot control system as well as the AOP was implemented on VxWorks platforms. To keep the systems compatible for the different robots it has been very difficult to introduce new control schemes for the different robots in the institute.

With the upcoming of the two armed "robonaut" systems it was clear that the control and the higher level programming interface must be redesigned in a way that allows much more flexibility.

The main functional design guidelines of the AOP approach, however, have been kept the same:

- decomposition of complex tasks in a set of elementary actions which can be executed autonomously on the robotic system, ideally guided by sensor information;
- the separation of the interfaces for robotic experts and control engineers and the simple and easy to use interfaces for application developers or payload experts in the space robotic environment.

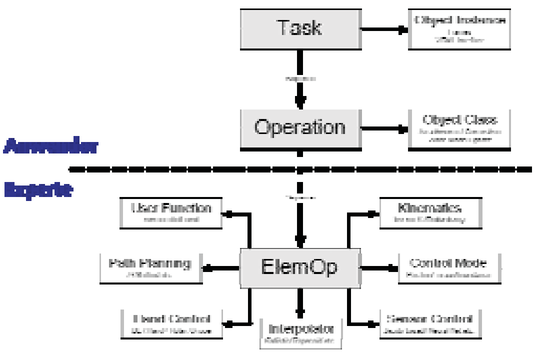

Fig. 208 User and expert level of the AOP and TOP programming environment

Requirements for the New System (TOP)

The system has to be integrated easily in very different and complex robotic systems like in JUSTIN or the envisioned space manipulator for DEOS (MARCO) or for teleoperating multiple robots. It must enable the real-time control of multiple robotic systems. Control strategies for the system have to be changed in a very flexible way. The integration of higher level robotic software components like motion planners or grasp planners, even reasoning components or logical planners should be straightforward.

At last the system should integrate well with the approach of rapid prototyping the control subsystem with Matlab/Simulink and Realtime Workshop.

Architecture and Implementation

The former hierarchical AOP approach has been extended by a stringent modularity at each execution layer: At the control layer Matlab/Simulink in combination with our aRD communication framework (see Sec. IV.1.2) allows a very fast integration of new control algorithms as well as interpolator functions.

Upon this hard real-time layer the TOP kernel is positioned, which autonomously controls and supervises the action planning and execution in soft real-time. Further on, this kernel delivers generic interfaces, e.g. to high-level action planning as well as collision-avoiding path planning algorithms.

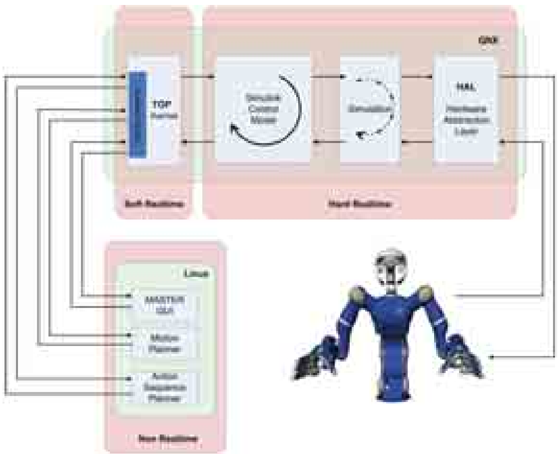

Fig. 209 System architecture of the TOP Environment

On the other hand this modular approach can also integrate easily in the Modular Automation and Robotics Controller Architecture (MARCO). This framework is developed in the context of future on-orbit servicing missions, in which the robotic systems (teleoperator) is part of the satellite payload [Stelzer 2007f]. This teleoperator needs fast data streams to other payload components and to the operator at the ground station.

These real-time data streams can be established by the operator during runtime between subsystems that need a fast and direct data transfer, for details see Chapter II.1.

Available User Interfaces for the TOP Environment

A variety of user interfaces can connect to the TOP kernel via a standardised low-bandwidth communication channel. Until now an easy-to-use GUI—including a graphical motion simulator—and a speech processing system are implemented.

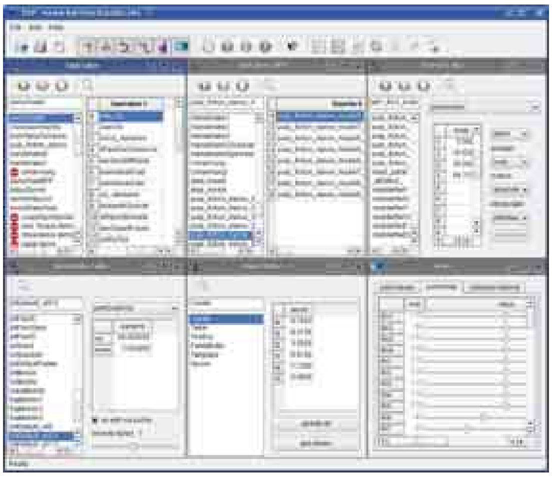

Fig. 210 Qt-based graphical TOP editor

Each user interface, as well as the TOP kernel, uses the same interface structure, based on a standard XML description of all the available actions, and a small aRD-based communication channel. Each of the active user interfaces is notified about the actions of the other ones. So it is possible to install a "supervisor" which can, for instance, stop the ongoing action or act as a FDIR instance.

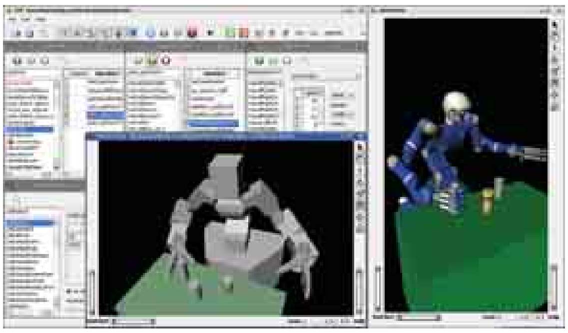

Fig. 211 Motion planning system integrated in the TOP Editor environment

For test purposes, the control module need not to be running with the real hardware behind, but can serve as a pure software simulator with the correct system behaviour.

Concerning an agile software development process, the TOP approach provides the necessary flexibility to make the robot programming cycle much faster and more adaptive than the former AOP system. Of course, all the TOP software modules are written platform-independent, partly based on the open Qt framework, which is also running on most of the common operating systems.

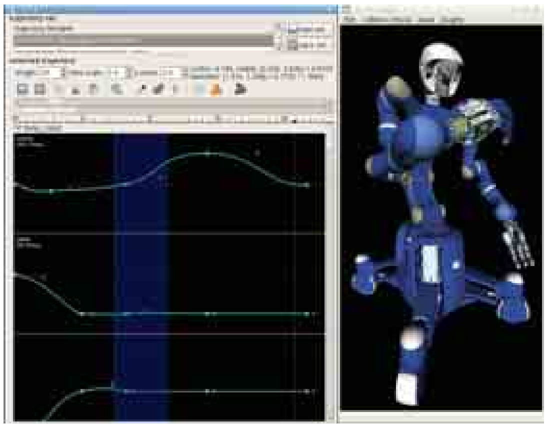

Fig. 212 Trajectory composer with offline integration to the TOP environment

5.3.2 World Model Update

Concerning a teleoperation scenario with different levels of autonomy – in contrast to the telepresence scheme, the teleoperator at the remote site has to cope with unknown or uncertain environments autonomously. At the master side, a virtual environment (world model) is presented, in which the operator can define tasks or operation and pre-simulate operations of the teleoperator. Based on the workspace representations and the simulation, the operator can evaluate the task execution in advance, before commanding the robot. On the other hand, this world model is used for the autonomous functionality of the system.

Updating Geometry of Remote Scene

The basis of the virtual simulation is the geometrical representation of the remote scene. Hereby often the geometry of the objects is known, but the pose has to be continuously determined, or at least once before a manipulation task has to be performed.

Our TOP system delivers a general interface to update the pose of the objects according to the task requirements (one-shot or continuously). All the Cartesian motions w.r.t.

the desired object poses are modified online, e.g., to grasp an object such as a bottle or intercept a free-flying object, such as a ball or a satellite.

The new poses are registered in the TOP data base, as well as shown in the 3-D model simulation for the operator's acceptance.

Fig. 213 World model update of known geometries according to 3-D point cloud

Furthermore, our on-going work will treat the case of fully unknown environments: a powerful combination of multiple sensors (stereo vision, 3-D scanner, force/torque sensor) deliver an amount of information to build a correct 3-D model of the visible objects. After that, sophisticated action [Zacharias *et al.* 2006[c]] and grasp planning algorithms generate a TOP operation, which decomposes the high-level command, e.g. "grasp the object on the left" into the corresponding elementary operations for execution.

Workspace Representations for Grasp- and Task-Planning

Besides the geometric properties of the scene, the workspace and the manipulability of the teleoperator is a limiting factor for the design of a task or operation – human or robot planned. The workspace is constrained by the obstacles in the world and the kinematic structure of the robot itself, which has to be evaluated in 3D, while planning a task or operation.

The obstacle representation developed for the object centred manipulation could be extended to the general 3-D manipulation case. The determination of the grasp region however is restricted to a 2-D reach-to-grasp problem. Therefore we have studied previous approaches on characterising the workspace of robotic arms. The most prominent representation is the manipulability ellipsoid, which describes how agile the robot arm is in a certain configuration. For the grasp and task planning issues, however, this representation does not help too much [Zacharias *et al.* 2007[c]].

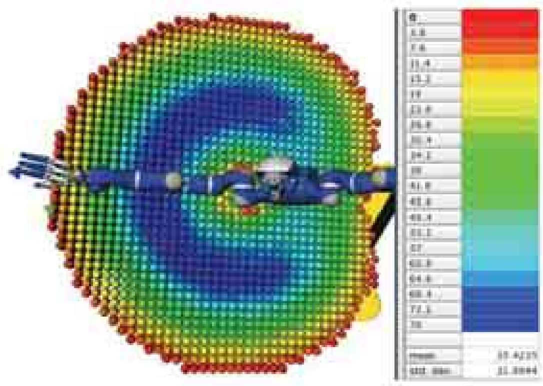

Fig. 214 Shows the reachability spheres across the workspace. The workspace representation was cut for better visibility of the structure.

Basically, one is interested in the size of the workspace and in the directional information on each Cartesian point in the workspace. This addresses the question from where a point in the workspace can be reached, which Cartesian configurations can be reached.

Fig. 215 Shows spheres from the border of the workspace moving inward (top). A close-up shows that the possible approach directions have a structure.

To achieve some insight in the workspace structure we discretised the workspace and calculated the inverse kinematics at each sampled Cartesian configuration. As a first representation we visualise the so-called reachability map. The spheres in Fig. 214 show the reachability in terms of percentage of discrete configurations that can be reached on the surface of the sphere. Blue spheres represent high reachability (max. 78%) and red spheres represent low reachability.

The underlying representation already includes the information that is needed to reason about the direction from where to grasp an object. However, it is not visualised in the reachability map. To directly visualise more of the directional structure of the workspace, we have analysed the directions from where a discrete region in the workspace (represented by a sphere) can be reached. As expected, different regions of the workspace show different structures.

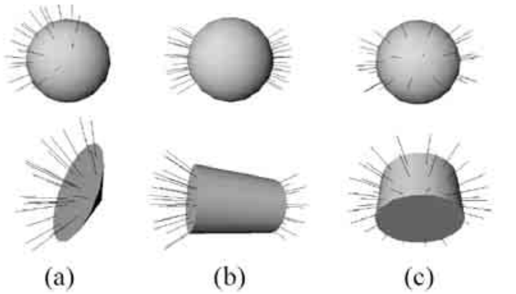

Fig. 216 Cones (a) and two cylinder types (b), (c) to capture structures

The regions on the outer limit of the workspace can be only reached from direction of the robot base, where in contrast the regions near the robot base can only be reached from directions pointing from the outer workspace to the robot base. To get a clear view of the workspace structure, we fit cones and cylinders to the spheres in the workspace. A cone can be reached from any direction of its base, whereas a cylinder can be approached from its shell. Fig. 216 shows the approximation of directional information in geometric primitives.

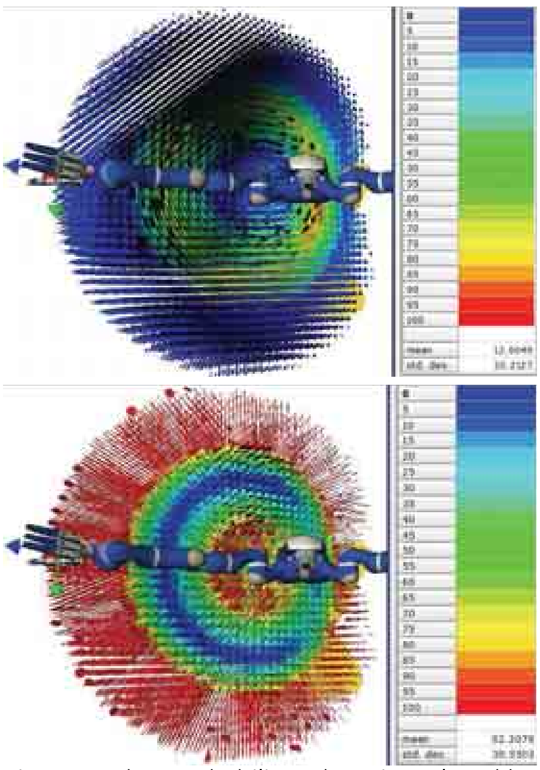

Fig. 217 The reachability sphere is replaced by the best fitting cone (top). The cylinder (type c) replaces the reach ability sphere (bottom). Blue areas mark low approximation errors.

To verify the approximation, we calculate the mean approximation error, which is only 7.2% for the mixed map approximated by cones and cylinders. In each point of the workspace, the best approximating primitive is chosen.

As expected, structure is present in the workspace, which can be visualised and exploited in planning tasks. This representation is called *capability map* as it represents the robot's kinematic capabilities. Having the capability maps at hand, a shared autonomy module can plan operations, such as grasp an object, or paths through the workspace or the human operator can use the visualisation for planning and analysis of tasks and operations.

5.3.3 Programming-by-Demonstration

The approach of tele-sensor programming used in former space teleoperation experiments, e.g. ROTEX or GETEX, is currently extended with a programming-by-demonstration paradigm (PbD). We are following hereby two approaches, including different level of autonomy.

In a first case the operator demonstrates the operations or elementary operations directly in the world model and the teleoperator executes them as close as possible. In PbD the operator demonstrates the task to the robot system directly or via a haptic feedback device in a virtual simulated world (Fig. 218). In this way a shared autonomy approach is implemented, where the operator can direct the robot in an intuitive task related framework. The sensor recordings from the haptic interface produce the sensor patterns, which parameterise the underlying elementary operations. This way generated sequence of operations and elementary operations are commanded to the remote robot for adaption to the remote environment and execution.

Despite the simplicity of the PbD compared to traditional robot programming, there are still certain robotic skills needed to generate suitable robotic programs by demonstration, e.g. respecting the robots capabilities or defining control parameters. Currently methods to support and train the operator to do so are developed [Schmirgel 2007[c]] within the EU project SKILLS.

Fig. 218 Immersive programming-by-demonstration of a robot in the world model

A major problem of such lower level PdB is that the topology of the scene has to be constant within a certain range. If the objects to be manipulated are arranged totally different the approach will fail. An approach which is often referred as programming-by-imitation might help in this case. In this approach a user demonstrates the task like grasp the carafe and pour water into a glass and a task sequencing system tries to segment the demonstration and label the different actions to higher level task descriptions. The robotic system then generates its own action sequences from the task plans learned form the human. Within the EU project DEXMART we try to integrate knowledge of the TU Karlsruhe on imitation learning into our teleoperated execution environment. To allow the robotic system to adapt the higher level task plans to different objects and scene topologies representations have been and are developed to allow reasoning about and parameterisation of planning and execution operations.

5.3.4 Shared Autonomy and Shared Control

Since the ROTEX Experiment, the Institutes' research pursues the idea of increasing the autonomy of robotic systems through the use of sensor information of the environment. At a very low abstraction level this starts sensor phases or skills, which encapsulate feedback control loops based on various sensor data, like laser distance, force and torque sensors as well as camera images. These basic operations can be aggregated to more complex compound operations and tasks. However the intelligence of the whole system is always dominated by human teleoperator which gives the commands (higher or lower level) to the robotic system.

In case of a shared control scenario the human operator delegates some delicate subtasks to the robot's controller to ease the task for the operator. Often a telerobotic scenario contains several sub-tasks, e.g. while capturing a satellite, collision between the servicer and the target satellite have to be avoided. In shared control the robot autonomously controls the distance between the two satellites and the operator controls only the grasping and berthing of the target. The two commands are superimposed to command the AOCS and the teleoperator.

An even more delicate example of the shared control approach comes from the field of minimally invasive robot assisted surgery. The delegated sub-task is the compensation of the beating hearts movement, based on the motion captured by the endoscopic camera inside the patient body [Ortmaier *et al.* 2005[j]]. A local controller superimposes the movement of the beating heart to the operator's motion, such that the heart virtually stands still, see Chapter VII.4 for details [Gröger & Hirzinger 2006a[c]].

5.3.5 Autonomous manipulation planning

For planetary exploration or service robotics on earth, however, the current systems still need too much input from intelligent operators. To further increase the autonomy of the robotic systems higher level planning modules are needed to allow the robot to interpret, reason, plan and parameterise actions itself without human intervention.

Fig. 219 A sample manipulation sequence: JUSTIN prepares instant tea

Task Planning on a Table

Since 2005 we actively work on the integration of grasp and motion planning to allow systems (e.g., our two-armed JUSTIN) to autonomously plan a certain manipulation action, involving a task that must be solved and senor-based scene information, e.g., stereo images. As a sample scenario we use the tea preparation scenario shown in Fig. 219.

In this scenario, the robot should grasp the tea bin, pass it to the second hand, and open the bin. Then some tea is tipped into the glass while the tea bin is held over the glass. Subsequently the bin is placed on the table, the water carafe is grasped and water is poured into the glass.

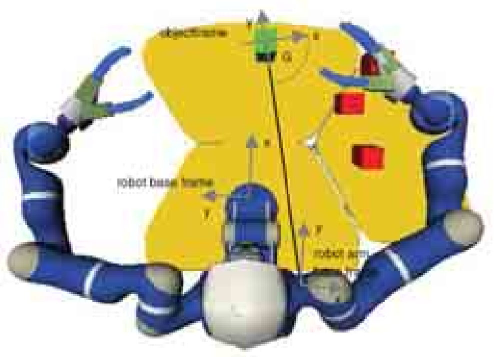

Fig. 220 JUSTIN approaches the green target object. The orientation of the target object frame depends on the robot position

Several motion and grasp planning problems can be studied with this exemplar manipulation. First we have concentrated on the problem of where to grasp an object, dependent on the kinematic constraints of the robot and the geometric constraints of the scene (object location and obstacles). For example, the same grasp on the carafe can be executed from any orientation around its symmetry axis. But which direction is beneficial for the subsequent motion planning operation. In [Zacharias *et al.* 2006[c]] we approach this problem with some heuristics in the 2-D case. Fig. 220 shows the underlying problem.

This problem is affected by the kinematic reachability of the arm and the red-coloured obstacles (other objects) on the desk. An inverse kinematics analysis shows that, for the right arm, the object is only reachable from the right side of the object. From a brute-force calculation of the reachability for objects in the workspace of JUSTIN, we derived a simple heuristic that calculates a circle segment from which the object can be reached (Fig. 221).

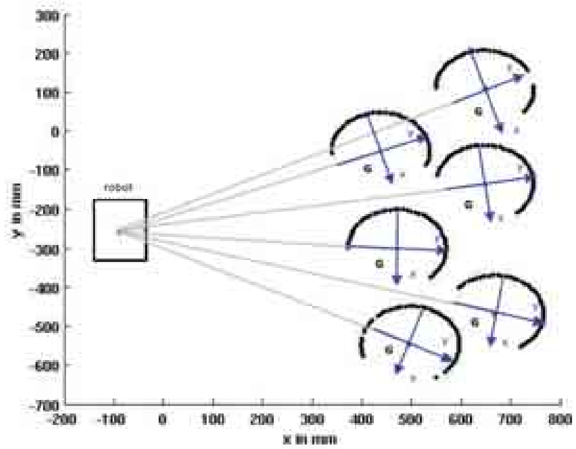

Fig. 221 A scenario where 6 objects are distributed across a table is analysed concerning kinematic reachability. The inverse kinematics is able to find solutions at those locations where to circle has gaps. The object frames (blue) resulting from the heuristic method are sketched into the plot.

To address the influence of obstacles in the scene on the grasping direction a representation for the 2-D case has been developed. This representation is also used to provide information if the scene should possibly be cleaned up before grasping the target object. Each obstacle is represented as a bivariate Gaussian function oriented to the target object. To determine the reachability of the target object a discrete polar histogram around the target object is built which accumulates the Gaussian obstacle representations for a certain approach vector segment. Fig. 222 shows the principle calculation of the polar histogram.

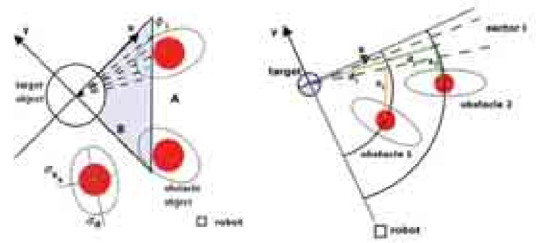

Fig. 222 (left) The region of influence (dashed ellipses) of obstacles (filled red circles) is illustrated. The goal object (empty black circle) is grasped in the shaded region. (right) Computation of the polar histogram in the grasp approach region.

Together with an empirically determined threshold a first task planning component has been developed and tested. As long as the polar histogram of the target object has no segment that is below the determined threshold, the object is considered as blocked by obstacles. To find a sequence to clean up the scene obstacles are to be removed from the desk.

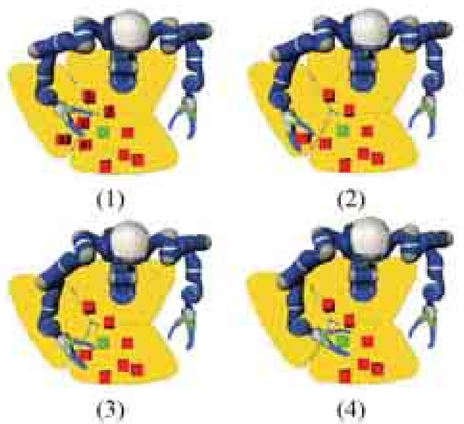

Fig. 223 The green object is to be grasped but is inaccessible. A space is cleared automatically to get to the object.

To determine which object can be removed, the scene is analysed with respect to the influence of object removals on the graspability of the target object. Each obstacle's accessibility is determined by the approach described above. A tree is built to find a sequence of valid obstacle removals. The tree building process stops as soon as the target object becomes accessible by one sequence of object removals. Tree nodes of the class leaf are inserted when the target object becomes accessible.

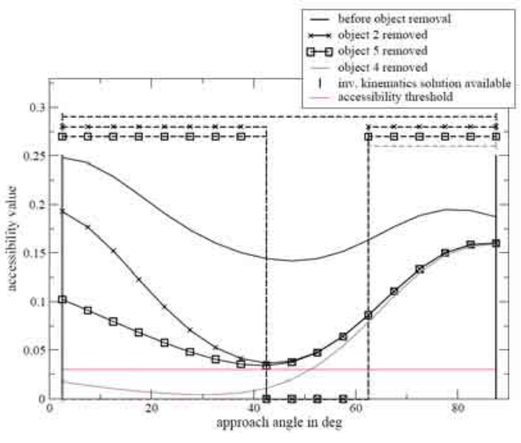

Fig. 224 The accessibility values are plotted across the determined approach angles. The red line represents the accessibility threshold. The black bars mark the area where an inverse kinematics solution is available. The dashed lines visualise if the robot arm would be in collision. Those intervals are free of collision where the dashed line falls to zero.

They terminate a valid solution path. To determine an optimal removal sequence that path to a leaf is searched, that results in a minimum value for the accessibility measure of the target object. Fig. 223 shows a sample scenario where the green object is blocked by some obstacles that are removed in three steps before grasping the target object. The accessibility values for the target object in each step are shown in Fig. 224.

Planning of Constrained Motions within the Arm Workspace

The directional workspace representation can be used to plan constrained manipulation actions. The opening of a drawer for example assumes that a linear constrained motion of at least 30 to 40 cm is possible at a certain position in the robots workspace. If one has a mobile manipulator as a service robot one can use the capability map to plan the position of the mobile base for a certain task [Zacharias *et al*. 2008[c]].

Fig. 225 Different gripper orientations w.r.t. the handle of the drawer. Trajectories lie in a plane perpendicular to the drawer handle.

As the constrained trajectory in the drawer case is in a plane, the corresponding plane in the reachability sphere map can be analysed. If we assume a fixed orientation of the robot gripper to the drawer handle during the execution of the movement we search for a line of spheres in the workspace which can be reached from the same direction. In Fig. 226 such a line of spheres is shown with the desired direction marked red.

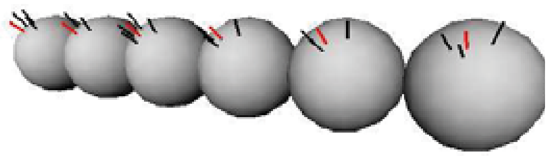

Fig. 226 Neighbouring spheres with the line corresponding to the vector (0,0,-1) coloured red

The search for these connected regions where the same approach directions are possible can be done with image processing algorithms. All possible approach directions in the manipulation plane (for the drawer) are stored as b/w images. The search for the linear opening trajectory is then a simple morphological operation.

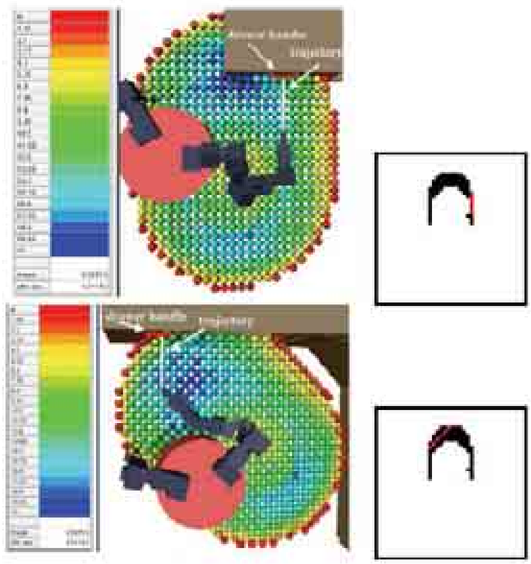

Fig. 227 (left) Trajectory in the robot arm workspace, (right) location of the trajectory in the binary map

Fig. 227 shows two different planned positions for a mobile service robot which allow the execution of the linear motion without moving the platform. The b/w images on the right show the projections of the corresponding reachability sphere map to a single gripper orientation. The red lines mark the desired trajectory found in the workspace representation.

Currently we address the problem of guiding the grasp planner with task and scene representations based on this workspace representation. This will allow the system to decide the sequence of manipulation actions as well as the grasp and motion trajectories fully autonomous.

5.4 Applications and Experiments

Based on the work described in the section before, applications and experiments were implemented and conducted. Those are summarised in the following.

5.4.1 On-Orbit Servicing Demonstrator

A testbed for on orbit servicing was developed [Artigas *et al.* 2006[c]]. It consists of an HMI, a communication simulation, a teleoperator, and a simulated environment. The HMI, depicted in Fig. 228, consists of an LWR-III configured as haptic device with a joystick handle mounted as end-effector, and a head-mounted display which provides the (stereo) visual channel to the user. The teleoperator is built up of an LWR-II with an industrial gripper as end effector and a stereo-camera mounted on a pan-tilt unit. The communication simulation is either an adjustable constant delay or the communication emulator described in Sec. III.5.2.1. The environment simulation consists of a task board mounted on a LWR-II.

Fig. 228 On-Orbit Servicing HMI

Fig. 229 The teleoperator environment, consisting of the teleoperator and the target satellite simulator holding the task board

The LWR-II can be controlled in two modes, the first one being a predetermined trajectory and the second one is according to the movement of a simulated satellite [Schätzle 2007[r]]. In the second mode, a force-torque sensor, mounted in between the task board and the robot, measures the contact forces and torques in the case of colliding teleoperator and task board and reacts according to the simulated satellite. This way, different satellites can be simulated. The teleoperator environment including the task board is depicted in Fig. 229. On this task board different assembly tasks can be accomplished, like changing cable connections as well as opening and closing the door. Capturing the simulated satellite is possible using the handle on the lower end of the task board.

5.4.2 ARTEMIS Experiment

The DLR On-Orbit Satellite Servicing (OOS) Telepresence Testbed, located in the Telepresence Laboratory, was used during this experiment to communicate master and slave robots through a geostationary satellite [Stoll *et al.* 2008[i]]. This involved the LRT ground station in Garching, Germany and the ESA ground station in Redu, Belgium. Both were connected via the geostationary ESA data relay satellite ARTEMIS, whereas operator and teleoperator were located on ground. The feasibility of telepresent OOS was evaluated, using the previous mentioned control architectures and different communication setups. The respective manipulation task was representative for OOS and supported real time feedback from the haptic-visual workspace with a mean time delay of 650ms. The tests showed that complex manipulations tasks, necessary for OOS operations, can be fulfilled by using geostationary data relay satellites (Fig. 230).

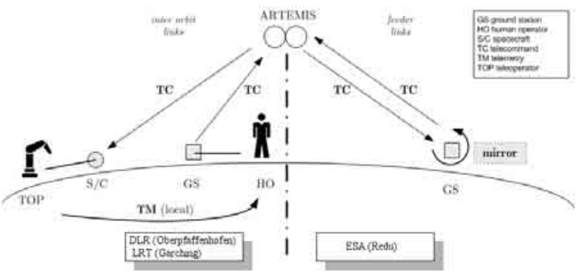

Fig. 230 ARTEMIS experiment: Satellite communication mirror setup

5.4.3 Exoskeleton Experiment

A different, dexterous haptic telepresence scenario is based on the PERCRO exoskeleton as master haptic device located in Pisa in the PECRO laboratory and the DLR Light-Weight Robot III (LWR-III) as slave device. Besides typical end effector Cartesian control, this setup exploits the DLR 7-DoF robot redundancy to allow bilateral mimicking between both robots. The system is suited for complex tasks where whole-arm dexterous manipulability is required. These developments are extended by a close cooperation with ESA/ESTEC and the evaluation of the new X-Arm 2 exoskeleton in a telepresence scenario.

5.4.4 Teleoperation Experiments with JUSTIN

The humanoid upper body JUSTIN has not only been used for advanced impedance control and telepresence experiments but also for teleoperation setups where the robot acts almost autonomously.

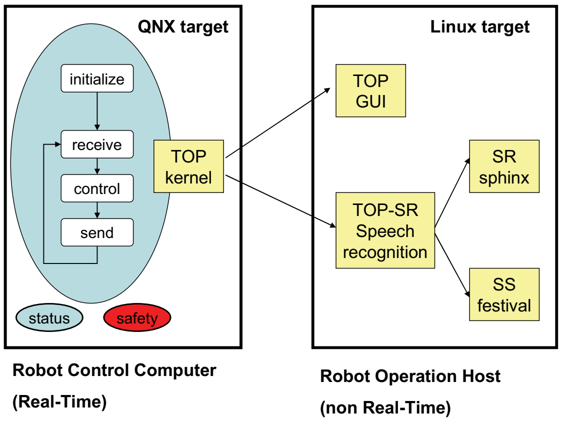

Fig. 231 Integrating Speech Recognition (SR, sphinx from CMU) and Speech Synthesis (SS, festival from University Edinburgh) systems in the Teleoperation Framework

The most demonstrated task is the Serving of Instant Tea. This task shows the autonomous execution of several operations aggregated to a complex task. To command such tasks as well as to teach new tasks aggregated by basic operations like Cartesian arm movements with different coordinate references, grasp operations and dual arm coordinated actions, a speech recognition system has been integrated.

The speech recognition module uses the same interface on the real-time robot controller as the Task Operation Programming environment TOP. It can start and stop elementary operations. Basically it consists of a python script starting a speech synthesiser which enables JUSTIN to give feedback on the received commands and on the actual state of operation. This way a single user can command and teach JUSTIN intuitively new tasks. For cooperative manipulations where JUSTIN and a human operator execute a task jointly like carrying a ladder such a command interface is required.

As the speech recognition system has a built-in grammar parser although variable commands like "go forward 5cm" can be commanded.

Fig. 232 Speech recognition used to teach JUSTIN new command sequences

5.4.5 JUSTIN as Telepresence Slave

A mobile bimanual telepresence system was realised using afore described bimanual multimodal HMI consisting of two LWR with two grasping force controllers, an optical tracking system, and an HMD coupled to the mobile JUSTIN. To enable the stationary HMI to control the mobile teleoperator, two modes of operation were implemented, one for the approach phase and one for the manipulation phase. During the approach phase one of the two arms is used as a speed source to control the movements of the platform. In the manipulation mode the robotic arms of the HMI are used to teleoperate JUSTIN's arms and the grasping force controllers are used to control the robotic hands. Both interfaces provide haptic feedback of the remote side. In both modes the tracking system is used to command the head of JUSTIN according to the head movements of the human operator.

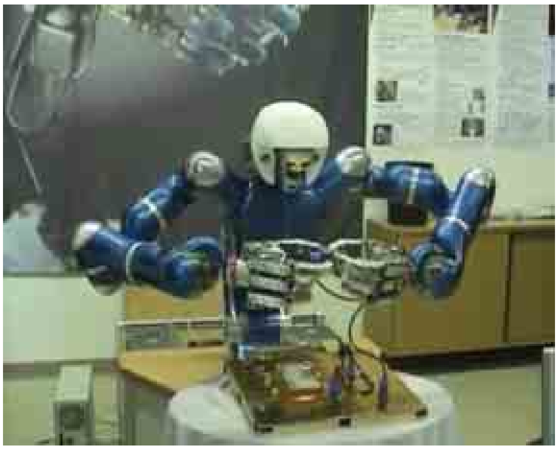

Fig. 233 Telepresent opening of a bayonet nut connector using JUSTIN

The stereo images of JUSTIN's cameras are fed back to the HMD. Using this setup, a task consisting of approaching the manipulation site, grasping a cable with a connector, which was no longer securely attached to its clamp, opening the connector, and closing it again, could be successfully conducted. The connector used was a bayonet nut. This type of connector requires a combined translational movement and, while still pulling, a rotational movement to open it (Fig. 233).

Virtual Assembly Verification

Using the haptics technologies developed in our lab (see Sec. III.3.5.1) it is possible to perform virtual assembly simulations like the one shown in Fig. 234. By means of the HMI, two objects can be moved simultaneously in the virtual world, while the user sees and feels all the collisions that happen even in extremely complex environments. As already commented in III.3.5.1, these and other simulations [Hulin *et al.* 2008b[c]] are of great interest for the automotive and aerospace industry, because they can test designs and train mechanics without building expensive physical prototypes.

Fig. 234 Virtual assembly simulation. A coolant tank moved by the left hand is assembled in the car and screwed with a drill operated by the right hand. Red arrows show movement paths, whereas green arrows highlight the object pairs whose interaction must be computed. Visual and haptic feedback is generated throughout the simulation.

5.4.6 Telerobot for Home Surveillance

Telerobotic concepts have been implemented on a small humanoid robot. In particular this robot (Fig. 235) has been equipped with a camera head and a wireless data connection to a host PC. The robot receives high-level movement commands (walk forward, turn, etc.) and feeds back the video stream. The host PC is connected to the Internet and a Web-Server offers the robot's service to a remote user either by browser interface or via mobile communication on a mobile phone.

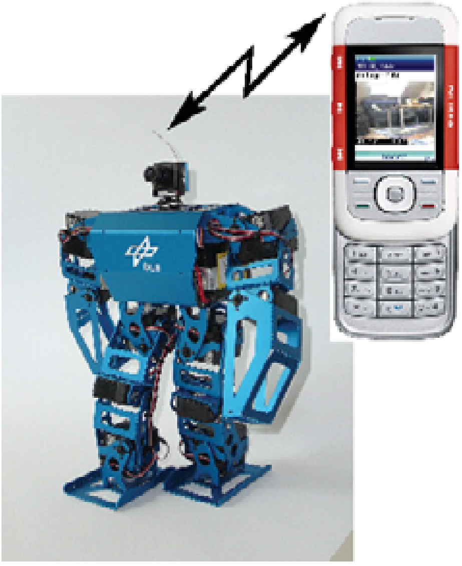

Fig. 235 Humanoid robot with cameral controlled via mobile phone

5.4.7 Further Experiments and Cooperations

Telerobotic and/or telepresence experiments have been conducted between the Institute and several partners worldwide, like the Institute of Automation and Control at the TU Munich (our partner in the DFG corporate research area "Realistic Telepresence") or the Biorobotics Laboratory of the Korean University of Technology.

As part of the ROKVISS space experiment telepresence methods and controllers have been applied to this system in the last years.

Further, ongoing work is taking place within a cooperation framework between the DLR and the ESA/ESTEC. The goal of this project is building a telepresence system integrating the ESA/ESTEC exoskeleton and the LWR-III as teleoperator.

6 Autonomous Systems

This chapter highlights various integrated autonomous systems developed in the institute or in cooperation with partners, demonstrating how such systems are integrated and used. Further information on the concepts involved is found in the corresponding chapters.

6.1 Flying Robots

Aerial imaging is an important data source for 3-D modelling and reconstruction of rural or urban environments, historic sites or even for indoor environments as for instance the interior of historic churches.

Fig. 236 6-rotor helicopter "AscTec Hornet"

Different types of multi rotor helicopters have been equipped with additional sensors and algorithms to get closer to a state, where they should complete such tasks without the interaction of a human pilot [Gurdan *et al.* 2007[j]].

Fig. 237 Octocopter "AscTec Falcon 8": eight rotors on a v-shaped carbon fibre structure and a stabilised digital camera

At this point, all our air vehicles are able to complete autonomous tasks in well known, obstacle free environments, where GPS is available. This was proven in a micro air vehicle competition EMAV08, where teams from all over Europe demonstrated the potential of their current research vehicles. The DLR team scored first places in all three categories they competed (Indoor flight dynamics, outdoor flight dynamics and outdoor autonomy), using the six-rotor helicopter called "AscTec Hornet".

To be able to fly autonomously with more precision even without perfect GPS reception or in indoor environments a visual odometry system was integrated in a quadrotor helicopter. The system shall be used to support GPS position estimates or even replace GPS completely during certain parts of a mission. Research is going on to fuse the data of the onboard IMU and GPS and the information gained by the optical system in order to get a solid and robust pose estimate in any situation.

A novel 8-rotor helicopter—or octocopter—was developed for experiments and missions, where a wide, undisturbed field of view of the camera is useful or necessary. Carried by this octocopter, a camera system can be tilted up and down for a total of 180°, and consequently an object can be visualised from any perspective.

Using this system, image data has been gathered enabling researchers to generate 3-D models of an outdoor environment.

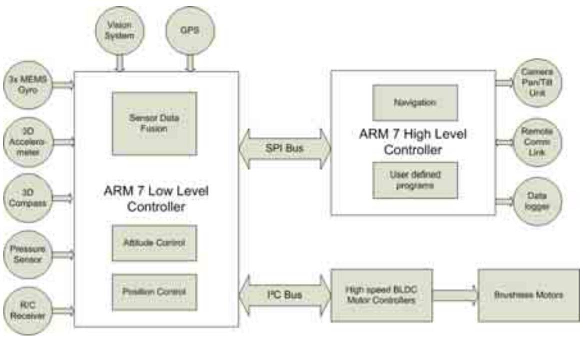

Fig. 238 Octocopter system overview

Current research also includes the conceptual design of mission planning algorithms considering constraints given by the operation environment, by the degree of knowledge about the environment and by the flight system itself. Ultimately, the airborne system conducting a mission like gathering data for 3-D reconstruction of a building must be able to avoid obstacles, choose a save and efficient flight path and to alter the mission based on decisions made by algorithms running on board. Consequently, another focus lies on the conceptual design, development and integration of additional sensor equipment, algorithms and software enabling the perception and interaction with the environment.

With the first successful field tests in an archaeological excavation area in Mongolia and the vision algorithms making rapid progress (see Sec. III.4.2) we are approaching one of our most challenging goals, the 3-D reconstruction and 3-D world modelling by just "flying around" with mono cameras.

First tests were realised and demonstrated at the AUTOMATICA 2008 in Munich by flying around a model church (Fig. 239).


Fig. 239 Model church at the 2008 AUTOMATICA fair

6.2 The Autonomous Airship ALUSTRA

Starting in 2005, we have used the HGF-construct "virtual institute" to push forward the field of photorealistic 3-D reconstruction from stationary and flying platforms in close cooperation with the University of Stuttgart (Institute of Flight Mechanics and Control, IFR) and the Technical University of Munich. The University of Stuttgart contributed essentially to the development of an autonomous airship ALUSTRA as multi-sensory platform, e.g., for high-precision cameras. We claim the result to be presumably the most mobile and controllable airship built to date. Its design was simultaneously aiming at a (low trajectory dynamics) hovering behaviour (similar to a helicopter) with rotation around the vertical axis, as well as lateral shift capability (perpendicular to main axis) and fast longitudinal flight. The request for very low trajectory dynamics was essential to avoid blurring in the pictures taken during flight. This leads to demanding requirements to the accuracy of the flown trajectory, added to which are even more demanding requirements for the performance of the navigation system.

Thus we provided the airship with in altogether 13 controllable actuators.

Fig. 240 Actuator configuration of ALUSTRA I

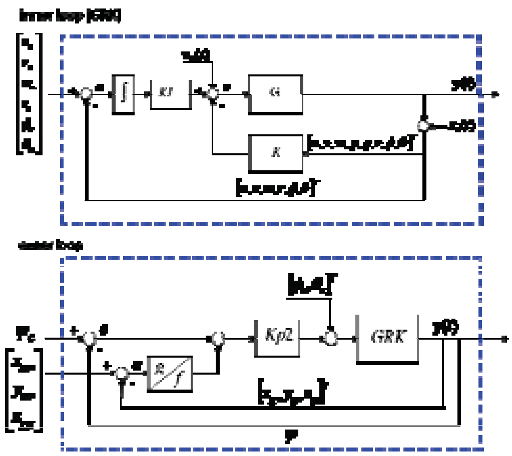

Fig. 241 Controller architecture

The actuator configuration is visualised in Fig. 240. In addition to the four aerodynamical steering actuators, the yaw rudder and two separately controllable pitch elevators, this blimp has as well six thrust vector actuators. Since the direction of thrust is the same for a main actuator couple, this results in 13 variables, which need to be handled by the controller. Thus the controller had to be designed as a multiple-input-multiple-output controller and is based on a linear quadratic regulator algorithm. The designed flight control algorithm needs special adjustments due to the susceptibility of a blimp. Hence it is possible to fulfil the mission even if some actuators reach their limits.

The controller architecture is shown in Fig. 241. It consists of an inner control loop for the translational velocities, the yaw rate and the angle of roll and pitch. Additionally a controller for the angle of yaw and the position is superimposed. The inner control loop can be operated as well as a Control-Augmentation-System. This makes simple tests possible concerning the behaviour of the controller. Furthermore it permits to train pilots on this blimp test carrier in an easy way.

Fig. 242 ALUSTRA with integrated ground station

The airship with a length of 15m, a maximal diameter of 3m and nearly 10kg extra load capacity for instruments was built up by help of the industrial partner AEE, a small aircraft electronics company. And a complex ground station was developed to monitor and control the flights on their way to autonomy (Fig. 242).

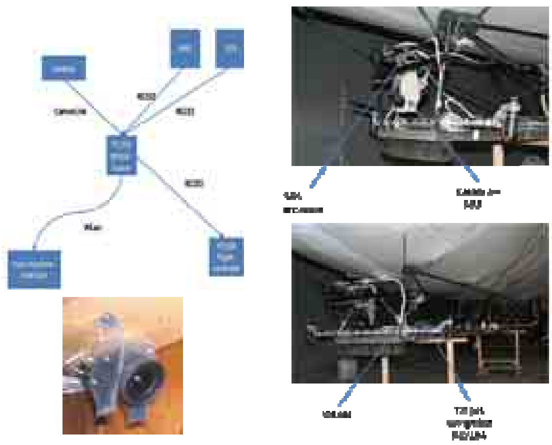

Fig. 243 Sensor architecture and mounting (IFR)

The navigational solution as developed by our IFR colleagues in close cooperation with our integral positional sensing (IPS) project is calculated by an Extended Kalman Filter Algorithm. The used measurement equipment are a GPS receiver, an inertial measurement unit and a camera, see also Fig. 243. The identified values are the translational and rotational velocity of the airship and its orientation and position in space.

Moreover the optical system provides the distance to the tracked points for the follow up flight control system. This information can be used to avoid collisions as well as for an estimation of the height with respect to the landing site.

In order to keep the weight low, the inertial platform consists of a low-cost, MEMS-based sensor. Like the GPS, the inertial platform is a commercial off-the-shelf component which provides processed measurement values. In addition image processing software for the optical sensor was developed in order to obtain the "visual" measurement values. These measurements consist of the coordinates of tracked points of the observed scene on the image sensor. A low level feature tracker based upon the Lucas Kanade tracker was applied to the sensor, given that it had to be designed for any arbitrary scene. Moreover a quality criteria was implemented for the reliability of the feature tracking, so that gradually drifting features can be corrected. The evaluation of information of the optical system within the data fusion is based on the focus of expansion and the epipolar constraint. The camera used is an industrial camera which transmits pictures by means of a camera link connection to a frame grabber on the target computer which then performs the data evaluation. Besides the image analysis this data processor also contains the fusion algorithm. Thus the complete sensor system is installed on board the airship and meets the aims and requirements of the project concerning autonomy. The airship is connected via radio link to the ground control station which visualises helpful information in real time, a feature that is especially useful during the development stage. Furthermore the ground station contains an instrument panel for the surveillance of the flight [Hirzinger & Fach 2008[c]].

The functionality of the navigation system was successfully verified on autonomous flights. The airship had to follow a pre-assigned trajectory circling around a virtual building on an open field, as shown in Fig. 244. On this pre-assigned trajectory—a square—the waypoints were reached exactly during the flight, the blimp stopped at the waypoints and turned to the next waypoint to proceed with the flight. In the meantime, highly efficient wind estimation algorithms are in preparation.

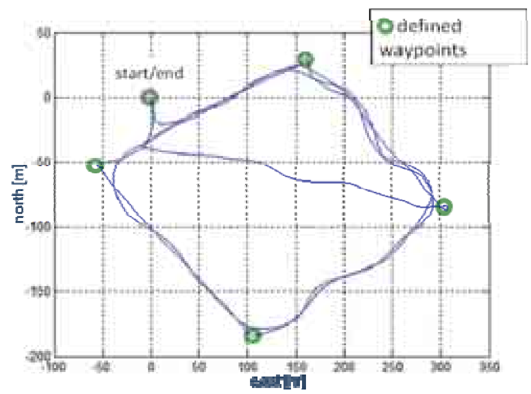

Fig. 244 Trajectory of an autonomous flight

6.3 Ball-Catching Robot

The DLR Robotic ball catcher, developed for the LWR-II, has been redesigned and modularised to fit into the new system architecture and control system.

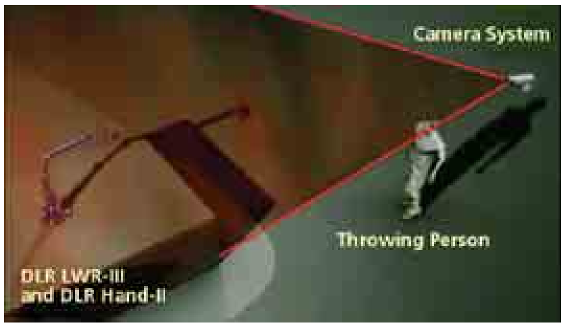

Fig. 245 General setup: Baseline approx. 1m throwing distance about 6m

It now consists of a stereo camera system with a large baseline mounted behind the throwing person, which tracks the ball comparing each image to a slowly adapting reference image (see Fig. 245). The image processing part and the prediction of the ball trajectory with an Extended Kalman Filter (EKF) is kept the same as for the previous system. As robotic arm the LWR-III is now used. It can move at higher joint velocities compared to LWR-II. This opens new prospects for the catching strategy, as now the robot usually arrives at the calculated catch point far before the thrown ball arrives.

In an early version of this demonstration experiment the catch point and the orientation for the hand were heuristically predefined. The robot has been commanded to reach the target position as fast as possible. This results in a lower catch rate. To increase the robustness of the system a new kinematic optimal catching strategy has been developed.

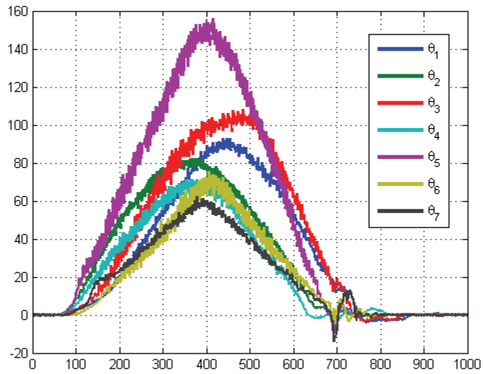

Fig. 246 Joint velocities during a "Soft Catch" attempt. It can be seen that the robot does not need to drive at maximum speed.

The new system takes the start configuration of the robot (joint positions and velocities) and the trajectory of the thrown ball as input. The catch point of the ball depends on one of three actually implemented strategies chosen.

Fig. 247 The Ball-catching robot during a "Cool Catch" attempt

The first strategy minimises the accelerations for the robot's joints to catch the ball. This strategy is called "Soft Catch". The goal function is defined as sum of the accelerations of each joint raised to the power of four. The constraints that have to be considered are the equality of TCP and ball position in the catch point and the inequality constraints of the joint limits, the joint velocity limits and the collision free trajectory. The kinematics and the collision constraints bring non-linearity into the optimisation.

The problem is therefore best solved by a state of the art nonlinear optimisation method. Here SQP is used. Fig. 246 shows the joint velocities for a catching attempt using this strategy. For any joint a maximum velocity is driven only for a very short amount of time. This results in very smooth robot movements. It should be stated that the catch position is optimised in a way that ensures slow trajectories.

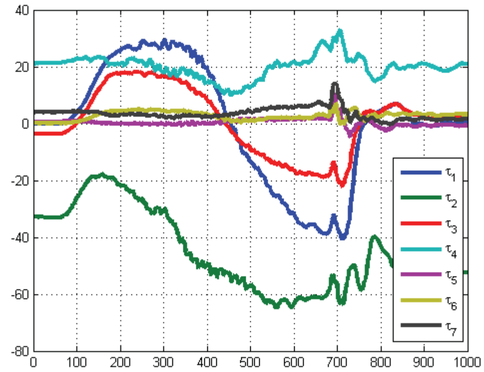

Fig. 248 Joint torques during "Soft Catch" attempt

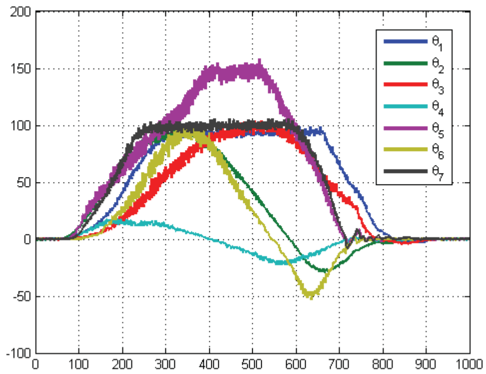

Fig. 249 Joint velocities during a "Cool Catch" attempt. It can be seen that the robot needs to drive at maximum speed.

This can be also seen in the plot of the measured joint torques. At time 700ms one can see the impact of the caught ball. So it can be seen that the whole interval is used to drive to the target position, even if the robot could have driven faster.

The second strategy produces more challenging and impressive trajectories. Here the goal function is tuned to catch the ball at the latest possible position. This normally leads to larger robot movements and therefore to larger accelerations. Fig. 249 shows the joint velocities of a "Cool Catch" approach. The maximal performance can be reached with high accelerations and a long period driving at maximal speed which can be reached by a trapezoidal interpolation.

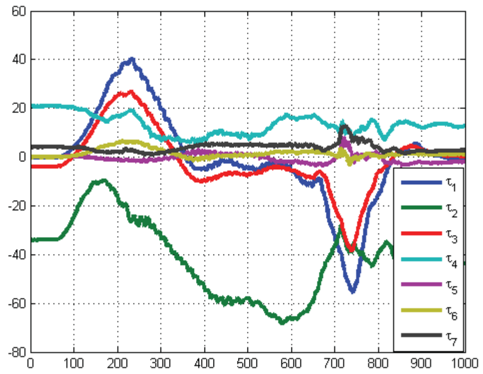

Fig. 250 Joint torques during "Cool Catch"

The according joint torques show that the stress on the robot is much higher using this subjective function (Fig. 250).

The last catch mode implemented is the "Latest Catch" which tries to start the robot at the latest possible moment in time. This mode is rarely shown in demonstrations as it is very sensitive to prediction errors of the image processing. In this mode the robot is started at the latest possible moment and then drives with maximum velocities. However if there is a correction proposed by the image processing component the robot cannot react on the trajectory change as it will arrive too late.

To allow the adaption of the trajectory in the first two strategies a pipelining mechanism for the trajectory optimisation has been implemented. Each run of the optimisation takes about 60ms and every 20ms a new trajectory prediction comes from the image processing unit. At the start of one try multiple instances of the optimiser are started to select the best local minimum solution. Then every 20ms a new optimisation is started predicting the joint positions and velocities at the time in future where the trajectory might change the movement of the robot taking the actual prediction of the image processing into account.

This approach depends on high real-time computing power which is provided here by four dual QuadCore boards running QNX. Fig. 251 shows the system architecture of the new demonstrator.

The half images delivered by the synchronised PAL cameras are processed on a standard Linux PC. The prediction of the trajectory is fed to the Motion Generator which assigns optimisation jobs to a pipeline of optimiser instances. This ensures new results every 20ms. The generated optimal trajectory is transferred to a joint interpolator. The interpolator directly moves the robot via the joint controllers. For the hand a fixed closing trajectory is predefined. Only the time to close is commanded from the Motion generator.

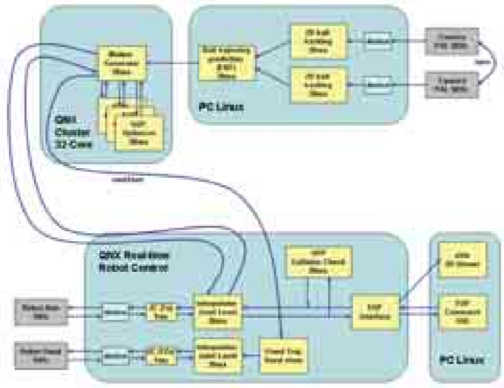

Fig. 251 System architecture of the new ball catch demonstrator

An interface for visualising the robot and the ball trajectory as well as a graphical tool to start and stop completes the system.

6.4 Vision and Force-Controlled Assembly

Combination of vision and force sensor data is an essential feature for versatile robot systems of the future, which should be able to reliably assemble parts despite of inaccuracies in the environment. To show the advanced robustness and flexibility that is achievable by such a system, a demonstration platform has been set up, consisting of a DLR/KUKA light-weight robot with an additional Firewire camera in an eye-in-hand configuration. The robot's task is to insert complex pieces into the appropriate holes in a plate lying on the table.

The setup is designed such that all difficulties met in industrial assembly applications have to be addressed:

- the pieces and the plate have to be localised on the table using a vision system, precise part feeders are missing;
- tight clearances ask for an intelligent insertion strategy and compliant robot behaviour;
- the variety of parts and their complexity make manual robot programming of this application tedious and error prone.

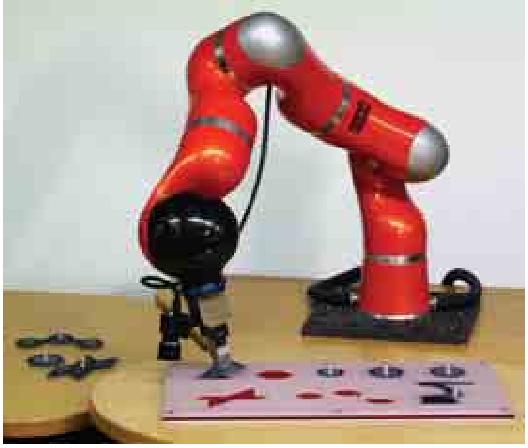

Fig. 252 The assembly demonstrator trying to insert a triangle piece into the plate

Using image-based visual servoing (IBVS) for detecting and tracking the objects, and the LWR's Cartesian impedance control for compliant assembly, the robot is able to insert the pieces quickly (below 15s on average per part) and robustly. The insertion strategy is planned automatically, based on the geometry of the parts. In the near future we see the chance that robots of this type might be faster than humans in assembly and thus might bring production facilities back to Europe, which in the past have been transferred to low-cost countries.

Fig. 253 Illustration of the Cartesian impedance control law used for aligning the pieces compliantly

IV Bridging Technologies

1 Concurrent Mechatronic Design

1.1 Infrastructure for Signal-Oriented Computing

The development of highly integrated "mechatronic" robotic systems is a multidisciplinary challenge. It is characterised by the tight collaboration of mechanic, electronics, software, and control designers (Fig. 18). However, each field has the focus on different specifications and uses its own language. Identical terms have a different meaning in a certain area. Nevertheless, certain pairs of designers need to agree on an explicit set of specifications.

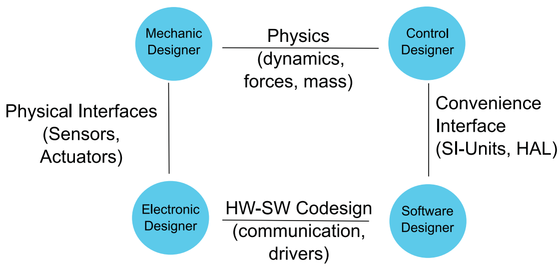

Fig. 254 Concurrent design of mechatronic systems

Mechanic designers and control designers naturally use one common language: physics. Depending on the robot's application, tangible physical parameters are specified, for example torque range, maximum end-effector speed, the kinematic layout, etc.

Designers of electronic components collaborate with mechanic designers on the physical interfaces, i.e. the implementation and placement of sensors and actuators. This involves the specification of measurement principles (e.g. strain gauges, potentiometers) and the definition of motor parameters.

Software designers and electronic designers are faced with a complex HW/SW co design problem. This involves modularisation, communication infrastructure and protocols.

For efficient feedback control programming, control designers and software designers have to determine a convenient interface. This involves the presentation of values as SI-Units, the implementation of a hardware abstraction (HAL) that represents the robot device in a suitable way.

Model driven design establishes a domain-specific "model" as a common language ("ubiquitous language") that is used for clear specifications between designers. For the domain of feedback control on mechatronic systems we use a signal-oriented model: Signals connect Sensors with Controllers and Actuators. Specifications between designers can be clearly devised within this abstract model.

The formal definition of such a view is known as Actor-oriented Design: Active components (Actors) communicate via Signals within a model of computation.

Mathwork's Simulink is an actor-oriented framework. Thus, control designers benefit from Simulink as it allows them to directly implement their algorithms within the design model.

We established a tool chain with Mathwork's Real-Time Workshop, RT-Lab by Opal-RT that allows the execution of Simulink models on real-time hosts. For FPGA platforms, we use Mathwork's HDL Coder and Xilinx's System Generator.

Additional to those tools for automatic code generation, we require a frame for the implementation of the mechatronic system consisting of distributed mechanical hardware, electronic components, computing nodes and software—a communication infrastructure.

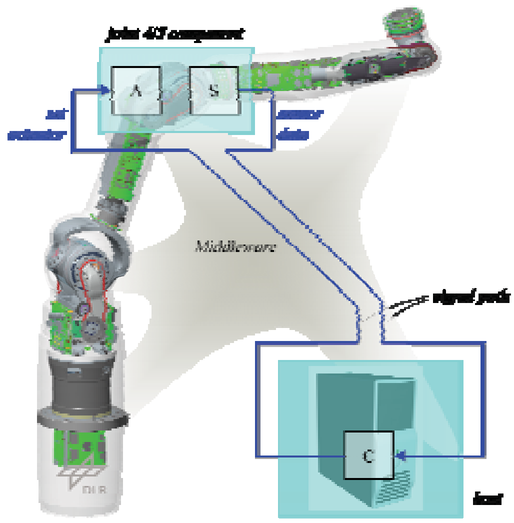

Fig. 255 Schematic signal flow from sensors and actuators to control system

The new surgical robotic system MIRO has been designed with the help of this tool chain. Fig. 255 shows the communication paradigm of this approach. The communication middle ware and the Hardware Abstraction Layer HAL provide a consistent view on each joint of the robot. All relevant data for the control designer is transparently transferred to a central real-time computing host.

1.2 Agile Robot Development

Similar to the infrastructure approach for the lower level hardware (sensor/actor) design also a new software framework design for the higher level control algorithms was mandatory [Bäuml & Hirzinger 2006c].

Our robot control software successfully used so far was originally designed for one robot arm with a gripper in a monolithic implementation. This design, however, not only made it increasingly harder to build more complex systems, but also led to proprietary extensions and further to several different versions of robot control systems. This, of course, had consequences with regard to maintenance and provoked incompatibilities.

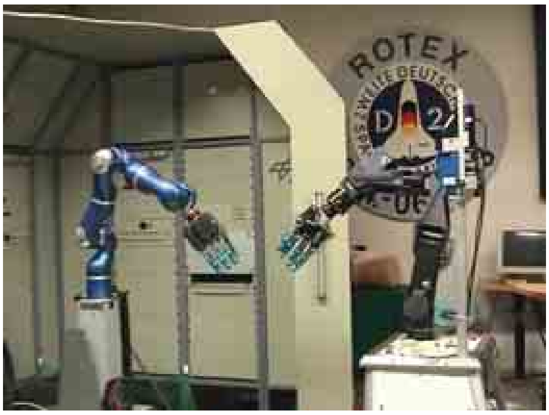

Fig. 256 Robotic testbed for the development of JUSTIN, allowing to evaluate the control strategies and the control framework for dual handed manipulation

In the process of analyzing the problems of increasing system complexity it became clear that the currently available computing power of commodity systems together with their fast communication links and high-speed buses between the robot components allows for a completely new view on the system architecture of a robot system. This also led to the insight that a mere re-design of the old robot control software was not an adequate solution, but that a completely new software concept which makes full use of modern hardware possibilities was necessary. The main idea to build the new system was to decouple the overall system architecture from the hardware details and to take a functional view on a robot system.

An appropriate software concept has to provide tools for designing this functional view and mechanisms to map this functional design onto the actual computing and robot hardware.

Another important point with strong influence on the requirements for a new software concept is the fact, that a complex robot system is developed by a heterogeneous team of researchers from various fields. This implies that the software concept has to support the specific tools from the different fields and allow working independently on different components, but should still remain simple and easy to use.

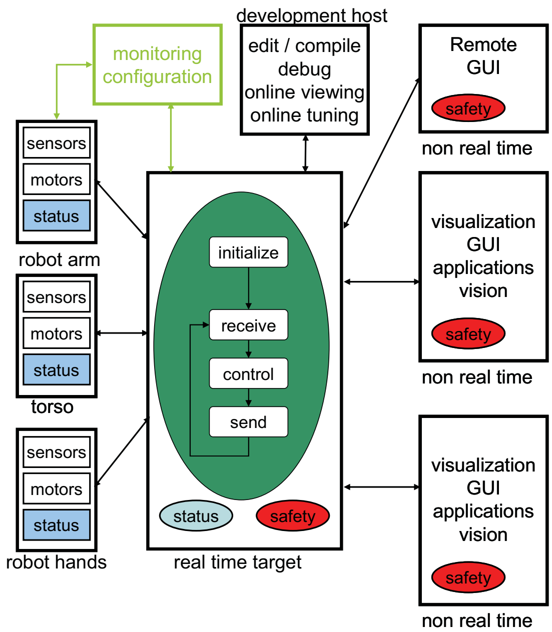

Fig. 257 General Architecture of JUSTIN with hardware, control system and higher level software components

Finally, for building complex systems it is highly advantageous that the software concept supports rapid prototyping to allow an iterative development process.

To find a good definition of a functional view we oriented the design and implementation of the new system on the development and needs of the humanoid upper body JUSTIN.

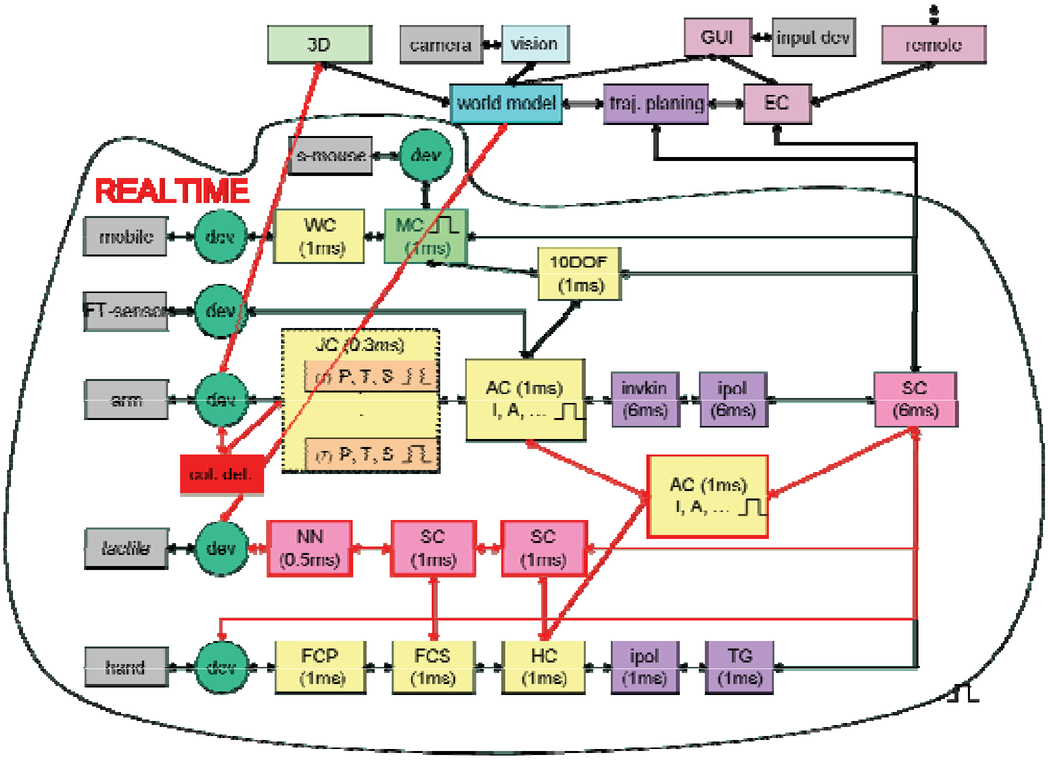

Fig. 258 Functional signal flow model of JUSTIN's control system

Such a system consists of a number of robot components connected to a real-time target running the controller loops. Applications for user interaction (e.g., 3-D viewer, GUI) and higher level intelligence (e.g. vision system, trajectory planning) are implemented on a network of non-real-time computers. Those applications can communicate with the real-time target and also possibly have a link to a remote command station, coupled by a WAN or the internet.

Additional hosts run tools for development (edit-compile-debug) and tools that allow for monitoring and profiling of the different parts of the system during runtime.

Leaving the details of the computer architecture aside and refining the structure of the functional modules one ends up with a scheme as in Fig. 258. All of the functionality of the system is now represented by blocks running in real-time or non-real-time. They perform calculations and communicate with each other. Typically the granularity of the real-time part is finer, as each block usually performs only a small amount of deterministic calculation. On the other hand, blocks in the non-real-time part represent more monolithic applications and can perform elaborate algorithms on complex internal representations.

It is therefore straightforward to see a robot system as a decentralised net of calculation blocks and communication links, in this way defining the functional view on the system.

1.2.1 Design Considerations

This abstraction not only helps in designing the architecture of a robot system, but also paves the way for a component based software engineering approach if supported by the software concept. The component-based approach is particularly well suited as a complex robot system is developed by a team of researchers. If in addition the concept allows changing the structure of the net in a simple and flexible way, rapid prototyping is also naturally supported.

Besides the wish for a simple and flexible software concept, one would pragmatically like to keep the implementation from becoming too complicated.

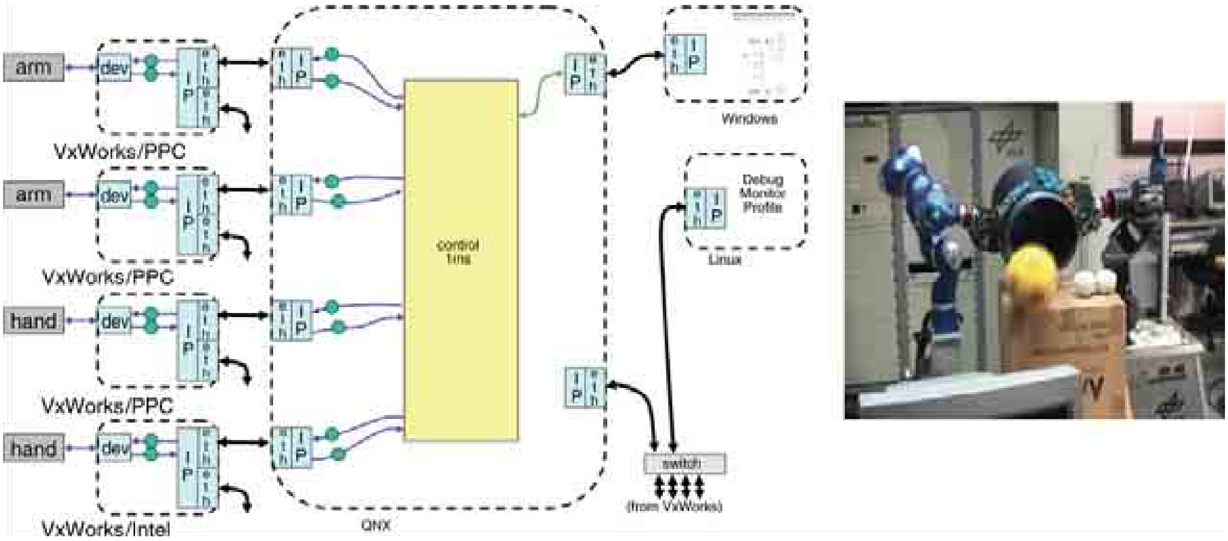

Fig. 259 Functional signal flow of the dual-arm test bed where the control schemes for JUSTIN have been developed before the JUSTIN hardware was available. The figure shows that various different real-time data collectors have been integrated.

Design considerations and requirements of the net of communicating blocks were:

1. *Equality of Blocks:* All blocks are equal in the sense, that they all can be sources and sinks for data and there is no distinction in client or server blocks. Also the connection scheme is arbitrary. A block's output port can be connected to any other block's input ports, as long as the data formats match.
2. *Execution Order:* Each block is an execution entity, e.g. a process or thread, and can have its own priority. This allows to schedule the available processing time between the blocks and implicitly defines the execution order. In practice it is often more efficient and simpler to aggregate blocks into groups, where each group is an execution entity and iterates through its blocks. The request of a synchronised data flow and set of blocks assures deterministic execution, simplifies the scheduling and priority adjustment while nearly not restricting the flexibility.
3. *Data Flow:* The data format of each port of each block can be different, but is static during runtime. This simplifies the implementation of a block, but also means that a block is less than an object or a component, where different methods with different parameters and return values can be called. Also the block's connection scheme is static at runtime. This design decision dramatically simplifies the implementation, not only of the single block but of the mechanisms for configuring the overall system. Instead of allowing to dynamically change the connection scheme it is possible to disable and enable blocks through input ports, where a disabled block does not consume computation time.

1.2.2 Requirements for Daily Use

The following considerations address the handling and development of such a system.

1. *Development Tools:* For complex systems consisting of a large number of blocks and links between them a *graphical development tool*, which allows organising the net of blocks in a *hierarchy* of meta-blocks is almost essential. The possibility for rapid prototyping was one of the main design aspects of the overall software concept. This should be supplemented by having a *quick edit-compile-debug cycle*. Tools for *monitoring and visualisation* of the data flow are also important for getting an insight into the runtime behaviour of a complex net of blocks and for finding bugs.
2. *Interfaces:* The aRD concept only provides a flexible communication

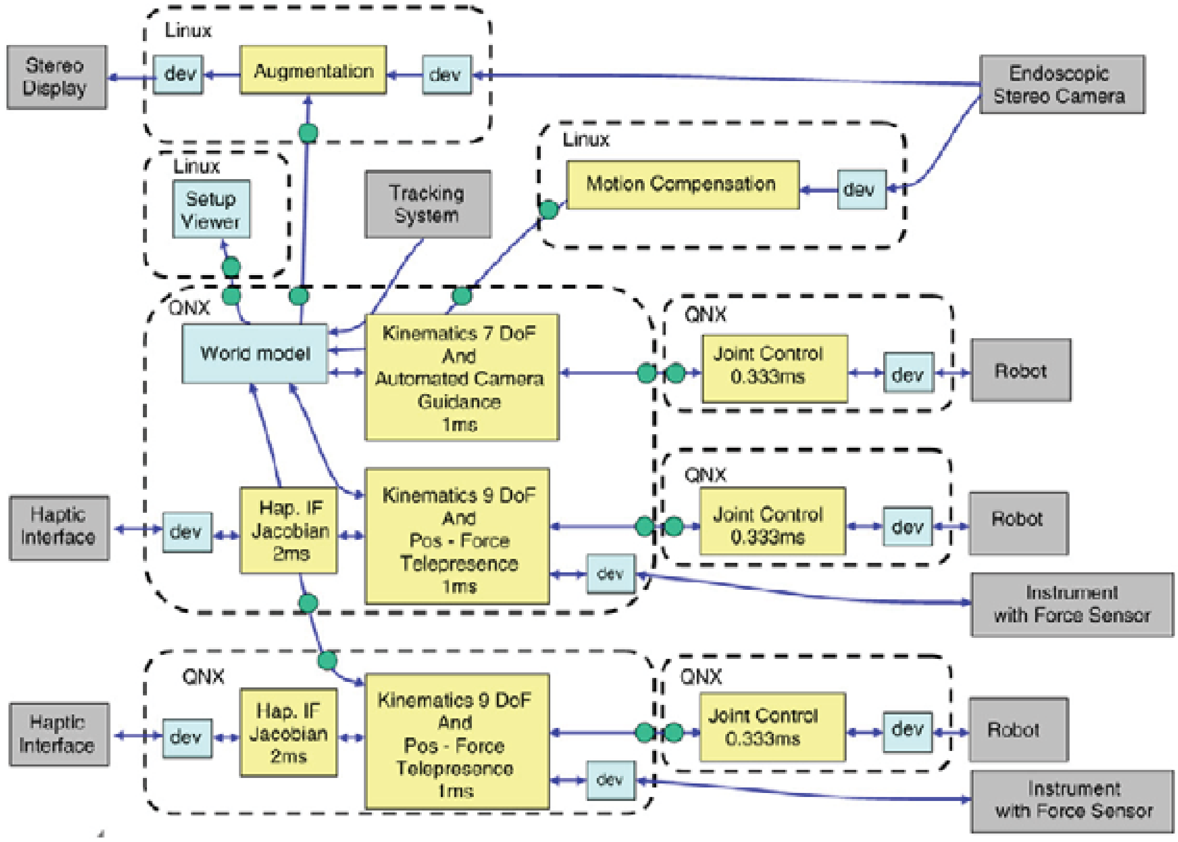

Fig. 260 Functional signal flow and mapping to dedicated computing resources of the MIRS demonstrator using aRDnet suite

infrastructure for the net of blocks. The functionality, however, is implemented *in* the blocks. Therefore it is very important that the *interface* for writing a block and integrating it in the net's communication structure should be *open* to arbitrary programming languages. This is especially important as in robotics the blocks are contributed by a team of experts from different fields, each requiring its specific tools and languages. The interface for writing a block should also be *simple*, as researchers are experts in their field but not necessarily software experts and are not willing to invest much time to understand sophisticated software frameworks.

1.2.3 Implementation

The current implementation of the aRD concept consists of aRDnet, a simple software suite developed at our institute and a tool-chain based on Matlab/Simulink/RTW and RTLab. As operating systems (OS) we use QNX Neutrino, a POSIX-compliant microkernel real-time OS, for the real-time target, Linux for the non real-time computers and Windows XP for the development hosts.

The aRDnet is laid out as a simple software suite that supports and standardises the communication between blocks. The suite consists of four parts:

- a library supporting the implementation of a block’s input and output ports;
- the aRDnet executable realising communication between blocks running on different computers;
- a template for writing Simulink stub blocks;
- tools for a coordinated start-up and shut-down of the system.

The aRDnet library provides a simple C/C++ interface, which allows us to easily build interfaces to other programming languages, e.g., by using SWIG.

At the institute, in almost all projects the aRD concept is used, now involving about 20 researchers working on more than 15 development seats (with >25 QNX PCs). Beside the already discussed humanoid robot JUSTIN, for which the aRD concept was originally developed, the projects range from testbeds for a new generation of robotic arms and hands, over telepresence and virtual reality setups up to space and medical robotics. These applications can easily reach the complexity of humanoid robots, as shows the minimally invasive robotic surgery setup with more than 30 actuated DoF and control rates of up to 3kHz.

2 Universal Drive Technology

In the recent years, the design and integration of high-power servo drives has been one of the driving factors in the Institute's hardware developments. In various projects the specialised motors were the key element for highly demanding applications. From automotive steer-by-wire projects with high-torque demands and space projects with high qualification levels to the latest medical applications, there was a broad range of developments.

Our innovative new motors RoboDrive have turned out to be not only attractive as lightweight robot joint and rover wheel drives, but also for wheel steering actuators in cars, actuators for electric brake systems (e.g., the mechatronic wedge brake), stabilisation platforms (e.g., for optical communication), and they are now in preparation for use as aeroplane flap and rudder actuators as well as in landing gears.

A tendency towards smaller motors became evident in the last three years. Although in this range (less than 100g in weight and 100mNm of torque) there are many commercial products available, yet none of these were able to fulfil all the requested requirements. Most of the commercial products were brushed motors, which show a lack in peak performance, reliability, endurance, and torque-to-mass ratio. Additionally this technology is not usable in vacuum, which is necessary for most space-applications.

The range of RoboDrive-Motors was therfore extended from 40Nm of peak-torque (with a 2.5kg motor) down to 24mNm continous torque. Many applications have been realised or are under development (see Fig. 261).

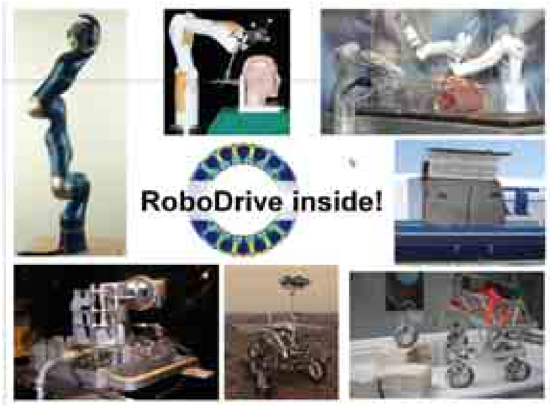

Fig. 261 Applications of RoboDrives motors

Application in the DLR Hand-Arm System

As a specific robotic example, we here describe the design of miniature servo drives for a humanoid hand-arm-System.

Fig. 262 ILM25 servo drive

For future humanoid robotic systems we are building robotic arms and hands which closely match human dimensions as well as dynamics. This can only be achieved by removing the finger actuators from the palm of the hands (their current position in DLR's modular hands). In the next generation, a large number of drives will be integrated into the robotic forearm. These will actuate the fingers in an antagonistic way to achieve inherent safety and compliance.

To this end, miniaturised servo motors with excellent torque characteristics and minimal thermal loss needed to be designed. Since the maximum available gear-ratio is given by the best commercially available harmonic-drive-gears (size 8 and size 5), these motors should be able to reach an accordingly high speed and dynamics.

In a first step, new materials have been tested with the geometry of the existing ILM50. The thermal losses at high speeds should be reasonably low, but also the torque-capability of the drives (which is proportional to the magnetic flux-density in the iron parts) should not be reduced. Prototypes of both materials have been investigated on a special test bench.

Since friction torques of the bearings in a test bench are in the same range as the expected torques induced by dynamic iron-losses, these needed to be cancelled.

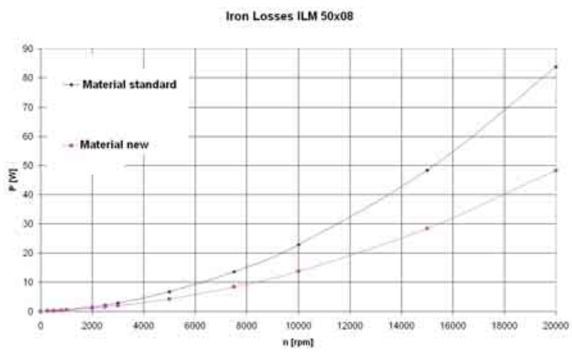

Fig. 263 Iron-loss of different materials for miniature drives

By removing and inserting the magnetic rotor on a linear slide while the motor was turning, a relative measurement of the torque was taken. Thereby the friction torque of the bearing and torque-transducer, which strongly depends on temperature, speed and state of the lubricant, was cancelled as an offset-value. Based on the results, a material was chosen which keeps the torque performance fairly equal (less than 3% deviation), but reduces the dynamic thermal loss in the iron to 50%. With these small motors, speeds of more than 20.000rpm can be reached.

Thermal Investigation and Model

Based on the results of the material investigation, a detailed thermal model and simulation was established. The assumed load-cycle is a full finger flexion with maximum fingertip force in less than 250ms. During the acceleration phase, the maximum available peak torque of the motor is applied for a few milliseconds. In the constant speed phase, the maximum allowed input speed of the gear unit is used. Later this cycle was repeatedly verified with the prototype on the test bench.

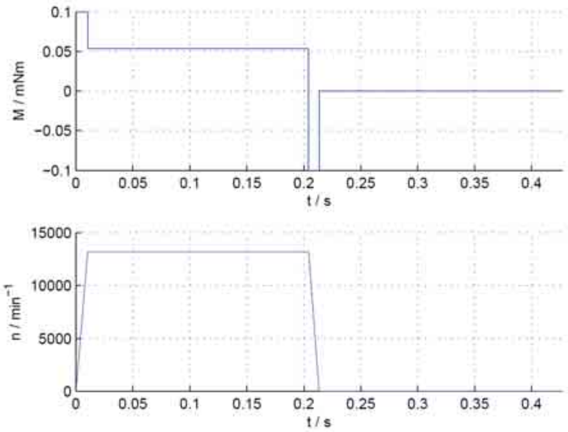

Fig. 264 Maximum load cycle of a finger actuator

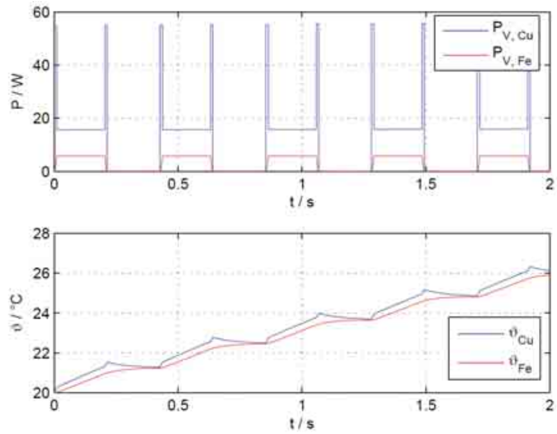

Fig. 265 Temperature rise of an ILM25 during 5 cycles in 2 seconds

It was successfully shown that the motor is able to run this cycle with minimum thermal loss. During a few of the short cycles, most of the thermal energy is stored in the motor itself. Nevertheless, it is a demanding problem to cool all the losses of 32 active motors in the forearm. This can probably only be achieved by partial water-cooling of the arm structure.

Design Process and Prototyping

By applying the Concurrent-Engineering-SW for motor-design, two types of mini motor were calculated. The smaller one, with 25mm diameter, will be used to drive the fingers. A larger unit with 38mm diameter is available to support antagonistic actuation of the hands flexion and the elbow's rotation. Relying on the positive experience with the ILM50, the tooling for those motors was designed and manufactured. Within a few months several prototypes were produced to verify the design and simulation process. The tools are capable to produce a larger number of motors for the hand-arm-systems in the institute.

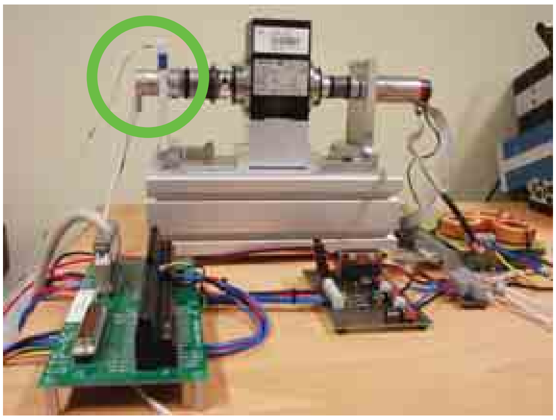

Fig. 266 ILM25 on test bench for thermal measurements

Measurements

The motors are intensively tested and measured on the test benches. The designed performance characteristics have been successfully reached. Some of the results are shown in the below table. Unfortunately, the error between motor design and prototype is higher than with the larger motors that have been realised in the LWR project. This will be further investigated to improve the design process. For the larger motors, the maximum error was less than 5% whereas with the mini-motors we found deviations in the range of 8% to 12%.

Technical Data

Both motors show very good performance in torque capability and speed characteristics. Due to the compact size and rather low inertia, acceleration rates to rated speed are only a few milliseconds. Both motors reach peak-torques of more than four times the rated torque.

Tests with Electronic Inverters

The latest tests with the electronic inverters designed in the MIRO project approved the motor measurements. The inverters were adapted to run a 100kHz PWM frequency, which is necessary because of the relatively low resistance and inductance of the new motors. The targeted motor speeds have been successfully reached. Additionally, the whole system is very efficient. This enables the foreseen high density integration of digital inverter and control logic with the motor units in the forearm of the new hand-arm-system.

Table 8 Technical Data ILM25 and ILM38

Motor Type	ILM25	ILM38
Power	60W	100W
Torque	24mNm	100mNm
Peak Torque	100mNm	400mNm
Voltage	24V	24V
Speed	24.000rpm	12.000rpm
Phase Current	3A	5,5A
Phase Resistance	250mV/A	180mV/A
Weight	15g	52g

3 Integral Positioning System

Introduction

Goal of the project IPS (Integral Positioning System) is the development of a system for determining the ego-motion of objects in unknown environments, e.g. robots, vehicles or measurement cameras. The measurement of position and attitude is calculated without external sensors primarily and should be suitable for indoor and outdoor applications.

Concept

IPS is based on a multi sensor approach. Sensors being able to provide position or attitude date or their derivates can be integrated into the system. Data of different sensors are received in the IPS box and time stamped. Complex filter algorithms are responsible for a state estimation in dependence on applications and motion models. IPS can be adjusted to accuracy, reliability and costs by goal-oriented choice of components. An optional external aiding by GPS/ Galileo provides absolute referencing in space and time domain. Due to its multi sensor approach IPS is able to provide six degrees of freedom robustly and reliably.

Sensors

A standard low-cost configuration consists of monocular or binocular cameras and inertial measurement units. Other sensors, e.g., laser range finder, tilt sensors, pseudolites, GPS, can be integrated on demand.

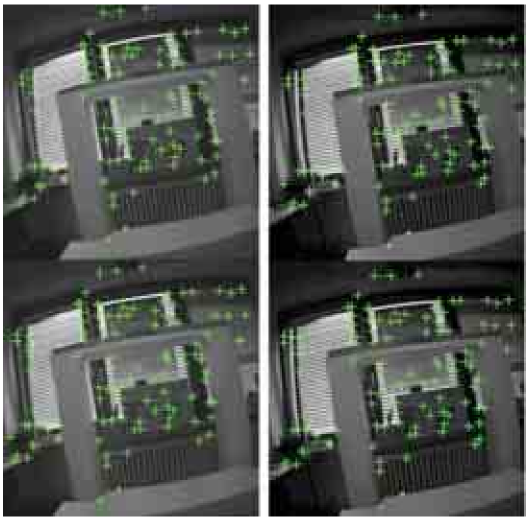

Fig. 267 Intra matching and inter matching, identical object points (green) detected in two stereo images (left and right) and at different times (top and bottom)

Fig. 268 IPS concept

IPS Box

Data acquisition is realised by the IPS box. A common time base of all single sensors is not necessary, data can arrive asynchronously. Core element of the IPS box is a FPGA card. Two CamLink interfaces and up to 10 serial RS232 ports are at the user's disposal. External and internal triggering is possible.

Software

More or less expensive data preprocessing steps are necessary depending on system configuration. The usage of cameras implies the development of complex image processing algorithms. Feature extraction and tracking are prerequisites for the determination of the ego-motion based on image sequences. Inter- and intra-matching methods assign image points for images captured from one camera at different times and for stereo images captured at the same time, respectively. This results in three dimensional object points and can be used to determine relative ego-motion as well.

Different Kalman filter approaches (e.g. extended Kalman filter, information filter, sigma point filter) allow an accurate and reliable state estimation.

Simulation and Evaluation

A complex software simulation environment was developed in order to deploy retrieval algorithms and state estimation procedures. A virtual three-dimensional textured model can be designed, in which a virtual IPS can be moved on any desired trajectory. Any sensor combination with certain properties can be simulated in order to optimise application dependent constellations. This way, a compliance matrix can be created, defining optimal IPS configurations for dedicated tasks.

Fig. 269 Motion simulator test bed with attached sensors (frontal view onto sensors)

Fig. 270 Motion simulator test bed with attached sensors (side view)

Calibration

Calibration of sensor systems has a big influence on the performance of an IPS system. Therefore, accurate sensor models are required. Within the IPS project innovative camera calibration methods were developed applying diffractive optical elements. Besides, the combination of different sensors relies on the knowledge of the alignment between theses sensors. Inter-sensor calibration strategies were developed.

And a robot system as a motion simulator has been configured in such a way that it may carry around the most different sensor systems in a dedicated way, while storing all measurements and time stamp data.

Application

Numerous applications can benefit from IPS navigation with robots, assistance systems in vehicles, guidance systems, and in-orbit-servicing in space.

4 Robots as Motion Simulators

In the last years we have started to develop interactive real time motion simulators, utilising a modified industrial KUKA robot. Due to its large workspace and outstanding mobility extreme manoeuvres such as overhead flights or vehicle rollovers also become feasible which are not possible with conventional (nevertheless expensive) hexapod based motion simulators. The available workspace compared to the simulator size and weight also exceeds that of a classical hexapod.

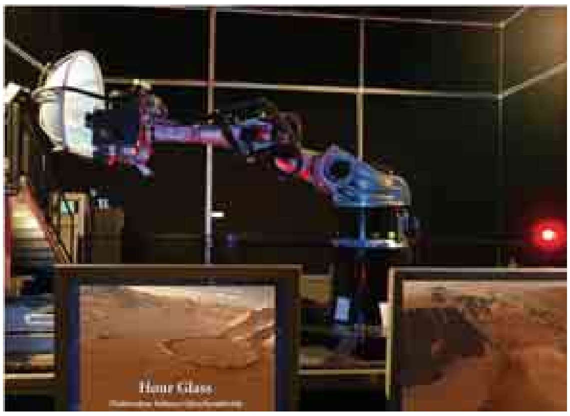

Fig. 271 The early Mars flight simulator with open dome projection 2005

4.1 Concept

The KUKA KR500/2 has been chosen as base mechanics for the DLR robot-based motion-simulator, it is capable of carrying up to 500 kg payload. The simulator cell is equipped with a visualisation and sound systems providing a transparent simulation environment.

This robot is, in a special modified and security certified variant called Robocoaster, available for public use as a fun ride in theme parks/leisure parks. In 2005 we presented for the first time a predefined flight path simulation in the Sony Center Berlin, where a Robocoaster, equipped with a projection dome, simulated a virtual flight over the Martian surface.

4.2 Interactive Motion-Simulations

However, these pre-calculated simulation runs provide no possibility for user interaction. In order to use the robot for interactive motion simulations, the research activity of the Institute aims for the implementation of interactive, real-time path planning algorithms. Here, the movement of the cell is calculated from the accelerations of a vehicle or aircraft model simulated in parallel. In the future the driver or pilot will steer a vehicle or aircraft and thus interact directly with the motion-simulation [Bellmann 2008[c]]. Appropriate in-house developed vehicle or aircraft models are generated with the object-orientated modelling language Modelica. These models consist, dependent on the detail of modelling, e.g. of complete vehicle models with powertrains or they include flexible elements like elastic aeroplane wings.

4.3 Real-Time Path Planning

The path planning has to consider every mechanical constraint of the robot during operation, for example the maximum or minimum joint angles or motor torques. This is necessary to assure that the planned trajectory can be retraced by the hardware. It is achieved by the use of optimisation algorithms, rendering a newly calculated trajectory, which matches the reference trajectory as close as possible, but which is in accordance with the robot constraints [Bellmann *et al.* 2007[c]]. And "wash-out-filters" are needed to take in account the human's sense of balance which has to be "cheated". Because of the limitations of the maximum cell weight, the possible equipment and instrumentation of the simulator cell is of course limited. While in commercial available simulators complete aircraft cockpits or vehicle interiors are reproduced, it is crucial for a robot-based motion simulator to avoid every unnecessary additional weight (Fig. 272).

Fig. 272 Different mountings of the simulator cell, suitable for different scenarios (left: automotive, aircraft simulations; right: helicopter hovering simulations)

4.4 Interactive Visualisation of Photorealistic 3-D Landscapes

We have developed different display techniques for visualising the scenery in which a pilot might fly. In addition to the open dome solution with projection technology as realised for the early Mars flight as mentioned above, we have developed closed carbon fibre shells with integrated 21'' displays as used in the avalanche simulator. And of course a crucial item of such a simulation system is the perfect synchronisation between robot motion and real-time visualisation of huge landscape data. The work flow necessary to create interactive 3-D models e.g. of large cities includes the efficient processing, mosaicing and radiometric correction of very high resolution digital aerial imagery (5-10 cm). 3-D building outlines are extracted and vectorised using semi automated processing. A custom-made software, developed by our industrial partner "reality maps", in cooperation with the Institute of Computer Science at the University of Bonn, allows the efficient visualisation of complex city models with hundreds of thousands buildings. Facades are extracted automatically from oblique viewing parts of the aerial images and mapped on the respective buildings.

The final goal of our research is the provision of a cost effective (because mass-produceable), highly flexible motion simulator, suitable for a wide range of dynamic simulation and telepresence scenarios, providing new simulation experiences like overhead flights, realisable due to the large workspace of the robot. Sensor-based and force-reflecting man-machine-interfaces will be integrated next for the realistic interactive control of simulated aeroplanes and vehicles. The robotic motion simulator topic covers many research items in the Institute, from dynamic modelling to fast sensor-based robot control including force reflection up to photorealistic synchronised 3-D visualisation based on our landscape modelling camera and stereo processing techniques.

Fig. 273 Avalanche simulation with DLR Robocoaster in *Les deux alpes*

Of course if interactivity is not requested, the alternative is to just generate a video e.g. of a skiing or snowboard descent including the recording of the corresponding accelerations and then display it with such a robot simulator. An application of this type has indeed been realised by us 2007 in the French Alps, where a simulated skiing experience ends up with an avalanche disaster. The simulator is now running in continuous operation for the public (Fig. 273).

5 System Modelling and Advanced Control

5.1 Multi-Engineering Modelling with Modelica

Modelling is a central topic in the Institute both for analysis of dynamic systems as well as being an integral part of advanced controllers. Since the software systems available on the market did not fulfil our needs, we founded the non-profit Modelica Association together with other partners from Europe and U.S.A. Since 1996 we have been jointly developing the component-oriented modelling language Modelica, as well as Modelica libraries in many engineering fields. For details see www.modelica.org. We are one of the driving forces behind Modelica, e.g., by leading the Modelica Association since 2000, as well as by organising the library development and the international Modelica conferences.

Modelica is based on differential, algebraic, and discrete equations and is targeted for system simulation using components from all engineering domains, see the schematic diagrams with components of free Modelica libraries in Fig. 274. The object-oriented nature of Modelica allows for one-to-one mapping of physical components and phenomena into model software components. Such components may be stored into engineering discipline-specific libraries for reuse in various applications.

Model construction from these libraries is done graphically, using drag and drop. Several innovative concepts have been introduced with Modelica not available in other simulators, e.g., "true" component-oriented modelling, robust simulation of coupled friction elements. Examples of the latter are clutches, brakes, gear mesh efficiency, or reliable bi-directional fluid flow, where the component models are independent of the medium model (e.g., a pipe model can be used with gases, water, oil).

The commercial tool Dymola acts as our Modelica simulation environment. Its highly efficient code generation and special integration algorithms represent the key to Modelica's success in the real-time simulation area. Dymola has been developed by the Swedish company Dynasim with which we have a close cooperation since 1992. One result of this cooperation was the porting of our formerly developed simulation kernel into Dymola. Dynasim was acquired in 2006 by Dassault Systèmes, a world leader in CAD and PLM, in order to integrate Dymola and Modelica in CATIA.

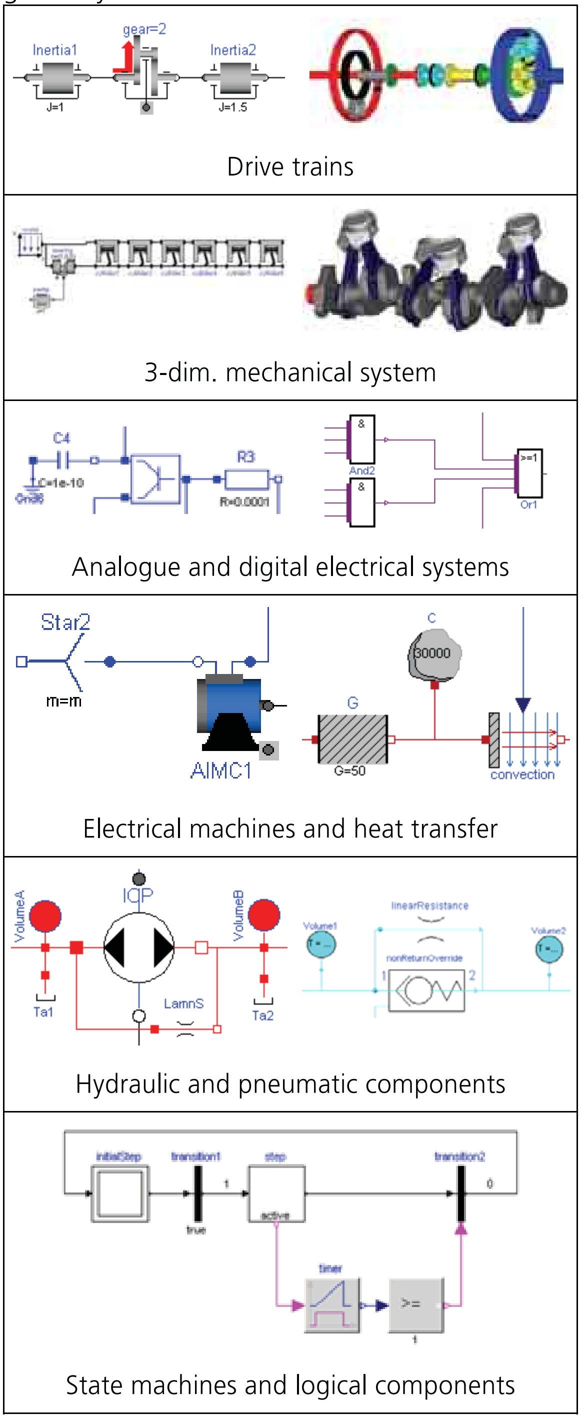

Fig. 274 Schematic diagrams with components of free Modelica libraries

We have developed essential parts of the free Modelica standard library such as libraries for multibody systems, drive trains, control blocks, and profits from free libraries developed by other partners, e.g., in the electrical, thermal, and fluid fields. Currently, three of our Modelica libraries—for vehicle power trains, for flexible bodies and for design optimisation—are sold commercially via Dassault Systèmes.

First industrial applications with Modelica and Dymola date back to the beginning of the year 2000. Since then, the usage is rapidly increasing. For example, most car manufacturers, such as BMW, Daimler, Ford, Toyota are now using it. Besides direct benefits in our work (e.g., hardware-in-the-loop simulation of stiff systems, or automatic inversion of non-linear dynamic systems for advanced controllers), our leading know-how of Modelica and Dymola helps us to acquire projects such as the POA and MOET projects (see Chapter V.2). There are also now large multi-national projects to further develop the Modelica technology:

EUROSYSLIB (2007–2010) is an ITEA2 project with 18 partners to develop about 30 free and commercial Modelica libraries in the mechanical, electrical, fluid, control, safety and automotive area and to improve the Modelica infrastructure. DLR-RM has organised this project together with Dassault Systèmes and is leader for the technical part of this project.

MODELISAR (2008–2011) is an ITEA2 project with 28 partners. The goal is to provide an open end-to-end solution for automotive systems modelling, embedded software generation and integrated simulation based design and testing, based on Modelica, AUTOSAR (the coming standard for embedded software in the automotive industry) and the product life cycle management of CATIA V6. The project leader is Dassault Systèmes.

FlexibleBodies Library

The commercial DLR *FlexibleBodies* library enables and supports the object-oriented and mathematically efficient modelling of flexible bodies as components of multibody and of arbitrary physical systems. It provides Modelica model classes to model beams and general flexible bodies exported from finite element programs, see [Heckmann *et. al*. 2006[c]].

The library is based on the "Standard Input Data of flexible bodies" (SID) which is an object-oriented data structure that was developed at the institute to generally describe the properties of elastic bodies.

In order to model beam-like structures the *FlexibleBodies* Library provides a graphical user interface which facilitates the definition of all necessary geometrical and physical data.

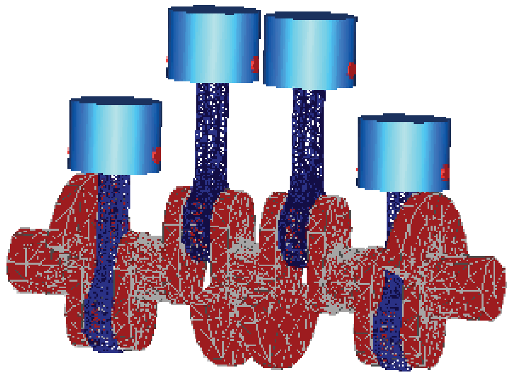

Fig. 275 Modelica FlexibleBodies model of a four-cylinder-combustion engine with an elastic crankshaft and elastic piston rods

Finite element data that are supposed to be used as part of a multibody model have to be pre-processed, so that the underlying SID structure is generated. We cooperate with the DLR spin-off company Intec GmbH for this step, which offers interfaces to all major commercial finite element tools and keeps track of their versions and upgrades.

The library is open for further developments and improvements. In the course of the EUROSYSLIB project, the modelling of an annular plate is about to be implemented in the same manner as the already existing beam-like structures.

The modelling and simulation of rotor-like structures will additionally be supported exploiting axially symmetric or axially cyclic properties and using the so-called ALE-approach, see Chapter VI.3.

A cooperation project with Knorr Bremse SfS GmbH on thermoelastic effects and related vibration problems of brake discs actually concerns railway vehicle brakes, but the results will also be introduced into a new Modelica *Multifield Library*, supposed to expand the *FlexibleBodies* library. Hence, the so-called modal multifield approach [Heckmann 2005[b]] will also be available for automotive brake systems.

5.2 Computational Methods for Control

Solving challenging control problems in the aerospace and robotics fields requires efficient and numerically reliable computational methods implemented in high-quality robust numerical control software. Collaborative efforts to develop numerical algorithms and implement high-quality robust numerical software have been pursued in the framework of several international and national cooperation projects such as the EU Thematic Network NICONET (Numerics In COntrol NETwork), and several research grants from the German and Swedish Research Foundation. In all these projects we played a leading role by contributing many control-relevant structure exploiting algorithmic developments (documented by a large number of journal and conference publications) as well as numerous software implementations. The software implemented within NICONET belongs to the control library called SLICOT. The maintenance and further development of the SLICOT library is now the task of the NICONET Association (NICONET e.V.), where DLR, as institutional member, is strongly involved in its leadership.

Based on SLICOT we developed several powerful and user-friendly toolsets for MATLAB. In long term efforts, toolboxes for descriptor systems, periodic and multirate systems, fault detection and LFT-modelling, have been developed. They go far beyond the state-of-the-art available in standard control software tools like MATLAB. The availability of these unique tools forms the basis of our projects for fault tolerant control (GARTEUR AG17, IMMUNE, ADDSAFE), satellite attitude control (cooperation with ASTRIUM) and helicopter vibration attenuation via periodic control (cooperation with EUROCOPTER).

Descriptor Systems

The descriptor system representation

$$\begin{aligned} E\dot{x} &= Ax + Bu \\ y &= Cx + Du \end{aligned}$$

arises when modelling interconnected systems or constrained mechanical systems (e.g., contact problems). Frequently, descriptor systems appear when solving standard computational problems, e.g., design of fault detection and isolation filters or manipulation of rational and polynomial matrices (e.g., factorisation).

For operations with descriptor systems and polynomial/rational matrices the Descriptor Systems Toolbox for MATLAB has been implemented. Besides providing an extended functionality to the Control Toolbox of MATLAB, the available functions allow a user-friendly operation to solve some of the most complicated dynamics analysis and synthesis problems using an object-oriented approach. Most of the structure-exploiting numerical computations are performed via MEX-functions. This toolbox has been continuously extended with new functions to cover the computational needs of fault detection applications.

Fault Detection and Health Monitoring

The detection and diagnosis of failures in engineering systems is of great practical importance. The quick and correct diagnosis of faulty components of such systems facilitates proper decisions in emergency situations and appropriate corrective actions or repairs. The large interest over several decades to solve fault detection problems led to many approaches which try to overcome the limitations of traditional hardware redundancy based methods or simple limit checking of supervised variables.

An important area is the model based fault detection, where especially for linear systems a large number of methods and approaches have been developed. A typical setup of a fault detection and diagnosis system is presented in Fig. 276, where typical faults (actuator, sensor, parametric), measured signals (control inputs $u(t)$, measured outputs $y(t)$), disturbance $d(t)$, residual $r(t)$, evaluation $\theta(t)$ and decision signals $i(t)$ are shown together with the corresponding processing blocks (residual generator, residual evaluator, decision making).

Surprisingly, there were only very few attempts to address in depth the involved computational aspects of the proposed synthesis algorithms. This explains why the vast majority of proposed methods are numerically unreliable and can not be used to solve practical problems with larger dimensions. To overcome this situation, in several projects focused on and involving fault detection, a systematic investigation of numerical aspects of the synthesis of linear residual generators for fault detection and isolation has been pursued. The results of this effort are new numerically reliable computational algorithms, which cover the main methodological approaches, see [Varga 2008d[r]] for a comprehensive survey and [Varga 2007d[c], 2008[c]] for the last developments. A distinctive features of the new algorithms is that they rely on a descriptor system formulation, which allows to solve the underlying problems in the most general setting, without any technical assumptions.

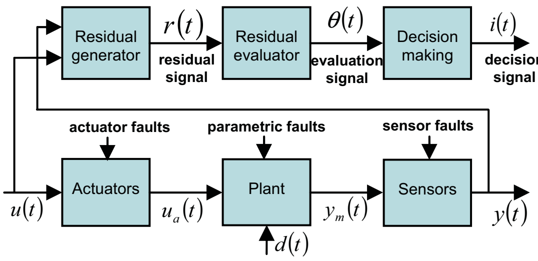

Fig. 276 Typical setup for fault detection and diagnosis

The proposed new methods have been implemented using tools of the Descriptor Toolbox, in a new Fault Detection Toolbox. This toolbox provides basic functionality to design linear residual generators for fault detection and isolation. It allows exploiting the complete parametric freedom of different problems via a user-friendly interface based on an object-oriented approach. A first version of the toolbox has been described in [Varga 2006b[c]].

Health monitoring is closely related to fault diagnosis. However, while fault diagnosis systems are after-the-failure approaches, the main focus in health monitoring is to predict and therefore prevent critical failures (e.g., arising from structural damages). Health monitoring is mainly used in situations where failures can lead to catastrophic situations (e.g. plane crash), or where a failure leads to high maintenance costs (e.g. involving production loss). The application of fault detection techniques to structural health monitoring problems is widely used, where the main aspect is the detection and localisation of *incipient faults*. New advances in signal processing, sensor and actuator technology are expected to revolutionise the way health monitoring for large electromechanical systems will be done in the future.

The Fault Detection Toolbox has been used to solve challenging fault diagnosis problems in flight control (within the GARTEUR AG17 and IMMUNE projects), will be the basis for the newly granted FP7 project ADDSAFE, is intended to be also used for the detection of incipient faults in electrical networks (within the MOET project) and for actuator health monitoring.

Periodic Systems

Many control applications arise as genuine periodic control problems such as satellite attitude control or helicopter forward flight control. In addition, periodic systems represent a general framework to analyse and design multirate-sampled data systems. The research to develop new structure exploiting and structure preserving numerically stable algorithms for the analysis and design of periodic control systems has been conducted in the framework of a cooperation project with the group of Prof. Bo Kågstrom from the Umeå University (Swedish Strategic Research Foundation Grant: Matrix Pencil Computations in Computer-Aided Control System Design: Theory, Algorithms and Software Tools, 2002–2008). The results of this research (7 published papers) are also described in the survey paper [Varga 2007e[c]].

Based on the new generation of structure preserving algorithms, we developed a Periodic Systems Toolbox [Varga 2005d[c]] for manipulation, analysis and design of discrete-time periodic systems. This toolbox is the first CACSD tool able to handle realistic practical problems where either the system order or the period is large. The toolbox has been used to solve several satellite attitude control problems in cooperation with the group of Prof. M. Lovera from the Politecnico di Milano [Lovera & Varga 2005[c]; Pulecchi *et al.* 2006[c], 2008[c]; Vigano *et al.* 2007[c]], and is envisaged to be used in the technology project INROS (Innovative Rotor Systems) to address active control of higher harmonic vibration attenuation using periodic control techniques. An increasing interest in applying periodic control methods is due to the availability for the first time of suitable computational tools.

LFT-Based Uncertainty Modelling

Modelling parametric uncertainties using linear-fractional transformations (LFTs) is necessary when applying advanced linear robust control synthesis techniques like μ. A typical procedure for parametric uncertainty modelling for robust control design is presented in Fig. 277.

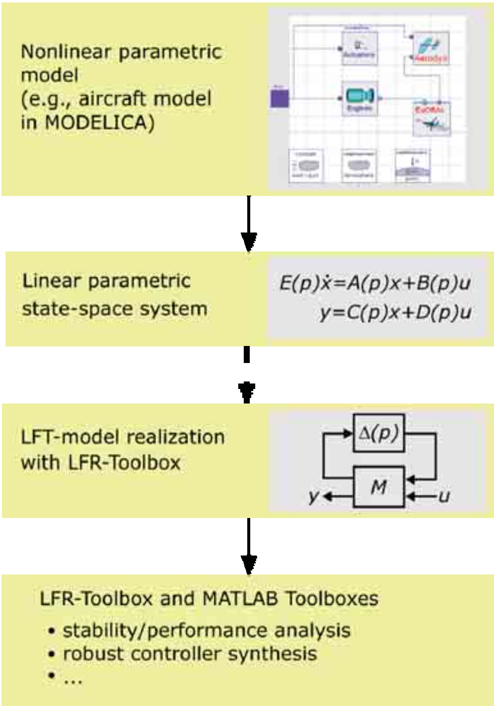

Fig. 277 Robust control design process: (1) starting from a nonlinear parametric model, linear parametric models are obtained via symbolic linearisation; (2) linear parametric models are transformed to LFT-form using the LFR-Toolbox; (3) robust analysis and synthesis methods from the LFR-Toolbox or related MATLAB toolboxes are applied.

The uncertainty modelling problem, i.e., to convert the parametric expressions of the system matrices into LFT-based representations of lowest possible orders, requires advanced computer aided generation tools. With our new LFR (Linear Fractional Representation) Toolbox [Hecker *et al.* 2005[j]], LFT-representations can be directly obtained from symbolic expressions or via object oriented manipulation of LFT-objects. A first version has been developed within the joint DLR/ONERA project HAFUN and includes many new developments and enhancements (e.g., more general LFT-definition, improved numerical order reduction, enhanced symbolic preprocessing) compared to the previous software tools available at DLR and ONERA. Further developments of the Toolbox [Hecker 2008[c]] are still ongoing.

Since the end of 2007 a special focus was put on the first step of the control design process, which involves the generation of linear parametric state-space systems from a nonlinear parametric model. In case that a symbolic description cannot be directly derived from e.g. a Modelica model, we developed very efficient algorithms and software tools for the generation of optimal linear parametric models, that depend continuously on the model parameters. These tools are important for nonlinear aeronautic models, where usually the aerodynamics or structural models are only given at a discrete set of grid points within the flight envelope. Therefore, a rational parametric approximation, which covers the grid-point models, must be generated to obtain the required linear parametric model.

These tools were successfully applied and allowed to generate linear parametric models and LFT-models of high accuracy and minimum complexity for a highly nonlinear missile model [Pfifer & Hecker 2008[c]] and a highly nonlinear model of a large transport aircraft [Hecker 2008[c]].

5.3 Nonlinear Model-Based Methods

The design of control laws for highly nonlinear systems (such as aircraft, robots, vehicles) using linear techniques can result in an elaborate, iterative process, involving multiple designs at a grid of operating points and integrating these with the help of gain schedules. For this reason, the institute has investigated, improved and successfully applied several nonlinear controller synthesis methods.

One promising approach is the use of originally linear controller structures based on inverse plant models, implementing inverted non-linear plant models instead. Examples are inverse models in the feed-forward path, or disturbance observers with an inverse model in the feedback path. Another approach is the use of controllers based on feedback linearisation (in aerospace known as Nonlinear Dynamic Inversion, NDI). In this case, the states in the inverse model equations are obtained from measurement or observers. Desired dynamic behaviour may be imposed via an additional linear outer feedback loop.

Automatic Model Inversion

Inverse models can be derived as the solution of higher-index differential-algebraic equations. This can be done automatically from a Modelica model of the system. To this end, the meanings of inputs and outputs are exchanged, after which the Modelica simulation tool Dymola performs the needed index reduction using symbolic algorithms, see Fig. 278.

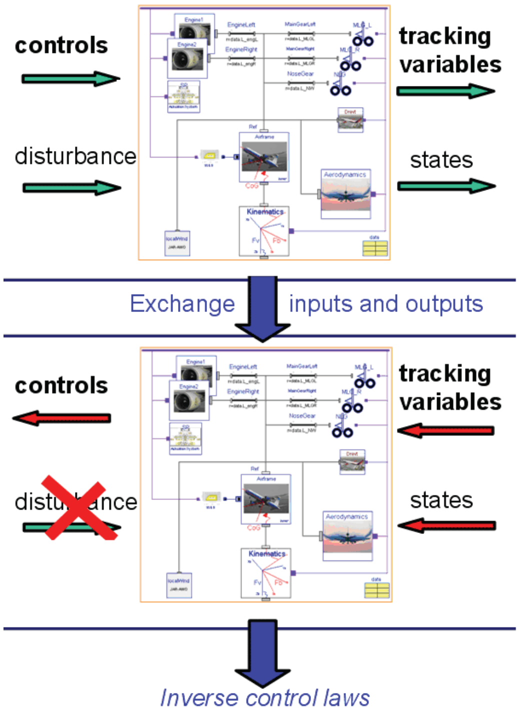

Fig. 278 Exchange of model inputs and outputs for automatic inversion

Automation of model inversion saves tedious and error-prone manual derivation of the inverse control laws, especially in case the system model is highly complex. This technique has been used especially for:

- robots, to implement a controller based on a detailed inverse nonlinear robot model, in which the elasticity of the robot is considered, permitting high performance tracking tasks. The generated code was successfully implemented in a standard rapid control prototyping environment (Matlab xPC);
- vehicles, to compute criteria for assessment of vehicle handling by means of inverse vehicle dynamics models;
- aircraft equipment, for evaluation and optimisation of new "more electric" aircraft system architectures (see Chapter V.2);
- aircraft dynamics, for the implementation of nonlinear dynamic inversion control laws for e.g. aircraft drive-by-wire control (see Chapter V.1).

Design for Robustness

The use of inverse model equations of course gives rise to robustness issues in case the actual system dynamics are not described sufficiently accurately. For this reason a new approach for achieving a robust design has been developed. Tolerances on parameters in the model namely also appear in the inverse equations. It has been shown that these parameters may be very effectively used as additional tuning parameters in multi-objective parameter optimisation. Robustness is hereby addressed by optimisation for multiple model parameter cases, as well as via robustness measures (e.g., gain and phase margins) as design criteria. As a result, the model is basically inverted at a location in the parameter space that provides the highest level of robustness [Looye 2008[t]], see Fig. 279.

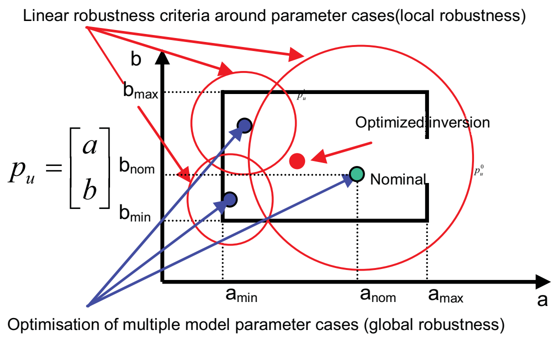

Fig. 279 Optimisation of the inversion point in the parameter space (a,b). Robustness is achieved using local robustness criteria and multi-case optimisation

5.4 Multi-Objective Parameter Synthesis

Multi-objective optimisation is a proven, well-known parameter tuning technique in engineering design especially suited to solve complex, multidisciplinary control design problems, like robust handling quality control of aerodynamically unstable aircraft, robust autopilot control of large transport aircraft, commissioning by robot-in-the-loop optimisation, etc. Applications in close cooperations with our partners in industries and research (KUKA, Airbus Germany/France, Bosch, TU Berlin, Univ. Stuttgart) showed the necessity for a homogeneous design environment, which engineers are familiar with. Our optimisation-based design environment, called MOPS (Multi-Objective Parameter Synthesis) is therefore implemented in the common engineering language MATLAB still using sophisticated proprietary optimisation algorithms.

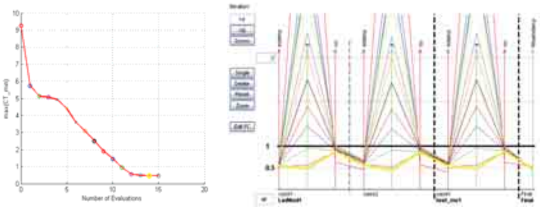

Fig. 280 Visualisation during optimisation run showing the progress of the overall objective function "maximum criteria value" (left diagram) and the progress of individual normalised criteria and constraints in parallel coordinates (right diagram). Both diagrams are interrelated.

MOPS is currently applied to various design and evaluation problems at DLR and in industry. The main fields of application are industrial robotics, flight control, power-optimised aircraft systems, and vehicles. Development and maturation of MOPS is an ongoing process. As an integrated semi-automatic parametric analysis and design engine MOPS provides a number of advanced features:

- in order to find global optimum solutions deterministic and stochastic search algorithms are now available both for continuous and mixed integer/continuous problems;
- the visualisation tools have been further improved. The effects of parameter variations for different model cases can now be displayed automatically on demand as well as the progression of the optimisation run, see Fig. 280;
- in order to assist design optimisation, higher-level functions are provided like multi-start optimisation to overcome local minima, and automatic search of Pareto bounds to exploit compromises as illustrated in Fig. 281;
- worst-case search based robustness analysis can be performed by anti-optimisation automatically derived from design problem setup;
- for parameter estimation, needed for modelling of robots, efficient bounded least squares algorithms are available;
- statistical analysis of design criteria via Monte-Carlo simulation is a supported feature as well. Statistical design criteria, like variances, risk probabilities etc., can be directly used within an optimisation process;
- robust control law synthesis for multi-disciplinary design problems is explicitly supported by a structured multi-model/multi-case/multi-objective problem setup;
- extensive optimisation runs, parameter studies or Monte-Carlo simulations can now be computed in parallel on a distributed network yielding a large benefit in computing time.

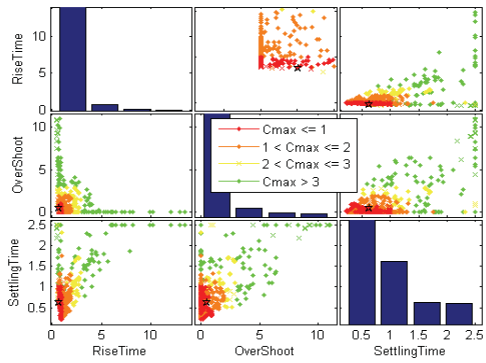

Fig. 281 Automatic generation of scatter plots indicating Pareto-bounds for compromising conflicting design criteria

5.5 Advanced Sensitivity Analysis

The equations of multidisciplinary models are typically described by discontinuous functions that simplify complex interrelations like Coulomb friction. Modelling of Coulomb friction in Modelica is based on model internal state machines that determine the valid slip or stick phase. An alternative way has been developed to simulate the discontinuous models. It follows the approach to numerically compute the generalised solution according to Filippov without any additional model setup. Hence, the corresponding component models are less complex—an advantage of the method.

An important task in system analysis and controller design is the identification of unknown model parameters by optimisation algorithms. Gradient oriented algorithms require derivative information of the simulated models. Therefore, detailed model-based investigations not only demand computing the solution of model equations, but also sensitivities (derivatives) with respect to model parameters. A general numerical approach relies on the simultaneous integration of the nominal system and the sensitivity differential equations. This approach was extended to hybrid systems with discontinuities in right-hand sides and states.

The developed software environment FISEMO [Pfeiffer 2008[t]] affords the direct numerical integration of discontinuous Modelica models with Filippov solutions. The implemented sensitivity analysis includes the numerical integration of the sensitivity equations as well as the consideration of state events and the Filippov solution. Results from parameter identification in robotics using MOPS as optimisation engine show the functionality and the advantages of the approach. Fig. 282 demonstrates the more efficient and reliable numerical optimisation using the newly implemented methods in comparison with the standard ones.

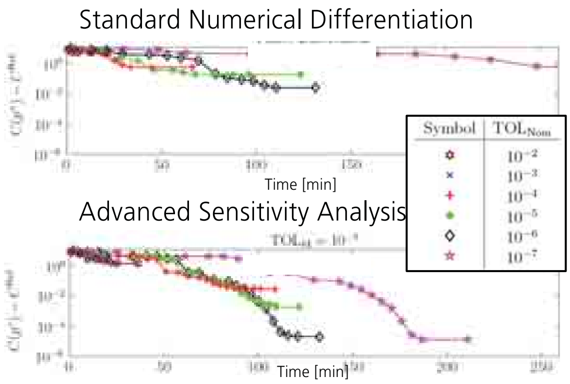

Fig. 282 Influence of standard and advanced sensitivity analysis on the optimisation results. Parameter identification in robot model: Distance to optimal objective function value over computing time for different integration error tolerances.

Within the ITEA-project EUROSYSLIB the optimisation kernel of MOPS is currently coupled with the developed advanced sensitivity analysis of discontinuous systems for gradient computations. The goal is to specify and run efficient optimisations directly in the modelling and simulation environment of Modelica.

V Aeronautics

The institute has long standing experience in the development and application of methods and tools for aircraft and systems modelling and simulation, design of primary and secondary flight control laws, multi-objective design optimisation, and (closed-loop) aircraft flight dynamics and systems assessment. During the reporting period, starting from end of 2004, these tools and methods, as well as their applications, have been considerably extended and are reported in Section "Flight Dynamics and Control".

The quality and versatility of the methods and tools developed by the institute is probably best illustrated by the fact that their application has grown rapidly beyond flight control system design only. Already during the previous reporting period, modelling and simulation of systems for more electric aircraft with the help of Modelica technology has become an important pillar of work. During this reporting period these activities have been further expanded, a.o. through the institute's leading role (on strong request by industrial partners) in the MOET project and are reported in Section "More Electric Aircraft Systems".

1 Flight Dynamics and Control

The institute has long standing experience in the development and application of methods and tools for multi-disciplinary aircraft flight dynamics modelling, flight control law synthesis, multi-objective design optimisation, and (closed-loop) aircraft flight dynamics and systems assessment. During the reporting period these tools and methods, and especially their applications, have been considerably extended.

The increasing need for addressing multi-disciplinary aspects in the design of flight control laws has led us to put considerable effort in multi-disciplinary model integration, resulting amongst others in the Modelica Flight Dynamics Library. Since 2000, the developed methods and tools, as well as resulting aircraft models, have increasingly found application in loads analysis on fully flexible aircraft and in real time flight simulation. During the reporting period, aircraft design analysis in the pre-design phase has become a new important field for our modelling tools. In order to standardise tool interfaces and to improve efficiency modelling activities were oriented towards a standardised modelling process.

For the design of primary and secondary flight control laws we propose an inherently multi-disciplinary, optimisation-based design process, based on the aforementioned method and tools. During the reporting period, active loads alleviation system design continued to be a major application for this design process. The excellent results in the MODYAS and AWIATOR projects led to heavy involvement in new projects like ACFA 2020, iGreen, and a key role in the Smart Fixed Wing Aircraft project within the European CleanSky Joint Technology Initiative (JTI).

Design of primary flight control functions found new application in missile flight control systems. Here techniques like LPV (Linear Parametrically Varying) controller synthesis are very promising, due to the highly nonlinear nature of missile flight dynamics.

An important new topic has been Fault Diagnosis. Here methods and tools for robust and efficient fault detection and isolation have been and will further be developed. These methods and tools found successful application within the DLR-ONERA project IMMUNE and in the GARTEUR FM(AG16) action group on Fault Tolerant Control.

In order to handle large scale analysis problems in flight control laws design, like clearance with respect to uncertainties over the full flight envelope, the institute has developed methods like optimisation based worst-case search, and implemented techniques like Monte-Carlo analysis in its MOPS (Multi Objective Parameter Synthesis) design environment. The highly successful application of optimisation based clearance in the GARTEUR FM(AG11) project, and the development of an extensive tool set for automatic transformation of nonlinear models in to LFT-form (required for many robustness analysis methods, like μ-analysis), led to a key role in the European COFCLUO project.

The quality and versatility of the methods and tools developed by the institute is probably best illustrated by the fact that, like in the case of flight dynamics modelling, their application has grown rapidly beyond flight control system design only. One example is the multi-objective optimisation of aircraft trajectories with respect to noise, emissions, and economical aspects in the frame of projects like IHK-HICON. These activities are now continued within JTI-CleanSky MTM (Management of Trajectories and Mission) work package. As another example, the statistical analysis part of MOPS has found extensive application for wake vortex analysis in the frame of projects like WakeScene or CREDOS where aircraft separations during take-off and landing have been investigated.

From the above it may be concluded that the institute's focus in the field of aeronautics has clearly widened from robust flight control in the mid-nineties to flight dynamics and aircraft systems analysis in general, both from an aircraft design as well as an operational point of view. In the following sections progress in the fields of method and tool development, as well as their applications in various projects will be discussed in more detail.

1.1 Aircraft Modelling and Simulation

Multi-disciplinary design of flight control laws (FCLs) implies that prime objectives of the control laws are addressed in coordination with their effects on other disciplines. For example, in case of manual fly-by-wire or autopilot flight control laws, accurate tracking of command variables may considerably influence structural dynamics of and aerodynamic loads on the airframe, as well as result in high effort by the control system hardware. On the other hand, in case of active loads alleviation control laws, it has to be made sure that the aircraft's handling qualities do not deteriorate to an unacceptable level.

The computation of all relevant numerical design criteria requires the availability of multi-disciplinary aircraft models. These models in the first place have to be sufficiently accurate in order to allow for reliable computation of all design criteria of interest. At the same time, models have to be "loop capable", i.e. allow for evaluation of thousands of flight cases in a short time. Finally, models must be available in various forms, depending on the type of analysis. Examples are nonlinear ordinary differential equations for simulations and Linear Fractional Transformation (LFT) for robustness assessment.

For these reasons, the institute follows a so-called model integration approach. This implies that multi-disciplinary aircraft models are developed by integrating model data, components and/or methods from involved specialist engineering departments. This avoids unnecessary repetition of work and at the same time ensures compatibility with discipline-specific models used within specialist engineering departments.

During the reporting period, the institute has considerably advanced its methods and tools for development of multi-disciplinary aircraft models. Three Ph.D. theses were successfully defended [Reschke 2006[t]; Looye 2008[t]; Reijerkerk 2008[t]] and a fourth is in a well advanced stage [Kier *et al.* 2007[c]]. Nine publications on the subject were presented at highly regarded conferences like the International Forum on Aeroelasticity and Structural Dynamics (IFASD), the annual conference of the German Aerospace Society (DGLR), and the annual Modelling and Simulation Technologies conference of the American Institute of Aeronautics and Astronautics (AIAA).

1.1.1 Dynamic Aircraft Model Integration Process

During the reporting period the diversity of applications of flight dynamics models developed in the institute has grown considerably. For example, besides FCL design, models were developed for flight loads analysis, mission simulation and aircraft pre-design analysis. At the same time a stronger emphasis on modelling of aircraft in the pre-design phase has emerged, requiring rapid model updates as the aircraft geometry is modified over sequential design iterations. For these reasons, it was decided to integrate all aircraft modelling tasks for the various applications within the institute and in cooperations with partners into a standardised Dynamic Aircraft Model Integration Process (DAMIP). As can be seen from the basic structure depicted in Fig. 283, the process covers key aspects such as:

- Handling and processing of model data (especially in case of flight loads analysis amounts of data can be huge);
- Integration of model data from various disciplines;
- Application of industry-standard and advanced modelling methods (e.g. FEM for structural modelling, aerodynamic methods like Doublet and Vortex Lattice);
- Suitable platforms for model implementation;
- Tools for model simulation and model analysis.

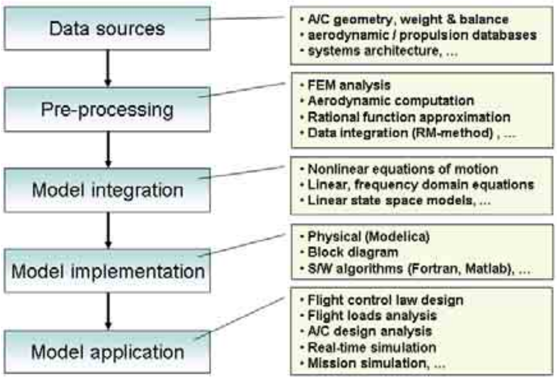

Fig. 283 DAMIP—Dynamic Aircraft Model Integration Process

The process further provides a standard framework and orientation for future tool development.

Besides the definition of DAMIP, the most important advances in flight dynamics modelling activities are in the individual process steps, as will be discussed in the following subsections.

1.1.2 Data sources and Preprocessing

The construction of integrated aircraft models requires the availability of various data sources, e.g. aerodynamic tables (or other forms, like neural networks), geometry of the airframe, weight and balance properties, etc. Therefore, interfaces to such data sources are the first step in DAMIP. The preferred database, especially in case of loads analysis applications is VarLOADS [Kier *et al.* 2007[c]]. In the frame of the DLR projects TIVA (Technology Integration for the Virtual Aircraft) and TIVA-II, an XML-based aircraft data structure is used, called CPACS (Common Parametric Aircraft Configuration Standard). Interfaces to CPACS have been developed, allowing aircraft aerodynamics, geometry and other data to be directly used in model components. For flight mechanics applications, first interfaces to the emerging AIAA-standard DAVE-ML (Dynamic Aerospace Vehicle Exchange Mark-up Language) have been developed.

In the early design stage of aircraft, only limited data are available, especially for aerodynamics. For this reason, own implementations of the Vortex and Doublet Lattice (VLM, DLM) methods have been programmed in highly efficient Matlab code. New approaches for Rational Function Approximations of unsteady aerodynamic data (computed in the frequency domain, e.g. using DLM) in the time domain have been developed [Kier *et al.* 2007[c]], which enhance reusability of the data and therefore considerably reduce computing time.

1.1.3 Model Integration

The nonlinear equations of motion (EOM) of flexible flight vehicles in combination with kinematic equations with respect to an Earth-Centred Inertial (ECI) reference frame form the backbone for the proposed model integration approach. Components like propulsion and aerodynamics physically interact with the EOM via kinematic constraints, as well as forces and moments. As body reference system so-called mean axes are used, allowing direct use of the same so-called free-free modal analysis results as used for e.g. gust loads analysis [Reschke 2006[t]]. During the reporting period detailed flexible airframe equations of motion (with loads equations) that include all inertial coupling effects, were derived and implemented. An example analysis result for a large passenger aircraft can be seen in Fig. 284 [Reschke 2006[t], 2005[c]].

One of the key integration issues in case of flexible aircraft is how to combine model data from the flight mechanics and aeroelasticity disciplines. Models developed in these disciplines are of very different nature, but also contain overlaps, like rigid body degrees of freedom in aeroelastic models, static aeroelastic corrections in flight mechanics models. Therefore, the institute has developed the so-called Residualised Model (RM) method [Looye 2005[c]; Reschke 2005[c]]. Besides its use in models developed in-house, the method is also used to integrate aeroelastic model data in tools of industrial partners.

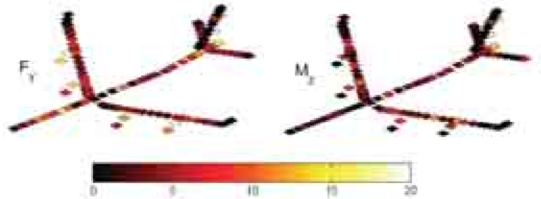

Fig. 284 Relative differences [%] of maximum nodal forces and moments over the airframe between inertially coupled and uncoupled equations of motion and loads equations during an EASA/FAR-25 design rolling manoeuvre (2.5g)

1.1.4 Model Implementation

For aircraft model implementation, the institute uses two platforms: the Modelica Flight Dynamics Library, developed in-house, and the Matlab/Simulink-based VarLOADS environment, developed in close cooperation with Airbus. In addition, components developed using the DAMIP process can be made available for use in tools of industrial partners.

The New Modelica Flight Dynamics Library

The Modelica-based DLR Flight Dynamics Library is the most important platform for implementation of multi-disciplinary aircraft models. The particular strength of the Modelica language is to code model components in their physical form, thus providing an ideal basis for multi-disciplinary model implementation. As an additional advantage, the physical implementation allows various types of runtime analysis models for various applications to be derived from a single implementation (e.g., nonlinear ODEs for simulation, inverse models for control laws, static models for mission simulation and trimming, etc.). This ensures consistency between the various model forms and saves considerable amounts of time.

During the reporting period, the Modelica Flight Dynamics Library has been redesigned and expanded. The reason is that the Modelica language specification has been considerably extended, allowing for more convenient physical structuring of aircraft models, see Fig. 285.

The most important features of the Flight Dynamics Library are:

- Standard components for aircraft airframe (flexible or rigid) and kinematics (body reference w.r.t. ECI, WGS84 position coordinates), environment models (atmosphere, rotating planet, terrain, etc.);
- Basic classes that allow for easy implementation of aircraft-specific components (aerodynamics, propulsion, systems, etc.);
- Airframes and components like landing gears may be constructed using the Modelica multibody library;
- Components may retrieve control commands (e.g. throttle setting for an engine) from, and transmit measured variables to, data buses, based on the Modelica expandable bus feature.

Important library extensions include landing gear models, allowing for landing, take-off and on-ground simulations, navigation equipment (e.g. GPS, VOR, DME). Also the automatic generation of inverse models has become more comfortable.

The Flight Dynamics Library will be publicly released and added to the growing palette of commercially available libraries that have been developed by the institute.

The VarLOADS Environment

Besides the Flight Dynamics Library, the institute has been closely involved in the development of the Airbus modelling environment VarLOADS (Fig. 287), intended for special flight loads related investigations. Modelling methods and integration techniques addressed above are extensively used in this implementation. Flight mechanics models only require total forces and moments around the vehicle's centre of gravity. Models used for loads analysis require the distribution of external forces over the airframe to be explicitly accounted for, allowing dynamic loads at specific locations of interest to be computed. The VarLOADS tool has been successfully used for flight clearance in the EU-project AWIATOR.

Furthermore, the institute made significant contributions to the further improvement and extension of VarLOADS in conjunction with the development of the next generation of long range Airbus aircraft. VarLOADS was used in early development stages to determine dimensioning load cases.

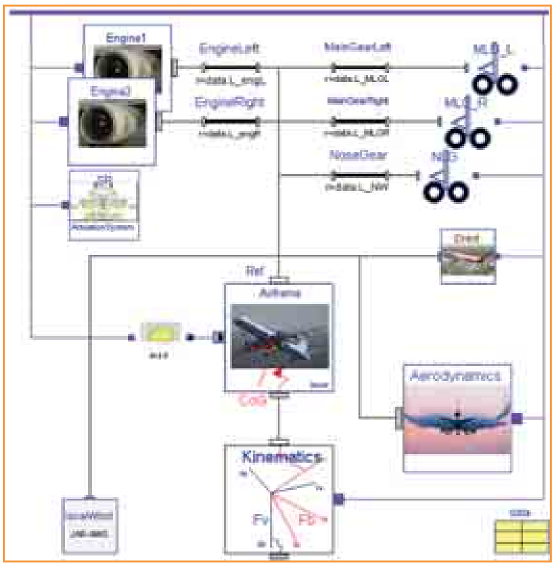

Fig. 285 Example aircraft model, including aerodynamics, engines and landing gears, constructed using the Modelica Flight Dynamics Library. The purple lines are connection to a central databus

VarLOADS will also play a major role in the EU Project "Clean Sky/Smart Fixed Wing", where it will be used to assess new loads reduction technologies.

In the near future, the VarLOADS environment will be extended to directly accommodate runtime models generated from the Modelica Flight Dynamics Library.

Model Implementation in Partner Tools

In the frame of the LuFo-III project MODYAS (Multi-Objective Dynamic Aircraft Synthesis) methods and tools from the DAMIP process were used to integrate and implement aeroelastic model components into simulation tools of Airbus.

For manoeuvre loads analysis flexible aircraft models were generated at flight and loading conditions of interest and integrated with the nonlinear quasi-flexible flight dynamics simulation in the Airbus production software LODEMA (Loads Design Manoeuvres), see Fig. 286. By using the aforementioned Residualised Model method, the existing flight mechanics part of the model only needs minor modification in the form of small additional forces and moments in the equations of motion. The extended simulation environment (LODEMA-Flex) allows for computing loads envelopes based on batch simulations at various flight and loading conditions and for various design manoeuvres, including the effects of dynamic structural deformation of the airframe.

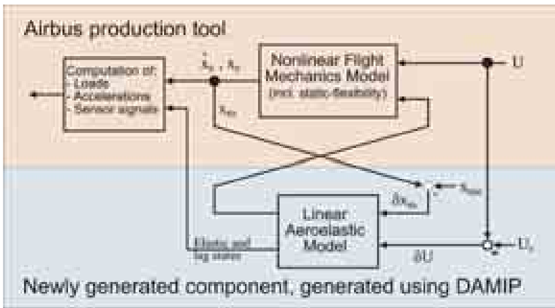

Fig. 286 Integration of aeroelastic model components in standard Airbus tools

Also in the frame of the MODYAS project, aeroelastic model components were generated for use in real time flight simulators. Especially the influences of gust disturbances, as well as excitations by gear and engine forces were modelled accurately. The fully integrated real-time model was successfully tested in fixed and moving base simulators in Hamburg and Berlin respectively.

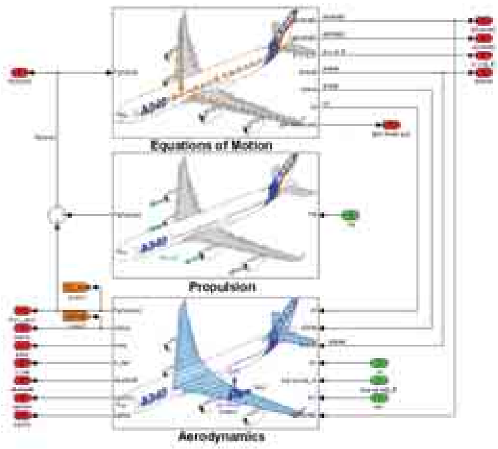

Fig. 287 VarLOADS flight loads model environment

1.1.5 Model Application

During the reporting period, the focus of model application has been clearly widened from flight control law (FCL) design analysis to over-all aircraft design analysis. Besides FCL design, the latter also includes for example loads analysis, preliminary stability and control analysis, and mission simulation.

Runtime Models from Modelica

As mentioned before, one of the most important advantages of the Modelica language is that model implementation and model application are independent to a large extent. Various types of runtime models may be automatically generated from a single model. During the reporting period, besides nonlinear differential equations for simulation, the ability of automatic generation of inverse models has been applied extensively. This has enabled the development of a rapid-prototyping process for flight control laws, based on the Nonlinear Dynamic Inversion control design method, see Fig. 288. More details can be found in [Looye 2008[t]].

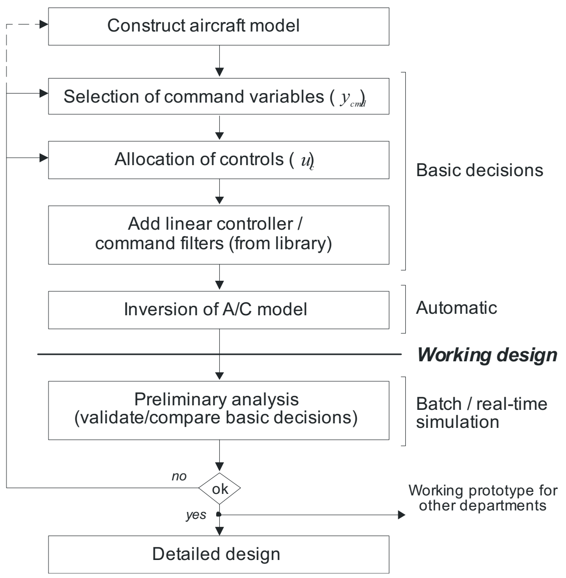

Fig. 288 Rapid prototyping process for flight control laws using automatic inversion from a Modelica model

In the frame of the DLR TIVA projects the institute used the Flight Dynamics Library (with the aforementioned newly developed interfaces to the CPACS database) to construct a model of an example aircraft configuration based on DLR's ATTAS aircraft. From this implementation, runtime models for various applications have been generated, like nonlinear differential equations for (real-time) simulation analyses, linear state space models for handling quality analyses, static inverse models for trim analyses (e.g. for loads computation), inverse models for preliminary control laws (based on Nonlinear Dynamic Inversion), and inverse models for mission simulation.

During the reporting period, mission simulation emerged as an important new model application. Mission simulation involves the quasi-static simulation of the aircraft along complete mission trajectories at given speeds. The simulation result includes equilibrium aircraft states and output variables along the trajectory segments, fuel usage (and decreasing over-all aircraft weight), etc. These results may for example be used for emission and noise computations, as well as aircraft performance assessment covering complete flight plans.

Fig. 289 Mission simulation of a 3-D spiralling approach to Munich Airport (EDDM), rwy. 08R

As an example, in the frame of TIVA-II several approach trajectories have been simulated for comparative calculation of noise in airport vicinity by the institute AS. One such approach is depicted in Fig. 289.

Flight Loads Analysis using VarLOADS

In the frame of the MODYAS project an aircraft model for flight loads analysis in the pre-design stage was developed. Emphasis was put on prediction of aerodynamic loads on specific structural parts, like the fin, during dynamic manoeuvres and during discrete gusts. These loads can now be computed with low effort, but with sufficient accuracy. Tolerances can be estimated for sensitivity and worst-case analyses.

The Vortex-Lattice Method (VLM) was used to estimate steady loads as a function of the current airframe configuration. Unsteady aerodynamic loads were computed using Doublet-Lattice Method (DLM) [Kier *et al*. 2005[c]].

For demonstration the geometry of the fin was modified. Based on aerodynamic loads computed with VLM/DLM the impact on gust and (lateral) manoeuvre loads, as well as flight mechanical aspects such as the minimum control speed were analysed, see Fig. 290.

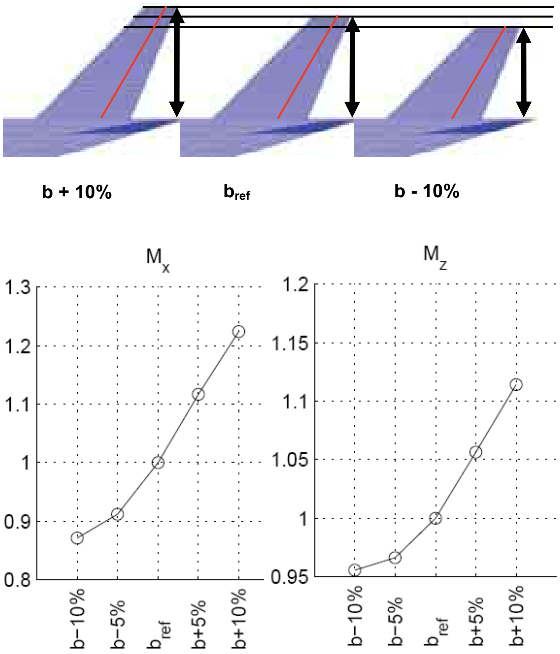

Fig. 290 Load calculation for variation of fin span from +10% to -10%, while the sweep remains constant

Tools for Trimming and Linearisation

Trimming is an important step in initialising models for nonlinear simulation and linearisation. The in-house developed algorithms for finding equilibrium points are based on nonlinear equation solvers and optimisation methods and have been considerably extended (e.g. handling of bounds on input variables). A graphical user interface for specifying trimming problems has been further improved.

Within the VarLOADS environment, our trimming tools have been used to compute so-called bookcase equilibrium manoeuvres (like 2.5g pull-up) for the aforementioned future long-range Airbus aircraft, in order to find dimensioning loads for the airframe structure.

Visualisation and Desktop Simulation

With increasing complexity of aircraft models, high-quality visualisation plays a very important role. For real-time visualisation (e.g. for interactive evaluation of flight control laws), the institute uses the visualisation software VisEngine from AeroLabs AG (http://www.aerolabs.de). Extensions exclusively developed for the institute include high-quality 3-D visualisation, as well as real-time visualisation of dynamic airframe deformation in flight. Also external loads on the airframe can be displayed, see Fig. 290. This feature has been very valuable for qualitative model validation. The interactive simulation of flexible aircraft in combination with 3-D stereo visualisation has further been demonstrated at various events and conferences, like ILA 2006 in Berlin, the Public Day 2008 in the Federal Chancellery, the ICAS 2006 conference in Hamburg and the CEAS 2007 conference in Berlin, attracting a lot of public interest.

Fig. 291 Realistic real-time aircraft visualisation, including stylistic display of aerodynamic, propulsion, and landing gear loads

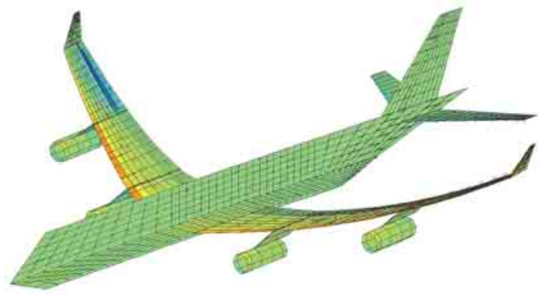

Fig. 292 Pressure distribution around a deformed aircraft, computed using DLM

For data analysis in the Matlab environment, dedicated tools have been developed to (dynamically) display airframe loads, deformation, aerodynamic pressure distributions, see Fig. 291.

1.2 Flight Control Design and Clearance

With each newly developed aircraft, flight control systems continuously increase in their functionality (e.g. automatic take-off, drive-by-wire on ground). In addition the increasing tendency towards "just-right" sizing of systems hardware and airframe structure leads to stronger inter-disciplinary interactions.

In order to handle future flight control problems efficiently, we propose an inherently multi-disciplinary flight control laws design process with a high level of automation. This design process is based on the long-standing experience of the System Dynamics and Control group in the fields of object-oriented modelling and multi-objective optimisation [Joos 2008a[f]].

The overall process is depicted in Fig. 293 where the principal steps of the design iteration are shown in the middle. The process is supported by software tools and methods indicated in the boxes on the right hand side. These tools have to be permanently maintained, extended and improved in order to successfully manage upcoming projects and tasks. Models required for multi-disciplinary design analysis and synthesis (left) are preferably generated from the DAMIP process, described in the previous section.

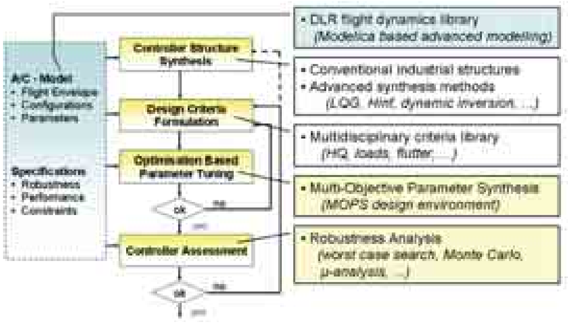

Fig. 293 Overall proposed design process and its support by analysis and synthesis tools

During the reporting period this process and its accompanying tools have been successfully applied and further improved within several projects concerning e.g. active loads control (Sec. 1.3), rapid prototype controller design, clearance of flight control laws, and drive-by-wire ground control.

1.2.1 Drive-by-Wire Ground Control

Within the GARTEUR NASTAC project we contributed to an aircraft-on-ground benchmark proposed by Airbus. Aircraft-on-ground control systems will reduce pilot work load (e.g. the aircraft will stay on its commanded track, even in case of cross wind), and provide the possibility to implement autopilot modes for on-ground operations, allowing for future automatic "gate-to-gate" operation of airliners. The control problem involved proper handling of redundant possibilities of steering the aircraft (rudder, nose wheel, differential brakes and thrust), and handling of severe nonlinearities and large uncertainties in tyre, braking and nose wheel steering dynamics. The advantages of rapid-prototyping control laws using nonlinear dynamic inversion and automatic model inversion from a Modelica environment (see Sec. 1.1) have been demonstrated. This allowed for quick comparison of different control strategies and pilot commands regarding performance and e.g. loads, see Fig. 294.

Fig. 294 Forces acting on the landing gears of a passenger aircraft in turn on ground equipped with drive-by-wire control laws

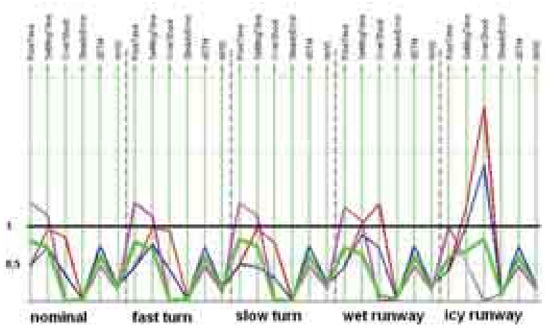

Fig. 295 Optimisation result (green line) of yaw rate control under various conditions, expressed in parallel coordinates (criteria are rise time, settling time, over shoot, steady error, control rate and deflection). Criteria values below one are satisfactory (green line).

The dynamic inversion controller worked reliably, in spite of the necessity of solving iteratively nonlinear equations for aerodynamics and propulsion models based on "black-box" neural networks implementations.

The MOPS environment has been successfully applied to robustly tune the control laws against uncertainty in aircraft-on-ground dynamics, as well as various runway and taxi way conditions (dry, wet, icy), see Fig. 295.

The work on aircraft-on-ground control will be continued within the CleanSky Smart Operations on Ground project. Intention of this project is to explore ways for reducing over-all fuel consumption and emissions during aircraft operations on the ground. The project covers both on-board solutions, like integrated electric motors in the wheels, as well as operational aspects like gate allocation optimisation, extended use of towing trucks, etc. Initially the institute will contribute a virtual aircraft test platform in Modelica for use by other partners to derive specifications for new electric devices for moving aircraft during taxiing on ground. In a later phase, models of such devices will be integrated into this test bed for analysing operational efficiency of the enhanced aircraft. For steering the aircraft on the ground, the wheel-integrated electric motors need to be coordinated properly. For this reason, drive-by-wire control laws will be developed using our proposed Flight Control Laws design process.

1.2.2 Clearance of Flight Control Laws

The aeronautical industry is faced with the formidable task of clearance of the flight control laws (CFCL). Before an aircraft can be tested in flight, it has to be proven to the authorities that the flight control system is safe and reliable and has the desired performance under all possible operational conditions as well as in the presence of failures. Current practise is an extremely time consuming task when trustworthy results should be achieved. This gives motivation to explore the benefits of new model-based analysis techniques for the clearance of flight control laws.

Optimisation-Based Clearance

The CFCL can be formulated as a robustness analysis problem, where a set of suitably defined clearance criteria must be checked to lie within certain limits for all admissible variations of aircraft parameters, pilot inputs and all flight conditions. The idea of optimisation based worst case clearance is to use available and efficient optimisation methods to find those parameter/input/flight conditions for which the criteria are violated or poorly satisfied.

Within two international projects (GARTEUR, COFCLUO), incorporating Airbus, the analysis results clearly demonstrated the high potential of the optimisation-based approach in reliably solving clearance problems with many simultaneous uncertain parameters. The potentials are its general usability for both frequency-domain and time-domain analysis, and for both linear and non-linear models and control laws including protections. Moreover, there is no limitation on the number of parametric uncertainties that can be investigated and the method does not itself add conservatism to the CFCL as many other alternatives do, mainly those based on approximations or simplifications.

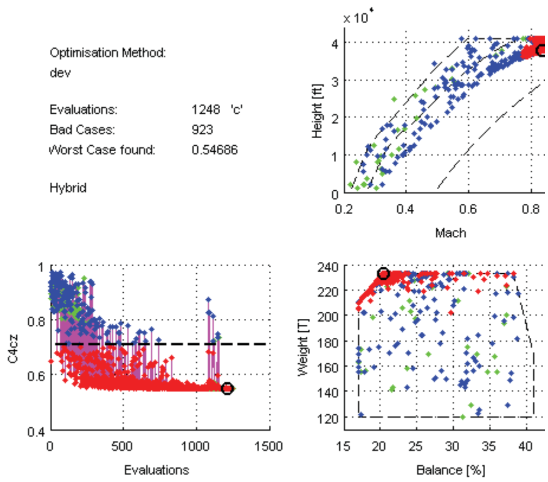

Fig. 296 Analysis results for the low speed manoeuvrability criterion (C4cz). Red marks in the flight domain indicate parameter combinations where the criterion is not matched. The worst-case found is marked by 'O'.

The difficulty with the optimisation based approach is not to find hidden weaknesses if they exist, but to confidently assert that no violation exists for all parameters/inputs/flight conditions. To assert this a global optimum solution has to be found. Our optimisation tool MOPS has therefore been enhanced by stochastic and deterministic global optimisation methods. Fig. 296 shows the clearance result for a low speed manoeuvre obtained by stochastic global search. The result indicates a clear violation of the clearance criterion.

In the context of optimisation based clearance a criteria library has been developed. The criteria cover Priority 1 certification aspects formulated by Airbus, with emphasis on the analysis of the closed-loop nonlinear aircraft with respect to protection violations [Varga 2008a[r]; Varga & Joos 2008[r]].

LFT-Model Based Clearance

For Linear Parameter Varying (LPV) models and their representation as Linear Fractional Transformation (LFT) models there exist powerful tools (e.g. μ-analysis) to analyse certain classes of clearance criteria. The advantage of this approach is that sufficient conditions for clearance (no violation of the criterion in a certain parameter domain) will be obtained with less computational effort compared to (global) optimisation or traditional gridding. However LPV/LFT models have to be approximated from the original nonlinear aircraft and controller models which may introduce unknown approximation errors. To keep these errors small and to ensure preferably large areas of validity we derived methods to generate a linear parametric state-space model [Hecker *et al.* 2005[i]], which approximates a nonlinear system (including neural networks) with high accuracy and is optimally suited for LFT-based robust stability analysis and control design, see Fig. 297. The very promising results have been reported in a COFCLUO Workshop .

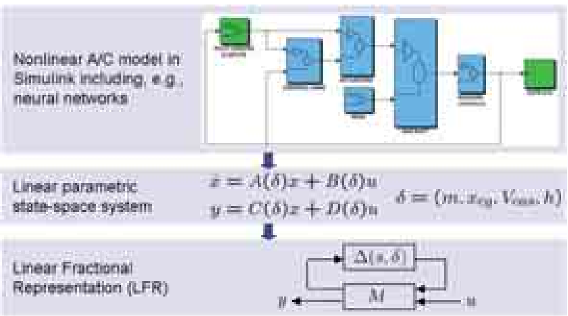

Fig. 297 Uncertainty modelling process

Fig. 298 EADS Mako/HEAT

These techniques of generating LPV/LFT based uncertainty models have been applied within a contract work with EADS Mako/HEAT (High Energy Advanced Trainer), see Fig. 298. Using our advanced LFT-model generation methods and tools, it was possible to generate LFT models of least complexity, which allowed performing a single LFT based analysis to prove robust stability of the controlled aircraft within a large region of the flight envelope, including also nonlinearities as e.g. saturations and state constraints.

1.2.3 LPV Analysis & Synthesis for Missiles

In cooperation with LFK-Lenkflugkörpersysteme GmbH, we demonstrated that our tools for the optimal generation of LPV/LFT models can cope with highly nonlinear missile dynamics. Low order LPV/LFT models with high accuracy could be derived [Pfifer & Hecker 2008[c]] and successfully used for robust stability analysis. Due to the high degree of nonlinearity, it is only possible to analyse a limited region of the flight envelope with a single linear parametric model. Therefore, the whole flight envelope is divided into various sub-regions. For each sub-region an individual parametric model is generated. By employing this strategy, it has been possible to prove stability of the missile model for a large region of the flight envelope by means of the structured singular value μ. One analysis is exemplarily shown in Fig. 299. The upper μ-value is smaller than 1 indicating that the system is robustly stable.

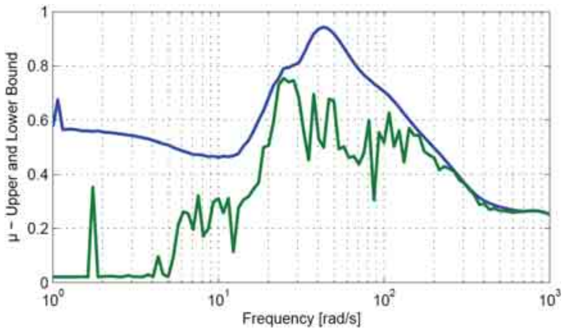

Fig. 299 μ-Analysis of a generic missile

In a next step the generated linear parametric models will be used as a basis for controller synthesis.

1.2.4 Flight Control Law Design for UCAVs

Within the scope of the DLR internal project UCAV-2010 (Unmanned Combat Aerial Vehicle) a numerical and experimental procedure for development and assessment of an unmanned tactical aircraft will be developed. Our contribution is aimed at the design of a flight control system that allows for best possible autonomous flight and manoeuvring.

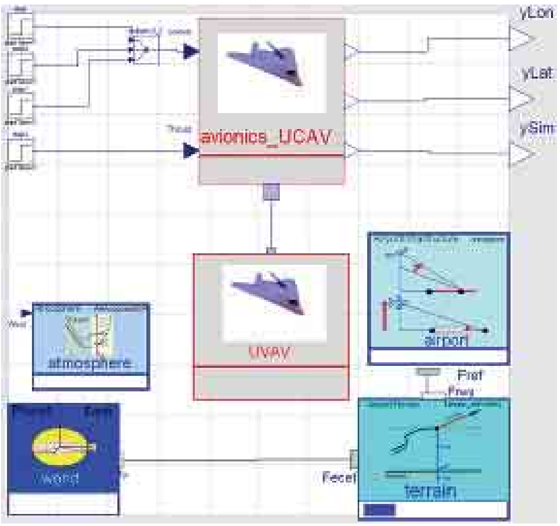

Fig. 300 Two-level Modelica implementation of a UCAV model using the Flight Dynamics Library

For fast and comfortable integration of model descriptions and data arising during the pre-design phase at different departments the interface between our Modelica flight dynamics library and the CPACS database, developed in the TIVA project, is used. Initial control laws are derived using the rapid prototyping process depicted in Fig. 288.

The specification of mission trajectories over realistic terrain incorporating rotation of the earth is now possible with the new Flight Dynamics Library and can be simulated, see Fig. 300.

1.3 Active Loads Control

In the field of flight control law design, considerable emphasis has been on active loads alleviation systems. These systems have the potential of considerable structural weight reduction by reducing aerodynamic peak loads on the airframe.

The institute's expertise in control law design led to the participation in several national and international projects where our technologies could be demonstrated successfully.

1.3.1 Improved Loads Control Design for Contemporary Aircraft Configurations

Within the MODYAS project (LuFo III) we provided models, methods and tools for joint synthesis of structural & load control function parameters to achieve lower loads, lower weight, higher comfort, higher crew & passenger safety and lower costs. This implies an interdisciplinary cooperation between structure, aeroelastics, loads, flight mechanics, handling quality and mass properties.

New Load Control Function Design Methodology

The loads control function (LCF) synthesis is primarily based on the multi-objective optimisation-based methodology MOPS (Multi-Objective Parameter Synthesis) which allows to directly formulate all related design objectives as a set of optimisation criteria. In former projects (Flexible Aircraft, LuFo II) this methodology proved to be well suited for load control function design. However, to ascertain best possible control function performance additional structural analysis has to be made in addition by determination of sensor and rudder effectiveness.

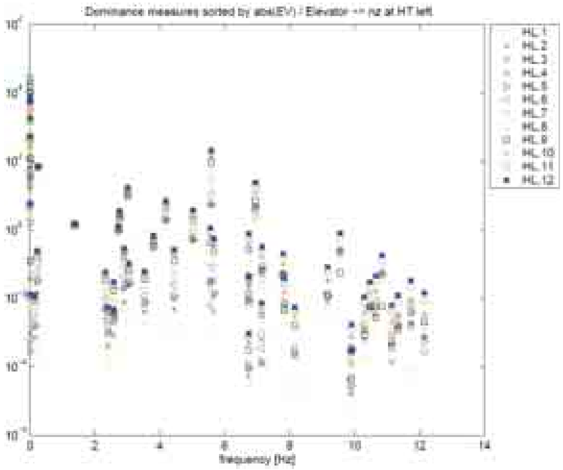

Fig. 301 Dominance measures derived from controllability and observability analysis for 12 stations (HL_1,...,HL_12) on horizontal tail plane. Station HL_12 has highest controllability and observability measures for almost all frequencies.

To find out best suited control surfaces and acceleration sensor locations on aircraft structure different approaches have been investigated in frequency and time domain. As a new contribution time domain dominance measures known from controllability and observability analysis have been applied to find the most effective control surface and sensor location, see Fig. 301.

In order to find appropriate scheduling variables and functions the effects of variables and parameters on design criteria has to be investigated. Statistical methods like "variance analysis" and "correlation analysis" have been applied to analyse dependencies of design goals from load variations and flight conditions.

Application of New Load Control Modelling and Load Control Function Design Methodology

The objective of this task is to demonstrate the loads reduction potential which can be achieved by additional load control functions (LCF). The LCFs have been designed by applying the improved multi-disciplinary loads models and the loads control function design methodology mentioned above for real aircraft problems. The loads control functions to be designed are required to be structurally simple filters as add-on functions to the basic EFCS, which remains unchanged but whose performance must not be deteriorated elsewhere.

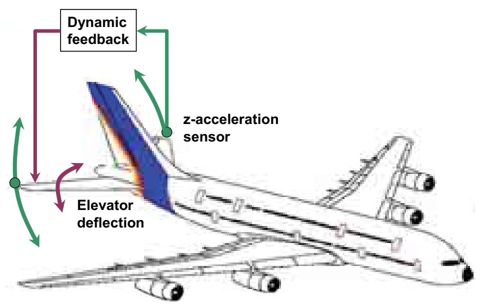

Fig. 302 Add-on load alleviation functions using conventional control surfaces. Example: reduction of rear fuselage loads via control of bending moment at horizontal tail plane root.

Additional sensors to measure accelerations at one or more aircraft structure stations could be positioned, whereas the available aircraft control surfaces should be used for control only (Fig. 302).

Among others a loads alleviation system (HLAS) for horizontal tail plane and rear fuselage was designed to reduce bending moments at horizontal tail plane root due to external disturbances or manoeuvres for a large Airbus aircraft [Joos 2005a[r], 2005b[r]]. In this application emphases was put on reduction of the RMS-value of the bending moment at horizontal tail plane root in a frequency range from 1.5–3.6Hz due to stochastic disturbances acting on the outboard elevator and on reduction of load peak value due to square pulse input also at outboard elevator, whereas bending moment in other frequency ranges and other loads at aircraft rear is not increased more than design value, see Fig. 303. The Dutch roll frequency response up to 1Hz is nearly unchanged indicating the minor impact of the HLAS on the A/C handling. The HLAS proposed is of simple structure using gain scheduling with respect to true airspeed.

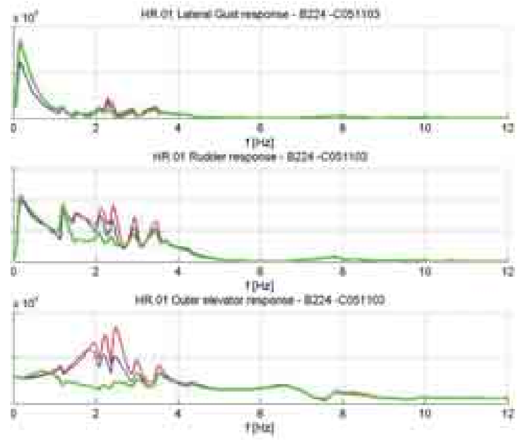

Fig. 303 Design results: Frequency response magnitude of bending moment for lateral gust, rudder and external disturbance input for original A/C (red) and two different LC functions (blue, green)

1.3.2 Integration of New Sensors and Control Surfaces in Active Loads Control Systems

Within the AWIATOR project we were involved in the development and flight testing of new control strategies for Gust Load Alleviation [Hecker & Hahn 2007[c]] with the focus on the usage of new direct-lift control devices (mini-TEDs) and a forward-looking LIDAR sensor for determination of wind turbulences ahead of the aircraft.

Gust Computation System (GCS)

One of our major contributions since 2004 was the development of a sensor fusion algorithm to improve the accuracy of the forward looking LIDAR sensor signal [Hecker, 2007[p]]. This was essential for the usage of the LIDAR signal as input to the control system, where a sensor signal error of less than 1m/s was required. As the pure LIDAR signal only had a measurement accuracy of 1.8m/s, we developed an algorithm for the fusion of this signal with the angle of attack sensor signal, which delivers vertical wind information at the aircraft nose. With this algorithm it was possible to combine the high accuracy of the angle of attack sensor with the forward looking property of the LIDAR sensor, yielding an accurate (40% improved accuracy compared to LIDAR signal, see Fig. 304), forward looking wind signal that could be used as input for our feed-forward control system.

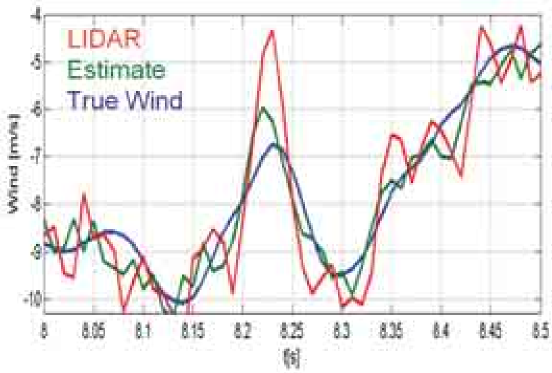

Fig. 304 Accuracy improvement of LIDAR signal using sensor fusion algorithm

Gust Load Alleviation System (GLAS)

Using the forward-looking wind information from the GCS, a feed-forward gust load alleviation system (GLAS (flex)) was developed by us, which also takes into account the structural flexibility of the aircraft. The GLAS (flex) allowed to reduce the peak wing bending moment Mx by 80% compared to the open-loop aircraft without controller.

Aeroelastic Model Identification of Winglet Loads from Flight Test Data

As part of the AWIATOR project we developed algorithms enabling the identification of flexibility effects on the outer wing within a manoeuvre loads context based on the Maximum Likelihood method. The models considered are based on distributed local data rather than on the net effect on aircraft performance. While this requires the size of the specific models to be much larger, the identified models allow a much more detailed physical interpretation of the observed performance benefits or penalties of winglets or wing tip devices. This identification algorithm was successfully applied using real flight test data [Reijerkerk 2008[t]].

1.3.3 Active Loads Control for Innovative Aircraft Configurations

Blended Wing Body Aircraft

Following the ACARE vision 2020, aircraft must become significantly cleaner and quieter so that the aeronautics sector's contribution to a sustainable environment is widely recognised. Significant improvements in aircraft efficiency and noise can be only achieved with major changes in aircraft configuration. The most promising concept is the blended wing body (BWB) aircraft with respect to efficiency improvement and potential noise reduction. In this context the European project ACFA 2020 (Active Control for Flexible 2020 Aircraft) has two main objectives: pre-design of the ACFA 2020 aircraft configuration, a marketable European ultra efficient 450 passenger BWB type aircraft, and providing solutions for the active control system of BWB type aircraft. The development of control systems reducing structural vibrations and loads are very challenging for BWB type aircraft and can only be solved by employing modern robust controller synthesis techniques.

Within the project we are leading the work package "Integrated control design" and we are responsible for the development of Linear Fractional Transformation based uncertainty models for the BWB aircraft. These models are the basis for all the modern robust control design techniques that will be applied by different partners to alleviate gust and manoeuvre loads, improve passenger comfort and to ensure some predefined flying qualities for this new type of aircraft.

Fig. 305 Blended Wing Body Aircraft

Ultra Green Transport Aircraft

The project iGreen (integrated Green Aircraft) shall deliver contributions required for a better design and integration of eco-technologies in an ultra-green transport aircraft. The project is focussed on a detailed investigation of global aeroelastic mechanisms for the reduction of drag and structural weight.

In this project we are involved in the design of turbulence and manoeuvre load alleviation controllers. These will be designed for an aeroelastic wing and tested on the corresponding wind tunnel model of an actuated and moving wing.

New Smart Fixed Wing Concepts

Within the JTI-Smart Fixed Wing Aircraft (SFWA) project, the purpose is to develop, validate and flight test innovative technologies, concepts and capabilities in the critical areas of fuel consumption and noise emissions.

As one of the key contributors in the area of active loads control in the AWIATOR project [Hecker & Hahn 2007[c]], we will have a leading role in this part of the JTI-SFWA project. In particular, we will be responsible for the design of integrated, fault-tolerant feed-forward and feedback control laws for manoeuvre and gust load alleviation.

In addition, the institute is responsible for the integrated modelling of an aeroelastic benchmark aircraft model, which is the basis for the investigation of smart wing concepts for active loads control. The Modelica DLR Flight Dynamics Library will be used for the modelling, which also allows generating a prototype flight control system, which is essential for the evaluation of the performance of the overall controlled aircraft system and could not be easily delivered by any other partner. We will also be involved in the aircraft modelling and algorithm testing on the EFCS test rig at DLR Braunschweig.

1.4 Fault Diagnosis

Flight control systems need to be more and more capable of handling of failures in sensors and actuators. To this end the reliable automatic detection of such failures is a prerequisite. The hardware-redundancy based fault detection and diagnosis (FDD) approach is nowadays the standard industrial practice and fits also into current aircraft certification processes. However, its applicability is becoming increasingly problematic when used in conjunction with the many innovative technical solutions being developed by the aeronautical sector to satisfy the More Affordable, Safer, Cleaner and Quieter imperatives being demanded by society. Our institute has been and continues to be involved in several challenging projects, addressing different facets of the applicability of advanced model-based methods to FDD of aircraft systems (GARTEUR AG16, Fault Tolerant Control; IMMUNE, Intelligent Monitoring and Managing of UNexpected Events; ADDSAFE).

Within the GARTEUR project our institute was involved in studying the applicability of FDD methods for the detection of primary actuator faults of a large transport aircraft (benchmark: Boeing 747-200). Our main focus was on developing numerically reliable computational methods for the design of residual generation filters to serve for fault detection and isolation, the development of associated robust software tools for the synthesis of residual generators, and the application of new methods to the project benchmark. The obtained results are summarised in a GARTEUR Technical Report [Varga 2008c[f]]. The main theoretical achievements have been presented in [Varga 2005a[c], 2007b[c], 2007d[c]], and the developed software tools formed the basis of a Fault Detection Toolbox [Varga 2006b[c]].

Fig. 306 Structural faults (surface/actuators) of an Airbus A300B4-203F Freighter hit by a surface-to-air missile (Nov. 2003)

From the practical applicability side, the main result of our analysis is the proof of feasibility of the complete isolation of all primary actuator/surface faults in the nominal case by using a minimal number of additional surface angle sensors. A typical step response of residual signals illustrating the detection and isolation of actuators faults for 4 elevators and 1 stabiliser is presented in Fig. 307. To achieve this, a minimal number of 3 surface angle measurements (2 elevators, 1 stabiliser) were only needed.

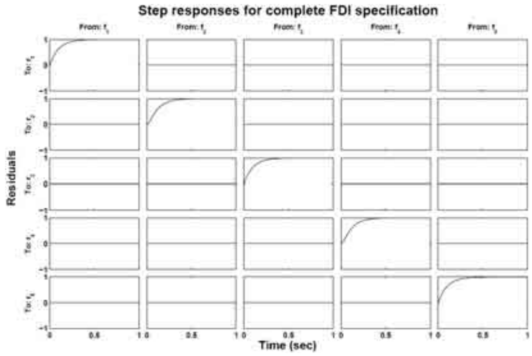

Fig. 307 Step responses from the faults with left elevators and stabiliser angles measurements

IMMUNE is an ONERA-DLR common research project to demonstrate the capability and viability of intelligent monitoring and managing of unexpected events during flight. The goal is to improve safety and autonomy, and reducing pilot workload. The main research problems to be solved concern the multi-disciplinary design and synthesis of advanced control laws with event driven reconfiguration capabilities. A main component of these control laws are fault diagnosis systems based on advanced FDD methods. Fig. 308 illustrates the overall architecture of a FDD based fault tolerant control system.

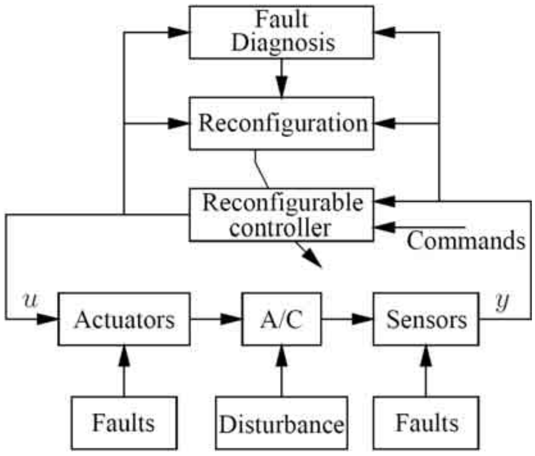

Fig. 308 Fault diagnosis based fault tolerant control

In the period 2006–2008 our institute was involved in the following main activities:

- Development of a benchmark model with actuator faults for 20 split control surfaces and a 3-D Visualisation environment [Hecker *et al*. 2008[c]]. The visualisation features for actuator/surface faults are illustrated in Fig. 309.
- Study of trimmability of the benchmark model in the case of primary actuator faults and determination of restricted flight envelopes [Schabreiter 2007[r]; Hecker *et al*. 2008[c]].
- Development of new null-space based methods for fault detection based on linearised models [Varga 2008[c]].
- Further development of computational tools available in the Fault Detection Toolbox developed in our group [Varga 2006b[c], 2008d[r]].
- Application of the developed methods and tools to the design of residual generators for the detection and isolation of selected events.

Fig. 309 3-D visualisation of actuator/surface faults

The work envisaged in the final phase of the project is the design of robust residual generators and of reliable residual signal evaluation schemes in the presence of parametric uncertainties.

Fig. 310 Wake Vortex Visualisation, NASA

Recently a FP7 Collaborative Project ADDSAFE has been evaluated and selected for EC founding. The aim of this project is to research and develop model-based fault detection and diagnosis methods for application by the aeronautic industrial sector to aircraft guidance and control systems. Our institute had a primordial role in the preparation of the proposal and setting up the consortium (formed of the core teams of the GARTEUR AG16, including Airbus).

1.5 Wake Vortex Scenario Analysis / Trajectory Optimisation

The methods and tools developed for flight control law design found applications in new areas like Wake Vortex Scenario Analysis and aircraft trajectory optimisation.

1.5.1 Wake Vortex Scenario Analysis

In the context of large civil aircraft like A380, the wake vortex (WV) problem came to the fore. Simulation and analysis of wake vortex scenarios near airports is a multidisciplinary task (physics of the atmosphere, flight guidance, flight physics) where our design and analysis environment MOPS can serve as an integrating platform.

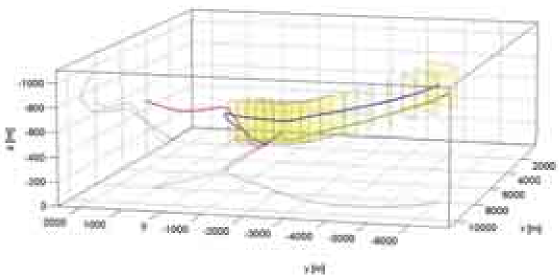

Fig. 311 WakeScene-D Simulation

WakeScene

WakeScene (Wake Vortex Scenario Simulation) is a package of software modules, developed by different DLR institutes, combined in and controlled by MOPS. The functionality includes aircraft traffic mix and trajectory generation, realistic meteorological data, WV evolution modelling and WV encounter identification. The first versions of WakeScene focussed on the landing scenario and were utilised in cooperation with Airbus in projects in 2004–2006.

Using the WakeScene tool, two different WV research topics can be addressed: i) research of WV encounter probabilities and ii) assessment of WV encounter severity.

Current and Future Wake Vortex Research

Further development of WakeScene in 2006 and 2007 resulted in a version for take-off and departure scenarios. This WakeScene-D version was developed for an EU project, CREDOS to investigate the possibility of reducing the WV separation in crosswind dominated weather scenarios. The modules in WakeScene-D were enhanced and include: i) a trajectory model by DLR-FL including a pilot model for departure by TU Berlin, ii) a meteorological database of one year in 10min increments for airport Frankfurt-Main by DLR-PA, iii) WV evolution models by DLR-PA and UCL (Université Catholique de Louvain, Belgium) and iv) a hazard area model by DLR-FT for WVE identification. All modules are embedded in MOPS, which performs central computations and controls parameter synthesis, data exchange and storage for extensive Monte-Carlo simulations in the range of up to 1 million departure simulations. The simulations are performed on the Linux 32-core cluster of our institute.

The software and results of the simulations were presented on the ICAS/ATIO 2008 congress [Holzäpfel *et al.* 2008[c]]. A 3-D illustration of a single simulation is shown in Fig. 311. The trajectory module provides the two trajectories for the generator (blue) and follower (magenta) aircraft. The evolution of the WV (red and green) is computed in planes (yellow) perpendicular to the generator trajectory.

WakeScene is being further developed for the landing scenario as well, especially for the DLR project "*Wetter und Fliegen*"—"weather and flying", the successor of the renowned DLR projects *Wirbelschleppe I + II* (1999–2006). The project is focussed on airport weather to enhance the (future) air traffic control (ATC) and advanced aircraft systems to improve safety.

In the weather part of the project, WakeScene will be utilised to develop reduced separation operations for different weather conditions and perform risk assessment and capacity gain estimation. For this purpose, the advanced trajectory module of WakeScene-D will be converted to include approach and landing capability.

Aircraft Trajectory Optimisation

Innovative technologies for high lift devices offer the possibility of flying new alternative approach or landing procedures in civil air transportation. Besides airport capacity, noise reduction is one of the most important goals of future air traffic. Within the LuFo III "*Verbundprojekt IHK-HICON: Untersuchung neuer Hochauftriebssysteme*" a systematic approach has been developed for objective evaluation of A/C performance regarding noise emission, fuel consumption, approach time and handling qualities of the piloted aircraft as well as for designing new optimal trajectories regarding all relevant evaluation criteria in order to exploit the benefit of high lift devices.

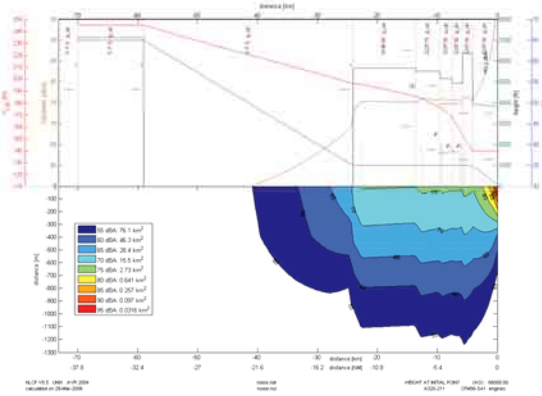

Fig. 312 Noise spread on ground for conventional approach with glide slope angle of at most 3°

For this the analysis and synthesis environment MOPS has been applied as methodological platform. Proprietary trajectory generation modules and evaluation models, e.g. for noise propagation, have been integrated in the MOPS environment [Joos 2006[r]]. Experimental noise criteria have been developed in order to adequately express air traffic noise spread on ground.

The utility of the developed evaluation models and tools has been demonstrated by designing optimal landing trajectories allowing steeper glide slope angles; see Fig. 312, Fig. 313 and Fig. 314. In addition, a robust glide slope controller was developed capable to fly the optimal trajectories automatically [Joos 2006[r]].

These activities can now be continued within CleanSky Systems for Green Operations ITD (launched in October 2008) where a "transversal optimisation framework" for mission and trajectories is envisaged. Our contribution to this tool will be an efficient trajectory generator for realistic flight paths. Moreover multi-objective optimisation and decision strategies and concepts will be investigated with respect to trajectory optimisation for green operations.

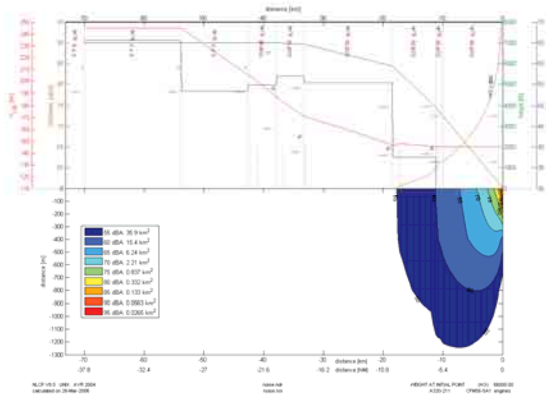

Fig. 313 Noise spread on ground for optimal approach with maximum allowed glide slope angle of 6°

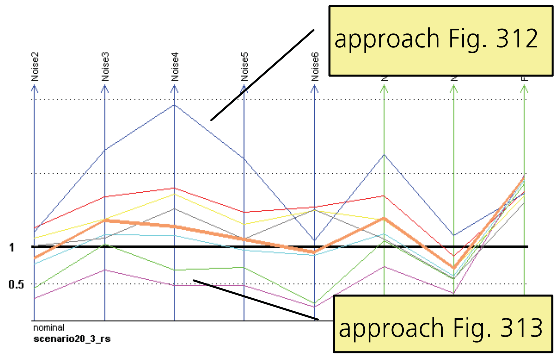

Fig. 314 Comparison of different noise measures and flight time for alternative approaches by means of parallel coordinates in MOPS. The blue line represents the criteria values of the approach in Fig. 312, the magenta coloured line correspond to that of Fig. 313.

2 More Electric Aircraft Systems

For next generation aircraft, electric energy will be of growing importance since it compares favourably to hydraulic or pneumatic supply systems with respect to performance, weight, integration and maintenance. Challenges are the design of suitable aircraft systems architectures and questions of electric network stability and power quality of the resulting complex electric supply systems.

At present, consumers being powered by central hydraulic or pneumatic supplies typically are flight controls, landing gears and environmental control (Fig. 315). If these consumers are electrified on a future aircraft, the electrical network has to take over the function of the former central hydraulic and pneumatic supplies, which then are removed. As a consequence, the electrical system has to generate more power, and has to be more reliable, since it supplies an increasing number of components having a safety critical function, e.g. flight control actuators.

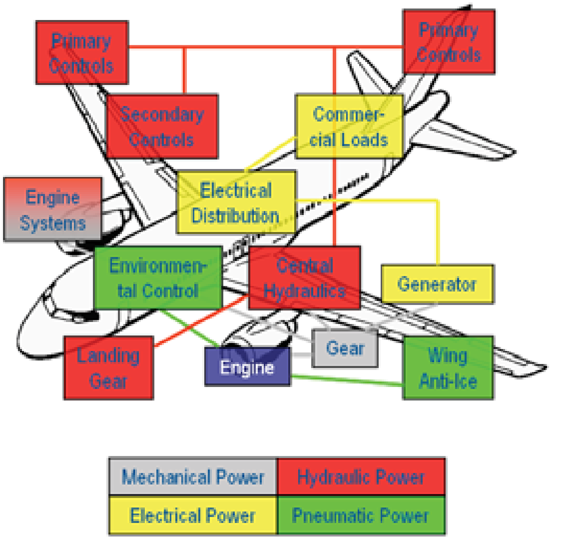

Fig. 315 Present aircraft systems architecture

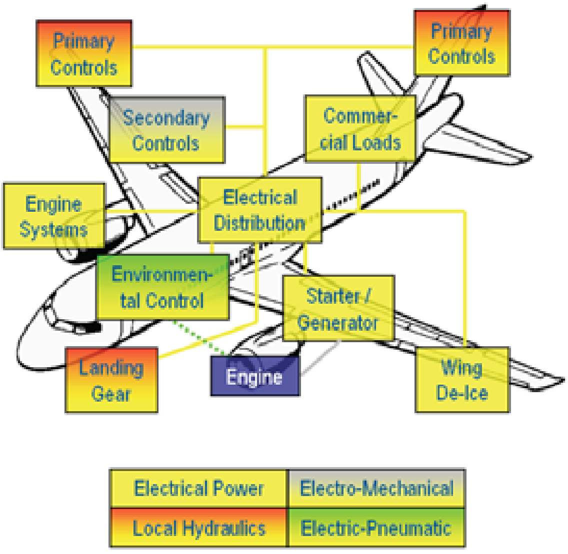

Fig. 316 A potential future More-Electric Aircraft systems architecture

Our core competence is to analyse, design and optimise power generation and distribution architectures and systems by use of modern multi-physics models expressed in the object oriented modelling language Modelica and optimisation tools like MOPS.

The research is conducted in several national (LuFo) and EU-funded projects working together with European airframers and suppliers.

2.1 Power-Optimised Aircraft

Our work in the field of more electric aircraft systems began with the POA ("Power-Optimised Aircraft") project, finished in 2006. The aim of POA was to identify, optimise and validate innovative aircraft equipment contributing to the reduction in consumption of non-propulsive power.

In the POA project, a contemporary large civil aircraft was defined as the reference. A set of so-called "feasible architectures" was considered with the introduction of novel technology equipment, and several feasible architectures were defined. The main focus was on several more- and fully-electrical aircraft architectures having engine-embedded starter/generators, reduced bleed or bleedless environmental control, reduced hydraulic or fully electrical flight control and landing gear actuation. All changes in non-propulsive power demand, weight, reliability, cost etc. involved with novel on-board systems and equipment were assessed in POA with regard to the reference aircraft.

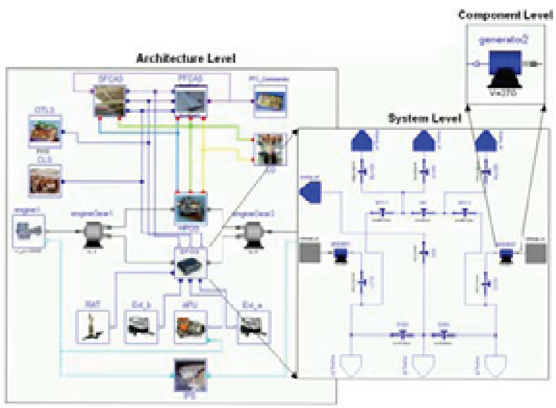

Fig. 317 Modelica diagram of a hierarchical aircraft model

The role of the Institute as one of the prime contractors was to set up a modelling and simulation environment, the so called Virtual Iron Bird (VIB). The VIB was used for the evaluation and optimisation of new "more electric" systems architectures at aircraft level, with respect to the POA project goals (reduction of non-propulsive power and weight).

The VIB model library was designed as an object-oriented Modelica library consisting of several levels. The hierarchy ends on the aircraft architecture level (the top level) that comprises the feasible and reference aircraft configurations. The generation of different aircraft level models can be realised in a very flexible and easy way by exchanging the accordant model classes. An example for an aircraft architecture model with its systems and components is shown in Fig. 317. The electrical power generation system (EPGS) is extracted from the aircraft architecture model and indicates one of the generators on component level. In Fig. 318 the flight control system model with its surface actuation components illustrates the complexity of the diverse aircraft system models.

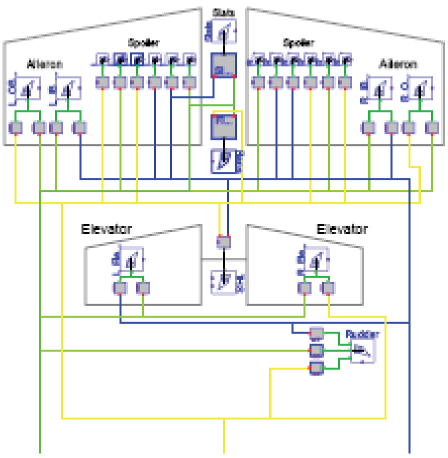

Fig. 318 Modelica diagram of the flight control actuation system

In addition to the off-line system simulation and optimisation environment VIB, the Institute was responsible for the real-time model development for the ASVR hardware-in-the-loop simulation facility (see Fig. 319) in co-operation with the University of Kassel.

Fig. 319 The POA aircraft system validation rig at Hispano Suiza in Paris

2.2 Electrical Network Simulation (VIVACE)

In the frame of the European concurrent engineering project VIVACE (Value Improvement through a Virtual Aeronautical Collaborative Enterprise) we developed novel methods and tools for detailed aircraft electrical systems simulation and design in cooperation with Airbus-France and Thales Electrical Systems.

The results of this project were a re-usable Modelica base library called NETCORE for aircraft electrical network simulation and a Multi-Level modelling approach for Right-sized Multi-domains simulation.

DLR NETCORE Library

As a major result delivered from VIVACE project, the NETCORE library developed by DLR provides main basic components and interfaces for building a complete electrical power system in the future more electric aircraft. With the park transformation feature of NETCORE library, it is feasible to design and simulate power system in ABC and DQ0 reference frames, so that effective simulation for both transient and steady state model can be undertaken. Additionally, the NETCORE library provides a perfect solution of the Right-sized simulation problem with the Multi-Level Modelling technique.

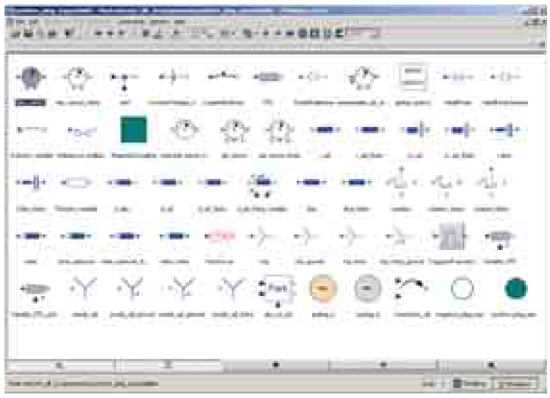

Fig. 320 An overview of DLR NETCORE library

Multi-Level Modelling Approach for Right-Sized Simulation

A multi-level concept used for aircraft electrical systems design was developed. The goal was to easily switch between three model levels in a complex system model, in order to arrive at dedicated models for the needed simulation tasks: a simple and super fast model for energy consumption design (so-called architectural level), a detailed model for fast network stability analysis (so-called functional model) and a very detailed model for network quality assessment (so-called behavioural level). Special care was spent on the modelling assumptions and a suitable Modelica library concept fitting to the needs.

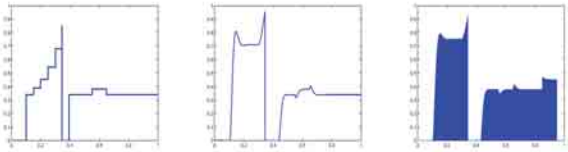

Fig. 321 Illustration of the 3 layer concept by means of simulations of a DC/DC buck converter

In Fig. 321 the tree-level concept is illustrated at hand of simulations of a DC/DC buck converter. The architectural layer input current shows large simulation steps neglecting the detailed effects which can be seen at the behavioural layer model simulation. The functional layer model covers the waveform of the detailed model without switching effects.

A test model for the chopper can be seen in Fig. 322.

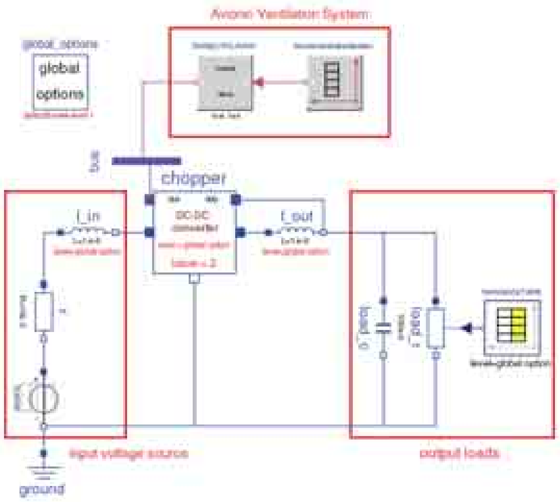

Fig. 322 Test circuit for chopper use case (for all 3 levels)

2.3 More Open Electrical Technologies

Following and building on POA and VIVACE the institute participates in the 3-year 6[th] framework EC program "More Open Electrical Technologies" (MOET). The aim of this project is to

- define and validate new electrical networks up to 1MW;
- resolve and validate the transformation of power users into all electrical solutions;
- develop and validate power electronics enabler technology;
- integration into the aircraft;
- develop a coherent design environment to supply PbW design and validation.

Our institute is responsible for leading the work package "Methods, Tools and Simulation". This package plays a central role in the objective of developing a coherent design environment to supply PbW (Power by Wire) design and validation.

2.3.1 Architecture Optimisation Tool

Based on the Virtual Iron Bird (VIB) from POA, one of the main tasks of our institute in this work package is the development of an integrated modelling and analysis tool for the evaluation of aircraft on-board electric power systems with regard to their weight, power behaviour and reliability. The novel tool is implemented in the Modelica language and intended for use in the conceptual design of such electric systems. Diverse methodologies are integrated with the tool, to cover the mentioned analysis aspects in a combined manner. The novel tool is an advancement of the VIB from the previous POA project, enhancing it with the capability to simulate different operating modes of an electric system architecture as well as visualisation and automated analysis features for component power sizing, weight, reliability.

Component Library

The tool comprises a dedicated model library containing object-oriented, physical models of electric power system components. The model library is hierarchically structured to accommodate various models of different complexity, such as interfaces (electric connectors, signal buses, etc.), basic electrical components (contactors, busbars, wiring, etc.), integrated electrical components (generators, rectifiers, converters, etc.), power users (motor drives, heatings, etc.) and entire system architectures. Each component model includes a physical representation of the component's failure behaviour and probability, as well as a parametric dependency of its weight on sizing parameters (e.g. nominal power, nominal speed). Thus, the library provides an infrastructure for the modelling of electric system architectures. An example of that can be viewed in Fig. 323.

Architecture Modelling

The graphical model editor of Modelica/Dymola supports, by simple drag and drop, an easy creation of electric system architecture models, which include numerous components and associated network contactor logics. The object-oriented modelling approach helps to create models that also have a concise appearance, similar to a schematic sketch of an electrical system.

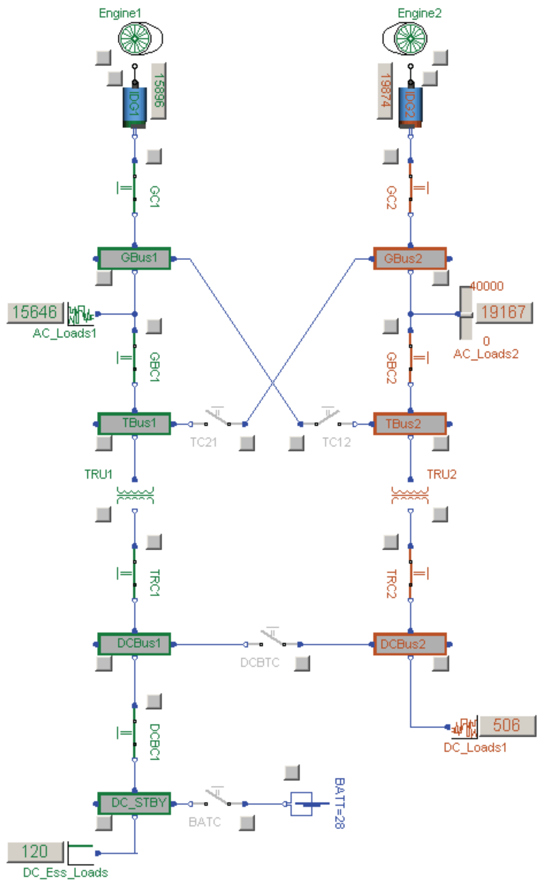

Fig. 323 Electric system model/schematic of a twinjet short-range aeroplane, normal operation in flight [Schallert 2007c]

The capability of an aircraft electric system to (re-)configure itself due to different operating modes (e.g. on-ground with external power, in-flight) or at the occurrence of component failures is also built into the respective architecture model. This is achieved by including the open/close logics of the various busbar contactors, which link (or disconnect) the power generators and users through the electric network. Thus, the system architecture models can be simulated for normal and various abnormal operating scenarios. Fig. 323 illustrates the example of a generic twinjet aeroplane, which is implemented in the new modelling and analysis tool.

Interactive Analysis and Simulation

The tool offers an interactive simulation mode. If a system architecture model is run in this mode, the tool shows dynamically and graphically the open/closed status of the miscellaneous contactors, as well as the resulting flow of electric power by different colours. The user can interactively change the operative/failed status of the electric system components, i.e. inject failures by mouse-click, and observe the resulting system behaviour that is graphically visualised in the architecture model scheme. In this manner, the model implementation of an electric system architecture can be checked easily and readily, i.e. to review if the model behaves as intended.

Automatic Power Sizing and Weight Analysis

To evaluate a modelled electric system architecture, the tool provides means of automatic determination of the highest electric power to be generated or carried by each component of the electric system. To achieve this, the so called power sizing analysis performs automated simulations of the electric system for various scenarios of normal and degraded operation. As a result, the dimensioning electric loads that occur during a flight cycle are provided for each component. Subsequently, the sizing parameters of each component are selected leading to the computation of the individual component weights, as well as the overall weight of an electric system architecture.

Automatic Reliability Analysis

Further more, an automated reliability analysis is offered by the tool as another means for electric system architecture evaluation. This analysis feature is implemented in the Modelica language as well, thus being fully integrated with the tool [Schallert 2008c]. Like the power sizing analysis, the reliability analysis procedure relies on the capability of a system architecture model to operate in normal and degraded modes, as well as to isolate and bypass failed components by system reconfiguration. For user defined system level events, such as the availability (or loss) of voltage and power on a single or several busbars, the analysis procedure automatically identifies the so called minimum path sets, i.e. combinations of intact components that cause the system to operate corresponding to the user defined event. Furthermore, the probability of occurrence of the event is computed, as well as the importances of system components. The importance of a component is a measure for its structural and probabilistic influence on the probability of occurrence of a system level event. Knowledge of the component importances helps to identify potential weak points or unnecessary redundancies in the electric system architecture.

The schematic in Fig. 324 depicts the kinds of design analyses offered by the tool and results computed.

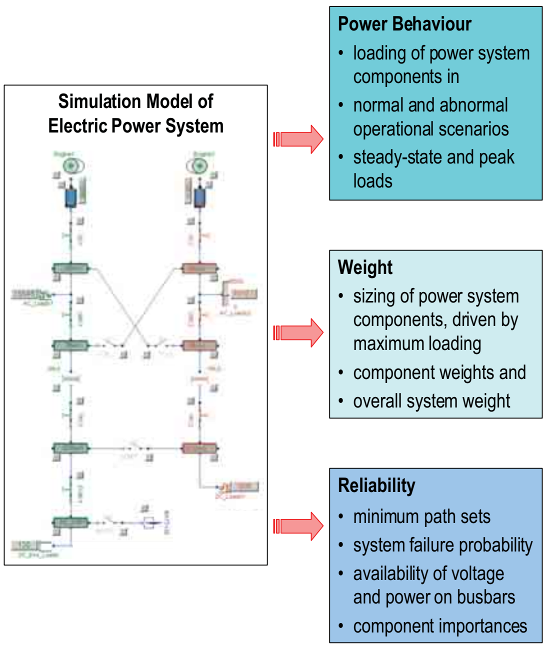

Fig. 324 Summary of the tool analysis instruments

Automatic Architecture Optimisation

Starting from the analysis capabilities it is possible to perform electric aircraft system and architecture optimisation [Schallert *et al.* 2006[c]]. The base of the optimisation tool is our multi-objective parameter synthesis tool MOPS.

The goals and criteria of electrical system architecture optimisation are the following:

- to minimise the sizing of electrical components, e.g. generators, wiring, in order to minimise the component weights and overall system weight;
- to minimise the system's power needs and losses;
- to optimise the availability of voltage and power on busbars w.r.t. the requirements imposed by the power users;
- to maximise the aircraft dispatch reliability.

The free design inputs, i.e. the tuners, in the optimisation of architectures are component design parameters, network (re-)configuration logics, handling of non-essential power demands and the architecture topology. Modification of the tuners is limited by the constraints that are imposed by architecture design rules and safety requirements.

These different types of analysis are all based on a single simulation model of the electric system. The advantages of having to create or adapt just a single system model are a lower change effort associated with system architecture modifications easier and more consistent management of analysis results. This is a technological advancement compared to existing analysis methods for weight, power and reliability, which require different representations or models of the system dedicated to each kind of analysis.

The newly developed tool enables to rapidly evaluate different electrical system concepts and to find the trade-offs between them. This supports the optimisation [Schallert *et al.* 2006[c]] of system architectures. Therefore, the tool is well suited to improve the design process of aircraft electric powersystems.

2.3.2 Electrical Network Stability and Power Quality Analysis

The new Power-by-Wire technologies require completely new concepts for the electrical networks on an aeroplane. A key issue will be to adequately specify network performances including the definition of users' requirements for such an electrical network. Starting from the experience of POA and the VIVACE project our institute participates in the investigation and development of new methods and tools for network stability

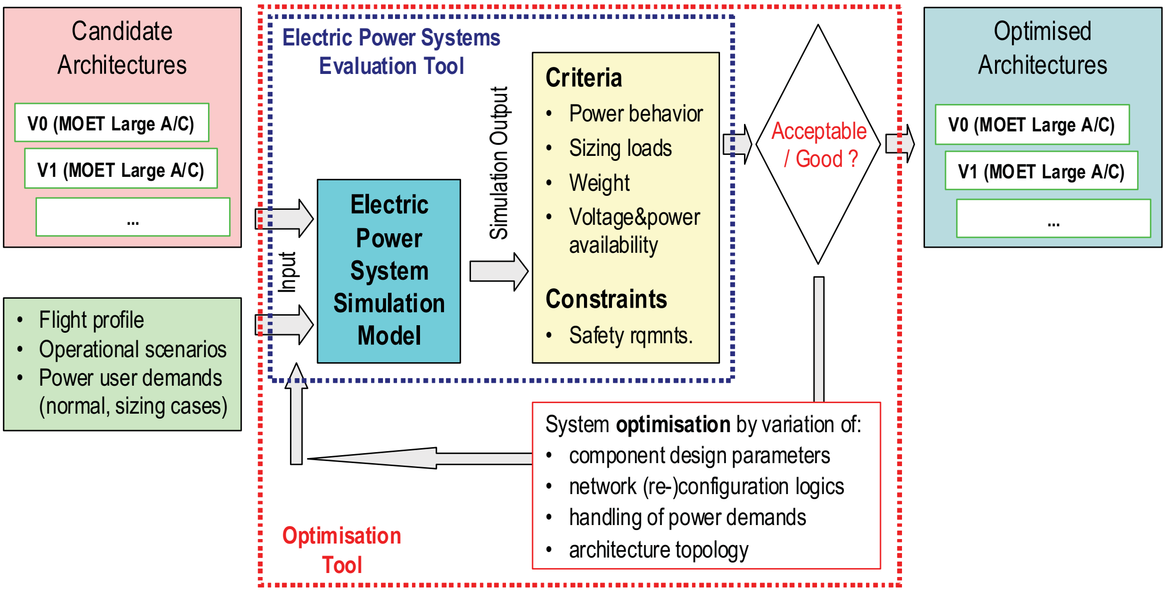

Fig. 325 Process overview of architecture evaluation and optimisation

and power quality analysis.

As an ongoing task, Modelica is under investigation for the future standard modelling tool for aircraft electrical systems. To demonstrate its maturity, the component models from MOET are made available as part of the "Modelica library for network stability studies within the project MOET". The library is based upon the "NETCORE library" which was licensed to University of Sheffield as the partner for the joint translation process.

Our tools applied to the task of aircraft electric system stability analysis within Moet are LFT based μ-analysis and nonlinear worst case analysis using anti-optimisation, where the multi-level modelling techniques are successfully applied [Kuhn *et al.* 2007[c], 2008a[c]]. For instance, a regulated buck converter is a typical critical component in a power system. Due to the negative resistance at low frequencies the regulated buck converter could be unstable in combination with the input filter. Therefore it is necessary to investigate the stability of the whole electric network both at small signal level for steady state conditions and large signal level for transients, impacts and network reconfiguration. The Multi-Level Modelling concept proposed above is a good tool for this purpose since validity of functional models can firstly be demonstrated by comparison of simulation results with the behavioural models. The Modelica functional models can be used for stability studies with methods for linear time invariant systems. For eigenvalue based methods, including modal analysis and eigenvalue sensitivity, the eigenvalues have to be calculated numerically by the simulation program. μ-analysis is a powerful method of robust control for stability investigations of parametric varying systems. The Modelica functional models can be directly applied for μ-analysis after extraction of the symbolic code and using it in Maple and Matlab. Compared with other methods for small signal stability, e.g. Middlebrook criterion and Modal Analysis, the μ-sensitivity approach gives a much more global and direct result for the influence of all components on stability. For details on the methods, see [Kuhn *et al.* 2008a[c]].

In contrast to these approaches, for industrial use, stability of a system often is defined as the ability of a system to keep a certain system variable within desired limits given by industrial standards. These are combined criteria of network stability, power quality and performance. This makes them difficult to proof with methods of linear control theory. Therefore a simulation based approach often is the only possibility to proof "industrial" stability and also large signal stability including failure protection devices. Instead of random or gridded parameter variation on the varying environment and system parameters, a better and faster method is to search for the most critical parameter combination directly. The basic idea is to use an optimiser to find the most critical criterion from the industrial specified standards and drive it to its worst performance by changing the uncertain parameters over the whole realistic operation range. In case the criterion is violated, stability / quality / performance has been shown to be not guaranteed. On the other hand, the tolerable design range for parameters could be investigated. This can be defined as the maximum parameter variations which still keep the system stable. An overview on the methods is shown in Fig. 326.

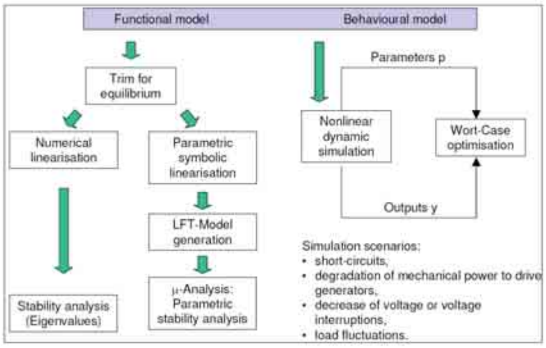

Fig. 326 Quality and stability studies overview

As tools, the object-oriented simulation environment Dymola and the DLR-developed Matlab-based multi-objective optimisation tool MOPS are used.

The methodology of anti-optimisation is demonstrated with a parametric variable model consisting mainly of a DC/DC buck converter in an aviation use case.

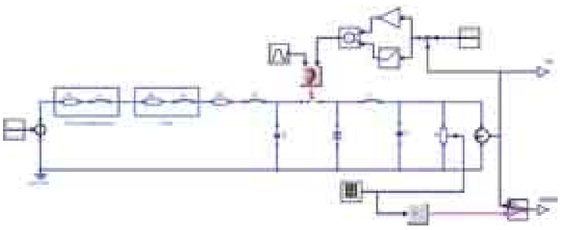

Fig. 327 “Behavioural” model of DC/DC buck converter

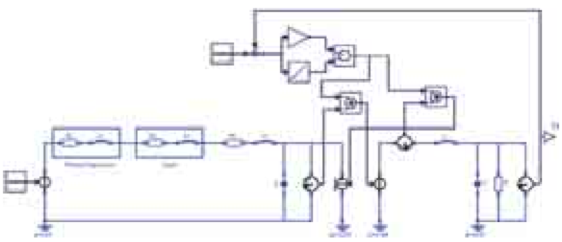

Fig. 328 “Functional” model derived from “behavioural” model

The behavioural model and the functional model can be seen in Fig. 327 and Fig. 328 respectively. The source voltage, feeder resistance and inductance and the load resistance are system variables which are variable in a predefined range. The design parameter is the Thévenin inductance.

For the behavioural model, instead of a variable load parameter, a load step is used and the limits are checked according to an industrial stability criterion.

For demonstration of the approach, three distance criteria are used: eigenvalue stability, eigenvalue damping, and the transient limits (see Fig. 329). The former two are evaluated with the functional model while the latter one is checked with the behavioural model.

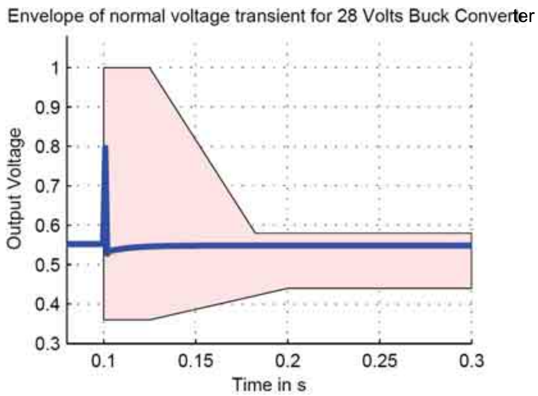

Fig. 329 Transient criterion

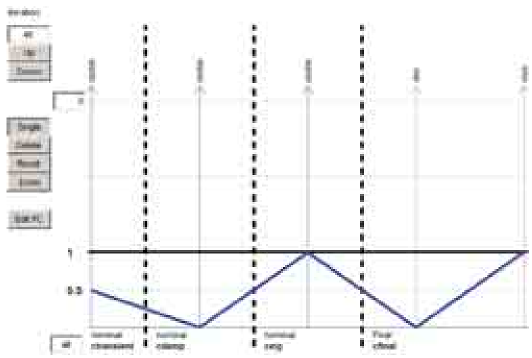

Fig. 330 Results as displayed by MOPS

From the MOPS result window in Fig. 330 one can see that the damping criterion was the most critical one (1 means “good” result). The other criteria are not violated.

In order to easily undertake power quality analysis and extract stability criteria e.g. total harmonic distortion according to the industrial specified standards, a Stand-Alone signal analysis tool with a graphical user interface for Dymola Modelica has been being developed, see Fig. 331. With this tool it is feasible to easily carry out comprehensive signal analysis by powerful signal processing like statistical computation and Fourier transformation.

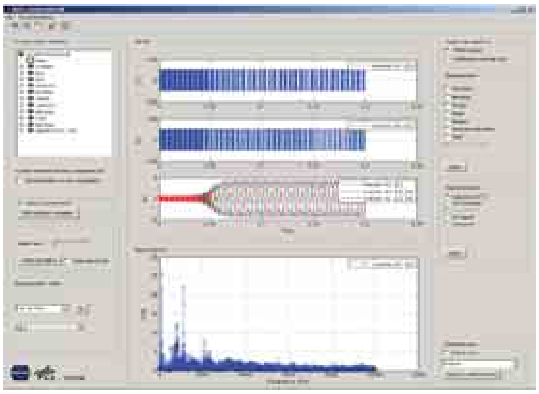

Fig. 331 Signal analysis tool for Dymola

2.3.3 Failure Mode Analysis

Our institute also participates in fault detection and isolation studies within the MOET project.

Starting with behavioural and functional Modelica models of the electrical network linearised models for fault detection analysis are generated. These linearised models are then extended by modelling predefined faults in our institute's FDI (fault detection and isolation) MatLab toolbox to synthesise appropriate fault detection filters. Basically these filters are residual generators allowing the declaration and isolation of faults, when certain residual levels are crossed.

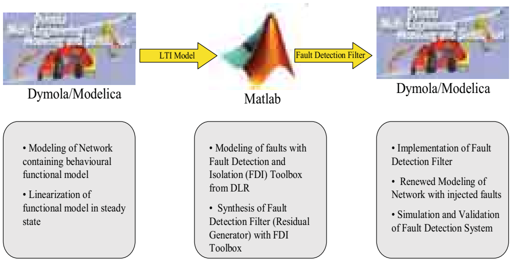

Fig. 332 Fault detection and isolation tool chain

The fault detection filters are then implemented in Modelica models and the overall electric system model is enhanced with the ability to inject faults into the systems. This enhanced model is then used to validate the fault detection and isolation filters via nonlinear system simulation.

2.4 Design Environment for ECS (DENECS)

In a bilateral research project with Airbus Deutschland GmbH, the Institute is developing a design and modelling environment for unconventional Environmental Control System architectures (ECS) for commercial aircraft. The environment provides both functional and behavioural models for conventional baseline ECS architectures as well as a modular toolkit to assemble unconventional architectures using air cycles, vapour compression cycles, or combinations thereof. These models allow evaluating potential ECS architectures in conceptual design with respect to system weight, required block fuel and performance metrics such as electrical power demand or engine bleed air mass flow. Building on these key criteria, optimisation tools are used to establish both unconventional ECS architectures themselves and their open-loop control logic.

A purpose-built model library is at the core of the tool. It is being implemented in the object-oriented modelling language Modelica and contains physical models in an acausal formulation. The library is modular and hierarchically structured. Therefore, basic component models are composed of elements of minimal complexity, such as control volumes or fluid inlets and outlets. In turn, they constitute component assemblies such as compressors, heat exchangers or cabin zone sub-models. Similarly, subsystem and system models are put together. The five key domains of a complete ECS architecture model are the "Fuselage" domain covering the cabin, flight deck, and under-floor, "Air Mixing and Distribution", the "Air Generation Unit", the "Ram Air Channel" and "Vapour Cycle and Electric Heating". Using this tool kit, users can plug together various conventional and advanced ECS architectures from Engine Bleed Air System or Cabin Air Compressor to the cabin using the graphical user interface of a Modelica environment.

For ECS architectures, the trade-off between subsystem weight and its energy efficiency cannot be solved a priori but has to be investigated for each design separately. Consequently, the architecture optimisation problem requires optimisation of the architecture itself and its open-loop control logic. This setup was implemented using the Multi-Objective Parameter Synthesis tool developed by the Institute, which allows executing the optimisations on the Institute's distributed computing facility.

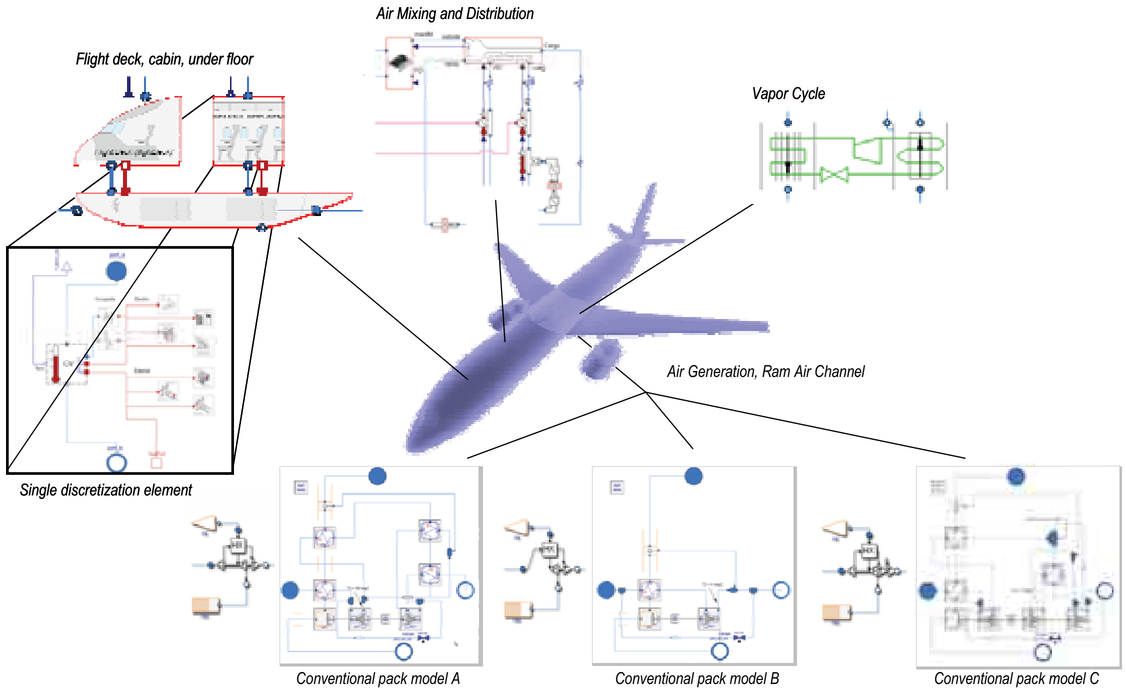

Fig. 333 Modelica model for environmental control system

VI Transportation

1 Introduction

When the DLR decided to initiate its new Research Program "Transportation" in 1999, the institute could already refer to a long tradition of related activities. Until then, the application of modelling and control techniques, the design, engineering and testing of complex mechatronic systems that had been applied to automotive and railway systems, was attributed to the topic "Technology Transfer".

In fact, the expertise in the field of highly complex mechatronic systems, the laboratory infrastructure and scientifically established methods, and tools for control engineering that originates from developments in aerospace, were and still are a strong part of our work associated to the field of transportation.

Today, modelling and control technologies originating from the transportation program are also used in aerospace applications. One demonstrative example is our vehicle dynamics modelling of Mars rovers.

A major contribution of the institute to transport issues concerns an integrated design approach in both automotive and railway domains. This approach is realised based on the standard *Modelica* and covers the modelling of vehicle dynamics together with energy systems and suitable integrated control strategies. Particular emphasis attains our Integrated Chassis Control and energy management approach which is aimed at contributing to more efficiency and vehicle accident avoidance for future vehicles.

The achievements during the reporting period are presented in the below Sections "Automotive" and "Railway Systems".

2 Automotive

Activities in the automotive field are mainly embedded in the DLR research area "Assistance for Traffic Participants". In the associated project "Mechatronic Chassis" we coordinate joint research with other DLR institutes.

Our excellence and work is focussed on control of vehicle dynamics and energy systems, multi-domain automotive modelling and simulation, and mechatronic components and their testing. These topics will be explained in the sequel.

2.1 Control Strategies

To develop strategies for chassis control we concentrate on the modelling and simulation of both chassis and powertrain systems. We are exploiting the synergies and interactions between the chassis and the power train to achieve optimal results for active safety, efficiency, and driving comfort at a low cost. Advanced optimisation techniques are used both in terms of control and as part of our design process.

2.1.1 Integrated Chassis Control

With the rising number of available active chassis systems the need for their adequate coordination increases, at the same time allowing for optimal exploitation of synergies. Moreover, the large amount of equipment options for mass production vehicles demand for an integrated control design approach which overcomes the confusing situation specific operation of present vehicle dynamics control systems.

Fig. 334 Model of innovative vehicle having wheel-individual steering and braking with integrated chassis control

A concept for integrated chassis control is in the focus of past and ongoing development at our institute [Bünte *et al.* 2006[c]; Bünte & Andreasson 2006[c]; Andreasson & Bünte, 2006[c]; Knobel *et al.* 2006[c]]. Targetting at a given vehicular motion request, the control signals are computed for the actual set of available chassis actuators (which may be deteriorated e.g. in case of a failure). The available actuator degrees of freedom are exploited in an optimal fashion to maximise the safety margin while minimising fuel consumption and tyre wear. The transparent control concept is characterised by the fact that it uses a single structure [Bajcinca & Bünte 2005[c]] and fixed parameters for all vehicle configurations and driving situations. Apart from real vehicle dynamics control, the approach may be used for assessing the benefit of novel mechatronic chassis systems.

2.1.2 Vehicle Energy Systems

This specific topic is organised in the DLR research area of the same name. The objective is to research on and to provide new concepts for propulsion technologies to substantially reduce fuel consumption and emissions and to investigate alternative fuels. The project is pursued jointly by several DLR institutes. The scientific questions along with this project aim at the further development of system-theoretical principles and process modelling concerning propulsion systems to increase the range, efficiency, and performance of alternative vehicles.

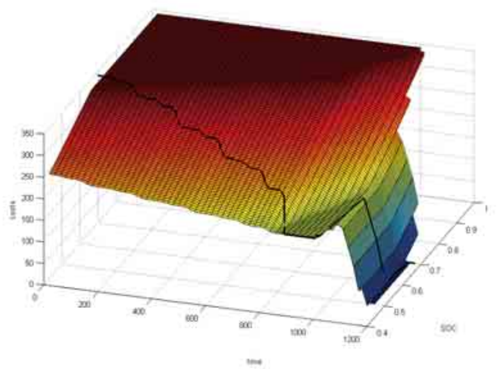

Fig. 335 Minimum cost table for the standardised New European Driving Cycle (NEDC)

Our contribution focuses on the system-theoretical and modelling aspects. Due to the extensive coupling of technological and systems-dynamics aspects, the development of low energy consumption and low-emission vehicle technologies requires the integration of mechatronic approaches to an increasing extent. These approaches need both theoretical principles of modelling and simulating combined with optimisation methods as well as the development and provision of appropriate tools. Therefore, the Modelica library *AlternativeVehicles* was initiated. Optimised operating strategies have been developed and tested, cf. Fig. 335, Fig. 338. In a next step, criteria relating to driving dynamics will also be taken into account.

Evaluation of Control Strategies for Fuel Cell Systems

In cooperation with a premium OEM and the DLR Institute of Vehicle Concepts the project "Evaluation of control strategies for fuel cell systems" considers and evaluates the different potential architectures of fuel cell systems for automotive application. Each single architecture necessitates a different operating strategy with different complexity and system-theoretical effort.

The institute of Robotics and Mechatronics is developing model based controllers for the different fuel cell systems and formulates criteria to evaluate the different architectures. The system models use components from the *AlternativeVehicles* library which already contains a fuel cell package with physical models and simplified models of fuel cell systems and sub-systems.

2.2 Integrated Vehicle Modelling and Simulation

Both simulation-based evaluation and model-based controller design require multidisciplinary modelling of the mechatronic chassis. It is therefore necessary to enhance and refine the modelling options with regard to all the above-mentioned aspects. To this end, we are developing a Modelica-based automotive model kit consisting of various compatible and complementary libraries that go far beyond mapping the pure driving dynamics. Moreover, interfaces and software for common standards as for tyre models and physical road definitions are included.

Fig. 336 Multibody vehicle model with hybrid drive

The compatibility of the different Modelica libraries each covering different disciplines or sub-systems allows for compilation of complex integrated models within a single framework and tool. Thus the former disadvantageous need for co-simulation is avoided. The details of the abovementioned libraries are explained in the next section.

Fig. 337 Demonstration of our activities in vehicle modelling and haptic feedback at FISITA 2008

They are complemented by the DLR-initiated EuroSysLib project, which aims at European leadership in system modelling and simulation through innovative Modelica libraries.

The integrative modelling of a complex mechatronic vehicle was demonstrated at the World Automotive Congress FISITA 2008. Here, we presented interactive hardware-in-the-loop (i.e. real-time) simulation of the multibody chassis with hybrid drive powertrain together with vehicle dynamics control such as anti-lock braking, rollover avoidance or yaw stabilisation, see Fig. 336. Involved was also a force-feedback steering wheel as well as high quality visualisation of vehicle, landscape and road. For virtual testing in the near future, robot-based motion simulation together with visualisation will allow a driving experience close to reality (see Fig. 337).

2.2.1 Modelica Component Libraries

In the sense of object-oriented modelling (and as consequence of our various modelling activities), it is essential to have libraries available which comprise components and assembled models. The main fields of our automotive modelling activities are vehicle dynamics, power trains (both conventional and alternative) and vehicle controls.

One important aspect in development of different libraries for automotive applications is interoperability. As a common effort of multiple (not only DLR) developers of Modelica automotive libraries, a general architecture for the modelling of vehicles was created with the scope to enable interoperability of developed libraries. The result-

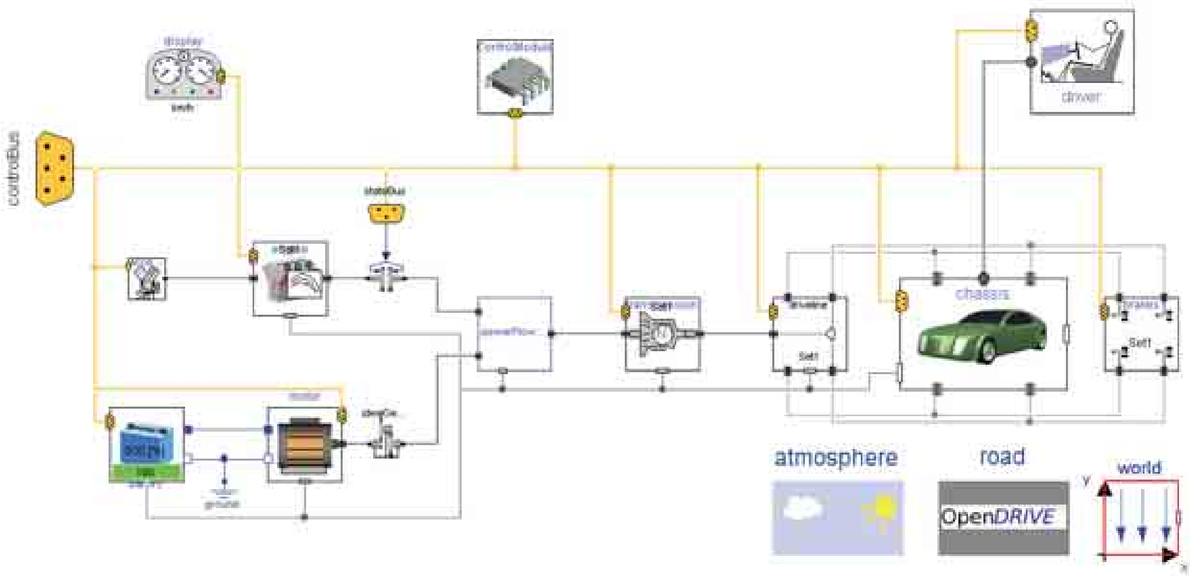

Fig. 338 Diagram view of a Modelica model of a parallel hybrid vehicle with optimised operating strategy

ing Modelica library called *VehicleInterfaces* was released by partners including DLR.

PowerTrain Library

The institute's expertise in the field of powertrain modelling started in 2000. The knowledge and experience was gathered steadily in a commercial Modelica library called *PowerTrain*. It is sold to automotive manufacturers and suppliers worldwide. Further development of the library led to its second version which was completed in 2007, see [Schweiger *et al.* 2005[c]; Tobolar *et al.* 2007[c]]. This version was significantly enhanced and completely redesigned (see Fig. 339 for a structure overview) to be able to interoperate with other automotive libraries on the base of the *VehicleInterfaces* library.

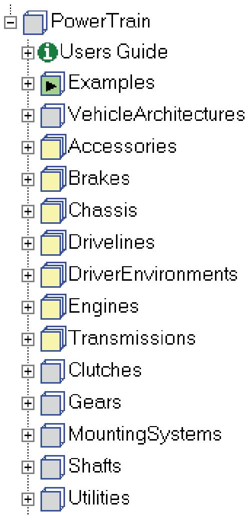

Fig. 339 Structure of the *PowerTrain* 2.0 library

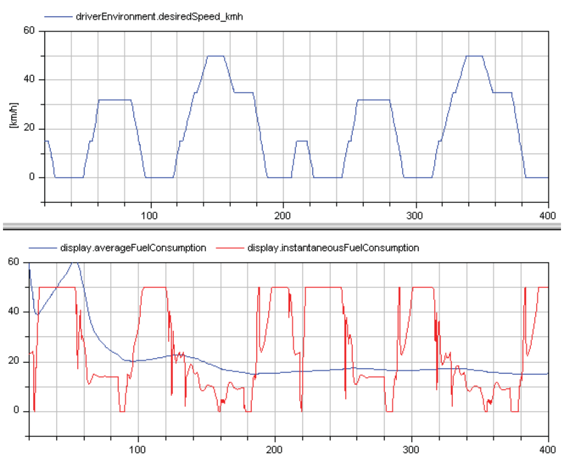

Fig. 340 Extract from results of the vehicle consumption simulation for vehicle with manual transmission. Upper diagram shows prescribed speed of typical drive cycle, lower graph focus on average (blue line) and instantaneous (red line) fuel consumption.

The *PowerTrain* library provides sophisticated models of manual transmissions, drivelines, drivers and other components. The range of examples was extended significantly including tests for both particular component models as well as complete vehicle architectures (e.g. for power consumption calculation and performance tests or analysis of shift strategies, see also Fig. 340).

VehicleControls Library

Simulation-based evaluation and model-based controller design for future mechatronic chassis require multidisciplinary modelling of both involved vehicle dynamics and its control systems. The *VehicleControls* library (currently at the beginning stage of development) will provide basic models of common vehicle dynamics control and driver assistant systems, such as anti-lock braking system (ABS), anti-slip regulation (ASR), electronic stability control (ESP), etc. The scope is to model the function principles rather than to mirror detailed (proprietary) systems.

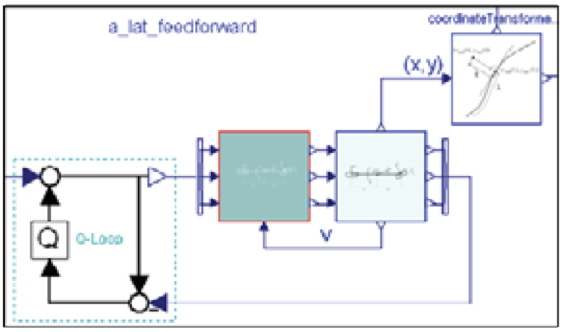

Fig. 341 Model of a simple vehicle dynamics control (based on single track model)

Future integrated control strategies (see Sec. 2.1.1) will as well be provided that are based on non-linear inverse vehicle models. Consequently, the necessary vehicle models will be provided as well. The vehicle model complexities vary from simplest single track model through double track up to sophisticated multibody models.

First tests of our new controller concepts have been carried out for yaw rate control based on a special "disturbance observer" (see Fig. 341) and for rollover avoidance via coordinated steering/braking.

The library *VehicleControls* is based upon the *VehicleInterfaces* library and is developed within the scope of project EuroSysLib.

AlternativeVehicles Library

Design and content of the *AlternativeVehicles* [Baur *et al*. 2006[c]] library focuses on powertrain concepts for today and future road and railway vehicles. The *AlternativeVehicles* library extends the *PowerTrain* library with models for batteries, electrical drives, power electronics and fuel cells and completes examples of non-conventional vehicle architectures like hybrid electric vehicles (e.g. parallel hybrid, serial hybrid or power-split hybrid), or fuel cell vehicles (fuel cell as well as fuel cell battery hybrid) which also include operating strategies, cf. Fig. 338. Furthermore, the library contains models of electric vehicles with in-wheel motors which can be controlled independently.

Hybrid electric vehicles (HEV) offer the opportunity of fuel reduction by torque allocation between the electric motor and the engine and by taking advantage of temporary energy storage in a battery. The ability of fuel reduction is based on the varying efficiencies of the propulsion aggregates. These efficiencies depend on the operating states, recuperation and boost which means, that the engine can be sized down when the motor supports to meet the peaks of power demand. In this context, the library also contains examples of fuel consumption optimised operating strategies.

2.3 Test Rigs

The research and development of new concepts and control strategies for mechatronic chassis require testing and model validation. Therefore, we have several different test rigs and measuring and visualisation systems.

2.3.1 Test Rigs for Steering Systems

Two steering test facilities offer testing of conventional and steer-by-wire steering systems und its components. They have been used in industrial projects. For advanced tests the laboratory was completed with a car mockup and a stereo visualisation system.

Steer-by-Wire

The steer-by-wire (SbW) test rig (see Fig. 342) is designed for testing of different wheel steering concepts complemented with different force-feedback steering wheel actuators. The formerly developed harmonic drive actuator as well as the recently launched SENSO-Wheel SD-LS from SENSODRIVE company and appropriate control strategies are analysed.

Fig. 342 Steer-by-wire test rig

Steering Wheel (SENSODRIVE)

The new version of the SENSO-Wheel SD-LC (Fig. 343) offers higher peak torque for even more realistic end stop simulation. The extremely high encoder resolution of 40,000 increments facilitates perfect simulation results.

Fig. 343 SENSO-Wheel SD-LC

Experimental Study of a Hydraulic Power Steering System

To update a numerical simulation model of a hydraulic power steering system from automotive industry partner a comprehensive test was performed at our lab. Two essential scenarios, the transfer dynamic behaviour of perturbation controlled system and the tracking control were analysed at different scenarios. The test rig (Fig. 344) and the power steering system were implemented with ten pressure sensors, two torque sensors, one force sensor, two angle sensors, one linear sensor, three temperature sensors and one current sensor. A hydraulic cylinder simulated the roughness of the street. Altogether, 960 measurements were performed and evaluated (see e.g. Fig. 345).

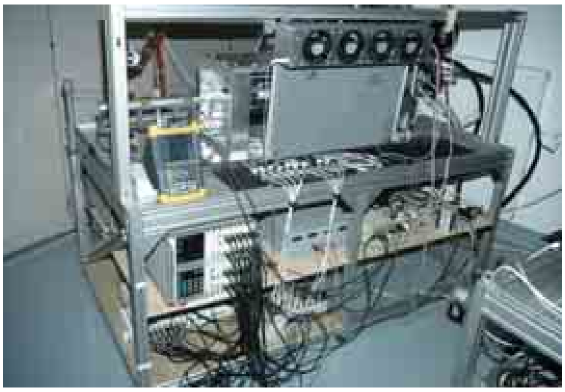

Fig. 344 Test rig for power steering system

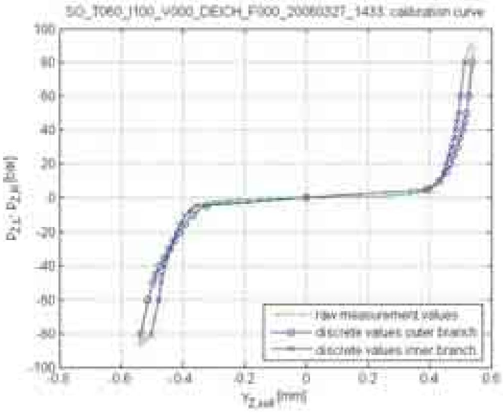

Fig. 345 Calibration curve of the steering rack

Fig. 346 Universal steering test rig

Parameter Identification of a Hydraulic Power Steering System

The test results gained by tests described previously were used for validation of the dynamic characteristics of the simulation model from another partner of automotive industry. The test rig has been designed to enable investigation of different steering systems (Fig. 346). The excitation of the steering wheel is carried out by an electric motor and by hand at different angles and frequencies. During the tests the following signals can be measured: Steering wheel angle, steering wheel moment, track rod force, track rod stroke, steering gear pressure, oil temperature and the acceleration of the air back box. A total of 60 measurements were performed and evaluated.

2.3.2 Vehicle Mockup and Visualisation System

Testing of Human-Machine Interfaces (HMI) such as force-feedback steering wheel actuators requires more than pure HiL tests. The vehicle mockup (Fig. 347) and the high quality visualisation system (Fig. 348) complement our test facilities for more realistic driving experience.

Fig. 347 Vehicle mockup

Fig. 348 Visualisation system

In view of using a Robocoaster as a future driving simulator, the car mockup is equipped also with pedals. Additionally, instruments and gear shift will be added.

The visualisation system uses polarising to get the impression of stereo viewing.

2.3.3 Scene Visualisation

Most visualisation systems operate independent from the simulation, which means that additional effort goes into the separate generation of the scene.

For this reason, we use a different approach for the visualisation of multibody systems: The visualisation control is fully integrated into the object oriented simulation language Modelica. External visualisation software, developed at the institute, displays the scene defined by the Modelica model. Fig. 336 was generated using our visualisation approach.

The simulation communicates via UDP with an external visualisation system based on the open source graphics engine called OpenSceneGraph. Every basic multibody element supported by the Modelica 3.0 standard is displayable, as well as common CAD data formats. Additionally, the visualisation of energy flows (useful especially for hybrid drive vehicles) is supported.

2.3.4 Models and Tools for HiL

Leaving the pure simulation of mechatronic systems behind, Hardware-in-the-Loop test rigs provide cost effective ways to test new control algorithms with existing hardware. For this purpose, Modelica models can be included into Simulink models. This hybrid model can be compiled and run on a xPC Target system, providing a hard real-time environment. Unlike workstation simulations, where the real-time condition can not be guaranteed because of operating system techniques like multi-threading and multi-processing, the real-time simulation assures the execution of the model with a constant simulation rate, which is essential for hardware control.

Using this real-time simulation system allows the safe, direct control of external hardware for HiL simulations and is used for example in the steer-by-wire test rig and for the test of robot control algorithms.

3 Railway Systems

The application of methods and tools from aerospace and robotics to railway vehicles has a tradition of more than 25 years at the institute and has even reached the industrial level in the meantime. In fact the virtual design of today's high-speed-trains such as the ICE relies on the multibody simulation environment Simpack, which has originally been developed at the institute and nowadays represents the technological and economical basis of the spin-off company Intec.

The present-day research activities in railway vehicles are focussed on vehicle dynamics and on energy systems. In details, our current work deals with

- improvements of the dynamic simulation methodologies in order to prepare ready-to-use technologies for a target-oriented vehicle design;
- a novel concept of a mechatronic running gear that will be qualified at our scaled M 1:5 roller rig;
- the transfer of methods from aeronautics that are based on the modelling language Modelica and are capable to model and design multi-domain energy systems in railway vehicles.

The activities are embedded in the DLR-Project "Next Generation Train" (NGT), see [Kurzeck *et al.* 2008[f]] and Fig. 338, in order to organise the cooperation with other DLR institutes on topics such as crosswind stability, noise and vibration engineering and operational energy management.

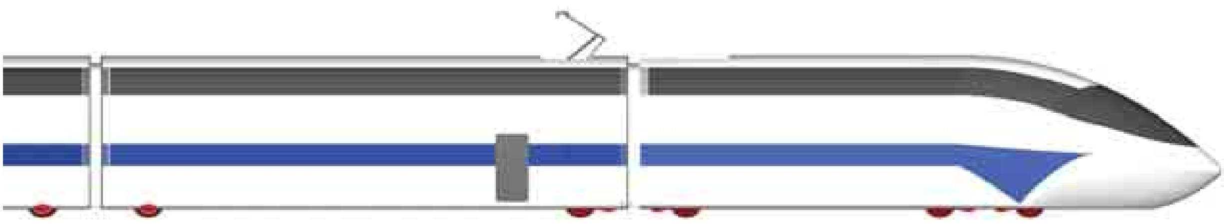

Fig. 349 DLR-Project Next Generation Train: side view of the high-speed multiple unit vehicle concept: double deck, Jacobs bogies, high-speed-low-floor running gears, optimised aerodynamics, light-weight

3.1 Dynamics and Simulation

3.1.1 Wheel/Rail Interface

Some important issues addressed by the project NGT are directly related to the wheel/rail interface: it is the origin of rolling noise, the major noise source below 200km/h, and the origin of wear. The associated maintenance costs are generated there and running safety as well relies on the wheel/rail forces, which therefore are the relevant quantities for the homologation of a railway vehicle.

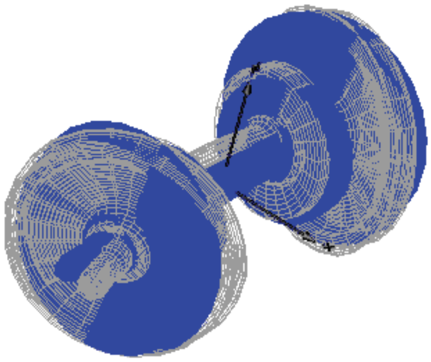

Fig. 350 Exemplary wheel-set bending mode that corresponds to 83Hz eigenfrequency

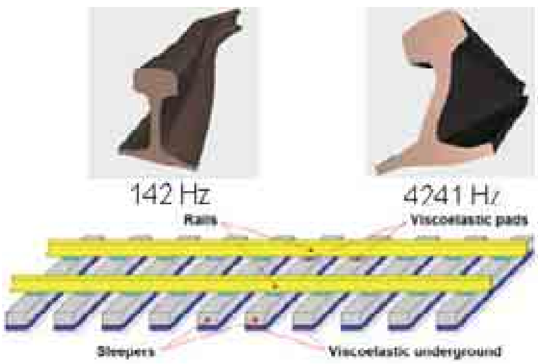

Fig. 351 Structure of the track model and 2 exemplary deformation modes of the rails

These problems are the essential motivation of our approach to extend and to improve the modelling of the wheel/rail interface by consideration in particular the structural dynamics of the wheel or wheel-sets and the rail or track system, respectively.

To become descriptive, this means that e.g. the bending modes of a wheel-set such as shown in Fig. 350 or the deformation behaviour of the rail visualised in Fig. 351 are introduced instead of assuming both contact partners to be rigid as it is the state-of-the-art today [Kaiser & Popp 2006[c]].

We could show that the so-called hunting motion, a dangerous running state of high-speed-trains, may occur at lower velocities, if the structural elasticity of wheel and rail are taken into account, i.e. neglecting the elasticity leads to a smaller reserve of safety related to the running behaviour.

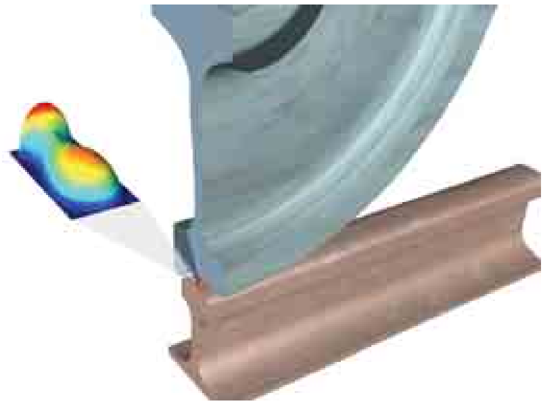

Fig. 352 Normal pressure distribution at the contact patch between wheel and rail.

We propose to use the so-called Arbitrary-Euler-Lagrange (ALE) description to de scribe the deformation of the rotating wheels [Kaiser *et. al.* 2007[c]]. This approach inter alia facilitates the modelling of rotor-like structures with non-rotating contact forces, as they are present at the wheel/rail interface, but also, e.g., at the brake-disc/pad- or the lathe/workpiece interface.

Contrary to other ALE-approaches inspired by fluid dynamics, we exploit the specific properties of axially symmetric or axially cyclic structures, so that the resulting formulation exposes a high computational efficiency, which is a requirement for the industrial application of the method.

In addition to the consideration of the structural dynamics the contact modelling itself also has to be refined in order to reasonably adjust the different model components. Due to the geometrical shape of wheel and rail, the wheel/rail interface has a non-elliptic contact patch, see Fig. 352, which may be solved using a fast iterative algorithm [Kaiser 2008[c]].

3.1.2 Acoustics

Besides an improved running dynamical design of railway vehicles, the modelling extensions also open the new field of acoustics that has been beyond the capabilities of the multibody methodology so far.

In addition to the approach presented above, structural dynamics models with high-frequency modes up to 6kHz for the wheel-sets and even 10kHz for the rails are taken into account together with appropriate excitation mechanism such as surface roughness or mode coupling [Kurzeck 2008[t]].

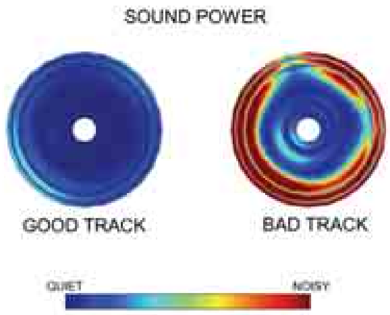

Fig. 353 Exemplary comparison of the structure-borne-noise level: the same wheel, running on two different tracks

On this basis a post-processing procedure of the multibody simulation results was defined that yields the structure-borne-noise level at the surface of the observed component. Fig. 353 shows exemplary results of the rolling noise of a wheel, excited by tracks with different surface roughness.

In the near future the post-processing procedure will be extended to evaluate the airborne-noise level e.g. in a distance of 7.5m when a train passes by.

3.1.3 Wear

From the point of view of the railway operator, two kinds of wear are to distinguish:

- the ordinary wear in lateral direction of the wheel and rail profiles, quite often addressed just as "wear", mainly defines the maintenance intervals;
- the non-uniformity of the wear in longitudinal direction such as rail corrugation or wheel polygons, see Fig. 354, is both the result and the cause of vibrations of the vehicle.

A lot of uncertain parameters influence the distribution of lateral wear of the wheel profiles, such as wheel and track profile, track irregularities, layout of the line, operation conditions, train performance and contact conditions. Hence, a current project in cooperation with the *Bayerische Oberlandbahn*, a local train operator, deals with the determination of theses parameters. The wear at the wheels of their train sets is evaluated calculating the local distribution of the work of friction in the corresponding contact patch in multibody simulations.

Additionally, the consideration of the structural dynamics of the wheel-sets and the rails and the refined contact description presented in Sec. 3.1.1 allows for a detailed analysis of the mechanism of friction induced oscillations, see e.g. [Kurzeck 2008[t]], and non-uniform wear in longitudinal direction such as corrugation or out-of-round wheels since this type of wear is related to higher frequency ranges.

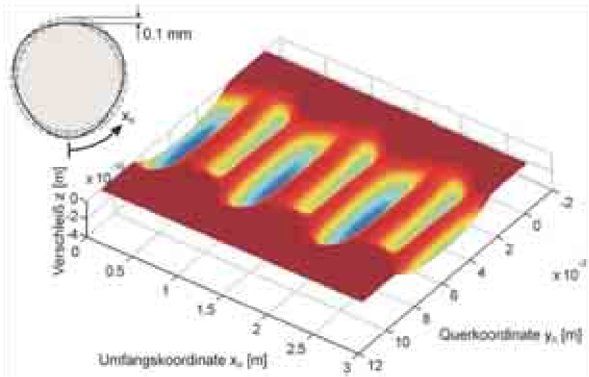

Fig. 354 Simulation result: polygonalisation of the wheel

Comprising, the key feature of the approach is the interplay of short time vehicle/track dynamics including the improved modelling of the wheel/rail interface and the long term behaviour of the vehicle and track components subject to wear. In principle even rolling contact fatigue phenomena might be taken into account this way.

3.1.4 Crosswind Stability

Railway vehicles are endangered by strong crosswinds, catastrophic accidents having already occurred in the history of railway transportation. This problem, aggravated by the continuous improvement of the lightweight characteristics of modern rolling stock, has eventually become a neuralgic point in the design and homologation of vehicles.

Accordingly, the project NGT includes a joined work package on this topic, in which DLR-Institute of Aerodynamics and Flow Technology contributes the aerodynamic design of the NGT including windtunnel measurements.

At our institute, the research is focussed on the effects of the aerodynamic forces on the running safety of the railway vehicle. In particular we have developed advanced probabilistic methods for crosswind risk analysis which are less conservative than currently used crosswind stability criteria for vehicle design and homologation.

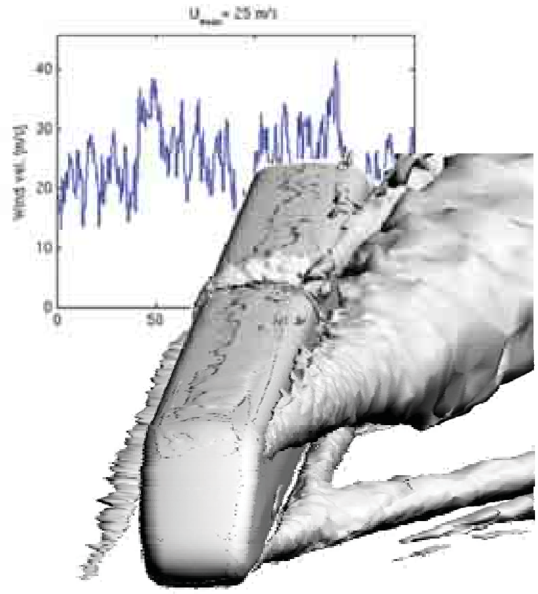

Fig. 355 Stochastic wind crosswind velocity for running safety analysis (related CFD results of the DLR-Institute of Aerodynamics and Flow Technology are given for visualisation)

In addition, passive and active countermeasures at the vehicle level, e.g. based on active suspension concepts, are investigated using simulation, risk analysis and optimisation tools.

3.1.5 Thermoelastic Brake Models

This working field has been initialised by a joined project of Knorr-Bremse GmbH, Siemens Mobility and our institute [Günther *et. al.* 2008[c]].

The goal of this project was to understand potential vibration mechanisms of brakes in high-speed trains. The study comprises a comprehensive multibody simulation study and its comparison to experimental results at the test rig of Knorr-Bremse in Munich, see Fig. 356.

It is a result of the project that the onset of a certain type of brake vibrations can only be explained if the thermoelasticity of the brake disc and system dynamics of the whole brake system including its mounting in the bogie is taken into account.

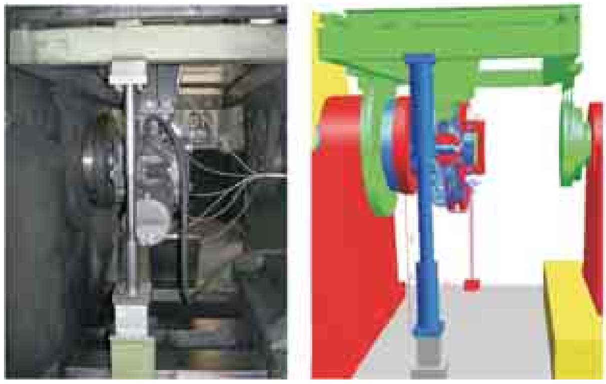

Fig. 356 Side view of the Knorr-Bremse brake test rig (photo and multibody model)

In cooperation with Knorr-Bremse, a succession project, scheduled for three years, has been defined in order to develop a brake model that is capable to explain this specific vibration behaviour. The model will use the so-called modal multifield approach to describe the coupling of the thermal and the mechanical field of the brake disc [Heckmann 2006[c]] and as well will take advantage of the ALE-description, that enables an easy brake-disc/pad contact formulation [Kaiser *et al*. 2007[c]].

The innovative simulation environment, whose first draft originates from a Simpack/Modelica project with Daimler [Busch 2007[r]] and is related to the ITEA2 Modelisar project, will combine the advantages of the multibody tool Simpack and the multi-domain modelling language Modelica.

In addition results of this project will be introduced into the commercial Modelica FlexibleBodies Library [Heckmann *et .al.* 2006[c]] and the new Modelica Multifield Library, that is developed in the ITEA2 EuroSysLib project.

3.1.6 Further Use Cases

Virtual Homologation

One of the most expensive and time consuming parts in the development of new rolling stock is the homologation, which is almost exclusively performed by means of tests on track. For this reason, a key research topic at DLR-RM is the enhancement of models and simulation techniques to replace the hardware tests as much as possible by computational ones, allowing the homologation to be performed with minimal efforts in terms of cost and time. Moreover, the so called "virtual" homologation would permit to integrate more closely the design process—which is already based to a very large extent on computer tools—and the homologation processes, reducing the number of necessary design iteration steps and optimising the overall process. The proposed modelling improvements are one step further towards the goal to enable virtual homologation.

Dissemination

It is the final goal of all modelling activities presented in Sec. 3.1 to organise their application in cooperations and third-party funded projects or to generate a software product ready for use in the industrial practise.

That is why the presented techniques are implemented twice, wherever it is reasonable. The introduction into the commercial Software Simpack aims at the railway industry, where Simpack has become a quasi-standard. By the implementation of methods in Modelica and related projects such as EUROSYSLIB the railway system team contributes bridging technology ready to be used in automotive and aerospace applications as well.

3.2 Mechatronics

3.2.1 High-Speed-Low-Floor-Running Gear

In order to extend the train capacity and reduce the energy consumption per passenger, the vehicle concept of the NGT is configured as a double-deck high-speed multiple unit train set according to the high level goals of the project. This leads to the following list of requirements. The running gears

- have to meet all safety standards e.g. concerning running stability;
- have to allow a planar alleyway for passengers at the lower level of a double-deck vehicle (low-floor design);
- have to contribute to the traction of the train set;
- have to reduce wear of the wheels and the rails;
- have to reduce rolling noise.

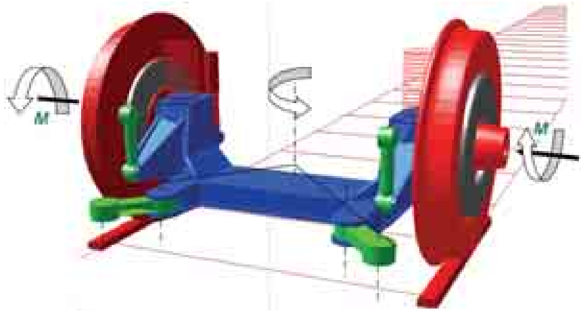

Fig. 357 Unit with carrier and independently torque-controlled wheels for the mechatronic running gear

Mechatronic systems for active steering and running gear control in principle offer an enormous potential for enhancements regarding this list of demands. Therefore, we have developed and assessed a special concept for a novel mechatronic running gear in low-floor-design, see Fig. 358.

Its major components are the feedback-controlled single wheels and the wheel carrier, which may be aligned along a curve radius. The wheel drives serve two purposes: they are traction systems and actuators, which may apply different torques on both wheels of one carrier. This way the carrier-wheels-unit may be adjusted to the middle of the track and may be steered into curves so that low-wear and -noise running characteristics are achieved.

A particular challenge of this project is to find an appropriate sensor concept that is reliable in daily train operation.

In the first step it is planned to design and to realise a first scaled prototype, so that advantages and disadvantages of the concept can be evaluated using the roller rig at our institute, see Fig. 358.

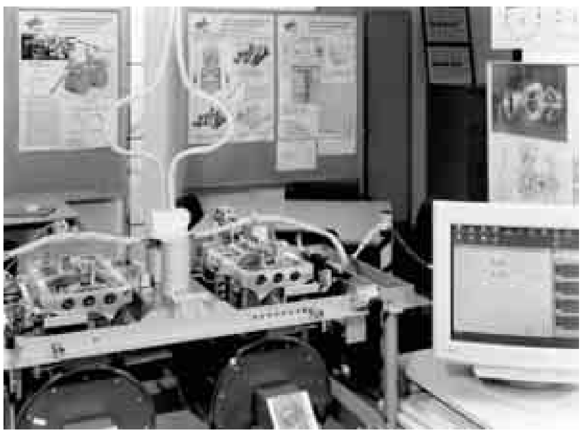

Fig. 358 Scaled roller rig M 1:5 at the institute

Beside the application to high-speed trains, we also see a high potential of the concept even for urban transport systems, where low-floor, low-noise and low-wear characteristics are highly relevant as well.

3.2.2 Brake Control

Currently, a pilot study is carried out that is initiated by an industrial partner. The goal of the study is to reveal potentials for innovating the brake control in passenger trains.

In principle a wide range of possible issues are taken into account, such as:

- improved longitudinal train set dynamics during braking;
- planning of braking trajectory and high-accuracy-halt;
- comfort improvement and brake noise reduction;
- slippage control;
- reduction of the braking distance;
- wear reduction at the wheel/rail interface;
- friction temperature control;
- monitoring and reliability;
- integrated drive train and brake control.

The achieved promising results of the pilot study will be discussed with the management of the partner and is supposed to initiate a succession project with a clear realisation horizon.

3.3 Energy Systems

The object-oriented multi-domain language Modelica has been applied very successfully in some prominent Aerospace projects such as POA or MOET und proved to be an adequate tool to describe heterogeneous energy systems consisting of electrical, electronic, hydraulic, pneumatic, thermo-dynamical and mechanical components.

In addition a prototype of a system simulation platform to represent the complex auxiliary power system in railway vehicles together with its onboard control system called TCMS was developed, see Fig. 359. The proposed environment is open to hardware- and software-in-loop applications.

Fig. 359 Overview on the ingredients of the system simulation platform for the auxiliary system

Regarding the DLR project "Next Generation Train" the institute cooperates with the DLR Institute of Vehicle Concepts in the NGT work package Energy-Management. The role of the institute is to provide methods and tools support, in particular regarding Modelica and high level analysis methods like optimisation, anti-optimisation, uncertainty-modelling and Monte-Carlo simulation.

VII Technology Transfer Examples

1 The DLR-KUKA Success Story Continues

The institute and the leading European robot manufacturer KUKA have jointly gone through an exciting technology transfer success story for more than 10 years. Essential improvements were transferred via research and development contracts from DLR to KUKA. Both sides greatly profit from this long lasting relationship. The success story is based on the technology transfer of advanced control algorithms for industrial robots and more recently on transfer of the light-weight robot technology.

1.1 LWR Technology Transfer

After years of intensive research cooperation with KUKA, the company decided to pick up the DLR concept of LWR-III and bring it to the robot market.

Fig. 360 LWR-III at the AUTOMATICA 2006

In a first step, KUKA reproduced 20 LWRs in their original form as developed at DLR to be familiarised with its concept. To build the robot, several DLR-manufactured components had to be transferred to industrial partners to reproduce them in industrial quantities and with the required documentation. DLR supported these efforts by finding manufacturers and working out specifications for the components.

Furthermore, the KUKA staff had to be convinced of the new torque controlled robot design, which pushes the modern concepts of “soft robotics” and touch sensitivity based on impedance control.

The KUKA LWR-III was first presented to the public at the AUTOMATICA 2006 robotics fair in Munich.

In the past two years, efforts were taken to modify the robot to increase its reliability and robustness, as well as to reduce the production costs. To come to serial status several tests had to be passed, e.g.:

- electromagnetic compatibility tests at Fujitsu-Siemens and DLR succeeded after DLR improving the electronics;
- long-term load tests were run for more than 4,000 hours with extended load at 100% speed.

By now, the second lot of 60 LWRs with minor improvements in the design are in production at KUKA.

Fig. 361 KUKA LWR-III at EMC test

On the software side, considerable effort was put into the seamless integration of the LWR's advanced features into the KUKA Robot Control (KRC). Although the KRC is designed for position-controlled industrial robots with up to six joints, it was a major goal to make the redundancy and compliant control modes of the robot easily available for the end user. In the integrated control solution, the LWR-specific control software is running as a separate module on the same computer as the high-level KUKA user interface. This way, a compact controller box with only one computer could be realised. The KUKA programming language KRL was extended to have easy access to all features and control modes of the light-weight robot (position control, impedance control, gravity-compensated torque control, collision detection, contact force estimation, virtual workspace limits).

Source code for the control of the LWR and the interaction with the KRC was transferred to KUKA but is still maintained by members of our institute, thus providing continued support and ensuring the integration of new features.

DLR accompanies the further development to maintain the concepts and to position the robot in the market as a prototype for a new generation of versatile robots.

1.2 Industrial Robot Control

The intensive and established cooperation in the field of advanced control algorithms for conventional KUKA industrial robots (see Fig. 363), which are sold about 8,000 times per year, was continued.

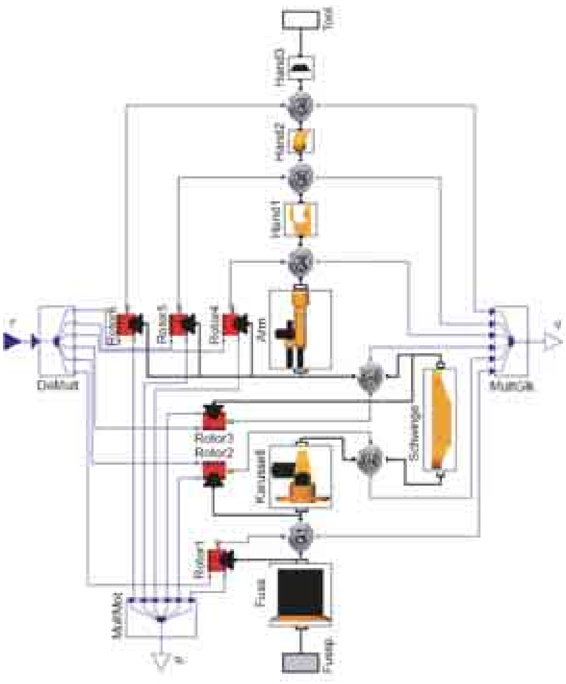

Fig. 362 Nonlinear dynamics of the 6-axis robot with elastic joints in Modelica/Dymola

New types of robot applications and the competition on the market urge the need for permanent improvements of the dynamic performance w.r.t. to speed and accuracy on the one side and cost reduction of the robots on the other side. To solve this conflict advanced control algorithms are of high strategic importance. They can be exploited for better performance or for cost reduction by using cheaper hardware components (gear boxes, light-weight mechanical parts).

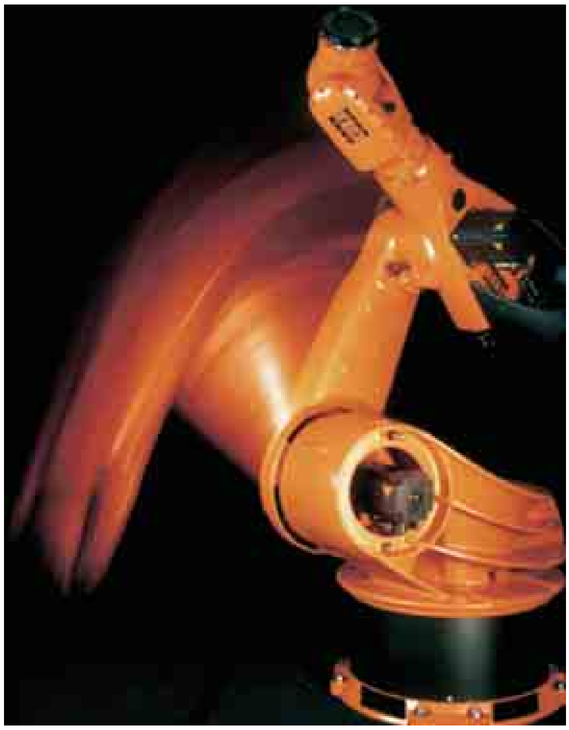

Fig. 363 Industrial Robot KR210

1.2.1 Nonlinear Robot Control

The robot is system-theoretically a nonlinear coupled system with multiple inputs and multiple outputs and a large operating range.

To achieve good performance for the complete operating range a model based controller is needed. It enables the decoupling of the control loops and the compensation of nonlinearities depending on operating conditions.

An essential prerequisite for application of advanced controllers is the estimation of internal states and parameters. Various algorithms have been designed, including an observer that uses the signals of acceleration sensors on the robot arm to achieve largely decoupled joints, reduce the model complexity and save computation time.

Alternatively nonlinear observers without additional sensors have been designed to estimate the non-measureable states.

To achieve a correct estimation it is essential to identify and compensate friction online, because it depends on operating condition. In this context an online identification and compensation of friction for nonlinear control systems with multiple inputs and multiple outputs is used.

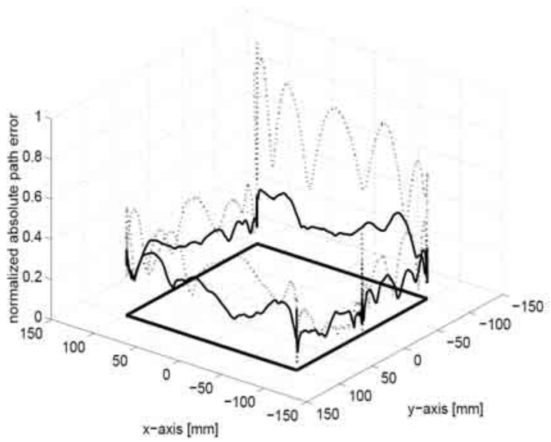

Fig. 364 Nonlinear controllers can greatly improve the tracking error, compared to a standard controller (dotted line)

The designed controllers are evaluated on a standard industrial robot using a special rapid control prototyping system and can significantly improve the robot control performance (see Fig. 364).

1.2.2 Structural Elasticity Compensation

To further improve the accuracy and achievable speed with industrial robots it is necessary to improve the mathematical models which are used inside the control algorithms. One important aspect is to not only consider the elasticity of the gearboxes in the joints of an industrial robot, but also the structural elasticity of the parts and links.

Fig. 365 shows an example of a deformed link of an industrial Robot, which connects axis 2 and 3 of the robot. These deformations occur under high load and high speed movement. If structural elasticity of the parts is taken into account in the control algorithms, the accuracy can be increased.

An important aspect is, that models used for control have to be calculated in real-time. So it is not possible to calculate complex FEM-models as part of a controller. As a result of this it is necessary, to reduce and approximate the models in their complexity, while still preserving the essential dynamic effects, which are necessary to compensate the dominant part of the structural elasticity of the robot in real-time.

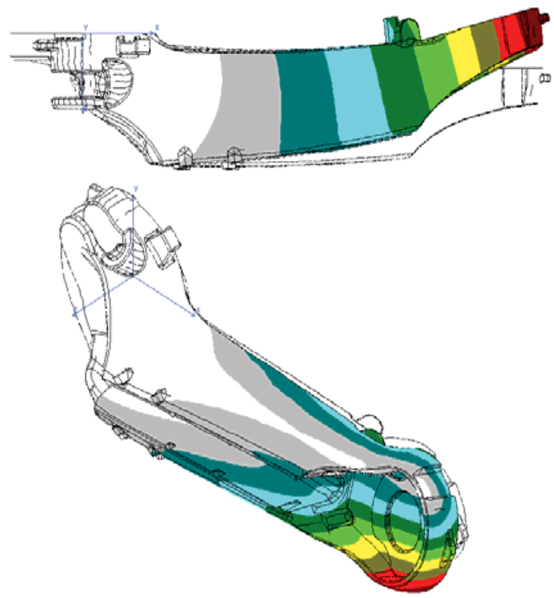
Fig. 365 Example of FEM-Data of a deformed part of an industrial robot

To attain accurate models of the robot it is necessary to identify the parameter of the models with measured data from the real physical robot. To accomplish this, a multi-step approach is applied which consists of direct measurements and nonlinear optimisation based grey-box identification (using the DLR-tool MOPS), resulting in accurate models.

These models can not only be used as part of a real-time control concept. They also can be used to generate time- or energy-optimal trajectories for the robot when considering the torque limits of its power trains, while taking the elasticity of the structure and gearboxes of the robot into account. This is done by a multiple-shooting optimisation with constrain conditions.

1.2.3 Robust Control of Robots with Elastic Joints

Modern linear and nonlinear robot control algorithms are model based. Model uncertainties have to be considered in case the actual system dynamics cannot be described sufficiently accurately. Suitable uncertainty models are necessary to apply modern robustness analysis and robust control synthesis methods.

A major cause for model uncertainty are inaccurately known load parameters of the tool (Fig. 366) which are essential for the more complex models like the one described in the Sec. 1.2.2.

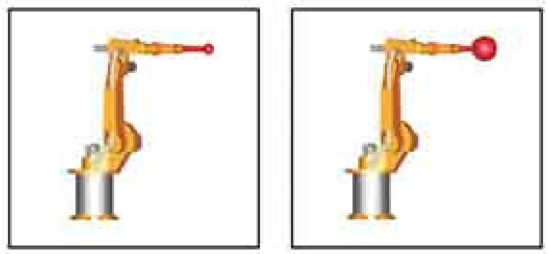

Fig. 366 Robot with different load

Due to the complex model of the robot containing nonlinear kinematics, friction and stiffness, the model has to be simplified for the controller synthesis. These simplifications and the errors appearing in the identification of the model parameters have to be considered as uncertainty, too.

Therefore uncertainty models have been developed which can describe the most important physical uncertainties and influences depending on operating conditions. The goal was to keep the uncertainty description as close as possible to the physical variations in order to avoid conservative control designs in applying robust control methods and tools to the uncertainty models.

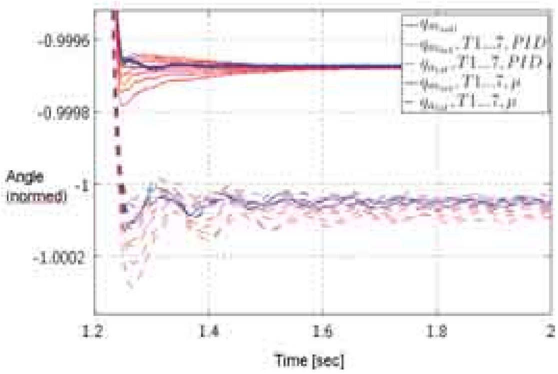

Fig. 367 Motor and gear position for different friction, blue μ, red PID control

Then modern robust control synthesis methods (H∞, μ, LPV, LFT, IQC, LMI) and tools, see Sec. IV.5.2, have been studied. As an example the robustness against friction, tested on a standard industrial robot, is shown in Fig. 367.

Due to the high nonlinear friction modern control algorithms tend to limit cycles. IQC based tools have been developed for limit cycle assessment of high performance controllers [Löhning *et al.* 2008[c]].

1.2.4 Periodic torque Ripple Rejection with Model-Based Controllers

The axes of today's industrial robots are often actuated with permanent magnet synchronous motors (PMSM). A bad property of these motors is that they generate parasitic oscillations (torque ripple). Unfortunately the gearbox of the robot also produces torque ripples with several harmonics which makes the robot oscillate at the tool centre point (TCP), see Fig. 368.

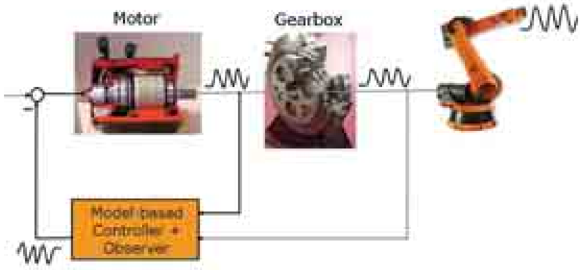

Fig. 368 TCP oscillations of the robot due to motor and gearbox ripples

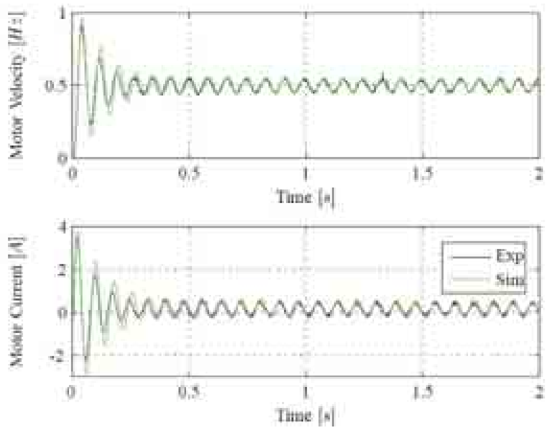

Fig. 369 Comparison between simulation and experiment. Step response of the PMSM

Torque ripple does not play an important role whenever the robot has to execute pick and place movements. For these tasks, the multi-body dynamics of the robot play the most important role. But whenever the robot operates quite slowly (applications are laser welding or gluing), the oscillation of the TCP is disadvantageous for the work piece.

In a first step models for motor and gearbox ripples have been developed and validated. A fit of the motor after a speed step is shown in Fig. 369. Different feed-forward and feedback periodic disturbance rejection methods are part of current research.

2 Assembly in Motion

Technology transfer to industrial robotics is not limited to control issues. In contrast to usual robot programs which represent fixed robot paths, the basic approach of sensor driven motion, which is a key technology of the institute, can be applied to industrial scenarios as well. While existing sensor applications predominantly determine a target pose at which the robot has to arrive, the project at hand combines sensor-based path specification and real-time control to realise an accurate motion of the robot end-effector along online sensed trajectories.

Fig. 370 Setup at *iwb* for mounting of wheels to a continuously moved car body

Trajectory control is crucial for motion along moving parts as in handling at a conveyor belt. Therefore, as a demonstration scenario an assembly line has been chosen in which wheels are assembled on a car body that is moved by a Power & Free conveyor. This set-up (Fig. 370) has been arranged at the project partner iwb, an institute of the Technical University of Munich. The developed approach is general enough to be applied to other assembly tasks as well [Werner *et al*. 2006[c]].

2.1 Sensor-Based Trajectory Planning

Assembly in motion cannot be implemented by simply perceiving the target motion and overlaying it to a robot motion that has been programmed for unmoved objects. The configuration has to be extended to allow the perception of objects whose pose is normally implicitly given by the program. This perception in particular has to include oscillations of the car body. As well, control errors of the robot have to be measured, which in the case of unmoved objects could be compensated by teaching slightly displaced poses. Furthermore, in industrial applications the requirements with respect to both accuracy and speed are usually higher than in service or space applications.

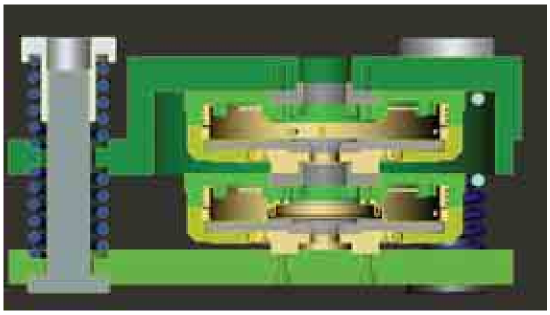

Fig. 371 Compliant force torque sensor for high forces and torques and high deflection (Exo-Compliance)

A setup of three kinds of sensors has proved to be generally useful. First, a coarse sensor that informs the system whether the car body is present. Second, a non-contact sensor that surveys the car body. A preferred realisation of this sensor is a CCD camera at the robot end-effector, since cameras are flexible sensors and this location leads to more accuracy and less occlusion. The output of the vision system will be used to let the robot end-effector approach the designated contact point. After the impact, the third sensor, a compliant force torque sensor, takes control. A compliance of at least one millimetre or degree is crucial, since conveyors are known to generate small scale oscillations, and also because the robot path accuracy is typically worse than the assembly tolerance.

Since compliant sensors of the required dimensions (1000N, 300Nm, 2mm) were not available, the institute has strengthened a small scale sensor by external springs and a second measuring unit, thus it fulfils the requirements (Fig. 371). Fig. 372 shows a prototype of the resulting multi-sensory end-effector, which includes five power screw drivers as well.

Trajectory planning is implemented by a Kalman filter that weighs all sensor information with their appropriate accuracies and by a heuristic scheme that defines the transient behaviour from the current to the sensed trajectory. More details can be found in [Lange *et al*. 2008a[c]].

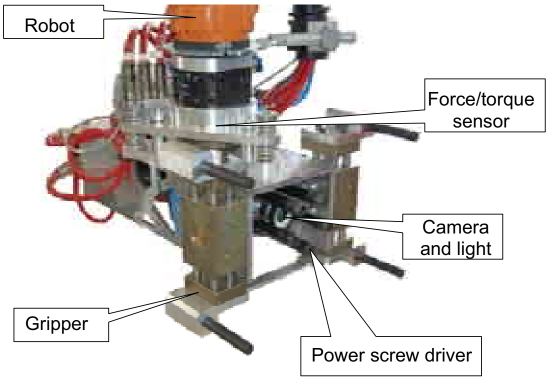

Fig. 372 Multi-sensory end-effector

2.2 Predictive Trajectory Control

Control within assembly lines is different from normal robot control since, first, small control errors have to be guaranteed at significant speed, and second, not only the robot path has to be controlled but also its synchronisation with respect to the conveyor. Finally the robot dynamics are more complex since a compliant and thus oscillatory end-effector is present.

Trajectory control is realized using model-based prediction of the sensed desired trajectory as input to a two-stage feed-forward filter (see below figure). The upper level is designed as an input shaping filter (see [Kamel *et al.* 2008b[c]]) to suppress any oscillation of the compliant sensor, while the lower level is realised by an adaptive feed-forward controller that compensates for the robot dynamics.

This approach allows very small control errors in spite of the robot dynamics as long as the predictions of the motion of the wheel rim are correct. This is arranged by a model of the conveyor and the car oscillations and by a proper calibration of the camera that prevents a hard impact. Fig. 374 shows images of the robot mounted camera during the approach to the wheel rim. Note the adjustment of the orientation.

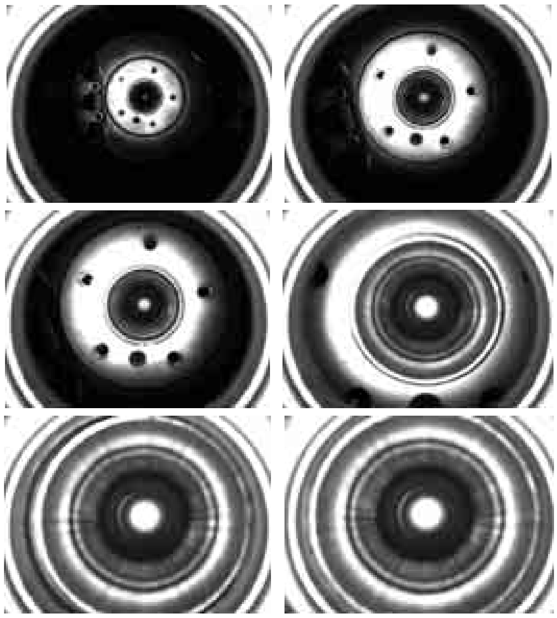

Fig. 374 Images of the robot mounted camera while approaching the wheel rim

The robotic setup includes a redundant linear axis to move the robot in parallel to the conveyor (Fig. 370). For dynamic reasons, the speed of this axis is not changed as long as the conveyor does not stop. In that case the robot completes assembly while its base is stopped.

2.3 Task Description and Programming

Applications for sensor-based control in assembly lines require programming techniques different from the typical industrial robot languages. In addition to the definition of the nominal robot path, for sensor-based tasks the application program has to incorporate the desired sensor values as well. These values usually vary, e.g. during vision-controlled motion towards the tracked object. Therefore, within this project both, the robot trajectory and the object trajectory are used for the online computation of the expected sensor values. In particular, the object motion (the car trajectory) is firstly extracted from the robot path, as-

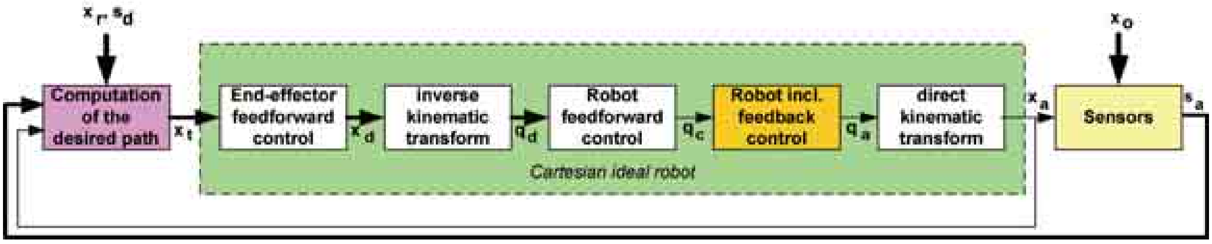

Fig. 373 Signal flow for predictive trajectory control of the robot

suming a conveyor-like motion with ideal contact in the contact phase. In this way, the existing robot languages can still be used with small extensions, e.g. to specify the active sensors or phases.

2.4 Impact

When the implemented prototype was first presented [Lange 2007c], it has attracted great interest by representatives of industry, above all by car manufacturers. Robust assembly in motion is assessed as a key technique for automation of production lines since currently manual work still predominates in final assembly lines. The qualification and experience of the institute, documented by several patent applications, can thus promote one of the most important industrial sectors in Germany.

3 The Mechatronic Wedge Brake

A rapid and intelligent braking system is one of the foundations for advancing the next generation of driver assistance systems. Mechatronic drive by wire systems are expected to replace existing hydraulic or pneumatic systems. Thus at the end of the last decade we had tried to develop a "dry" electromechanical brake following the most obvious concepts, namely actuating the braking disks by a motor-spindle combination (Fig. 375).

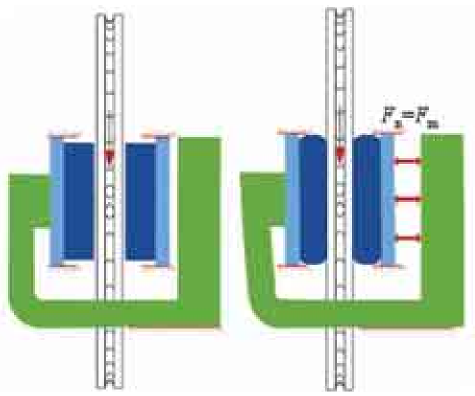

Fig. 375 Classical motor spindle concept for a "dry" brake

Such a solution seemed particularly interesting for us, as we had developed a high-reduction, low friction roller spindle gear drive.

This patented spindle concept is today produced and marketed by our license company Narr (Fig. 376).

Fig. 376 DLR's linear actuators based on planetary roller spindles, commercialised by Narr

And indeed our motor-spindle concept proved its applicability in a train-brake system which we developed in contract for the company Knorr. However soon it became clear that in the automotive sector it would be necessary to change from 12V supply to 42V supply, as all the braking energy with forces up to 30kN and more would have to be supplied by the batteries.

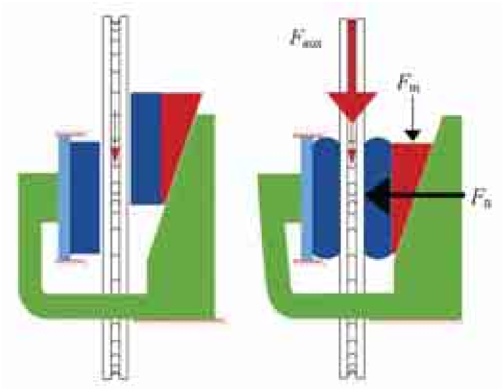

Fig. 377 Wedge brake principle

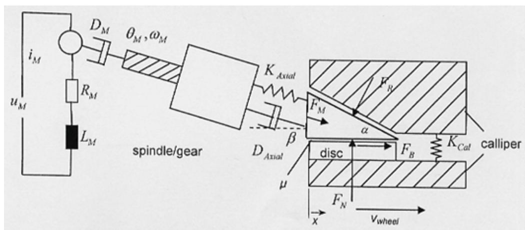

Fig. 378 Simplified model of the Electronic Wedge Brake

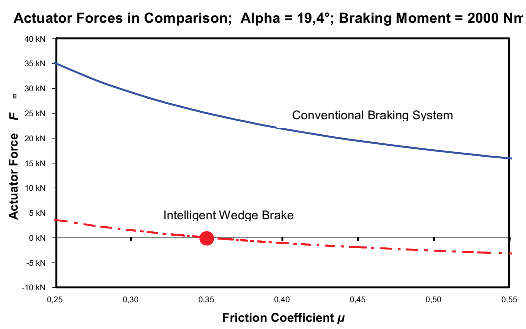

Fig. 379 Comparison of actuator forces needed for braking with alternative electro-mechanical braking systems

After an extensive brainstorming phase we decided to develop a new, self-amplifying wedge brake, where most of the braking energy (around 97%) is taken from the car's kinetic energy (see Fig. 377–Fig. 379).

The wedge principle had been used by the coachmen 200 years ago; he had to accept jamming effects but today with mechatronic concepts (force sensing and high-dynamic actuation of the wedge, realised via rollers, using our light-weight robot motor RoboDrive) it is possible to prevent the wedge from jamming. The first prototypes were realised in our institute.

In 2000, several of our employees founded the spin-off company eStop. In 2004, the wedge brake received the highly acknowledged HERMES award at the opening of the Hannover fair, and since then Siemens VDO bought our spin-off company and our former co-workers installed a major division of around hundred engineers for the improvement and preparation of the automotive mass market. Several redesigns of the system were realised (see Fig. 381–Fig. 386, courtesy of Siemens VDO).

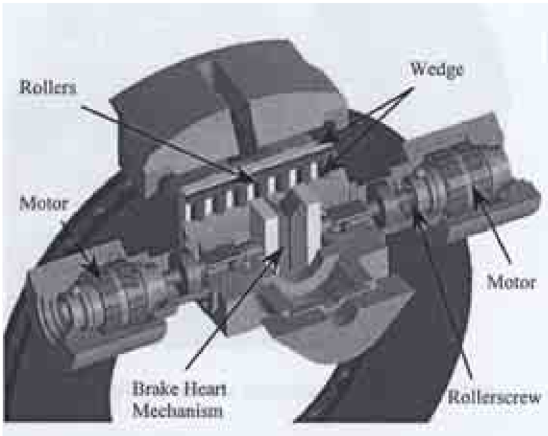

Fig. 380 Dual motor solution as used in the alpha prototype, the brake-heart mechanism is shown

Control theoretic solution had to be found for achieving robust, very high self-reinforcement factors despite of large fluctuations in the friction coefficient. The first (alpha and beta) prototypes used two motors (dual solution) to solve the problem of backlash (Fig. 380 and Fig. 381) while the final 90kN prototype (Fig. 382, Fig. 383, and Fig. 384) mastered the backlash problem while using only one motor to control the wedge mechanism. Parking brake, wear adjustment and failsafe function were realised via a second motor.

Fig. 381 Beta prototype of Siemens VDO (40kN/2500Nm)

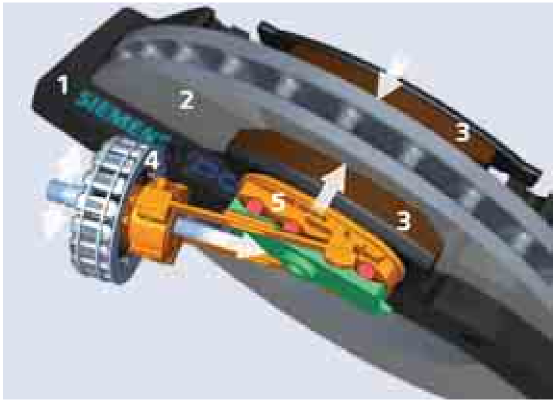

Fig. 382 Single motor actuation for the service brake

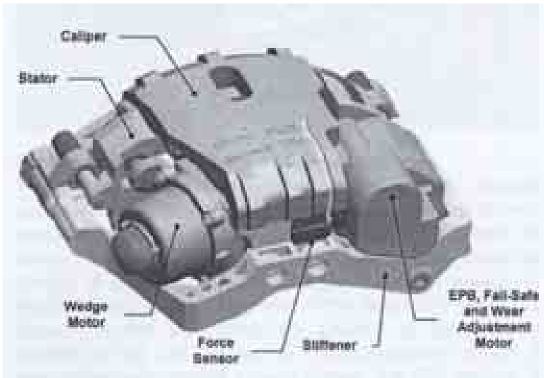

Fig. 383 PT1 prototype of Siemens VDO (90kN/4500Nm)

The mechatronic wedge brake with its challenging self-reinforcement feature would not have been realisable a few decades ago, since neither the control technology nor the basic technical prerequisites existed. These are characterised as follows:

- monitoring of the system within the closed servo loop, including fast acquisition of information and feedback to the control unit;

- real-time processing of the sensor signals to generate the necessary control demands;
- controller optimisation based on a validated plant model;
- implementation of control demands with sufficient bandwidth to guarantee system stability by an appropriate actuation system.

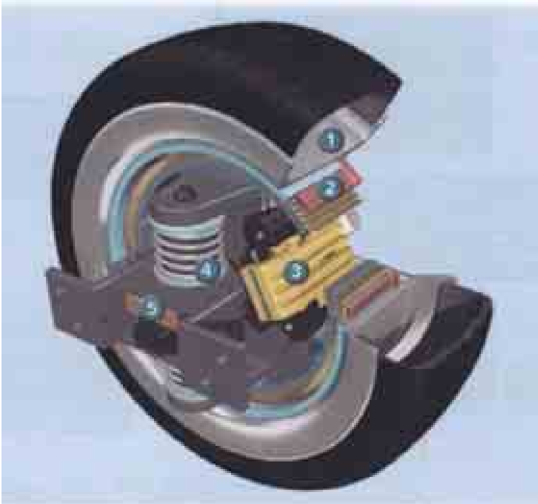

Fig. 384 Wedge Brake integrated into a "wheel robot" with electrical hub motor

It is only possible to stabilise the system if the whole servo loop can react to system changes faster than these changes can develop.

Because of the above requirements, it seems logical that a development such as the Electronic Wedge Brake would rather come from a mechatronics research establishment than from the classical braking industry.

From 2004 to 2007, numerous tests with standard cars, where only the brake system was replaced, were performed, to a great extent in Scandinavian countries in winter and on frozen lakes (Fig. 385).

Reduction of braking distance of up to 15% on dry streets were reported by many of the automotive journals who watched the tests. Experts stated that part of the superior performance of the new "dry" brake was due to the high dynamics of our RoboDrive actuator positioning the wedge, especially in the ABS situation (Fig. 386).

Fig. 385 Half braking distance on frozen lakes: AUDI with classical brake (left) and wedge brake (right)

Nevertheless, in 2007 Siemens VDO was bought by Continental, a market leader in "wet" brakes, and thus we have to wait what will happen with our fascinating brake concept, which often has been denoted as one of the most important automotive innovations of the last ten years (indicated e.g. by the Frost & Sullivan award 2006 and the Wall Street Journal award 2007).

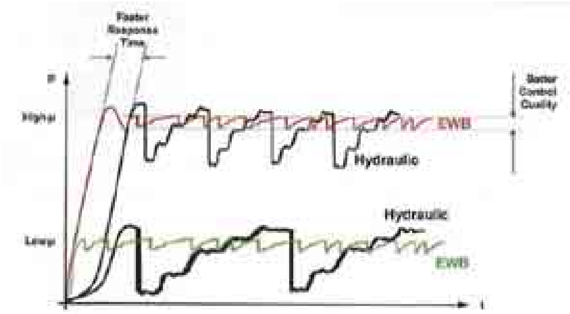

Fig. 386 ABS performance compared over the last ten years

4 Medical Device Technologies

Robotics and mechatronics are key technologies for the development of new medical devices. The institute transfers its expertise on telerobotics, mechatronic design and vision to two medical fields: surgical robotics and mechatronic implants. All projects in this field are third-party funded.

4.1 Surgical Robotics

Besides projects in the field of mechatronic implants (see Sec. 4.2) the research group focuses on the field of surgical robotics. Robotic systems can benefit surgical treatment by increasing precision, overcoming barriers, enabling new instrument designs, and enhancing ergonomics. Surgical procedures can vary by each patient, surgeon, and clinic. Therefore, and in contrast to specialised robotic systems, the central design paradigm for the institute's research is versatility, enabling rapid prototyping of new approaches and making the results available for a wide range of surgical applications. The need for versatility in a robotic system is a direct result of the experiments in space robotics where the system is operated at a place which is not accessible and mostly unknown. Due to this lack of predictability, the robotic system must be capable of performing its tasks in different adaptable ways. Developed space technologies such as telepresence, multi-modal sensors, and new robot control modes are, therefore, the basis of the surgical robotics development at the institute.

4.1.1 The DLR KINEMEDIC Robot

The DLR KINEMEDIC was the first generation of light-weight robots for surgery developed at the institute and funded by industry cooperation with BrainLAB AG. It has been designed to meet the requirements of a broad range of surgical applications. By adding specialised instruments the KINEMEDIC robot can be adapted to different applications in orthopaedic surgery and neurosurgery. Moreover, integrated multi-modal sensors and different control modes allow system configurations for telepresence as well as for autonomous and soft robotics applications. To simplify the integration of one or multiple DLR KINEMEDIC robots into the crowded operating room (OR), the design of the arm aims at compact dimensions and different mounting solutions [Frumento *et al.* 2006[c]].

Besides functionality, the aspect of safety during close interaction with patient and user is a central design issue. The reduction of accelerated masses through light-weight design, multi-modal sensors, and the application of enhanced control methods significantly reduce the severity of collisions between man and machine [Haddadin *et al.* 2007d[c]].

The close interaction demands for an inherent predictability of the system actions for the user. To achieve this, a serial kinematics with seven degrees of freedom (DoF) which resembles those of the human arm has been developed and optimised for medical procedures by means of gradient methods and genetic algorithms.

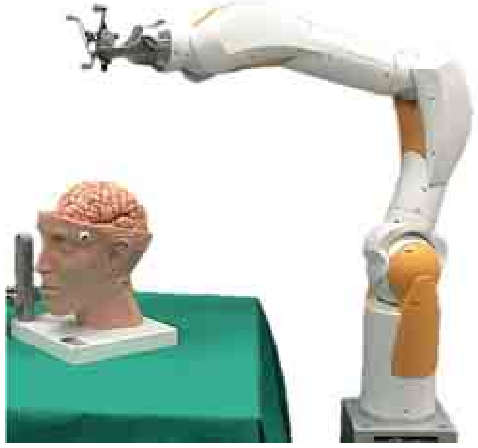

Fig. 387 The DLR KINEMEDIC in a setup for robot assisted biopsy

As a prototypic application, a navigated, robot-assisted biopsy for neurosurgery has been implemented [Konietschke *et al.* 2006b[c]]. The development of the DLR KINEMEDIC prototype has been completed in 2006. The system is in the commercialisation phase at BrainLAB AG.

4.1.2 The Second Generation MIRO

Based on the technologies introduced with the DLR KINEMEDIC, the institute developed the second generation DLR MIRO (see Fig. 388), enhancing performance, size, safety and electromagnetic compatibility.

Fig. 388 The DLR MIRO light-weight robot for surgical applications

With its low weight (<10kg) and dimensions similar to those of the human arm, the MIRO robot can assist the surgeon directly at the operating table where space is limited. The hardware of the DLR MIRO integrates 7 torque-controllable joints and all features established by the DLR Light-Weight Robot (torque and position sensors, safety brakes, integrated electronics, etc.) in a yet more slim design [Hagn *et al.* 2008[j]].

Fig. 389 The DLR MIRO: overlay of extremal pitch joint configurations with plot of maximum reach

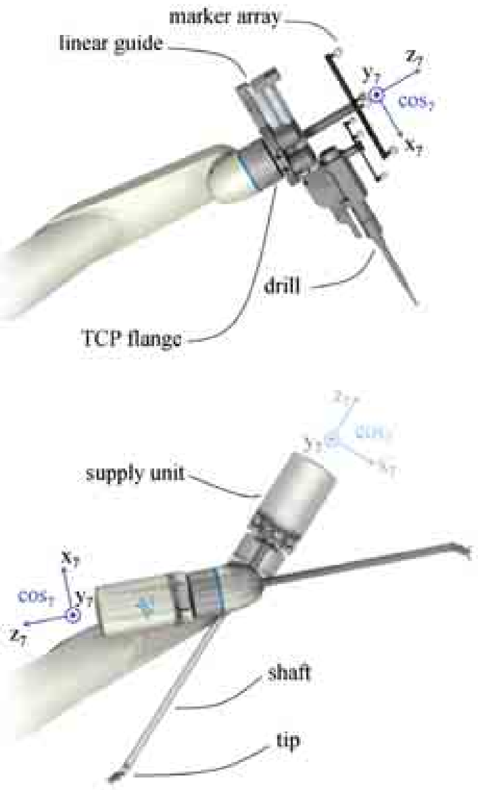

Fig. 390 The DLR MIRO wrist: conventional instrument (above) and endoscopic instrument (below)

Compared to the DLR KINEMEDIC joint ranges (see Fig. 389) and dimensions have been significantly enhanced for endoscopic surgery with the DLR MIRO.

To form compact groups of joints with intersecting axes, coupled joints with 2 DoF, based on differential gears, have been developed. A new compact wrist design allows the use of endoscopic and conventional instruments (see Fig. 390). The instruments are connected by a new electro-magnetic quick changing system integrated into the last axis of the MIRO.

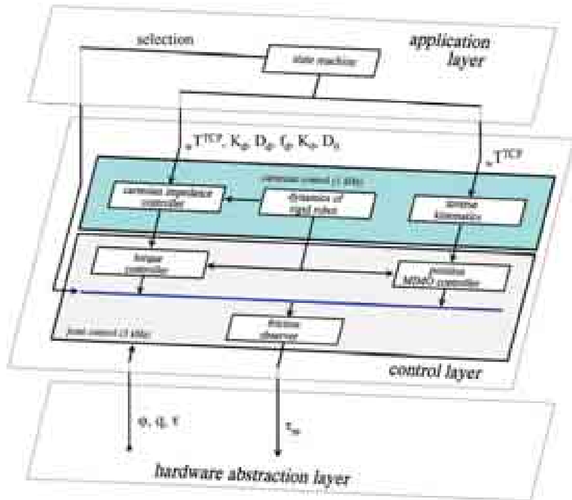

Fig. 391 The layered control architecture of the DLR MIRO

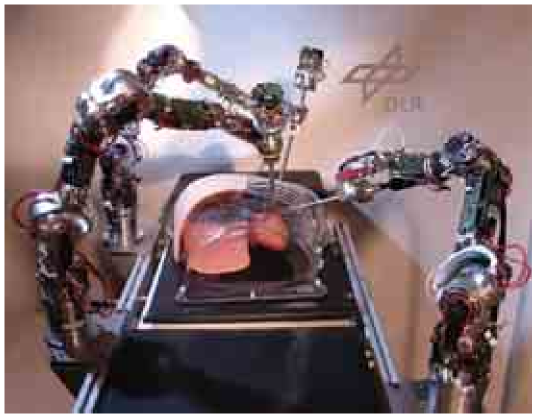

Fig. 392 Three DLR MIRO robots without housings in a telepresence setup for endoscopic surgery

The control structure of the MIRO robot has been developed according to the principles of platform-based design. The application is designated to configure and parameterise the platform for a specific task. To achieve the demanded versatility of the system it is necessary to cover as many system constraints as possible by the configuration due to the faster optimisation cycles in application design compared to platform design. Fig. 391 shows the layered structure of the control architecture [Jörg *et al.* 2006[c]], offering two main control modes [Le-Tien *et al.* 2007[c]], which can be selected by the application. Beside classical position control a compliant control mode is available enabling so-called "hands-on" robotics applications [Albu-Schäffer *et al.* 2007b[j]].

The DLR MIRO is targeted at applications in endoscopic surgery, neurosurgery and ortho-surgery. Currently three DLR MIRO robots are in the evaluation phase (see Fig. 392).

4.1.3 The DLR MICA Instrument

An actuated instrument for minimally invasive robotic surgery (MIRS) was developed, the DLR MICA (see Fig. 393).

In conventional minimally invasive surgery (MIS) the surgeon operates with long, slender instruments through small incisions in the patient's skin. Dexterity for the surgeon as well as kinaesthetic feedback is greatly diminished as compared to open surgery. To overcome these drawbacks an actuated and sensor integrated instrument was developed at our institute. It re-establishes full intra-corporeal dexterity and can measure tissue interaction forces.

Instrument

The instrument provides 2 articulated degrees of freedom (DoF) at the tip and one functional DoF. Interaction forces and torques can be measured distally by means of a miniaturised force-torque sensor. Actuation of the instrument tip is provided by a compact drive unit with integrated motor and sensor electronics. The distal end of the instrument is in direct patient contact and, therefore, has to be steam sterilisable since autoclavation is the standard sterilisation process in daily clinical use. Due to the fact that most electromechanical parts of the drive unit are unstable with respect to autoclavation conditions, the propulsion unit was designed to be separable: the proximal part containing all unstable devices (drive unit) is not in direct patient contact and can be decoupled from the autoclavable, distal part [Kübler *et al.* 2005[j]].

Based on the experiences with this drive train and with the design of the MIRO robot a new version was designed recently, shown in Fig. 394. Based on a simplified and modularised design it will provide over all better performance (power, precision and dynamics) at reduced weight and diameter.

Fig. 393 The DLR MICA, an actuated instrument for minimally invasive robotic surgery

Fig. 394 The new drive unit for the DLR MICA Instruments

Force Sensing

True tissue interaction forces can only be measured at the instrument tip close to the actual operation site. Hence, the force sensor needs to be small enough (diameter <10mm) to be integrated into the instrument, yet mechanically stiff and able to withstand conditions inside the human body and during sterilisation. A design based on a Stewart platform was selected, shown in Fig. 395. It offers straightforward scalability and allows for integration of mechanical drive elements required to actuate the functional end of the instrument. The current sensor design provides 9 bit of usable resolution over a measuring range of 10N in 6 DoF [Seibold *et al.* 2008[b]].

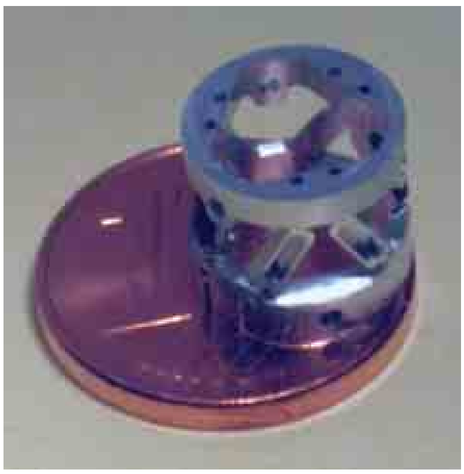

Fig. 395 Stewart platform structure of the miniaturised force sensor

Basic research concerning the applicability of fibre-optic sensors for force measurement in MIRS is being performed within a DFG project ("Faseroptische Sensorik in der Medizinrobotik").

Tactile Ultrasound Sensor

Since the presented force-torque sensor is mainly intended for kinaesthetic feedback, a new, ultrasound based sensor is being developed within the DFG project SFB453/I3 to capture tactile information (see Fig. 396). This unidirectional Doppler ultrasound sensor for MIRS application allows feedback of very important tactile information in surgery—the perception of vessels beneath covering tissue—to prevent unintentional bleedings after blunt dissection. The detected pulsation of vessels can then be displayed, e.g. on force-reflecting input devices as a smooth bucking.

Fig. 396 Doppler ultrasound sensor for tactile sensing of blood vessels

4.1.4 Heart Motion Simulator

A simulator has been developed to simulate the motion of the beating heart surface. It is intended to be used for experiments with the MIROSURGE telepresence setup (see Fig. 397) for heart surgery providing a reproducible test environment for motion compensation (see Sec. 4.1.7). Trajectories of motion gained from motion tracking of the human heart in real surgical procedures [Gröger *et al.* 2005b[c]; Ortmaier *et al.*, 2005] can be replayed by the simulator.

Fig. 397 DLR heart motion simulator

A modified delta-mechanism-based assembly provides three DoF to simulate a simplified trajectory of the human heart surface. An upper platform unites three drive linkages allowing planar and vertical movements. On this platform an artificial heart model is mounted. The actuation of the simulator consists of three light-weight RoboDrive servo motors (Sec. VII.7.2) and power converters developed by the institute's spinoff SENSODRIVE.

4.1.5 Telepresence Application

In 2008 the institute integrated a telepresence system for robotic endoscopic surgery – the DLR MIROSURGE. The development of this system has been funded by the *Bayerische Forschungsstiftung*. For this purpose, three DLR MIRO robot arms are combined with DLR MICA instruments and an endoscopic camera (see Fig. 398).

Fig. 398 The DLR MIROSURGE robotic setup integrating three MIRO robots, two MICA instruments, an endoscopic stereo camera and the heart simulator

The surgeon controls the motion of the instruments and robots by a remote master station with haptic handcontrollers and a 3-D display (Fig. 401). In addition, the manipulating forces exerted are rendered as so called force-feedback [Seibold *et al.* 2008[c]; Ortmaier *et al.* 2007[b]]. The haptic interface is realised as shown in Fig. 401 by the integration of two "omega.7" devices (Force Dimension, Switzerland). The whole setup with three MIRO, two MICA, and two haptic devices has 41 DoF [Hagn *et al.* 2008[c]].

Control Architecture

The control system is able to handle different operating modes and various control loops such as joint control, force-feedback control, or collision avoidance of the robotic arms. Due to computational limitations and robustness the control system has to be distributed to several computers.

The control architecture grants an efficient execution of control loops while still being flexible and expandable. The system is easy to modify and adaptable to changing prototypic hardware.

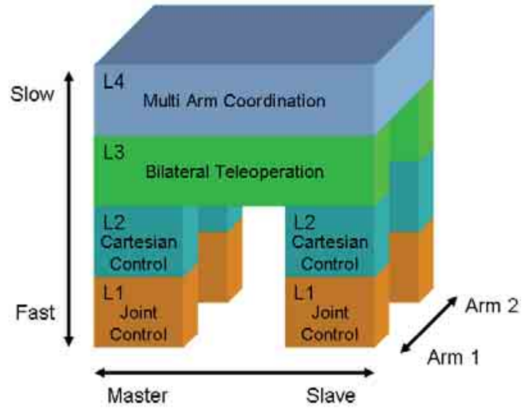

Fig. 399 Architecture of the control system for minimally invasive surgery

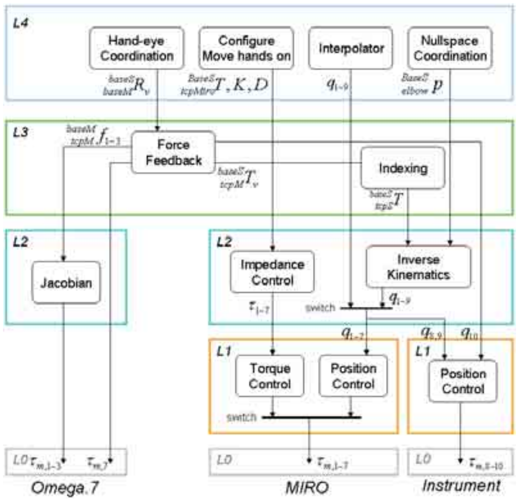

Fig. 400 Control Architecture as demonstrated at the AUTOMATICA Trade Fair in June 2008

The focus so far was to establish a conceptual architecture that gives a group of researchers a common understanding of the system. The architecture organises the control components in different layers according to their demand in execution time and amount of affected hardware (Fig. 399).

Beside the classic position control mode during teleoperation the compliant control mode of the DLR MIROs is used for introducing the instruments into the patient. The control system (Fig. 400) includes local controllers for the MIRO and the sensorised instruments as well as force-feedback control and a first approach of collision avoidance of the MIRO arms.

Fig. 401 The MIROSURGE remote master station with two haptic devices and a user testing the force feedback with a beating heart

Bilateral Teleoperation

In bilateral teleoperation the dynamics of two mechatronic devices are coupled together (see Chapter III.5). The goal is to give a human operator holding the master device a sensation of the environment of the slave device. In MIS the surgeon needs force feedback for palpation of tissue or for suturing. The bilateral control is implemented with a position-force scheme were positions are sent from the master to the slave and forces are sent back. The system takes care of workspace limitations and joint limits. It automatically decouples when the user moves out of the workspace and couples in again when moving back. The entry point into the patient is respected and collisions of the arms are avoided. An analytic inverse kinematics solution for the end effector and the entry points guarantees an exact result. A numeric solution optimises the null space of the MIRO to avoid singularities and collisions. The user can concentrate on his task without concern of what is outside the endoscopes view. In demonstrations the users on the master station could feel the beating of an artificial heart (see Sec. 4.1.4).

System Integration

The control system was developed with Matlab/Simulink/RealtimeWorkshop for rapid prototyping and automatic code generation. The control software is implemented in different models that are communicating with the agile robot development (aRD) [Bäuml & Hirzinger 2006c] software suite. The system is distributed over six PCs running the QNX real time operating system.

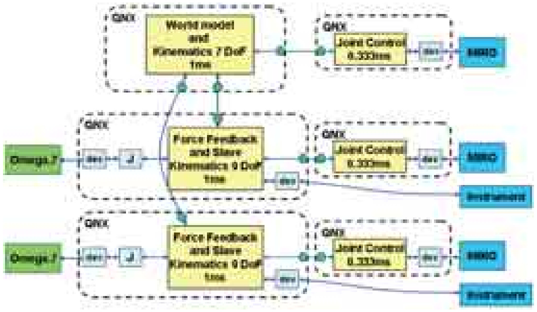

Fig. 402 Distributed control software for minimally invasive surgery

The system provides proper hand-eye coordination in 6+1 DoF for each hand. Bimanual force-feedback was implemented in four degrees of freedom per hand.

4.1.6 Shared Control Applications

Beside telepresence setups, the research group works on single-arm applications based on the shared-autonomy principle.

Robot Assisted Placement of Pedicle Screws

Pedicle screws are used in spine surgery to add stabilisations to damaged vertebrae. Exact placement of the screws is critical due to vital structures nearby (spinal cord, aorta). The position of the screws is planned on pre-operative CT scans.

During the operation, the robot arm displays the planning data in a haptic way. Additionally, the pose of the robot tool-centre point is tracked by an optical navigation system serving as an external reference source. Therefore, it is possible to measure and to compensate deviations between the intraoperative and the preoperatively planned pose.

Fig. 403 The DLR KINEMEDIC prototype in a setup for navigated placement of pedicle screws

The KINEMEDIC arm is impedance controlled (see Chapter III.3). This allows for a new intuitive man-machine-interface as the joint units are equipped with torque sensors: the robot can be moved just by pulling/pushing its structure by the surgeon, who has full control of the robot at every step of the intervention. The hand-eye-coordination problems known from manual pedicle screw placement can be omitted. The drilling machine is connected by a passive slider to the robot and the surgeon feeds the driller manually, while the robot holds the instrument in the correct position. Sharing the tasks in this way still gives the surgeon the haptic sensation while drilling without overcharging him with the accurate positioning [Ortmaier *et al.* 2006a[c]]. This project has been funded by the *Bayerische Forschungsstiftung*.

Robot Assisted Navigated Biopsy

Based on the experiments on pedicle screw placement, a setup for navigated biopsy has been developed integrating a prototype of BrainLAB's VectorVision navigation system as shown in Fig. 404.

Fig. 404 The DLR KINEMEDIC in a setup for navigated biopsy in neurosurgery

In a pre-operative planning step, the tumour is localised in CT-scans of the human brain. During biopsy, the navigation system is used for referencing the posture of the patient's head and the tool centre point of the robot. Utilising a compliant control mode, the surgeon can move the robot by exerting forces on its structure whereas the robot limits the free motion towards the planned posture where the tool directly points to the tumour. If this posture is reached, the robot automatically switches to position control keeping this desired position and orientation. The tool fixed to the tip of the robot is a guide jacket bearing a biopsy needle which the surgeon feeds manually until a mechanical end stop is reached. This manual component of the procedure is demanded by the surgeons to keep haptic sensation [Konietschke *et al.* 2006b[c]].

Automated Endoscope Guidance

An automated endoscope guidance system for minimally invasive surgery has been developed. It assists the surgeon by automatically moving the endoscope mounted on a robotic arm such that the view of the camera remains centred to the field of surgery [Gröger *et al.* 2008[b]].

The system is based on real-time colour stereo segmentation. Colour markers which clearly differ from colours appearing in the human abdomen, are attached near the instrument tip. These markers are robustly tracked in 3D via a stereo endoscope. This 3-D position is used to servo the robot holding the endoscope (see Fig. 405).

Fig. 405 Automated endoscope guidance using instruments with colour markers

The core technology of the system had already been developed prior to this report period involving an AESOP surgical robot and was successfully tested on 30 patients in a Munich hospital (*Klinikum rechts der Isar*). As a result, the automated robotic endoscope guidance system was found to be working more reliably, enduringly, and accurately than any human assistant.

With the new design of a DLR medical robot system the focus of work in this report period has been on the transfer of the endoscope guidance system to the new DLR MIRO robot and the improvement of the performance and stability of the system.

4.1.7 Vision

Minimally invasive surgery involves an endoscopic camera system to provide the surgeon with a view of the operation site inside the closed body of the patient. Next to the importance of high quality visual feedback to the surgeon the camera image stream enables visual servoing techniques. These provide the robot system with information about the operation site, which can be used to derive semi-autonomous applications such as automated endoscope guidance or motion compensation of the beating heart.

Visual Feedback

Since direct access to the operation site is lost in minimally invasive surgery, visual feedback to the surgeon has to be provided by an endoscopic camera system. To achieve 3-D vision as in open surgery a stereo endoscope is used. The stereo image stream in the DLR MIROSURGE setup (see Sec. 4.1.5) is captured by a video server. The resulting stereo image stream can be distributed via Ethernet to a flexible number of clients. This client-server approach enables the easy integration of various 3-D output devices, e.g. standard 3-D displays with special glasses, ocular systems or autostereoscopic displays [Hagn *et al.* 2008[c]].

Stereoscopic 3-D Display Based on Polarisation

One of the stereo displays used is a stereoscopic LCD display (Miracube, Pavonine Inc., Korea). The 3-D impression is created by polarisation which is why the viewer needs to wear special glasses with circular polarisation filters. To integrate this display into the MIROSURGE scenario the images from the endoscope are scaled and converted to an interlaced stereo image which contains alternating lines of the left and the right images. The resulting image displayed by the LCD monitor is polarised by a filter. The viewer's special glasses are required to filter the polarised image content, thus separating the images for the left and right eyes.

Autostereoscopic Display (ASD)

The autostereoscopic display integrated in MIROSURGE provides spatial 3-D vision without the need for special glasses and enables free movement of the viewer by tracking the position of his eyes in real-time. The hardware principle of the autostereoscopic display manufactured by SeeFront GmbH, Hamburg, is based on a lenticular screen in front of an LCD display. Accurate eye-tracking algorithms are developed by us to estimate the position of the viewer in 3D in real-time (Sec. III.4.1.1).

Visual Force Feedback by Augmentation

Besides haptic feedback of the contact forces in the MIROSURGE master station (see Fig. 401) the orientation and the magnitude of the forces measured at the tool tip are visually represented in the endoscopic stereo images.

Fig. 406 Autostereoscopic display and augmented force arrow feedback

This is achieved by the augmentation of force vectors into synchronously grabbed stereo images. Combined with adequate stereo displays the viewer is able to seize a visual impression of the applied forces. In Fig. 406 the force arrow corresponding to the orientation and magnitude of the force at the right tool is displayed in the lower right region of the screen. [Ortmaier *et al.* 2007[b]]

Heart Motion Tracking and Compensation

Compensation of organ motion can help to facilitate surgical procedures or to enable the performance of complicated tasks using MIS techniques. To achieve the goal of motion compensation, motion is detected from endoscopic images, which can be used as a feedback to the robot system to compensate for this motion [Gröger *et al.* 2005b[c], 2008[c]; Ortmaier *et al.* 2005[j]]. Research in this project has been funded in part by the DFG (*Deutsche Forschungsgemeinschaft*).

Especially in the challenging case of beating heart surgery, motion compensation can help surgeons considerably. Besides minimal invasiveness, heart patients benefit greatly if the surgical procedure can be carried out on the beating heart, as this does not require arresting the heart and using a heart lung machine to circulate the blood.

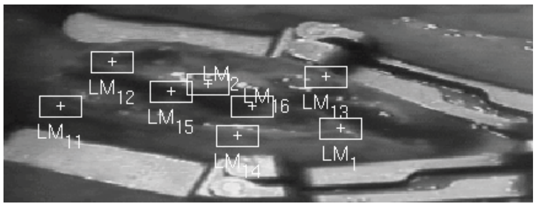

Fig. 407 Heart surface with landmarks for motion tracking and compensation

Concerning visual feedback to the operating surgeon, motion vectors gained from endoscopic images can be used for motion correction to provide stabilised images to the surgeon. Motion is detected by tracking natural landmarks on the surface of the beating heart. The strategy used is able to cope with disturbances by specular reflections [Gröger *et al.* 2005a[c]; Gröger *et al.* 2005b[c]]. Also, using a multi-sensory prediction scheme [Ortmaier *et al.* 2005[j]], the strategy can bridge short-time gaps in motion tracking e.g. due to occlusion caused by instruments. Based on this strategy special algorithms have been designed to stabilise images of the beating heart in real-time. The stabilisation strategies involve the concurrent tracking of several landmarks (see Fig. 407). Experiments on real video data of the beating heart acquired during heart surgery show that a significant reduction of image motion is possible [Gröger & Hirzinger 2006b[c], 2006a[c]].

As a result, the scene provided to the surgeon can be stabilised for major parts of the occurring motion of the beating heart in order to ease the task of robot assisted surgery on the beating heart.

4.1.8 Planning Procedure for the Telerobotic Surgery Setup

A preoperative planning (outside the OR) and computer-assisted setup procedure (inside the OR) as depicted in Fig. 408 was developed in the last four years at our institute and is presented in the following. After preoperative planning in virtual reality (VR), the setup is aligned with the situation in the OR just before the operation (intraoperatively). In case of short notice changes the surgeon can repeat the planning and after final verification the setup data S_{intra} is transferred to the control part.

The goal of the procedure is to achieve an optimised setup of robots relative to the patient in the OR. The developed procedure takes the robot kinematics into account and helps to decrease setup times in the OR as well as error sources during the intervention. For the latter, the robot positioning is optimised considering criteria to avoid collisions, singularities, and workspace boundaries throughout the operation. This research is part of the project AccuRobAs (6th EU Framework Programme for Research and Technological Development).

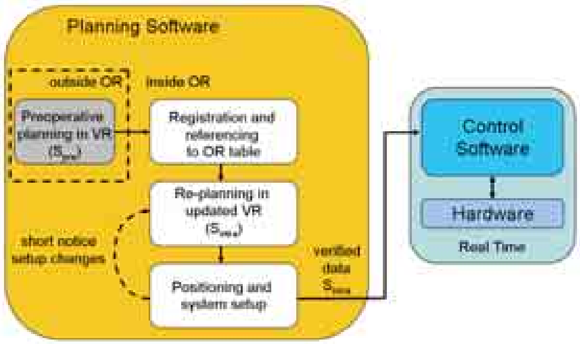

Fig. 408 Phases of the DLR planning procedure for MIRS

Preoperative Planning

Preoperatively, planning is done based on virtual reality and patient data such as segmented CT/MRI images [Konietschke 2008[t]]. The surgeon provides details about the operating field inside the patient and the area of possible entry points into the patient. An optimisation algorithm that uses a combined Genetic Algorithm and gradient-based method then yields several setups which sufficiently satisfy the optimisation criteria throughout the operating field.

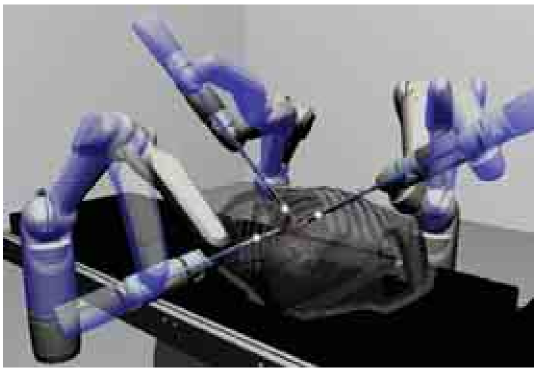

Fig. 409 Optimised setup: The transparent robots are shown in the approach pose from where the surgeon moves the robots through the trocar to the working pose (solid robots).

This preoperative phase of the planning procedure takes place before the intervention and outside the operating room and, therefore, is less time critical. An optimised setup is shown in Fig. 409: Robot base positions and entry points into the patient are suggested. In the next steps of the planning procedure, the data has to be adapted from the virtual world to the real situation in the OR.

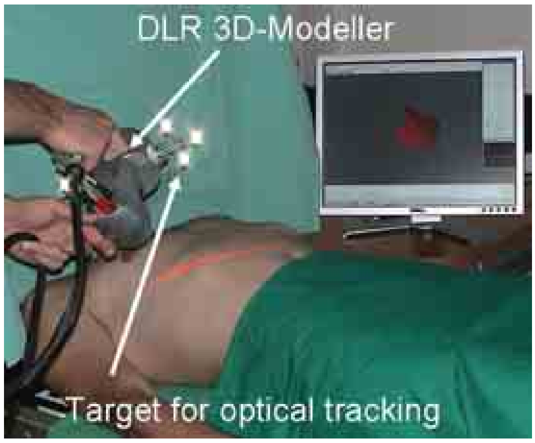

Fig. 410 Patient registration with the DLR 3D-Modeller

Transfer of Planning Results into the OR

Preoperative planning is usually based on MRI/CT images of the patient. Intraoperatively, deviations might therefore occur due to e.g. soft tissue displacement. These differences have to be taken into consideration. Eventually, the automatically optimised configuration of the robotic arms has to be verified by the surgeon and transferred into the OR. An assisting tool for the alignment of trocar positions and robot bases is inevitable to reduce setup time.

Patient registration is obtained through a surface scan of the upper body using the handheld 3D-Modeller (Sec. III.4.2) as shown in Fig. 410 and a robust feature-based algorithm according to [Rink 2006[r]] to match the patient surface with preoperative data. The position of the patient relative to the OR table is measured with the same optical tracking system as used for the 3D-Modeller [Konietschke *et al.* 2007a[c]]. Therefore, a tracking target is attached to the operating table. The medical robots are mounted to the operating table and can be positioned relative to the table. Since the patient will be in a slightly different pose relative to the OR table than preoperatively planned, the optimal OR setup has to be recalculated taking into consideration the registration and table referencing results. However, since good initial solutions are known from the preoperative planning, this step only takes about 20s and thus consumes only little of the valuable time in the OR.

Fig. 411 Display of trocar point with the DLR AutoPointer

Eventually, the robots have to be positioned and the trocars set. To show the calculated positions of trocars and robot bases to the surgeon, the AutoPointer [Konietschke *et al.* 2007c[c]] is used: this optically tracked hand-held device automatically projects the relevant data onto the patient respectively the OR table as shown in Fig. 411. In case the surgeon decides on short notice to arrange robots or trocars different from the planned configuration, the updated trocar positions or robot base poses are measured using an optically tracked probe and fed back to the planning software to calculate new valid data for e.g. q_{app} and ${}_{elbow}p$. This way, the complete setup data S_{intra} as realised in the OR is available for the control part described in Section 4.1.5.

The developed planning procedure includes the complete workflow from patient specific preoperative planning based on MRI/CT data to the current setup of the robots relative to the patient in the OR. The preoperative planning is the most time consuming part of the procedure. It takes about 15 min. Since it is done outside the OR, this is not time critical. Use of the software is easy and intuitive. The user just has to mark the operating field as well as an area for the entry points into the patient in the VR and then gets several proposals for the setup. Inside the OR, patient registration and re-planning take only few minutes. With the AutoPointer, the results of the planning procedure are projected directly onto the patient and the OR staff can set up the robots very conveniently. First tests with an experimental setup confirm the potential of the chosen approach. Registration is very robust and works also with incomplete patient scans. In the optimised setups chosen so far, the robots could operate without problems in the considered operating field.

4.2 The DLR Heart Assist Device

A new implantable left ventricular assist device (VAD) for regeneration and support of severe cardiac insufficiency belongs to the most outstanding mechatronic developments of the institute and has attained several international awards, latest the Klee Innovation Award in 2008 (see Fig. 412).

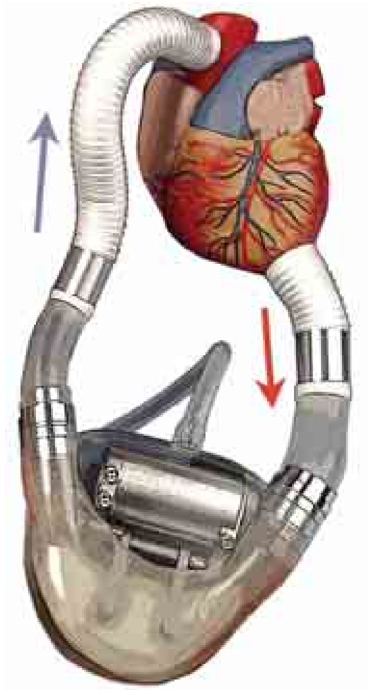

Fig. 412 The novel artificial heart distinguished with the Klee Innovation Award in 2008

The DLR Heart is designed to connect to the left heart chamber and the blood supply. It transports blood back to the aorta using high pressure coordinated with the beating heart.

The device works on a pumping principle of simultaneous suction and forward pumping two elastic chambers that lie on top of each other. This concept enables that blood is let in and pumped out at the same time as one chamber is compressed and the other is released simultaneously.

For actuation, a very thin pusher plate is integrated between the chambers as shown in Fig. 413. The two chambers lie very close together so that only when one is compressed the other one can fully expand. This allows for an extremely compact design.

Fig. 413 Pumping principle of the DLR Heart: two flexible chambers are alternately compressed by a thin pusher plate

4.2.1 A Novel Drive for Long-Term Support

An innovative drive unit has been developed for the DLR Assist Device with the focus on a maximised life-span of up to 10 years. The new design integrates an almost frictionless hydraulic pump as shown in Fig. 414. By means of a transmitter-fluid, the pump chambers are compressed without impact on mechanical parts. The compact design allows implantation even in small adults and children. The developed pump is primarily targeted at bi-ventricular assistance applications.

The optimisation of the pump chamber geometry is one of the main issues in the design process of a new VAD-system. By avoidance of turbulent flow and non-flow phenomena, energy loss and the risk of thrombembolism can be significantly reduced. One key issue was the identification and elimination of areas with reverse flow and high shear stress [Schiller *et al.* 2006[j]]. Extensive fluid mechanics simulations helped to find an excellent first approach for the shape of pump chamber and tubes (see Fig. 415) [Schmid *et al.* 2006[j]].

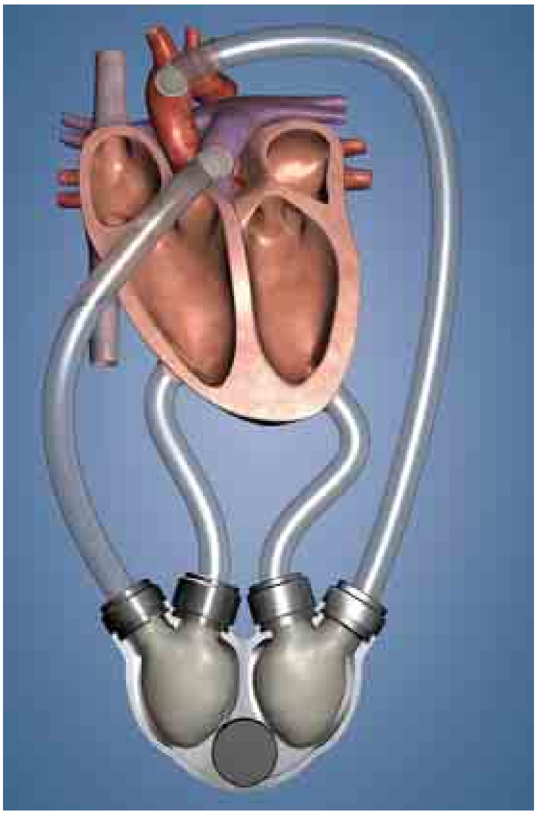

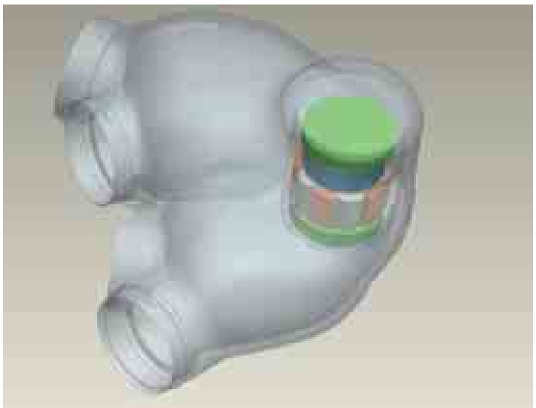

Fig. 414 The DLR Bi-Ventricular Assist Device with a novel, hydraulic drive unit for long term support as an alternative to heart transplantation

In subsequent experimental studies, flow visualisation with a birefringent fluid compared with velocity measurements (Particle Image Velocimetry, PIV) [Schmid *et al.* 2005[j]]. This comparison led to further improvements of the pump chamber's geometry and the kinematics of the pump membrane. The VAD has been tested in circulatory mock loops as well as in vivo (pigs). Long term animal studies (calves) are performed since 2008. With a modification of in- and outflow-adapters, the system will assist both ventricles (bi-ventricular assist device). Besides a version for adults, a smaller version for children has been developed. To reduce the risk of thrombus formation, the biocompatibility of different poly(ether)urethane (PUR) as a base material for the pump chambers of the DLR-VAD was evaluated together with the Clinic for Heart Surgery, University of Regensburg.

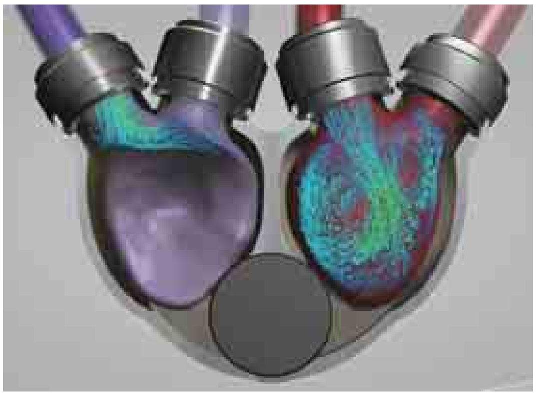

Fig. 415 A new design of pump chamber enables flow-structure similar to the native heart; shear stress and recirculation are reduced to a minimum

Inside the pump chambers, human saphenous vein endothelial cells (HSVEC) and a mouse fibroblast cell line (L929) were cultivated with different PUR specimens. The cell layer should work as biocompatible contacting surface to the blood.

Fig. 416 The DLR wireless energy and data transmission system (TET)

For the artificial heart a wireless, inductively working energy and data transmission system has been developed (Fig. 416), which (slightly modified) may be used for many other implants [Vodermayer *et al.* 2005[j]]. In contrast to known energy systems, the DLR-TET (Transcutaneous Energy Transfer) works with two coreless coils, thus being light and the surrounding tissue is well supplied with blood. In addition the system permanently adapts itself to the implant's energy demand, to minimise electromagnetic stress and increase the long term durability of the electronic components.

5 Autostereoscopic Displays

The 3-D visualisation of 3-D content gains increasing importance not only in the domain of the entertainment industry but also for professional use. With respect to conventional 2-D display technologies, 3-D visualisation offers more information allowing, e.g., surgeons, design engineers, and teleoperators to interface more efficiently with computers in general and robots in particular.

Autostereoscopy plays a special role among the techniques used for 3-D visualisation since it removes the need for head-mounted devices, e.g., glasses. Autostereoscopic displays achieve the desired effect by separating a spatially-interlaced stereo image through an optic material (the lenticular lens; see Fig. 417). Accordingly, the eyes of a person see distinct images, i.e., views on a scene, provided the person is located at a suitable position with respect to the display.

In order to allow the person to freely choose a comfortable position, an accurate eye-tracker and an accurate and appropriate registration procedure have been developed at the institute. The tracker consists of two cameras and one infrared light-source integrated in a single housing. The eyes of the operator are tracked in real-time and in 3-D using the approaches described in Sec. III.4.1.1. These 3-D positions are transformed into coordinates relative to the display through a prior, accurate registration of both coordinate systems. Finally, the accordingly transformed 3-D positions are used to dynamically control the focus of the display with respect to the position of the viewer.

We cooperate in this field with the companies SeeFront GmbH, Hamburg, and Spatial View GmbH, Dresden within the projects MIROSURGE and EU-project SKILLS. The eye-tracker is also part of the HGF-founded project Fahrerassistenzsysteme within the DLR programmatic pillar transportation.

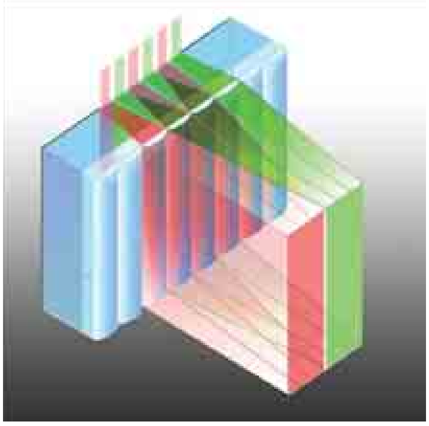

Fig. 417 Schematic drawing of the separation of interlaced stereo-images with a lenticular lens (left to right) into two spatially distinct images (red and green) (Courtesy SeeFront GmbH)

Fig. 418 Autostereoscopic display equipped with the DLR eye-tracker

6 From ASURO to ASUROnaut

The ASURO (Another Small and Unique Robot from Oberpfaffenhofen) is a mechatronic/robot development kit that was developed in 2003 for use as robotics experiment at the DLR School_Lab in Oberpfaffenhofen. It consists of about 130 standard electronic and mechanic components, including an 8-bit processor, two motors, gears and wheels, different sensor systems (collision detection, line following unit, odometric sensors) and an infrared transceiver unit for wireless communication with a standard PC. The kit is kept very simple, so that the part costs stay low and so that it can easily be assembled with standard electronic tools by students of ages of 16 up.

The completely assembled robot includes a pre-programmed self test that helps verifying all of the features and simplifies debugging in case one or more components were placed incorrectly. Freeware C-compiler and editor allow programming of the robot and a special flash tool is used to transfer the compiled code to the robot's processor. Although C is not the best programming language for beginners, it was chosen because a C-compiler exists for almost every processor and microcontroller. To ease the use of the language for beginners, all of the robot's functionality can be accessed via predefined functions. Because of this, ASURO can be regarded as a tutorial for real world robotics.

Fig. 419 ASURO kit and students during assembly

Encouraged by the great acceptance of the kit by the School_Lab customers, the search for a licensee started and resulted in an ASURO license to AREXX Engineering, a small company in the Netherlands that manufactures and sells educational electronic toys worldwide and also to German resellers such as Conrad, Farnell and Reichelt. Since the beginning of the sales in 2004, more than 25,000 kits have been sold. Multiple homepages, forums and videos on the internet show the high acceptance of the robot in the community.

Based on the ASURO concept the institute has now created another School_Lab experiment which addresses younger students and demonstrates the possibilities of telepresence. In this experiment two mobile robots called ASUROnaut are used. These robots are the upgraded version of the ASURO featuring a pan-tilt unit with synchronised stereo video camera, an RF link for real-time video stream and control commands, a 2-axis accelerometer, photo interrupters for collision detection and a small gripper. The achievable low control latency of less than 100ms is ideally suited for telepresence. The robot, as well as the control station, has been designed as simple and cheap as possible resulting in a complex telepresence experiment at moderate cost.

Fig. 420 Assembled ASURO

The robot is able to drive through an artificial landscape that was especially designed for the experiment. Computer controlled lighting in the room generates a realistic "deep-space" mood. The ASUROnaut can be controlled from the room next door (without the option of looking directly) generating the impression of a long distance between the operator and the robot. An operator steers the robot with a commercial force feedback joystick and the accelerations measured by the robot due to vibrations, collisions and tilting are used to generate a haptic feedback.

The stereo video from the robot's camera can be watched by the operator through a head-mounted display. A tracker senses the orientation of the operator's head and makes the ASUROnaut camera head look in the same direction as the operator.

During the experiment, it is the operator's job to rescue a few "probes" from a "planet's surface". The images of two additionally placed cameras and telemetric data from the robot are displayed on separate screens so that the other students in the team can supervise the success of the "mission". An additional delay can be added in the data link to show the effects of latency on the controllability of a telepresence system.

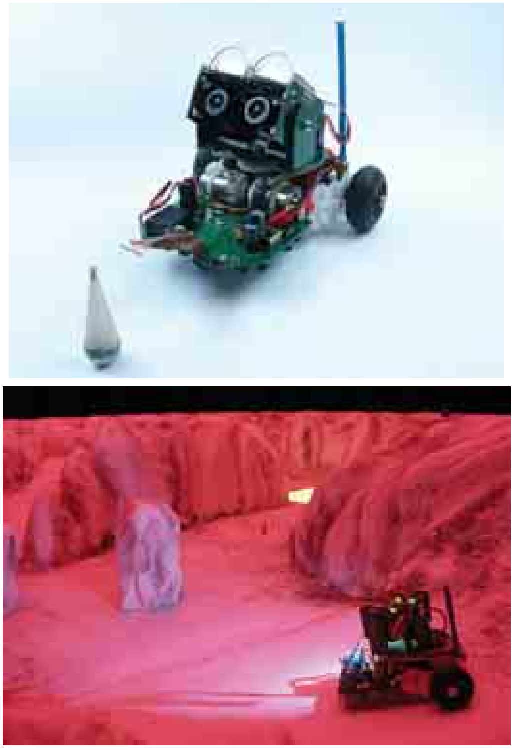

Fig. 421 ASUROnaut

The experiment will start in December 2008 but first tests proved that even ten-year olds are able to successfully operate the robot.

7 SpinOffs

7.1 DUALIS

On basis of the successful development of innovative robot systems, the institute transfers its experience into medical technologies. As well as in space flight, medical products are requiring high standards concerning quality, reliability and long term durability.

With the foundation of the DUALIS MedTech GmbH, a platform is prepared to transfer the developed technology into commercial application. DUALIS combines the innovative know how and is acting as a development, research and sales company. The vision of DUALIS is the development of innovative medical products, particularly active implants. DUALIS developed a network of cooperating companies and institutes in the medical field (Lt. GORE, Edwards Inc., em-tec GmbH, Osypka GmbH). In cooperation with the University of Freiburg, DUALIS is developing the telemetry and wireless energy system for a completely implantable sphincter system.

Fig. 422 The DUALIS Minipump with a novel hydraulic drive unit

The new technology of the DLR Heart Assist Device offers a real alternative for heart transplant patients, suffering on severe heart insufficiency. The drive unit of the device is based on the long term experience and development of light-weight robots. The novel pumping technique reduces the power consumption of the device to a minimum, flow optimised pump chambers are minimising the risk of thrombembolism. The DUALIS wireless energy and data transfer system enables an early mobilisation of patients and prevents the risk of inflammation. All the DUALIS technologies have been tested in laboratory as well as in animal studies.

7.2 RoboDrive

ROBODRIVE

Founded in 2005, RoboDrive is a young and innovative spinoff company of the Institute located in Seefeld next to DLR.

RoboDrive develops and produces electric servo motors for highly demanding applications, such as medical devices, aerospace equipment and robotics. The product line offers motor kits from the sizes 115mm down to 25mm diameter. The unique features of these brushless servo motors are highest torque and power-density for a given volume and weight. All motors are available with a hollow shaft for conducting media or power-lines or to integrate mechanical parts, e.g. spindle-drives to achieve linear motion.

The smallest motor offers a nominal speed of 22,000rpm at 24V DC-link-voltage with 24mNm of torque. Thus it can provide up to 60 Watts of mechanical power at the shaft with only 15g of weight in its active components. The largest product weighing 2.5kg is able to exert a peak-torque of 40Nm with extreme linearity. The torque-ripple is reduced to only 30mNm amplitude. RoboDrive assists its customers in all questions of drive-technology and state-of-the-art servo-drive-controllers.

The ultra-compact drive-units directly contribute to the precision and dynamics shown with DLR's light-weight robots, the robotic hands or the medical robot systems MIRO and KINEMEDIC.

7.3 STA

Reacting to the need for high-performance computing solutions for applications, STA Chipdesign Ltd. was cofounded in 2008 by members of the Institute with the goal of designing and producing high-performance processors based on the *Synchronous Transfer Architecture*®.

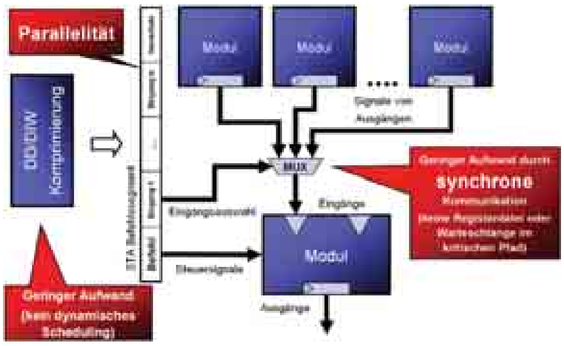

Fig. 423 Architecture of the STA chip

The cooperation between STA and DLR was cemented in the Bavarian Project "STAR", funded by the *Bayerischen Forschungsstiftung*, running from April 2008 until March 2010. In this project, STA and DLR cooperate on the design and application of an FPGA-implemented version of the STA-Chip, applied to various problems such as 3-D reconstruction and eye tracking for the autostereoscopic display.

The first design of the chip has demonstrated, in simulation, its ability to solve the computational requirements for DLR's 3-D reconstruction algorithm SGM in real-time, thus marking a new era in the applicability of these algorithms.

VIII Research Network

1 Projects

HGF Projects

ARGOS

Event and disaster management applying airborne sensor systems is main goal of DLR-internal project ARGOS. RM provides services and engineering support for the compact airborne multi-sensor system ANTAR, which is able to derive traffic parameters in real time.

Fahrerassistenzsysteme

This project aims to the development and evaluation of several assistance functions for vehicles in order to improve safety and comfort aspects. DLR-RM is involved in different sub-projects, e.g. sensor networks, SimWorld and dynamic chassis, and designs and deploys systems for sensing (e.g. cameras) and acting (e.g. control loops). This project is led and coordinated by DLR-TS.

iGreen

The iGreen (integrated Green Aircraft) focuses on detailed investigations of global aeroelastic mechanisms for the reduction of drag and weight as an enabling technology contribution to the design of future ultra-green transport aircraft configurations. The institute's participation involves the design of load alleviation control laws. Participating DLR institutes are AE (project lead), AS, AT, RM, FLT, and SHT.

Next Generation Train

All DLR research activities that concern railway vehicles are integrated to the project Next Generation Train, in which 8 DLR-institutes contribute their railway relevant know-how in running and structural dynamics, aerodynamics, material design, lightweight construction, energy-efficiency and mechatronics. The high-level goals of this project are the reduction of energy consumption, CO_2 emission, noise and wear, increasing the use of alternative fuels and improving safety, comfort and economic efficiency. In detail, the department SR participates in the NGT work-packages "Energy Management" and "Noise and Comfort", organises the work-package "Running-Safety and Wear" and essentially contributes to the specification of vehicle concept.

On-Orbit-Verification

German Aerospace Agency started this project to enable low-budget technology developments for space applications. RM-OS is responsible for know-how transfer relying in BIRD satellite and involved in the deployment of small satellite components (structure, attitude control).

Planetary Evolution and Life

Under lead management of our planetary scientists in Berlin (DLR-PF), DLR has been awarded the establishment of a HGF-Alliance within a timeframe of five years starting in 2008, with the major goal to study the interactions between life and the evolution of planets. The vision goes beyond the solar system by including the challenges that life would face in other solar systems. The institute participates with its robotics expertise in order to investigate the efficient use of different kind of robotic tools to support the scientific community for exploration and habitability purposes. The major topics concern the study of mobility on various celestial bodies of interest, on manipulability and skills, perception and autonomy. The work is being performed by two Ph.D. students.

RaiCe

Airport management implies safety and security tasks. Cameras play an important role for surveillance. Within this project different sensor systems will be applied for monitoring airport ramps and detecting relevant objects. DLR-FL is responsible for the project.

RCAS

Railway collision avoidance system (RCAS) is a system for an infrastructure independent approach for train-to-train-communication. Our institute provides camera systems and image processing algorithms for high precision navigation and obstacle detection. Partners are DLR-KN and DLR-TS.

TIVA and TIVA-II

Objective of the TIVA (Technology Integration for the Virtual Aircraft) and follow-on TIVA-II project is to strengthen DLR's capability in multidisciplinary design and assessment of new aircraft configurations. The institute's main contributions are the integration of flight dynamics models for various types of analysis (including mission simulation), generated using the Modelica Flight Dynamics Library. Participating institutes are AE, AS (project leader), AT, BK, FA, FT, RM, FW, and SC.

UCAV-2010

Objective of the DLR internal project UCAV-2010 (Unmanned Combat Aerial Vehicle) is the development of technologies for design and assessment of unmanned combat aircraft. The project extensively uses the framework tool developed in the TIVA projects. The institute integrates data from the various disciplines into several types of UCAV flight dynamics models and develops high performance flight control laws. The following institutes are involved: AS (project leader), AE, AT, FT, HR, SC, RM, and MF.

Virtuelles Institut

The project aiming at close cooperation between DLR and the universities of Munich and Stuttgart was funded by the HGF between 2005 and 2007. It was focused on automation of photorealistic 3-D modelling. The DLR developed methods for automatic registration of multiple scans and colour images and for the generation of photorealistic 3-D models. Furthermore, the combination of data from different sensors (small scale, terrestrial scale and aerial images) has been researched. The consortium in cooperation with aerospace industry developed the autonomous airship as multi-sensory flying platform (see Sec. III.6.2).

WALES

DLR-PA proposed and designed an airborne LIDAR system for water vapour measurements. DLR-RM developed an end-to-end simulator, mechanical constructions and high precise wavelength stabilisation.

Wetter & Fliegen

The DLR project Wetter & Fliegen includes partners from several DLR institutes (Physik der Atmosphäre, Flugsystemtechnik, Flugführung, Lufttransportkonzepte und Technologiebewertung) and is mainly concerned with the influence of weather phenomena on aircraft and air traffic. The Institute's participation involves wake vortex scenario analysis as well as design of flight control laws for improved flight in disturbed atmosphere (turbulences, wake vortices).

National Projects

Active Light-weight Chassis

In July 2008 a project "Active Light-weight Chassis" (ALF) started with support by the Federal Ministry of Education and Research (BMBF) aiming at the development of a novel light-weight chassis for road vehicles based on fibre composite materials and mechatronic systems. Our Institute is contributing to work packages on modelling techniques and vehicle dynamics control.

Compensation of Heart Motion

This project is funded by the DFG and started in 2008. The central goal of the project is the compensation of beating heart motion by image stabilisation and robot guidance in telerobotic heart surgery.

CoTeSys

In 2005, the DFG started an initiative to honour excellent research in Germany by funding a limited number of "Clusters of Excellence". From October 2006, 37 Clusters of Excellence were funded; among the first was *CoTeSys*, an Initiative between the DLR, LMU, MPG, TUM, and UniBW. DLR's participation was key in the funding of CoTeSys. Within this initiative, DLR was awarded a junior research group as well as three other cooperative research projects between 2006 and 2008. DLR hardware forms the basis of a central CoTeSys demonstrator.

DEOS

is funded by the German Space Agency. In the phase A study the institute contributes with image processing, motion estimation, telepresence operation, path planning as well as the development of a manipulator, based on the ROKVISS joints. Main contractor for the study is the SpaceTech GmbH.

DFG Laserscanner

In this project methods for non-invasive head registration for cranio-facial surgery using optical sensors have been developed by the DLR and the University of Heidelberg. The project was funded by the DFG between 2006 and 2008.

ELBASYS

This research project was part of the German aerospace research agenda LUFO IV. Herein, the Institute collaborated with Airbus Deutschland GmbH in order to optimise conventional und unconventional environmental control systems (ECS) for use in commercial aircraft built of composite materials. Among the key drivers are changes in aircraft system architecture and material constraints.

EOSYS

The LuFo III project EOSYS (2003-2006) had as subject the optimisation of aircraft systems with respect to energy consumption. The institute's contribution was the development of a mechatronic design process for electrically actuated landing gear systems. Partners were Liebherr-Aerospace, EADS, ESW Wedel, AOA Gauting, LEG, TU Dresden, TU München.

ForBAU - Virtual Building Site

The development of a digital construction site model is the central idea of the research association which includes institutes of TUM, University of Regensburg, DLR and numerous companies. The goal is a universal planning and progress-monitoring instrument, which can be used in every stage of a big construction project (e.g. bridges, new highways, etc.). DLR is supposed to provide technologies for 3-D terrain modelling via new stereo line camera developments, as well as "flying robot" technologies for the permanent update of the construction.

FOSFOR

In this project fibre bragg grating sensors are evaluated regarding the applicability in force-torque-sensors for minimally invasive robotic surgery instruments. The project funded by the DFG started in 2008 and will be completed in 2010.

GASS

The "German Artificial Sphincter System–GASS" is an implantable sphincter muscle prosthesis for the treatment of patients suffering fecal and urinary incontinence, developed at the University of Freiburg in cooperation with IMTEC and DLR. Goal of the DLR working group is the development, integration and evaluation of the control, data- and energy transmission for GASS.

IHK-HICON

The LuFo III project IHK-HICON (2003-2007) had as subject the investigation of innovative high lift devices. The institute's contribution was the development of a design and assessment tool for evaluation of innovative high lift components regarding noise, handling and aircraft separation during take-off and landing. Partners were Airbus-D, TU Hamburg Harburg, DLR-FT.

KATO

This research project has taken place in 2003-2007 and is part of the German aerospace research programme LUFO III. DLR-RM has participated in KATO TP07 in order to improve the control system of civil aircraft air conditioning systems for improved comfort.

Lynkeus

The Lynkeus project is funded by the BMBF and focuses on advanced environment analysis by using real time 3-D cameras. It started in 2006 and will end in 2009. The DLR participates as a subcontractor of KUKA, focusing on bin-picking of complex parts, real time environment modelling, and sensor-base collision free planning

MiB (Assembly in motion)

Technology transfer within the project MiB (assembly in motion, see Chapter VII.2) has been funded from 2005 to 2007 by the Bayerische Forschungsstiftung. The consortium consisted of 7 partners who are still in contact to improve and promote sensor driven assembly in industrial applications. DLR and TUM act as a research institute and a university while the other partners are companies, leaders of their respective sectors as BMW and KUKA, and smaller companies as Schunk, QUISS, and Sturm.

Ministry of Defence

Ordered by the Bundeswehr, 8 areas have been captured between 2006 and 2007 with an UltraCam camera. Orthographic images and high resolution elevation models have been processed from the data. The creation of interactive 2.5-D models, based on the DLR models, has been supported by the RSS GmbH in cooperation with the University Bonn.

MIROSURGE

This project has been funded by the Bayerische Forschungsstiftung. The central research subject is the development of a universal robotic system for endoscopic telesurgery. It comprises research in the fields of robot and instrument design, control, telerobotics and vision. The project started in 2006 and will be completed in 2009.

MODYAS

The LuFo IV project MODYAS (2004-2006) had as subject the Multi-Objective Dynamic Aircraft Synthesis. Our main contributions were the design of multi-disciplinary loads control functions; investigations on interaction of structural and control design optimisation; flexible A/C modelling for control law design. Partners were Airbus-D, DLR-AE, DLR-FT, TU Hamburg Harburg, RTW Aachen, Uni Stuttgart, Uni Rostock, TU Braunschweig, ZFB, NLR, HSVA.

OLEV

This project aims for the extension of the operational phases of telecommunication satellites. Within the project (Phase A and B) the institute was responsible for the development of a space qualified version of the capture tool, development of docking strategies by means of manual guidance or visual servoing as well as the simulation of the entire docking process. For this project the institute was subcontracted by Kayser-Threde.

SFB453

The cooperative research centre on "High-Fidelity Telepresence and Teleaction" (SFB453), including DLR and Munich universities, started 1999 and has been prolonged until 2010 (4^{th} period). Within the project basic research on multimodal man machine interaction, bilateral control and human factors for telepresence is performed and applications in the fields of multi agent, space and medical telerobotic systems are developed.

TECSAS

Technology Satellite for Demonstration and Verification of Space Systems was funded by the German Space Agency. The institute contributed with manipulator development, image processing and teleoperation concepts.

TET

Small satellite TET is the core element of DLR's On-Orbit Verification Program (OOV), which aims at testing new space technologies in a space environment. The project is mainly funded by the German Space Agency. The Institute develops core elements of the satellite bus and payload.

Virtueller Wald

The project is a subcontract by the group of Prof. Rossmann, RWTH Aachen. The project goal was the automatic detection and classification of trees from aerial images and elevation models. The DLR captured aerial images of 900 km^2 of forest using the HRSC camera and computed a high resolution orthographic image and the elevation model.

International Projects

ACFA 2020

The European project ACFA 2020 (Active Control for Flexible 2020 Aircraft) has two main objectives: pre-design of a marketable European ultra efficient 450 passenger Blended Wing Body (BWB) type aircraft, and providing solutions for the active control system of BWB type aircrafts. The team consists of 13 partners and is lead by EADS-IW. Within the project the institute is leading the work package "Integrated control design" and is involved in the design of flight control systems.

AccuRobAs

This Specific Targeted Research or Innovation Project (STREP) is part of the 6th EU Framework Programme for Research and Technological Development (FP6). AccuRobAs officially started in October 2006 and ends in October 2009. DLR is involved in this international cooperation with research topics on surgical robotics. The main goals are: Increasing the accuracy of compliant light-weight robots through multi-sensory concepts and robot assisted laser osteotomy.

AWIATOR

The EU funded project AWIATOR (2002-2007) with 23 partner organisations from all over Europe and led by Airbus-Deutschland aimed at the integration of new technologies in the fields of noise regulation, limitation of gaseous emissions, increase of aircraft frequency and demand on passenger comfort. In cooperation with Airbus, ONERA, Israel Aircraft Industries and the DLR Institute of Flight Systems, our institute developed new control strategies for gust load alleviation.

COFCLUO

In the FP6 European project COFCLUO (Clearance Of Flight Control Laws Using Optimisation, 2007–2010), a consortium of several research teams under the leadership of University of Linköping and with Airbus France as industrial partner, investigates the potentials of the optimisation based clearance approach in the enhancement of present day certification process for civil aircraft. Our contributions are covering aspects like uncertainty modelling for robustness analysis, development of a clearance criteria library, or optimisation-based worst-case determination using parallel optimisation techniques.

CREDOS

The objective of the European research project is a safe reduction of WV separation in crosswind dominated weather scenarios for take-off and departure under the coordination of Eurocontrol. DLR-RM contributes with the development of sophisticated analysis software for simulation of departure scenarios under realistic weather conditions in close cooperation with other DLR-institutes (FL, FT, PA).

DEXMART

DEXMART (2008-2012) is a large-scale integrating project which is funded under the European Community's 7th Framework Programme. DEXMART has the ambition to fill the gap between the use of robots in industrial environments and the use of future robots in everyday human and unstructured environments, contributing to reinforce European competitiveness in all those domains of personal and service robotics where dexterous and autonomous dual-hand manipulation capabilities are required. The main goal of DLR is the integration of dual-hand manipulation control with more abstract planning levels.

Enactive

In the European Network of Excellence on Enactive Interfaces (2004-2007), researchers from nearly 30 European and Canadian research facilities developed the concept of enactive systems as a new way to interact between human and computer. As a prolonging result the Enactive Conference series has been established attracting researchers from all over the world. In the newly founded *European Institute of Enactive Systems* the future efforts will be coordinated.

EURON

The European Robotics Research Network was established in 1999 as way of uniting robot researchers throughout Europe. It was set up under the Future and Emerging Technologies Framework Programme 5 and continues under Framework Programme 6. The aim was to implement a network of excellence which encouraged the coordination of research, teaching and education, in the area of robotics. In addition, the Network seeks to strengthen academic and industrial collaboration. The institute has played a prominent role in EURON since the beginning, and has received various awards (Girault Ph.D. Award; Technology Transfer Award) therefrom.

EUROP

The European Robotics Technology Platform (EUROP) was officially launched in 2006. The DLR Institute of Robotics and Mechatronics is founding member of this initiative to maintain Europe's leadership in robotics and to supply networks to meet the new technological needs. The mission of EUROP is the concerted strategic planning, the coordination and the facilitation of pre-competitive robotics industrial and research activities in Europe, encompassing education, basic research, applied research and development. To this end, EUROP will discuss industrial, scientific, technical, political, social and economic objectives.

EUROSYSLIB

This is an ITEA2 project with 18 partners to develop 30 free and commercial Modelica libraries in the mechanical, electrical, fluid, control, safety and automotive area and to improve the Modelica infrastructure. DLR-RM has organised this project together with Dassault Systèmes and is leader for the technical part of the project. Duration is Oct. 2007 – March 2010.

GARTEUR AG16

This action group on *Fault Tolerant Control* (FTC) investigated in the period 2003-2007 how new FTC technologies can be used to improve on and supplement existing reconfiguration schemes of the aircraft control laws. An important activity in this group (also the main focus of DLR) was the study of the applicability of fault diagnosis methods as basis of control reconfiguration techniques. The results of AG16 for a benchmark application have been demonstrated within pilot simulation studies on a high performance flight simulator.

GARTEUR AG 17

The institute has been partner of the Flight Mechanics Action Group FM AG17 "Nonlinear Analysis and Synthesis Techniques in Aircraft Control" (2004-2007): This action group investigated how the flight control law design process can be improved by application of nonlinear analysis and synthesis techniques. Main partners were Airbus, ONERA, NLR, LAAS, EADS-MAS, FOI, SAAB, University of Bristol, University of Leicester, University of Liverpool, The Montfort University.

HYCON

Hybrid Control: Taming Heterogeneity and Complexity of Networked Embedded Systems (HYCON) is a Network of Excellence of 23 universities and research institutes, with an international scientific council and industrial advisory board (2004-2008).

IMMUNE

IMMUNE (Intelligent Monitoring and Managing of UNexpected Events) is an ONERA-DLR common research project, with the objective to demonstrate the capabilities of intelligent monitoring and managing of unexpected events during flight with the aim to improve aircraft safety and autonomy. The main research problems to be solved concern control laws with event driven reconfiguration capabilities and advanced fault diagnosis systems. The project started in June 2006 and will terminate in December 2009.

JTI Clean Sky – SFWA and SGO ITDs

The JTI (Joint Technology Initiative) Clean Sky is the framework of the Integrated Technology Demonstrator project called SFWA (Smart Fixed Wing Aircraft) with a large number of partners all over Europe. The purpose of the Smart Fixed Wing Aircraft flying demonstrator is to develop and validate innovative technologies, concepts and capabilities in the critical areas of fuel consumption and noise emissions. The institute is a core partner in the areas of fault tolerant active loads control and flexible aircraft modelling.

The Systems for Green Operations (SGO) Integrated Technology Demonstrator will create value for improved aircraft operation through the management of aircraft energy and the management of mission and trajectory. The institute is leader of the methods and tools work package for management of energy, participates in trajectory optimisation activities, and is responsible for a Modelica based design environment for smart ground operations using wheel integrated electrical motors.

Kompsat-3

This satellite, funded by the Korean Space Agency, will carry a high-resolution optical payload which is developed by EADS, Astrium, and RM-OS.

MERTIS

MERTIS is an imaging spectrometer working in the infrared part of the electromagnetic spectrum. This payload as developed by RM-OS is part of ESA's Bepi Colombo mission which will be launched in 2014 to planet

Mercury. Prof. Jessberger (University Münster) is principal investigator (PI), DLR's institute of planetary research is our scientific partner.

MODELISAR

This is an ITEA2 project with 28 partners. The goal is to provide an open end-to end solution for automotive systems modelling, embedded software generation and integrated simulation based design and testing, based on Modelica, AUTOSAR (the coming standard for embedded software in the automotive industry) and the product life cycle management of CATIA V6. The project leader is Dassault Systèmes. Duration is July 2008 – June 2011.

MOET

The 6th Framework European integrated project "More Open Electrical Technologies" (MOET) with more than 60 partners lead by Airbus France deals with design, analysis and optimisation of the electric power generation and distribution system of future aircraft. Our institute is work package leader for "Methods, Tools and Simulation" within the MOET project. The main cooperation partner in this work package is Airbus France. In particular the institute is responsible for development of the electrical aircraft architecture analysis, simulation and optimisation tool. In addition we contribute to fault detection and mitigation studies and methods and tools for electrical power quality and network stability coordinated by Airbus France.

NEUROBOTICS

The European Integrated Project NEUROBOTICS, focusing on robot control through neural interfaces, was funded by the EC between 2004 and 2008. Being the second largest partner, DLR led one of the three central scenarios, focusing on prostheses and neural interfaces. The review meetings confirmed the scientifically leading role of DLR in the project.

NEUROBOTICS research contacts have led to two subsequent EC projects (SENSOPAC [2006-2010] and STIFF [2009-2011]) and various international cooperations. It was a major source of finance for the DLR Integrated Hand-Arm system.

PHRIDOM

The EURON-2 Perspective Research Project "Physical Human-Robot Interaction in Anthropic Domains" (PRHIDOM; 2006) was about charting the new "territory" of physical Human-Robot Interaction (pHRI). Human-machine interaction and safety-dependability issues in mechatronic systems were addressed. This project was the predecessor of the PHRIENDS project.

PHRIENDS

This FP6-Strep started in 2006 and will end in 2009. It is about developing key components of the next generation of robots designed to share the environment and to physically interact with people. The internationally awarded results of DLR in designing control strategies for collision detection and reaction and for biomechanical evaluation of potential human injury during interaction with robots is a key feature for the commercialisation of the light-weight robot and attracted wide medial interest.

POA

The European integrated project POA (Power Optimised Aircraft) running from 2002 to 2006 was aiming at identification, optimisation and validation of innovative "more electric" aircraft equipment in order to reduce the consumption of non-propulsive power. Within POA the institute was responsible for the development of the central "Virtual Iron Bird" aircraft systems simulation environment, which was used for the assessment of new aircraft systems architectures

SENSOPAC

The European Integrated Project SENSOPAC started in 2006, with DLR as the second largest partner. Receiving non-sufficient reviews after year 1, DLR took the leading role over, became the largest partner by increasing its budget by over 50%, and saved the project from being discontinued. Since then, it is a landmark in EC funding, integrating neuroscience, neural network, and robotics research in Europe. It is a major source of finance for the DLR Integrated Hand-Arm system.

SKILLS - Multimodal Interfaces for Capturing and Transferring of Skill

The goal of the project is to capture human skills focused on manual abilities by technical means, store them in a database and transfer them to a novice in that field. Besides the fundamental research on detection, representation, capturing and rendering of skills seven demonstration activities ranging from sports and entertainment over surgical and rehabilitation to industrial applications.

SMErobot

The European Robot Initiative for Strengthening the Competitiveness of SMEs (Small Medium Enterprises) in Manufacturing is an Integrated Project within the 6th Framework Programme to create a new family of SME-suitable robots and to exploit its potentials for competitive SME manufacturing. For the first time, the five major European robot manufacturers have joined forces in SMErobot™, in close cooperation with key component manufacturers, leading research institutes, universities and consultants for multidisciplinary R&D, dissemination and training efforts.

STIFF, VIACTORS

Following the development work of NEUROBOTICS and SENSOPAC, SME-ROBOT, PHRIDOM and PHRIENDS, and the integrated hand-arm system that is partly funded by those projects, two new EC projects were initiated. Starting in 2009, the DLR-led projects will focus on variable impedance control of human and robotic arms (STIFF) and robotic hands, arms, legs (VIACTORS).

VIVACE

The 6th Framework European integrated project "Value improvement through a virtual aeronautical collaborative enterprise" (VIVACE) aimed to define the future European Aeronautical Collaborative Design Environment. Our institute participated in the task "electrical system application" by improving the simulation process and tools currently used for design and validation of the Aircraft Electrical System. Partners were Airbus France and Thales AES.

2 Scientific Cooperations

Germany

DFKI Deutsches Forschungszentrum für Künstliche Intelligenz

A cooperation is planned with the Robotic research group (Prof. F. Kirchner) of the DFKI Bremen.

Fraunhofer IBMT

From NEUROBOTICS, IBMT (Prof. Klaus-Peter Hoffmann) and DLR (Bionics) initiated a cooperation in 2007 on the development and application of implantable electrodes.

Fraunhofer IGD

The cooperation with the IGD yields to combine the complementary competences in visual and haptic rendering for virtual reality simulations. Both institutions are also involved in the SKILLS project.

Fraunhofer IOF

The cooperation aims at the development of optical elements and systems for space applications. Project MERTIS was starting point for common activities.

Fraunhofer PYCO

PYCO (Prof. Bauer) and DLR investigate the usability of polymer materials for optical elements and surfaces structure for spaceborne systems.

Humboldt University Berlin

Several projects were completed between DLR and Humboldt University (Prof. Reulke) in the last years. The work was focused on image processing and camera calibration.

Klinikum Rechts der Isar (RdI) / Klinikum Grosshadern (GH)

Starting in 2008, DLR (Bionics), RdI and GH initiated a cooperation on the control of prosthetic hands and on feedback of robotic proprioceptive data through peripheral nervous system interfaces.

Leibnitz University Hannover

Two Ph.D.-projects on multibody methodology and multi-sensory modelling have been completed with the Institute of Robotics and Mechatronics (Prof. Dr. Heimann).

RWTH Aachen

Within the project “Virtueller Wald”, the DLR cooperated with Prof. Rossmann for the automatic detection and classification of trees from aerial images.

Martin-Luther University Halle-Wittenberg

Various Ph.D.-projects on numerics and simulation methodology have been completed with the Institute of Mathematics (Prof. Dr. Arnold) and have led to a collaborated work in the ITEA –project MODELISAR.

Technical University Berlin

Small satellite activities at DLR and TU Berlin (Prof. Briess) are the baseline of a cooperation for a long time. Based on the common experiences in the BIRD project new methods and technologies are investigated.

The *Institut für Luft- und Raumfahrt, Fachgebiet Flugmechanik, Flugregelung und Aeroelastizität* (Prof. Luckner) is in cooperation in the field of wake vortex assessment and multi-objective optimisation based design.

The railway systems group is cooperating with the Institut für Land- und Seeverkehr, Fachgebiet Schienenfahrzeuge (Prof. Dr. Hecht). Ph.D.-projects on crosswind stability and vehicle-track vibrations have been accomplished together.

Technical University Clausthal

DLR started a cooperation on benchmarking collision detection and haptic rendering algorithms with TU Clausthal (Prof. Zachmann) in 2007.

Technical University Ilmenau

DLR (Bionics) initiated a cooperation in 2008 with the TU Ilmenau (Prof. Witte/Prof. Haueisen) on the creation of novel surface EMG electrodes.

Technical University of Hamburg-Harburg (TUHH)

Since 2002, the Institute cooperates with the Institute of Aircraft Systems Engineering of the TUHH—Prof. Carl (retired) and Prof. Thielecke—in the European Power Optimised Aircraft (POA) and More-Open Electrical Technologies (MOET) projects. In the field of more electric aircraft environmental control systems and object-oriented modelling of thermo-fluid systems with Modelica DLR cooperates with the Institute of Thermo-Fluid Dynamics (Prof. G. Schmitz), while in the field of robust control methods for industrial robots DLR cooperates with the Institute of Control Systems (Prof. H. Werner).

Technical University Munich (TUM)

Many cooperations between TUM and DLR exist at all levels. Joint projects, professorships, lectures, student exchanges, and so on define combined goals on a daily basis. There is much cooperation between DLR and TUM within the DFG-Funded Excellence Cluster CoTeSys. The demonstrator of the project MiB (see above), led by DLR, is with the application centre of the Institute for Machine Tools and Industrial Management (*iwb*) of TUM in Augsburg. The institute cooperates with various institutions of the TUM in the SFB453: with the Institute of Communication Networks (LKN) on the integration of a platform independent communication framework, with the Institute for Data Processing (LDV) on immersive presentation of acoustic information, and the German Heart Centre Munich (DHC) on an interface for remote teleoperation and with the Institute for Robotics and Embedded Systems on haptic user interfaces, 3-D vision in medical applications, force sensing in robotics and operation-room setup. In the FOSFOR project together with the Institute of Measurement System and Sensor Technology (MST) fibre-optic sensor systems are developed for their use in force-feedback-aided robotic surgery. The institute also cooperates with the *Lehrstuhl für elektrische Antriebssysteme und Leistungselektronik* in the field of control of industrial robots.

In the field of system dynamics and control, intense cooperation took place with several departments, both in the framework of national and international projects, as well as in joint supervision of Ph.D. research projects. In particular, cooperation on flight dynamics and control took place with the *Lehrstuhl für Leichtbau* (Prof. Baier) and *Lehrstuhl für Flugsystemdynamik* (Prof. Holzapfel), cooperation on robust control with the *Lehrstuhl für Steuerungs- und Regelungstechnik* (Prof. M. Buss) and *Lehrstuhl* *für Regelungstechnik* (Prof. Lohman), and cooperation on elastic robots and contact mechanics with the *Lehrstuhl für Angewandte Mechanik* (Prof. Ulbrich), cooperation in the field of control of industrial robots with the *Lehrstuhl für elektrische Antriebssysteme und Leistungselektronik* (Prof. Schröder).

University of Bonn

Prof. Klein, the RSS GmbH and the DLR cooperate in the field of visualisation of interactive rendering of huge terrain models. The group of Prof. Klein is developing the interactive viewer component.

University of the Federal Armed Forces Munich

Cooperation with the Institute for Human Factors in the special research field SFB453: evaluation of impressiveness regarding presentation of information in different modalities.

Cooperation with the Institute of System Dynamics in the field of vehicle dynamics and control with the group of Prof. F. Svaricek.

University of Hamburg, Cardiovascular Surgery Department and Clinic

One of the main goals of the group is the development of new surgical techniques using a minimally invasive approach. The cooperation with DLR is well established and currently focuses on motion compensation for beating heart surgery.

University Karlsruhe (UNIKARL)

The aim of the cooperation with UNIKARL (Prof. Wörn) in the scope of the European project AccuRobAs is to develop and implement laser osteotomy with robotic assistance, a worldwide novelty. While DLR brings in the robotic knowledge and hardware, UNIKARL is in charge of the development and customisation of the laser unit.

University of Münster

Prof. Jessberger (Institute for Planetology) is principal investigator of MERTIS, an imaging infrared spectrometer for ESA's BepiColombo mission to planet Mercury.

University of Stuttgart

The Institute is closely co-operating with the Institute of Flight Mechanics and Flight Control (Prof. Dr.-Ing. W. Fichter) and the Institute of Aerodynamics and Gas Dynamics (Prof. Dr.-Ing. E. Krämer) in the frame of various Master's thesis projects, national projects (Flexible Aircraft II,III, MODYAS), and the HGF construct "virtual institute" (airship ALUSTRA). One employee received his Ph.D. from the Institute of Flight Mechanics and Flight Control (advisor: Prof. K.H. Well, Ph.D.).

Europe

CNES, Toulouse, France

The CNES is responsible for navigation and environment modelling on the ESA ExoMars rover. The DLR and CNES cooperate on (1) the integration of advanced range sensor technologies for improved collision avoidance and simultaneous environment modelling, and on (2) rover mobility dynamics modelling and simulation on uneven terrain while making use of their respective testbed facilities.

CEIT, San Sebasitan, Spain

CEIT and DLR are collaborating in European projects (Enactive, SKILLS) and beyond in the field of haptics, telerobotics and assembly verification. There has been exchange of scientific personnel in the last years.

College de France, Paris (CdF), France

The CdF (Prof. Berthoz) and DLR (Bionics) have had a long-standing cooperation on conducting biophysics experiments and using their results in robotics environments.

DEIMOS, Spain

Cooperation between DEIMOS and RM-SR in the preparation of proposal of the recently granted FP7 Collaborative Project ADDSAFE (Theme 7: TRANSPORT, including AERONAUTICS).

Erasmus Medical Centre, Rotterdam (EMC), Netherlands

To facilitate the access to biological material and clinical experimenting, a long-term cooperation was setup between the EMC and DLR (Bionics).

ESA/ESTEC, Netherlands

DLR and ESTEC is cooperating in the fields of haptic interfaces and telerobotic control. DLR has supervised thesis performed at ESTEC and hosts a guest scientist for the mechatronic integration of the X-Arm2 and the evaluation in telepresence experiments. Moreover, very recently DLR has agreed in a cooperation with the Development Department of the Human Spaceflight Directorate in order to assist with their robotics expertise in the ESA Roadmap development for space exploration. For this reason, a member of the institute will stay with ESTEC for several weeks, and furthermore an exchange of guest scientists and students is agreed upon.

ETHZ, Eidgenössische Technische Hochschule, Zürich, Switzerland

Institute of Robotics and Intelligent Systems, Autonomous Systems Lab of Prof. R. Siegwart. With the ETH (Prof. Siegwart) we cooperate in the Swiss-German consortium which is supposed to develop the ExoMars Rover. Cooperations related to object-oriented modelling and Modelica developments took place with the Institute of Computational Science (Prof. F. Cellier).

International Space University (ISU), Strasbourg, France

On basis of visiting lectured contributions DLR supports ISU's educational programme in space studies and space management with certain topics on advanced space robotics and planetary exploration, involving student exchange.

LAAS, Toulouse, France

In 2006 cooperation work was formally initialised with the LAAS (CNRS, France). The scope of this work is to develop a robot motion planning tool, based on a combination of nonlinear optimisation and sampling-based heuristics.

Lund University (LU), Sweden

Within the project SENSOPAC, LU and DLR cooperate on the application of cerebellar models for robot control. This cooperation involves frequent visits and exchanges.

National Technical University of Athens (NTUA), Greece

The NTUA (Prof. Kyriakopoulos) and DLR (Bionics) were involved in student exchanges in 2006 for applying control and adaptive algorithms to the DLR hand.

ONERA, France

Cooperation took place between ONERA and RM-SR in the European Projects COFCLUO, AWIATOR, JTI-SFWA, ACFA2020, GARTEUR AG17 and ONERA-DLR Project IMMUNE.

Politecnico di Milano. Italy

Cooperation between Politecnico di Milano (Prof. M. Lovera) and RM-SR on periodic control of satellite attitude via magnetic torquers.

Russian State Scientific Center for Robotics and Technical Cybernetics Saint Petersburg (RTC), Russia

RTC (Prof. Alexander Kondratev) and DLR-RM cooperate on telepresence control of the space robotic system ROKVISS over internet.

Scuola Superiore St. Anna (SSSA), Italy

PERCRO (Prof. Massimo Bergamasco) and DLR have had a long-lasting cooperation in the field of haptic interfaces, man-machine interaction and telerobotics (Enactive; SKILLS), involving many personnel exchanges.

Brought together in NEUROBOTICS, SSSA and DLR (Bionics) cooperate on EMG systems and other biomorphic approaches in robotics.

Simon Fraser University, Vancouver, Canada

The group of Prof. Kamal Gupta and DLR cooperate in the field of sensor-based exploration with fixed-base robot manipulators.

Technical University of Catalonia, Barcelona, Spain

The GRINS Lab and DLR develop approaches to physical human-robot interaction in complex scenarios, enhancing the interaction capabilities of LWR-III with external sensing.

Technical University Delft (TU Delft), *Netherlands*

TU Delft (Prof. Frans van der Helm) and DLR (Bionics) initiated various personnel exchanges, to combine the DLR hand-arm system and TU Delft human arm models.

In the field of system dynamics and control, during the last year two employees of the institute received their Ph.D. from the TU-Delft, faculty of Aerospace Engineering (Control and Simulation group. Prof.dr.ir. J.A. Mulder). Several students from this group performed their Master’s thesis work at the institute. Further co-operation is performed in the frame of projects, like GARTEUR FM(AG16) and ADDSAFE.

Umeå University, Sweden

Within the projects NEUROBOTICS and SENSOPAC, Umeå (Prof. Roland Johannson) and DLR (Bionics) cooperate on creating skin-like touch sensors.

Cooperation in the framework of the Swedish Strategic Research Foundation Grant: “Matrix Pencil Computations in Computer-Aided Control System Design: Theory, Algorithms and Software Tools” between Prof. B. Kågstrom’s group and RM-SR.

Universitá degli Studi di Verona (UVR), Italy

In the scope of the European project AccuRobAs, cooperation with UVR covers surgery simulation and development of haptic feedback consoles for telepresence in minimally invasive robotic surgery.

Universitá di Pisa (UNIPI), Italy

The cooperation with Prof. Bicchi at the University of PISA is on the design of variable impedance actuators and on safety in robotics. Joint projects are PHRIDOM, PHRIENDS (led by UNIPI) and VIACTORS (led by DLR). The cooperation further included co-organisation of workshops on major international robotics conferences and joint publications.

Universitá di Roma, La Sapienza (UOR), Italy

The cooperation with the University of Rome included a sabbatical of Prof. Alessandro de Luca (Editor in Chief IEEE Trans. On Robotics) at DLR, long-time Ph.D. and Postdoc visits, the cooperation in the European projects PHRIDOM, and PHRIENDS, organisation of common tutorial at the ICRA conference. The joint work on robot control emerged in several publications, the last one awarded the Best Application Paper Award at the IROS 2008 conference.

Université Montpellier II (UM2) and Université Pierre et Marie Curie -Paris VI (UPMC), France

UM2 and UPMC join the European project AccuRobAs and contribute new algorithms for force- and vision-based motion compensation in minimally invasive robotic surgery.

UPMC (Dr. Angelo Arleo) and DLR (Bionics) exchanged students in 2008, working on interpreting skin data. This cooperation is based on the SENSOPAC project.

Université Montpellier I (UM1), France

DLR and UM1 are collaborating in the field of human motor control and bimanual coordination. Within the SKILLS project research on human-agent interaction started.

Univeristy of Barcelona, Spain

DLR supports the education at the university of Barcelona receiving regularly graduate students under the European mobility programs.

University of Cambridge (UCam), England

Within SENSOPAC, UCam (Prof. Daniel Wolpert) and DLR cooperate on transferring statistical human data to robotic systems. This cooperation involved personnel exchanges in 2008.

University of Edinburgh, Scotland

Cooperating in the projects SENSOPAC and STIFF, researchers from Edinburgh University (Prof. Sethu Vijayakumar) have visited DLR (Bionics) to apply their neural network-based algorithms to the dynamics of the LWR-III.

University of Genova, Italy

This University (Prof. Giulio Sandini) and DLR (Bionics) cooperate on learning algorithms for EMG. This cooperation involved student visits in 2007.

University of Naples, Italy

The cooperation with Prof. Siciliano (President of the IEEE Robotics and Automation Society) is in the field of human-robot interaction control and dexterous manipulation control. Joint work with visiting Ph.D. students was done within the projects PHRIDOM, PHRIENDS, and DEXMART.

University of Sheffield, England

Within the EC funded project MOET, DLR cooperates with the University of Sheffield on the translation process of the MOET component models into Modelica.

University of Twente, Netherlands

The cooperation with University of Twente (Prof. Stramigioli) was in the area of impedance control of flexible joint robots, in particular of the DLR arms and resulted in several publications. The joint work will be continued in the new VIACTORS project, led by DLR.

World

Australian National University (Canberra)

A cooperation with the group of Prof. Brian Anderson takes place on optimal continuous-time periodic control.

Brown University, RI, USA

Following up on NEUROBOTICS, DLR and Brown University (Providence, RI) started a cooperation on robot control via central nervous system implants.

Canadian Space Agency (CSA)

Since 2002 already CSA and DLR have signed a MoU in the field of Space Robotics; recently this cooperation has been continued until 2011. The mutual interests are focused on (1) ground operations and robot autonomy, (2) space manipulator dynamics, simulation and control, and recently on (3) planetary rover mobility modelling and simulation. Particular achievements so far have been obtained by the ROKVISS contact dynamics experiments at the ISS.

Instituto Tecnológico de Aeronáutica, Brasil

Cooperation with the Dept. of Electronics (group of Prof. K.-H. Kienitz) on flight control, satellite attitude control and modelling of mechatronics systems.

Harbin Institute of Technology (HIT), China

The DLR and HIT have jointly developed a multi-sensory four-fingered dexterous hand DLR/HIT Hand I and a five-fingered humanoid robot hand DLR/HIT Hand II; furthermore, a prosthetic version is under development.

Instituto Nacional de Pesquisas de Espaciais (INPE), Instituto Tecnológico de Aeronáutica (ITA), Sao Jose dos Campos, Brazil

Cooperation with INPE and ITA (Prof. Luiz Carlos Goes) is in the area of dynamics, control and simulation of flexible space structures, specifically in space robotics.

Korean Institute of Science and Technology (KIST)

A common research approach between DLR and KIST (Prof. Ryu) on bilateral control and telerobotics has been developed. Personnel of KIST visited DLR regularly.

Middlebury College, VT, USA

Prof. Daniel Scharstein and DLR cooperate in the field of stereo reconstruction with the goal of improving the reconstruction from images with radiometric differences.

Musashi Institute of Technology, Japan

Professor Nenchev visited the DLR for a two month period in 2008 to carry out cooperation work on nonlinear control for the JUSTIN robot and for free-flying robots. A student exchange is now foreseen.

Tohoku University, Space Robotics Lab, Sendai, Japan

Professor K. Yoshida and DLR work together on modelling of impact dynamics for free-floating robots. The cooperation involves experimental and simulation data exchange, mutual use of respective testbeds for rendezvous and docking simulations, as well as student exchange.

University of Alberta, Canada

Prof. Martin Jägersand and DLR cooperate on new methods for photorealistic rendering by mixing image-based and geometry-based approaches. In 2006, during his sabbatical, he worked as a visiting scientist at the institute and applied his "dynamic texture" methods.

University of Auckland, NZ

The cooperation between DLR and the University of Auckland (Prof. Klette) was established in the middle of the 1990s, focusing on imaging systems and image processing. The panoramic camera is an outstanding example of the excellent collaboration.

University of Delaware, USA

In 2005 a cooperation was started with Professor S. Agrawal from Delaware University. Joint work was carried out in the field of nonlinear control of free-floating robots.

University of Massachusetts (UMass), USA

Starting 2008, DLR (Bionics) and UMass (Prof. Rod Grupen) are cooperating on new approaches to tactile sensing.

University of Southern California (USC), USA

USC (Prof. Gerald Loeb) and DLR (Bionics) cooperate on artificial skin prototypes and implantable electrodes since 2008, combining efforts on biomimetic sensing.

University of Washington (UoW), USA

DLR and UoW (Prof. Hannaford) jointly worked in the field of time domain passivity controllers.

3 Industrial Cooperations

Airbus, Loads and Aeroelastics, Germany

DLR-RM has a continuing, long-term cooperation with the Airbus loads department in Hamburg. This partnership involves mainly flexible aircraft modelling and load alleviation systems design. The frame of this cooperation covers many areas, ranging from research projects, over aircraft development in the pre-design stage to active support of current aircraft projects.

Airbus, Electrical Systems, France

We have a continuing cooperation with Airbus France, Electrical Systems in the field of more electric aircraft development. The main projects for this cooperation were POA and MOET.

Airbus, Stability and Control, France

The institute has a continuing, long-term cooperation with the Airbus Stability and Control department in Toulouse. The cooperations, mainly within European projects, cover the field of aircraft control and aircraft clearance with emphasis on method and tools.

A.R.T.

The Advanced Realtime Tracking GmbH (A.R.T.) is a manufacturer of optical tracking systems. In cooperation with the DLR, the use of tracking systems in new fields, e.g. surgery (see DFG Laserscanner) or instrument tracking is analysed. Additional cooperation has occurred in the new field of providing tactile feedback to the human hand.

Astro- und Feinwerktechnik Adlershof GmbH

Astro offers integrated solutions for mechanical and electro-optical components and systems. The company played an important role during the deployment of the camera MFC (Chapter III.4) and within the TET project (above).

The optical payload of the Korean satellite Kompsat-3 is developed in cooperation between EADS Astrium and the department of Optical Information Systems.

BrainLAB

The BrainLAB AG Munich is a vital partner for the surgical robotics research group (see Sec. VII.4.1). The company provides know-how in the fields of navigation systems in operating rooms, clinical workflows and risk analysis of medical devices. BrainLAB funded the development of the KINEMEDIC robot arm for medical applications. This project has been completed in 2006. Additionally BrainLAB is an active member in various research projects like MIROSURGE and AccuRoBas.

BMW AG

With BMW the institute has a long history of cooperation, mainly in the areas of mechatronic components (e.g., actuators for wheels and steering wheels) and man-machine interfaces, integrated mechatronic chassis control, and vehicle systems modelling with Modelica.

Bombardier Transportation

The so called path-following technique is a specific simulation methodology that enables the automated bifurcation analysis of complex technical systems, in particular railway vehicles. This methodology has been developed at our institute and its advantages will be demonstrated together with Bombardier Transportation (BT) using a rolling stock model provided by us.

Daimler AG, Stuttgart

Daimler has selected the Semi-Global Matching (SGM) stereo method as the base for driver assistance tasks. They have already implemented SGM on an FPGA for real-time processing and work together with the DLR for improving SGM.

There exist also cooperations in such fields as vehicle system simulation, fuel cell control or testing of power steering systems.

Furthermore, we cooperate with Daimler within the ITEA project MODELISAR to develop a new standard for model-in-the-loop and software-in-the-loops simulations ("functional mockup interface").

Dassault Systèmes, Paris, France

Dassault Systèmes is a world-leader in CAD systems (CATIA, SolidWorks) and PLM solutions. Due to the acquisition of Dynasim AB in 2006, a cooperation with DLR-RM is performed in the fields of behavioural modelling and embedded control systems. Especially, two large ITEA projects (EUROSYSLIB, MODELISAR) have been jointly organised and Dassault Systèmes became a distributor of DLR-RM Modelica libraries.

Dynasim AB, Lund, Sweden

Dynasim develops the commercial simulation software Dymola which is based on the modelling language Modelica. DLR-RM has a close cooperation with Dynasim since it was founded in 1992. On a scientific level, collaborative work is performed to improve the underlying modelling language and the needed transformation algorithms. On a commercial level, the DLR-RM simulation engine is used within Dymola and DLR-RM Modelica libraries are commercially sold.

EADS Astrium

Astrium is Europe's largest enterprise in the fields of space transportation, satellite systems and services. The optical payload of the Korean satellite Kompsat-3 is developed in cooperation between EADS Astrium and the department of Optical Information Systems. The ROKVISS project was realised in close cooperation with EADS Bremen.

EADS- MAS (Military Air Systems)

MAS is a division of EADS Defence & Security and deals with fighter aircraft (Eurofighter), jet trainers and UAVs. The institute supports EADS-MAS with methods and tools in the area of flight control mainly for the analysis and clearance of flight control laws. Continuous close co-operation exists in the frame of various GARTEUR Action Groups, like FM(AG08), FM(AG11), and FM(AG17).

EADS Military Flight

EADS MF and DLR are cooperating for the evaluation of virtual training methods for maintenance task in aircraft.

HOLOEYE Photonics AG

HOLOEYE's diffractive optical elements are applied for camera calibration. This innovative technology can be used for very accurate line of sight measurements. DLR and HOLOEYE were joined in several projects, e.g. DIOPTER (Sec. II.2.2.5).

Intec GmbH

As a spin-off company of our institute, a tight collaboration with Intec GmbH has been graduated signing a Memorandum of Understanding, that defines a basis to bring DLR, railway industry and Intec together at one table and discuss, how simulation methods can be finally polished for industrial use.

Kayser-Threde GmbH

Space related projects are a main part of the company's business portfolio. DLR and Kayser-Threde GmbH cooperate in a number of projects, e.g. TET, MERTIS, EuMap and ROKVISS (see above).

Knorr-Bremse GmbH

The vehicle dynamics and control group of the institute could establish a close cooperation to Knorr-Bremse, which is the world's leading supplier of railway brake systems. The projects accomplished concern the analysis of brake vibrations at high-speed-trains such as ProSID [Vaculin *et al.* 2005[f]] and MAVela [Günther *et al.* 2008[c]]. Today, Knorr Bremse sponsors one Ph.D.-project on the consideration of thermoelastic effects in dynamical brake models (Sec. VI.3.1.5) and retained us to perform a study on the potential of advanced brake control in passenger trains (Sec. VI.3.2.2).

KUKA Roboter GmbH

KUKA is our main partner with respect to industrial robotics; see also Chapter VII.1. Besides these projects and the licensed commercialisation of our light-weight robot, KUKA is a partner in the field of medical robotics. In the project MIROSURGE, KUKA contributes know-how on the design of commercial products and safe robot control. KUKA and the institute cooperate in this project regarding the commercialisation of the KINEMEDIC robot. In mid of 2008, we have formalised a big strategic cooperation for the next years in the field of advanced and service robotics.

Liebherr Aerospace, Lindenberg

We have long running cooperations with Liebherr Aerospace. In the POA project Liebherr was the main provider for models for ECS (Environmental Control System) and one provider for electrical actuator models for DLR's virtual iron bird (VIB). Within MOET Liebherr is the main partner concerning ECS models. In this cooperation also a HM (health monitoring) project is carried out.

LSE Space

DLR, LRT (TUM) and LSE Space have been collaborating for the simulation of space communications for telerobotic systems. Based on the requirements and experiments LSE designed a simulator software for CCSDS communication.

MBDA Missile Systems

MBDA is a multinational group and world leader in missile and missile systems. In cooperation with its German subsidiary LFK-Lenkflugkörper Systeme GmbH the institute develops tools for robust stability analysis and LPV controller design of missiles.

OEM

In cooperation with a premium OEM and the DLR Institute of Vehicle Concepts the project "Evaluation of control strategies for fuel cell systems" was arranged in 2008. The aim was to evaluate the different potential architectures of fuel cell systems for automotive application.

Within a scope of two industrial projects the improvement and identification of models of hydraulic power steering systems made by different German car manufacturers was conducted. To improve and identify the models comprehensive tests were performed at our lab.

Dr. Ing. h.c Porsche AG

In a joint advance development project with Porsche over several years, a DLR chassis control concept was adapted to two different vehicle types and successfully tested for both. The final stage of development was judged by Porsche as "close-to-production".

QUISS GmbH & Co KG

QUISS is a small company that cooperates with DLR in developing and improving the vision system of MiB (see above).

Richard Wolf GmbH

Wolf is a medical device manufacturer involved in the project MIROSURGE. Wolf supplies new 3-D endoscopes and auxiliary video equipment for the telerobotic system. Additionally WOLF advises the development of the instruments (DLR MICA, see Sec. VII.4.1.3) from the industry point of view.

Robert Bosch GmbH

With the Corporate Sector "Research and Advance Engineering" the institute has a close co-operation on the field of multi-objective design optimisation.

Rotec Engineering

Rotec Engineering is a company specialised to advanced automation solutions for research and industry. The DLR and Rotec Engineering cooperate on the evaluation of a product development for the DLR 3-D sensor technology.

RSS GmbH

Prof. Klein, the RSS GmbH and the DLR co-operate in the field of visualisation of interactive rendering of huge terrain models. The RSS GmbH is responsible for annotating the interactive data with symbolic information (e.g. streets, touristic attractions, names of mountains, etc.) and also for marketing the data.

Schunk GmbH & Co KG

Schunk is the licence holder and manufacturer of the institute's compliant force torque sensor. And the DLR/HIT Hand I has been distributed by Schunk since 2006.

SeeFront GmbH, Hamburg

SeeFront GmbH is a DLR project partner within the MIROSURGE project, which provides the hardware for an autostereoscopic display (ASD). The ASD enables 3-D vision for the user without additional special glasses. DLR develops robust real-time eye-tracking algorithms for the ASD to allow for free movement of the viewer.

Siemens Mobility

The railway systems team accomplished a project on brake vibrations of a Siemens high-speed-train [Günther *et al.* 2008[c]] and co-operates in the field of multidomain railway system simulation with Modelica.

Volkswagen AG, Konzernforschung, Virtual Reality Lab

The institute cooperates with the Virtual Reality Laboratory of Volkswagen in the field of virtual assembly verification with focus on haptics.

VRCOM (ICIDO)

VRCOM (now joint with ICIDO) is Germany's leading provider for VR systems. DLR implements the haptic rendering and control of handcontrollers in the *Virtual Design* software framework. The evaluation goes along with the virtual assembly verification.

ZF Friedrichshafen

ZF Friedrichshafen AG is the project leader of the BMBF – project *Active Light-weight Chassis (ALF)* which started in July 2008 (see section on *National Projects* above).

Zoller und Fröhlich

Zoller und Fröhlich is a leading manufacturer of terrestrial laser-scanner systems. DLR and Z+F cooperate on the integration of colour cameras and on the automation of 3-D modelling methods. Furthermore, Z+F funds an external employee for strengthening the cooperation.

4 Other

CACSD 2006

Andreas Varga was the General Chair of the 2006 IEEE Symposium on Computer Aided Control Systems Design held in Munich in Sep. 2006 and Simon Hecker was the Local Arrangements Chair of this conference.

CCA 2006

Andreas Varga was the General Chair of the 2006 IEEE Conference on Control Applications held in Munich in Sep. 2006; Local Arrangements Chair: Simon Hecker.

EIES

In the European Institute of Enactive Systems Carsten Preusche acts as a member of the Board of Directors.

ICRA 2007

Alin Albu-Schäffer co-organised the tutorial "Nonlinear Control of Flexible Joint Robots" Full Day Tutorial, Int. Conf. on Robotics and Automation, Rome 2008

ICRA 2008

Roberto Lampariello was co-organiser of the workshop "Collision-free motion planning for dynamic systems" at the ICRA 2008.

ISC Industrial Simulation Conferences (organised by EUROSIS)

Since 2005 Bernd Schäfer is member of the IPC and is responsible chairman for session track "simulation in multibody systems".

ISIC 2006

Andreas Varga was the General Chair of the 2006 IEEE International Symposium on Intelligent Control held in Munich in Sep. 2006; Local Arrangements Chair: Simon Hecker.

Handbook of Robotics

The Springer Handbook of Robotic covers under the editors Bruno Siciliano and Oussama Khatib all aspects of robotic research. Patrick van der Smagt, Carsten Preusche and Gerd Hirzinger co-authored two of the 64 chapters: "Telerobotics" and "Neurorobotics: From Vision to Action".

Modelica Association

The Modelica Association is a non-profit, non-governmental organisation with the aim of developing and promoting the Modelica modelling language for modelling, simulation and programming of physical and technical systems and processes. Partners: 11 organisational members (including DLR), 70 individual members. DLR chairs this association since 2000 and is also a co-organiser and program chair for all 6 International Modelica Conferences hold since 2000.

MOVIC 2008

Patrick van der Smagt was a co-organiser of the MOVIC conference, held in Munich in September 2008.

MSC 2008

Andreas Varga was a plenary speaker of the 2008 IEEE Multi-conference on Systems and Control held in San Antonio, Texas, in Sep. 2008 and Simon Hecker was the Registration Chair of this conference.

NEUROBOTICS Summer School

Sami Haddadin, Patrick van der Smagt: Overview of man-made actuators. Neurobotics Summer-School 2006, Umea, Sweden, 2006.

NICONET Association

The NICONET Association is a non-profit, non-governmental organisation with the aim of developing and promoting reliable numerical computational methods in system and control, with a special focus on maintaining and further development of the SLICOT control software library. The NICONET Association has presently 2 institutional members (including DLR) and 20 individual members. The DLR representative Andreas Varga is vice-chair of the association.

OptecBB Association

OptecBB is an initiative of companies, universities and scientific institutes to strengthening the economic power of the Berlin-Brandenburg region through joint activities using the potential of the optical technologies. DLR is active member since 2000.

RO-MAN 2008

Patrick van der Smagt acted as a co-organiser and exhibition chair of the RO-MAN 2008 conference held in Munich from August 1-3, 2008. Within this conference Carsten Preusche co-organised a workshop on capturing and transferring of human skill.

RSS 2008

Alin Albu-Schäffer co-organised the workshop "Design and Control of Variable Impedance Actuators for Physical Interaction of Robots with Humans and Their Environment" at the Robotics: Science and Systems conference, 2008. Sami Haddadin co-organised the workshop "Robot Manipulation: Intelligence in Human Environments" at this conference.

IX Documentation

1 Lectures at Universities

Lecturer	University	Subject	2005	2006	2007	2008
Albu-Schäffer	TU München	Regelungstechnische Methoden in der Robotik			x	x
Börner	FH Nordhausen	Grundlagen der digitalen Bildverarbeitung	x	x	x	x
Borst	Hochschule München (HM)	Grundlagen der Bildverarbeitung			x	x
Eckardt	Universität Stuttgart	Digitalkameras und elektronische Verarbeitung	x	x	x	
Hirzinger	TU München	Sensorgeführte Roboter	x	x	x	x
Kübler	Uni Stuttgart	Biomedizinische Gerätetechnik		x	x	x
Kübler Ortmaier	TU München	Computer und Robotereinsatz in der Chirurgie (Ringvorlesung Medizintechnik)	x	x	x	
Mangoldt		Grundlagen der digitalen Druckvorstufe			x	x
Ortmaier	TU München	Echtzeitbildverarbeitung für die Robotik			x	x
Otter	TU München	Objektorientierte Modellierung mechatronischer Systeme	x	x	x	x
Preusche	TU München	Bilaterale Regelung von Master-Slave Systemen mit Totzeit (Regelungstechnisches Seminar)			x	
Schäfer	Hochschule München (HM)	Technische Mechanik	x	x	x	x
Schäfer	ISU International Space University, Strasbourg	Advanced Space Robotics and Planetary Exploration (visiting lecture, two days per year)	x	x	x	x
Schmid	Hochschule München (HM)	Technische Mechanik	x	x	x	x
Schmid	Hochschule München (HM)	Maschinenelemente / mechanische Konstruktion	x	x	x	x

Schlotzhauer	Universität Potsdam	Optische und spektrophotometrische Methoden der Fernerkundung				x
van der Smagt	TU München	Bionik (Ringvorlesung sensorgeführte Roboter)				x
van der Smagt	TU München	Learning Robotic Systems (Ringvorlesung Learning)			x	x
Steinhauser	Uni Bw München	Regelungstechnik	x	x		
Steinhauser	Hochschule München (HM)	Signale und Systeme			x	
Steinhauser	Hochschule München (HM)	Methoden in der Robotik				x

2 Awards

Year	Award	Institution	Name
2005	Preis des Fördervereins Für eine hervorragende Diplomarbeit in Informatik	Förderverein des Forschungszentrums Informatik Karlsruhe	F. Zacharias
2005	Pioneer in Robotics and Automation Award	IEEE Robotics and Automation Society For his pioneering research in mechatronic devices, teleoperation, articulated hands, and light-weight robots, and his leadership in space robotics programs in Europa	G. Hirzinger
2005	Finalist –ICRA Best Video Proceedings	IEEE International Conference on Robotics and Automation (robots get closer to humans)	C. Ott, C. Borst, U. Hillenbrand, B. Brunner, B. Bäuml, G. Hirzinger
2005	Best Paper Award Mechatronik 2005	VDI Wissensforum IWB GmbH	T. Ortmaier,C. Ott, H. Weiß, U. Hagn, M. Grebenstein, M. Nickl, A. Albu-Schäffer, S. Jörg, R. Konietschke, G. Hirzinger, Essenreiter, Bertram
2005	Erna-Schäffler-Förderpreis	Soroptimist International-Club Karlsruhe/Universität Fridericiana Karlsruhe In Anerkennung ihrer herausragenden wissenschaftlichen Leistung der Diplomarbeit	F. Zacharias
2005	Goldene Wernher-von-Braun-Medaille	Internationaler Förderkreis für Raumfahrt Hermann Oberth – Wernher von Braun e.V.	K. Landzettel
2005	Honorary Professor of Bu-	Budapest Tech	G. Hirzinger

	dapest Tech		
2005	2. Preis Münchner Business Plan Wettbewerb	Münchener Business Plan Wettbewerb „TechVenture Stage“ für den Businessplan DUALIS	T. Schmid
2005	Innovationspreis 2005 Medizintechnik	Bundesministerium für Bildung und Forschung für die Entwicklung eines neuartigen, voll implantierbaren künstlichen Herzens Verliehen am 16.11.2005 auf der MEDICA, Düsseldorf	T. Schmid
2005	Preis des Vorsitzenden	Erstmalig verliehen durch die Gesellschaft von Freunden des DLR bei der JHV 01.12.2005. Für den jüngsten Kandidaten, dem im Vorjahr ein Patent erteilt wurde	U. Seibold
2005	Best Paper Award 2005	Bester Beitrag des Jahrgangs 2005, der wichtigsten deutschsprachigen Zeitschrift für Regelungstechnik und Automatisierung at „Kartesische Impedanzregelung von Robotern mit elastischen Gelenken“	C. Ott, A. Albu-Schäffer, A. Kugi, S. Stramigioli, G. Hirzinger
2006	curac, Die Deutsche Gesellschaft für Computer- und Roboterassistierte Chirurgie e.V.	First presentation award “On the Accuracy of Robot Assisted Placement of Pedicle Screws with Soft Robotics”	T. Ortmaier
2007	iF Product design award 2007	SAH/DLR-HIT-Hand Multisensor Robothand	P. Meusel
2007	IEEE Field Award Robotics and Automation	“for contributions in robot mechatronics, telerobotics, man-machine interface research, and space robotics”	G. Hirzinger
2007	IEEE Best Video Award Robotics and Automation	IEEE International Conference on Robotics and Automation (ICRA2007)	C. Borst, C. Ott, T. Wimböck, B. Brunner, F. Zacharias, B., Bäuml, Ulrich Hillenbrand, Sami Haddadin, Alin Albu-Schäffer, G. Hirzinger
2007	Euron Technology Transfer Award 2007	DLR/HIT Hand European Robotics Forum	H. Liu, G. Hirzinger, P. Meusel
2007	Euron Technology Transfer Award 2007	KINEMEDIC European Robotics Forum	U. Hagn, T. Ortmaier, R. Wohlgemuth
2007	Enactive Mobility Award	Network of Excellence on Enactive Interfaces	J. Artigas

2007	Innovationspreis 2007	Gesellschaft von Freunden des DLR, Jahreshauptversammlung, 28./29.11.2007 in Göttingen	O. Eiberger, A. Beyer, M. Schedl, A. Albu-Schäffer, G. Plank, G. Schreiber
2007	DLR-Wissenschaftspreis 2007	awarded by the Vorstand des DLR for his scientific work "A Unified Passivity-based Control Framework for Position, Torque and Impedance Control of Flexible Joint Robots"	A. Albu Schäffer
2007	E'ON Future Award	awarded by E'ON Energie in cooperation with TUM for his Master Thesis „Entwicklung und Auswertung eines taktilen Sensor nach biologischem Vorbild - Künstliche Haut für Roboter- und Prothesenhände"	M. Strohmayr
2007	E'ON Future Award	vergeben von E'ON Energie in Kooperation mit der TUM für seine Masterarbeit „Raumfahrt-Kommunikation für Telepräsenzanwendungen"	G. Schroth
2008	European Mirco Air Vehicle Conference, MAV	-Indoor Flight Dynamics – Rotary Wing -Outdoor Autonomy Competition -Outdoor Flight Dynamics – Rotary Wing	D. Gurdan, J. Stumpf
2008	Nichols Medal 2008	IFAC 2008 International Federation of Automatic Control	G. Hirzinger
2008	Innovationspreis 2008 der Stiftung Familie Klee	DGBMT-Preis 2008 der Stiftung-Familie-Klee zur Förderung des wissenschaftlichen Nachwuchses für die Arbeit „Doppelpulsatiles Herzunterstützungssystem"	T. Schmid
2008	Best Application Paper Award	IEEE/RSJ International Conference on Intelligent Robots and Systems President of ICROS	S. Haddadin, A. Albu-Schäffer, G. Hirzinger (DLR) A. De Luca (Univ.Roma)
2008	3. Preis (Beitragspreis)	ICCAS/Herzzentrum Leipzig CURAC 7. Jahrestagung der Deutschen Gesellschaft für Computer und Robterassistierte Chirurgie e.V. Betragspreis „DLR MIRO-SURGE-Towards Versatility in	A. Tobergte, U. Hagn, M. Nickl, S. Jörg, B. Kübler, G. Passig, M. Gröger, F. Fröhlich, U. Seibold, R. Konietschke, L. Le-Tien, A. Albu-Schäffer, M. Grebenstein, T. Ortmaier, G. Hirzinger

		Surgical Robotics"	
2008	Industrial Robot Innovation Award – Highly Commended	CLAWAR 2008 Int. Conf. on Climbing and Walking Robots and Support Technologies for Mobile Machines	M. Görner, G. Hirzinger
2008	Outstanding Paper Award	Emerald Literati Network (Industrial Robot, Vol. 34, No. 5, 2007)	A. Albu-Schäffer, S. Haddadin, C. Ott, Andreas Stemmer, T. Wimböck, G.Hirzinger
2008	Ernennung zum Mitglied in die Leopoldina	Deutsche Akademie der Naturforscher Leopoldina, in Anerkennung hervorragender wissenschaftlicher Leistungen	G. Hirzinger
2008	Förderungspreis Initiativprogram Ideenwettbewerb BIONIK	Förderungspreis der TUM für den Beitrag „Implementierung von Kokontraktion und mehrgelenkiger Muskeln in die Robotik"	P. van der Smagt *et al.* (Böhm, Senner, Ulbrich, Lindemann/TUM)
2008	Finalist Best Conference Paper	ICRA 2008 Finalist Best Conference Paper "Employing Wave Variables for Coordinated Control of Robots with Distributed Control Architecture"	C. Ott, Y. Nakamura (Univ. Tokyo)
2008	Preis des Vorsitzenden der Gesellschaft von Freunden des DLR e.V.	„Raumtransporter mit einer Vorrischtung zum Andochen an einen Satelliten"	A. Baumann
2009	iF Product Design Award	DLR MIRO robot for surgical applications was honoured in the category "advanced studies"	
2009	iF Product Design Award	DLR-HIT-Hand II	

3 Scientific Exchange

3.1 Guest Scientists

Guest	Home Institution	Country	Year
Abiko, Satoko, Dr.	Tohoku University, Sendai	Japan	2005-2006
Agrawal, Sunil	University of Delaware	USA	2005
Avdeenko, Tatyana, Prof.	Novosibirsk State Technical University	Russia	2007
Borghesan, Gianni	DEIS, Univ. of Bologna	Italy	2007
Botturi, Debora	University of Verona	Italy	2005-2006
Castellini, Claudio	University of Genova	Italy	2007
Chen, Zhaopeng	Harbin Institute of Technology, Robot	China	2008-2010

	Research Institute		
Cobzas, Dana	University of Alberta	Canada	2006-2007
De Luca, Aleassandro, Prof.	Universita di Roma "La Sapienza"	Italy	2005-2006
De Santis, Agostino	University of Naples	Italy	2005-2006
Fenili, Andre, Dr.	INPE Instituto Nacional de Pesquisas Espaciais, Sao Jose dos Campos	Brazil	2007
Fernandez, Xavier	Université Pierre et Marie Curie Paris	France	2008
Gadelha de Souza, Luiz Carlos, Dr.	INPE Instituto Nacional de Pesquisas Espaciais, Sao Jose dos Campos	Brazil	2005, 2007
Garcia Aracil, Nicolas	Universitas Miguel Hernández	Spain	2006
Gil, Jorge Juan, Dr.	Universidad Navarra	Spain	2006
Giralt, Xavier	Technical University of Catalonia, GRINS Laboratory, Barcelona	Spain	2008-2009
Hassmann, Carlos	INPE Instituto Nacional de Pesquisas Espaciais, Sao Jose dos Campos	Brazil	2005
Howard, Ian	Cambridge University	UK	2008
Iskakov, Renat	University of St. Petersburg	Russia	2005-2008
Jagersand, Martin, Prof.	University of Alberta, Computer Vision and Robotics Research Group, Edmonton	Canada	2006-2007
Kienitz, Karl-Heinz, Prof.	ITA Instituto Tecnologico de Aeronautica, Sao Jose dos Campos	Brazil	2004-2005
Lamiraux, Florent	LAAS CNRS	France	2006
Le-Tien, Luc	Hanoi University of Technology	Vietnam	2002-2006
Liu, Yiwei, Dr.	Harbin Institute of Technology	China	2005
Lutun, Jeremie	ENSIAME	France	2004-2005
Mitrovic, Djordje	University of Edinburgh, Scotland	UK	2007-2008
Nenchev, Dragomir, Prof.	Musashi Institute of Technology	Japan	2008
Palli, Gianluca	DEIS, University of Bologna	Italy	2006
Panagiotis, Artemiadis	National Technical University of Athens	Greece	2006
Perez Vidal, Carlos	Universitas Miguel Hernández	Spain	2006
Prod'Homme, Richard	Ecole centrale de Nantes	France	2006
Robuffo Giordano, Paolo	Universita di Roma "La Sapienza"	Italy	2007-2008
Schiele, Andre, Dr.	European Space Research and Development Centre, ESA/ESTEC	The Netherlands	2008-2009
Shiriaev, Anton, Prof.	University of Umea	Sweden	2007
Wu, Ke	Harbin Institute of Technology, Robot Research Institute	China	2007-2010

3.2 Leaves

Member	Foreign Host Institution	Country	Year
Artigas, Jordi	PERCO-Laboratory, Scuola Superiore Sant'Anna, Pisa	Italy	2007-2008
Jörg, Stefan	EDALAB Electronic Design Automation Laboratory, Universita degle Studi di Verona	Italy	2006
Konietschke, Rainer	University of Hawaii, Honolulu	USA	2004-2005
Lampariello, Roberto	LAAS (CNRS), Toulouse	France	2006
Nickl, Mathias	EDALAB Electronic Design Automation Laboratory, Universita degle Studi di Verona	Italy	2006
Ott, Ch., Dr.	University of Tokyo	Japan	2007-2009
Otter, Martin, Prof.	Dassault Systèmes, Paris	France	2007
Seibold, Ulrich	University of British Columbia (UBC), Vancouver	Canada	2003-2009

4 Membership in External Professional Committees

Many members of the Institute are frequent reviewers and for most conferences and journals on the topics of, control, mechatronics, neuroscience, numerics, robotics, vision, and so on. Below we list activities beyond such reviewing work.

A. Albu-Schäffer

Associate Editor for IEEE Transactions on Robotics

Organiser of Workshop "Design and Control of Variable Impedance Actuators for Physical Interaction of Robots with Humans and Their Environment" at the Robotics: Science and Systems conference, 2008

J. Bals

PC-Member of several conferences

Member of international Ph.D. committees

S. Hecker

Local Arrangements Chair, IEEE Conference on Control Applications Munich, Sep. 4-6, 2006

Local Arrangements Chair, IEEE Symposium on Computer Aided Control System Design, Sep. 4-6, 2006

Local Arrangements Chair, IEEE Symposium on Intelligent Control, Sep. 4-6, 2006

Registration Chair, IEEE Multi-conference on Systems and Control, San Antonio, USA, Sep. 3-5, 2008

S. Haddadin

Organiser of Workshop "Robot Manipulation: Intelligence in Human Environments" at the Robotics: Science and Systems conference, 2008

G. Hirzinger

Officer of the Int. Federation of Robotics Research (IFRR, German Representative)

Member of the LEOPOLDINA (national Academy of Sciences)

Executive Board Member: Cluster of Excellence "Cognitive Technical Systems" of the Technical University of Munich

Consulting and Board assignments for the Bayer. Wissenschafts- und Wirtschaftsministerium

DFG Reviewer

Permanent Advisory Board of ICAR (Int.

Conference on Advanced Robotics)

Reviewer of Swiss National Fonds Program COME (Medical Technologies)

Board Member Forum MedTech and Pharma until 2005

Member IEEE Award Nomination Committee

Award Committee Member for:

- ICRA 2005 (International Conference on Robotics and Automation)
- WHC 2005 (World Haptics Conference)

Speaker of the Board of BKM (Bayerisches Kompetenz-Netzwerk Mechatronik) until 2005

Secondary SFB speaker 453 "Wirklichkeitsnahe Telepräsenz und Teleaktion"

Member of the management advisory board of the DGR (Deutsche Gesellschaft für Robotik)

Member of the jury of the 2005 science award "Medizintechnik", Wissenschaftszentrum Nordrhein-Westfalen

Ph.D. reviewer for many national and international dissertations

PC-Member of nearly all major international robot conferences

M. Otter

Chairman of the non-profit International Modelica Association since year 2000 (www.Modelica.org, 70 members, 11 organisational members)

Reviewer for the following dissertations:

- Reichl G. (2005). Optimierte Bewirtschaftung von Kläranlagen basierend auf der Modellierung mit Modelica. Fakultät für Informatik und Automatisierung. Technische Universität Ilmenau.
- Thümmel M. (2007). Modellbasierte Regelung mit nichtlinearen inversen Systemen und Beobachtern von Robotern mit elastischen Gelenken. Lehrstuhl für Elektrische Antriebssysteme, TU München.
- Kurze M. (2008). Modellbasierte Regelung von Robotern mit elastischen Gelenken ohne abtriebsseitige Sensorik. Lehrstuhl für Elektrische Antriebssysteme, TU München.
- Schweiger Ch. (2008). Objektorientierte Modellierung und Echtzeitsimulation von Kraftfahrzeug-Antriebssträngen. Institut für Steuer- und Regelungstechnik, Universität der Bundeswehr München.

Program-Chair of International Modelica Conferences: 4th Modelica Conference 2005 (Hamburg-Harburg), 5th Modelica Conference 2006 (Vienna), 6th Modelica Conference 2008 (Bielefeld)

C. Preusche

Program Co-Chair, 3rd Enactive Conference, Montpellier, France, 2006

Co-organiser of Workshop on "Multimodal Interfaces for Capturing and Transferring of SKILLS" at RO-MAN 2008

Associate Editor, World Haptics Conference 2009

B. Schäfer

Senior Member AIAA (American Institute of Aeronautics and Astronautics)

Member of GAMM (Ges. für Angewandte Mathematik und Mechanik)

Chair (since 2005) "Simulation in Multibody Systems" of the annual ISC (Industrial Simulation Conference), organised by EUROSIS

M. Sielemann

Member of the International Modelica Association

P. van der Smagt

EC-FP7-IST Advisor

Editor for *Neural Networks*

Book Editor (Europe) for *Neural Networks*

Editor of *Progress in Neural Networks*

Exhibition Chair for the 2008 RO-MAN Conference

Chair for the 2008 MOVIC Conference

Examination board member for the Ph.D. thesis "Object manipulation and force control by using tactile sensors", Somrak Petchartee, Uni BW Munich

A. Varga

Fellow IEEE (since 2003)

Member of SIAM (since 1995)

Vice-chairman of the NICONET Association (e.V.)

Guest Editor of *Linear Algebra and Its Applications*, vol.415, Issues 2-3, 2006: Special Issue on "Order Reduction of Large-Scale Systems"

General Chair, IEEE Conference on Control Applications Munich, Sep. 4-6, 2006

General Chair, IEEE Symposium on Computer Aided Control System Design, Sep. 4-6, 2006

General Chair, IEEE Symposium on Intelligent Control, Sep. 4-6, 2006

Plenary Speaker IEEE Multi-conference on Systems and Control, San Antonio, USA, Sep. 3-5, 2008

5 Publications

In this chapter, the Institute's publications from the period 2005–2008 are listed, sorted per type of publication: journal papers (Sec. 5.1), conference papers (5.2), book chapters (5.3), books (5.4), patents (5.5), Ph.D. theses (5.6), and technical reports (5.7). Note that the in-text references distinguish, per reference via a superscripted letter, whether the said publication is a "j"ournal paper, "c"onference paper, "b"ook chapter, "B"ook, "p"atent, Ph.D. "t"hesis, or technical "r"eport. Thus you will encounter references to, e.g., [Author 2008[c]], and can find them in the corresponding list.

Some publication years are distinguished with a lower-case letter (e.g., 2008a, 2008b), in order to uniquify a literature reference thereto.

5.1 Articles in Refereed Journals ("j")

Below you will find 75 references to publications in internationally refereed journals:

Abmayr T., Härtl F., Hirzinger G., Burschka D., and Fröhlich C. (2008). A Correlation Based Target Finder for Terrestrial Laser Scanning. *Journal of applied Geodesy*, 2(3):31–38.

Albu-Schäffer A., Eiberger O., Grebenstein M., Haddadin S., Ott C., Wimböck T., Wolf S., and Hirzinger G. (2008). Soft robotics: From Torque Feedback Controlled Lightweight Robots to Intrinsically Compliant Systems. *IEEE Robotics and Automation Magazine*, 15(3):20–30.

Albu-Schäffer A., Haddadin S., Ott C., Stemmer A., Wimböck T., and Hirzinger G. (2007a). The DLR Light-weight Robot Design and Control Concepts for Robots in Human Environments. *Industrial Robot-An International Journal*, 34(5):376–385.

Albu-Schäffer A., Ott C., and Hirzinger G. (2007). A Unified Passivity Based Control Framework for Position, Torque and Impedance Control of Flexible Joint Robots. pages 5–21.

Albu-Schäffer A., Ott C., and Hirzinger G. (2007b). A Unified Passivity Based Control Framework for Position, Torque and Impedance Control of Flexible Joint Robots. *International Journal of Robotics Research*, 26(1):23–39.

Bajcinca N. (2005). Rasch geregelt. *Design & Elektronik*, 03:30–33.

Bajcinca N., Cortesao R., and Hauschild M. (2005). Robust Control for Steer-by-Wire Vehicles. *Autonomous Robots*, 19:193–214.

Bajcinca N. and Hulin T. (2005). Menge aller robust stabilisierenden PID-Regler: Methodik und Software (Teil I). *at - Automatisierungstechnik*, 53(11):556–564.

Bajcinca N. and Hulin T. (2006). Menge aller robust stabilisierenden PID-Regler: Methodik und Software (Teil II). *at - Automatisierungstechnik*, 54(5):240–246.

Bajcinca N. and Hulin T. (2006). Menge aller robust stabilisierenden PID-Regler: Methodik und Software (Teil III). *at - Automatisierungstechnik*, 54(10):515–519.

Bäuml B. and Hirzinger G. (2007). When Hard Realtime Matters: Software for Complex Mechatronic Systems. *Robotics and Autonomous Systems: Special Issue on Humanoid Technologies*.

Bellmann T. (2008). Bewebungssimulationen - Roboterbasierte Simulatoren als Alternative zu Hexapoden. *Automobiltechnologie in Bayern*, pages 16–17.

Börner A. (2006). Optische Sensoren für Fahrzeuge. *VDI-Berichte*, 1944:37–48.

Carrarini A. (2007). Reliability based analysis of the crosswind stability of railway vehicles. *Journal of Wind Engineering and Industrial Aerodynamics*, 95:493–509.

Castellini C. and Smagt van der P. (2008). Suface EMG in Advanced Hand Prosthetics. *Biological Cybernetics*.

da Silva A., Schäfer B., and de Souza L. (2007). Joint Dynamics Modeling and Parameter Identification for Space Robot Applications. *MPE open access journal*.

Dryia C., Schmid T., Stock M., Schopka S., Schmid C., and Lehle K. (2008). Cell-Type Specific Evaluation of the Biocompatibility of Polyurethanes used as a base Material for Ventricular Assist Devices. *International Journal of Artificial Organs*, 31(7):625.

Frese U., Larsson P., and Duckett T. (2005). A Multilevel Relaxation Algorithm for Simultaneous Localization and Mapping. *IEEE Transactions on Robotics*, 21(2):196–207.

Gonzalo J., Martin de Mercado G., Lorenz E., Oertel D., Casanova J. L., Aguirre M., Leibrandt W., and Billig G. (2005). Demonstration of a semi-operational firerecognition service using BIRD micro-satellite - DEMOBIRD. *Small Satellites for Earth Observation - Selected Proceedings of the 5th International Symposium of the International Academy of Astronautics, Berlin 4-8, 2005, H.-P. Röser, R. Sandau, A. Valenzuela (eds.), ISBN:3-11-018851-1*, V:110–118.

Grebenstein M. and Smagt van der P. (2008). Antagonism for a Highly Anthropomorphic HandArm System. *Advanced Robotics*, (22):39–55.

Haddadin S., Laue T., Frese U., Wolf S., Albu-Schäffer A., and Hirzinger G. (2008). Kick it like a Safe Robot: Requirements for 2050. *Robotics and Autonomous Systems: Special Issue on Humanoid Soccer Robots*.

Hagn U., Nickl M., Jörg S., Passig G., Bahls T., Nothhelfer A., Hacker F., Le-Tien L., Albu-Schäffer A., Konietschke R., Grebenstein M., Warpup R., Haslinger R., Frommberger M., and Hirzinger G. (2008). The DLR MIRO: A versatile light-weight robot for surgical applications. *Industrial Robot: An International Journal*, 35(4):324–336.

Hecker S. (2008). Improved mu-analysis results by using low order uncertainty modelling techniques. *AIAA Journal of Guidance, Control and Dynamics*, 31(4).

Hecker S. and Varga A. (2006). Symbolic manipulation techniques for low order LFT-based parametric uncertainty modelling. *International Journal of Control*, 79(11):1485–1494.

Hecker S., Varga A., and Magni J.-F. (2005). Enhanced LFR-toolbox for MATLAB. *Aerospace Science and Technology*, 9:173–180.

Heckmann A., Arnold M., and Vaculin O. (2005). A modal multifield approach for an extended flexible body description in multibody dynamics. *Multibody System Dynamics*, 13:299–322.

Heipke C., Oberst J., Albertz J., Attwenger M., Dorninger P., Dorrer E., Ewe M., Gehrke S., Gwinner K., Hirschmüller H., Kim J. R., Kirk R. L., Mayer H., Muller J.-P., Rengarajan R., Rentsch M., Schmidt R., Scholten F., Shan J., Spiegel M., Wählisch M., and Neukum G. (2007). Evaluating Planetary Digital Terrain Models - The HRSC DTM Test. *Planetary and Space Science*, 55:2173–2191.

Helbert J., Arnold G., Benkhoff J., Hirsch H., Maturilli A., Formisano V., and Giuranna M. (2005). Comparison of surface temperatures measured by the Planetary Fourier Spectrometer (PFS) on Mars Express with predictions from the Berlin Mars near Surface Thermal model (BMST) for the BEAGLE 2 landing site in Isidis Planitia. *Advances in Space Research*.

Hetzheim H. (2007). Automated contrail and cirrus detection using stochastic properties. *International Journal of Remote Sensing*, 28(9):2033–2048.

Hetzheim H. and Tuchscheerer W. (2007). An image processing based traffic estimation system. *Transport Science and Technology*, pages 275–284.

Hillenbrand U. (2007). Consistent parameter clustering: definition and analysis. *Pattern Recognition Letters*, 28(16):1112–1122.

Hirschmüller H. (2008). Stereo Processing by Semi-Global Matching and Mutual Information. *in IEEE Transactions on Pattern Analysis and Machine Intelligence*, 30(2):328–341.

Hirzinger G. (2007). Eine neue Robotergeneration für Raumfahrt, Dienstleistung und Chirurgie. *it - Information Technology*.

Hirzinger G. and Albu-Schäffer A. (2008). Light-Weight Robots. *Scholarpedia*, 3(4):3889.

Hirzinger G., Bals J., Otter M., and Stelter J. (2005). The DLR-KUKA Success Story. *IEEE Robotics & Automation Magazine*, 12(3):16–23.

Holzäpfel F., Frech M., Gerz T., Tafferner A., Hahn K.-U., Schwarz C., Joos H.-D., Korn B., Lenz H., Luckner R., and Höhne G. (2007). Aircraft Wake Vortex Scenarios Simulation Package - WakeScene. *Aerospace Science and Technology*.

Kaiser I. (2005). Modellierung und Simulation des Laufverhaltens von elastischen Radsätzen auf elastischen Schienen. *Der Eisenbahningenieur*, 56(7):67–71.

Kienitz K. H. (2005). On the Implementation of the Eigenvalue Method for Limit Cycle

Determination in Nonlinear Systems. *Nonlinear Dynamics*.

Kienitz K. H. and Bals J. (2005). Pulse modulation for attitude control with thrusters subject to switching restrictions. *Aerospace Science and Technology*, 9:635–640.

Kübler B., Seibold U., and Hirzinger G. (2005). Development of actuated and sensor integrated forceps for minimally invasive robotic surgery. *International Journal Medical Robotics and Computer Assisted Surgery*, 1(3):96–107.

Lagerkvist C.-I., Moroz L., Nathues A., Erikson A., Lahulla F., Karlsson O., and Dahlgren M. (2005). A Study of Cybele asteroids II. Spectral properties of Cybele asteroids. *Astronomy and Astrophysics*, 432:349–354.

Landzettel K. (2006). Weltraumrobotik, Aufgaben und Entwicklungsstand. *Zeitschrift: Raumfahrt Concret*, 42.

Landzettel K. (2006). Weltraumrobotik (Helfer im Weltraum). *Mobiles*.

Lange F. and Werner J. (2008). Montage am laufenden Band. *Computer and Automation*, (9):74–77.

Liu H., Meusel P., Hirzinger G., Jin M., Liu Y., and Xie Z. (2008). The Modular Multisensory DLR-HIT-Hand: Hardware and Software Architecture. *Transactions on Mechatronics*, 13:461–469.

Looye G. and Joos H.-D. (2006). Design of Autoland Controller Functions with Multiobjective Optimization. *AIAA Journal of Guidance, Control, and Dynamics*, 29(2):475–484.

Lorenz E. and Jahn H. (2005). BIRD: More than 3 years experience in orbit. *Small Satellites for Earth Observation - Selected Proceedings of the 5th International Symposium of the International Academy of Astronautics, Berlin 4-8, 2005, H.-P. Röser, R. Sandau, A. Valenzuela (eds.), ISBN:3-11-018851-1*, V:102–109.

Lübberstedt H., Penné B., Sandau R., and Oertel D. (2005). EKOSAT-IR - ecology-related earth observation and hot spot detection. *Acta Astronautica*, 56(1-2):81–88.

Maturilli A., Helbert J., Witzke A., and Moroz L. (2006). Emissivity Measurements of Analogue Materials for the Interpretation of data from PFS on Mars Express and MERTIS on Bepi-Colombo. *Planetary and Space Science*, 54(11):1057–1064.

Mischke S., Zhang C., and Börner A. (2007). Bias of ostracod stable isotope data caused by drying of sieve residues from water. *Journal of Paleolimnology*.

Oertel D., Lorenz E., Zhukov B., and Csiszar I. (2005). BIRD fire recognition and comparison with Terra/MODIS. *Small Satellites for Earth Observation - Selected Proceedings of the 5th International Symposium of the International Academy of Astronautics, Berlin 4-8, 2005, H.-P. Röser, R. Sandau, A. Valenzuela (eds.), ISBN:3-11-018851-1*, V:23–30.

Ortmaier T., Gröger M., Böhm D., Falk V., and Hirzinger G. (2005). Motion estimation in beating heart surgery. *IEEE Transactions on Biomedical Engineering*, 52(10):1729–1740.

Ott C., Albu-Schäffer A., Kugi A., and Hirzinger G. (2008). On the Passivity Based Impedance Control of Flexible Joint Robots. *IEEE Transactions on Robotics*, pages 416–429.

Otter M. (2008). Modellierung von Fahrzeugsystemen mit Modelica. *Automobiltechnologie in Bayern*, pages 44–46.

Pfeiffer A. and Arnold M. (2005). Numerical analysis of structure preserving Nyström methods for Hamiltonian systems. *Applied Numerical Mathematics*, 53:391–408.

Preusche C. and Hirzinger G. (2007). Haptics in Telerobotics. *The Visual Computer*, 23(4):273–284.

Reinhart G., Werner J., and Lange F. (2008). Robot Based System for the Automation of Flow Assembly Lines. *Annals of the German Academic Society for Production (WGP)*.

Ryu J.-H., Preusche C., Hannaford B., and Hirzinger G. (2005). Time domain passivity control with reference energy following. *IEEE Transactions on Control Systems Technology*, 13(5):737–742.

Schiller W., Schmid T., Spiegel K., Donisi S., Probst C., Kowacz A., Flacke S., Liepsch D., and Oertel H. (2006). Computational Simulation of Blood Flow in the Human Left Ventricle. *Journal Biomech*, 39(1):297.

Schmid T., Schiller W., Spiegel K., Stock M., Liepsch D., Hirzinger G., Oertel H., and Welz

A. (2006). Optimization of Ventricle-Shaped Chambers for the Implantable DLR Assist Device. *Biomechanics and Modelling in Mechanobiology*, 39(1):250.

Schmid T., Schiller W., Vodermayer B., Liepsch D., Welz A., and Hirzinger G. (2007). The completely implantable DLR-LVAD: System innovations and improvements. *International Journal of Artificial Organs*, 30(8):676.

Schmid T., Stock M., Donisi S., Schiller W., Liepsch D., Hirzinger G., Welz A., , and Oertel H. (2008). Development and verification of ventricle-shaped chambers for the DLR Assist Device. *International Journal of Artificial Organs*, 28(9):875.

Schmid T., Stock M., Donisl S., Schiller W., Liepsch D., Laschka B., Hirzinger G., Welz A., and Oertel H. (2005). Development and verification of ventricle-shaped chambers for the DLR assist device. *The international Journal of Artificial Organs, Speciall issue Abstracts of the XXXII ESAO Congress, Bologna, Italy 5-8October 2005*, 28(9):875–.

Stoll E., Artigas J., Preusche C., Kremer P., Letschnik J., Pongrac H., and Walter U. (2008). Ground Verification of the Feasibility of Telepresent On-Orbit Servicing. *Journal of Field Robotics*.

Stuffler T., Kaufmann H., Hofer S., Forster K.-P., Schreier G., Müller A., Eckardt A., Bach H., Penne B., Benz U., and Haydn R. (2007). The EnMAP hyperspectral imager-An advanced optical payload for future applications in Earth observation programmes. *Acta Astronautica*, 61:115–120.

Suppa M. and Hirzinger G. (2005). Ein Hand-Auge System zur multisensoriellen Rekonstruktion von 3D-Modellen in der Robotik. *at - Automatisierungstechnik*, 53(7):322–331.

Suppa M. and Hirzinger G. (2007). Multisensorielle Exploration von Roboterarbeitsräumen. *TM-Technisches Messen*, 74(3):139–146.

Terzibaschian T. (2005). Experiences with the BIRD magnetic coil system for wheel desaturation, satellite rate damping and attitude control - the concept of virtual wheel systems. *Small Satellites for Earth Observation - Selected Proceedings of the 5th International Symposium of the International Academy of Astronautics, Berlin 4-8, 2005, H.-P. Röser, R. Sandau, A. Valenzuela (eds.), ISBN:3-11-018851-1*, V:361–368.

Tetzlaff A., Zhukov B., Hirner A., Kuenzer C., and Voigt S. (2005). Coal fire quantification and detection using the DLR experimental bi-spectral infrared detection (BIRD) small satellite. *Small Satellites for Earth Observation - Selected Proceedings of the 5th International Symposium of the International Academy of Astronautics, Berlin 4-8, 2005, H.-P. Röser, R. Sandau, A. Valenzuela (eds.), ISBN:3-11-018851-1*, V:255–262.

Varga A. (2008). On solving periodic Riccati equations. *Numerical Linear Algebra witih Applications*, 15:809–835.

Vodermayer B., Gruber R., Schmid T., Schiller W., Hirzinger G., Liepsch D., and Welz A. (2005). Adaptive transcutaneous energy transfer system (TET) for implantable devices. *The international Journal of Artificial Organs, Speciall issue Abstracts of the XXXII ESAO Congress, Bologna, Italy 5-8October 2005*, 28(9):885–.

Vodermayer B., Gruber R., Schmid T., Schiller W., Hirzinger G., Liepsch D., and Welz A. (2006). PID vs Fuzzy Logic Control for New Adaptive Transcoutaneous Energy Transmission System (TET) for Implantable Devices. *Journal Biomech*, 39(1):250.

Walter I., Brieß K., Bärwald W., Lorenz E., Skrbek W., and Schrandt F. (2005). A microsatellite platform for hot spot detection. *Acta Astronautica*, 56(1-2):221–229.

Zäh M., Werner J., and Lange F. (2006). System zur vollautomatisierten förderbandsynchronen Montage. *Werkstatttechnik wt-online*, 96(9):592–596.

Zhukov B., Briess K., Lorenz E., Oertel D., and Skrbek W. (2005). Detection and analysis of high-temperature events in the BIRD mission. *Acta Astronautica*, 56(1-2):65–71.

Zhukov B., Lorenz E., Oertel D., Wooster M., and Roberts G. (2006). Spaceborne detection and characterization of fires during the bi-spectral infrared detection (BIRD) experimental small satellite mission (2001-2004). *Remote Sensing of Environment*, 100(1):29–51.

5.2 Conference Papers (“c”)

Below you will find 348 references to publications presented at national and interna-

tional conferences:

Abiko S. and Hirzinger G. (2007a). An Adaptive Control for a Free-Floating Space Robot by Using Inverted Chain Approach. In *Proc. IEEE/RSJ Int. Conf. on Intelligent Robots and Systems (IROS)*.

Abiko S. and Hirzinger G. (2007b). On-line Parameter Adaptation for a Momentum Control in the Post-Grasping of a Tumbling Target with Model Uncertainty. In *Proc. IEEE/RSJ Int. Conf. on Intelligent Robots and Systems (IROS)*.

Abiko S. and Hirzinger G. (2008). Computational efficient Algorithms for Operational Space Formulation of Branching Arms on Space Robots. In *Proc. IEEE/RSJ Int. Conf. on Intelligent Robots and Systems (IROS)*.

Abiko S., Lampariello R., and Hirzinger G. (2006). Impedance Control for a Free-Floating Robot in the Grasping of a Tumbling Target with Parameter Uncertainty. In *Proc. IEEE/RSJ Int. Conf. on Intelligent Robots and Systems (IROS)*, pages 1020–1025. IEEE/IROS International Conference on Intelligent Robots and Systems.

Abmayr T., Dalton G., Härtl F., Hines D., Liu R., Hirzinger G., and Fröhlich C. (2005). Standardization and Visualization of 2.5D Scanning Data and Color Information by Inverse Mapping. In *Proc. 7th Conference on Optical 3-D Measurement Techniques*.

Abmayr T., Härtl F., Hirzinger G., Burschka D., and Fröhlich C. (2008). Automatic Registration of Panoramic 2.5D Scans and Color Images. In *EuroCOW 2008, International Calibration and Orientation Workshop*.

Agrawal S., Pathak K., Franch J., Lampariello R., and Hirzinger G. (2006). Design of a Differentially Flat Open-Chain Space Robots with Arbitrarily Oriented Joints and Two Momentum Wheels at the Base. In *Proc. IEEE Int. Conf. on Robotics & Automation (ICRA)*, pages 3867–3872.

Albu-Schäffer A., Bertleff W., Rebele B., Schäfer B., Landzettel K., and Hirzinger G. (2006). ROKVISS - Robotics Component Verification on ISS Current Experimental Results on Parameter Identification. In *Proc. IEEE Int. Conf. on Robotics & Automation (ICRA)*, pages 3879–3884.

Albu-Schäffer A., Bicchi A., Chatila R., Luca De A., Giralt G., Hirzinger G., Mattone R., Oriolo G., Schiavi R., Siciliano B., Tonietti G., Vendittelli M., and Villani L. (2005). Physical Human-Robot Interaction in Anthropic Domains: Safety and Dependability. In *Proc. 4th IARP/IEEE-RAS/EURON Workshop on Technical Challenges for Dependable Robots in Human Environments*.

Albu-Schäffer A., Ott C., and Hirzinger G. (2005). Constructive Energy Shaping Based Impedance Control for a Class of Underactuated Euler-Lagrange Systems. In *Proc. IEEE Int. Conf. on Robotics & Automation (ICRA)*, pages 1399–1405. IEEE.

Andreasson J. and Bünte T. (2006). Global Chassis Control Based on Inverse Vehicle Dynamics Models. In *Proc. International Association for Vehicle System Dynamics Symposium (IAVSD)*, number 44.

Arnold G., Helbert J., Hiesinger H., Hirsch H., Jessberger E. K., Peter G., Walter I., and MERTIS-Team (2007). MERTIS - MErcury Radiometer and Thermal Infrared Spectrometer- a novel thermal imaging spectrometer for the exploration of Mercury. In *Proc. International Conferecen on Advanced Infrared Technology and Applications (AITA)*.

Artigas J., Kremer P., Preusche C., and Hirzinger G. (2006a). Testbed for Telepresent On-Orbit Satellite Servicing. In *Proc. Human Centered Robotic Systems (HCRS)*.

Artigas J. and Preusche C. (2005). Time-delayed Telepresence Introduction to passivity based bilateral control. In *Europaeisches Virtuelles Seminar*.

Artigas J., Preusche C., Borghesan G., and Melchiorri C. (2008). Bilateral Energy Transfer in Delayed Teleoperation on the Time Domain. In *Proc. IEEE Int. Conf. on Robotics & Automation (ICRA)*, pages 671–676.

Artigas J., Preusche C., and Hirzinger G. (2007). Time Domain Passivity for delayed Haptic Telepresence with Energy Reference. In *Proc. IEEE/RSJ Int. Conf. on Intelligent Robots and Systems (IROS)*, pages 1612–1617.

Artigas J., Vilanova J., Preusche C., and Hirzinger G. (2006b). Time Domain Passivity Control Based Telepresence with Time Delay. In *Proc. IEEE/RSJ Int. Conf. on Intelligent Robots and Systems (IROS)*, pages 4205–4210. IEEE/IROS International Conference on Intelligent Robots and Systems.

Bajcinca N. (2005). A necessary stabilization condition for PID control. In *Proc. American Control Conference (ACC)*.

Bajcinca N. (2005). Robust Autonomous Car Steering Based on Vehicle Dynamics Inversion. In *Proc. IEEE International Conference on Control Applications (CCA)*.

Bajcinca N. (2005). Robuste Regelung für Steer-by-Wire Lenksysteme. In *39. Regelungstechnisches Kolloquium*.

Bajcinca N. and Bünte T. (2005). A novel control structure for dynamic inversion and tracking. In *Proc. 16th IFAC World Congress*.

Bajcinca N. and Naunin D. (2005). Two Degree of Freedom Resonant Structure for Robust Current Control and Active Power Filtering. In *Proc. 11th European Conference on Power Electronics and Applications (EPE)*.

Bajcinca N., Schürmann N., and Bals J. (2005). Two degree of freedom motion control of an energy optimized aircraft ram air inlet actuators. In *Proc. International Conference on Control and Automation (ICCA)*.

Bals J., Hofer G., Pfeiffer A., and Schallert C. (2005). Virtual Iron Bird - A Multidisciplinary Modelling and Simulation Platform for New Aircraft System Architectures. In *DGLR Jahrestagung*.

Bals J. and Kienitz K. H. (2005). A Comprehensive Approach to Pulse Modulation for Attitude Control with Thrusters Subject to Switching Restrictions. In *DGLR Jahrestagung*, volume I & II.

Bauer M., Börner A., Jahn H., Scheele M., Schischmanow A., and Schuster R. (2006). Dynamische Beugungsmuster als Passpunktfelder für die geometrische Kalibration. In *DGPF-Jahrestagung 2006*, volume 2006, pages 303–310. DGPF.

Bäuml B. and Hirzinger G. (2006). Agile Robot Development (aRD): A Pragmatic Approach to Robotic Software. In *Proc. IEEE/RSJ Int. Conf. on Intelligent Robots and Systems (IROS)*, pages 3741–3748. IEEE/IROS International Conference on Intelligent Robots and Systems.

Baur M., Ungethüm J., Treffinger P., Otter M., and Schweiger C. (2006). Alternative Vehicles - Modelica Bibliothek zur Simulation von alternativen Fahrzeugkonzepten. In *Proc. Steuerung und Regelung von Fahrzeugen und Motoren - AUTOREG 2006*, volume 1931. VDI Verlag GmbH.

Bellmann T. (2008). An Innovative Driving Simulator: Robocoaster. In *Proc. FISITA 2008*.

Bellmann T., Otter M., Heindl J., and Hirzinger G. (2007). Realtime pathplanning for an interactive and industrial robot based motion simulator. In *Proc. Motion Simulator Conference*.

Bitzer S. and Smagt van der P. (2006). Learning EMG control of a robotic hand: Towards Active Prostheses. In *Proc. IEEE Int. Conf. on Robotics & Automation (ICRA)*, pages 4179–4186.

Bodenmüller T., Sepp W., Suppa M., and Hirzinger G. (2007). Tackling Multi-sensory 3D Data Acquisition and Fusion. In *Proc. IEEE/RSJ Int. Conf. on Intelligent Robots and Systems (IROS)*, pages 2180–2185. IEEE.

Börner A., Catala Prat A., Ernst I., Grießbach D., Krutz D., Lethaus F., Rataj J., Rollenhagen F., and Wohlfeil J. (2008). Sensor Fusion Approaches for High Precision Location Applications. In *Proc. FISITA World Automotive Congress 2008*, volume 8, pages 1–6. Springer Automotive Media.

Börner A., Hirschmüller H., Neidhardt M., Scheibe K., Wohlfeil J., and Zuev S. (2007). Ableitung photogrammetrischer Produkte mit der MFC-Kamera. In *Dreiländertagung 2007, Gemeinsame Jahrestagung der SGPBF, DGPF und OVG*.

Börner A., Hirschmüller H., Scheibe K., Suppa M., and Wohlfeil J. (2008). MFC - a modular line camera for 3D world modelling. In *Proc. Robot Vision, International Workshop RobVis 2008*, pages 319–326. Springer.

Börner A., Kiemle C., and Wirth M. (2006). A simulation approach for airborne DIAL systems. In *Proc. SPIEs Remote Sensing Europe Symposium*, volume 6376. SPIE.

Börner A., Suppa M., Abmayr T., Bodenmüller T., Eckardt A., Hirschmüller H., Scheibe K., and Strackenbrock B. (2006). Ein modulares Sensorsystem zur multiskalaren Erfassung von dreidimensionalen Objekten. In *DGPF-Jahrestagung 2006*, volume 15, pages 319–326. DGPF.

Borst C., Ott C., Wimböck T., Brunner B., Zacharias F., Bäuml B., Hillenbrand U., Haddadin S., Albu-Schäffer A., and Hirzinger G.

(2007). A humanoid upper-body system for two-handed manipulation. In *Proc. IEEE Int. Conf. on Robotics & Automation (ICRA)*, pages 2766–2767. IEEE.

Bucher T. (2007). Atmospheric correction of HRSC-AX line scanner data using the Dark-Pixel-Profile (dpp) method: A summary after 2 years. In *Proc. Remote Sensing for Environmental Monitoring, GIS Applications, and Geology VII*, volume 6749, pages 1–7. SPIE.

Bucher T. (2007). Die DPP-Methode: ein einfacher empirischer Ansatz zur Korrektur atmosphärischer Effekte in HRSC-AX Scannerdaten. In *Dreiländertagung SGPBF, DGPF und OVG, 27. Wissenschaftlich-Technische Jahrestagung der DGPF 2007*, volume 16, pages 181–188.

Bünte T. and Andreasson J. (2006). Integrierte Fahrwerkregelung mit minimierter Kraftschlussausnutzung auf der Basis dynamischer Inversion. In *Steuerung und Regelung von Fahrzeugen und Motoren - Autoreg 2006*, volume 1931. VDI Verlag GmbH.

Bünte T., Andreasson J., and Knobel C. (2006). On Road Vehicle Motion Control striving towards synergy. In *Proc. 8th International Symposium on Advanced Vehicle Control - AVEC*.

Bünte T., Sahin A., and Bajcinca N. (2005). Inversion of Vehicle Steering Dynamics with Modelica/Dymola. In *Proc. 4th International Modelica Conference*, pages 319–328.

Burschka D. (2006). Robust Feature Correspondences for Vision-Based Navigation with Slow Frame-Rate Cameras. In *Proc. IEEE/RSJ Int. Conf. on Intelligent Robots and Systems (IROS)*, pages 947–952. IEEE/RSJ International Conference on Intelligent Robots and Systems.

Busam A., Suppa M., Konietschke R., Bodenmüller T., Boesecke R., Wiechnik J., Eggers G., Ortmaier T., Hirzinger G., Mühling J., and Marmulla1 R. (2007). Risikoanalyse für einen handgeführten Laserscanner zur Patientenregistrierung in der navigierten MKG-Chirurgie. In *Proc. Jahrestagung der Deutschen Gesellschaft für Computer- und Roboterassistierte Chirurgie*.

Carrarini A. (2006). Reliability based analysis of the crosswind stability of railway vehicles. In *SIMPACK User Meeting*.

Carrarini A. (2006). Zuverlässigkeitsbasierte Analyse der Seitenwindstabilität von Schienenfahrzeugen. In *Proc. 8. Internationale Schienenfahrzeugtagung "Rad Schiene 2006"*.

Carrarini A. (2007). Efficient models and techniques for the computational analysis of railway vehicles in crosswinds. In *Proc. International Association for Vehicle System Dynamics Symposium (IAVSD)*.

Casella F., Otter M., Proelss K., Richter C., and Tummescheit H. (2006). The Modelica Fluid and Media Library for Modeling of Incompressible and Compressible Thermo-Fluid Pipe Networks. In *Proc. 5th International Modelica Conference*, pages 631–640.

Castellini C., Smagt van der P., Sandini G., and Hirzinger G. (2008). Surface EMG for Force Control of Mechanical Hands. In *Proc. IEEE Int. Conf. on Robotics & Automation (ICRA)*, pages 725–730.

Conradt M. (2005). Derivation and visualization of the real dynamic spacecraft orientation of BIRD. In *Proc. 5th Symposium on Small Satellites for Earth Observation*, volume V, pages 377–381. Wissenschaft & Technik Verlag.

De Luca A., Albu-Schäffer A., Haddadin S., and Hirzinger G. (2006). Collision Detection and Safe Reaction with the DLR-III Lightweight Manipulator Arm. In *Proc. IEEE/RSJ Int. Conf. on Intelligent Robots and Systems (IROS)*, pages 1623–1630.

De Santis A., Albu-Schäffer A., Ott C., Siciliano B., and Hirzinger G. (2007). The skeleton algorithm for self-collision avoidance of a humanoid manipulator. In *Proc. International Conference on Advanced Intelligent Mechatronics*.

Dempsey M., Gäfvert M., Harman P., Kral C., Otter M., and Treffinger P. (2006). Coordinated automotive libraries for vehicle system modelling. In *Proc. 5th International Modelica Conference*, pages 33–41.

Eckardt A., Börner A., Jahn H., Hilbert S., and Walter I. (2006). Neue optische Sensorsysteme für die Erdbeobachtung. In *Proc. 26. Wissenschaftlich-Technische Jahrestagung der DGPF*, volume 2006, pages 327–334. DGPF.

Eckardt A., Börner A., Jahn H., Hilbert S., and Walter I. (2006). New optical sensor systems for photogrammetry and remote sensing. In *Proc. SPIE European Symposium on Remote Sensing*, volume 6361, pages U45–U52. SPIE.

Eckardt A., Börner A., Jahn H., and Reulke R. (2008). Space instrument performance traceability for high resolution satellite systems. In *Proc. Earth Observing Systems XIII, Conference 7081*.

Eckardt A., Börner A., and Lehmann F. (2007). New optical sensor systems for high-resolution satellite, airborne and terrestrial imaging systems. In *Proc. SPIE Europe Symposium on Remote Sensing*, volume 6744, pages 74408–74408. SPIE.

Eckardt A., Walter I., and Schuster R. (2005). Low Light Panoramic Camera. In *Proc. Panoramic Photogrammetry Workshop*, volume XXXVI-5/W8, pages 1–5.

Eckardt A., Walter I., and Schuster R. (2005). Neue Generation einer 360° Panoramakamera. In *Proc. 25. Wissenschaftlich-Technische Jahrestagung der DGPF*, volume 14, pages 439–446.

Eckert S., Ritzmann S., Eckler J., and Bärwald W. (2007). On orbit verification with an technology test carrier TET. In *Proc. 6th Symposium on Small Satellites for Earth Observation*, volume VI, pages 33–36. Wissenschaft und Technik Verlag Berlin.

Elmqvist H., Olsson H., Mattsson S. E., Brück D., Schweiger C., Joos H.-D., and Otter M. (2005). Optimization for Design and Parameter Estimation. In *Proc. 4th International Modelica Conference*, pages 255–266.

Ernst I. and Hirschmüller H. (2008). Mutual Information based Semi-Global Stereo Matching on the GPU. In *Proc. the International Symposium on Visual Computing*, volume LNCS 5358, Part 1, pages 228–239.

Fenili A., Gadelha de Souza L., and Schäfer B. (2005). The Determination of the Velocities after Impact for the Constrained Bar Problem. In *Proc. 18th International congress of Mechanical Engineering*.

Fenili A., Gadelha de Souza L., and Schäfer B. (2005). A Mathematical Model to Investigate Contact Dynamics in Constrained Robots. In *Proc. XI DINAME: XIth International Symposium on Dynamic Problems of Mechanics*.

Foeckersperger S., Lattner K., Kaiser C., Eckert S., Bärwald W., Ritzmann S., Mühlbauer P., Turk M., and Willemsen P. (2008). TET-1 - A German microsatellite for technology on-orbit verification. In *Proc. 4S Symposium*, pages 1–11.

Frumento S., Michelini R., Konietschke R., Hagn U., Ortmaier T., and Hirzinger G. (2006). A Co-Robotic Positioning Device for Carrying Surgical End-Effectors. In *Proc. International Conference ASME-ESDA*, pages 1–8.

Fuchs S. and Hirzinger G. (2008). Extrinsic and Depth Calibration of ToF-cameras. In *Proc. Computer Society Conference on Computer Vision and Pattern Recognition*.

Gao X., Jin M., Xie Z., Jiang L., Ni F., Shi S., Wei R., Zhu Y., Cai H., Liu H., Beyer A., Krämer E., Landzettel K., Schott J., and Hirzinger G. (2006). Development of the Chinese Intelligent Space Robotic System. In *Proc. IEEE/RSJ Int. Conf. on Intelligent Robots and Systems (IROS)*. IEEE/RSJ International Conference on Intelligent Robots and Systems.

Gibbesch A. (2006). Multibody System Modelling and Simulation of Planetary Rover Mobility on Soft Terrain. In *SIMPACK User Meeting*.

Gibbesch A. and Schäfer B. (2005). Multibody System Modelling and Simulation of Plenetary Rover Mobility on Soft Terrain. In *Proc. International Symposium on Artificial Intelligence, Robotics and Automation in Space*.

Gibbesch A. and Schäfer B. (2006). Modelling of planetary rovers by means of a dynamical system approach with respect to mobility requirements. In *Proc. 10th European Conference of the ISTVS 2006*.

Gibbesch A., Schäfer B., and Michaud S. (2006). 3D Simulation and Validation of RCL-E and MER Rover Types Mobility. In *ESA Workshop on Advanced Space Technologies for Robotics and Automation (ASTRA)*.

Gil J., Sanchez E., Hulin T., Preusche C., and Hirzinger G. (2007). Stability Boundary for Haptic Rendering: Influence of Damping and Delay. In *Proc. IEEE Int. Conf. on Robotics & Automation (ICRA)*. IEEE.

Görner M. and Hirzinger G. (2008). The

DLR-Crawler: Gaits and Control of an Actively Compliant Hexapod. In *Proc. International Conference on Climbing and Walking Robots (CLAWAR)*.

Görner M., Wimböck T., Baumann A., Fuchs M., Bahls T., Grebenstein M., Borst C., Butterfass J., and Hirzinger G. (2008). The DLR-Crawler: A Testbed for Actively Compliant Hexapod Walking Based on the Fingers of DLR-Hand II. In *Proc. IEEE/RSJ Int. Conf. on Intelligent Robots and Systems (IROS)*, pages 1525–1531.

Grenzdörffer G. and Zuev S. (2007). Bestimmung des photogrammetrischen Genauigkeitspotentials des Online-Systems ANTAR zur luftgestützten Verkehrsdatenerfassung. In *Dreiländertagung 2007, Gemeinsame Jahrestagung der SGPBF, DGPF und OVG*.

Gröger M., Arbter K., and Hirzinger G. (2006). Analysis of colour distributions of anodised titanium clips and the heart surface for tracking. In *Proc. Bildverarbeitung für die Medizin*, pages 355–358. Springer.

Gröger M. and Hirzinger G. (2006a). Image stabilisation of the beating heart by local linear interpolation. In *Medical Imaging 2006: Visualization, Image-Guided Procedures, and Display*, volume 6141 of *Proceedings of SPIE*, San Diego, USA.

Gröger M. and Hirzinger G. (2006b). Optical flow to analyse stabilised images of the beating heart. In *Proc. International Conference on Computer Vision Theory and Applications (VISAPP)*, pages 237–244. INSTICC Press.

Gröger M., Ortmaier T., and Hirzinger G. (2005a). Structure tensor based substitution of specular reflections for improved heart surface tracking. In *Proc. Bildverarbeitung für die Medizin*, pages 242–246. Springer.

Gröger M., Sepp W., and Hirzinger G. (2005b). Structure driven substitution of specular reflections for realtime heart surface tracking. In *Proc. IEEE International Conference on Image Processing (ICIP)*, volume 2, pages 1066–1069.

Grunwald G., Borst C., and Zöllner M. J. (2008). Benchmarking dexterous dual-arm/hand robotic manipulation. In *Proc. IEEE/RSJ IROS 2008 Workshop on Performance Evaluation and Benchmarking for Intelligent Robots and Systems*.

Grunwald G., Plank G., Reintsema D., Zimmermann U. E., and Bischoff R. (2008). Communication, Configuration, Application: The three layer concept for Plug-and-Produce. In *Proc. International Conference on Informatics in Control, Automation & Robotics (ICINCO)*.

Günther F., Schroeder-Bodenstein K., Heckmann A., Kurzeck B., and Carrarini A. (2008). Analysis of Nonlinear Vibration Phenomena in Trains During Breaking. In *Proc. 9th International Conference on Motion and Vibration Control (MOVIC)*.

Gurdan D., Stumpf J., Achtelik M., Doth K.-M., Hirzinger G., and Rus D. (2007). Energy-efficient Autonomous Four-rotor Flying Robot Controlled at 1 kHz. In *Proc. IEEE Int. Conf. on Robotics & Automation (ICRA)*, pages 361–366.

Haddadin S., Albu-Schäffer A., De Luca A., and Hirzinger G. (2008a). Collision Detection and Reaction: A Contribution to Safe Physical Human-Robot Interaction. In *Proc. IEEE/RSJ Int. Conf. on Intelligent Robots and Systems (IROS)*, pages 3356–3363.

Haddadin S., Albu-Schäffer A., De Luca A., and Hirzinger G. (2008b). Evaluation of Collision Detection and Reaction for a Human-Friendly Robot on Biological Tissues. In *Proc. IARP International Workshop on Technical challenges and for dependable robots in Human environments*.

Haddadin S., Albu-Schäffer A., Frommberger M., and Hirzinger G. (2008d). The Role of the Robot Mass and Velocity in Physical Human-Robot Interaction - Part II: Constrained Blunt Impacts. In *Proc. IEEE Int. Conf. on Robotics & Automation (ICRA)*, pages 1339–1345.

Haddadin S., Albu-Schäffer A., and Hirzinger G. (2007a). Approaching Asimov's 1st Law: The Role of the Robot's Weight Class, Robotics. In *Proc. Manupulation Workshop, Robotics: Science and Systems Conference*.

Haddadin S., Albu-Schäffer A., and Hirzinger G. (2007b). Dummy Crash-Tests for the Evaluation of Rigid Human-Robot Impacts. In *Proc. International Workshop on Technical Challenges for Dependable Robots in Human Environments*.

Haddadin S., Albu-Schäffer A., and Hirzinger G. (2007c). Safe Physical Human-Robot Interaction: Measurements, Analysis and New Insights. In *Proc. International Symposium on Robotics Research*, pages 439–450.

Haddadin S., Albu-Schäffer A., and Hirzinger G. (2007d). Safety Evaluation of Physical Human-Robot Interaction via Crash-Testing, Robotics. In *Proc. Robotics: Science and Systems Conference*, pages 217–224.

Haddadin S., Albu-Schäffer A., and Hirzinger G. (2007e). Approaching Asimov's 1st Law. In *Proc. 2nd ACM/IEEE International Conference on Human-Robot Interaction*, pages 177–184.

Haddadin S., Albu-Schäffer A., and Hirzinger G. (2008c). The Role of the Robot Mass and Velocity in Physical Human-Robot Interaction - Part I: Unconstrained Blunt Impacts. In *Proc. IEEE Int. Conf. on Robotics & Automation (ICRA)*, pages 1331–1338.

Haddadin S., Albu-Schäffer A., Strohmayr M., Frommberger M., and Hirzinger G. (2008e). Injury Evaluation of Human-Robot Impacts. In *Proc. IEEE Int. Conf. on Robotics & Automation (ICRA)*, pages 2203–2204.

Haddadin S., Albu-Schäffer A., and Hirzinger G. (2008f). Safety in Human-Robot Interaction. In *Proc. Manipulation Workshop, Robotics: Science and Systems Conference*.

Haddadin S., Laue T., Frese U., and Hirzinger G. (2007e). Foul 2050: Thoughts on Physical Interaction in Human-Robot Soccer. In *Proc. IEEE/RSJ Int. Conf. on Intelligent Robots and Systems (IROS)*, pages 3243–3250.

Hagn U., Nickl M., Jörg S., Tobergte A., Kübler B., Passig G., Gröger M., Fröhlich F., Seibold U., Konietschke R., Le-Tien L., Albu-Schäffer A., Grebenstein M., Ortmaier T., and Hirzinger G. (2008). DLR MiroSurge–towards versatility in surgical robotics. In *Proc. 7. Jahrestagung der Deutschen Gesellschaft für Computer- und Roboterassistierte Chirurgie e.V.*, pages 143–146.

Hähnle M. and Sporer N. (2005). Drehmomentgeregelte Servoantriebe für Industrie, Fahrsimulatoren und Steer-by-Wire. In *Proc. Internationales Forum für Mechatronik (ifm)*, pages 195–204.

Halle W. and Schlicker M. (2007). Echtzeitbildverarbeitung zur Fernüberwachung von kleinen Flughäfen. In *Proc. 52. Internationales Kolloquium an der TU Ilmenau*.

Hausamann D. and Kaiser I. (2005). Das DLR_School_Lab Oberpfaffenhofen ein außerschulischer Lernort aus der Luft- und Raumfahrtforschung. In *Proc. 69. Jahrestagung der Deutschen Physikalischen Gesellschaft*, volume 40, page 111.

Hecker S. (2006). Robust H-based vehicle steering control design. In *Proc. IEEE International Conference on Control Applications (CCA)*.

Hecker S. (2007). Enhanced symbolic factorization for low order LFT-modelling and improved -analysis for RCAM. In *Proc. AIAA Guidance, Navigation and Control Conference*.

Hecker S. (2008). Generation of LPV and LFT-models for the COFCLUO nonlinear aircraft model. In *Proc. Workshop on Clearance of Flight Control Laws*.

Hecker S. and Hahn K.-U. (2007). Advanced gust load alleviation system for large flexible aircraft. In *CEAS European Air and Space Conference*.

Hecker S. and Varga A. (2005). Symbolic techniques for low order LFT-modelling. In *Proc. 16th IFAC World Congress*.

Hecker S., Varga A., and Looye G. (2008). A desktop environment for assessment of fault diagnosis based fault tolerant flight control laws. In *Proc. IEEE International Symposium on Computer-Aided Control Systems Design (CASCD)*.

Heckmann A. (2006). A Brake Model with Thermoelastic Disc for the Analysis of Vehicle Judder Vibrations. In *Proc. International Association for Vehicle System Dynamics Symposium (IAVSD)*, volume 44, pages 360–367.

Heckmann A. and Arnold M. (2005). Flexible Bodies with Thermoelastic Properties in Multibody Dynamics. In *Proc. ECCOMAS Thematic Conference*.

Heckmann A., Otter M., Dietz S., and López J. D. (2006). The DLR FlexibleBody library to model large motions of beams and of flexible bodies exported from finite element programs. In *Proc. 5th International Modelica Conference*, pages 85–95.

Heindl J., Otter M., Hirschmueller H., Fromberger M., Siegert F., and Heinrich H. (2006). The Robocoaster simulation platform, path and video generation for an authentic mars flight simulation. In *Proc. Joint Conference on Robotics / ROBOTIK (ISR)*.

Helbert J., Jessberger E., Benkhoff J., Arnold G., Banaszkiewicz M., Bischoff A., Blecka M., Calcutt S., Coangeli L., Coradini A., Erard S., Fonti S., Killen R., Knollenberg J., Kührt E., Mann I., Mall U., Moroz L., Peter G., Rataj M., Robinson M. S., Spohn T., Sprague A., Stöffler D., Taylor F., and Warrell J. (2005). MERTIS - A Thermal Infrared Imaging Spectrometer for the Bepi-Colombo Mission. In *Proc. XXXVI Lunar and Planetary Science Conference*, volume 1234, page 1753. Lunar and Planetary Institute, Houston, TX.

Helbert J., Jessberger E. K., Benkhoff J., Arnold G., Lorenz E., Peter G., Spohn T., Venus H., Walter I., and investigator Team T. M. C. (2005). MERTIS The MERcury Thermal infrared Imaging Spectrometer for the Bepi-Colombo mission. In *Proc. European Geosciences Union General Assembly*, volume 7, pages abstract EGU05–A–07503.

Helbert J., Jessberger E. K., Benkhoff J., Arnold G., and Team T. M. C.-I. (2005). MERTIS? A Thermal infrared imaging spectrometer for the Bepi-Colombo mission. In *Proc. Asia Oceania Geosciences Society's 2nd Annual Meeting (AOGS)*.

Herrnberger M., Heller M., Paul R., Hecker S., and Sachs G. (2007). Advanced Uncertainty Modeling and Robustness Analysis for the Basic Flight Control System of a Modern Jet Trainer. In *Proc. AIAA Guidance, Navigation and Control Conference*.

Hillenbrand U. (2008). Pose Clustering From Stereo Data. In *Proc. VISAPP International Workshop on Robotic Perception*, pages 23–32.

Hillenbrand U. and Lampariello R. (2005). Motion and Parameter Estimation of a Free-Floating Space Object from Range Data for Motion Prediction. In *Proc. 8th International Symposium on Artificial Intelligence, Robotics and Automation in Space*.

Hirschmüller H. (2005). Accurate and Efficient Stereo Processing by Semi-Global Matching and Mutual Information. In *Proc. IEEE Conference on Computer Vision and Pattern Recognition (CVPR)*, volume 2, pages 807–814. IEEE.

Hirschmüller H. (2006). Stereo Vision in Structured Enviroments by Consistent Semi-Global Matching. In *Proc. IEEE Conference on Computer Vision and Pattern Recognition (CVPR)*, pages 2386–2393.

Hirschmüller H., Mayer H., and Neukum G. (2006). Stereo Processing of HRSC Mars Express Images by Semi-Global Matching. In *Proc. International Archives of Photogrammetry, Remote Sensing and Spatial Information*, volume XXXVI, Part 4.

Hirschmüller H. and Scharstein D. (2007). Evaluation of Cost Functions for Stereo Matching. In *Proc. the IEEE Conference on Computer Vision and Pattern Recognition*. IEEE.

Hirschmüller H., Scholten F., and Hirzinger G. (2005). Stereo Vision Based Reconstruction of Huge Urban Areas from an Airborne Pushbroom Camera (HRSC). In *Proc. Pattern Recognition, 27th DAGM Symposium*, volume LNCS 3663, pages 58–66. Springer.

Hirzinger G. (2005). Robotik und Mechatronik. In *Innovationskongress der deutschen Hochschulmedizin*.

Hirzinger G. (2005). Weltraum-Robotik im DLR - Ergebnisse, Perspektiven und terrestrische Spin-Offs. In *Kolloqium Universität Würzburg, Lehrstuhl Informatik VII, 27.06.2005*.

Hirzinger G. (2006). Advancements in Robotics and Mechatronics. In *Proc. International Workshop on Robotics in the Alpe-Adria-Danube Region (RAAD)*.

Hirzinger G., Bodenmüller T., Hirschmüller H., Liu R., Sepp W., Suppa M., Abmayr T., and Strackenbrock B. (2005). Photo-realistic 3D modelling - From robotics perception towards cultural heritage. In *Proc. International Workshop on Recording, Modeling and Visualization of Cultural Heritage*.

Hirzinger G. and Fach M. (2008). Airship ALUSTRA and other flying robots. In *7th International Airship Convention 2008, DGLR, Celebrating the centenary of Luftschiffbau Zeppelin*.

Hirzinger G., Landzettel K., Reintsema D., Preusche C., Albu-Schäffer A., Rebele B., and Turk M. (2005). ROKVISS ROBOTICS COMPONENT VERIFICATION ON ISS. In *Proc. International Symposium on Artificial Intelligence, Robotics and Automation in Space*.

Höbinger M. and Otter M. (2008). Planar-MultiBody - A Modelica Library for Planar

Multi-Body Systems. In *Proc. 6th International Modelica Conference*, pages 549–556.

Hofer G., Ayeb M., and Theuerkauf H. (2006). Einsatz von Echtzeitsimulationen zur Integrstion elektrischer Flugzeugsysteme an einem Flugzeugsystemprüfstand. In *Proc. Deutscher Luft- und Raumfahrtkongress 2006*.

Hofer S., Kaufmann H., Stuffler T., Penné B., Schreier G., Müller A., Eckardt A., Bach H., Benz U., and Haydn R. (2006). EnMAP Hyperspectral Imager: an advanced optical payload for future applications in Earth observation programs - art. no. 63660E. In *Proc. Remote Sensing for Environmental Monitoring, GIS Applications and Geology VI*, volume 6366, pages E3660–E3660.

Holzäpfel F., Frech M., Tafferner A., Hahn K.-U., Schwarz C., Joos H.-D., Korn B., and Lenz H. (2005). Quantitative Risk Assessment: Wake Vortex Scenarios Simulation Package - WakeScene. In *Proc. 3rd annual WakeNet2 Europe Workshop*.

Holzäpfel F., Kladetzke J., Amelsberg S., Lenz H., Schwarz C., and De Visscher I. (2008). Aircraft Wake Vortex Scenarios Simulation for Take-Off and Departure. In *Proc. AIAA ICAS/ATIO 2008 Conference*.

Hosseini A., Artigas J., Preusche C., Brunberg A., and Hirzinger G. (2008). Online Passive Reconstruction -Based Bilateral Control under Time-Varying Communication Delay and Packet-Loss. In *Proc. 5th International Conference on Enactive Interfaces*.

Huang H., Jiang L., D.W. Z., J.D. Z., Cai H., Liu H., Meusel P., Willberg B., and Hirzinger G. (2006). The Development on a New Biomechatronic Prosthetic Hand Based on Under-actuated Mechanism. In *Proc. IEEE/RSJ Int. Conf. on Intelligent Robots and Systems (IROS)*. IEEE/RSJ International Conference on Intelligent Robots and Systems.

Hulin T., Gil J. J., Sanchez E., Preusche C., and Hirzinger G. (2006a). Experimental Stability Analysis of a Haptic System. In *Proc. ENACTIVE/06 Enaction & Complexity*, pages 157–158.

Hulin T., Kremer P., Scheibe R., Schätzle S., and Preusche C. (2007). Evaluating Two Novel Tactile Feedback Devices. In *Proc. 4th International Conference on Enactive Interfaces*.

Hulin T., Preusche C., and Hirzinger G. (2005). Haptic rendering for virtual assembly verification. In *Proc. World Haptics Conference (WHC)*.

Hulin T., Preusche C., and Hirzinger G. (2006b). Stability Boundary and Design Criteria for Haptic Rendering of Virtual Walls. In *Proc. SYROCO, 8th International IFAC Symposium on Robot Control*.

Hulin T., Preusche C., and Hirzinger G. (2006c). Stability Boundary for Haptic Rendering: Influence of Physical Damping. In *Proc. IEEE/RSJ Int. Conf. on Intelligent Robots and Systems (IROS)*, pages 1570–1575.

Hulin T., Preusche C., and Hirzinger G. (2008a). Stability Boundary for Haptic Rendering: Influence of Human Operator. In *Proc. IEEE/RSJ Int. Conf. on Intelligent Robots and Systems (IROS)*.

Hulin T., Sagardia M., Artigas J., Schätzle S., Kremer P., and Preusche C. (2008b). Human-Scale Bimanual Haptic Interface. In *Proc. 5th International Conference on Enactive Interfaces*.

Iskakov R., Albu-Schäffer A., Schedl M., Lopota V., and Hirzinger G. (2007). Influence of sensor quantization on the control performance of robotics actuators. In *Proc. IEEE/RSJ Int. Conf. on Intelligent Robots and Systems (IROS)*, pages 1085–1092. IEEE.

Jöhl K., Preusche C., Reintsema D., and Hirzinger G. (2005). High Fidelity USB Force Feedback Joystick. In *Proc. World Haptic Conference (WHC)*.

Jörg S., Nickl M., and Hirzinger G. (2006). Flexible Signal-Oriented Hardware Abstraction for Rapid Prototyping of Robotic Systems. In *Proc. IEEE/RSJ Int. Conf. on Intelligent Robots and Systems (IROS)*, pages 3755–3760. IEEE/RSJ International Conference on Intelligent Robots and Systems.

Kaiser I. (2008). A Fast Iterative Solution of the Wheel-Rail Contact. In *Proc. XXII ICTAM*.

Kaiser I., Heckmann A., and van der Linden F. (2007). On an ALE-Approach for Rotating Elastic Structures. In *Proc. ECCOMAS Thematic Conference*.

Kaiser I. and Popp K. (2005). Interaction of Elastic Wheelsets and Elastic Rails: Modelling and Simulation. In *Proc. International Association for Vehicle System Dynamics Symposium (IAVSD)*.

Kaiser I. and Popp K. (2006). Interaction of Elastic Wheelsets and Elastic Rails: Modelling and Simulation. In *Proc. International Association for Vehicle System Dynamics Symposium (IAVSD)*, pages 932–939.

Kamel A., Lange F., and Hirzinger G. (2008a). An Industrial-Robots Suited Input Shaping Control Scheme. In *Proc. 9th International Conference on Motion and Vibration Control (MOVIC)*. Springer Verlag.

Kamel A., Lange F., and Hirzinger G. (2008b). New Aspects of Input Shaping Control to Damp Oscillations of a Compliant Force Sensor. In *Proc. IEEE Int. Conf. on Robotics & Automation (ICRA)*, pages 2629–2635.

Kienitz K.-H. (2005). Schaltende Aktuatoren mit Schaltungseinschränkungen in Lageregelungssystemen. In *Proc. GMA-Kongress 2005: Automation als interdisziplinäre Herausforderung*, pages 865–873. VDI-Verlag.

Kier T. (2005). Comparison of Unsteady Aerodynamic Modelling Methodologies with Respect to Flight Loads Analysis. In *Proc. AIAA Atmospheric Flight Mechanics Conference*.

Kier T., Looye G., and Hofstee J. (2005). Development of Aircraft Flight Loads Analysis Models with Uncertainties for Pre-Design Studies. In *Proc. International Forum on Aeroelasticity and Structural Dynamics (IFASD)*.

Kier T., Looye G., Scharpenberg M., and Reijerkerk M. (2007). Process, methods and tools for flexible aircraft flight dynamics model integration. In *Proc. International Forum on Aeroelasticity and Structural Dynamics (IFASD)*.

Knobel C., Pruckner A., and Bünte T. (2006). Optimized Force Allocation - A General Approach to Control and to Investigate the Motion of Over-Actuated Vehicles. In *Proc. 4th IFAC Symposium on Mechatronic Systems*.

Konietsche R., Hirzinger G., and Yan Y. (2006a). All Singularities of the 9-DoF DLR Medical Robot Setup for Minimally Invasive Applications. In *Proc. Advances in Robot Kinematics*.

Konietschke and Hirzinger G. (2006). A Registration-Free Intraoperative Procedure to Optimally Position the Ports and the Robots in MIRS. In *Proc. 5th World Congress on Biomechanics*.

Konietschke R., Busam A., Bodenmüller T., Ortmaier T., Suppa M., Wiechnik J., Welzel T., Eggers G., Hirzinger G., and Marmulla R. (2007a). Accuracy Identification of Markerless Registration with the DLR Handheld 3D-Modeller in Medical Applications. In *Proc. Jahrestagung der Deutschen Gesellschaft für Computer- und Roboterassistierte Chirurgie*.

Konietschke R., Busam A., Bodenmüller T., Ortmaier T., Suppa M., Wiechnik J., Welzel T., Eggers G., Hirzinger G., and Marmulla R. (2007b). Potential, Limitations and Challenges of Markerless Registration with the DLR 3D-Modeller in Medical Applications. In *Proc. International Congress and Exhibition of Computer Assisted Radiology and Surgery (CARS)*.

Konietschke R. and Hirzinger G. (2006). Registration-Free Intraoperative Procedure to Optimally Position the Ports and the Robots in MIRS. In *Proc. 5th World Congress on Biomechanics*.

Konietschke R., Knöferle A., and Hirzinger G. (2007c). The Autopointer: A New Augmented-Reality Device for Transfer of Planning Data into the Operating Room. In *Proc. International Congress and Exhibition of Computer Assisted Radiology and Surgery (CARS)*, volume 2, page 503.

Konietschke R., Ortmaier T., Ott C., Hagn U., Le-Tien L., and Hirzinger G. (2006b). Concepts of Human-Robot Cooperation for a new Medical Robot. In *Proc. Human Centered Robotic Systems (HCRS)*, pages 1–6.

Krenn R. and Hirzinger G. (2008). Contact Dynamics Simulation for Space Robotics Applications. In *Proc. IEEE/RSJ Int. Conf. on Intelligent Robots and Systems (IROS)*.

Kübler B., Passig G., Seibold U., and Hirzinger G. (2006). Prototypic setup of a surgical forced feedback instrument for minimally invasive robotic surgery. In *Proc. Jahrestagung der Deutschen Gesellschaft für Computer- und Roboterassistierte Chirurgie*.

Kuhn M., Ji Y., Joos H.-D., and Bals J. (2008a). An Approach for Stability Analysis of Nonlinear Electrical Network using Antioptimization. In *Proc. Power Electronics Specialists Conference (PESC)*.

Kuhn M., Ji Y., and Schröder D. (2007). Stability Studies of Critical DC Power System Component for More Electric Aircraft using Sensitivity. In *Proc. 15th Mediterranean Conference on Control and Automation*.

Kuhn M., Otter M., and Raulin L. (2008b). A Multi Level Approach for Aircraft Electrical Systems Design. In *Proc. 6th International Modelica Conference*.

Kurze M., Weiß M., and Otter M. (2006). Methods and Tools to Design and Test Robot Control Systems. In *Proc. Joint Conference on Robotics / ROBOTIK (ISR)*.

Kurzeck B., Hecht M., and Kaiser I. (2008). Erweiterte Simulationsmodelle zur Abbildung der höherfrequenten Fahrzeug/Fahrweg-Interaktion und Schwingungsausbreitung im Fahrzeug. In *Proc. 9. Internationale Schienenfahrzeugtagung*.

Lampariello R., Abiko S., and Hirzinger G. (2008). Dynamic Modeling of Structure-Varying Kinematic Chains for Free-Flying Robots. In *Proc. IEEE Int. Conf. on Robotics & Automation (ICRA)*, pages 1207–1212.

Lampariello R., Heindl J., Koeppe R., and Hirzinger G. (2006). Reactionless Control for Two Manipulators Mounted on a Cable-Suspended Platform. In *Proc. IEEE/RSJ Int. Conf. on Intelligent Robots and Systems (IROS)*, pages 91–97. IEEE/IROS International Conference on Intelligent Robots and Systems.

Lampariello R. and Hirzinger G. (2005). Modeling and Experimental Design for the On-Orbit Inertial Parameter Identification of Free-flying Space Robots. In *Proc. International Design Engineering Technical Conferences & Computers Information in Engineering Conference*.

Landzettel K., Preusche C., Albu-Schaffer A., Reintsema D., Rebele B., and Hirzinger G. (2006). Robotic On-Orbit Servicing - DLR's Experience and Perspective. In *Proc. IEEE/RSJ Int. Conf. on Intelligent Robots and Systems (IROS)*, pages 4587–4594.

Lange F. (2005). Robotersteuerung mit online Bahnvorgabe durch Kraftsensorik und / oder Bildverarbeitung. In *Proc. Fachausschusses 4.13 der GMA*. GMA.

Lange F. (2007). Montage in Bewegung - Konzept und Implementierung. In *Cluster Mechatronik & Automation*.

Lange F., Frommberger M., and Hirzinger G. (2006). Impedance-Based Smoothing for Visual Servoing along Edges. In *Proc. Joint Conference on Robotics / ROBOTIK (ISR)*.

Lange F., Frommberger M., and Hirzinger G. (2006). Is Impedance-Based Control Suitable for Trajectory Smoothing? In *Proc. SYROCO, 8th International IFAC Symposium on Robot Control*.

Lange F. and Hirzinger G. (2005). Calibration and Synchronization of a Robot-Mounted Camera for Fast Sensor-Based Robot Motion. In *Proc. IEEE Int. Conf. on Robotics & Automation (ICRA)*, pages 3911–3916. IEEE.

Lange F. and Hirzinger G. (2005). Stability Preserving Sensor-Based Control for Robots with Positional Interface. In *Proc. IEEE Int. Conf. on Robotics & Automation (ICRA)*, pages 1712–1717. IEEE.

Lange F., Kamel A., Hirzinger G., and Werner J. (2008a). Sensorfusion und Regelung eines Roboters am kontinuierlich bewegten Band. In *Proc. Kongress Automation 2008*.

Lange F., Strobl K., Langwald J., Jörg S., Hirzinger G., Gruber B., Klein J., and Werner J. (2008b). Kameragestützte Montage von Rädern an kontinuierlich bewegte Fahrzeuge. In *Proc. Fachtagung Robotik 2008*.

Lange F., Willberg B., Meusel P., Langwald J., Jörg S., Frommberger M., Hirzinger G., and Werner J. (2008c). Montage am kontinuierlich bewegten Band - Sensorkonfiguration und Programmierung. In *Proc. Fachtagung Robotik 2008*.

Le-Tien L. (2008). Modellierung, Identifikation und Entkopplungsregelung für das mechanisch gekoppelte Doppelgelenk des DLR-Medizinroboters. In *Proc. VDI-Workshop*.

Le-Tien L., Albu-Schäffer A., De Luca A., and Hirzinger G. (2008). Friction Observer and Compensation for Control of Robots with Joint Torque Measurement. In *Proc. IEEE/RSJ Int. Conf. on Intelligent Robots and Systems (IROS)*, pages 3789–3795.

Le-Tien L., Albu-Schäffer A., and Hirzinger G. (2007). MIMO state feedback controller for a flexible joint robot with strong joint coupling. In *Proc. IEEE Int. Conf. on Robotics & Automation (ICRA)*, pages 3824–3830. IEEE.

Liu H., Meusel P., Willberg B., Hirzinger G., Jin M., Liu Y., Wei R., Xie Z., and Cai H. (2006). The modular mulitsensory DLR-HIT-hand: Hardware and software architecture. In *Proc. Joint Conference on Robotics / ROBOTIK (ISR)*.

Liu H., Wu K., Meusel P., Seitz N., Hirzinger G., Jin M., Liu Y., Fan S., and Chen Z. (2008). Multisensory Five-Finger Dexterous Hand: The DLR/HIT Hand II. In *Proc. IEEE/RSJ Int. Conf. on Intelligent Robots and Systems (IROS)*.

Liu R., Burschka D., and Hirzinger G. (2007a). A Novel Approach to Automatic Registration of Point Clouds. In *Proc. International Geoscience and Remote Sensing Symposium (IGARSS)*. IEEE.

Liu R., Burschka D., and Hirzinger G. (2007b). On the Way to Water-tight Mesh. In *Proc. 3D-ARCH*.

Liu R., Burschka D., and Hirzinger G. (2007c). Real Time Landscape Modelling and Visualization. In *Proc. International Geoscience and Remote Sensing Symposium (IGARSS)*. IEEE.

Liu R., Burschka D., Hirzinger G., and Strackenbrock B. (2007d). Real Time Fully Automatic 3D-Modelling of HRSC Landscape Data. In *Proc. Joint Workshop on Remote Sensing and Data Fusion over Urban Area, GRSS/ISPRS*. IEEE.

Liu R. and Hirzinger G. (2005a). Marker-free Automatic Matching of Range Data. In *2nd Panoramic Photogrammetry Workshop*.

Liu R. and Hirzinger G. (2005b). Matching-Tree - A Novel Data Structure for Global Automatic Matching. In *7th Conference on Optical 3D Measurement Techniques*.

Liu R., Suppa M., Hirzinger G., and Burschka D. (2007e). Modelling the World in Real Time. In *Proc. 8th Conference on Optical 3D Measurement Techniques*.

Löhning M., Ruder J., and Bals J. (2008). Robust Stability Analysis with Integral Quadratic Constraints (IQCs): A Design Example. In *Proc. IEEE Multi-conference on Systems and Control*.

Looye G. (2005). Integration of Rigid and Aeroelastic Aircraft Models using the Residualised Model Method. In *Proc. International Forum on Aeroelasticity and Structural Dynamics (IFASD)*.

Looye G. (2008). The New DLR Flight Dynamics Library. In *Proc. 6th International Modelica Conference*.

Looye G., Hecker S., Kier T., and Reschke C. (2005). FlightDynLib: An Object-Oriented Model Component Library for Constructing Multi-Disciplinary Aircraft Dynamics Models. In *Proc. International Forum on Aeroelasticity and Structural Dynamics (IFASD)*.

Looye G., Hecker S., Kier T., Reschke C., and Bals J. (2005). Multi-Disciplinary Aircraft Model Development Using Object-Oriented Modelling Techniques. In *DGLR Jahrestagung*.

Lorenz E. and Jahn H. (2005). BIRD: More than 3 years experience in orbit. In *Proc. 5th Symposium on Small Satellites for Earth Observation*, volume V, pages 121–124. Wissenschaft & Technik Verlag.

Lorenz E., Oertel D., Zhukov B., Wooster M., Roberts G., Perry G., and Csiszar I. (2005). Lessons Learned from Dedicated Active Fire Remote Sensing. In *Proc. 31st International Symposium on Remote Sensing of Environment (ISRSE) - Global Monitoring for Sustainability and Security*, volume CD-ROM, pages 4 p.–.

Lovera M. and Varga A. (2005). Optimal discrete-time magnetic attitude control of satellites. In *Proc. 16th IFAC World Congress*.

Lura F., Biering B., Lötzke H. G., Studemund H., and Baturkin V. (2007). BIRD micro satellite thermal control system - 5 years of operation in space. In *Proc. 6th Symposium on Small Satellites for Earth Observation*, volume VI, pages 207–210. Wissenschaft und Technik Verlag Berlin.

Maier S. and Smagt van der P. (2008). Surface EMG suffices to classify the motion of each finger independently. In *Proc. 9th International Conference on Motion and Vibration Control (MOVIC)*.

Malmheden M., Elmqvist H., Mattsson S. E., Henriksson D., and Otter M. (2008). ModeGraph - A Modelica Library for Embedded Control Based on Mode-Automata. In *Proc. 6th International Modelica Conference*, pages 255–267.

Maturilli A., Helbert J., Moroz L., and Witzke A. (2006). The Berlin Emissivity Database (BED). In *Mars Dialogue*.

Maturilli A., Helbert J., Witzke A., Arnold G., and Moroz L. (2005). Emissivity Measurements of Analog Materials for the Interpretation of Data from PFS on Mars Express and MERTIS on BepiColombo. In *Proc. European Geosciences Union General Assembly*, volume 7, pages abstract EGU05–A–07579.

Maturilli A., Helbert J., Witzke A., Arnold G., and Moroz L. (2005). Emissivity Measurements of Analog Materials for the Interpretation of Data from PFS on Mars Express and MERTIS on BepiColombo. In *Proc. 2nd General Assembly of the European Geosciences Union*, volume 7, page 07579.

Maturilli A., Witzke A., Helbert J., Moroz L. V., Arnold G., and Wagner C. (2005). Emissivity Spectral Measurements of Particulate Planetary Analog Materials. In *Proc. XXXVI Lunar and Planetary Science Conference*, volume 1234, page 1770. Lunar and Planetary Institute, Houston, TX.

Mesquita A. R. and Kienitz K.-H. (2005). Persistent Motion and Chaos in Attitude Control with Switching Actuator. In *Proc. 16th IFAC World Congress*.

Michaud S., Gibbesch A., Thueer T., Krebs A., Lee C., Despont B., Schäfer B., and Slade R. (2008). Development of the ExoMars Chassis and Locomotion Subsystem. In *Proc. International Symposium on Artificial Intelligence, Robotics and Automation in Space*.

Michaud S., Hoepfinger M., Lee C., Thueer T., Krebs A., Despont B., and Gibbesch A. (2008). Lesson Learned from ExoMars Locomotion System Test Campaign. In *ESA Workshop on Advanced Space Technologies for Robotics and Automation (ASTRA)*.

Michaud S., Richter L., Thueer T., Gibbesch A., Huelsing T., Schmitz N., Weiss S., Krebs A., Patel N., Joudrier L., Siegwart R., Schäfer, and Ellery A. (2006). Rover Chassis Evaluation and Design Optimisation using the RCET. In *ESA Workshop on Advanced Space Technologies for Robotics and Automation (ASTRA)*.

Oczipka M., Bucher T., Moder F., and Lehmann F. (2008). Classifying high resolution image data in Southeast Asian urban areas using MFC line scanner data. In *GEOgraphic Object-Based Image Analysis for the 21st Century (GEOBIA)*.

Oczipka M., Bucher T., and Trosset A.-M. (2008). Mapping and updating maps in dense urban regions using high resolution digital airborne imagery, surface models and object-based classification. In *Proc. International Society for Photogrammetry and Remote Sensing (ISPRS) Congress*, volume XXXVII, pages 551–555.

Oertel D., Halle W., Lorenz E., Skrbek W., Venus H., Walter I., Zhukov B., and Wooster M. (2005). BIRD - Wegbereiter für das zukünftige IR Element der ESA. In *25. Wissenschaftlich-Technische Jahrestagung der DGPF*, volume 14, pages 453–460.

Oertel D., Lorenz E., Zhukov B., and Cziszar I. (2005). BIRD Fire Recognition and Comparison with Terra/MODIS. In *Proc. 5th Symposium on Small Satellites for Earth Observation*, volume V, pages 23–26. Wissenschaft & Technik Verlag.

Olsson H., Otter M., Mattsson S. E., and Elmqvist H. (2008). Balanced Models in Modelica 3.0 for Increased Model Quality. In *Proc. 6th International Modelica Conference*, pages 21–33.

Ortmaier T. (2005). Minimally Invasive Robotic Surgery of the Future - Introducing Autonomy into the OR. In *Proc. IEEE Int. Conf. on Robotics & Automation (ICRA)*.

Ortmaier T., Deml B., Passig G., Reintsema D., and Seibold U. (2007). Advances in Telerobotics, chapter Robot Assisted Force Feedback Surgery. In *Proc. IEEE Int. Conf. on Robotics & Automation (ICRA)*, page 18. Springer.

Ortmaier T. and Konietschke R. (2006). Image Guided Robotic Surgery - Towards Less Invasive Therapy. In *Proc. IEEE Int. Conf. on Robotics & Automation (ICRA)*.

Ortmaier T., Morel G., and Vitrani M. (2005a). Real-Time Instrument Tracking in Ultrasound Images for Visual Servoing. In *Proc. Bildverarbeitung für die Medizin*, pages 232–236. Springer Verlag.

Ortmaier T., Vitrani M., Morel G., and Pinault (2005b). Robust Real-Time Instrument Tracking in Ultrasound Images. In *Proc. SPIE Medical Imaging Conference*.

Ortmaier T., Vitrani M., Morel G., and Pinault S. (2005c). Robust Real-Time Instrument Tracking in Ultrasound Images for Visual Servoing. In *Proc. IEEE Int. Conf. on Robotics & Automation (ICRA)*.

Ortmaier T., Weiß H., Hagn U., Grebenstein M., Nickl M., Albu-Schäffer A., Ott C., Jörg S., Konietschke R., and Hirzinger G. (2005d). Ein neuer Roboter zum navigierten Setzen von Pedikelschrauben. In *Proc. Internationales Forum für Mechatronik (ifm)*, pages 673–699.

Ortmaier T., Weiß H., Hagn U., Nickl M., Albu-Schäfer A., Ott C., Jörg S., Konietschke R., Le-Tien L., and Hirzinger G. (2006a). A Hands-on-Robot for Accurate Placement of Pedicle Screws. In *Proc. IEEE Int. Conf. on Robotics & Automation (ICRA)*, pages 4179–4186.

Ortmaier T., Weiss H., Hagn U., Grebenstein M., Nickl M., Ott C., Albu-Schäffer A., Hirzinger G., Essensreiter R., and Bertram M. (2005e). Ein neuer Roboter zum navigierten Setzen von Pedikelschrauben. In *Proc. VDI Wissensforum - Mechatronik*, pages 661–686.

Ortmaier T., Weiss H., Hagn U., Ott C., Hirzinger G., Essenreiter R., and Bertram M. (2005f). Ein neues System zum robotergestützten, navigierten Setzen von Pedikelschrauben. In *Proc. XXVII Münchner Symposium für Experimentelle Orthopädie*.

Ortmaier T., Weiss H., Ott C., Hirzinger G., and Schreiber G. (2006b). A soft robotics approach for navigated pedicle screw placement First experimental results. In *Proc. Computer Assisted Radiology and Surgery, 20th International Congress and Exhibition (CARS)*.

Ott C., Albu-Schäffer A., and Hirzinger G. (2006a). A Cartesian Compliance Controller for a Manipulator Mounted on a Flexible Structure. In *Proc. IEEE/RSJ Int. Conf. on Intelligent Robots and Systems (IROS)*, pages 4502–4508. IEEE/IROS International Conference on Intelligent Robots and Systems.

Ott C., Bäuml B., Borst C., and Hirzinger G. (2007). Autonomous opening of a door with a mobile manipulator: A case study. In *Proc. IFAC Symposium on Intelligent Autonomous Vehicles*.

Ott C., Borst C., Hillenbrand U., Brunner B., Bäuml B., and Hirzinger G. (2005). The Robutler: Towards Service Robots for the Human Environment. In *Proc. IEEE Int. Conf. on Robotics & Automation (ICRA)*, pages 1399–1405.

Ott C., Eiberger O., Friedl W., Bäuml B., Hillenbrand U., Borst C., Albu-Schäffer A., Brunner B., Hirschmüller H., Kielhöfer S., Konietschke R., Suppa M., Wimböck T., Zacharias F., and Hirzinger G. (2006b). A Humanoid Two-Arm System for Dexterous Manipulation. In *Proc. International Conference on Humanoid Robots*, pages 276–283.

Otter M. (2006). The LinearSystems Library for Continous and Discrete Control Systems. In *Proc. 5th International Modelica Conference*, pages 529–538.

Otter M., Elmqvist H., and López J. D. (2005). Collision Handling for the Modelica MultiBody Library. In *4th International Modelica Conference*.

Otter M., Årzén K.-E., and Dressler I. (2005). StateGraph A Modelica Library for Hierarchical State Machines. In *Proc. 4th International Modelica Conference*, pages 569–578.

Paetsch W., Hirzinger G., and Schäfer B. (2006). Explorationsmissionen in unserem Sonnensystem - Bedeutung von Robotersystemen. In *Konferenz 'Exploration in unserem Sonnensystem'*.

Palli G., Melchiorri C., Wimböck T., Grebenstein M., and Hirzinger G. (2007). Feedback linearization and simultaneous stiffness-position control of robots with antagonistic actuated joints. In *Proc. IEEE Int. Conf. on Robotics & Automation (ICRA)*, pages 4367–4372.

Panzer H., Eiberger O., Grebenstein M., Schäfer P., and Smagt van der P. (2008). Human motion range data optimizes anthropomorphic robotic hand-arm system design. In *Proc. 9th International Conference on Motion and Vibration Control (MOVIC)*.

Paproth C., Lorenz E., Jahn H., Säuberlich T., and Helbert J. (2007). Conception and State of an End-To-End Simulator for the Mercury Radiometer and Thermal Infrared Spectrometer (MERTIS). In *Proc. International Conferecen on Advanced Infrared Technology and Applications (AITA)*.

Peter G., Rohbeck U., Berlin R., Ruß N., and Ulmer B. (2006). Spacewire Interface Simulation. In *Proc. Conference on Space Mission Challenges for Information Technology (SMC-IT)*.

Pfifer H. and Hecker S. (2008). Generation of Optimal Linear Parametric Models for LFT-based Robust Stability Analysis and Control Design. In *Proc. IEEE Conference on Decision and Control (CDC)*.

Poschlad K., Remelhe M., and Otter M. (2006). Modeling of an Experimental Batch Plant with Modelica. In *Proc. 5th International Modelica Conference*, pages 651–660.

Preusche C., Reintsema D., Landzettel K., and Hirzinger G. (2006). Robotics Component Verification on ISS ROKVISS - Preliminary Results for Telepresence. In *Proc. IEEE/RSJ Int. Conf. on Intelligent Robots and Systems (IROS)*, pages 4595–4601. IEEE.

Preusche C., Reintsema D., Ortmaier T., and Hirzinger G. (2005). The DLR Telepresence Experience in Space and Surgery. In *Proc. Joint International COE/HAM-SFB453*, pages 35–40. The 21st Century COE Project Office (Japan).

Pulecchi T., Lovera M., and Varga A. (2006). Optimal discrete-time design of magnetic attitude control laws. In *Proc. 6th International ESA Conference on Guidance, Navigation and Control Systems*.

Pulecchi T., Lovera M., and Varga A. (2008). Classical vs modern magnetic attitude control design: A case study. In *Proc. 7th ESA GNC Conference*.

Rebele B., Schäfer B., Albu-Schäffer A., Bertleff W., and Landzettel K. (2006). Robotic Joints and Contact Dynamics Experiments: Lessons learned from ROKVISS. In *ESA Workshop on Advanced Space Technologies for Robotics and Automation (ASTRA)*.

Reicke L., Kaiser I., and Kröger M. (2006). Identification of the Running-State of Railway Wheelsets. In *Proc. International Conference of Noise and Vibration Engineering (ISMA)*.

Reiner M., Heckmann A., and Otter M. (2008). Inversion based control of flexible body systems. In *Proc. 9th International Conference on Motion and Vibration Control (MOVIC)*.

Reintsema D., Landzettel K., and Hirzinger G. (2007). DLRs Advanced Telerobotic Concepts and Experiments for On-Orbit Servicing. In *Proc. Jahrestagung der Deutschen Gesellschaft für Computer- und Roboterassistierte Chirurgie*, page 22. STAR - Springer.

Reschke C. (2005). Flight Loads Analysis with Inertially Coupled Equations of Motion. In *Proc. AIAA Atmospheric Flight Mechanics Conference*.

Reschke C. and Looye G. (2005). Comparison of Model Integration Approaches for Flexible Aircraft Flight Dynamics Modelling. In *Proc. International Forum on Aeroelasticity and Structural Dynamics (IFASD)*.

Robuffo Giordano P., Stemmer A., Arbter K., and Albu-Schäffer A. (2008). Robotic Assembly of Complex Planar Parts: An Experimental Evaluation. In *Proc. IEEE/RSJ Int. Conf. on Intelligent Robots and Systems (IROS)*, pages 3775–3782.

Roemer S., Terzibaschian T., Wiener A., and Bärwald W. (2007). Experiences with the BIRD ACS test facility and the resulting design of a state of the art mini-and microsatellite ACS test facility. In *Proc. 6th Symposium on Small Satellites for Earth Observation*, volume VI, pages 165–168. Wissenschaft und Technik Verlag Berlin.

Ruhe M., Kühne R., Ernst I., Zuev S., and Hipp E. (2007). Air Borne Systems and Datafusion for Traffic Surveillance and Forecast for the Soccer World Cup. In *Proc. TRB (86. Annual Meeting)*.

Sagardia M., Hulin T., Preusche C., and Hirzinger G. (2008). Improvements of the Voxmap-PointShell Algorithm - Fast Generation of Haptic Data-Structures. In *Proc. 53. Internationales Wissenschaftliches Kolloquium der TU Ilmenau*.

Säuberlich T., Lorenz E., and Skrbek W. (2006). Conception and State of the Radiometric Analysis Breadboard (RAB) for the Mercury Radiometer and Thermal Infrared Spectrometer (MERTIS). In *Proc. Optics & Photonics*, volume 6297, pages 62970Y–1–62970Y–12. SPIE.

Säuberlich T., Lorenz E., Skrbek W., Walter I., Paproth C., and Helbert J. (2007). Development of a calibration concept for the MErcury Thermal Infrared Spectrometer. In *Proc. International Conferecen on Advanced Infrared Technology and Applications (AITA)*.

Schäfer B. (2005). Raumfahrt-Robotik und Planetare Rover: Dynamik, Modellierung und Simulation; aktuelle Raumfahrtprojekte. In *Kolloquium für Mechanik und Regelungstechnik*.

Schäfer B. (2007). Applications of Robotics and Mechatronics for Space Structures. In *Proc. Mechanics Applications at UNESP*.

Schäfer B. (2007). Planetary Rover Mobility: Wheel-Soil Interaction based on Multibody System Approach. In *Proc. 17th IFAC Symposium on Automatic Control in Aerospace*.

Schäfer B. (2007). Raumfahrt-Robotik: Simulation und Anwendung. In *Virtuelle Produktentwicklung für Raumfahrtsysteme*. DLR (Systec).

Schäfer B., Gibbesch A., and Krenn R. (2008). Planetary Rover Mobility Performance on Soft and Uneven Terrain. In *Proc. XXII ICATM International Congress of Theoretical and Applied Mechanics, SM 14 - Multibody and Vehicle Dynamics*.

Schäfer B., Gibbesch A., Krenn R., and Rebele B. (2008). Planetary Rover Mobility Performance Simulation Tool. In *Proc. SESP 2008 - 10th International Workshop on Simulation for European Space Programmes*.

Schäfer B., Gibbesch A., Krenn R., and Rebele B. (2008). Verification and Validation Process on 3D Dynamics Simulation in Support of Planetary Rover Development. In *ESA Workshop on Advanced Space Technologies for Robotics and Automation (ASTRA)*.

Schäfer B., Rebele B., and Krenn R. (2005). Actual End Effector Trajectories Computation for Redundant Free-Floating Space Manipulators. In *Proc. International Symposium on Artificial Intelligence, Robotics and Automation in Space*.

Schäfer B., Rebele B., and Krenn R. (2006). Free-Floating Space Robots: Two Approaches for Dynamics Computation. In *Proc. ECT-2006: 5th International Conference on Engineering Computational Technology*.

Schäfer B., Rebele B., and Krenn R. (2006). On Free-Flying Redundent Space Robots with Nonholonomic Constraints. In *Proc. 5th Vienna Symposium on Mathematical Modelling*.

Schäfer B., Rebele B., and Krenn R. (2006). Time-Efficient Algorithm for Computation of Free-Flying Redundant Space Robot Dynamics. In *Proc. EUROMECH 476: Real-time Simulation and Virtual Reality Applications of Multibody Systems*.

Schäfer B., Rebele B., Schedl M., Görner M., Wedler A., Krenn R., Seeni A., and Hirzinger G. (2008). Light-Weight Mechatronics and Sensorics for Robotic Applications: A DLR Perspective. In *Proc. International Symposium on Artificial Intelligence, Robotics and Automation in Space*.

Schallert C. (2007). A Novel Tool for the Conceptual Design of Aircraft On-Board Power Systems. In *Society of Automotive Engineers Aerotech Congress*.

Schallert C. (2008). Incorporation of Reliability Analysis Methods with Modelica. In *Proc. 4th International Modelica Conference*, pages 103–112.

Schallert C., Pfeiffer A., and Bals J. (2006). Generator Power Optimisation for a More-Electric Aircraft by Use of a Virtual Iron Bird. In *Proc. International Congress of the Aeronautical Sciences (ICAS)*.

Schätzle S., Hulin T., Preusche C., and Hirzinger G. (2006). Evalution of Vibro-Tactile Feedback to the Human Arm. In *Proc. EuroHaptics 2006*, pages 557–560.

Schedl M. (2005). Systemintegrierte Leistungselektronik für Aktuatorik und Robotersysteme. In *Kooperationsforum Leistungselektronik*.

Scheele M., Krüger S., and Schuster R. (2005). New Calibration Scheme for Panoramic Line Scanners. In *Panoramic Photogrammetry Workshop*, volume XXXVI-5/W8, pages 1–4.

Schmidt M., Rudolph M., Werther B., and Fürstenau N. (2007). Development of an Augmented Vision Videopanorama Human-Machine Interface for Remote Airport Tower Operation. In *Proc. Conference on Human-Computer Interactino (HCII)*, volume LNCS 4558, pages 1119–1128. Springer Verlag.

Schmirgel V., Zimmermann U. E., Hulin T., and Preusche C. (2007). Position Paper: Human Skills for Programming-by-Demonstration of Robots. In *Skills - scientific workshop*.

Schroth G., Preusche C., and Hinterseer P. (2007). Astronautic Communication for Telepresence Applications. In *Proc. 13th IASTED International Conference on Robotics and Applications*.

Schwarzer H., Börner A., Degen K.-H., Eckardt A., and Scherbaum P. (2008). Dynamic PSF and MTF measurements on a 9k

TDI CCD. In *Proc. SPIE Europe, Remote Sensing, Sensors, Systems, and Next-Generation Satellites XII, volume 7106*.

Schwarzer H., Börner A., Fix A., Günther B., Hübers H.-W., Raugust M., Schrandt F., and Wirth M. (2007). Development of a wavelength stabilized seed laser system for an airborne water vapour lidar experiment. In *Proc. SPIE Optics+Photonics 2007 - Remote Sensing*, page 6681. SPIE.

Schweiger C., Dempsey M., and Otter M. (2005). The PowerTrain Library: New Concepts and New Fields of Application. In *Proc. 4th International Modelica Conference*, pages 457–466.

Schweiger C. and Otter M. (2005). Modelica-Modellbibliothek zur Simulation der Dynamik von Schaltvorgängen bei Automatikgetrieben. In *Dynamik und Regelung von automatischen Getrieben, VDI-Schwingungstagung 2005*, pages 105–124. VDI Verlag GmbH.

Seeni A., Schäfer B., and Rebele B. (2007). Investigation of Robotic Vehicle Locomotion Concepts for Unmanned Lunar Missions. In *Proc. 9th ILEWG International Conference on Exploration and Utilisation of the Moon*.

Seeni A., Schäfer B., and Rebele B. (2007). Manipulation Concepts for Human-Robot Cooperative Lunar Exploration. In *Proc. 9th ILEWG International Conference on Exploration and Utilisation of the Moon*.

Seeni A., Schäfer B., and Rebele B. (2007). Radioisotope Power Systems A Valuable Resource for European Polar Moon Missions and Beyond. In *Proc. 9th ILEWG International Conference on Exploration and Utilisation of the Moon*.

Seeni A., Schäfer B., Rebele B., and Krenn R. (2008). Lunar Rover with Multiple Science Handling Capability. In *Proc. 59th International Astronautical Congress, A.3 Space Exploration Symposium - 2.B Moon Exploration*.

Seeni A., Schäfer B., Rebele B., and Tolyarenko N. (2008). Robot Mobility Concepts for Extraterrestrial Surface Exploration. In *Proc. IEEE Aerospace Conference*.

Seibold U., Kübler B., and Hirzinger G. (2005). Prototype of Instrument for Minimally Invasive Surgery with 6-Axis Force Sensing Capability. In *Proc. IEEE Int. Conf. on Robotics & Automation (ICRA)*, pages 498–503.

Seibold U., Kuebler B., Passig G., and Hirzinger G. (2006). Development of Actuated and Sensor Integrated Forceps for Minimally Invasive Robotic Surgery. In *Proc. 5th World Congress on Biomechanics*.

Sepp W. (2005). A direct method for real-time tracking in 3-d under variable illumination. In *Proc. 27th Pattern Recognition Symposium, DAGM 2005*, number 3663 in Lecture Notes In Computer Science, pages 246–253, Vienna, Austria. Deutsche Arbeitsgemeinschaft für Mustererkennung (DAGM), Springer Verlag.

Sepp W. (2006). Efficient tracking in 6-dof based on the image-constancy assumption in 3-d. In *Proc. International Conference on Pattern Recognition*, volume 3, pages 59–62. International Association for Pattern Recognition (IAPR).

Sepp W., Fuchs S., and Hirzinger G. (2006). Hierarchical Featureless Tracking for Position-Based 6-DoF Visual Servoing. In *Proc. IEEE/RSJ Int. Conf. on Intelligent Robots and Systems (IROS)*, pages 4310–4315.

Sielemann M., Giese T., Öhler B., and Otter M. (2007). A Flexible Toolkit for the design of environmental control system architectures. In *CEAS European Air and Space Conference*.

Smagt van der P. (2006). Cognitive Robotics. In *Proc. IST*.

Smagt van der P. and Hirzinger G. (2006). NEUROBOTICS: The fusion of neuroscience and robotics. In *Proc. Joint Conference on Robotics / ROBOTIK (ISR)*.

Smagt van der P. and Stillfried G. (2008). Using MRT data to compute a hand kinematic model. In *Proc. 9th International Conference on Motion and Vibration Control (MOVIC)*.

Sparchholz C., K. S., Strackenbrock B., and Heindl J. (2005). 3D Visualization - Using High Resolution Multi.Sensor Data. In *Panoramic Photogrammetry Workshop*, volume XXXVI-5/W8, pages 1–5.

Stemmer A., Albu-Schäffer A., and Hirzinger G. (2007). An Analytical Method for the Planning of Robust Assembly Tasks of Complex Shaped Planar Parts. In *Proc. IEEE Int. Conf. on Robotics & Automation (ICRA)*, pages 317–323.

Stemmer A., Schreiber G., Arbter K., and Albu-Schäffer A. (2006). Robust Assembly of Complex Shaped Planar Parts Using Vision and Force. In *Proc. International Conference on Multisensor Fusion and Integration for Intelligent Systems, MFI*, pages 493–500.

Stoll E., Letschnik J., Walter U., Preusche C., and Hirzinger G. (2006). Concept of an Algorithm to Determine the Signal Delay Time for Telepresence Space Applications. In *Proc. IEEE Aerospace Conference*.

Strackenbrock B., Tsuchiya B., and Scheibe K. (2005). 3d-Modelling and Visualisation from 3D-Laser Scans and Panoramic Images. In *Panoramic Photogrammetry Workshop*, volume XXXVI-5/W8.

Strobl K. and Hirzinger G. (2008). More Accurate Camera and Hand-Eye Calibrations with Unknown Grid Pattern Dimensions. In *Proc. IEEE Int. Conf. on Robotics & Automation (ICRA)*, pages 1398–1405.

Strobl K. H. and Hirzinger G. (2006). Optimal Hand-Eye Calibration. In *Proc. IEEE/RSJ Int. Conf. on Intelligent Robots and Systems (IROS)*, pages 4647–4653. Proc. IEEE/RSJ International Conference on Intelligent Robots and Systems.

Stuffler T., Kaufmann H., Hofer S., Förster K.-P., Schreier G., Müller A., Eckardt A., Penné B., and Haydn R. (2007). The German Hyperspectral Satellite EnMAP - The Next Generation in Optical Remote Sensing (Abstract). In *Proc. 6th Symposium on Small Satellites for Earth Observation*, volume VI, page 59. Wissenschaft und Technik Verlag Berlin.

Suppa M. (2006). Multisensorielle Exploration von Roboterarbeitsräumen. In *Expertenforum*.

Suppa M., Kielhöfer S., Langwald J., Hacker F., Strobl K., and Hirzinger G. (2007). The 3D-Modeller: A Multi-Purpose Vision Platform. In *Proc. IEEE Int. Conf. on Robotics & Automation (ICRA)*. IEEE.

Terzibaschian T. (2005). Experiences with the BIRD magnetic coil system for wheel desaturation, satellite rate damping and attitude control - the concept of virtual wheel systems. In *Proc. 5th Symposium on Small Satellites for Earth Observation*, volume V, pages 441–444. Wissenschaft & Technik Verlag.

Tetzlaff A., Hirner A., Zhukov B., Kuenzer C., and Vogt S. (2005). Coal Fire Quantification and Detection Using the DLR Experimental Bi-Spectral Infrared Detection (BIRD) Small Satellite. In *Proc. 5th Symposium on Small Satellites for Earth Observation*, volume V, pages 307–311. Wissenschaft & Technik Verlag.

Thümmel M., Looye G., Kurze M., Otter M., and Bals J. (2005). Nonlinear Inverse Models for Control. In *Proc. 4th International Modelica Conference*, pages 267–279.

Thümmel M., Otter M., and Bals J. (2005). Vibration Control of Elastic Joint Robots by Inverse Dynamics Models. In *Proc. IUTAM Symposium on Vibration Control of Nonlinear Mechanisms and Structures*, pages 343–353.

Tobolar J. (2005). Advances in macro-joint based suspension model for real-time model of vehicle. In *Computational mechanics*, volume II, pages 597–604.

Tobolar J., Otter M., and Bünte T. (2007). Modelling of Vehicle Powertrains with the Modelica PowerTrain Library. In *Dynamisches Gesamtsystemverhalten von Fahrzeugantrieben (Haus der Technik Essen)*, pages 204–216.

Varga A. (2005a). Numerically reliable methods for optimal design of fault detection filters. In *Proc. IEEE Conference on Decision and Control (CDC)*.

Varga A. (2005b). On solving discrete-time periodic Riccati equations. In *Proc. 16th IFAC World Congress*.

Varga A. (2005c). On solving periodic differential matrix equations with applications to periodic system norms computation. In *Proc. IEEE Conference on Decision and Control (CDC)*.

Varga A. (2005d). A Periodic Systems Toolbox for MATLAB. In *Proc. 16th IFAC World Congress*.

Varga A. (2006a). Computation of H-infinity norm of linear discrete-time periodic systems. In *Proc. International Symposium on Mathematical Theory of Networks and Systems (MTNS)*.

Varga A. (2006b). A Fault Detection Toolbox for MATLAB. In *Proc. IEEE International Symposium on Computer-Aided Control Systems Design (CASCD)*.

Varga A. (2006c). On computing frequency-responses of periodic systems. In *Proc. International Symposium on Mathematical Theory of Networks and Systems (MTNS)*.

Varga A. (2007a). Computation of minimal order dynamic covers for periodic systems. In *Proc. European Control Conference (ECC)*, Kos, Greece.

Varga A. (2007b). Fault detection and isolation of actuator failures for a large transport aircraft. In *CEAS European Air and Space Conference*.

Varga A. (2007c). On computing minimal realizations of periodic descriptor systems. In *Proc. IFAC Workshop on Periodic Control Systems*, St. Petersburg, Russia.

Varga A. (2007d). On designing least order residual generators for fault detection and isolation. In *Proc. 16th International Conference on Control Systems and Computer Science*, pages 323–330.

Varga A. (2007e). An overview of recent developments in computational methods for periodic systems. In *Proc. IFAC Workshop on Periodic Control Systems*, St. Petersburg, Russia.

Varga A. (2008). On computing nullspace bases - a fault detection perspective. In *Proc. 17th IFAC World Congress*.

Varga A., Johansson S., K. B., and Shiriaev A. (2007). Comparing one-shot and multi-shot methods for solving periodic of Riccati differential equations. In *Proc. IFAC Workshop on Periodic Control Systems*.

Viganò L., Lovera M., and Varga A. (2007). Optimal periodic output feedback control: a continuous-time approach. In *Proc. IFAC Workshop on Periodic Control Systems*, St. Petersburg, Russia.

Vitrani M., Morel G., and Ortmaier T. (2005). Automatic Guidance of a Surgical Instrument with Ultrasound Based Visual Servoing. In *Proc. IEEE Int. Conf. on Robotics & Automation (ICRA)*.

Vitrani M., Ortmaier T., and Morel G. (2005). Automatic Guidance of a Surgical Instrument with US Based Visual Servoing. In *Proc. Surgetica 2005; 1st International Congress, Computer Assisted Medical and Surgical Interventions*.

Walter I., Hirsch H., Jahn H., Knollenberg J., and Venus H. (2006). MERTIS - a highly integrated IR imaging spectrometer. In *Proc. Optics & Photonics*, volume 6297, pages 62970X–1–62970X–11. SPIE.

Walter I., Hirsch H., Knollenberg J., Jahn H., Säuberlich T., Venus H., and Skrbek W. (2006). MERTIS - the design of a highly integrated IR imaging spectrometer. In *EGU, General Assembly*.

Wei R., Jin M., Xia J., Xie Z., Shi J., and Liu H. (2006). High Fidelity Distributed Hardware-in-the-Loop Simulation For Space Robot on CAN-based Network. In *Proc. IEEE/RSJ Int. Conf. on Intelligent Robots and Systems (IROS)*. IEEE/RSJ International Conference on Intelligent Robots and Systems.

Werner J., Zäh M., and Lange F. (2006). System to Realize a Conveying Belt Synchronous Assembly. In *Proc. 17th International DAAAM Symposium: Intelligent Manufacturing & Automation: Focus on Mechatronics and Robotics*.

Wimböck T., Ott C., Albu-Schäffer A., and Hirzinger G. (2008a). Analysis and Experimental Evaluation of the Intrinsically Passive Controller (IPC) for Multifingered Hands. In *Proc. IEEE Int. Conf. on Robotics & Automation (ICRA)*, pages 278–284.

Wimböck T., Ott C., Albu-Schäffer A., Kugi A., and Hirzinger G. (2008b). Impedence Control for Variable Stiffness Mechanisms with Nonlinear Joint Coupling. In *Proc. IEEE/RSJ Int. Conf. on Intelligent Robots and Systems (IROS)*, pages 3796–3803.

Wimböck T., Ott C., and Hirzinger G. (2006). Passivity-based Object-Level Impedance Control for a Multfingered Hand. In *Proc. IEEE/RSJ Int. Conf. on Intelligent Robots and Systems (IROS)*. IEEE/IROS International Conference on Intelligent Robots and Systems.

Wimböck T., Ott C., and Hirzinger G. (2007). Impedance Behaviors for Two-handed Manipulation: Design and Experiments. In *Proc. IEEE Int. Conf. on Robotics & Automation (ICRA)*, pages 4182–4189.

Wolf S. and Hirzinger G. (2008). A New Variable Stiffness Design: Matching Requirements of the Next Robot Generation.

In *Proc. IEEE Int. Conf. on Robotics & Automation (ICRA)*, pages 1741–1746.

Yoon Z. and Terzibaschian T. (2008). Optimal three-axis attitude control design, simulation and experimental verification for small satellites using magnetic actuators. In *Proc. 4S Symposium*, pages 46–47.

Zacharias F., Borst C., Beetz M., and Hirzinger G. (2008). Positioning Mobile Manipulators to Perform Constrained Linear Trajectories. In *Proc. IEEE/RSJ Int. Conf. on Intelligent Robots and Systems (IROS)*, pages 2578–2584.

Zacharias F., Borst C., and Hirzinger G. (2006). Bridging the Gap between Task Planning and Path Planning. In *Proc. IEEE/RSJ Int. Conf. on Intelligent Robots and Systems (IROS)*, pages 4490–4495. IEEE/RSJ.

Zacharias F., Borst C., and Hirzinger G. (2007). Capturing Robot Workspace Structure: Representing Robot Capabilities. In *Proc. IEEE/RSJ Int. Conf. on Intelligent Robots and Systems (IROS)*, pages 3229–3236. IEEE.

Zhao J., Xie Z., Jiang L., Cai H., Liu H., and Hirzinger G. (2005). Levenberg-Marquardt Based Neural Network Control for a Five-fingered Prosthetic Hand. In *Proc. IEEE Int. Conf. on Robotics & Automation (ICRA)*, pages 4493–4498.

Zhoa J., Xie Z., Jiang L., Cai H., Liu H., and Hirzinger G. (2006). EMG Control for a Five-fingered Underactuated Prosthetic Hand Based on Wavelet Transform and Sample Entropy. In *Proc. IEEE/RSJ Int. Conf. on Intelligent Robots and Systems (IROS)*. IEEE/RSJ International Conference on Intelligent Robots and Systems.

5.3 Book Chapters (“b”)

Below you will find 23 references to chapters in refereed published books:

Arbib M., Metta G., and Smagt van der P. (2008). *Neurorobotics: From Vision to Action*, In Siciliano B. and Khatib O., editors, *Handbook of Robotics*, pages 1453–1480. Springer-Verlag.

Arnold M. and Heckmann A. (2007). *From Multibody Dynamics to Multidisciplinary Applications*, In Garcia Orden J., Goicolea J., and Cuadrado J., editors, *Multibody Dynamics, Computational Methods and Applications*. Springer Verlag.

Artigas J., Reintsema D., Preusche C., and Hirzinger G. (2006). *DIMSART: A Real Time Device Independent Modular Software Architecture For Robotic And Telerobotic Applications*, In Braz J., Araújo H., Vieira A., and Encarnaçao B., editors, *Informatics in Control, Automation and Robotics I*. Springer.

Bucher T. (2007). *Identification and mapping of materials containing hydrocarbons by merging the data from two remote sensing platforms*, In Knödel K., Lange G., and Voigt H.-J., editors, *Environmental Geology. Handbook of field methods and case studies*, pages 149–150. Springer Berlin.

Eckardt A. (2005). *Zeitliche Auflösung und kinematische Eigenschaften (Kap. 2.8)*, In Sandau R., editor, *Digitale Luftbildkamera - Einführung und Grundlagen*, pages 105–109. Herbert Wichmann Verlag, Hüthig GmbH & Co. KG, Heidelberg.

Gröger M., Arbter K., and Hirzinger G. (2008). *Motion Tracking for Minimally Invasive Robotic Surgery*, In Bozovic V., editor, *Medical Robotics*, pages 117–148. I-Tech Education and Publishing, Vienna, Austria.

Hilbert S. (2005). *Optoelektronische Wandler (Kap. 4.4) und Sensornahe Elektronik (Kap. 4.6)*, In Sandau R., editor, *Digitale Luftbildkamera - Einführung und Grundlagen*, pages 197–226,–230–239. Herbert Wichmann Verlag, Hüthig GmbH & Co. KG, Heidelberg.

Hirzinger G., Landzettel K., and Kaiser C. (2007). *Neue Technologien und Robotik*, In Hallmann W., editor, *Handbuch der Raumfahrttechnik*. Hanser Verlag.

Höpler R. (2005). *A Unifying Object-oriented Methodology to Consolidate Multibody Dynamics Computations in Robot Control*, In *Fortschritt-Berichte VDI*, volume 1054, pages 1–115. VDI Verlag.

Jahn H. (2005). *Einleitung Grundlagen und Definitionen, Grundlegende Eigenschaften des Lichts, Fouriertransformation, Lineare Systeme, Signalabtastung, Radiometr. Auflösung und Rauschen, Farbe (Kap. 2.1-2.7)*, In Sandau R., editor, *Digitale Luftbildkamera - Einführung und Grundlagen*, pages 33–105. Herbert Wichmann Verlag, Hüthig GmbH & Co. KG, Heidelberg.

Lange F. and Hirzinger G. (2007). *Spatial Vision-Based Control of High-Speed Robot Arms*, In Cubero S., editor, *Industrial Robotics - Theory, Modelling and Control*, pages 693–712. pro literatur Verlag, Mammendorf, Germany.

Liu R. and Hirzinger G. (2005). *Matching-Tree - A Novel Data Structure for Global Automatic Matching*, In Grün A. and H. K., editors, *Optical 3-D Measurement Techniques VII*, volume II.

Liu R., Suppa M., and Hirzinger G. (2007). *Modelling the World in Real Time*, In Grün A. and H. K., editors, *Optical 3-D Measurement Techniques VIII*, volume I.

Looye G. (2007). *Rapid prototyping using inversion-based control and object-oriented modelling*, In Bates D. and Hagström M., editors, *Nonlinear analysis and synthesis techniques for aircraft control*. Lecture Notes in Control and Information Sciences. Springer Verlag.

Maibaum O., Montenegro S., and Terzibaschian T. (2008). *Robustness as Key to Success for Space Missions*, In Schuster A., editor, *Robust Intelligent Systems*, pages 233–250. Springer.

Niemeyer G., Preusche C., and Hirzinger G. (2008). *Telerobotics*, In Siciliano B. and Khatib O., editors, *Handbook of Robotics*, pages 741–757. Springer Verlag.

Ortmaier T., Deml B., Kübler B., Passig G., Reintsema D., and Seibold U. (2007). *Robot Assisted Force Feedback Surgery*, In Ferre M., Buss M., Aracil R., Melchiorri C., and Balaguer C., editors, *Advances in Telerobotics*, pages 361–379. Springer Tracts in Advanced Robotics (STAR) series book.

Otter M., Elmqvist H., and Mattsson S. E. (2007). *Multi-Domaiin Modeling with Modelica*, In Fishwick P., editor, *CRC Handbook of Dynamic System Modeling*, pages 36.1–36.27.

Preusche C., Hulin T., and Hirzinger G. (2008). *Haptic Rendering and Control*, In *Human Haptic Perception: Basics and Applications*. Birkhäuser Basel.

Radi M., Artigas J., Preusche C., and Hirzinger G. (2008). *Transparency Measurement of Telepresence Systems*, In *Haptics: Perception, Devices and Scenarios*. Springer Berlin / Heidelberg.

Rauer H., Erikson A., Hatzes A. P., Pätzold M., Wuchterl G., Berlin R., Carone L., Eigmüller P., Eislöffel J., Gahr A., Guenther E., Kabath P., Krutz D., Lehmann H., Peter G., Rohbeck U., Russ N., Ulmer B., Voss H., and Zecha T. (2006). *The German Contribution to the CoRoT Mission*, In *The CoRoT Mission*, volume 1306, pages 123–127. ESA Science Publications.

Seibold U., Kuebler B., and Hirzinger G. (2008). *Medical Robotics, chapter Prototypic force feedback instrument for minimally invasive robotic surgery.*, In Bozovic V., editor, *Medical Robotics*, pages 377–400. I-Tech Education and Publishing, Vienna, Austria.

Varga A. (2005). *Controller reduction using accuracy-enhancing methods*, In Benner P., Mehrmann V., and Sorensen D., editors, *Dimension Reduction of Large-Scale Systems, Lecture Notes in Computational Science and Engineering*, volume 45, pages 225–260. Springer Verlag.

5.4 Books (“B”)

Heckmann A. (2005). *The Modal Multifield Approach in Multibody Dynamics*, volume 398. VDI.

Huang F., Klette R., and Scheibe K. (2008). *Panoramic Imaging - Sensor-Line Cameras and Laser Range-Finders*. Wiley.

5.5 Patents (“p”)

The following 124 patents were filed or granted in the reporting period:

Albu-Schäffer A., Hagn U., Ott C., and Ortmaier T. (2007). Verfahren zur Regelung eines Roboterarms sowie Roboter zur Durchführung des Verfahrens, Patent Germany: 102005054575B3, USA: pending.

Albu-Schäffer A., Schreiber G., and Sporer N. (2007). Verfahren zur Bewegungskommandierung eines Roboters, Patent Germany: 10137955,IPC B25J 9/22.

Arbter K., Sepp W., and Fuchs S. (2008). Verfahren und Vorrichtung zur Bestimmung der Lage eines Kamerasystems relativ zu einem Objekt, Patent pending.

Bajcinca N. and Bünte T. (2006). Verfahren und Vorrichtung zur Steuerung oder Regelung von Prozessgrößen sowie zur näherungsweisen Inversion dynamischer Systeme, Patent Germany: 10 2005 004 632 B3.

Baumann A. (2008). Vorrichtung zum Andocken an Satelliten, Patent pending.

Baumann A., Gruber R., and Kielhöfer S. (2008). Anordnung optischer Sensoren zur Lagebestimmung in Satellitendüsen, Patent pending.

Bodenmüller T., Kielhöfer S., Hagn U., Konietschke R., Suppa M., and Hacker F. (2008). Intelligenter Triangulationsscanner zur autonomen oder teilautonomen Erfassung von 3D Oberflächen und zur Anzeige von positionsgebundenen Informationen in der Realität, Patent pending.

Börner A. (2006). Positions- und Lagebestimmung in Innenräumen, Patent Germany: 202004000000.

Börner A. (2008). Optisches Abbildungssystem mit Autofokus und Verfahren zur automatischen Fokussierung eines Objektes, Patent pending.

Börner A. (2008). Optisches System sowie ein Verfahren zur Bildaufnahme, Patent pending.

Börner A., Eckardt A., and Lehmann F. (2008). Digitale Zeilenkamera, Patent pending.

Börner A., Eckardt A., Walter I., and Hilber S. (2008). Fokalebene und Verfahren zur Justage einer solchen Fokalebene, Patent Germany: 102005000000.

Börner A., Scheele A., and Schichmanow M. (2007). Verfahren und Vorrichtung zur Bestimmung der Punktverschmierungsfunktion eines optischen Sensorsystems, Patent Germany: 102005056188.

Börner A., Scheele M., and Schuster R. (2008). Optisches System mit veränderlichen Abbildungseigentschaften und Verfahren zur Einstellung veränderlicher Abbildungseigenschaften, Patent pending.

Dietrich J., Grebenstein M., Lange T., Schedl M., and Neumann P. (2006). Vorrichtungen für Roboterantriebseinheiten, Patent Europe: EP000001293024B1.

Eckardt A. (2008). Erdbeobachtungssatellit mit einem Spiegelteleskop, Patent Germany: 102006000000.

Eckardt A. (2008). TDI-Zeilendetektor und Detektoranordnung unter Verwendung von TDI-Zeilendetektoren, Patent pending.

Eckardt A. (2008). Vorrichtung zur digitalen Abtastung von farbigen Bildvorlagen, Patent Switzerland: 697319.

Eckardt A. and Börner A. (2008). Sensoren zur indirekten Erzeugung von höchstauflösenden Multispektralbildern, Patent pending.

Eckardt A., Börner A., and Jahn H. (2008). Verfahren und Vorrichtung zur Bestimmung der LSF und/oder MTF eines photosensitiven Zeilen- oder Matrix-Sensors, Patent pending.

Eckardt A., Börner A., Schichanov A., Rollenhagen F., and Schanvaski V. (2008). Verfahren und Vorrichtung zur Kalibration und zum Test von Sternkameras, Patent Germany: 102006000000.

Eckardt A. and Dobler C. (2007). Film-Scanner, Patent USA: 7217943.

Eckardt A. and Drischer H. (2008). Side-view or rear-view mirror for a motor vehicle, Patent pending.

Eckardt A. and Hirzinger G. (2008). Panorama-Bildprojektor, Patent pending.

Eckardt A., Hirzinger G., and Lehmann F. (2008). Kamerasystem zur Aufnahme verschiedener Spektraler Bilder einer Szene, Patent pending.

Eckardt A., Sandau R., and Dittel R. (2008). Vorrichtung und Verfahren zur Informationsaufbereitung von Umgebungsdaten und/oder Fahrzeugzustandsdaten eines Kraftfahrzeuges, Patent pending.

Eiberger O. (2008). Gelenkmechanismus, Patent pending.

Eiberger O. (2008). Roboter-Manipulator-Gelenkantrieb, Patent pending.

Eiberger O., Eiband K., and Heinzl A. (2008). Elektromagnetische Bremse für Handlingssysteme, Patent pending.

Friedl W., Hagn U., Kielhöfer S., Hacker F., and Suppa M. (2007). Triangulationsscanner, Patent Germany: 102006001382B3.

Fuchs M. (2008). Industrieroboter-Anordnung, Patent pending.

Fürstenau N., Hetzheim H., Halle W., Rudolph M., Schmid t. M., Werther B., and Tuchscheerer W. (2008). Flugverkehr-Leiteinrichtung, Patent pending.

Grebenstein M. (2006). Sitz, Patent Germany: 000010034289B4.

Grebenstein M. (2007). Antagonistische Schwenkvorrichtung, Patent pending.

Grebenstein M. (2008). Gelenkeinheit für einen Roboter, Patent Germany: 102004059235B3, USA: Pending.

Grebenstein M. (2008). Joint unit for a robot, Patent pending.

Grebenstein M. (2008). Kupplung zum Ausgleichen eines Achsversatzes, Patent pending.

Grebenstein M. (2008). Robotergelenk, Patent pending.

Grebenstein M. and Fischer M. (2008). Roboterhand, Patent Germany: 102006006322B3, Europe: 000001820610A1.

Gruber R. (2008). Energieversorgungsvorrichtung, Patent pending.

Gruber R. (2008). Verfahren zur Minimierung von Rippelströmen, Patent pending.

Gruber R. and Baumann A. (2008). Robuster kapazitiver Abstandssensor, Patent pending.

Gruber R. and Knorr M. (2005). Verfahren und Einrichtung zur Positions- und Lagebestimmung eines Objekts unter Verwendung von elektromagnetischen Wellen, Patent pending.

Gruber R. and Kunze K. (2008). Flachkabel zur Energiedurchleitung, Patent pending.

Gruber R. and Lemke P. (2008). Abgasreinigungsvorrichtung für Brennstoffaggregate, Patent pending.

Gruber R. and Lemke P. (2008). Abgasreinigungsvorrichtung für Brennstoffaggregate, Patent pending.

Gruber R. and Nickl M. (2008). Drehkupplung zur berührungslosen Übertragung von elektrischen Signalen, Patent pending.

Gruber R. and Passig G. (2008). Modulationsverfahren zur Datenübertragung auf Stromleitungen, Patent pending.

Gruber R., Schott J., and Tegtmeier B. (2008). Verfahren zum Detektieren und zum Löschen von Latch-Ups sowie Anordnungen der Verfahren, Patent Germany: 102005000000, USA: 7310211, France: 1751800, Netherlands: 1751800.

Gruber R. and Sedlmayr H.-J. (2008). Redundantes elektromotorisches Antriebssystem, Patent Europe: 1764907.

Gruber R. and Seitz N. (2008). Elektrische Spannungsversorgungseinheit zur Erzeugung mindestens einer Ausgangsgleichspannung aus einer Versorgungsgleichspannung, Patent pending.

Hagn U. (2008). Device for connecting conventional or laparoscopic instruments to a robot, Patent Germany: 102004054866B3, USA: pending.

Hagn U. (2008). Roboterarm sowie Roboter-Tragstruktur, Patent Germany: 30546322.

Hagn U. (2008). Tastatur für Computer, Patent pending.

Hagn U., Albu-Schäffer A., Grebenstein M., Joehl K., Nickl M., Ortmaier T., Hacker F., Jörg S., and Konietschke R. (2007). Anthropomorpher medizintechnischer Roboterarm mit Bewegungseinschränkung, Patent Europe: EP000001754448B1, USA: Pending.

Hagn U. and Schreiber G. (2008). Handhabungsroboter und Verfahren zur Steuerung eines Handhabungsroboters, Patent pending.

Hassenpflug H., Markgraf M., Ettl J., and Toner P. (2008). Intelligentes GPS Antennen System bei spinnstabilisierte Höhenforschungs-Raketen für fehlerfreien GPS Empfang, Patent pending.

Hecker S. (2007). Sensoreinrichtung zur Windturbulenzmessung sowie Verfahren zur Windturbulenzmessung, Patent Germany: 10 2006 003 199.

Hetzheim H. (2007). Verfahren und Vorrichtung zum Erkennen und zur Größenvermessung von Bereichen gleicher Textur in einem Digitalbild, Patent Germany: 102005000000, Germany: 102006000000.

Hetzheim H. (2008). Verfahren und Vorrichtung zum Auffinden und Unterscheiden von Personen, Tieren oder Fahrzeugen mittels automatischer Bildüberwachung digitaler oder digitalisierter Bilder, Patent pending.

Hetzheim H. (2008). Verfahren und Vorrichtung zur Bestimmung der Geschwindigkeit von Verkehrsteilnehmern bei bildgebenden Verfahren, Patent Germany: 10 2004 036 157.

Hetzheim H. (2008). Verfahren und Vorrichtung zur Bestimmung des aktuellen Hintergrundes in einem Digitalbild mit zumindest temporär beweglichen Objekten, Patent pending.

Hetzheim H. (2008). Verfahren und Vorrichtung zur Verkehrsüberwachung, Patent Germany: 102 39 026.

Hübers H., Eckardt A., and Drischer H. (2008). Film scanner for color originals, Patent pending.

Jahn H., Eckardt A., and Börner A. (2008). Optisches Sensorsystem und Verfahren zur Ansteuerung eines optischen Sensorsystems, Patent pending.

Kielhöfer S., Gruber R., Schott J., Nickl M., and Hacker F. (2008). Elektrostatisch angetriebener Mikroaktor, Patent pending.

Konietschke R. (2008). Verfahren und System zum Übertragen von positionszugeordneten Informationen aus einer virtuellen in eine tatsächliche Realität und zum Anzeigen dieser Informationen in der tatsächlichen Realität, Patent pending.

Kübler B., Passig G., Gruber R., Prepbar S., and Wegel C. (2008). Ultraschallkopf mit Ultraschall-Doppler-Anordnung, Patent pending.

Kübler B. and Seibold U. (2008). Rachenraum-Hüllschlauch, Patent Germany: 20 2007 012 842 U.

Kübler B., Seibold U., and Hagn U. (2008). Chirurgisches Manipulationsinstrument, Patent Germany: 10 2006 045 865.

Lange F. (2008). Radmontage-Industrieroboter und Verfahren zur Montage eines Rades durch einen Radmontage-Industrieroboter, Patent pending.

Lange F., Frommberger M., Jörg S., Langwald J., Meusel P., Willberg B., and Werner J. (2008). Radmontage-Roboter, Patent pending.

Lange F., Jörg S., Frommberger M., Langwald J., Meusel P., and Riegel S. (2006). Industrieroboter, Patent Germany: 10 2006 057 843.

Lange F., Jörg S., Meusel P., Langwald J., Frommberger M., and Lange F. (2006). Anordnung zur Montage eines Anbauteiles an ein bewegtes Basisbauteil, Patent Germany: 10 2006 011 341.

Lange F. and Riegel S. (2008). Radmontage-Industrieroboter und Verfahren zum Betrieb eines Radmontage-Industrieroboters, Patent pending.

Lemke P. (2008). Magnetischer Längensensor, Patent pending.

Lemke P. and Eiberger O. (2008). Elektromagnetmetallkern aus Einzelblechen, Patent Germany: 102006000000.

Lemke P. and Gruber R. (2008). Verfahren und Schaltung zur Messung des einem stromgesteuerten Verbraucher zugeführten oder des von einer stromgesteuerten Quelle abgeführten Stromes, Patent pending.

Lemke P. and Seibold U. (2008). Winkel-Messanordnung, Patent pending.

Mertens V., Knollernber J., Behnke T., Kührt E., Gräser G., Jock A., Krane U., Neus H., and Vogel H. (2008). Verfahren für die Überwachung von Territorien zur Erkennung von Wald- und Flächenbränden, Patent Turkey: 1817759B1, Slovenia: 1817759B1, Portugal: 1817759B1, Poland: 1817759B1, Netherlands: 1817759B1, Letland: 1817759B1, Italy: 1817759B1, Chech Republic: 1817759, Cyprus: C08/1100380, Switzerland: 1817759B1, Bulgaria: 1817759B1, Estonia: 1817759B1, Germany: 502005000000, France: 1817759B1, Greece: 20080401031, Spain: 1817759B1.

Meusel P. and Liu H. (2008). Roboterfinger sowie Roboterhand, Patent Germany: 402008000000.

Meusel P., Liu H., Willberg B., and Seitz N. (2008). Roboter-Hand, Patent Germany: 202005000000.

Meusel P., Willberg B., and Bryzgalski M. (2008). Opto-elektronischer Kraft-Momenten-Sensor, Patent pending.

Meyer zu Hörste M., Pelz M., Börner A., and Wohlfeil J. (2008). Videobasiertes Verfahren für eine gleisselektive Ortungsinformation, Patent pending.

Nagel J., Kübler B., and Ortmaier T. (2007). Verfahren zum Aufspüren und Lokalisieren von im Inneren eines Materials oder Gewebes vorhandenen, besonderen Strukturen, Patent Germany: 10 2005 045 480 B4.

Oertel D., Jahn H., Lorenz E., Bärwald W., Halle W., Terzibaschian T., Venus H., and Zhukov B. (2008). Verfahren zur Erkennung von heißen Zielen am Erdboden, Patent pending.

Ortmaier T., Jacob A., and Neff T. (2008). Verfahren zur Kühlung hochintegrierter Roboter mittels Peltierelemente, Patent pending.

Ortmaier T., Jacob A., and Neff T. (2008). Verfahren zur Vereinfachung der Planung und des Aufbaus in der navigierten und/oder robotergestützten Chirurgie, Patent pending.

Ortmaier T., Jacob D., Heinzl A., and Neff T. (2008). Patientenregistrierung durch robotergetragene Sensorsysteme, Patent pending.

Ortmaier T., Jacob D., Heinzl A., and Neff T. (2008). Sterilbarriere für einen chirurgischen Roboter mit Drehmomentsensoren, Patent pending.

Ortmaier T., Neff T., and Jacob D. (2008). Anpassung des Robotermodells eines chirurgischen Roboters an ein montiertes Werkzeug mittels RFID-Technik, Patent pending.

Ortmaier T., Neff T., Ueberle M., and Summerer A. (2008). Kameragestützte virtuelle Wände bei Robotern in der Chirurgie, Patent pending.

Ortmaier T., Passig G., and Jacob D. (2008). Augmented Reality Interface für die robotergestützte Chirurgie, Patent pending.

Ortmaier T. and Ueberle M. (2008). Anpassung des Arbeitsbereiches in sicherer Technik zur Erfüllung von Performanzanforderungen, Patent pending.

Riegel S. and Lange F. (2006). Roboter sowie Roboter-Schutzeinrichtung, Patent Germany: 10 2006 044 071.

Schallert C. (2008). Verfahren zur Analyse der Zuverlässigkeit technischer Anlagen mit Hilfe von physikalischen Modellen, Patent pending.

Schreiber G., Albu-Schäffer A., and Sporer N. (2005). Kalibrierverfahren für einen Roboterarm, Patent Germany: 10143753, IPCB25J 9/22.

Schroth A., Hornbostl A., Konovaltsev A., Steingast A., Eckardt A., and Venus H. (2008). Signal-Simulationseinrichtung, Patent Europe: 1715359, UK: 1715359, Finland: 1715359, France: 1715359, Germany: 502006000000, Switzerland: 1715359.

Schwarzer H., Eckardt A., Pausmann H., and Hofer S. (2007). Verfahren und Vorrichtung zur Kalibration von Hyperspektralinstrumenten sowie ein Hyperspektralinstrument, Patent Germany: 102005000000.

Sedlmayr H.-J. and Gruber R. (2008). Testvorrichtung zur Überwachung des Stroms in einem einer Strahlungsbelastung ausgesetzten, zu testenden elektrischen Bauteil, Patent pending.

Seibold U. (2008). Chirurgie-Roboter-Anordnung, Patent pending.

Seibold U., Hagn U., and Sturm M. (2008). Roboterstruktur, Patent Germany: 10 2006 059 952 B3.

Seibold U., Haslinger R., and Passig G. (2008). Kraft-Moment-Sensor zum Messen von mindestens drei orthogonalen Belastungen, Patent pending.

Seibold U. and Weiß H. (2008). Greifbediengerät, Patent pending.

Skbek W., Sandau R., and Gerzer R. (2008). Verfahren und Vorrichtung zur Ermittlung der arteriellen Gefäßreagibilität, Patent pending.

Smagt van der P. (2007). Taktiler Flächensensor, Patent Germany: 10 2006 016 662.

Smagt van der P. (2008). Taktiler Flächensensor, Patent Germany: 10 2006 016 661.

Smagt van der P., Strohmayr M., and Harms A. (2008). Aufnehmer zur Erfassung von Biopotentialen, Patent pending.

Sporer N. (2008). Verfahren zum Schalten einer elektromagnetischen Bremse sowie elektromagnetische Bremse, Patent Germany: 502005000000, France: 1754448, UK: 1754448, Italy: 1754448.

Strohmayr M., Smagt van der P., and Krampe E. (2008). Taktiler Flächensensor, Patent Germany: 10 2007 020 131.

Tschhernjawski V., Rollenhagen F., Grunert U., Neidhardt M., Zender B., and Trautenberg H. (2008). Verfahren und Vorrichtung zum Liefern eines phasensprungarmen Uhrsignals beim Umschalten zwischen zwei Frequenzstandards, Patent Germany: 102005000000.

Uhlig M., Eckardt A., and Neidhardt M.

(2008). Film scanner and a scanning method for surpressing brightness variations of a radiation source, Patent pending.

Vodermayer B. and Schmid T. (2007). Einrichtung zum Unterbringen und Positionieren von Einheiten zur drahtlosen Energie- und Datenübertragung zu Implantaten, Patent Germany: 202007000000.

Vodermayer B. and Schmid T. (2008). Kunstherz, Patent pending.

Vodermayer B. and Schmid T. (2008). Übertragungs-Anordnung, Patent pending.

Vodermayer B., Wagner H., Schmid T., and Schiller W. (2008). Herzunterstützungsvorrichtung, Patent pending.

Vodermayer B., Wagner H., Schmid T., and Schiller W. (2008). Implantierbares Zweikammersystem zum Unterstützen des linken Herzventrikels, Patent pending.

Walter I. and Zender B. (2008). Vorrichtung zur Digitalisierung von Filmmaterial, Patent pending.

Willberg B. (2008). Zweiachsiger Momentensensor, Patent pending.

Willberg B. and Baumann A. (2007). Raumtransporter mit einer Vorrichtung zum Andocken an einen Satelliten, Patent Germany: 102006009001.

Willberg B., Lange F., Riegel S., and Meusel P. (2008). Messeinrichtung, Patent Germany: 10 2006 034 481.

Willberg B., Meusel P., and Liu H. (2008). Vierfinger-Roboterhand, Patent pending.

Willberg B. and Strobl C. (2008). Kalibriervorrichtung sowie Kalibrierverfahren zum Kalibrieren von Kraft-Momenten-Sensoren, Patent pending.

Wolf S. (2008). Roboter-Manipulatorarm-Gelenkantrieb, Patent pending.

5.6 Ph.D. Theses ("t")

A total of 22 Ph.D. theses were finished in the reporting period:

Bajcinca N. (2006). *Robust Control Methods with Applications to Steer-by-Wire Systems*. Ph.D. thesis, TU Berlin.

Ballauf C. (2008). *Dämpfung aeroelastischer Strukturen mit modelladaptiver Regelung*. Ph.D. thesis, TU München.

Carrarini A. (2006). *Reliability based analysis of the crosswind stability of railway vehicles*. Ph.D. thesis, TU Berlin.

Hecker S. (2006). *Generation of low order LFT Representations for Robust Control Applications*. Ph.D. thesis, TU München.

Heckmann A. (2005). *The Modal Multifield Approach in Multibody Dynamics*. Ph.D. thesis, Universität Hannover.

Konietschke R. (2008). *Planning of Workplaces with Multiple Kinematically Redundant Robots*. Ph.D. thesis, TU München.

Krutz D. (2006). *Ein Betriebssystem für konfigurierbare Hardware*. Ph.D. thesis, HU Berlin.

Kurze M. (2008). *Modellbasierte Regelung von Robotern mit elastischen Gelenken ohne abtriebsseitige Sensorik*. Ph.D. thesis, TU München.

Kurzeck B. (2008). *Methoden zur Minderung mittelfrequenter Schwingungen bei Bogenfahrt im Schienennahverkehr*. Ph.D. thesis, TU Berlin.

Looye G. (2008). *An Integrated Approach to Aircraft Modelling and Flight Control Law Design*. Ph.D. thesis, TU Delft, Netherlands.

Pfeiffer A. (2008). *Numerische Sensitivitätsanalyse unstetiger multidisziplinärer Modelle mit Anwendungen in der gradientenbasierten Optimierung*. Ph.D. thesis, Martin-Luther Universität Halle-Wittenberg.

Reijerkerk M. (2008). *Aeroelastic Model Identification of Winglet Loads from Flight Test Data*. Ph.D. thesis, TU Delft, Netherlands.

Reschke C. (2006). *Integrated Flight Loads Modelling and Analysis for Flexible Transport Aircraft*. Ph.D. thesis, TU Stuttgart.

Saiger P. (2007). *Entwicklung, Implementierung und Erprobung eines planetaren Informationssystems auf Basis von ArcGIS*. Ph.D. thesis, Universität Potsdam.

Scheibe K. (2006). *Design and Test of Algorithms for the Evaluation of Modern Sensors in Close-Range Photogrammetry*. Ph.D. thesis, Universität Göttingen.

Schmid T. (2007). *Doppelpulsatiles Herzunterstützungssystem*. Ph.D. thesis, TU München.

Schreiber G. (2005). *Steuerung für redun-*

dante Robotersysteme: Benutzer- und aufgabenorientierte Verwendung der Redundanz. Ph.D. thesis, Universität Stuttgart.

Schweiger C. (2008). *Objektorientierte Modellierung und Echtzeitsimulation von Kraftfahrzeug-Antriebssträngen*. Ph.D. thesis, Universität der Bundeswehr München.

Sepp W. (2008). *Visual Servoing of Textured Free-Form Objects in 6 Degrees of Freedom*. Ph.D. thesis, TU München.

Suppa M. (2008). *Autonomous robot work cell exploration using multisensory eye-in-hand systems*. Ph.D. thesis, Universität Hannover.

Thümmel M. (2007). *Modellbasierte Regelung mit nichtlinearen inversen Systemen und Beobachtern von Robotern mit elastischen Gelenken*. Ph.D. thesis, Lehrstuhl für Elektrische Antriebssysteme TU München.

Tobolar J. (2005). *Reduktion von Fahrzeugmodellen zur Echtzeitsimulation*. Ph.D. thesis, Czech Technical University in Prague.

5.7 Technical Reports ("r")

136 Technical reports, including Master and other theses, were filed:

Ackermann J. (2005). Entkopplung und Dämpfungsvorgabe bei der Autolenkung. Technical Report DLR-IB 515-2005/16.

Apfelbeck M. (2008). Modellierung eines virtuellen Rad-Boden Prüfstandes für einen Mars Rover in Modelica und Identifikation der Rad-Boden-Parameter. Technical Report DLR IB 515-08-15.

Bader R. (2006). Redesign des Linksventrikulären DLR Herzunterstützungssystems. Technical Report DLR-IB 515-2006/7.

Bajcinca N. and Hulin T. (2005). RobSin: Software-Werkzeug zum Entwurf robuster PID-Regler. Technical Report DLR-IB 515-2005/18.

Bals J., Schedl M., Kuhn M., Schweiger C., and Lemke P. (2007). EOSYS Mechatronische Systeme. Technical Report DLR-IB 515-07-38.

Bauer M. (2008). Sensorkalibrierung mit diffraktiv optischen Elementen. Technical report.

Baumann A. (2006). Berechnung und Konstruktion einer weltraumtauglichen Mechanik zum Ergreifen eines Satelliten. Technical Report DLR-IB 515-2006/4.

Beier G. (2006). Entwicklung eines Filterrades für eine IR-Signaturkamera. Technical report.

Bellana J. (2007). Design and Implementation of an Encountered-type Haptic Display: "What You See Is What You Feel". Technical Report DLR IB 515-07-10.

Bellmann T. (2008). Echtzeitbahnplanung für einen innovativen, roboterbasierten, interaktiven Bewegungssimulator. Technical Report DLR IB 515-08-19.

Benner M. (2008). Robuster Reglerentwurf mithilfe der µ-Synthese und Analyse am Prüfstand. Technical Report DLR-IB 515-08-14.

Bertleff W. (2007). Entwicklung und Implementierung eine Algorithmus zur trägheitsabhängigen Parametrierung des Zustandsreglers am DLR Leichbauroboter III. Technical Report DLR-IB 515-2007/1.

Bliem T. (2008). Entwicklung eines grafischen Analyse-Tools für Dymola. Technical Report DLR IB 515-08-38.

Bochert T. (2007). Modellierung und Simulation von Flugzeugsystemen. Technical Report DLR-IB 515-07-39.

Brüßhaber C. (2005). Können HRSC-Aufnahmen zur Aktualisierung der ALK genutzt werden? Untersuchung von HRSC-Daten mit Wewel-Prozessierung und der ALK - ein Beispiel aus Berlin -. Technical report.

Brüßhaber C. (2008). Genauigkeiten digitaler flugzeuggestützter Bilddaten matrix- und zeilenbasierter Sensorsysteme - Untersuchung am Beispiel der HRSC-AX, UltraCamD und MFC 3 -. Technical report.

Buder M. (2007). Verlustfreie Kompression in rekonfigurierbarer Hardware. Technical report.

Burger R. (2005). Analyse von Verfahren zum parallelen Betrieb von Echtzeit- und Standard-Betriebssystemen auf einer CPU am Beispiel der Steuerung der DLR-Hand-II. Technical Report DLR-IB 515-05-13.

Burger R. (2007). Anbindung und Evaluierung von Sensorik zur Erzeugung von Umgebungsmodellen in Robotersteuerungen. Technical Report DLR-IB 515-2007/15.

Busch M. (2007). Entwicklung einer SIMPACK-Modelica/Dymola Schnittstelle. Technical Report DLR IB 515-07-02.

Carrarini A. (2008). Numerical Analysis of Railway Rolling Noise Generation. Technical Report DLR IB 515-08-27.

Carrarini A. (2008). SimSound - A Multibody-Simulation Based Tool for Acoustic Analysis. Technical Report DLR IB 515-08-26.

Chaudhari T. (2008). Modeling and Analysis of an antagonistically driven robot hand. Technical Report DLR-IB 515-2008/05.

Chen C.-C. (2005). Simulation of free-floating robots based on superposition of satellite base and manipulator motions. Technical Report DLR-IB 515-2005/3.

Chen C.-C., Schäfer B., and Rebele B. (2005). Simulation of free-floating robots based on superposition of satellite base and manipulator motions. Technical Report DLR-IB 515-05-03.

Dasse-Hartaut S. (2008). Motion planning as a nonlinear programming problem with B-splines and collision avoidance. Technical Report DLR-IB 515-2008/20.

Diener M. (2005). Spezifikation und Implementierung eines Protokolls zur Konfiguration von telepräsenzfähigen Geräten. Technical Report DLR-IB 515-2005/12.

Dietl S. (2006). Integration eines robotergeführten Hand-Auge-Systems zur Umgebungsexploration und Vergleich von Explorationsverfahren. Technical Report DLR-IB 515-2006/19.

Fabel S. (2007). Robotergestützte Verfolgung des Blutgefässverlaufs mittels Doppler-Ultraschall. Technical Report DLR-IB 515-2007/21.

Fähse M. (2007). Entwicklung einer Steuerelektronik für den DLR kraftreflektierenden Joystick. Technical Report DLR-IB 515-2007/4.

Fenili A. and Schäfer B. (2007). Contact Dynamics Investigations. Technical Report DLR-IB 515-2007/29.

Fiedler S. (2005). Paramatrische Modellierung und Simulation eines elastischen Flugzeuges. Technical Report DLR-IB 515-2005/24.

Fleischmann H. (2006). Algorithmen zur Bestimmung von Objekteigenschaften in konfigurierbarer Hardware. Technical report.

Fröhlich F. (2006). Untersuchung zur synchronen Akquisition endoskopischer Stereobilder. Technical Report DLR-IB 515-2006/8.

Frommholz D. (2008). Beschleunigung von Matchingverfahren durch 3D-Laserdaten zur schnellen und präzisen Objektrekonstruktion. Technical report.

Fuchs M. (2005). Untersuchung und Entwicklung eines hochgenauen Drehwinkelsensors. Technical Report DLR-IB 515-2005/9.

Fuchs M. (2008). Konzeption der Engergieversorgung und Antriebssteuerung für ein mobiles Roboter-Plattformsystem. Technical Report DLR-IB 515-2008/06.

Fuchs S. (2006). Autonomes Greifen bekannter Objekte in freier Bewegung. Technical Report DLR-IB 515-2006/5.

Gesenhues R. (2008). Aktive Schwingungsdämpfung für mobile Serviceroboter. Technical Report DLR-IB 515-2008/22.

Glässer J. (2006). Untersuchung zur Verfolgung der Herzbewegung durch ein Robotersystem. Technical Report DLR-IB 515-2006/9.

Gmeiner H. (2008). Entwicklung eines elektro-hydraulischen Antriebssystem für das DLR-Kunstherz. Technical Report DLR-IB 515-2008/08.

Gobert C. (2007). Aufbereitung der Eingangsdaten zu POALib: Dokumentation der Untersuchung verschiedener Interpolations- / Approximationsmethoden und Entwicklung einer Methode zur Approximation durch Splines. Technical Report DLR-IB 515-07-40.

Görner M. (2007). Entwurf eines mechatronischen Konzepts für einen Krabbelroboter basierend auf der DLR-Hand Fingertechnologie. Technical Report DLR IB 515-07-09.

Grössl M. (2007). Test von weltraumtauchlicher Hardware mittels Boundary Scan. Technical Report DLR-IB 515-2007/6.

Haberhauer U. (2005). Bewertung von Algorithmen zur Bewegungskorrektur in Bildsequenzen des schlagenden Herzens. Technical Report DLR-IB 515-2005/14.

Haddadin S. (2006). Bewertungskriterien und Regelungsstrukturen für eine sichere Mensch-Roboter Interaktion. Technical Report DLR-IB 515-2006/1.

Hähnle M. and Sporer N. (2005). Drehmomentgeregelte Servoantriebe für Industrie, Fahrsimulatoren und Steer-by-Wire. Technical Report DLR-IB, 515-05-03.

Hao X. (2007). Modellierung und Positionsregelung des Roboterfingers der DLR/HIT Hand. Technical Report DLR-IB 515-2007/35.

Hecker S. and Peterson D. (2008). Report on State-of-the-art techniques for generation of LFT models. Technical Report DLR IB 515-08-34.

Heckmann A. and Bals J. (2007). Entwicklung von Entwurfs- und Berechnungsmethoden sowie Aufbau eines Conceptual Design Labors. Technical Report DLR IB 515-07-03.

Heger M. (2006). Entwicklung und Simulation einer Fly-by-Wire-Steuerung per DLR-Spacemouse für ein Kleinluftschiff. Technical Report DLR-IB 515-2006/15.

Hiltner J. Z. (2008). Visuelle 3D-Lagebestimmung der DLR-Sensorzange für die endoskopische Chirurgie. Technical Report DLR-IB 515-2008/11.

Hirzinger G. (2005). BKM - Forschungsnetzwerk für die Industrie. Technical Report DLR-IB, 515-05-03.

Hirzinger G., Schedl M., and Sporer N. (2005). Leichtbaudesign in der Robotik. Technical Report DLR-IB 15-05-03.

Holzäpfel F., Frech M., Tafferner A., Hahn K.-U., Schwarz C., Joos H.-D., Korn B., and Lenz H. (2005). Wake Vortex Scenarios Simulation Package 2. Technical Report DLR-IB 553-1/2005.

Holzer S. (2006). Stereobildauswertung zur 3D-Lagebestimmung auf der Herz-Oberfläche. Technical Report DLR-IB 515-2006/18.

Hosseini A. (2008). Bilateral Telerobotics in Presence of Time-Varying Delays and Packet-Loss. Technical Report DLR-IB 515-2008/3.

Jahn H. (2008). Beiträge zur Bild- und Signalverarbeitung. Technical report.

Ji Y. (2007). Stability and Quality Tests of an Electric Network for a More Electric Aircraft Architecture. Technical Report DLR-IB 515-07-44.

Joos H.-D. (2005a). HTP-Modes Control (HLAS) Bending Moment A380. Technical Report DLR IB 515-05-21.

Joos H.-D. (2005b). Zusammenfassung der HBLAS-Berichte Biegemeoment HTP-root A380. Technical Report DLR IB 515-05-20.

Joos H.-D. (2006). Untersuchungen zur Optimierung Lärmarmer Anflugbahnen mit MOPS. Technical Report DLR IB 515-06-10.

Joos H.-D. (2008a). MOPS Multi-Objective Parameter Synthesis User's Guide V 5.3. Technical Report DLR IB 515-08-37.

Joos H.-D. (2008b). Specification of an optimisation based clearance tool based on parallel computation. Technical Report DLR IB 515-08-36.

Joos H.-D., Hecker S., Varga A., and Mouyon P. (2008). Trimming and Linearization Tools for Criteria Evaluation. Technical Report DLR IB 515-08-33.

Kamel A. (2007). Dämpfung von Schwingungen eines Industrieroboters mit nachgiebigem Kraft-Momenten-Sensor. Technical Report DLR-IB 515-2007/36.

Knöferle A. (2007). Entwicklung eines automatischen Laserprojektionssystems zum Einsatz in der AR-unterstützten Chirurgie. Technical Report DLR-IB 515-2007/17.

Krüger N. (2006). Entwicklung einer humanoiden Ball-Fang-Strategie für ein Roboter-Hand-Arm-System. Technical Report DLR-IB 515-2007/13.

Kulkarni S. (2008). Development and Realization of an autonomous driving concept for planetary vehicles. Technical Report DLR-IB 515-2008/13.

Kurzeck B., Carrarini A., and Heckmann A. (2007). Projekt MAVela. Technical Report DLR-IB 515-07-26.

Kurzeck B., Loose S., Heckmann A., Meyer zu Hörste M., Kopp G., Ungethüm J., and Nickel J. (2008). Fahrzeugkonzept und Auslegungsdaten zum Next Generation Train. Technical Report DLR IB 515-07-45.

Looye G. (2008). Development of a generic GUI-based software environment for aircraft trimming. Technical Report DLR IB 515-08-32.

Martin G. (2007). Entwurf eines mechatronischen Konzepts für einen Krabbelroboter basierend auf der DLR-Hand Fingertechnologie. Technical Report DLR-IB 515-2007/9.

Meißner H. (2007). Untersuchung und Evaluierung von Methoden zur Kalibrierung optischer Sensoren in Verbindung mit Lagesensoren. Technical report.

Nölle A. (2008). Untersuchung der Genauigkeit von Objektgeschätzern. Technical Report DLR-IB 515-2008/10.

Nothelfer A. (2006). Modeling and Simulation of High-Energy Synchronous Machines. Technical Report DLR-IB 515-2006/13.

Oddoy T. (2006). Anbindung einer FPGA-Plattform an einen PC mittels USB-Schnittstelle unter Benutzung eines VHDL-Betriebssystems. Technical report.

Oertel D. (2006). Instrumente für die Raumfahrt Made in Adlershof (Editorial) Instruments for space-travel Made in Adlershof (Editorial). Technical report.

Otterbach M. (2005). Software-Werkzeug zur Diskretierung virtueller 3D-Objekte. Technical Report DLR-IB 515-2005/5.

Pfifer H. (2008). Generation of Optimal Linear Parametric Models for LFT-based Robust Stability Analysis. Technical Report DLR IB 515-08-17.

Plafka A. (2007). Entwicklung eines Treibers für den integrierten DLR-Kraft-Momentensensor. Technical Report DLR-IB 515-2006/22.

Potdar A. (2007). Modelling and Design of soft fingertips of a dexterous robot hand. Technical Report DLR-IB 515-2007/12.

Pügner T. (2005). Erstellung und Implementierung eines Kommunikationskonzeptes für den multisensoriellen 3DModellierer-R. Technical Report DLR-IB 515-2005/6.

Quasem M. (2006). Investigation of non-holonomic characteristics in free-floating space robots. Technical Report DLR-IB 515-2006/6.

Radi M. (2006). Transparency Measurements of Telepresence Systems. Technical Report DLR-IB 515-2006/20.

Raugust M. (2008). Entwicklung und Evaluation eines Softwarepakets zur Regelung eines Seedlasersystems (Engl.: Development und evualation of a softwarepaket to controll a seed laser system). Technical report.

Reijerkerk M. (2006). Inter report: Winglet Loads Investigation. Technical Report DLR IB 515-06/11.

Reijerkerk M. (2007). DARIUS FACT Validation for Reference case. Technical Report DLR-IB 515-07-24.

Reijerkerk M. (2007). FACT Validation using TLS data, Part II Comparsion with linear flexible procedure. Technical Report DLR-IB 515-07-23.

Reijerkerk M. (2007). Study of winglet aerodynamics for static aero-elastic purposes. Technical Report DLR-IB 515-07-41.

Ries M. (2005). Entwicklung eines hochdynamischen Robotersystems zum Abfangen eines schnell bewegten Objekts. Technical Report DLR-IB 515-2005/2.

Rink C. (2006). Merkmalbasierte Registrierung homogener Dreiecksnetze. Technical Report DLR-IB 515-2006/17.

Ritter M. (2006). Midi-basiertes Klavierspielen unter Berücksichtigung der Anschlagdynamik mit der impedanzgeregelten DLR-Roboterhand. Technical Report DLR-IB 515-2006/16.

Roos C., Döll C., Hecker S., and Varga A. (2008). Preliminary LFT models for nonlinear behaviour and complete model of aircraft linear dynamics. Technical Report DLR IB 515-08-35.

Rosenthal C. (2006). Feature Detection und Matching Verfahren zur Positions- und Lagebestimmung. Technical report.

Ruder J. (2008). Robuste Stabilitätsanalyse mit Integral Quadratic Constraints. Technical Report DLR IB 515-08-16.

Rybak A. (2008). Entwicklung eines elektrohydraulischen Herzunterstützungssystems. Technical Report DLR-IB 515-2008/07.

Sagardia M. (2008). Enhancements of the Voxmap-PointShell Algorithm. Technical Report DLR-IB 515-08/4.

Sahin A. (2005). Inversion of Vehicle Dynamics with Modelica. Technical Report DLR-IB 515-2005/01.

Schabreiter H. P. (2007). Aufbau einer interaktiven Desktop-Simulationsumgebung für den Entwurf und die Evaluierung von Fehlererkennungsalgorithmen und fehlertoleranten Regelungen. Technical Report DLR-IB 515-07-42.

Schätzle S. (2006). Entwicklung eines vibrotaktilen Feedback-Geräts für den Unterarm. Technical Report DLR-IB 515-2006/12.

Schätzle S. (2007). Aufbau und Regelung eines Satelliten Simulators für On-Orbit Servicing. Technical Report DLR IB 515-07-8.

Scherbaum P. (2007). Entwicklung und Verifikation eines Testplatzes für TDI-Kameras, Deployment and verification of a test site for TDI cameras. Technical report.

Schimanek T. (2005). Analyse der Lagegenauigkeit und Design von aktiven Markern eines optischen Trackingsystems. Technical Report DLR-IB 515-2005/19.

Schischmanow A. (2005). Analyse des Straßenverkehrs mit verteilten optoelektronischen Sensoren. Technical report.

Schmidt F. (2007). Realisierung eines Demonstrators für Servicerobotik: Lösen eines Rubiks-Cube mit dem anthropomorphen Roboter JUSTIN. Technical Report DLR-IB 515-2007/19.

Schott K. and Gschwilm J. (2007). Experimentelle Unersuchung einer hydraulischen Servolenkung. Technical Report DLR IB 515-07-07.

Schroth G. (2006). Raumfahrt-Kommunikation für Telepräsenzanwendungen. Technical Report DLR-IB 515-06-21.

Schürmann N. (2005). Energieoptimale Regelung eines Ram Air Inlet Actuators. Technical Report DLR-IB 515-2004/38.

Schwerin T. (2008). Scanwinkelmessung bei einem MEMS-basierten Laser-Entfernungsmesser. Technical Report DLR-IB 515-2008/01.

Seeni A. (2007). Systems Study for Robotic Moon Missions. Technical Report DLR-IB 515-2007/28.

Sparchholz C. (2005). Stereoskopie – Wahrnehmung, Techniken und Verfahren. Technical report.

Stelzer M. (2007). Entwurf einer generischen Daten- und Kommandoschnittstelle zur Steuerung von Teilsystemen orbitaler Service-Satelliten. Technical Report DLR-IB 515-2007/32.

Stemmer A. (2005). Entwurf und Implementierung robuster Fügestrategien für impedanzgeregelte Roboter. Technical Report DLR-IB 515-2005/11.

Stillfried G. (2008). Modellierung menschlicher Fingergelenke als Scharniergelenke mit geneigter Drehachse. Technical Report DLR-IB 515-08-12.

Strohmayr M. (2007). Development and Analyses of a bio-inspired Tactile-Sensor. Technical Report DLR-IB 515-2007/20.

Stude J. (2007). Drehzahlmessung an Mikroreaktionsrädern zur Satellitensteuerung. Technical report.

Stumpf J. (2006). Entwicklung einer miniaturisierten multisensoriellen Elektronik mit Standardkomponenten zur Verwendung in mechatronischen Systemen. Technical Report DLR-IB 515-2006/2.

Thielmann S. (2008). Antriebseinheit für ein robotergeführtes minimal invasives Instrument. Technical Report DLR-IB 515-2008/09.

Tolstoi W. (2007). 3D-Modellierung ausgehend von Laserscandaten. Technical Report DLR-IB 515-2007/47.

Trommer C. (2007). Entwicklung eines mehr-achsigen Hals-Moduls für einen humanoiden Roboter. Technical Report DLR-IB 515-2007/5.

Vaculin O., Schupp G., Kaiser I., and Heckmann A. (2005). ProSiD - Final Report. Technical Report DLR-IB 515-05-07.

van der Linden F. (2007). Modeling of an Elastic Wheelset in a Multibody Environment. Technical Report DLR-IB 515-07-25.

Varga A. (2008a). Basic Software for Trimming. Technical Report DLR IB 515-08-31.

Varga A. (2008b). Clearance criteria for civil aircraft. Technical Report DLR IB 515-08-29.

Varga A. (2008c). Design of Least Order Residual Generators for Fault Detection and Isolation with Application to Monitoring Actuator/Surface Faults for a Boeing 747 100/200 Aircraft. Technical Report DLR IB 515-08-28.

Varga A. (2008d). Linear FDI-Techniques

and Software Tools. Technical Report DLR IB 515-08-18.

Varga A. and Joos H.-D. (2008). Clearance criteria library. Technical Report DLR IB 515-08-30.

Vilanova J. (2005). Time Domain Passivity - based Bilateral Control Design. Technical report.

Villanova i Buxó J. (2005). Time Domain Passivity-based Telepresence with Time Delay. Technical Report DLR-IB 515-2005/15.

Vogler A. (2007). Modellierung und Analyse eines anthropomorphen Roboterfinger. Technical Report DLR-IB 515-2007/11.

Vogler A. (2008). Entwicklung eines prototypischen Instrumentes für die robotergestützte, minimal invasive Erkennung und Verfolgung der Brustwandarterie zur teilautonomen Koronarrevaskularisation. Technical Report DLR-IB 2007/46.

Waldo A. (2007). Numerische Sensitivitätsanalyse bei der Parameteridentifizierung multiphysikalischer Systeme. Technical Report DLR-IB 515-07-43.

Wilhelm A. (2006). Design of a mobile robotic platform with variable footprint. Technical Report DLR-IB 515-2007/33.

Wu Z. (2007). Adaption of the Inverse Kinematics of the DLR Light Weight Robot for Its Use as Haptic Device. Technical Report DLR-IB 515-2007/37.

Zhukov B., Lorenz E., Oertel D., Wooster M., and Roberts G. (2005). Experience of detection and quantitative characterization of fires during the experimental small satellite mission BIRD. Technical Report 2005-04.

6 Acknowledgements

Putting together such a report is not a fun or rewarding thing, really. In giving birth to a document like this, the role of the editor is twofold. One the one hand, one has to make sure that the *function*, the contents, is selected, gathered, and ordered so that the reader can easily pick the right crumb here and there, or read a whole consecutive part. On the other, to present it in a *form* which is inconspicuous, not deviating the reader's mind from the contents; thus reducing syntactic and semantic mishaps: from inserting missing verbs to knowing the difference between an en-dash and an em-dash, and winning hopeless software fights.

Both of these arduous tasks could not have been realised without the input and assistance of many, many people in the institute, reading, correcting, and complaining. Apart, of course, from the department and institute heads, that long list of people includes Alin Albu-Schäffer, Klaus Arbter, Tobias Bellmann, Tim Bodenmüller, Anko Börner, Christoph Borst, Tilman Bünte, Andreas Eckardt, Oliver Eiberger, Werner Friedl, Martin Görner, Markus Grebenstein, Sami Haddadin, Ulrich Hagn, Andreas Heckmann, Johann Heindl, Ulrich Hillenbrand, Hans-Dieter Joos, Simon Kielhöfer, Philipp Kremer, Nadine Krüger, Roberto Lampariello, Klaus Landzettel, Friedrich Lange, Frank Lehmann, Liu Hong, Matthias Löhning, Mathias Nickl, Martin Otter, Britta Platt-van der Smagt, Carsten Preusche, Matthias Rainer, Bernd Schäfer, Manfred Schedl, Thomas Schmid, Wolfgang Sepp, Andreas Stemmer, Michael Suppa, Jakub Tobolár, Holger Urbanek, Andreas Varga, Thomas Wimböck, and Sebastian Wolf [and, of course, those whose input I have overseen]. A very special "thank you" goes to the secretarial team, who spent a large portion of their time on putting this beast together: Gabriele Beinhofer, Monika Köhler, Jessica Laskey, and Doris Volkmer.

the editor

6 Acknowledgements

Putting together such a report is not a fun or rewarding thing, really. In giving birth to a document like this, the role of the editor is twofold. One the one hand, one has to make sure that the *function*, the contents, is selected, gathered, and ordered so that the reader can easily pick the right crumb here and there, or read a whole consecutive part. On the other, to present it in a *form* which is inconspicuous, not deviating the reader's mind from the contents; thus reducing syntactic and semantic mishaps: from inserting missing verbs to knowing the difference between an en-dash and an em-dash, and winning hopeless software fights.

Both of these arduous tasks could not have been realised without the input and assistance of many, many people in the institute, reading, correcting, and complaining. Apart, of course, from the department and institute heads, that long list of people includes Alin Albu-Schäffer, Klaus Arbter, Tobias Bellmann, Tim Bodenmüller, Anko Börner, Christoph Borst, Tilman Bünte, Andreas Eckardt, Oliver Eiberger, Werner Friedl, Martin Görner, Markus Grebenstein, Sami Haddadin, Ulrich Hagn, Andreas Heckmann, Johann Heindl, Ulrich Hillenbrand, Hans-Dieter Joos, Simon Kielhöfer, Philipp Kremer, Nadine Krüger, Roberto Lampariello, Klaus Landzettel, Friedrich Lange, Frank Lehmann, Liu Hong, Matthias Löhning, Mathias Nickl, Martin Otter, Britta Platt-van der Smagt, Carsten Preusche, Matthias Rainer, Bernd Schäfer, Manfred Schedl, Thomas Schmid, Wolfgang Sepp, Andreas Stemmer, Michael Suppa, Jakub Tobolàr, Holger Urbanek, Andreas Varga, Thomas Wimböck, and Sebastian Wolf [and, of course, those whose input I have overseen]. A very special "thank you" goes to the secretarial team, who spent a large portion of their time on putting this beast together: Gabriele Beinhofer, Monika Köhler, Jessica Laskey, and Doris Volkmer.

the editor